SOVIET PHYSICS

JETP

A translation of the Zhurnal Éksperimental'noĭ i Teoreticheskoĭ Fiziki.

Vol. 12, No. 3 pp. 365-625 (Russ. orig. Vol. 39, No. 3, pp. 521-901, Sept., 1960) March, 1961

INVESTIGATION OF PARAMAGNETIC RELAXATION IN MAGNETICALLY DILUTE SYSTEMS

K. P. SITNIKOV

Kazan' State University

Submitted to JETP editor July 4, 1959; revised May 16, 1960

J. Exptl. Theoret. Phys. (U.S.S.R.) 39, 521-526 (September, 1960)

The internal magnetic field H_i and the splitting δ are evaluated for some paramagnetic substances on the basis of measured values of the specific heat b of the spin-system and of its electric component b_e. It is experimentally demonstrated that by means of magnetic dilution it is possible to distinguish between the effects on the specific heat of the interaction between the magnetic ions and the electric and magnetic crystalline fields. It is also shown that the spin-lattice relaxation time depends on the concentration of the magnetic ions in the paramagnetic substance.

1. CALCULATION OF THE SPECIFIC HEAT

FOR ions of elements of the iron group situated in a crystalline lattice the interaction with the surroundings may be considered weak and may be treated as a perturbation: the interaction energy $\epsilon_i \ll kT$ (cf., for example, references 1 and 2). Crystalline hydrates and their solutions are suitable materials in which such conditions are realized.

In crystals of salts of elements of the iron group the lowest orbital energy level of the ion E_1 lies lower than the next level E_2 by an amount $E_2 - E_1 \gg kT$. Moreover, the orbit of the ground level should be considered as fixed by the electric field of the crystal, and the orbital angular momentum should be taken as $L = 0$. Consequently, there remains the orbital singlet which is $(2S + 1)$ -fold degenerate with respect to spin. This level is subject to the influence of the internal electric and magnetic fields, as a result of which the degeneracy is removed completely. The difference in energy between the highest and the lowest sublevels of the multiplet is $\epsilon - \epsilon_0 \ll kT$.

By setting up on the basis of the concepts of a free ion and of multiplet structure the spin partition function

$$Z^{sp} = \sum e^{-\epsilon_i/kT} \Omega(\epsilon_i)$$

[where $\Omega(\epsilon_i)$ is the multiplicity of the sublevel ϵ_i] we can with the aid of the usual statistical formulas calculate the free energy, the entropy, and the specific heat. Let us discuss several concrete cases.

Spin $S = \frac{1}{2}$. In this case the electric field does not affect the spin, and the remaining Kramers degeneracy is removed by the magnetic field of the crystal. Consequently, the specific heat will have its origin in the interaction of the magnetic ion with the magnetic field of the crystal. Then we have

$$Z^{sp} = 1 + e^{-\Theta_1/T},$$

where $\epsilon_1 - \epsilon_0 = k\Theta_1$ is the splitting of the sublevels of the multiplet in the magnetic field of the crystal. On taking into account the fact that $\Theta_1 \ll T$ we obtain the following approximate expression for the molar specific heat of the spin system:

$$c = b_m T^{-2}, \qquad b_m = 0.25 R\Theta^2. \tag{1}$$

Spin S = 1. Let the electric field have rhombic symmetry. Then the degeneracy will be already completely removed by the electric field. In this case the specific heat of the spin system has its origin in the interaction of the magnetic ions with the electric field of the crystal. In accordance with the symmetry of the field and with the value of the spin we have

$$Z^{sp} = 1 + e^{-\delta_1/T} + e^{-\delta_2/T},$$

where δ_i is the splitting of the sublevels of the multiplet by the crystalline electric field. For the specific heat we obtain

$$c = b_e T^{-2}, \qquad b_e = 0.222 R(\delta_1^2 + \delta_2^2 - \delta_1\delta_2). \tag{2}$$

Spin S = $\frac{3}{2}$. In this case the magnetic interactions are superimposed on the electric ones. On taking into account the value of the spin and the fact that the degeneracy is completely removed by the electric and the magnetic fields of the crystal, we can write

$$Z^{sp} = 1 + e^{-\Theta_1/T} + e^{-\delta_1/T} + e^{-(\delta_1+\Theta_2)/T},$$

where Θ_i and δ_i are the splittings of the sublevels respectively due to the magnetic and the electric fields of the crystal. From this we obtain the following expression for the specific heat

$$c = bT^{-2},$$

$$b = \tfrac{3}{16} R\left\{\Theta_1^2 + \Theta_2^2 - \tfrac{2}{3}\Theta_1\Theta_2 - \tfrac{4}{3}\delta_1(\Theta_1 - \Theta_2) + \tfrac{4}{3}\delta_1^2\right\}. \tag{3}$$

If in the case S = $\frac{3}{2}$ we take into account the interaction of the ion with only the electric crystalline field (for example, of trigonal symmetry), then the partition function assumes the form

$$Z^{sp} = 2(1 + e^{-\delta_1/T}).$$

From this we obtain for the specific heat

$$c_e = b_e T^{-2}, \qquad b_e = 0.25 R\delta_1^2. \tag{4}$$

Spin S = $\frac{5}{2}$. We consider first the case when the degeneracy is removed completely by the electric and the magnetic fields of the crystal. On taking into account the value of the spin and the effect of the fields the partition function must be written in the form

$$Z^{sp} = 1 + e^{-\Theta_1/T} + e^{-\delta_1/T}(1 + e^{-\Theta_2/T}) + e^{-\delta_2/T}(1 + e^{-\Theta_3/T}),$$

where Θ_i and δ_i are, as before, the splittings of the sublevels due to the magnetic and the electric fields respectively. From this we obtain the following formula for the total specific heat of the spin-system

$$c = bT^{-2},$$

$$b = \tfrac{5}{36} R\left\{\Theta_1^2 + \Theta_2^2 + \Theta_3^2 - \tfrac{2}{5}(\Theta_1\Theta_2 + \Theta_1\Theta_3 + \Theta_2\Theta_3) - \tfrac{4}{5}(\delta_1 + \delta_2)(\Theta_1 + \Theta_2 + \Theta_3) + \tfrac{12}{5}(\delta_1\Theta_2 + \delta_2\Theta_3) + \tfrac{8}{5}(\delta_1^2 + \delta_2^2 - \delta_1\delta_2)\right\}. \tag{5}$$

We can obtain an approximate formula for the electric component of the specific heat of the spin system for the same ion by setting in (5) $\Theta_1 = \Theta_2 = \Theta_3 = 0$:

$$c_e = b_e T^{-2}, \qquad b_e = 0.222 R(\delta_1^2 + \delta_2^2 - \delta_1\delta_2). \tag{6}$$

2. DEPENDENCE OF THE SPECIFIC HEAT OF THE SPIN SYSTEM ON THE CONCENTRATION OF MAGNETIC IONS

We have investigated the paramagnetic absorption in parallel fields at room temperature. The object of the investigation was to find the dependence of the specific heat b and the spin-lattice relaxation time ρ on the concentration of magnetic ions in paramagnetic substances.

The thermodynamic theory of paramagnetic relaxation in parallel fields due to Shaposhnikov[3] leads to the following formula for the imaginary part χ'' of the complex susceptibility:

$$\chi''/\chi_0 m = F/\rho\nu + (1 - F)^2 \rho_s \nu, \qquad F = H_c^2/(b/C + H_c^2), \tag{7}$$

where χ_0 is the equilibrium susceptibility, m is the mass of the substance being investigated, ρ is the spin-lattice relaxation time, ρ_S is the spin-spin relaxation time, ν is the frequency of the alternating field, H_C is the constant external field, and C is the Curie constant. Formula (7) refers to the case when $\rho_S \ll \rho$, $\rho_S\nu \ll 1$ and $\rho\nu \gg 1$. When ρ_S and ρ differ sufficiently from one another it is possible to choose the frequency ν so large that the first term of formula (7) is much smaller than the second one. Then absorption will take place in accordance with the following formula

$$\chi''/\chi_0 m = (1 - F)^2 \rho_s \nu \tag{8}$$

and will be due only to internal relaxation. This is exactly what occurs at the 600 Mc/sec which we used.

Formula (8) has been checked in a number of investigations,[4,5] and has been found to agree well with experiment if we assume that ρ_S does not depend on the constant field H_C. Formula (8) enables us to evaluate the constant b/C from the absorption curve.

The absorption curve whose ordinates are proportional to χ'' was obtained by utilizing the

grid current method proposed by Zavoĭskiĭ.[6] A detailed description of the oscillator used by us has been given by Salikhov.[7]

On assuming that the electric field of the crystal retains its symmetry on dilution (isomorphism) and that, consequently, the contribution to the specific heat due to the interaction of the magnetic ions with the electric field of the crystal does not depend on the concentration of the magnetic ions, we can measure this specific heat by eliminating the magnetic component by means of magnetic dilution of the paramagnetic substance.[8]

For this purpose we prepared solid solutions of potassium chrome alum in which chromium ions are replaced by aluminum ions:

$$[CrK(100-n)+n\,AlK](SO_4)_2\cdot 12H_2O,$$

and also of the hydrate of manganese sulphate, in which manganese ions are replaced by magnesium ions:

$$[Mn(100-n)+n\,Mg]\,SO_4\cdot 4H_2O$$

(n is the concentration of the diamagnetic Al^{3+} and Mg^{2+} ions in these solutions). A single crystal grown in a solution of appropriate concentration was pulverized prior to the experiment and an ampoule containing this powder was placed inside the coil that produced the high-frequency field. This coil was placed in the gap of a magnet parallel to the constant field. The chromium and manganese concentrations in the solutions were determined chemically.

The absorption curves obtained as functions of the constant field H_C in solutions of chrome alum with different concentrations of the magnetic ions are shown in Fig. 1. It turns out that these curves are in good agreement with formula (8), and this allows us to evaluate the constant b/C.

The values of the constant b/C obtained for different concentrations of the magnetic ions are shown in Fig. 2. It may be seen from the figure that the constant b/C falls off rapidly with the magnetic dilution approaching the value

$$(b/C)_e = 0.22\cdot 10^6\ \text{oe}^2. \qquad (9)$$

Thus, in the case of chrome alum the following quantities are obtained from the measurements: the values of the total constant b/C (cf. reference 5) and of its electric component $(b/C)_e$. Then, on taking into account the additive properties of specific heat, we can also obtain the magnetic component of this quantity:

$$b/C = (b/C)_m + (b/C)_e. \qquad (10)$$

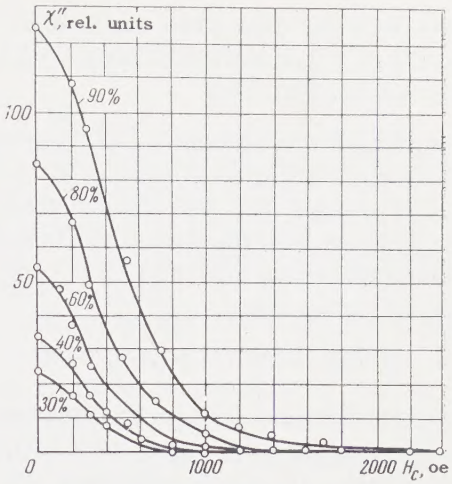

FIG. 1. Absorption curves in solid solutions of potassium chrome alum. Numbers beside the curves indicate the concentration of magnetic ions in solution; $\nu = 600$ Mc/sec.

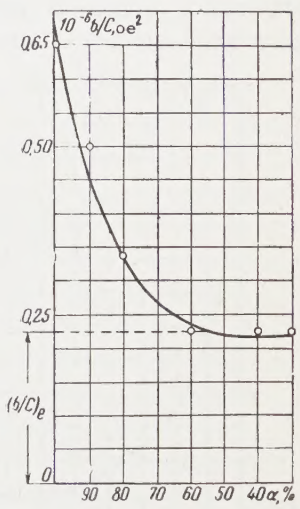

FIG. 2. Dependence of the constant b/C for the spin system on the concentration α of magnetic ions in solutions of potassium chrome alum. Circles indicate measured values of b/C.

The values of these quantities are shown in Fig. 2.

The paramagnetic absorption curves in solutions of the hydrate of manganese sulphate with a concentration of magnetic ions equal to 90, 80, 60, 50, 20, and 10% are similar to the curves of Fig. 1; we do not reproduce them here.

The dependence of b/C on the concentration of magnetic ions is shown in Fig. 3. From this figure it can be seen that in this case b/C falls off rapidly with magnetic dilution, approaching the constant value

$$(b/C)_e = 0.40\cdot 10^6\ \text{oe}^2. \qquad (11)$$

Thus experiments have shown that it is possible to distinguish between the effects on the specific heat of a spin-system due to the interaction of the magnetic ions with the electric and the magnetic fields of the crystal.

3. DEPENDENCE OF THE SPIN-LATTICE RELAXATION TIME ON THE CONCENTRATION OF THE MAGNETIC IONS

At sufficiently low frequencies paramagnetic absorption in parallel fields is determined only by spin-lattice relaxation (cf. Sec. 2) and takes place in accordance with the first term in formula (7), the exact expression for which (cf. reference 9) is of the following form

$$\chi''/\chi_0 m = \rho\nu F/(1+\rho^2\nu^2). \qquad (12)$$

We have utilized formula (12) for the measurement of ρ in solid magnetic solutions of $CrK(SO_4)_2 \cdot 12H_2O$ and $MnSO_4 \cdot 4H_2O$ (cf. reference 10). The absorption in these salts was studied at 7 and 13 Mc/sec respectively. The absorption curves in potassium chrome alum are shown in Fig. 4. The absorption curves in manganese sulphate are just as representative of spin-lattice relaxation as those shown in Fig. 4, and are therefore not reproduced here.

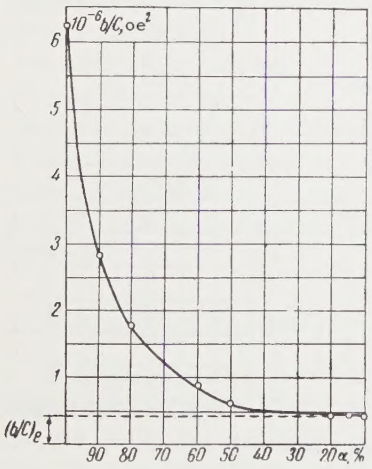

FIG. 3. Dependence of the constant b/C for the spin system on the concentration α of magnetic ions in manganese sulphate.

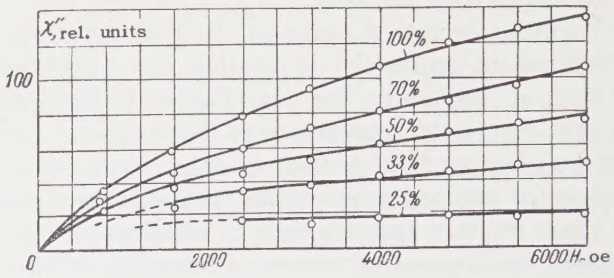

FIG. 4. Absorption curves in solid solutions of potassium chrome alum. Numbers beside the curves indicate the concentration of magnetic ions in solution; ν = 7 Mc/sec.

The calculated values of ρ for different concentrations of magnetic ions in the solutions, and for different values of the constant field H_C are given in Tables I and II for potassium chrome alum and for manganese sulphate respectively. It can be seen from the tables that the spin-lattice relaxation time increases as the concentration of magnetic ions in solution is decreased. The observed increase in the spin-lattice relaxation time ceases in chrome alum at a magnetic dilution by a factor of approximately two, and in manganese sulphate by a factor of approximately four, which is evidently related to the concentration of magnetic ions in the initial material. It should be noted that the observed effect is more pronounced in weak fields.

4. EXAMPLES OF THE EVALUATION OF THE CONSTANTS δ AND H_i

$CrK(SO_4)_2 \cdot 12H_2O$. Let us evaluate the splitting of the sublevels by the electric field of the crystal

TABLE I. Spin-lattice relaxation time ρ in potassium chrome alum for different concentrations α of Cr^{3+} ions

H_c	ρ, 10^{-8} sec					H_c	ρ, 10^{-8} sec				
	α = 100%	70%	50%	33%	25%		α = 100%	70%	50%	33%	25%
800	0.3	0.5	0.6			4000	1.2	1.4	1.6	1.5	1.7
1600	0.5	0.8	0.9	1.0	1.0	4800	1.3	1.5	1.6	1.8	1.8
2400	0.8	1.0	1.2	1.3	1.3	5600	1.4	1.6	1.9	2.0	2.1
3200	1.0	1.2	1.4	1.5	1.6	6400	1.4	1.9	2.3	2.4	2.3

TABLE II. Spin-lattice relaxation time in manganese sulphate for different concentrations of Mn^{2+} ions

H_c	ρ, 10^{-7} sec					H_c	ρ, 10^{-7} sec				
	α=100%	60%	33%	25%	10%		α=100%	60%	33%	25%	10%
800	3.4	11.0	13.9	14.1		4000	7.5	14.1	19.8	20.5	21.0
1600	4.1	12.5	17.0	18.0		4800	8.6	15 6	20.5	21.0	22.0
2400	5.2	13.0	18.4	18.3	18.2	5600	9.6	16.0	21.0	22.0	22.0
3200	6.4	13.4	18.7	20.0	20.0	6400	10.0	16.6	21.0	22.0	22.0

in this salt. On comparing (4) and (9), and on utilizing the value C = 1.87 for the Curie constant, we obtain $\delta_1 = 0.14°$, which agrees with the value $\delta_1 = 0.17°$, obtained by other investigators.[11,12]

On substituting into formula (3) the numerical values $b/C = 0.66 \times 10^6$, C = 1.87, $\delta_1 = 0.14°$, and on setting in accordance with Hund's rules $\Theta_1 = \sqrt{15}\beta H_i/k$ and $\Theta_2 = \sqrt{3}\beta H_i/k$ (β is the Bohr magneton), we obtain $H_i = 1170$ oe.

$MnSO_4 \cdot 4H_2O$. In accordance with formula (6) we obtain for the value of the splitting $\delta_{eff} = 0.30°$ (the Curie constant is C = 4.37). In formula (6) we have set $\delta_1 = \delta_2$. This is possible because $\delta_1, \delta_2 \ll T$ and the sublevels may be regarded as coincident. The value of δ_{eff} for $MnSO_4 \cdot 4H_2O$ is apparently measured here for the first time.

For the evaluation of the internal field H_i in the same salt we again set $\delta_1 = \delta_2$ in formula (5). Further, on substituting the numerical values $b/C = 6.20 \times 10^6$, C = 4.37, $\delta_{eff} = 0.30°$ and on setting in accordance with Hund's rules $\Theta_1 = \sqrt{35}\beta H_i/k$, $\Theta_2 = \sqrt{15}\beta H_i/k$ and $\Theta_3 = \sqrt{3}\beta H_i/k$, we obtain $H_i = 3913$ oe.

$CuSO_4 \cdot 5H_2O$. On substituting into formula (1) the numerical value $b/C = 0.47 \times 10^6$, and the Curie constant C = 0.37 we obtain $H_i = 790$ oe.

In accordance with Gorter's estimate[9] made on the basis of the concept of dipole-dipole interaction, the internal field H_i in $CrK(SO_4)_2 \cdot 12H_2O$, $MnSO_4 \cdot 4H_2O$, and $CuSO_4 \cdot 5H_2O$ is respectively equal to 310, 1200, and 370 oe.

[1] Ya. G. Dorfman, Магнитные свойства и строение вещества (Magnetic Properties and the Structure of Matter), Gostekhizdat, 1955.

[2] S. V. Vonsovskiĭ, Современное учение о магнетизме (Modern Theory of Magnetism), Gostekhizdat, 1952.

[3] I. G. Shaposhnikov, JETP **18**, 533 (1948).

[4] N. S. Garif'yanov, JETP **25**, 539 (1953).

[5] K. P. Sitnikov, JETP **34**, 1093 (1958), Soviet Phys. JETP **7**, 757 (1958).

[6] E. K. Zavoĭskiĭ, Doctoral Thesis, Physics Institute, Academy of Sciences, U.S.S.R., 1944.

[7] S. G. Salikhov, JETP **17**, 1070 (1947).

[8] K. P. Sitnikov, Thesis, Kiev State University, 1954.

[9] C. J. Gorter, Paramagnetic Relaxation, Elsevier, N. Y. 1947.

[10] K. P. Sitnikov, JETP **34**, 1090 (1958), Soviet Phys. JETP **7**, 755 (1958).

[11] M. H. Hebb and E. M. Purcell, J. Chem. Phys. **5**, 338 (1937).

[12] Gordy, Smith, and Trambarulo, Microwave Spectroscopy, Wiley, N. Y., 1955.

Translated by G. Volkoff
105

SECONDARY CAPTURE OF LITHIUM NUCLEI BY LEAD

WANG YUNG-YÜ, V. V. KUZNETSOV, M. Ya. KUZNETSOVA, V. N. MEKHEDOV, and V. A. KHALKIN

Joint Institute for Nuclear Research

Submitted to JETP editor March 12, 1960

J. Exptl. Theoret. Phys. (U.S.S.R.) 39, 527-535 (September, 1960)

The formation of $At^{211,210,207}$ in lead under bombardment by 80 — 660 Mev protons, 75 — 370 Mev deuterons and 210 — 810 Mev alpha particles has been studied by radiochemical means. The astatine isotopes result from secondary capture of lithium nuclei produced through disintegrations and having kinetic energies exceeding the Coulomb barrier. The At^{211} yield under alpha-particle bombardment reaches 0.3 microbarn and is practically independent of the alpha-particle energy. Under proton and deuteron bombardment the yield increases with particle energy, especially when the proton energy exceeds 400 Mev, and attains 0.2 microbarn at 660 Mev. The At^{211} yield is independent of lead target thickness in the 0.3 — 1.6 mm range and decreases for thicknesses smaller than 0.3 mm. The production cross section for the captured lithium fragments is computed and their energy spectrum is estimated on the basis of the astatine yield from lead. The cross section for production of "over-Coulomb" lithium fragments by 660-Mev protons is 3 — 6 millibarns.

INTRODUCTION

THE most interesting aspect of the fragmentation process,[1-6] by which we mean the ejection of lithium, beryllium and heavier fragments from excited nuclei, is the emission of fragments having energies that exceed the Coulomb barrier. No satisfactory theoretical explanation has thus far been advanced for this phenomenon. None of the known mechanisms of nuclear reactions can account for the fact that an aggregate of nucleons may, without being disrupted, receive an amount of kinetic energy which sometimes exceeds the total binding energy of the nucleons in the fragment.

Radiochemical investigations of "secondary" reactions[7-11] provide one method for the study of this process. These secondary reactions are produced in nuclei of the target by secondary "over-Coulomb" fragments. In the present work we have studied the formation of astatine isotopes in the secondary reaction $_{82}Pb(Li, xn)_{85}At$ when lead is bombarded with high-energy protons, deuterons or alpha particles. Lead was chosen as the target material for two reasons. The undesirable bismuth, uranium and thorium impurities can be removed relatively easily from lead. Also, despite the very low reaction yield (cross section) of $10^{-30} — 10^{-32}$ cm^2 the astatine end-product can be detected conveniently by means of its alpha emission. Chemical removal of beta- and gamma-active contamination from the reaction products is considerably simplified.

EXPERIMENTAL PROCEDURE

For reliable observation of a secondary reaction, the lead target must not contain more than 10^{-3}, 10^{-4} or 10^{-5}% of bismuth, uranium, or thorium, respectively.[10] This level of purity was attained as follows. The original chemically pure lead carbonate was used to prepare lead nitrate, which was recrystallized twice from a 75% solution (by volume) of methyl alcohol and once from concentrated nitric acid. The nitrate was heated and the resulting lead oxide was reduced to the metal by means of sucrose at 700 — 800° C. The original lead carbonate contained 10^{-2}% bismuth, but the lead metal revealed no trace of bismuth ($< 10^{-3}$%).* Uranium and thorium impurities in the metallic lead were estimated from the Ra^{223} yield under bombardment by 120-Mev protons and amounted to $< 10^{-5}$% if we assume a ~10-millibarn cross section for the formation of Ra^{223} from these elements.[12]

The targets were bombarded with 80 — 660 Mev protons, 75 — 370 Mev deuterons and 210 — 810 Mev alpha particles. The bombarding energy was varied by placing the target at different radial dis-

*Bismuth impurity in the lead was determined spectroscopically by M. Farafonov of the GEOKhI (Institute of Geochemistry and Analytical Chemistry), to whom the authors wish to express their appreciation.

tances in the beam path. In order to obviate the loss of astatine through target heating by the proton or deuteron beam, the lead samples, which weighed about 1 gram, were sealed in quartz ampoules with an outside diameter of 4 mm, 30 mm length and 0.5 — 0.6 mm wall thickness. Irradiation periods varied from 0.2 to 2 hours.

For the purpose of determining the astatine yield, 660-Mev protons were used to bombard lead foils of different thicknesses placed on the end faces of plates forming the magnetic extracting channel[13] of the synchrocyclotron. The proton beam was greatly diffused at the plates and the flux was attenuated by a factor of 50 — 100 compared with the circulating beam. All of the foils (each measuring 3 × 40 mm) were placed in a row in a single plane perpendicular to the proton beam and were bombarded simultaneously during 2 — 10 hours.

Diisopropyl ether was used to extract astatine from the irradiated lead dissolved in hydrochloric acid. For further purification, the radioactive impurities were coprecipitated with elemental tellurium from an alkaline solution, and the astatine was coprecipitated with elemental tellurium from a hydrochloric acid solution. (Details of the chemical technique for separating astatine are given in reference 14.) As a control some lead samples were treated by the procedure described in reference 10, which is based entirely on the coprecipitation of astatine with tellurium; the astatine yields agreed, within experimental error, with those of the extraction procedure.

Our measuring technique and apparatus have been described in reference 15. In all experiments both 7.5 -hour and ~ 140-day alpha activity were detected, which we assigned to At^{211} and Po^{210}. In some experiments activity with a half-life of about 2 hours was observed and was assigned to At^{207}.

The intensity of the bombarding beam was determined through the yield of Na^{24} from the aluminum foil in which the samples were wrapped during irradiation. The technique for measurements on Na^{24} was the same as that described in reference 15. The cross sections for N^{24} formation from Al^{27} under different bombarding energies was taken from references 16 — 19. For deuterons with > 200 Mev and alpha particles with > 400 Mev, the cross sections for Na^{24} formation were determined by extrapolating the excitation curves of Na^{24} yield given in references 16 and 17. In the case of deuterons this cross section was taken to be 22 millibarns, while for 585- and 810-Mev alpha particles it was estimated at 18 and 13 millibarns, respectively.

Possible errors in beam monitoring during irradiation of the ampoules were determined by comparing the cross sections for astatine formation at 660 Mev, in the case of irradiation at the magnetic channel with and without ampoules and in the circulating beam at reduced intensity. The yields in all three cases agreed within experimental error.*

EXPERIMENTAL RESULTS

The yields of At^{211} and At^{210}, and the relative yield At^{207}/At^{211} at different proton energies, are given in Table I, where (as everywhere below) the averages of at least three determinations are given. A single determination was obtained only in the case of ~ 80-Mev protons. Random errors for the astatine yield given in Table I do not exceed ±30%. The relative yield of At^{207} takes the 90% K-capture branching fraction into account.

TABLE I

Proton energy, Mev	Yield (cross section), microbarns		At^{207}/At^{211}	Total yield (cross section), microbarns
	At^{211}	At^{210}		
660	0.17	0.21	~1.3	~1.3
500	0.06	0.10	–	~0.35
340	0.03	0.08	–	~0.2
120	0.005	0.01	~1.1	~0.03
~80	~0.01	–	–	–

$At^{205}(\alpha, K)$ with $T_{1/2}$ = 25 min was detected in one run with 660-Mev protons, and its relative yield was estimated. When K capture is neglected we have $At^{205}/At^{211} \sim 0.1$.

The At^{211} and At^{207} yields are almost identical for 660- and 120-Mev protons. For 500 — 120 Mev, the At^{210} yield is about twice as large as that of At^{211}. The yields of the different astatine isotopes decrease with decreasing proton energy in approximately the same manner. The At^{210}/At^{211} ratio averaged over all proton energies is 1.5 ± 0.5. The last column of Table I gives the total yield of isotopes from At^{207} to At^{211}. The yields of At^{209} and At^{208} were interpolated from the yields of At^{211}, At^{210}, and At^{207}. Random errors included in the total yield do not appear to exceed ±50%.

The At^{211} yield at different proton, deuteron, and alpha-particle energies are shown in Fig. 1.

*In the present work all targets were thick enough to make the yield independent of target thickness, with the exception of the experiments which were specifically intended to determine the dependence on target thickness.

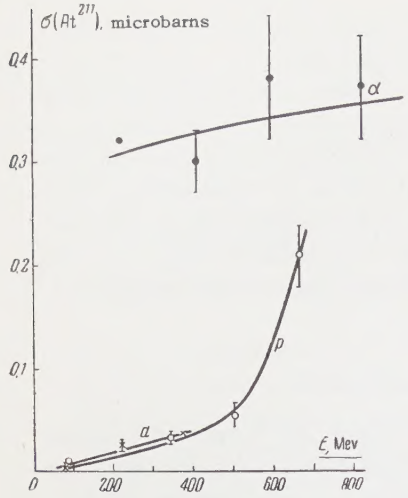

FIG. 1. At^{211} yield as a function of bombarding energies for alpha particles (α), deuterons (d) and protons (p).

The highest At^{211} yield (~ 0.3 microbarn) was detected under alpha-particle bombardment and varies only slightly with increasing alpha-particle energy. For deuterons and protons up to 400 Mev the At^{211} yields are almost identical, and are approximately one-tenth as large as for alpha-particles. Above 400 Mev, protons produce a strong increase of the At^{211} yield, which for 660-Mev protons becomes more than half of that for alpha particles.

It should be noted that in the case of high-energy alpha particles At^{211} can also be formed through alpha-particle capture by Pb^{208} followed by π^- and neutron emission, and also through capture by Pb^{207} followed by π^- emission. However, the figure shows that these reactions, if they do occur, are weak and not decisive.

Figure 2 shows the At^{211} yield from lead foils of different thicknesses. Almost no change is observed in the range 0.3 — 1.6 mm. Below 0.3 mm the yield decreases gradually and for 0.03 mm it amounts to half of the plateau value.

DISCUSSION

The observed quantity of astatine could not have been formed through the disintegration of any possible uranium, thorium, or bismuth impurities. It is estimated in the case of 120-Mev protons that these impurities could not account for more than one-tenth of the At^{211} and At^{210} yields. For protons with energies above 120 Mev this fraction becomes even smaller. The observed astatine activity therefore results almost entirely from the secondary reaction of lithium-capture reaction.

In Fig. 3 the proton-energy dependence of the total yield of astatine from lead is compared with an analogous curve for the formation of iodine from tin.[9] The curves are similar and at 660 Mev the astatine and iodine yields coincide.

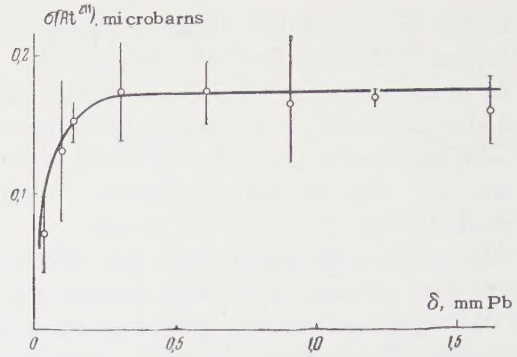

FIG. 2. At^{211} yield from lead foils of different thicknesses δ compared with a calculated curve.

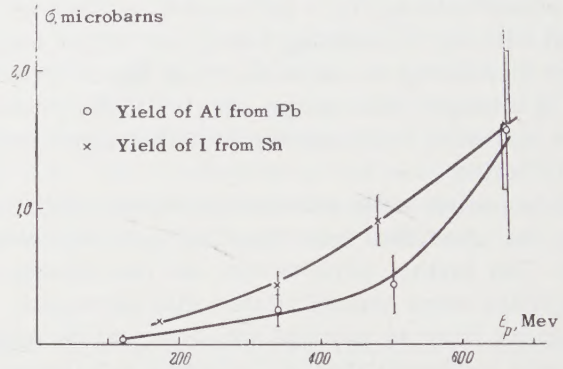

FIG. 3. Total cross section for the formation of astatine isotopes from lead and of iodine isotopes from tin as a function of proton energy.

The total astatine yield (~ 0.2 microbarn) which we obtained with 340-Mev protons agrees satisfactorily with the analogous yield of lead from gold (0.36 microbarn) obtained with 380-Mev protons.[11]

The procedure described in reference 10 was used in conjunction with the yields of secondary-reaction products to compute the energy spectrum of the lithium fragments and the cross sections for their formation from lead under bombardment by high-energy protons. The experimental yield ratios At^{210}/At^{211} and At^{207}/At^{211} had to follow from the selected lithium spectrum in conjunction with the given excitation functions for the reactions Pb(Li, xn)At(x = 1, 2, 3, . . . , 8) and the known losses of energy through ionization. The spectrum was then used to compute the cross section for lithium formation. On the basis of the data in reference 5 the lithium fragment spectrum was represented by*

$$P(E)\,dE = \tau^{-2}(E - V)\,e^{-(E-V)/\tau}\,dE \qquad (1)$$

with suitable values of the parameters V and τ.

*We attach no physical significance to this shape of the energy spectrum. $P(E)dE = E^{-h}dE$, with $h \approx 2$, could also be used, but the selected formula furnishes a somewhat better approximation of all known experimental data.

It was assumed that the energy spectra for Li^6, Li^7, and Li^8 are identical.[5] The excitation functions for the capture of lithium fragments by lead isotopes were calculated separately for Li^6, Li^7, and Li^8 by means of Jackson's formulas,[20] while Babikov's formula was used to calculate the cross section for lithium capture by lead.

Figure 4 shows the calculated excitation functions for the principal reactions in the formation of At^{211}, At^{210}, and At^{207} when Li^6 and Li^7 are captured by different lead isotopes. 25 out of 43 possible reactions were considered. In each instance we took into account the abundance of the lead isotope, and the relative yields of Li^6, Li^7, and Li^8 from lead were taken to be 0.55 : 0.41 : 0.043 as in the case of gold.[11] Familiar formulas[22] were used to calculate the ranges of different fragments in lead.

Table II gives the calculated relative yields

TABLE II

V		At^{210}/At^{211}	At^{207}/At^{211}	σ_{Li}, mb
6	11,5	1,67	0,9	6,0
	10,5	1,63	0,79	6,1
	9,5	1,57	0,63	6,7
10	11,5	1,7	0,86	5,7
	10,5	1,65	0,8	6,0
	9,5	1,57	0,63	6,7
15	6,5	1,39	0,28	9,4
	5,5	1,27	0,15	11,4
	4,5	1,16	0,09	14,5

At^{210}/At^{211} and At^{207}/At^{211} together with the cross section for the formation of lithium fragments with > 30 Mev in the case of 660-Mev protons, for different values of V and τ. The critical quantity determining the energy spectrum is seen to be the relative yield At^{207}/At^{211}, whereas At^{210}/At^{211} and $\sigma_{Li}(E_{Li} > 30$ Mev) change very little as V and τ are varied. V = 15 Mev and $\tau = 4.5 - 6.5$ Mev correspond to relative yields At^{207}/At^{211} that differ strongly from the experimental results (Table I). V = 6 — 10 Mev and $\tau = 10.5 - 11.5$ Mev in (1) furnish the energy spectra that best satisfy all experimental data, including those in the literature. Figure 5 shows the spectrum of lithium fragments with energies above 30 Mev (τ = 11.5 Mev, V = 6 Mev). Satisfactory agreement is found between the shape of our spectrum and the calculated spectrum of lithium fragments from secondary reactions in gold.[11] However, the cross section for the formation of lithium nuclei with > 54 Mev from gold was four times as large as our result obtained with 340-Mev protons (σ_{Li} = 1 mb from gold; 0.27 mb from lead).

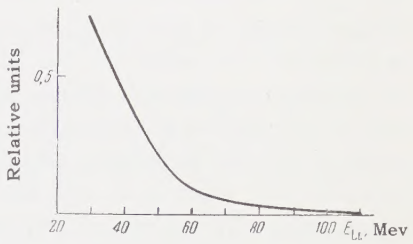

FIG. 5. Spectrum of lithium fragments with energies >30 Mev, calculated from the secondary-reaction yield in lead.

The approximate constancy of the relative yield At^{207}/At^{211} for 660-Mev and 120-Mev protons (Table I) indicates that the spectrum of over-Coulomb lithium fragments is either independent of proton energy or is only very slightly dependent. As a check, the calculated probability of At^{211} formation as a function of lead-foil thickness was compared with the experimental curve. For the purpose of the calculation we estimated the effective ranges of lithium nuclei in foils of different thicknesses, using the angular distributions of fast lithium fragments given in reference 5. The probability of At^{211} formation in lead of thickness δ was computed as the difference between the probability w_0 of formation by a fragment of the given energy in infinitely thick lead and the probability w of formation by a fragment with this same amount of energy remaining after it had traversed a lead layer of thickness δ. We have

$$w_0 = \sum_{i=1}^{n} N_0 \sigma_i \Delta l_i, \qquad (2)$$

where N_0 is the number of lead atoms per cm^3,

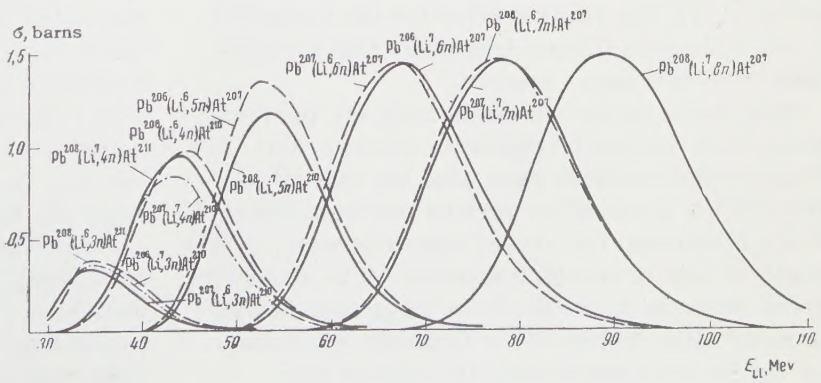

FIG. 4. Excitation functions for the principal reactions in the formation of $At^{211,210,207}$ when Li^6 and Li^7 are captured by different lead isotopes.

σ_i is the cross section for lithium capture leading to At^{211} formation, Δl_i is the ionization range of a fragment in lead within the energy range ($E_i + \Delta E_i$; E_i). The probability of At^{211} formation was integrated numerically over the entire lithium energy spectrum for each thickness δ.

The curve in Fig. 2 represents the calculated dependence of the probability of At^{211} formation; agreement with experiment is found at thicknesses beginning with 0.24 mm. The curve satisfactorily represents the falling-off of experimental values for small lead thicknesses. The postulated identity of the spectra of different lithium isotopes and the assumption of a value for the $Li^6 : Li^7 : Li^8$ ratio, as well as the possible differences between the calculated and actual excitation functions, somewhat reduce the reliability of the conclusions reached with respect to both the spectrum and the dependence of the yield on foil thickness. These conclusions must therefore be regarded as only qualitative.

Our experimentally observed dependence of the probability of At^{211} formation on lead-foil thickness permits an independent estimate of the cross section for the production of over-Coulomb lithium nuclei. This cross section, which we denote by σ^p_{Li}, is obtained from the relationship

$$B = N_0 \sigma^p_{Li} \overline{\sigma^{Li}_{At}} \Delta l. \quad (3)$$

Here B is the astatine yield for a given proton energy, $\overline{\sigma^{Li}_{At}}$ is the energy-averaged cross section for lithium capture by lead isotopes with subsequent astatine (At^{211}) formation. B and Δl are obtained directly from Fig. 2: B is the ordinate of the curve at saturation, and Δl represents roughly half of the lead thickness at which the probability of At^{211} formation begins to decrease from saturation. $\overline{\sigma^{Li}_{At}} = 0.1$ barn was calculated from the excitation functions for the reactions resulting in At^{211} formation, taking into account the abundances of the lead isotopes and the yields of different lithium nuclei. Substitution into (3) gives σ^p_{Li} 3 — 4 millibarns, which agrees satisfactorily with the cross section for the formation of over-Coulomb lithium fragments that is calculated from the energy spectra.

Some remarks on the mechanism for the formation of over-Coulomb fragments are in order. Although certain authors have used the statistical model[23,24] to account for various characteristics of fragmentation, this model cannot account for the origin of over-Coulomb fragments. The statistical model accounts for most of the fragments having energies close to that of the Coulomb repulsion, but not for the considerable fraction of over-Coulomb fragments. This can be seen from reference 4, for example, where emulsions were used to study the energy spectra of fragments. The authors of this paper discuss the partial success of evaporation theory and point to the need for some new mechanism. Our own work also shows that the energy spectrum of over-Coulomb fragments cannot be explained by means of the statistical model. If the parameter $\tau = 10.5 — 11.5$ Mev is given the physical meaning of a nuclear temperature, as is required in evaporation theory, we arrive at the absurd result that the excitation energy of the nucleus is several times greater than the energy of the bombarding particles. On the other hand, when we insert into (1) the values V = 15 Mev and $\tau = 4.5 — 5.5$ Mev, which are reasonable from the point of view of evaporation theory, we see from Table II that At^{207}/At^{211} is considerably below the experimental value.

The formation of over-Coulomb fragments cannot be accounted for within the statistical model by any possible "local" superheating of a nucleus as a result of pion creation and absorption, for example.[25,26] Figure 1 shows that over-Coulomb fragments are also produced at bombarding energies lying considerably below the threshold for meson production.

Over-Coulomb fragments are in all likelihood ejected before nuclear heating occurs, so that the statistical treatment is altogether unsuitable. This is indicated, for example, by the relationship between the yield of high-energy fragments and the number of cascade particles in disintegrations,[4] as well as by the high degree of forward emission of over-Coulomb fragments which has been noted in almost all studies of fragments in emulsions. We consider it more promising to regard the formation of over-Coulomb fragments as the result of direct many-particle interactions between nucleons of the target nucleus and both the bombarding particle and cascade nucleons.[27] Such interactions seem possible if we assume that the distance of nucleon separation in nuclear matter fluctuates so that nucleons can briefly come much closer than the average distance. Under these conditions an incoming particle could interact with a fluctuating group of nucleons as a whole and transfer to the latter a considerable fraction of its energy. However, we do not believe that we can apply the fluctuating-compression model of nuclear matter in the form that has been developed to account for the emission of high-energy deuterons.[28] This model yields a very small probability for the formation of over-Coulomb fragments and does not at all account for the fact

that we have observed the fragment yields to depend differently on proton and alpha-particle energies.

It must be noted that if many-particle interactions are responsible for the formation of over-Coulomb fragments, then reactions with multiply-charged ions should produce instances of the inverse event wherein the energy of an incoming ion is transferred to single nucleons. The fact that Karamyan and Pleve[29] have observed events in which the entire excitation energy (~ 60 Mev) was transferred to two nucleons indicates that such inverse many-particle interactions may occur.

The authors wish to thank E. N. Sinotov for experimental assistance and B. V. Kurchatov for valuable critical comments.

[1] D. H. Perkins, Proc. Roy. Soc. (London) **A203**, 399 (1950).

[2] O. V. Lozhkin and N. A. Perfilov, JETP **31**, 913 (1956), Soviet Phys. JETP **4**, 790 (1957).

[3] V. M. Sidorov and E. L. Grigor'ev, JETP **33**, 1179 (1957), Soviet Phys. JETP **6**, 906 (1958).

[4] Nakagawa, Tamai, and Nomoto, Nuovo cimento **9**, 780 (1958).

[5] O. Skjeggestad and S. O. Sörensen, Phys. Rev. **113**, 1115 (1959).

[6] S. Katcoff, Phys. Rev. **114**, 905 (1959).

[7] Batzel, Miller, and Seaborg, Phys. Rev. **84**, 671 (1951).

[8] A. Turkevich and N. Sugarman, Phys. Rev. **94**, 728 (1954).

[9] Kuznetsova, Mekhedov, and Khalkin, Атомная энергия (Atomic Energy) **4**, 455 (1958).

[10] Kurchatov, Mekhedov, Chistyakov, Kuznetsova, Borisova, and Solov'ev, JETP **35**, 56 (1958), Soviet Phys. JETP **8**, 40 (1959).

[11] A. E. Metzger and J. M. Miller, Phys. Rev. **113**, 1125 (1959).

[12] M. Lindner and R. N. Osborne, Phys. Rev. **103**, 378 (1956).

[13] Dmitrievskiĭ, Danilov, Denisov, Zaplatin, Katyshev, Kropin, and Chestnoĭ, Приборы и техника эксперимента (Instruments and Exptl. Techniques) 1, No. 11 (1957).

[14] Belyaev, Wang Yung-Yü, Német, Sinotova, and Khalkin, Preprint, Joint Institute for Nuclear Research; Радиохимия (Radiochemistry), in press.

[15] Wang Yung-Yü, Kuznetsov, Kuznetsova, and Khalkin, JETP **39**, 230 (1960), Soviet Phys. JETP **12**, 166 (1961).

[16] M. Lindner and R. N. Osborne, Phys. Rev. **91**, 342 (1953).

[17] Batzel, Crane, and O'Kelley, Phys. Rev. **91**, 939 (1953).

[18] Yu. D. Prokoshkin and A. A. Tyapkin, JETP **32**, 177 (1957), Soviet Phys. JETP **5**, 148 (1957).

[19] Friedlander, Hudis, and Wolfgang, Phys. Rev. **99**, 263 (1955).

[20] J. D. Jackson, Can. J. Phys. **34**, 767 (1956); **35**, 21 (1957).

[21] V. V. Babikov, JETP **38**, 274 (1960), Soviet Phys. JETP **11**, 198 (1960).

[22] B. Rossi, High-Energy Particles, Prentice-Hall, 1952.

[23] J. Hudis and J. M. Miller, Phys. Rev. **112**, 1322 (1958).

[24] K. J. Le Couteur, Nuclear Reactions, North-Holland Publ. Co., Amsterdam, 1959.

[25] Wolfgang, Baker, Caretto, Cumming, Friedlander, and Hudis, Phys. Rev. **103**, 394 (1956).

[26] N. T. Porile and N. Sugarman, Phys. Rev. **107**, 1422 (1957).

[27] M. Verdet, Anthology, Structure of the Atomic Nucleus, IIL, 1959.

[28] D. I. Blokhintsev, JETP **33**, 1295 (1957), Soviet Phys. JETP **6**, 995 (1958).

[29] A. S. Karamyan and A. A. Pleve, JETP **37**, 654 (1959), Soviet Phys. JETP **10**, 467 (1960).

Translated by I. Emin
106

MAGNETOACOUSTIC RESONANCE IN A PLASMA

A. P. AKHMATOV, P. I. BLINOV, V. F. BOLOTIN, A. V. BORODIN, P. P. GAVRIN, E. K. ZAVOĬSKIĬ, I. A. KOVAN, M. N. OGANOV, B. I. PATRUSHEV, E. V. PISKAREV, V. D. RUSANOV, G. E. SMOLKIN, A. R. STRIGANOV, D. A. FRANK-KAMENETSKIĬ, P. A. CHEREMNYKH, and R. V. CHIKIN

Submitted to JETP editor April 2, 1960

J. Exptl. Theoret. Phys. (U.S.S.R.) 39, 536-544 (September, 1960)

The work is devoted to the experimental study of magnetoacoustic vibrations in a cold plasma. It is shown that under certain conditions a high frequency electromagnetic field strongly penetrates into the plasma with an attendant resonance absorption of energy of the field. Results of the investigation of resonance at frequencies of 12.5 Mc/sec and 50 Mc/sec by various methods are described. These results are compared with the theoretical predictions.

1. For the investigation of the interaction of plasma with a variable electromagnetic field, it is first necessary to investigate the conditions for the appearance of vibrations inside the plasma. It is well known that in the absence of a static magnetic field, an electromagnetic field with a frequency lower than the plasma is reflected from the boundary of the plasma and does not penetrate inside. According to the theory, a static magnetic field should make possible the penetration into the plasma of vibrations with frequencies below the plasma frequency. In the present research, the problem was to investigate the appearance of vibrations perpendicular to the static magnetic field in a plasma. The physical picture of the phenomenon reduces in this case to compression and dilatation of the material together with the field "frozen" in it. The intensity of the field inside the plasma does not change as a consequence of the penetration of the external field but as a result of the compression and dilatation of the field "frozen" in the plasma. In its physical mechanism the process is analogous to ordinary sound vibrations, except that the fundamental role is played by the magnetic pressure $H^2/8\pi$ rather than the gas pressure. Therefore, the plasma oscillations that are investigated are known as magnetoacoustic.

As is known from theory, the velocity of propagation of magnetic "sound" in a cold plasma is close to the Alfvén velocity $H_0/\sqrt{4\pi\rho}$, where H_0 is the intensity of the static magnetic field and ρ is the density of the plasma. Under certain relations between H_0, ρ, the angular frequency of the vibration ω, and the radius of the plasma cylinder R, magnetoacoustic resonances should be observed.[1]

The resonance condition can be put in the form

$$\alpha H_0/\omega R\sqrt{4\pi\rho} = 1, \quad (1)$$

where α is a dimensionless number characterizing the type of vibration. If the frequency ω were less than the collision frequency, then the quantity ρ would represent the total density of the gas. Under our conditions, the frequency ω is large in comparison with the collision frequency, so that only charged particles take part in the vibrations. In this case ρ in Eq. (1) represents only the density of the charged particles of the plasma.

In the idealized case of purely radial vibrations of an infinite plasma cylinder,[2] where the wave vector is perpendicular to the direction of the magnetic field, penetration of the vibrations into the plasma should remain impossible for frequencies higher than the "hybrid" frequency,[3] which is close to the geometric mean of the electronic and ionic cyclotron frequencies. Here, anomalous dispersion should be observed close to the "hybrid" frequency. However, a small component of the wave vector along the magnetic field[1] is sufficient to prevent the anomalous phenomena pointed out above.

The spatial distribution of the amplitudes over the radius of the plasma cylinder should, according to theory,[1,2] be expressed in terms of Bessel functions of first order. If the static magnetic field is directed along the axis of the cylinder while the wave vector is almost perpendicular to it, then the fundamental role will be played by the axial component of the variable magnetic field $\tilde{H}_z \sim J_0(kr)$ and the azimuthal and radial components of the electric field E_φ, $E_r \sim J_1(kr)$.

The boundary condition is that E_φ vanish on the internal surface of the metallic housing. Since the velocity of propagation of the wave is much greater

in the vacuum than in the plasma, one can consider the same condition to be satisfied on the lateral surface of the plasma cylinder. Then the radial wave number k is determined from the condition that kR be the root of the Bessel function of first order.

The amplitude of the velocity of the radial motion of the plasma is estimated as

$$v_r \approx \tilde{H} u_{ph} / H_0 \approx \tilde{H} / \sqrt{4\pi\rho},$$

where u_{ph} is the phase velocity of the magnetic "sound." In first approximation, the ions and electrons move in the radial direction together. Moving in the azimuthal direction are essentially the electrons; their motion has a drift character with a velocity amplitude that can be estimated as $v_\varphi \approx \omega_i v_r / \omega$, where ω_i is the ionic cyclotron frequency.

2. In the experiment we investigated the interaction of a high-frequency electromagnetic field with a cold plasma in a cylindrical volume in the presence of an axial quasi-static magnetic field H_0 (see Fig. 1).

It must be noted that the plasma was generated by the same high-frequency field whose interaction with the plasma was being studied. This led to a marked change in the density of charged particles in the plasma under resonance conditions. Consequently, the experiments were carried out under essentially nonlinear conditions.

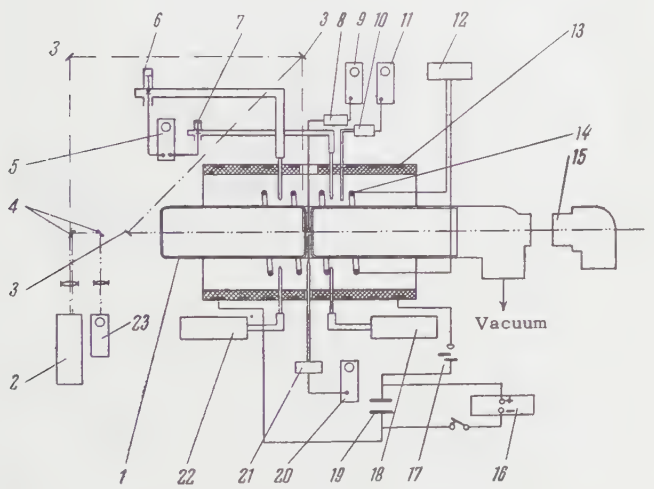

FIG. 1. Block diagram of the experimental setup. 1 – vacuum chamber; 2 – electron-optical light amplifier; 3, 4 – mirror projecting the illumination of the plasma and the time marker from the screen of the oscillograph 23 on the electron-optical light amplifier; 5, 9, 11, 20 and 23 – OK-17M oscillographs; 6, 7 – high-frequency detectors; 8 – magnetic probe; 10 – photomultiplier; 12 – self-excited generator (f = 12.5 Mc/sec); 13 – solenoid of the quasi-static magnetic field (H_{0max} = 12 koe); 14 – tank circuit of the generator 12; 15 – spectrograph; 16 – charging system; 17 – discharger; 18 and 22 – probe-signal generators with wavelengths 3 cm and 8 mm; 19 – capacitor bank; 21 – optical probe.

The plasma was prepared in a glass tube 7 or 10 cm in diameter and 175 cm long. The field H_0 was generated by an oscillating discharge of a capacitor bank through a solenoid.

The experiments were conducted under two arrangements. The period of vibration of the field H_0 was 6.25×10^{-3} sec in the first arrangement, and 8×10^{-3} sec in the second. The high-frequency magnetic field $\tilde{H}$ was excited parallel to the direction of the field H_0 by means of an induction coil mounted on the discharge tube. In the first arrangement, the coil was 20 cm long, composed of four windings, and formed the inductance of the high-frequency oscillator tank circuit. The generator operated at a frequency of 12.5 Mc/sec and had a power of approximately 20 kw.

In the second arrangement, the coil of the high-frequency magnetic field consisted of a single winding and was a copper tube 60 cm long with an axial cut to which was attached the capacitance of the circuit. This circuit was excited at a frequency of 50 Mc/sec from an independent generator. The power from the generator was of the order of 200 kw and was supplied through a coaxial line of length $(3/4)\lambda$.

Various methods were employed for the investigation of the character of the charge under observation.

With the aid of a FÉU-19 photoelectric multiplier and an OK-17M oscillograph, the time sweep of the glow of the plasma was observed, and the distribution of the brightness over the radius of the discharge column was studied. In the latter case a miniature photoconductor lying along the radius of the discharge tube was used as the optical probe 21.*

The penetration of the high-frequency vibrations into the plasma and the distribution of amplitude of the high-frequency magnetic field along the radius were studied by means of a magnetic probe 8, which moved along the radius of the discharge tube (see footnote).

In the arrangement with frequency f = 12.5 Mc/sec, the load of the high-frequency generator during the discharge process was determined by means of the grid and anode currents.

The discharge glow was swept by means of an electron-optical light amplifier through a small slit diaphragm (see reference 4). The time scan

*A thin glass tube which isolated the probe from the volume of the plasma was employed for this purpose.

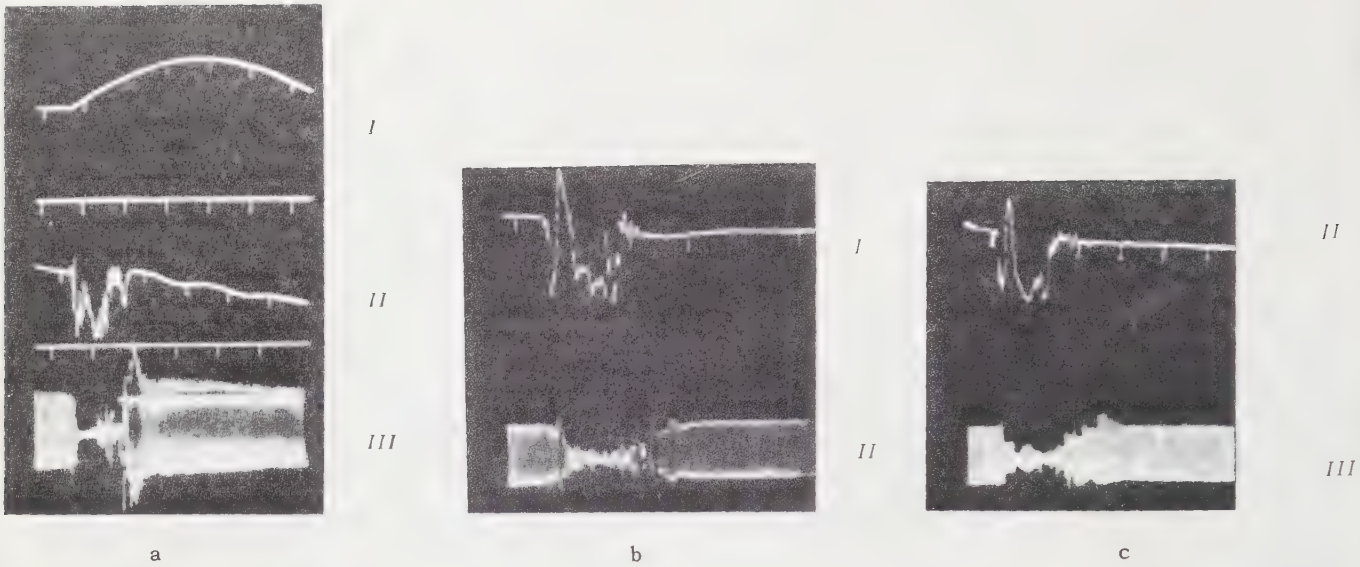

FIG. 2. The results of observation of the discharge in hydrogen (a), air (b), and argon (c) for a frequency of 50 Mc/sec. The pressure was 8×10^{-4} mm of mercury (a, b) and 3×10^{-3} mm of mercury (c). The amplitude of the magnetic field in the oscillator circuit was 27 oe (a), 13.5 oe (b) and 15 oe (c). The amplitude of the quasi-static magnetic field $H_0 = 5.3$ koe with a period of 8×10^{-3} sec. The time markers on all the oscillograms are 5×10^{-4} sec apart: I – oscillogram of the field H_0; II – oscillogram of the voltage on the magnetic probe placed in the center of the discharge chambers; III – the oscillogram of the high-frequency probing signal with wavelength $\lambda = 8$ mm.

of the discharge spectrum was observed and the Doppler half-width of the line $H\beta$ was measured by the same method.

The plasma was probed with plane polarized microwaves of wavelengths 3 cm and 8 mm to estimate the concentration of the charged particles. In this case the direction of the electric vector was parallel to H_0. The experiments were carried out on hydrogen, helium, argon, and air in the range of initial pressures from 10^{-4} to 6×10^{-3} mm of mercury.

The most interesting result of these experiments was the discovery in the range of magnetic fields from 300 oe to 5 koe of characteristic resonance phenomena, which were accompanied by a sharp increase in the brightness of the plasma radiation, by an increase in the concentration of charged particles, by penetration of the high frequency vibrations into the plasma, and by an increase in the loading of the generator. These peculiarities of the process are clearly seen in the photographs of Figs. 2 and 3. Figure 2 shows an oscillogram of the magnetic probe and an oscillogram of the passage of radio waves of wavelength 8 mm through the plasma. These were obtained in the arrangement with frequency of 50 Mc/sec for a discharge in hydrogen (a), argon (b), and air (c). Figure 3 shows the different experimental results obtained in the other arrangement (f = 12.5 Mc) for discharge in hydrogen.

It is seen in these photographs that for a certain (resonance) value of the quasi-static magnetic field $H_0 = H_p$, the loading of the high-frequency generator increases sharply while the high-frequency oscillations penetrate up to the axis of the discharge. In this case the illumination of the discharge increases rapidly and the microwave probe is cut off. This picture is repeated periodically, twice every half cycle of the magnetic field H_0.

The characteristic resonance interaction of the high-frequency electromagnetic field with the plasma also appears clearly in the brightness of the individual spectral lines, see Fig. 4, where streak photographs are shown of the individual parts of the hydrogen spectrum.

It can be noted in the photographs that, in addition to the lines of the atomic and molecular hydrogen in resonance, there is a number of admixture lines (for example, the lines 4794.5, 4810.1, and 4819.5 A). It is interesting that the time of their light emission constitutes only a part of the time of the passage through resonance from the side of low values of H_0. Since the admixture lines appear because of the interaction of the plasma with the walls of the discharge tube, the latter circum-

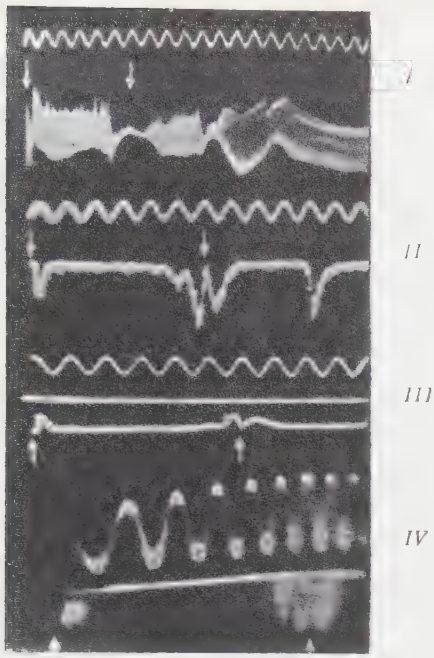

FIG. 3. The results of observation of discharge in hydrogen at a frequency of 12.5 Mc/sec obtained in a single experiment. The pressure was 10^{-4} mm of mercury. The amplitude of the quasi-static magnetic field H_0 and of the high-frequency magnetic field in the oscillator circuit $\tilde{H}$ were equal to 3.43 koe and 30 oe, respectively. The times of passage of H_0 through zero are marked by arrows. The time scale (period of sinusoidal vibrations) on all oscillograms was 0.5 msec. I – oscillogram of the high-frequency testing signal with wavelength $\lambda = 3$ cm; II – oscillogram of the signal from the photoelectric multiplier which recorded the brightness of the plasma in the center of the discharge tube; III – the oscillogram of the anode current of the high-frequency generator; IV – streak photograph of the illumination obtained with the help of the light amplifier. The photography was carried out perpendicular to the direction of H_0 through a narrow slit diaphragm located perpendicular to the axis of the discharge tube.

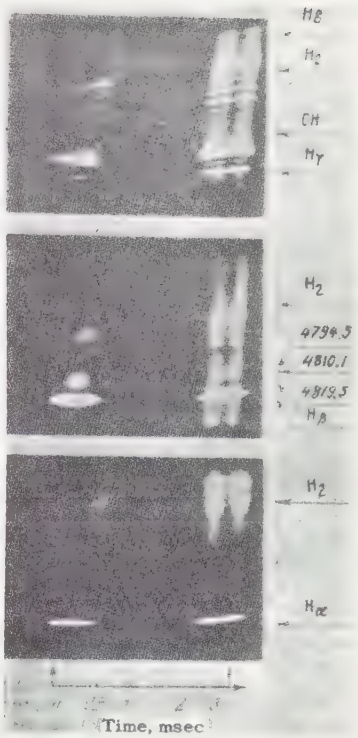

FIG. 4. Streak photographs of the separate parts of the discharge spectrum in hydrogen under conditions of resonance (f = 12.5 Mc/sec) obtained by means of a light amplifier and an ISP-51 spectrograph. The arrows denote the instants of the passage of H_0 through zero.

stance means that in resonance, during the time when the admixture lines are not radiating, the plasma has not reached the walls of the tube.

The dependence of the resonance magnetic field Hp on the amplitude of the high-frequency magnetic field H in the circuit in the absence of plasma was discovered and investigated in these experiments. In the arrangement with frequency 50 Mc/sec, the following experimental results were obtained for discharge in hydrogen:

$\tilde{H}$	13.5	16.5	19.5	22.2	27.3	33.3 oe
H_p	1300	1500	1750	2050	2850	3400 oe

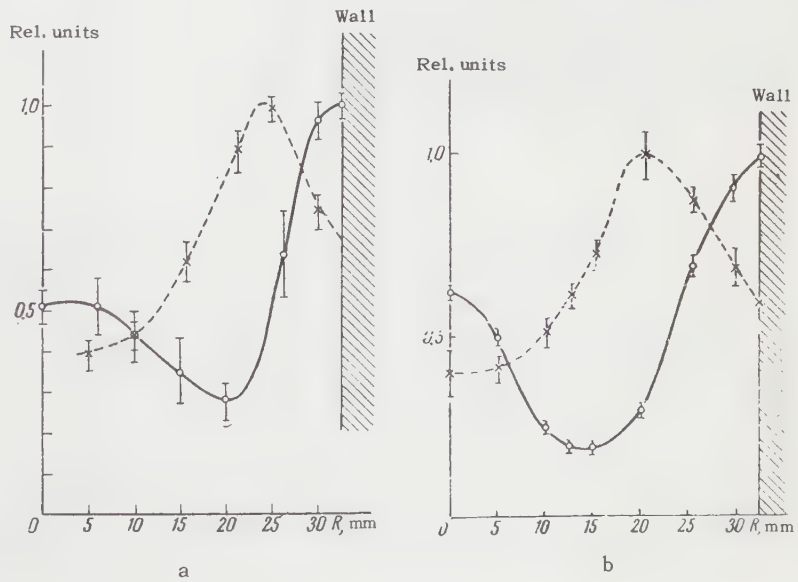

FIG. 5. Amplitude distribution of the high-frequency magnetic field (solid line) and of light (dashed line) along the radius: a – discharge in hydrogen ($p = 9 \times 10^{-4}$ mm mercury); $H_p \approx 800$ oe; b – discharge in argon ($p = 3 \times 10^{-3}$ mm mercury); $H_p \approx 1000$ oe.

One can see from these data that the field H_p increases with increasing $\tilde{H}$.

The dependence of H_p on the mass M of the ions taking part in resonance was also studied. For investigation of this dependence, experiments were carried out on hydrogen, helium, argon, and air under approximately the same conditions. An increase of H_p with increase in M was established in this case.

In Fig. 5a are shown the radial distributions of amplitude of the high-frequency magnetic field and the light emission of the plasma for resonance in hydrogen, obtained in the arrangement with a frequency of 50 Mc/sec. In Fig. 5b are shown the similar distributions for resonance in argon. It can be seen that the amplitude of the magnetic field has a relative maximum on the axis of the discharge, passes through a minimum approximately in the middle of the radius, and reaches its maximum value at the boundary of the plasma.

Attention should be paid also to a peculiarity of the phenomenon — the fine structure of the resonance. It can be noted in all the photographs shown in Figs. 2 and 3. It is most clearly evident in the streak photographs of the plasma shown in Fig. 6. This resonance in the second quarter of

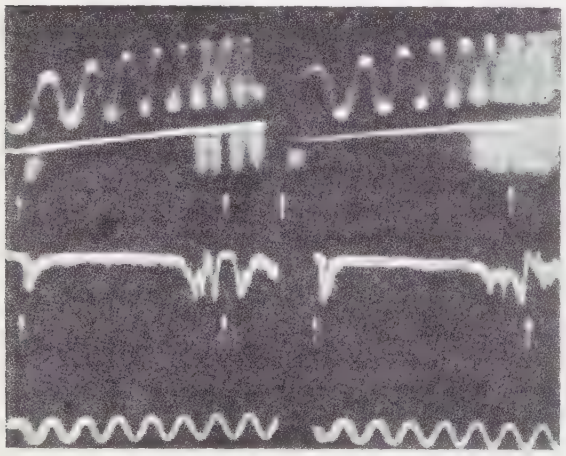

FIG. 6. Splitting of the resonance into two (a) and three (b) narrow resonances. I – streak photograph of the discharge obtained by means of the light amplifier. The photography was carried out in the direction perpendicular to H_0 through a narrow slit located perpendicular to the axis of the discharge tube; II – oscillogram of the signal from the photoelectric amplifier which records the light emission of the plasma in the center of the discharge tube. The pressure of the hydrogen: a – 3.5×10^{-5} mm mercury; b – 10^{-4} mm mercury. The amplitudes H_0 and $\tilde{H}$ are respectively equal to 3.43 koe and 74 oe. The arrows indicate the times of passage of H_0 through zero. The time scale (period of the sinusoidal oscillations) in all the photographs is equal to 0.5 msec.

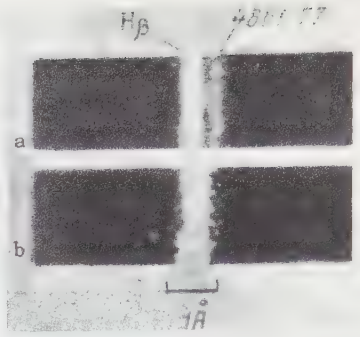

FIG. 7. Photograph of the $H\beta$ line obtained by means of the light amplifier and the ISP-51 spectrograph (focal length of the camera 1300 mm); a – in the spectrum of a standard DVS-25 hydrogen tube; b – in the high-frequency discharge (without the field H_0).

the period of the field H_0 is divided in one case (a) into two, and in the other case (b) into three separate narrow resonances. The nature of this effect, which appears at lowered initial pressures in the discharge tube, was investigated.

An estimate of the high-frequency energy absorbed at resonance was carried out in the arrangement with frequency 12.5 Mc/sec. At a generator power of 20 kw, the plasma absorbed about 10 kw of energy. This power is evidently mainly expended in ionization of the gas.

In the energy balance an important role must be played by the charge exchange with neutral atoms by means of which the energy absorbed by the plasma reaches the wall of the discharge chamber. From this point of view there is interest in the measurement of the temperature of neutral atoms in the discharge. Such measurements, based on the Doppler width of the $H\beta$ line, were carried out with the aid of a light amplifier for the high-frequency discharge outside the resonance conditions (in the absence of the field H_0).* The results of the measurements are shown in Figs. 7 and 8. In this case the Doppler broadening of the $H\beta$ line in the discharge was shown to be equal to ~ 0.6 A, which corresponds to a gas temperature of 2.5 ev (in energy units).

3. The experimental material just given makes it possible to draw the conclusion that a magnetoacoustic resonance was observed in the experi-

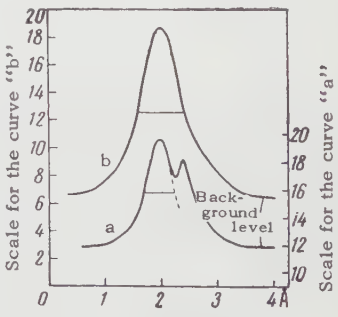

FIG. 8. Results of photometry of the negative of photographs shown in Figs. 7a and b. Light intensity is plotted along the ordinate in arbitrary units (the same for a and b). Thin horizontal lines indicate the half-width of the spectral lines.

*In this case the ion density in the discharge was $\lesssim 10^{12}$ cm^{-3} and the Stark broadening of the line was much smaller than the Doppler broadening.

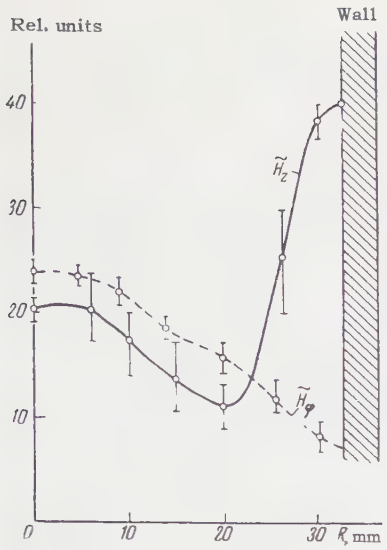

FIG. 9. Radial distribution of the components $\tilde{H}_z$ and $\tilde{H}_\varphi$ of the amplitude of the high-frequency magnetic field obtained in the arrangement with frequency 50 Mc/sec for $H_p \sim 800$ oe in hydrogen ($p = 9 \times 10^{-4}$ mm of mercury).

ments we have described. The phenomenon can be ascribed neither to electronic nor to ionic cyclotron resonance, since the observed resonance frequency lies far from the corresponding cyclotron frequencies. The dependence of the resonance field H_p on the amplitude of the variable field $\tilde{H}$ becomes understandable if we keep it in mind that the preliminary ionization in our experiments was brought about by the same high-frequency field whose interaction with the plasma was studied. This means that the change of the amplitude of the high-frequency field should lead to a change in the density n of charged particles which was established before the initial resonance. Consequently, the experimental results given above qualitatively reflect the dependence of H_p on the density n according to Eq. (1). The observed dependence of H_p on the mass M of the ion agrees qualitatively with this formula.

For quantitative comparison of Eq. (1) with experiment, an exact measurement of the quantity $\rho = nM$ is required. Such measurements were not carried out. The microwave testing made it possible to establish only the limiting values of the electron density, equal to 10^{12} and 1.6×10^{13} cm^{-3}, respectively, for the three-centimeter and eight-millimeter probes. An even larger inaccuracy is attributable to the mass M, inasmuch as in the process of discharge a considerable amount of impurity gas from the walls of the chamber enters into the discharge.

It can be assumed that qualitative agreement with theory is obtained also for the radial distribution of amplitude of the high frequency magnetic field at resonance (Fig. 5a), if we assume that the damping is sufficiently large (a Q of ~ 3).

Experiments with argon shown in Fig. 5b are of interest inasmuch as they were carried out in a range of frequencies known to be above the "hybrid." In the case of purely radial vibrations in this region there should be no penetration of the variable field into the cold plasma. However, experiment shows that penetration does exist and in its character it differs slightly from what takes place at a frequency below the "hybrid." One can therefore draw the conclusion that under experimental conditions transverse magnetoacoustic vibrations are observed with the direction of propagation not exactly perpendicular to the field H_0. This is confirmed by probe measurements of the azimuthal magnetic field $\tilde{H}_\varphi$ (see Fig. 9). One should note one more fact of qualitative agreement of theory with experiment which takes place behind the region of magnetoacoustic resonance, on the side of higher magnetic fields. Here, as follows from the evidence of the magnetic probe, for an increase of H_0 above a certain limiting value, the variable field begins to penetrate freely into the region of the discharge chamber, as in a vacuum. Simultaneously, the power loss to the plasma and the intensity of the radiation of the plasma falls off sharply.

The limiting field corresponds approximately to the conditions in which the azimuthal drift velocity of the electrons

$$v_\varphi = (\omega / \omega_i) \tilde{H} / \sqrt{4\pi\rho}$$

becomes insufficient for effective ionization.

In conclusion, the hope can be expressed that the observed magnetoacoustic resonance in which an intensive penetration of the high frequency vibrations into the plasma takes place is of interest from the point of view of the heating of a dense plasma.

The authors take note of the constant interest and cooperation displayed by Academician I. V. Kurchatov toward the completion of the present work.

[1] D. A. Frank-Kamenetskiĭ, JETP **39**, 669 (1960), this issue p. 469.

[2] K. Korper, Z. Naturforschung **12a**, 815 (1957).

[3] Auer, Hurwitz, and Miller, Phys. Fluids **1**, 1501 (1958).

[4] Zavoĭskiĭ, But-slov, Plakhov, and Smolkin. Атомная энергия (Atomic Energy) **4**, 34 (1956); Zavoĭskiĭ, But-slov, and Smolkin, Dokl. Akad. Nauk SSSR **111**, 996 (1956), Soviet Phys.-Doklady **1**, 743 (1957).

Translated by R. T. Beyer
107

CROSS SPIN RELAXATION IN THE HYPERFINE STRUCTURE OF ELECTRON PARAMAGNETIC RESONANCE OF Co^{2+} IN CORUNDUM

G. M. ZVEREV and A. M. PROKHOROV

Nuclear Physics Institute, Moscow State University

Submitted to JETP editor April 9, 1960

J. Exptl. Theoret. Phys. (U.S.S.R.) 39, 545-547 (September, 1960)

Cross spin relaxation has been detected in the hyperfine structure of electron paramagnetic resonance of Co^{2+} ions in corundum. The cross-relaxation time T_{12} has been measured and found to be 0.27 sec and independent of the temperature.

CROSS spin-spin interaction, i.e., interaction between spins with different resonance frequencies, plays an essential role in the dynamics of spin systems. In particular, it is of great significance in processes occurring in paramagnetic amplifiers.

The question of cross spin relaxation was recently analyzed in detail by Bloembergen et al.[1] who gave an explanation for the previously observed[2] effect of cross saturation of hyperfine structure components of electron paramagnetic resonance of copper ions in a single crystal of Tutton salt.

Cross-relaxation is prominent in systems of spins with not very different resonance frequencies. A group of closely spaced transitions occurs, for example, in the case of the Co^{2+} ion in corundum. For this ion the effective electron spin is $S' = 1/2$ and the nuclear spin is $I = 7/2$. The electron paramagnetic resonance lines for this ion have a well resolved hyperfine structure of eight components.[3,4]

We have investigated the cross spin relaxation of transitions corresponding to different orientations of the nuclear spin. The sample of corundum containing cobalt used by us had a low concentration of cobalt (10^{-2}%); the spin-lattice relaxation time T_1 at a temperature of 4.2°K was 1.2 sec. For the crystal orientation in the external magnetic field (H parallel to the trigonal crystal axis) used by us the width of an individual hyperfine structure component was 7.5 oe, the separation between the components was 30 oe.

The experiment was carried out in the following manner. The sample under investigation was placed into a rectangular resonator tuned simultaneously to two closely spaced frequencies ν_1 and $\nu_2 \sim 9200$ Mc/sec. The resonator had a nearly square cross section; oscillations of TE_{011} and TE_{101} type were excited in it. The sample was placed at a position of a maximum of the high frequency magnetic field in the resonator in such a way that the transitions between the levels would be induced by the high frequency field due to both types of oscillations. By means of a superheterodyne microwave spectroscope electron paramagnetic resonance lines were observed at the frequency ν_1 at a power level which excluded the possibility of saturation (10^{-10} w). Saturating pulses were applied at the frequency ν_2. The use of different frequencies for saturation and for observation enabled us to avoid interruption in the operation of the receiver due to the effect of the saturating pulse. The recovery of the intensity of the lines after the saturating pulse was turned off was recorded by a movie camera.

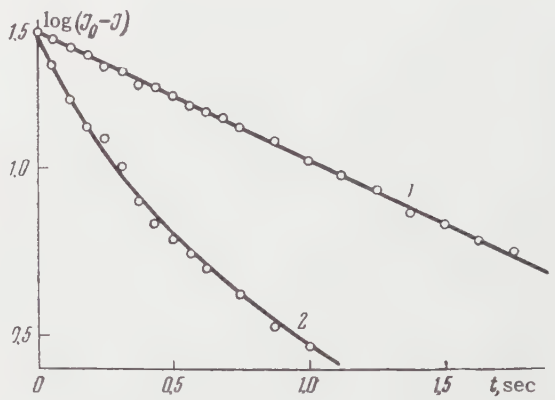

The diagram shows the dependence on the time of $\log (J_0 - J)$ for two different cases; J is the intensity of absorption which is proportional to the population difference between the spin levels n, while J_0 is the intensity of absorption in the case of thermal equilibrium.

In the case corresponding to curve 1 all eight hyperfine structure components were saturated to the same degree. Curve 2 corresponds to the case

when only one outermost component was saturated by a short pulse. In the first case the relaxation process is described by a single exponential

$$n_0 - n = A e^{-t/T_1}. \qquad (1)$$

In the second case due to the cross spin-spin interaction the relaxation occurs more rapidly; the saturation of a single component immediately leads to partial saturation of other components, and only after a certain time the spin system regains equilibrium and relaxes as a whole according to the exponential law (1). The relaxation process in the second case can be easily calculated under the following assumptions: a) the cross-relaxation between each pair of neighboring components is described by the single parameter T_{12}, the cross-relaxation time, b) cross spin-spin interaction is taken into account only for neighboring components. In this approximation the relaxation of the populations of the eight pairs of spin sublevels differing in the values of the components of nuclear spin is described by the system of the following kinetic equations:

$$\begin{aligned}
\frac{dn_1}{dt} &= \frac{n_0 - n_1}{T_1} + \frac{n_2 - n_1}{T_{12}}, \\
\frac{dn_2}{dt} &= \frac{n_0 - n_2}{T_1} + \frac{n_3 - n_2}{T_{12}} + \frac{n_1 - n_2}{T_{12}}, \ldots \qquad (2) \\
&\ldots\ldots\ldots\ldots\ldots\ldots \\
\frac{dn_8}{dt} &= \frac{n_0 - n_8}{T_1} + \frac{n_7 - n_8}{T_{12}}.
\end{aligned}$$

The solution of this system is a sum of eight different exponentials:

$$n_0 - n_i = \sum_{j=1}^{8} A_{ji} e^{-\lambda_j t}, \qquad \lambda_j = 1/T_1 + c_j/T_{12},$$

where the cj are constants. The coefficients Aji depend on the initial conditions.

Calculations show that the theoretical relaxation of a single hyperfine structure component agrees well with the experimental results if we take $T_{12} = 0.27$ sec. The results of such calculations are shown in the diagram by the curve, and the experimental values by points.

We note that the relaxation process at several different temperatures (1.8, 2.15, and 4.2° K) is characterized by different values of T_1 (3.0 sec at 1.8° and 1.2 sec at 4.2° K), while the same values are obtained for the parameter T_{12}.

In the case of saturation by a long pulse (of duration $\sim T_{12}$) the process is described by a similar system of kinetic equations, but the nature of the concrete relaxation process depends strongly on the amplitude and the duration of the saturating pulse.

[1] Bloembergen, Shapiro, Pershan, and Artman, Phys. Rev. **114**, 445 (1959).

[2] Giordmaine, Alsop, Nash, and Townes, Phys. Rev. **109**, 302 (1958).

[3] G. M. Zverev and A. M. Prokhorov, JETP **36**, 647 (1959) and **39**, 57 (1960), Soviet Phys. JETP **9**, 451 (1959) and **12**, 41 (1961).

[4] J. E. Geusic, Bull. Am. Phys. Soc. II, **4**, 261 (1959).

Translated by G. Volkoff
108

COMPOSITION OF SLOW IONS PRODUCED DURING THE IONIZATION OF GASES BY NEGATIVE IONS

Ya. M. FOGEL', A. G. KOVAL', Yu. Z. LEVCHENKO, and A. F. KHODYACHIKH

Physico-Technical Institute, Academy of Sciences, Ukrainian S.S.R.

Submitted to JETP editor April 9, 1960

J. Exptl. Theoret. Phys. (U.S.S.R.) 39, 548-555 (September, 1960)

The composition of slow ions produced by 10 to 50 kev H^- and O^- ions in He, Ne, Ar, Kr, Xe, H_2, N_2, and O_2 is analyzed with a mass spectrometer. The data of the present investigation, as well as those of a previous study by the authors in which the total cross sections for positive ion formation were measured, have been employed to calculate the cross sections for ionization involving the detachment of a definite number of electrons from the atom. The effective cross sections for production of slow ions with various charges by H^- and H^+ ions are compared.

INTRODUCTION

WHEN an atom of nuclear charge Z is ionized by negative ions, slow ions are produced with charges from e to Ze. By means of a method of collecting these ions on the plate of a measuring capacitor, the value σ^+ of the total cross section for the production of positive ions can be determined. This type of measurement for the ionization of a number of gases by H^- and O^- ions has been made in our previous work.[1]

The cross section σ^+ represents the sum $\sum_{n=1}^{Z} n\sigma_{0n}^i$, where σ_{0n}^i is the cross section for ionization with the detachment of n electrons from the atom.* It is of interest to measure the cross sections σ_{0n}^i, for which it is necessary to study the charge composition of the slow positive ions that are produced. An investigation of the composition of similar ions when fast positive ions pass through gases has been carried out in a number of experiments by Fedorenko and co-workers.[2-5]

Attention should be directed to one important difference in the processes of production of slow positive ions by fast positive and negative ions passing through gases. In the case of positive ions traveling through the gas, a positive ion of given charge is produced as a result of pure ionization processes, and also as a result of electron capture processes or processes of ionization with electron capture.[6] In this case, the cross sections for the production of slow ions are the sums of the cross sections of all the above processes. Negative ions cannot capture electrons from the gas particles and, as a result, when negative ions travel through the gas, slow positive ions are produced only in pure ionization processes. This fact makes it of interest to determine the cross sections σ_{0n}^i for negative ions. In the present work, measurements were made of the cross section σ_{0n}^i for the ionization of gases of He, Ne, Ar, Kr, Xe, H_2, N_2, and O_2 by 10 to 50 kev H^- and O^- ions.

*Here and in what follows, we shall use the notation for cross sections introduced by Fedorenko and Afrosimov.[2]

APPARATUS AND METHOD OF MEASUREMENT

The source of negative ions and the collision chamber in which the interaction between the negative ions and gas particles takes place have been described previously;[1,7] therefore, we give here only a description of the analyzer of the charges of slow ions (Fig. 1).

The slow positive ions produced in the path of the negative ion beam are accelerated by an electric field towards plate 1 of the third capacitor of the chamber (see Fig. 1 in reference 1), having a 20 × 20 mm opening covered by a grid with a transmission of 97%. The ions, upon passing through the grid, enter the space between the plate and end plane of electrode 2. This electrode is a tube 18 mm in diameter and 175 mm long. In this space the ions are additionally accelerated by the difference in potential V_a applied between plate 1 and electrode 2. Upon passing through a slit of dimensions 2 × 10 mm in the end plane of electrode 2, the ions are then focused by the electric field V_f in the gap between electrode 2 and the chamber of the magnetic mass spectrometer 6. Electrode 2

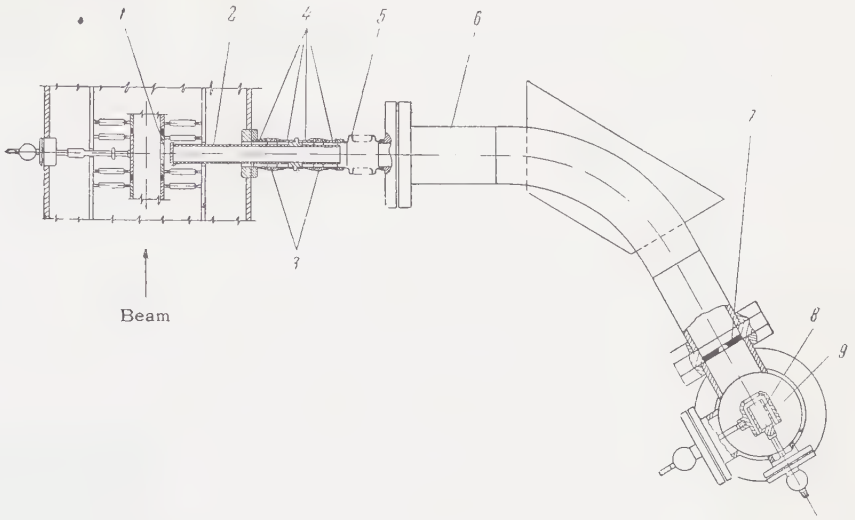

FIG. 1. Diagram of charge analyzer.

is insulated from the housing of the collision chamber and mass-spectrometer chamber by glass insulators 3 welded to kovar cylinders 4. Electrode 2 is soldered to the middle of these cylinders. The system supporting electrode 2 was joined to the mass-spectrometer chamber through bellows 5, which made it possible to adjust the position of the mass spectrometer with respect to the beam of ions coming from the ionization zone.

The charge analysis of the slow ions was carried out by means of a magnetic mass spectrometer with a beam deflection angle of 60° and a mean trajectory radius of 16.4 cm. The height of the gap between the poles of the electromagnet was 50 mm. The maximum field intensity in the gap was 6000 oe. The brass chamber of the mass spectrometer was insulated from the poles of the electromagnet by two Plexiglas plates 5 mm thick. The measurement of current in the Faraday box 8 at the mass-spectrometer exit was carried out by an ÉMU-3 vacuum-tube electrometer of sensitivity 10^{-14} amp/division. In order to deliver the secondary emission from the Faraday box to electrode 9, a potential of -50 volts was used. In front of the Faraday box was a slit 7, 20 mm high. The slit width could be adjusted from 0 to 20 mm without disturbing the vacuum.

The primary beam current on a Faraday box situated after the exit channel of the collision chamber was measured by a mirror galvanometer of sensitivity 10^{-10} amp/division. The currents in the Faraday box of the mass spectrometer and in the primary beam were measured simultaneously, which substantially reduced the error associated with current fluctuations in the primary beam.

Additional evacuation of the mass-spectrometer chamber was provided on the exit side by an MM-40 oil-diffusion pump, insulated from the chamber by a porcelain ring 18 mm high. The pressure in the mass-spectrometer chamber when the gas was let into the collision chamber was 5×10^{-6} mm Hg.

The method of determining the slow-ion charge composition will be described here only briefly, since this method is presented in great detail in the article of Fedorenko and Afrosimov.[2]

The value of σ^i_{0n} was calculated from the formula

$$\sigma^i_{0n} = \alpha_n \sigma^+ / n, \qquad (1)$$

where α_n is the relative intensity of the line spectrum of ions of charge n.

As has been shown previously,[2] the value of α_n correctly describes the actual slow-ion composition in the zone of interaction between the primary beam and the gas only when it is independent of the "extracting" potential difference V_e (potential difference between the condenser plates), V_a, V_f, and the slit width at the mass-spectrometer exit. For each combination of a primary ion with a molecule of the gas and for each primary ion energy, the value of α_n depends on the above-mentioned factors. The working values of V_e, V_a, V_f, and the slit width were chosen on the "plateau" of the respective curves, and were usually equal to the following: $V_e = 100$ volts, $V_a = (0.85 - 1)$ kv, $V_f = (1.25 - 1.5)$ kv, slit width $9 - 20$ mm for H^- ions; and $V_e = (150 - 200)$ volts, $V_a = (0.85 - 1.2)$ kv, $V_f = (1.25 - 1.5)$ kv for O^- ions.

To determine the collision chamber gas pressure which would ensure the condition for single collisions, we plotted the ratio $I^{n+}/I_0^- = f(p)$ (I^{n+} is the current of ions of charge n, I_0^- is the primary beam current), and the working pressure was chosen on the linear part of this curve. Most

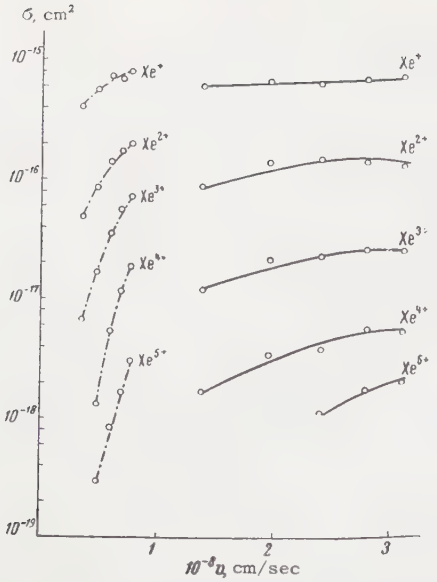

FIG. 2. Variation of cross sections for production of different ions of Xe by fast O^- ions (dash-dot curve) and H^- ions (solid curve); v is the primary ion velocity.

of the measurements were made at a gas pressure of (1 to 1.5) × 10^{-4} mm Hg. The error in the measurement of the value of σ^i_{0n}, consisting of the errors in measurements of the values of σ^+ and α_n, was equal to ±15% for cross sections (10^{-16} — 10^{-17}) cm^2 and ±25% for cross sections (10^{-18} — 10^{-19}) cm^2. In order to check the method as a whole, the cross sections for the production of argon ions of charge one to three by 30-kev protons were measured. The results of the measurements agreed with previous results[2] within the limits of experimental error.

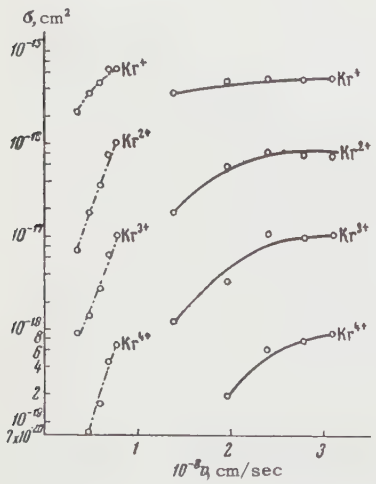

FIG. 3. Cross sections for production of different ions of Kr. Notation the same as in Fig. 2.

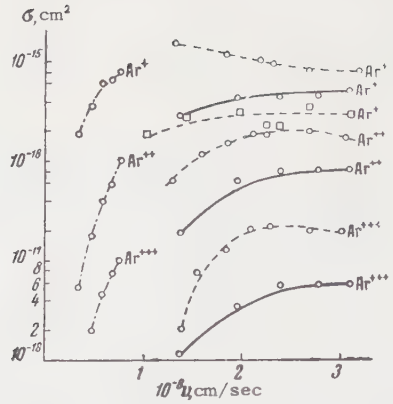

FIG. 4. Cross sections for production of different ions of A by fast O^- ions (dash-dot curve) and H^- ions (solid curve); dotted curve — for the primary H^+ ion (from data of reference 3); □ — σ^i_{01} curve (from data of reference 3).

RESULTS OF THE MEASUREMENTS

The dependence of the cross sections σ^i_{0n} on the velocity v of the H^- and O^- ions is shown in Figs. 2 — 6 for the ionization of five inert gases. In the case of Xe, it was possible to measure the cross sections for ions of charge one to three; for Kr, from one to four; for Ar and Ne, from one to three; for He it was, of course, impossible to produce ions of charge greater than two. The velocity dependence of the cross sections σ^i_{0n} was different for H^- and O^- ions. In the case of O^- ions, the cross sections σ^i_{0n} for all gases increase quite rapidly with an increase in the ion velocity. The rate of increase of σ^i_{0n} rises with an increase in the charge multiplicity of the slow ion produced, which is particularly visible on the curves of $\sigma^i_{0n}(v)$ for Xe. The cross sections σ^i_{0n} for H^- ions increase with the ion velocity much more slowly than for O^- ions. For ions of small charge,

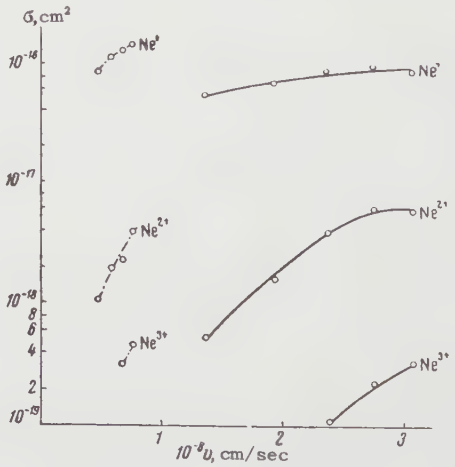

FIG. 5. Cross sections for the production of different ions of Ne.

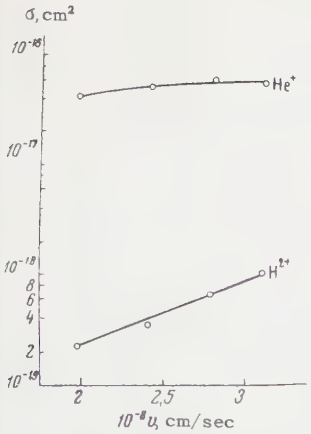

FIG. 6. Cross section for production of ions of He by fast H^- ions.

the $\sigma^i_{0n}(v)$ curves attain a flat maximum. The shape of the $\sigma^i_{0n}(v)$ curves for H^- ions permit one to conclude that the maximum of the curve shifts towards the larger velocities with an increase in the slow-ion charge.

When one considers the $\sigma^i_{0n}(v)$ curves, it should be borne in mind that each cross section σ^i_{0n} is the sum of the cross sections for ionization processes with no change in charge of a negative ion and with the detachment one, two, etc. electrons from a negative ion. Owing to this, the $\sigma^i_{0n}(v)$ curve is the resultant of a number of curves corresponding to the above-mentioned processes. From this viewpoint, the strongly diffused maximum on the $\sigma^i_{0n}(v)$ curves is apparently explained by the fact that the individual curves from whose sum the $\sigma^i_{0n}(v)$ curve is obtained, have maxima at different points.

The cross sections σ^i_{0n} depend on both the type of primary ion and on the type of gas atom.

Although the investigated velocity intervals for H^- and O^- ions do not coincide, one may conclude, however, from consideration of the shape of the $\sigma^i_{0n}(v)$ curves that for the same velocities the cross sections σ^i_{0n} are considerably greater for the O^- ion than for the H^- ion.

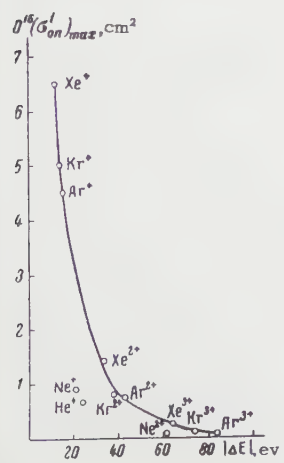

FIG. 7. Maximum cross sections for production of ions versus sum of ionization potentials ΔE.

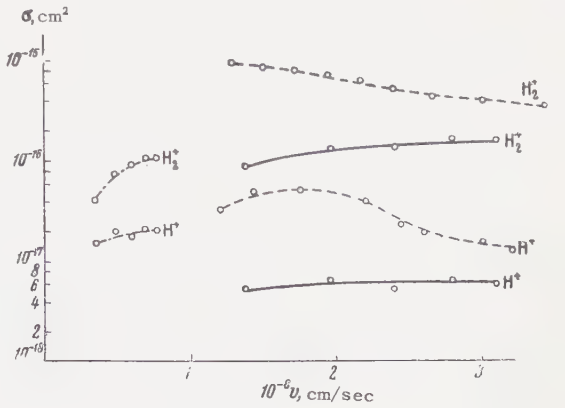

FIG. 8. Cross sections for production of various ions on molecular hydrogen by fast O^- ions (dot-dash curve) and H^- ions (solid curve); dotted curve – for the primary H^+ ion (data of reference 4).

Moreover, the cross section for ionization with the detachment of a given number of electrons increases with an increase in the atomic number of the gas. Thus the dependence of the cross section σ^i_{0n} on the type of primary ion and gas atom is in agreement with the assumption that the ionization cross section increases with an increase in the number of electrons in the electron shells of the colliding particles.

Examination of the $\sigma^i_{0n}(v)$ curves for H^- ions leads to the conclusion that the maximum values $(\sigma^i_{0n})_{max}$ rapidly decrease with an increase in the multiplicity of ionization, i.e., with an increase in the value of ΔE (ΔE is the sum of the ionization potentials). This circumstance is illustrated in Fig. 7. It is seen that the individual points for the Xe, Kr, and Ar atoms lie nicely on one smooth curve. Points for the Ne and He atoms lie off this curve.

The composition of slow ions produced during the ionization of gas by H^- and O^- ions were also studied for the molecular gases H_2, N_2, and O_2. In the slow-ion spectrum in hydrogen, the ions H_2^+ and H^+ were observed; in nitrogen and oxygen, apart from singly-charged molecular and atomic

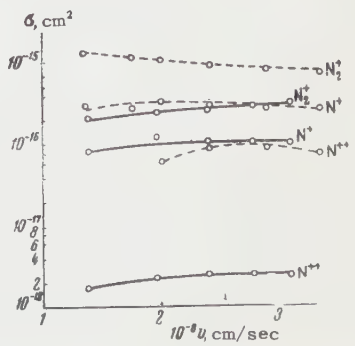

FIG. 9. Cross sections for production of various ions on molecular nitrogen. Solid curve – for H^- ions; dotted curve – for H^+ ions (data of of reference 5).

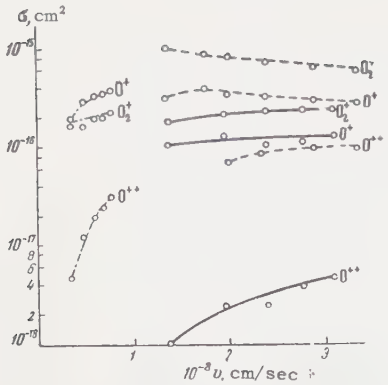

FIG. 10. Cross sections for production of various ions on molecular oxygen. Solid curve – for H^- ions; dotted curve – for H^+ ions (data of reference 5); dot-dash line for O^- ions

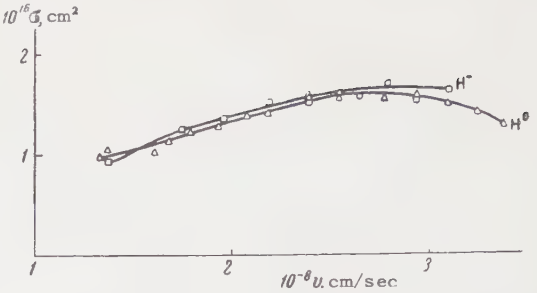

FIG. 11. Total cross sections for ionization of H_2 by H atoms (Δ – data of reference 8) and H^- ions (□ – data of the authors).

ions, doubly-charged atomic ions were also observed. The dependence of the cross section for the production of slow ions on the primary ion velocity is shown in Figs. 8 – 10. Examination of these curves leads to the following conclusions:

1. In the case of molecular gases, as well as in the case of atomic gases, the ionization cross sections for the same ion velocities are greater for O^- than for H^- ions.

2. The above-mentioned differences in the shape of the cross section curves for ionization of inert gases by H^- and O^- occur when molecular gases are ionized by these ions.

3. For all the investigated pairs, apart from the pair $O^- - O_2$, the cross section for the production of singly-charged molecular ions is greater than the cross section for the production of singly-charged atomic ions, and their ratio for ionization by O^- is less than in the case of H^- ions. The cross sections for the production of doubly-charged ions are much smaller than for singly-charged ions.

The cross sections for the production of singly-charged molecular ions depend comparatively weakly on the type of gas, while the cross section for the production of the H^+ ion is much smaller than for N^+ and O^+. Similar peculiarities are observed for the production of singly-charged ions of hydrogen, nitrogen, and oxygen by protons.[4,5]

The cross section for the production of slow ions in Ar, H_2, N_2, and O_2 when H^- ions pass through these gases can be compared with the corresponding cross sections for protons measured in references 3 – 5. From Figs. 4, 9, 10, 11, it is seen that the curves of the cross section for the production of a given slow ion versus the primary-ion velocity for protons lie above the corresponding curves for H^- ions and are of different shape. This becomes understandable if one bears in mind that for protons the cross section for the production of a slow ion is the sum of the cross sections for pure ionization and ionization with capture.

A comparison can be made between the cross sections for pure ionization with the production of singly-charged ions by protons and by H^- ions if it is assumed that the cross section for one-electron charge-exchange of protons σ_{01}^{ic} is much greater than the cross sections σ_{02}^{ic}, σ_{03}^{ic}, etc. for charge-exchange processes with simultaneous ionization of the atom.

In fact, (see reference 2)

$$\sigma_{01} = \sigma_{01}^{i} + \sigma_{01}^{ic}, \qquad \sigma_0 = \sigma_{01}^{ic} + \sigma_{02}^{ic} + \sigma_{03}^{ic} + \ldots \qquad (2)$$

if $\sigma_{01}^{ic} \gg \sigma_{02}^{ic}$ and $\sigma_{01}^{ic} \gg \sigma_{03}^{ic}$, etc., then from formula (2) we obtain

$$\sigma_{01}^{i} = \sigma_{01} - \sigma_0. \qquad (3)$$

The values of the cross section for the production of singly-charged ions (σ_{01}) and the total cross section for electron capture for protons (σ_0) in A were measured by Fedorenko et al.[3] The $\sigma_{01}^{i}(v)$ curve constructed from the data of this work is shown in Fig. 4. Comparison of this curve with the $\sigma_{01}^{i}(v)$ curve for H^- ions indicates that the cross sections for pure ionization with detachment of one electron for protons and H^- ions do not differ very much from one another. Comparison of the total cross sections for ionization by protons and H^- ions[1] leads to a similar conclusion.

Thus, the difference in the sign of the charge of H^+ and H^- ions does not have a basic effect on the value of the cross sections for ionization by these ions. A slight influence of the charge on the value of the ionization cross sections is confirmed by data in the recent work of Schwirzke,[8] in which it was shown that the total cross sections for ionization of hydrogen by H atoms and H^+ ions differ from one another by no more than a factor of two.

Using the data of the present work and the data of Schwirzke,[8] one can compare the total cross sections for ionization of hydrogen by H^- ions and H atoms. Such a comparison is shown in Fig. 11, where plots of the total cross sections for ioniza-

tion of hydrogen versus the velocity of H^- ions and H atoms are shown. The fact that these curves coincide indicates that the influence of the weak binding of the additional electron of the H^- ion on the ionization process of the hydrogen molecule is small.

We express our sincere gratitude to Professor N. V. Fedorenko and V. V. Afrosimov for valuable advice on the method of studying the composition of slow ions produced by fast particles passing through gases, and also to Professor A. K. Val'ter for constant interest in, and attention to, this work.

[1] Fogel', Koval', and Levchenko, JETP **38**, 1053 (1960), Soviet Phys. JETP **11**, 760 (1960).

[2] N. V. Fedorenko and V. V. Afrosimov, J. Tech. Phys. (U.S.S.R.) **26**, 1941 (1956), Soviet Phys. -Tech. Phys. **1**, 1872 (1957).

[3] Afrosimov, Il'in, and Fedorenko, J. Tech. Phys. (U.S.S.R.) **28**, 2266 (1958), Soviet Phys.-Tech. Phys. **3**, 2080 (1959).

[4] Afrosimov, Il'in, and Fedorenko, JETP **34**, 1398 (1958), Soviet Phys. JETP **7**, 968 (1958).

[5] Il'in, Afrosimov, and Fedorenko, JETP **36**, 41 (1959), Soviet Phys. JETP **9**, 29 (1959).

[6] Fedorenko, Afrosimov, and Kaminker, J. Tech. Phys. (U.S.S.R.) **26**, 1929 (1956), Soviet Phys.-Tech. Phys. **1**, 1861 (1957).

[7] Fogel', Koval', and Timofeev, J. Tech. Phys. (U.S.S.R.) **29**, 1381 (1959), Soviet Phys.-Tech. Phys. **4**, 1270 (1960).

[8] F. Schwirzke, Z. Physik **157**, 510 (1960).

Translated by E. Marquit
109

ENERGY SPECTRUM OF THE FRAGMENTS FROM THE TRIPLE FISSION OF U^{235}

V. N. DMITRIEV, L. V. DRAPCHINSKIĬ, K. A. PETRZHAK, and Yu. F. ROMANOV

Radium Institute, Academy of Sciences, U.S.S.R.

Submitted to JETP editor April 14, 1960

J. Exptl. Theoret. Phys. (U.S.S.R.) 39, 556-562 (September, 1960)

Data are presented on the energy distribution of fragments from the triple fission of U^{235}. It is shown that the ratio of the probability for triple fission to the probability for double fission does not depend on the ratio of fragment masses. We establish the relation (1) between the total kinetic energy of the fragments in triple and double fission and the energy of the long-range α particle. The mechanism of triple fission is discussed.

INFORMATION on the mechanism of nuclear fission can be obtained from the study of fission events in which a long-range α particle is emitted. This is because the α particle is emitted at the very beginning of the fission process and so characterizes the state of the nucleus at the moment of fission. This subject is reviewed in an article by Perfilov, Romanov, and Solov'eva.[1]

Until recently, the energy distribution of the fragments from triple fission had not been adequately studied. The most commonly used method for studying triple fission, that of emulsion stacks, can only give approximate information on the energy distribution of the fragments. Allen and Dewan[2] were the first to use an ionization chamber and grid to study the energy distribution of fragments from triple fission. The U^{235} target was placed in a double ionization chamber, one half of which detected fission fragments while the other half registered the α particles emitted during triple fission. Triple fission events were identified by coincidences between the two chambers. Unfortunately, this method has a fundamental drawback in that the results are distorted by the angular correlation between the fission fragments and the α particle. It is known that the most probable angle between the direction of emission of the α particle and the direction of emission of the lightest fission fragment is about 80°. Since the hemisphere associated with a heavy fragment contains fewer long-range α particles than does the hemisphere associated with a light fragment, coincidences between heavy fragments and α particles were detected with a higher efficiency than were coincidences between light fragments and an α particle. For this reason, the area of the peak corresponding to the group of heavy fragments is considerably larger than the area of the peak corresponding to light fragments, so that the distribution obtained is only a crude approximation to the real one.

We undertook a more detailed investigation of the energy spectrum of fragments from the triple fission of uranium.[3] The conditions of the experiment were such that the results were insensitive to angular correlations. It was found that the height of the peak corresponding to light fragments was greater, not smaller, than the height of the peak corresponding to the heavy fragments, while the half-widths of the peaks were approximately the same. The most probable value for the sum of the kinetic energies of the fragments in triple fission, plus the kinetic energy of the α particle, turned out to be approximately equal to the most likely value for the total kinetic energy of the fragments in double fission.

In a recently published paper, Mostovoĭ et al.[4] describe an experiment using the first method, but in which a correction was applied for the angular correlation between the fission fragments and the α particle. This correction is based on an extrapolation of data on the distribution of light fragments and also involves the angular distribution of the α particles, this latter distribution only being known with poor statistical accuracy. There is satisfactory agreement between the results quoted in references 3 and 4.

The work being reported upon here was carried out in order to get more detailed and reliable data on the energy spectrum of fragments from the triple fission of U^{235}. In order to do this, we measured the energies of pairs of fragments.

EXPERIMENTAL SETUP

In making measurements of the energy distribution of fragments from triple fission, the effect of angular correlation between the α particle and

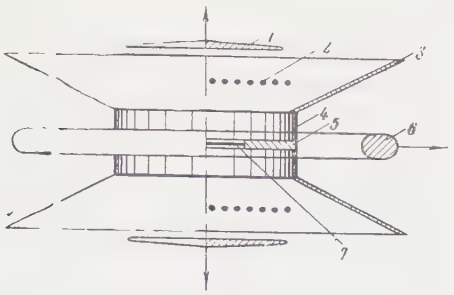

FIG. 1. Positions of the electrodes in the triple ionization chamber: 1 – collector for the fission chamber; 2 – grid for the fission chamber; 3 – cone; 4 – grid; 5 – common electrode for the fission chambers; 6 – collector for the α chamber; 7 – target.

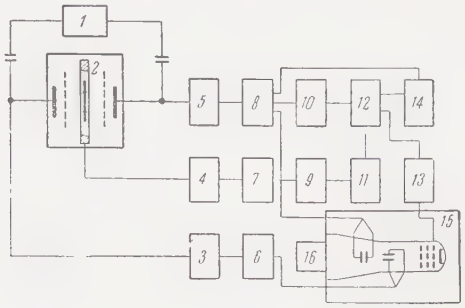

FIG. 2. Block diagram of the electronic circuitry: 1 – generator for calibrating pulses; 2 – chamber; 3, 4, 5 – preamplifiers; 6, 7, 8 – amplifiers; 9, 10 – discriminators; 11 – delay; 12 – coincidence circuit; 13 – brightness control; 14 – 63-channel pulse-height analyzer; 15 – oscilloscope; 16 – camera.

the fragments can be excluded by counting α particles on both sides of the target containing fissionable material. We have built a triple ionization chamber, together with its associated electronic circuitry.

The ionization chamber is shown schematically in Fig. 1. The chamber has cylindrical symmetry. The volume of the α chamber (the chamber for detecting long-range α particles) is defined by the cones and a metallic grid, the two together being one electrode of the α chamber. The other electrode of the α chamber is a metal ring. The electrode common to the two fission chambers and the first electrode of the α chamber were at ground potential. The supports and insulators were made of fluoroplastic.[5] The chamber was filled with argon at a pressure of two atmospheres. This pressure was high enough that α particles from naturally radioactive uranium could not reach the α chamber, which counted only long-range α particles with energies of 10 to 24 Mev.

The target of fissionable material was fastened to the common electrode of the fragment chambers. It was supported by a polyvinylchloride-acetate film[6] 5μg/cm^2 thick. Both sides were covered with ~ 6μg/cm^2 of gold by vacuum deposition. The U^{235} was deposited on one side of its support by a sputtering technique,[7] the thickness of the layer being ~ 10μg/cm^2.

A block diagram of the electronics is shown in Fig. 2. After passing through amplifying and pulse-shaping circuits, pulses from the fission chambers were fed onto the vertical (channel 1) and horizontal (channel 2) deflecting plates of an oscilloscope tube. The beam in the tube could be cut off so that no pulses were displayed unless there was a pulse from the α particle – fission fragment coincidence circuit. The position of the deflected beam was recorded photographically. When there were no pulses, the beam was focused on a point in the lower left hand corner of the field of view, this point being the origin of coordinates. When pulses were produced by the fission fragments and by the coincidence circuit, a dot would appear in the field of view, the distance of the dot from the vertical and horizontal axes being proportional to the amplitude of the first and second pulses. When observing fragments from double fission, the α channel was disconnected.

The photography was in the following sequence. The output of a calibrating generator was fed into the preamplifiers for the fission channels, the purpose of the calibrating generator being to illuminate three dots on the scope face, the dots defining the two coordinate axes and the origin. The stability of the entire apparatus was monitored by these three dots. The diameter of the dots was less than 1% of the full scale deflection the beam could undergo, so that one frame on the film could record about 80 – 100 dots (pairs of pulses). After these were recorded, the next frame would advance into position and the process would be repeated. Data taken this way were conveniently analyzed and were not subject to errors due to motion of the film while data was being recorded, or to the motion of the film in the projector while data was being analyzed.

The nonlinearity of the fission channels – from the input of the preamplifiers to the film – was less than 2%. After 30 min of warm-up time, the apparatus was stable to better than 2% over many hours.

The fraction of accidental coincidences was determined by the background pulses arising from neutron bombardment of the contaminants in the gas and of the α-chamber walls. To minimize this effect, the neutron beam was well collimated and was directed so as to miss the α-chamber walls. The effects of neutron scattering were

minimized by admitting the beam to the fragment chamber through a thin aluminum window, and by placing a second window at the exit of the neutron beam from the fragment chamber. Under these conditions, the accidental coincidences amounted to less than 3% of the true coincidences and were neglected in the analysis.

RESULTS

The work being described was carried out with the research reactor of the U.S.S.R. Academy of Sciences. The U^{235} target was irradiated by neutrons whose spectrum was that of the pile neutrons. About 8000 cases of triple fission and 6000 cases of double fission were observed.

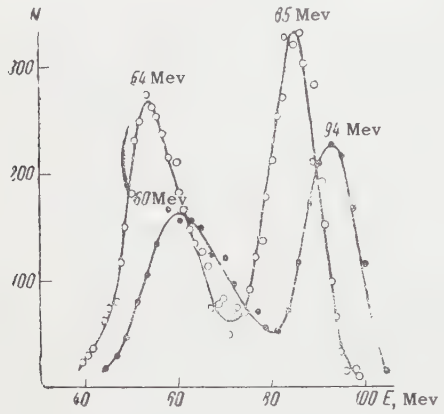

FIG. 3. Energy distribution of fragments from ○ – triple and ● – double fission of U^{235}. No correction for ionization effect.

Figure 3 shows the spectrum of fragments from triple and double fission, as obtained from observations on the chamber on the U^{235} side of the target. These data are corrected for the ionization produced by long-range α particles in passing through the fission chambers. It is clear from the diagram that the two distributions are displaced with respect to each other. The peak corresponding to light fragments is displaced (9.0 ± 0.5) Mev in the direction of lower energy, while the displacement of the peak corresponding to heavy fragments is (6.0 ± 0.5) Mev.

The half-widths of the light and heavy fragment peaks in triple fission are less than the corresponding half-widths for double fission. The spectra obtained from the second fission chamber are similar to the spectra shown in Fig. 3. A shift of ~ 2 Mev was observed and ascribed to energy loss in the target backing.

Figure 4 shows the yield of fragments from triple and double fission as a function of the total kinetic energy of the fragments. These curves are

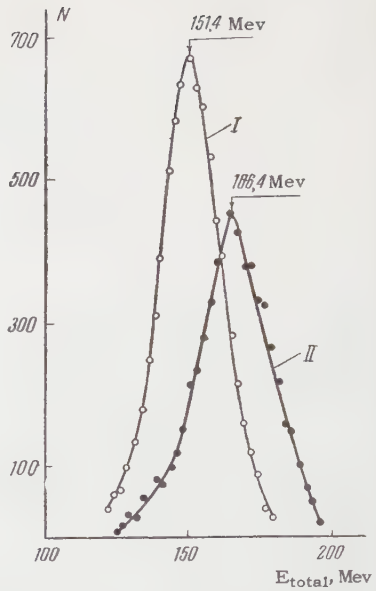

FIG. 4. Number of events as a function of total kinetic energy for ○ – triple and ● – double fission (with correction for ionization defect).

corrected for the ionization defect, which amounts to 12.4 Mev.[8] The difference between the most probable energies in double and triple fission is (15.0 ± 0.5) Mev. The half-width of the peak corresponding to triple fission is 3 Mev less than the half-width for the peak corresponding to double fission. The distributions are Gaussian to a good approximation.

The data were reduced to yield the dependence of the yield in both double and triple fission on the mass ratio of the fragments. Since the correction for the momentum of the α particle was small, it was assumed that the relation $M_1E_1 = M_2E_2$ held for triple as well as for double fission. The ioni-

FIG. 5. The yield η of double (●) and triple (○) fission as a function of the ratio of fragment masses. The yield is given in arbitrary units.

zation defect was assumed to be a linear function of the mass of the fragment: $\Delta E(M) = (4.0 \pm 0.019 M)$ Mev.[9] Upon normalizing the distributions to equal area it was found that the two distributions agreed within the statistical errors (Fig. 5). Both peaks occur at a mass ratio $M_1/M_2 = 1.4$. The half-widths of the distributions are the same and amount to ~ 16 mass units.

Finally, Fig. 6 shows the most likely total kinetic energy and the dispersion of the total kinetic energy of the fragments as a function of mass ratio. According to Protopopov, Baranov et al.[10], the maxima at mass ratio 1.3 can be explained in terms of shell structure.

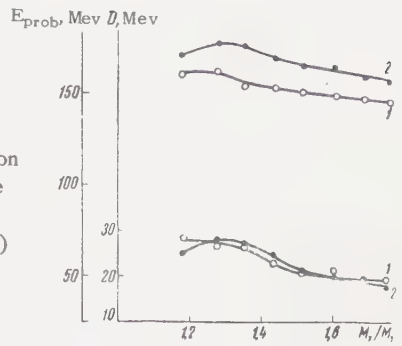

FIG. 6. The most probable total kinetic energy (E_{prob}) and the accompanying dispersion (D) as a function of the fragment mass ratio for triple (1) and double (2) fission.

DISCUSSION OF RESULTS

We have found that the half-widths of the energy distributions for fragments from double and triple fission differ from each other (Fig. 3). It might be suggested that the narrower peak observed for triple fission might be connected with a mass distribution which is more asymmetric for triple fission than it is for double fission. However, this does not agree with the observed mass distributions for triple and double fission, since these mass distributions are identical (to within the mass of the α particle) (Fig. 5). In other words, the probability of triple fission relative to double fission does not depend on the mass ratio. This disagrees with Hill's conclusion that triple fission should favor the formation of fragments with approximately equal masses.[11]

Our data show that the relation

$$E_d = E_{tr} + E_\alpha, \qquad (1)$$

holds, E_d and E_{tr} being the total kinetic energies of the fission fragments in double and triple fission respectively, while E_α is the energy of the α particle. For the most likely energy in double and triple fission we have, in particular, $E_d = 166.4$ Mev, while $E_{tr} + E_\alpha = 151.4 + 14.8 = 166.2$ Mev. All the fundamental data obtained in this and in previous work can be explained on the basis of equation (1).

First of all, the relation (1) implies that

$$(\Delta E_d)^2 = (\Delta E_{tr})^2 + (\Delta E_\alpha)^2,$$

where ΔE_d, ΔE_{tr} and ΔE_α are the half-widths of the corresponding distributions. From this it is clear why the half-width of the total kinetic energy distribution for triple fission is less than the corresponding half-width for double fission. The same relation leads to information about the energy spectrum of the long-range α particles. Since $\Delta E_d = 28$ Mev, and $\Delta E_{tr} = 25$ Mev, it follows that $\Delta E_\alpha = 13$ Mev. The maximum of this distribution should occur at 15 Mev. These numbers are in good agreement with the experimental data on the energy distribution of the long-range α particles: $\Delta E_\alpha = 11$ Mev and E_α (most likely) = 14.8 Mev[12].

According to Fong's theory,[13] the ratio of the probabilities for double and triple fission is determined by the difference between the total excitation energies of the fragments. Calculations show that when (1) is satisfied, then the difference between the total excitation energies of the fission fragments in double and triple fission depends but little on the fragment mass ratio and is about 4 Mev. Hence the probability for triple fission relative to double fission should not depend on the mass ratio. This explains the fact that the mass distributions in triple and double fission are the same (to within the mass of the α particle).

Decreasing excitation energy leads to a decrease in the probability for triple fission relative to that for double fission. Furthermore, a decrease in excitation energy should lead to the emission of fewer neutrons and γ rays in triple fission. Experimentally, it has been found[4] that the average number of prompt neutrons per triple fission is $\bar{\nu}_{tr} = 1.77 \pm 0.09$ for $E_\alpha \geq 9$ Mev, which is significantly less than the corresponding number for double fission. In reference 14, it was found that $\bar{\nu}_{tr} = 1.79 \pm 0.13$ for $E_\alpha \geq 22$ Mev. In the light of our assumptions, it is clear why the mean number of neutrons per triple fission does not depend on the energy of the α particles: the point is that in the act of fission there is a redistribution of the kinetic energy among the fragments and the α particle, but the excitation energy remains the same.

The equality (1) shows that the Coulomb energy of the system just before fission is the same in the two cases, i.e., there is no difference between the nuclear configurations just before double and triple fission and the α particle does not develop from a special "necking" process.

The mechanism for triple fission might be pictured as follows: just before fission, the potential barrier near the neck of the deformed nucleus becomes lower. During fission, the particles at the surface of the nucleus are strongly accelerated, which leads to a further lowering of the barrier because of "inertial forces" and so enhances the probability for emission of an α particle. Right up to the instant of fission, the nucleus "does not know" whether to split into two or three parts, which makes it plausible that the various quantities plotted in Figs. 3 — 6 are the same for double and triple fission. This picture suggests that the probability for triple fission does not change markedly from nucleus to nucleus, and this is observed experimentally.[15] The decrease in the probability for triple fission observed as the energy of the bombarding neutrons is increased presumably is due to competition from other processes (for example, neutron emission at the moment of fission).

The mechanism for triple fission which has just been described offers a qualitative explanation both for the observed anisotropy in the angular distributions of the long-range α particles and fission fragments, and also for the decrease in anisotropy for higher energy α particles.[16-18]

In conclusion it should be stressed that the study of triple fission leads to a number of detailed and interesting insights into the fission process in general.

The authors would like to thank M. A. Bak and S. S. Kovalenko for valuable discussions. They are also grateful to S. A. Gavrilov and A. P. Shilov for help in carrying out the experiments on the research reactor of the U.S.S.R. Academy of Sciences.

[1] Perfilov, Romanov, and Solov'eva, Usp. Fiz. Nauk, in press.

[2] K. W. Allen and J. T. Dewan, Phys. Rev. **80**, 181 (1950).

[3] Dmitriev, Drapchinskiĭ, Petrzhak, and Romanov, Dokl. Akad. Nauk SSSR **127**, 531 (1959), Soviet Phys.-Doklady **4**, 823 (1960).

[4] Mostovoĭ, Mostovaya, Sovinskiĭ, and Saltykov, Атомная энергия (Atomic Energy) **7**, 372 (1959).

[5] Dmitriev, Drapchinskii, and Romanov, Приборы и техника эксперимента (Instruments and Exptl. Techniques), in press.

[6] B. D. Pate and L. Jaffe, Can. J. Chem. **33**, 15 (1955).

[7] Gorodyskiĭ, Romanov, Sorokina, and Yakunin, op. cit. ref. 5, No. 5, 128 (1959).

[8] R. B. Leachman, Phys. Rev. **87**, 444 (1952).

[9] J. Fraser and J. Milton, Phys. Rev. **93**, 818 (1954).

[10] Protopopov, Baranov, Selitskiĭ, and Éĭsmont, JETP **36**, 1932 (1959), Soviet Phys. JETP **9**, 1374 (1959).

[11] D. L. Hill, Second UN International Conference on the Peaceful Uses of Atomic Energy, **15**, 244 (1958) [Paper P/660].

[12] C. Fulmer and B. Cohen, Phys. Rev. **108**, 370 (1957).

[13] P. Fong, Phys. Rev. **102**, 434 (1956).

[14] Apalin, Dobrynin, Zakharova, Kutikov, and Mikaélyan, op. cit. ref. 4, **7**, 375 (1959).

[15] Dmitriev, Drapchinskiĭ, Petrzhak, and Romanov, JETP **38**, 998 (1960), Soviet Phys. JETP **11**, 718 (1960).

[16] Tsien, Ho, Chastel, and Vigneron, J. Phys. Radium **8**, 165 (1947).

[17] E. Titterton, Nature **168**, 590 (1951).

[18] N. A. Perfilov and Z. I. Solov'eva, JETP **37**, 1157 (1959), Soviet Phys. JETP **10**, 824 (1960).

Translated by R. Krotkov
110

PICKUP REACTIONS ON F^{19}, P^{31}, *AND* S^{32} *NUCLEI*

G. E. VELYUKHOV, A. N. PROKOF'EV, and S. V. STARODUBTSEV

Leningrad Physico-Technical Institute, Academy of Sciences, U.S.S.R.

Submitted to JETP editor April 16, 1960

J. Exptl. Theoret. Phys. (U.S.S.R.) 39, 563-565 (September, 1960)

A telescope consisting of two proportional counters and a scintillation counter was employed to study the energy and angular distributions of deuterons from the reactions $F^{19}(n, d)O^{18}$, $P^{31}(n, d)Si^{30}$, $S^{32}(n, d)P^{31}$, and $Ne^{20}(n, d)F^{19}$. The cross sections and angular distributions for transitions to the ground states of the O^{18}, Si^{30}, and P^{31} nuclei are derived. The total cross section for the reaction $Ne^{20}(n, d)F^{19}$ is estimated. The reduced transition widths are computed from Butler's theory.

In our previous work[1] we pointed out that O^{18} and Si^{30} have the same differential cross sections for the reactions $F^{19}(n, d)O^{18}$ and $P^{31}(n, d)Si^{30}$ in transitions to the ground state if the incident neutron energy is 14.1 Mev. If it is assumed that this equality is connected with the fact that, according to the nuclear shell model, the last proton of F^{19} is in the same state as that of P^{31}, then analogous transitions can be expected in the reactions $Ne^{20}(n, d)F^{19}$ and $S^{32}(n, d)P^{31}$, because there the last protons are in the state $2S_{1/2}$. In connection with this it was of interest to conduct simultaneous investigations of (n, d) reactions on F^{19}, P^{31}, and S^{32}, because the comparison of reduced widths in this case could give relative characteristics of the wave properties of the nuclear surface.

We developed a method which is new compared to that[1] used before, and which improved the resolution of the deuteron groups. We carried out the investigation with the help of a telescope composed of two proportional counters and a scintillation counter. The proportional counters measured the ionization energy loss dE/dx, and the scintillation counter measured the energy of the deuterons. The separation of the deuteron groups was achieved with an electronic system which was based on the fact that $EdE/dx \sim M^{0.8}Z^2E^{0.2}$, i.e., it is only weakly dependent on the energy of the particle and depends almost linearly on its mass.

In the investigation of the reaction $S^{32}(n, d)P^{31}$ we used a target of a natural mixture of the isotopes of sulfur. We obtained the energy spectrum of the deuterons (Fig. 1) and their angular distribution. In the energy spectrum is observed a strong group of deuterons corresponding to the transition to the ground state of P^{31}. From an

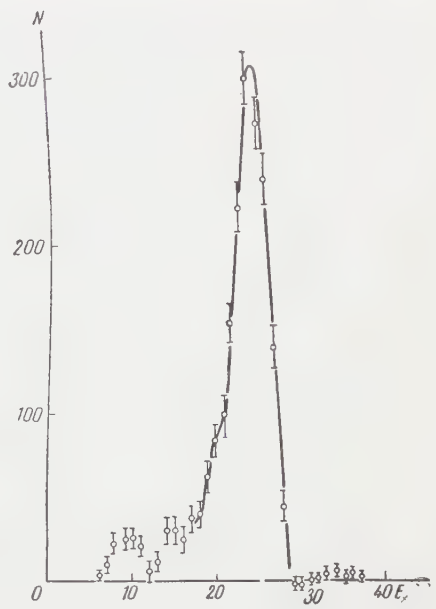

FIG. 1. Energy spectrum of deuterons from the reaction $S^{32}(n, d)P^{31}$ at the angle $\theta = 0°$ (in the laboratory system); E is the channel number.

analysis of the line shape corresponding to this transition it is clear that, in addition to the transition to the ground state, transitions also take place to the first excited state of P^{31}; however, their intensity is too weak to permit a quantitative estimate. From the form of the angular distribution it follows that proton capture takes place from the S state. The differential cross section for the angle $\theta = 0^0$ (in the laboratory system) is $(20.4 \pm 1.5) \times 10^{-27}$ cm^2/sr; the Q-value for this reaction is (-7.7 ± 0.1) Mev.

In the study of the reaction on F^{19}, a target of the fluorocarbon $4(CF_2 = CF_2)$ was used. The energy spectrum of the deuterons and their angular distribution were obtained. From the angular dis-

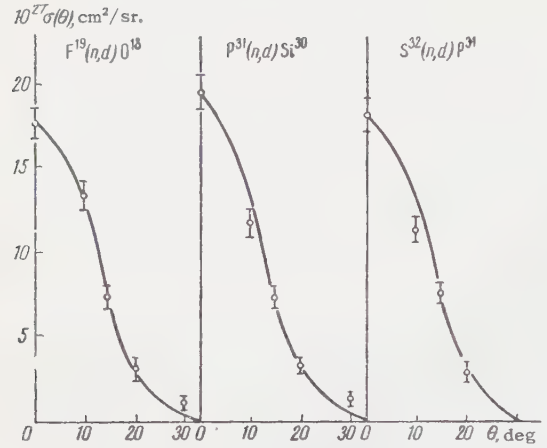

FIG. 2. Angular distribution of deuterons corresponding to transitions to the ground state in (n, d) reactions, in the center-of-mass system.

tribution it follows that a proton with $l_p = 0$ is captured in the transition to the ground state of O^{18}. The differential cross section for the same transition at the angle $\theta = 0^0$ (in the laboratory system) equals $(21.4 \pm 1.1) \times 10^{-27}$ cm²/sr, and the Q-value equals (-5.9 ± 0.3) Mev.

In the study of the reaction on P^{31}, the target was prepared by deposition of red phosphorus on a tantalum backing. The transition to the ground state of the nucleus Si^{30} was observed, and an angular distribution was obtained for this. The transition corresponds to $l_p = 0$. The differential cross section of the reaction for the transition to the ground state of Si^{30} at $\theta = 0^0$ (in the laboratory system) is $(21.8 \pm 1.2) \times 10^{-27}$ cm²/sr; the Q-value is (-5.2 ± 0.2) Mev.

The angular distribution of deuterons corresponding to transitions to the ground state of the final nuclei in the reactions $F^{19}(n, d)O^{18}$, $P^{31}(n, d)Si^{30}$, and $S^{32}(n, d)P^{31}$ (Fig. 2) were analysed on the basis of Butler's theory.[2] For the normalization of the theoretical values of the differential cross sections at the angle $\theta = 0^0$ we used the following values of the reduced transition widths (i.e., the quantities $\theta^2 = 2\mu_0 r_0 \gamma^2/3\hbar^2$)

$F^{19}(n, d)O^{18}$:

$\theta^2 = 0.011$ (0.012 according to reference 3),

$P^{31}(n, d)Si^{30}$: $\theta^2 = 0.012$,

$S^{32}(n, d)P^{31}$: $\theta^2 = 0.011$

(the measurement errors amounted to 15% in all cases).

Thus it appears that the differential cross section and the reduced width of the transition to the ground state of the nucleus in the reaction $S^{32}(n, d)P^{31}$ coincide, within the limits of experimental error, with the values of these quantities in the reactions $F^{19}(n, d)O^{18}$ and $P^{31}(n, d)Si^{30}$. The theoretical angular distributions fit the experimental results for the same interaction radius $r = 5.1 \times 10^{-13}$ cm.

Evidently this agreement is connected with the fact that in all three cases the proton is captured from the same state. If the reduced width is interpreted as the probability of the presence of the proton on the nuclear surface, then it follows that the contribution of S waves to the state of the last proton in the nuclei F^{19}, P^{31}, and S^{32} is identical.

However, a somewhat different point of view may be taken: since the nucleus S^{32} contains two protons in a $2S_{1/2}$ state, one would expect the probability of the presence of the proton on the nuclear surface to increase. Because this is not observed, it is necessary to find reasons for the lower probability of capture of a proton by the neutron. One of these reasons may be the increase of binding energy of the proton in S^{32} in comparison with P^{31} (S^{32} is an even-even nucleus). This assumption could be verified by investigating the reaction $Ne^{20}(n, d)F^{19}$, since Ne^{20} also contains two protons in the state $2S_{1/2}$ and has a proton binding energy greater than in S^{32}. We conducted such an investigation by the method described above, but because of bad conditions (high negative Q-value for the reaction and a gas target) we were able only to estimate the upper limit of the cross section of the reaction $Ne^{20}(n, d)F^{19}$ for the transition to the ground state of F^{19}. This estimate was 5×10^{-27} cm²/sr.

At present we are continuing the study of this reaction by another method. According to our preliminary data, the estimate given is at least five times too high.

The authors wish to thank A. P. Pulin and A. M. Tsvetkov for help in conducting the experiment.

[1] Velyukhov, Profof'ev, and Starodubtsev, Dokl. Akad. Nauk SSSR **127**, 781 (1959), Soviet Phys.-Doklady.

[2] S. T. Butler, Proc. Roy. Soc. **A208**, 36 (1951).

[3] F. L. Ribe, Phys. Rev. **106**, 767 (1957).

Translated by C. S. Littlejohn
111

TEMPERATURE HYSTERESIS OF DOMAIN STRUCTURE IN SILICON IRON CRYSTALS

YA. S. SHUR AND I. E. STARTSEVA

Institute of Metal Physics, Academy of Sciences, U.S.S.R.

Submitted to JETP editor April 16, 1960

J. Exptl. Theoret. Phys. (U.S.S.R.) 39, 566-573 (September, 1960)

The domain structure of silicon iron crystals before and after heating from room temperature up to 550°C was studied by the powder pattern technique. Irreversible changes of the domain structure were detected following a temperature cycle. The size, shape and number of closure domains change and the boundaries between basic domains are displaced; temperature hysteresis of the domain structure is observed. This behavior is explained using the domain theory of ferromagnetic structure.

I. INTRODUCTION

THE domain structure of a ferromagnetic substance is known to depend on its basic properties (magnetic saturation, the anisotropy and magnetostriction constants), its shape and size, and different kinds of lattice defects (residual strains, impurities, discontinuities, etc.). Since the basic properties are temperature-dependent we may expect the domain structure to vary with temperature. We may also expect that the magnetic structure will not return to its original form following a temperature cycle, since both reversible and irreversible changes may accompany temperature variations. Temperature hysteresis of the domain structure should therefore be observed.

The present work was performed to detect the temperature hysteresis of domain structure in silicon iron crystals and to establish the most general laws of this effect. We are not aware of any previous special investigation of this type.

II. DESCRIPTION OF SAMPLES AND EXPERIMENTAL TECHNIQUE

The magnetic structure was observed by means of the powder-pattern technique.[1] Both single crystals and polycrystalline samples of silicon iron (3.5% Si) 15 mm in diameter and 0.3—0.7 mm thick were used. The investigated surface of the single crystals was approximately parallel to the (011) plane. In the case of polycrystalline samples, which consisted of large grains 0.5—3.0 mm in diameter, the domain structure was observed on single grains having surfaces close to (001) or (011). The samples were etched from sheet silicon iron, and after mechanical grinding and polishing were vacuum annealed at 1250°C. The magnetic structure of some samples was studied immediately following this high-temperature annealing, while other samples were subjected to supplementary electrolytic polishing. For the purpose of studying the effect of a temperature cycle on the form of the magnetic structure, the samples were heated from room temperature to different temperatures up to 550°C and were then cooled to the initial temperature. The samples were heated in a special device placed within a vacuum chamber (Fig. 1) that was fastened to the microscope stage. A copper core 2 bearing a sample 3 on its upper end was inserted into a double-wound electric furnace 1. A copper cover 4 was provided for temperature equalization. A thermocouple 5 was fitted into the copper core. The furnace was fastened by means of the supports 6 to a heavy water-cooled iron plate 7. For the purpose of preventing oxidation during heating the furnace together with the sample was placed inside a vacuum chamber consisting of a heavy iron dome 8 and base 7, which at the same time provided magnetic screening for the sample. Thus the samples were both heated and cooled in a vacuum which was free of external magnetic fields.

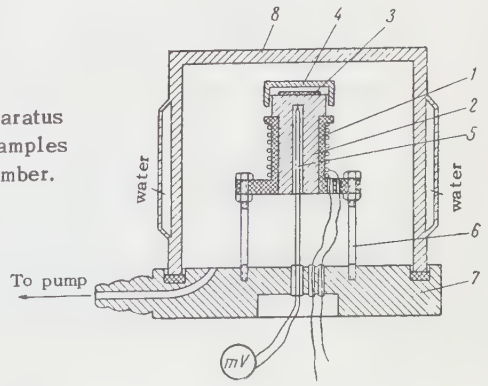

FIG. 1. Apparatus for heating of samples and vacuum chamber.

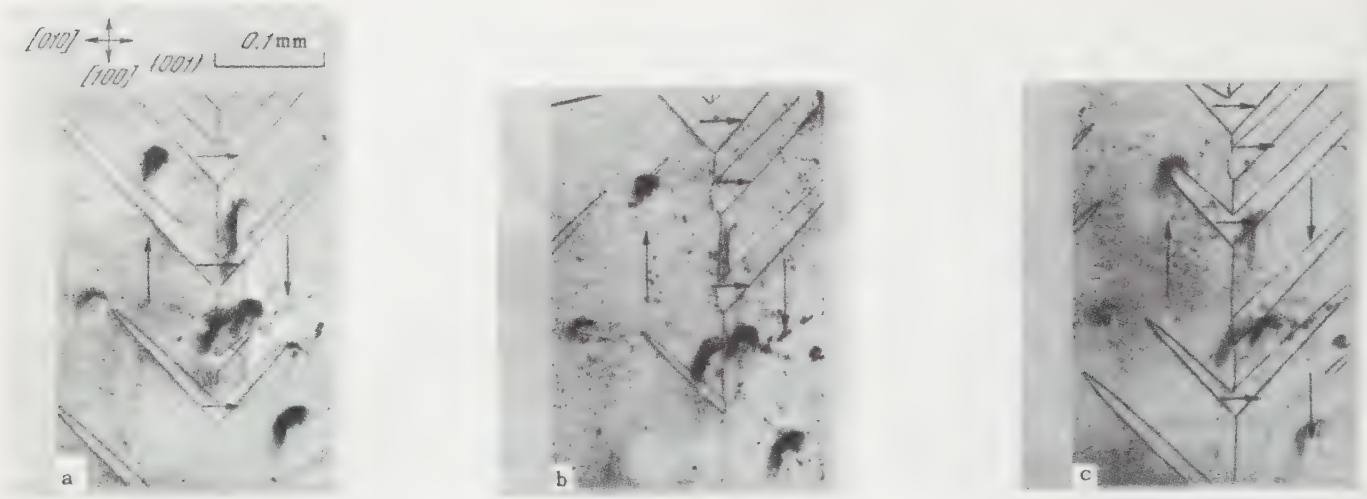

FIG. 2. Powder pattern on a crystal surface approximately parallel to the (001) plane (type A structure); a – after demagnetization, b – after heating to 400°C, c – after re-demagnetization.

Prior to observation of the domain structure each sample was demagnetized in a solenoid by means of a field which varied smoothly from 600 oersteds to zero. The sample was then placed upon the heating core 2. A magnetic colloidal suspension was applied to the surface of the sample; the powder pattern was then observed and photographed. After the suspension had been carefully wiped off the sample was covered with the copper cap 4, and the dome 8 was fastened to the plate 7. After a vacuum had been established the sample was gradually heated to the required temperature, at which it was maintained during 30 min. When the sample and furnace were subsequently cooled to room temperature the magnetic suspension was again applied to the surface of the sample and the powder pattern was photographed in exactly the same area as before heating.

The sample was thereupon demagnetized by a variable field and the powder pattern on its surface was again photographed. In the case of monocrystalline disks the powder pattern was photographed along a diameter perpendicular to the direction of easy magnetization lying in the plane of the sample. Repeated observations of the powder patterns following successive alternations of careful wiping and applying of the suspension showed that this procedure does not affect the magnetic structure.

For the purpose of detecting temperature hysteresis of the domain structure we compared the powder-pattern photographs of the same area a) after the first demagnetization, b) after heating and cooling and c) after the second demagnetization process.

III. EXPERIMENTAL RESULTS

Heating from 20 to 200°C followed by cooling to 20°C produced no essential changes in the domain structure. With heating to higher temperatures irreversible movements of boundaries between the basic domains became clearly distinguishable, accompanied by readjustment of the surface domains of closure. Reorganization of the domain structure was studied carefully following heating up to 400–550°C; the existence of temperature hysteresis was definitely established. Although subsequent demagnetization in a variable magnetic field restores the original type of domain structure, the boundaries of the basic domains and the domains of closure do not occupy exactly the same positions that are observed following the first demagnetization process prior to heating. This irreproducibility follows consistently; after each re-demagnetization at room temperature the magnetic structure is, as a rule, not entirely reproduced in all details.

The photographs of powder patterns in Figs. 2, 3, 5, and 6 show how the domain structure is modified in some of the simplest cases following a temperature cycle. Figure 2 shows powder patterns on a crystal having its surface approximately parallel to the (001) plane. In the demagnetized state (Fig. 2a) two basic domains are visible, separated by a 180° boundary, and the surface closure domains exhibit a "Christmas tree" structure.[1] The arrows in the photographs indicate the direction of magnetization I_s in the domains. Following heating to 400°C and subsequent cooling to the original room temperature the 180° boundary is observed to move irreversibly to the right (Fig.

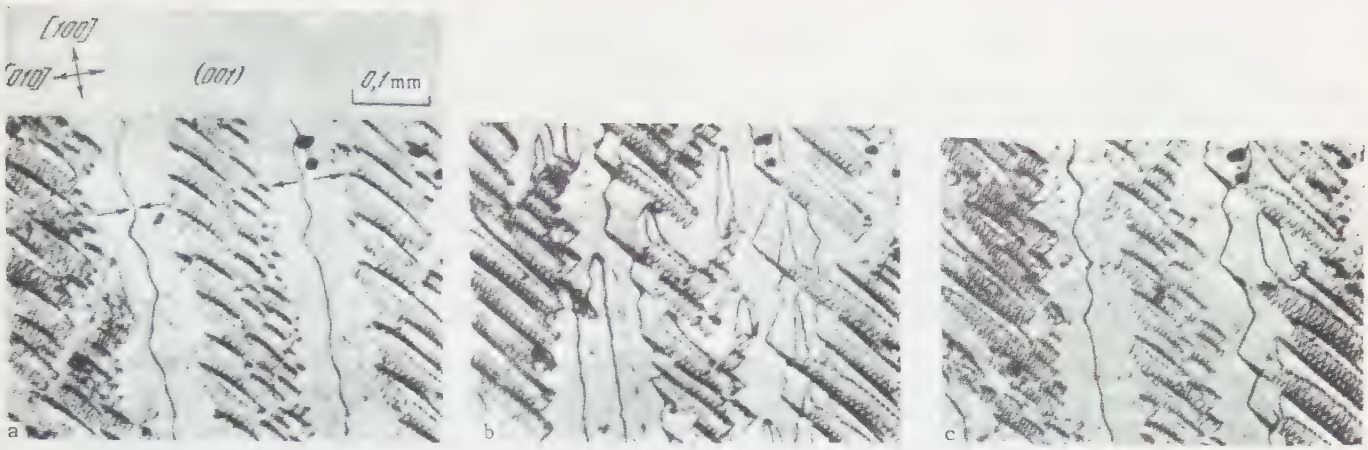

FIG. 3. Powder pattern on a crystal surface approximately parallel to the (001) plane (type B structure): a – after demagnetization, b – after heating to 400° C, c – after re-demagnetization.

2b) and the number of domains of closure (tree branches) is reduced. Re-demagnetization (Fig. 2c) returns the 180° boundary to its original position, while the number of closure domains increases and their original appearance is approximated.

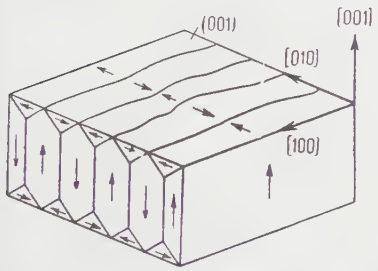

FIG. 4. Diagram of type B structure.

The powder patterns in Fig. 3 also belong to a crystal with its surface approximately parallel to (001), but differ from the preceding case by exhibiting type B structure (Fig. 3a) in the initial demagnetized state.[2] This means that the basic domains are located inside the crystal, while the observed surface reveals the bases of triangular-prism closure domains separated by zigzag boundaries. Type B structure is illustrated schematically in Fig. 4. In addition, smaller "comb-like" domains of closure are observed within the prismatic domains of closure.[2] Heating to 450° followed by cooling to room temperature considerably modifies the closure domain structure (Fig. 3b); the "combs" increase in size but decrease in

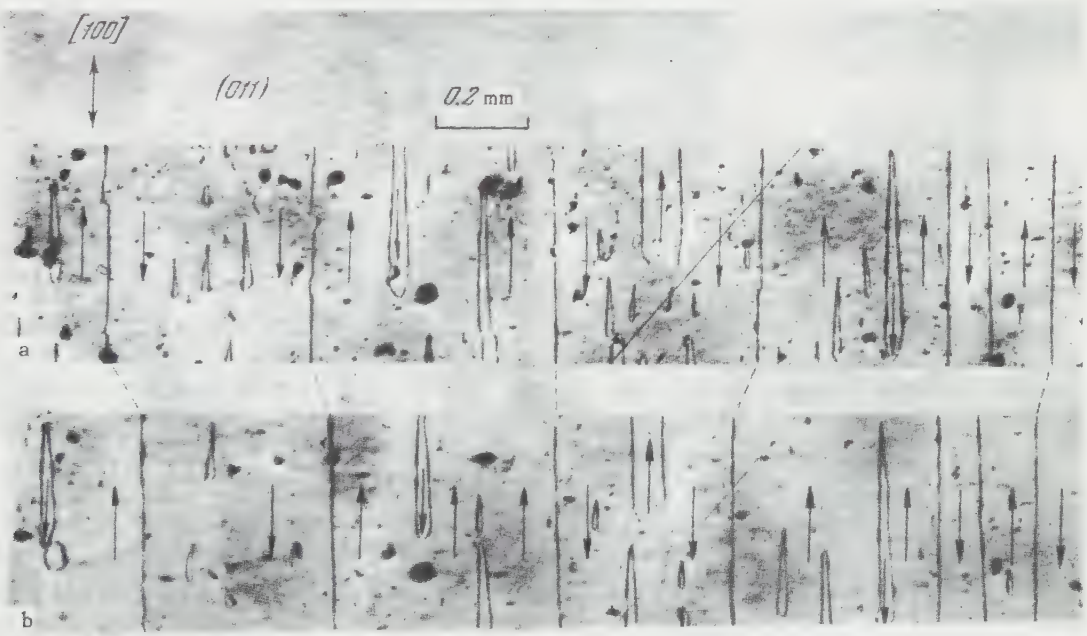

FIG. 5. Powder pattern on a crystal surface approximately parallel to the (011) plane: a – after demagnetization, b – after heating to 550° C.

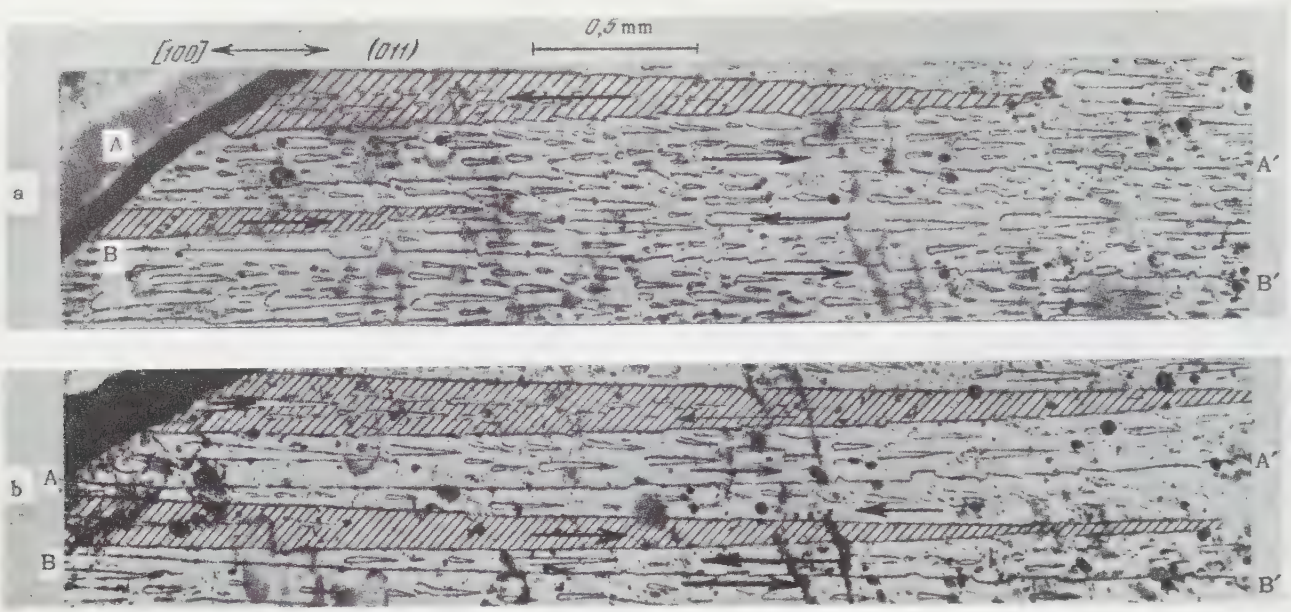

FIG. 6. Powder pattern on a crystal surface approximately parallel to the (011) plane: a – after demagnetization, b – after heating to 550°C.

number. Following the re-demagnetization, however, the original appearance of the domain structure is restored (Fig. 3c).

Figure 5 shows photographs of powder patterns on a single-crystal surface approximately parallel to (011). The plane of the sample contains one direction of easy magnetization; in the initial demagnetized state (Fig. 5a) the crystal is divided into oppositely magnetized domains separated by 180° boundaries. The surface also reveals a small number of closure domains shaped like drops of a liquid.[2] Heating to 550°C followed by cooling to room temperature induces an irreversible change of the magnetic structure (Fig. 5b) in which the boundaries of the basic domains are shifted while the drop-shaped regions change in size and decrease in number. The dashed lines connecting boundaries of the basic domains before and after heating show the extent to which the boundaries are shifted as a result of the temperature cycle.

Figure 6 also shows the powder pattern on the edge of a monocrystalline disk the surface of which is also approximately parallel to the (011) plane. Here the easy direction of magnetization closest to the crystal surface forms a larger angle with the latter than in the preceding case. In the demagnetized state (Fig. 6a) the sample is also divided into plane-parallel domains separated by 180°C boundaries that exhibit jogs (AA′ denotes the upper boundary and BB′ denotes the lower boundary). The surface reveals a large number of drop-shaped closure domains, as well as relatively large (hatched) dagger-shaped regions starting at the edge of the crystal. Figure 6b shows the domain structure after heating to 550°C.

A comparison of Figs. 6a and 6b shows that the temperature cycle does not induce an appreciable shift of the boundaries between the basic domains. These boundaries become more distinct and straighter. At the same time the closure domains are considerably reorganized; the drop-shaped domains decrease in number but some of them increase in size. The greatest change is exhibited by the dagger-shaped domains of closure located at the edge of the crystal. These domains grow much larger as a result of the temperature cycle and new dagger-shaped domains appear. Within the expanded upper dagger-shaped domain in Fig. 6b a new but smaller domain of the same type appears with antiparallel magnetization.

The experimental results thus show that a temperature cycle between 20 and 400—500°C induces considerable irreversible change of magnetic structure in monocrystalline and polycrystalline silicon iron. These changes can be summarized as follows: The surface domains of closure change in size and shape, and some of them disappear; the dagger-shaped domains of closure at the edge of the crystal increase in size; the boundaries between the basic regions are shifted.

IV. ANALYSIS OF RESULTS

We shall now attempt to account for the observed irreversible changes of the domain structure. We shall first determine what changes of magnetic structure could be expected when the temperature of silicon iron crystals is elevated. At room tem-

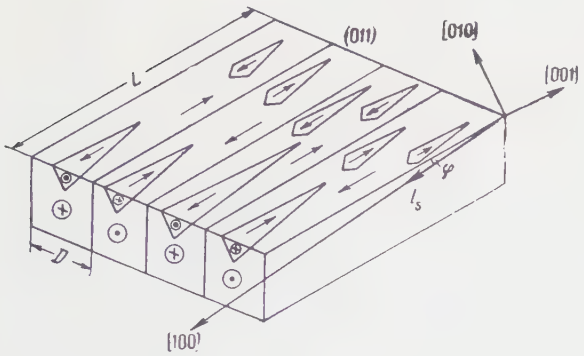

FIG. 7. Diagram illustrating type A structure. φ – angle between the [100] direction and the crystal surface.

perature a crystal having its surface approximately parallel to (011) is usually divided into basic domains separated by 180° boundaries; magnetization of these regions is oriented along the [100] tetragonal axis closest to the surface of the sample and forming an angle φ with the latter. This type of structure is represented schematically in Fig. 7. On the surface and edges of this crystal stray magnetic fields appear, whose energy is reduced through the formation of closure domains (drop-shaped domains on the surface and dagger-shaped domains on the edge). Energy is expended for the formation of the closure domains because boundaries are developed between these domains and the basic domains within which the former appear. Thus the sizes and shapes of closure domains are determined by the relationship between the stray-field energy and the wall energy. With weakening of the stray fields these domains should be reduced in size, but their size should increase when the wall energy is reduced.

The energy of the stray fields on the crystal surface that is approximately parallel to the (011) plane is, according to Kittel,[3]

$$F_1 = 0.85\, I_s^2 D \sin^2\varphi / (1+\mu^*), \tag{1}$$

where D is the width of the basic domains (Fig. 7) and $\mu^* = 1 + 2\pi I_S^2/K$. Through study of the domain structure by means of powder patterns it has been found that in silicon iron crystals having surfaces approximately parallel to (011), the magnetization I_S is parallel to the [001] axis in both the basic and closure domains. D can therefore be calculated by means of the formula derived for a uniaxial magnetic crystal:[3]

$$D = (\gamma L / 1.7 I_s^2)^{1/2}, \tag{2}$$

where L is the length of the basic domains. We thus obtain

$$F_1 = \frac{0.33 I_s \sin^2\varphi \sqrt{L\gamma}}{1+\pi I_s^2/K}. \tag{3}$$

$\gamma \sim \sqrt{aK + b\lambda_S^2 E}$ is the density of the wall energy;[4] here a and b are constants of the order of unity, λ_S is the saturation value of the magnetostriction and E is the elastic modulus. In our samples of silicon iron $K \gg \lambda_S^2 E$ (since $K \approx 3\times10^5$ erg/cm^3, (reference 5), $\lambda_{[100]} \approx 2\times10^{-5}$ (reference 6) and $E \approx 2\times10^{12}$ dyne/cm^2). We shall therefore hereinafter assume $\gamma \sim \sqrt{K}$. Equation (3) shows that F_1 depends on a number of temperature-sensitive ferromagnetic parameters: I_S, K, γ.

Our samples were heated from room temperature up to 400—550°C. By this process the saturation magnetization of silicon iron is not greatly (10—20%) reduced, but the anisotropy constant K is reduced by a factor of 3—6.[5] For silicon iron $I_S = 1600$; therefore $\pi I_S^2/K \gg 1$. It follows that $F_1 \sim K^{5/4}/I_S$. In view of the fact that with increasing temperature the decrease of I_S is insignificant compared with that of K, we take

$$F_1(T) \sim K^{5/4}(T). \tag{4}$$

The temperature dependence of the wall energy density is

$$\gamma(T) \sim K^{1/2}(T). \tag{5}$$

It follows from (4) and (5) that since F_1 decreases more strongly than γ, the surface drop-shaped closure domains must diminish in size, so that some of them may even disappear.

Both reversible and irreversible changes of the domain structure may occur when the crystals are again brought down to room temperature. The irreversible changes should partially conserve all characteristics of the domain structure reorganization which result from the higher temperature. In the present specific case we may expect the irreversibility to be manifested by a different size of the closure domains compared with the initial state prior to heating. In addition, some of the disappearing closure domains may not reappear because nuclei of new regions are formed with difficulty. Figures 5 and 6 contain the experimental evidence for these conclusions.

We shall now consider how a temperature rise should affect the appearance of the dagger-shaped closure domains at the crystal edge (Figs. 6 and 7). The stray-field energy on the lateral crystal surface is

$$F_2 = 0.85\, I_s^2 D \cos^2\varphi. \tag{6}$$

Equation (6) does not contain μ^* because this quantity may be neglected for large angles between I_S and the crystal surface in question.[1] Substituting D from (2) into (6) and considering that in our case I_S is only slightly temperature-dependent, we have

$$F_2(T) \sim K^{1/4}(T). \quad (7)$$

A comparison of (7) and (5) indicates that with rising temperature F_2 will decrease more slowly than the wall energy density. As a result the dagger-shaped closure domains on the edge should grow; they may also increase in number. Assuming that with a reduction to room temperature the structure may not return to its original condition (before heating), we may expect a growth of the dagger-shaped regions as a result of a temperature cycle. This is confirmed experimentally by the powder patterns given in Fig. 6, where it is shown how the temperature cycle brings about a considerable growth and multiplication of the dagger-shaped domains.

We may similarly consider how a higher temperature affects the structure of closure domains on a crystal surface approximately parallel to the (001) plane. When the surface is accurately parallel to (001) the magnetic domain structure predicted by Landau and Lifshitz appears.[7] This structure is shown schematically on the end surface in Fig. 4, where the basic domains and the triangular closure domains on the edges are represented. When the crystal surface is slightly inclined to (001) stray fields appear on the surface, and the energy of these fields may be reduced through the formation of surface closure domains (trees, tree trunks, etc.). For this structure, according to Kittel,[3] the width of the basic domains is calculated taking the magnetoelastic energy into account:

$$D = (4\gamma L / \lambda^2_{[100]} c_{11})^{1/2}, \quad (8)$$

where c_{11} is the elastic modulus. As the temperature of a silicon iron crystal increases to 500°C, $\lambda_{[100]}$ can only increase[6] while c_{11} decreases slightly. D will therefore diminish with rising temperature because of the growth of $\lambda_{[100]}$ as well as the reduction of K. From (1) and (8) we obtain $F_1(T) \sim K^{5/4}(T)$. We should therefore observe a reduction of closure domain size when a crystal having its surface approximately parallel to (001) is heated. This reconstruction of the closure domains may also follow a temperature cycle, as can be seen from the powder patterns in Fig. 2.

A temperature rise can also affect the appearance of the basic domains. The boundaries between these regions tend to assume the positions for minimum wall energy. This remains true if the total energy of the crystal is not enhanced through increases in other forms of energy. With rising temperature the regions of minimum γ are rearranged; the boundaries may thus be shifted. The boundaries of closure domains may be shifted for the same reason.

It follows from (2) and (8) that a temperature rise will also change the equilibrium width D of the basic domains. For example, in the case of the domain structure represented in Fig. 7 we may assume $D \sim \gamma^{1/2} \sim K^{1/4}$ according to (2), since in our experiments I_s changes very little with temperature. Higher temperatures may therefore break down the basic domains; in the present instance this may be brought about through growth of the dagger-shaped closure domains and through their transformation into basic domains.*

It follows from our analysis that the magnetic structure of silicon iron crystals should change when their temperature is elevated.† It may be expected that when the original temperature of these crystals is restored some of the changes are conserved. The existing theory is unable to predict the extent of this irreversibility of the magnetic structure. Only experiments such as those described in the present paper can supply pertinent information. We have shown that a temperature cycle is accompanied by a boundary displacement of the basic domains.

It is reasonable to expect that the domain structure of a heated sample will be metastable after being restored to its original temperature. Therefore if a heated sample is demagnetized by a variable field the magnetic structure should on the whole return to the original form exhibited by the demagnetized sample before heating. This conclusion is confirmed by the photographs in Figs. 2 and 3.

The temperature hysteresis of domain structure which we have described in the case of silicon iron crystals should also occur in all other ferromagnetic materials possessing a multidomain magnetic structure.

*Strictly speaking, we cannot consider changes of the closure domains and basic domains independently, since all the domains of a crystal are interrelated. In polycrystalline samples this interrelation also exists between domains located in different grains, especially between those which are in contact. Our treatment is adequate, however, for the discovery of qualitative laws.

†Kirenskiĭ and Degtyarev[8] used the Kerr effect to observe the magnetic structure on the oxidized (011) plane of a silicon iron crystal which was heated from 20 to 700° C. No changes of the magnetic structure were detected. Since these observations were made under very low magnification, small heat-induced changes of the magnetic structure may have been overlooked.

[1] Williams, Bozorth, and Shockley, Phys. Rev. **75**, 155 (1949).

[2] Ya. S. Shur and V. R. Abel's, Физика металлов и металловедение (Physics of Metals and Metallography) **5**, 11 (1955).

[3] C. Kittel, Revs. Modern Phys. **21**, 541 (1949).

[4] S. V. Vonsovskiĭ and Ya. S. Shur, Ферромагнетизм (Ferromagnetism), Gostekhizdat, 1949, p. 301.

[5] L. A. Shubina, Izv. Akad. Nauk SSSR, Ser. Fiz., **11**, 527 (1947).

[6] D. A. Shturkin, Izv. Akad. Nauk SSSR, Ser. Fiz., **11**, 664 (1947).

[7] L. D. Landau and E. M. Lifshitz, Sow. Phys. **8**, 153 (1935).

[8] L. V. Kirenskiĭ and I. F. Degtyarev, JETP **35**, 584 (1958), Soviet Phys. JETP **8**, 403 (1959).

Translated by I. Emin
112

LONGITUDINAL POLARIZATION OF BETA ELECTRONS

P. E. SPIVAK and L. A. MIKAÉLYAN

Submitted to JETP editor April 20, 1960

J. Exptl. Theoret. Phys. (U.S.S.R.) 39, 574-583 (September, 1960)

Values of the longitudinal polarization of β electrons from P^{32}, In^{144}, Sm^{153}, Lu^{177}, Ho^{166}, and Au^{198} nuclei have been measured at 300-340 kev by the method of Mott scattering (involving the transformation of longitudinal into transverse polarization). Differences up to 10% have been detected in the degree of polarization of the isotopes investigated. It has also been found that the absolute values of the polarization lie in the range $(0.86-0.97)$ v/c. The error in the absolute measurements ($\pm 3\%$) does not include any possible inaccuracies in the theoretical calculation which relates the values of the polarization and of the scattering asymmetry.

INTRODUCTION

As is well known, the discovery of the non-conservation of parity in weak interactions[1,2] has led to a reinvestigation of our description of β decay. In particular, it has turned out that in accordance with the two-component neutrino theory[3-5] the electrons emitted in β decay of unpolarized nuclei must be longitudinally polarized. This effect was then soon discovered experimentally.[6-8] It was shown that the magnitude of the effect agrees within an accuracy of $\pm(15-20)\%$ with the calculated value $\mp$ v/c for electrons and positrons respectively. During the next three years more than twenty papers have been published (cf. reference 9) in which different methods of measurement were utilized, and nuclei with different Z and with different types of transitions were studied. A considerable part of this work has been carried out with an accuracy not exceeding 15%. The majority of the results of the remaining articles (for example, references 10 — 17) which have higher accuracy happens to fall approximately in the range of values $(0.9-1.0)$ v/c.

An opinion that has been expressed most frequently is that the observed deviations of the effect from v/c are most likely due to systematic experimental errors, and that as experiments become more refined it will be shown that the polarization of electrons emitted by different nuclei is the same, and is equal to v/c (except for special cases of which RaE can be taken as an example). However, at present several authors claim an accuracy of 3 — 5% for their measurements and, moreover, while the value $P = -(1.0 \pm 3\%)$ v/c has been obtained[12] in the case of P^{32}, the ratio of electron polarizations for Au^{198} and Co^{60} has turned out[13] to be equal to $0.87 \pm 5\%$.

In the present work we have taken for our main aim the task of obtaining with the highest possible degree of precision an answer at least to the question of whether the polarization of electrons from β decay of different nuclei is different. The accuracy of the relative measurements attained by us has turned out to be sufficient to demonstrate that such differences actually do occur both in cases of allowed transitions in P^{32} and In^{114}, and also in the Coulomb transitions in Au^{198}, Lu^{177}, Sm^{153}, as well as in Ho^{166}. With respect to the deviations of the polarization from the value v/c, a discussion is given of the accuracy of the absolute measurements which have also been carried out.

1. METHOD

The method of Mott scattering has been utilized in the present investigation: with the aid of crossed electric and magnetic fields the longitudinal polarization was transformed into a transverse one, and the latter was measured by measuring the scattering asymmetry.

In this case the polarization P is related to the scattering asymmetry Δ by the following expression

$$\frac{P}{\beta} = \frac{\Delta}{\beta S}, \qquad \Delta = \frac{I_1/I_2 - 1}{I_1/I_2 + 1},$$

where I_1 and I_2 are the "right" and "left" scattering intensities, and S is a function of angle and of energy. With an optimum choice of the energy (300 — 500 kev), of the angle of observation of the scattered electron (110 — 140°) and of the scatterer thickness (several tenths mg/cm^2), the ratio of the scattering intensities is $I_1/I_2 \sim 1.6$.

The relatively large value of the scattering asymmetry makes this method more attractive compared to others. However, even in this case a measurement of the polarization with high pre-

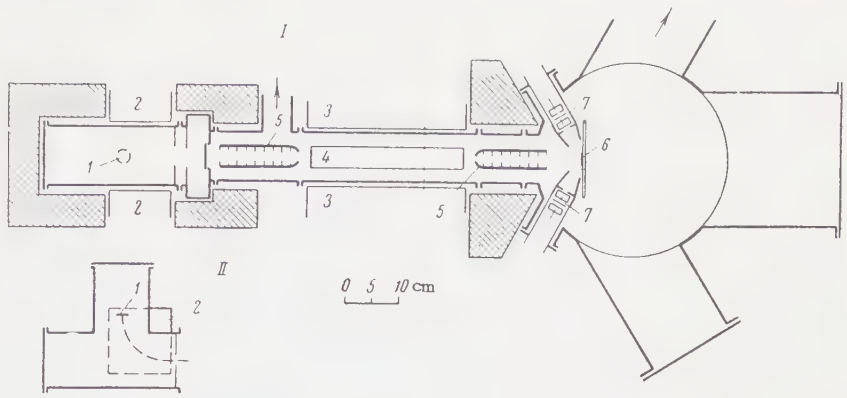

FIG. 1. Schematic diagram of the apparatus: I – horizontal cross section, II – vertical cross section of the chamber containing the source. 1 – source, 2 – magnet poles of the preliminary analyzer, 3 – magnet poles of the crossed fields system, 4 – capacitor plates of the crossed fields system, 5 – magnetic guides with diaphragm, 6 – scatterer, 7 – counters.

cision, for example, ±3%, is a very difficult problem. Indeed, the accuracy of the results is limited primarily by systematic error: lack of precise knowledge of the asymmetry of the apparatus, of multiple scattering, of depolarization in the source, and of other factors. At the same time, in order to determine all these quantities it is necessary to carry out repreated measurements of the scattering asymmetry, the relative error in the magnitude of which is approximately equal to double the error in the ratio of the scattering intensities I_1 and I_2 for $I_1/I_2 = 1.6$.

In other known methods the required accuracy of measurement is even higher, due to the smaller difference in the readings of the indicators of polarized or unpolarized electrons.

However, relative measurements can be carried out with greater accuracy if the depolarization in the source is small, and the energy and the angular distributions of the electrons incident on the scatterer do not depend on what source is being investigated. In this case the uncertainties in the numerous corrections, which enter into the absolute measurements, become negligibly small if the ratio of the polarizations is evaluated.

2. PRINCIPAL CHARACTERISTICS OF THE EXPERIMENTAL ARRANGEMENTS AND CONTROL EXPERIMENTS

1. Description of the Apparatus. A schematic diagram of the apparatus is given in Fig. 1. The β emitters were situated at a distance of approximately 10 cm above the axis of the apparatus in the position shown in the figure. Electrons that were rotated by a transverse magnetic field through an angle ~90°, passed through a collimator enclosed in an iron tube – a magnetic guide – and entered the region of the crossed fields. Then the transversely polarized electron beam again passed through the magnetic guide containing the collimator and fell on the scatterer. The scattered electrons were recorded by counters whose axes were placed at an angle of 120° with respect to the direction of the electron beam. Each of the counters consisted of two counters placed behind one another and connected in coincidence. Between them there was a filter of thickness ~25 mg/cm^2. The bodies of the counters were made of Plexiglas rings (10 – 12 mm high and 20 and 25 mm in diameter), coated with a conducting graphite layer. The working volume of the counters was separated from vacuum by a thin film of thickness ~0.3 mg/cm^2. The sources and the scatterers were placed in an exactly specified position, and they could be changed without breaking the high vacuum.

2. Calibration of the System of Crossed Fields. The values of the magnetic field H and of the electric field E required to rotate the spin of electrons of momentum p and of speed β through an angle φ were obtained from the following relations

$$\varphi = eHL\sqrt{1-\beta^2}/pc, \qquad E = \beta H,$$

where L is the length of the region of the crossed fields (~300 mm). The device which determined the magnitude of the potential difference between the plates was calibrated by using known values of the magnetic field and of the energy of conversion electrons passing through the crossed fields (we utilized the 187-kev line of In^{114}). The magnitude of the applied fields corresponded to a rotation of the spin by 90°. Therefore, a relatively large error in specifying the angle of rotation of the spin which could be made as a result of an error in the determination of the effective length L of the crossed fields, should lead to no appreciable error in the measured value of the asymmetry. A control experiment in which the angle of rotation of the spin deviated from 90° by ±15° has shown that the choice of the value of the fields had indeed been made correctly: in both cases the asymmetry was reduced by 3 ± 2%.

3. Sources. All the β sources were deposited on an aluminum foil 6μ thick and had a diameter of 20 mm. All the sources made of Sm, Lu, Ho, and In were prepared from unactivated low dispersion powders of the oxides of these elements with the Sm and In sources being enriched in the Sm^{152} isotope (98%) and the In^{113} (75%) isotope. The layers were deposited by evaporating suspensions of these powders in alcohol to which a small quantity of bakelite was added. The layers obtained in this manner after being dried at a temperature of approximately 200°C were sufficiently firmly attached to the backing. The Au source was obtained by sputtering in vacuum. All the sources were hermetically sealed into aluminum containers and were irradiated in a reactor. The P^{32} source was prepared by repeated application and evaporation of an active nitrate solution. The thickness of the sources varied in the range $0.6 - 1.3$ mg/cm^2. The low aperture of the apparatus did not allow us to carry out measurements using sources of low specific activity. The most intense Sm source had an activity up to 3 C. The activity of the In source amounted to approximately 100 mC.

4. Electron Spectra. The energy spectrum of each source was carefully investigated to verify the absence within the selected range of energies of conversion lines whose appearance might be associated with an impurity due to foreign elements. Relative measurements of the polarization were carried out at an energy of 340 kev for all the sources (with the exception of gold). This energy was close to the maximum energy which we could select by crossed fields with the spin being rotated through 90°. The spectrum of electrons entering the region of crossed fields extended approximately from 240 to 440 kev. Figure 2 shows, as an example, the spectra for the In^{114} source. Due to a preliminary energy analysis the spectrum of the electrons incident on the scatterer did not depend on the shape of the source spectrum, and had a line shape standard for all the sources with a half-width of ~40 kev and with a relative intensity less than 1% outside the selected (340 ± 40) kev region. This enabled us to avoid corrections which would be difficult to estimate, and which would have arisen if sources having sharply different shapes of spectra were compared.

5. Elimination of Differences in Counter Efficiency. Measurements of the electron scattering asymmetry must take into account differences in counter efficiencies. The method of crossed fields enables us to eliminate easily the effect of counter

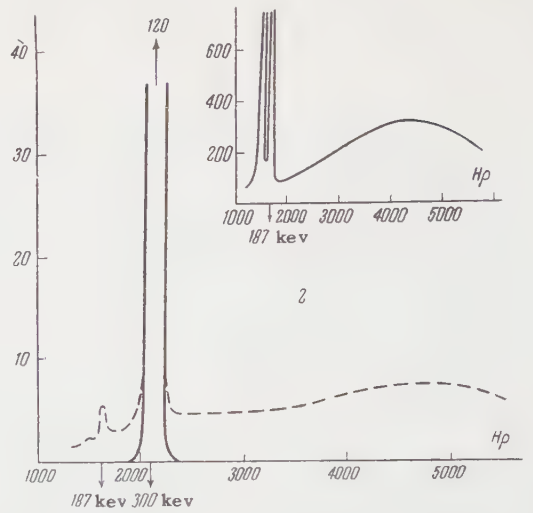

FIG. 2. Electron spectra. 1 – spectrum of electrons from In^{114}; 2 – spectrum of electrons from In^{114} which have passed through the crossed fields system: solid curve – including preliminary analysis with respect to energy, dotted curve – without preliminary analysis.

efficiency on the results obtained. If the signs of both the electric and the magnetic fields are reversed the spin of the electrons incident on the scatterer is flipped over from the "up" (↑) position into the "down" (↓) position. The ratio of the scattering intensities I_1/I_2, determined from the ratio

$$I_1 / I_2 = \sqrt{(J_l / J_r)\uparrow \cdot (J_l / J_r)\downarrow},$$

(where J_l and J_r are the counting rates of the left and the right counters) does not contain an coefficients characteristic of counter efficiency. Effects of slow variations in counter efficiency (which in the course of the experiment might attain values of 3 – 5%) were eliminated by carrying out many series of measurements with the signs of the fields alternately reversed.

6. Counter Background. The low sensitivity of the counter to γ rays, and good screening of the source and of the counters enabled us to obtain a low background level: 60 – 70 coincidences per hour. The magnitude of the background was determined primarily by cosmic rays and by radioactive contamination, and varied little even when the most intense sources were investigated. Owing to the use of preliminary analysis of electrons by the transverse magnetic field the scatterer could not be directly "seen" from the source, and therefore γ rays from the source could not reach the scatterer. Control experiments have shown that the magnitude of the background remains the same when measured by two different methods: a) the beam enters the chamber, the scatterer is removed, b) the scatterer is placed in position,

the direction of one of the fields is reversed, and the beam is not passed through.

The low background level made possible measurements with relatively weak sources and with thin scatterers, and to a certain extent compensated for the low aperture of the apparatus.

7. The Spread in the Experimental Results. In utilizing the method of transforming the longitudinal polarization of the electrons into a transverse one by means of crossed fields it is necessary to take precautions which will guarantee that the angular spread of electrons incident on the scatterer, and consequently the magnitude of the asymmetry introduced by the apparatus, will not depend on the position of the source and on the magnitude of the fields. One of the methods by means of which this can be attained is sufficiently strong collimation of the beam, and this was in fact used in the apparatus described. A sufficient degree of collimation of the beam, and the proper adjustment of the apparatus were achieved as a result of experiments in which we measured the dependence of the magnitude of the asymmetry on the position of the source, and on the deviations in the values of the fields from the prescribed values. These experiments were carried out using the most intense Sm^{153} source which enabled us to obtain the required statistical accuracy within a short time. As a result, a situation was achieved in which the magnitude of the asymmetry varied by not more than $1-1.5\%$ when the current in the magnet used for the preliminary analysis was varied by $\pm 15\%$, and remained constant within 1% when the field strengths of the crossed fields were changed by an amount which exceeded by a factor of several fold the possible error in determining them.

Carefully performed experiments have shown that the magnitude of the asymmetry is practically independent of the accuracy with which the source is placed in its operating position. For a sufficiently large displacement of the source a sharp decrease in the intensity of the beam reaching the scatterer occurred due to the strong collimation. But there was no noticeable accompanying change in the scattering asymmetry. As a result of the foregoing experiments on the investigation of the constancy of the asymmetry introduced by the apparatus, and of subsequent measurements in which the asymmetry in the scattering of electrons from Sm^{153} was compared with the asymmetry in the case of other sources, we could analyze approximately twenty measurements of the scattering asymmetry for β electrons from Sm^{153}, each of which had a statistical error of approximately 2%. This analysis has demonstrated the presence of a spread of non-statistical character whose maximum value was estimated as $\pm 1\%$.

8. Depolarization of Electrons in Sources. A determination of the amount of depolarization in sources was carried out in several control experiments. A comparison of Sm sources of thickness 0.8 and 0.2 mg/cm^2 and of Au sources of the same thickness showed no difference in the magnitude of the asymmetry within the accuracy of measurement ($\pm 2\%$). In subsequent experiments layers of gold, silver and aluminum of different thicknesses up to 10 mg/cm^2 were placed on a Sm source of thickness 0.8 mg/cm^2 (both from the backing side and from the active layer side). The observed decrease in asymmetry enabled us to obtain a more accurate estimate of the amount of depolarization in the sources which has turned out to be equal to

Source	Au	Sm	In	Lu	Ho	P
Thickness, mg/cm^2	0,8	0,9±0,2	1.6±0,3	0.9±0,2	0,8±0,2	1.8±0.3
Depolarization, %	1.7±0,5	1±0,5	1.2±0,5	1,3±0,5	1±0,5	0.8±0,5

9. Role Played by Electrons Scattered from the Walls of the Apparatus. In order to reduce the scattering of electrons the walls of the chambers in which the sources and the scatterer were placed were lined with Plexiglas the surface of which was covered with graphite and grounded. A number of control experiments has shown that scattering of electrons in the chamber in which the source was placed and scattering at the edges of the first diaphragms lead to a depolarization whose magnitude was estimated as 0.5%.

Considerably greater difficulties had to be overcome in order to reduce the role played by scattering by the walls of the chamber in which the counters and the scatterer were situated. Practically all the beam electrons passing through the gold layer reach the walls, and the probability of their entering the counters (either directly or through the scatterer) on being scattered from the walls is not as small as it appeared initially. For the data on the absolute values of the polarization, published by us earlier,[18] this effect had to be taken into account and a correction of $(3 \pm 1.5)\%$ had to be introduced. In the apparatus now being described the dimensions of the chamber were considerably enlarged: it was in the form of a cylinder of 350 mm diameter and approximately 400 mm high with deep traps situated opposite each of the counters in the path of the beam. In order to determine the role played by the scattering by the walls of this chamber under conditions close to those under which the

asymmetry was measured, a number of control experiments was performed. Experiments of very great sensitivity showed that as a result of the above effect corrections must be applied to the magnitude of the asymmetry: 0.4% due to the scattering from the walls of the chamber and 0.1% due to the scattering from the Plexiglas counter tips.

3. MEASUREMENTS AND RESULTS

1. Relative Measurements of Polarization. Relative measurements of polarization were obtained by comparing the magnitude of the scattering asymmetry for each of the sources investigated with the magnitude of the scattering asymmetry for Sm^{153}. The measurements were carried out using the same scatterer, the same energy and with the spin rotated by 90°. The results of the control experiments described earlier showed that the spectra of the electrons falling on the scatterer and the value of the asymmetry introduced by the apparatus are not altered when sources are changed. This allows us to assume that the comparison of the polarizations was carried out under strictly identical conditions.

From three to five series of measurements were carried out for each source at different times in the course of several months. Each series included measurements for the source under investigation with an accuracy of 2 or 3%, and measurements for Sm^{153} which were carried out at the beginning, in the middle, and at the end of the series. Table I gives relative values of the polarization obtained from the relation $P/P_{Sm} = \Delta/\Delta_{Sm}$.

Table I

Energy	340 kev					240 kev	
Isotope	Sm^{153}	P^{32}	In^{114}	Lu^{177}	Ho^{166}	Sm^{153}	Au^{198}
P_i/P_{Sm}	1	1.05	0.96	0.95	0.94	1	0.97
Error, %		±1.8	±3.2	±1.8	±1.8		±1.8

These ratios have been corrected for the differences in the value of the depolarization in the sources in accordance with the values given earlier. The errors in the ratios of polarizations obtained in this manner include: a) an error in the determination of Δ_{Sm}, equal to ±1%; b) an error in the value of Δ, equal to 1.5% in the case of Lu, Ho, P, and Au, and 2.5% in the case of In; c) an error in the relative values of the depolarization in the sources, equal ±0.5%. The quoted ratios of the polarizations do not require any corrections, since the corrections for the asymmetry due to the apparatus, for the depolarization of the electrons on the way from source to the scatterer, for the finite angle of observation of the scattered electrons, etc. are completely eliminated from the ratio of two values of polarization.

2. Absolute Measurements. Absolute measurements were carried out for one source — the most intense Sm^{153} source. These measurements were carried out for an electron energy of 300 kev. They consisted of determining the role played by multiple scattering in the scatterer, and the magnitude of the asymmetry due to the apparatus.

The asymmetry due to the apparatus was determined by means of experiments in which the gold scatterer was replaced by an aluminum scatterer. Since the angular distributions in the scattering by gold and by aluminum differ from one another it was necessary to achieve such conditions that the asymmetry due to the apparatus would be close to zero (as is shown later, in the final measurements its magnitude was 0.01).

Preliminary experiments showed that thick layers of aluminum (of the order of 5 mg/cm^2) are completely unsuitable for a correct measurement of the magnitude of the asymmetry due to the apparatus. Therefore, experiments were carried out in which the asymmetry due to the apparatus was varied artificially by an amount of approximately 5%, and these changes were monitored by means of a very thin (0.5 mg/cm^2) aluminum scatterer. Simultaneously the asymmetry due to the apparatus was also measured by means of thicker scatterers (2, 3, and 5 mg/cm^2). As a result of these experiments it was shown that a scatterer of thickness 2 mg/cm^2 can still correctly reproduce the variations in the asymmetry due to the apparatus, a measurement by means of a 3 mg/cm^2 scatterer already leads to a small error, while the results obtained with the aid of 0.5 mg/cm^2 and 5 mg/cm^2 scatterers differed by an amount ~0.1.

The observed effects are explained by the distortion of the angular distribution of the scattering due to multiple scattering of electrons in aluminum. This is confirmed by the fact that only for sufficiently thin layers does the intensity increase practically linearly with the thickness of the scatterer (the absolute values of the thickness were determined by weighing with an accuracy greater than 1%). For a scatterer of thickness 3 mg/cm^2, for which the distortions of the results of measuring the asymmetry due to the apparatus are already noticeable, the deviations from a linear dependence amount to ~15%.

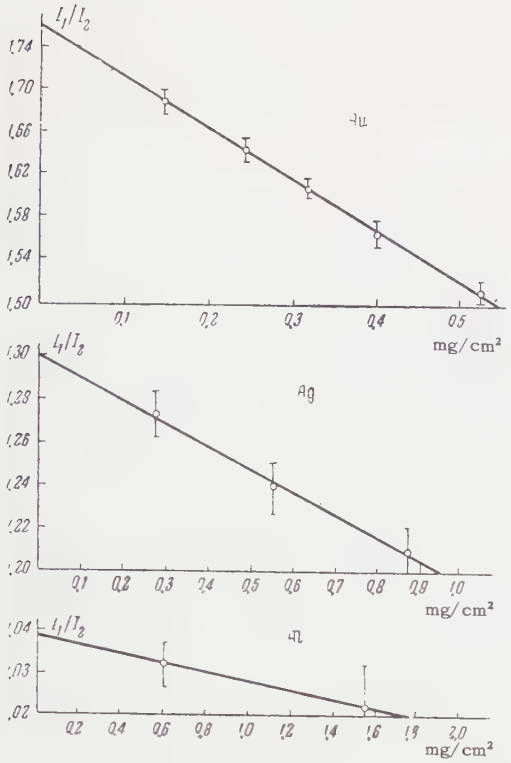

FIG. 3. Ratio of the "left-right" scattering intensities as a function of the thickness l of gold, silver, and aluminum scatterers.

In the case of gold scatterers the absolute values of the thickness could not be determined with a sufficiently high degree of accuracy by weighing. However, in order to achieve the correct extrapolation to zero it is necessary to know only the relative thickness of the layers. In order to obtain the relative thickness the intensities from different scatterers were compared with each other at the working energy (300 kev) and at a higher energy (500 kev). In the course of this those scatterers were identified for which the deviations from a linear increase in intensity are not yet very large.

In measuring the asymmetry we restricted ourselves to maximum thickness of scatterer equal to 1.6 mg/cm² in the case of aluminum, and to 0.5 mg/cm² for gold, for which the deviations described earlier do not exceed 8 — 10%.

Figure 3 shows the results of the measurements of the ratio of the intensities I_1/I_2 for gold, silver, and aluminum scatterers. The counting rates for the thinnest scatterers amounted to approximately 120, 60, and 30 counts per minute respectively for gold, silver, and aluminum. From the values of I_1 and I_2 we subtracted the background, the effect due to the film which was the scatterer backing, and the effect due to scattering by the walls of the chamber, which together did not exceed 2% of the values of I for the thinnest gold layer. The extrapolated values of I_1/I_2 and the corresponding values of the asymmetry Δ are given in Table II.

Table II

Scatterers	Au	Ag	Al
I_1/I_2	1.765 ± 0.8%	1.305 ± 1%	1.039 ± 0.8%
Δ	0.277 ± 1.6%	0.132 ± 5%	0.019 ± 20%
S for $\beta = 0.776$	0.427	0.208	0.038
$\Delta_T = \beta S$	0.331	0.161	0.0295

There we have also given the values of S for $\beta = 0.776$ and the value of $\beta S = \Delta_T$ taken from Sherman's tables.[19] The following corrections were applied to the values of the polarization obtained from the data of Table II.

for depolarization in the source: (1 ± 0.5)%
for depolarization along the path from the source to the scatterer: (2 ± 1)%
for the finite size of the scatterer, and for the spread in the angles of observation: (1.5 ± 0.5)%
for the error in the determination of the effective value of βS: 1%

In the final result the polarization of the electrons emitted in the β decay of Sm^{153} of energy 300 kev turned out to be equal to $-0.92\,\beta \pm 2.7\%$. The asymmetry due to the apparatus was not great in these measurements: − 0.01. The value of the asymmetry for a silver scatterer gives the same value of the polarization but with lower accuracy, specifically 6 — 7%.

Table III gives absolute values of the magnitude of the longitudinal polarization of the electrons

Table III

Isotope	Sm^{153}	P^{32}	In^{114}	Lu^{177}	Ho^{166}	Au^{198}
$-P/(v/c)$	0.92	0.97	0.88	0.87	0.86	0.89
Error, %	±2.7	±3.4	±4.2	±3.4	±3.4	±3.4

for the isotopes investigated which were obtained with the aid of the results of relative measurements. We recall in this connection that the relative measurements for Au^{198} were carried out at an energy of 240 kev, while in the case of all the other isotopes they were carried out at an energy of 340 kev.

4. DISCUSSION OF RESULTS

Results of relative measurements show that the polarizations of the electrons for the isotopes investigated are not the same. It is of interest to note that the polarizations for P^{32} and In^{114}, for which the transitions are allowed and are of the Gamow-Teller type, differ from each other by

approximately 10%. The results obtained for P^{32} and Au^{198} agree within experimental error with the results of references 12 and 13.

In spite of the fact that we attempted to determine in the most careful manner all the possible causes which might lead to an underestimate of the degree of polarization, it seems to us that the absolute values obtained by us cannot yet be regarded as finally established. First of all, it is necessary to check the correctness of the theoretical calculations of the function S which gives the relation between the scattering asymmetry and the degree of polarization. Unfortunately, experiments on double scattering of unpolarized electrons still do not give for the quantity S an accuracy higher than 10%. We intend to repeat these experiments in the near future for electrons of energy 200—300 kev. In doing this we also hope to check whether we have correctly estimated the magnitude of the depolarization along the path of the beam from the source to the scatterer in the apparatus utilized in the present work.

It is impossible to predict in advance the results of these experiments. If it should turn out that the corrections to the polarization are large and amount to 10%, then in this case the spread in the values of the polarization will be shifted into the range $(0.95-1.05)$ v/c. Then the deviations from the value of v/c would not exceed 5%, and this would apparently make it significantly easier to explain this effect by the influence of nuclear structure. However, if the true values of the polarization are close to those obtained in the present work, then it would be very interesting to carry out a measurement of the longitudinal polarization for the simplest nucleus T (for the neutron this is, apparently, practically impossible). These measurements could show whether the effect of nuclear structure is the only reason for the observed deviations, provided, of course, that it would be possible to show that in the case of T, just as in the case of the neutron,[20] one should expect very small deviations from v/c. We would like to express the wish that such quantitative calculations for T should be carried out.

The authors express their gratitude to V. I. Levin and his collaborators who prepared the P^{32} source, and to the crew of the RFT reactor who have carried out the irradiation of the sources over a long period.

[1] T. D. Lee and C. N. Yang, Phys. Rev. **104**, 254 (1956).

[2] Wu, Ambler, Hayward, Hoppes, and Hudson, Phys. Rev. **106**, 1361 (1957).

[3] L. D. Landau, JETP **32**, 405, 407 (1957), Soviet Phys. JETP **5**, 336, 337 (1957); Nuclear Phys. **3**, 127 (1957).

[4] T. D. Lee and C. N. Yang, Phys. Rev. **105**, 1671 (1957).

[5] A. Salam, Nuovo cimento **5**, 299 (1957).

[6] Frauenfelder, Bobone, von Goeler, Levine, Lewis, Peacock, Rossi, and de Pasquale, Phys. Rev. **106**, 386 (1957).

[7] Alikhanov, Eliseev and Lyubimov, JETP **34**, 785 (1958), Soviet Phys. JETP **7**, 541 (1958).

[8] Vishnevskiĭ, Grigor'ev, Ermakov, Nikitin, Pushkin, and Trebukhovskiĭ, Nuclear Phys. **4**, 271 (1957).

[9] Ya. A. Smorodinskiĭ, Usp. Fiz. Nauk **57**, 44 (1959).

[10] Geiger, Ewan, Graham, and Mackenzie, Phys. Rev. **112**, 1684 (1958).

[11] Alikhanov, Eliseev, and Lyubimov, JETP **34**, 1045 (1958), Soviet Phys. JETP **7**, 723 (1958); Nuclear Phys. **7**, 655 (1958).

[12] Ketelle, Brosi, Galonsky, and Willard, Bull. Am. Phys. Soc. **4**, 76 (1959).

[13] Turner, Gard, and Cavanagh, Bull. Am. Phys. Soc. **4**, 77 (1959).

[14] R. L. Gluerstern and V. W. Hughes, Bull. Am. Phys. Soc. **4**, 76 (1959).

[15] Bernardini, Brovertto, Ferrani, and Pasquarelly, Nuovo cimento, **14**, 787 (1959).

[16] U. Amaldi, Nuovo cimento **11**, 415 (1959).

[17] Cavanagh, Turner, Colemans, Gard, and Ridley, Phil. Mag. **2**, 1105 (1959).

[18] L. A. Mikaélyan and P. E. Spivak, JETP **37**, 1168 (1959), Soviet Phys. JETP **10**, 831 (1960).

[19] N. Sherman, Phys. Rev. **103**, 1601 (1956).

[20] Bilen'kiĭ, Ryndin, Smorodinskiĭ, and Hc Tso-Hsiu, JETP **37**, 1758 (1959), Soviet Phys. JETP **10**, 1241 (1960).

Translated by G. Volkoff
113

TWO-CASCADE GAMMA TRANSITIONS IN THE Nd^{144} *NUCLEUS, ACCOMPANYING THE CAPTURE OF THERMAL NEUTRONS*

V. R. BURMISTROV and V. P. RADCHENKO

Submitted to JETP editor April 26, 1960

J. Exptl. Theoret. Phys. (U.S.S.R.) **39**, 584-586 (September, 1960)

The γ radiation accompanying the capture of the thermal neutrons by the Nd^{143} nucleus was investigated by the sum-coincidence method[1] with scintillation counters. Four two-cascade γ transitions have been determined. An energy level scheme that includes the well-known 0.69-Mev level in the Nd^{144} nucleus is proposed. The corresponding states are identified by the relative cascade intensities.

THE γ radiation that accompanies the capture of thermal neutrons by a natural mixture of neodymium isotopes was investigated by the so-called sum-coincidence method.[1] This method consists of feeding the pulses from two counters in parallel to a coincidence circuit and to a linear pulse-adding circuit. If the pulses coincide in time and their sum corresponds to the energy of the nuclear level, from which the investigated two-cascade transition originates, then the pulses from one of the counters are let through for analysis. The scintillation counters used were NaI (Tl) crystals measuring 40 × 40 mm. The apparatus employed was the same as described earlier,[2] except that four crystals pairwise connected in parallel were used.

Neodymium in the form of oxide was placed in an aluminum cartridge weighing 0.26 g. Two targets with 0.74 and 0.42 g of oxide were used. Chemical analysis showed that the investigated substance contained 99.1% of neodymium oxide and 0.2% of oxides of other rare earths.

The greatest contribution to the absorption of thermal neutrons by a natural mixture of neodymium is made by Nd^{143}, and the capture is due to a single resonance with negative energy.[3] The binding energy of the neutron in the Nd^{144} nucleus, equal to 7.8 Mev,[4] is the highest among the binding energies of the other neodymium isotopes, so that the γ transitions are easier to identify.

In the investigation of the γ radiation that arises during the capture, the 'window' of the control channel was set to the binding energy of the neutron in the Nd^{144} nucleus, and the coincidence spectrum was investigated in the analyzed channel. Figure 1 shows a sample of a neodymium γ spectrum, obtained by the sum-coincidence method with the window of the control channel set to 7.8 Mev; the width of the window is 0.55 Mev. A similar spectrum is obtained in a pulse analyzer in a single step. In order to investigate the unresolved region of energies below 1 Mev, the gain of the analyzed channel is increased and additional measurements are made. The spectrum given here is the average of four measurements, each lasting approximately 12 hours. The figure shows also the random-coincidence spectrum, obtained by introducing a delay of 6×10^{-7} sec in one of the channels of the coincidence circuit ($\pi = 0.8 \times 10^{-7}$ sec).

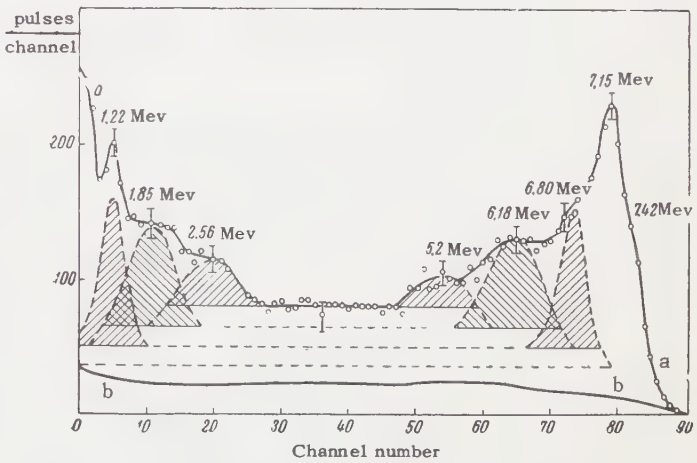

FIG. 1. a – Coincidence spectrum of captured γ radiadiation of Nd^{144}, occurring when the capture is in the energy range 1–8 Mev (rms errors); b – spectrum of random coincidences under the same conditions.

The dotted lines in Fig. 1 shows the resolution of the spectrum into components. In determining the relative intensities, we started out with the shaded areas and used formula (3) of the paper by Hoogenboom.[1] We calculated here the efficiency of registration of γ rays of corresponding energies, as well as the photo contribution of the crys-

stals, determined experimentally up to 2.76 Mev and extrapolated to higher energies.

In the resolution of the γ spectrum into components, we were guided by the fact that each pair of peaks corresponding to the two-cascade transition is accompanied by a more or less uniform momentum distribution between the peaks. The entire spectrum we obtained consisted essentially of four cascades of approximately equal intensity. Therefore the area under the flat part of the spectrum between 3 and 5 Mev (after subtracting the random coincidences) was cut in four horizontal parts of equal thickness. There is no need for a more exact subdivision in our case. Each of these parts was assumed to be the pulse distribution between a pair of corresponding peaks. Then, starting with the internal pair of peaks at 2.56 and 5.2 Mev, we plotted the distributions of the pulses for all pairs of peaks.

As the result of such an analysis of the γ spectrum, obtained by the coincidence method, we determined the following two-cascade transitions with a total energy of about 7.81 Mev (all the energies are in Mev): $(7.42 \pm 0.07) - (0.48 \pm 0.02)$, $(7.15 \pm 0.10) - (0.69 \pm 0.03)$, $(6.80 \pm 0.10) - (1.22 \pm 0.03)$, $(6.18 \pm 0.15) - (1.85 \pm 0.12)$, and $(5.2 \pm 0.15) - (2.56 \pm 0.15)$. The coincidence spectrum contains also a peak of energy (0.34 ± 0.02) Mev, which should be supplemented by a (7.57 ± 0.18)-Mev peak, which is not observed, however, possibly because of the insufficient resolution of the apparatus. The intensities of the aforementioned γ ray cascades are related as 0.3: 0.8: 1: 1.4: 1.1: 0.1, respectively. The error in the determination of the relative intensities, amounts to 40%.

The $7.42 - 0.48$ Mev and $7.57 - 0.34$ Mev cascade transitions do not belong to Nd^{144}, for on changing the width of the control channel (i.e., on changing the width of the energy region responsible for the transitions) the relative intensities of these cascades change whereas all other cascades remain constant, within the accuracy limits of the experiment. It is possible that the observed $7.42 - 0.48$ Mev cascade is due in fact to the $7.0 - 0.46$ Mev cascade of Nd^{146} and appears because the (7.48 ± 0.18) Mev binding energy of the neutron in Nd^{146} (reference 5) is close to the investigated energy (7.81 Mev) of Nd^{144}. The cascade in which the 0.34-Mev γ line participates is possibly due to the γ transitions of Sm^{150} through the 0.337-Mev energy level. The samarium content of the investigated substance was not measured but its presence among the rare-earth oxides is not excluded.

Assuming that in all the observed cascades a high-energy γ quantum, is emitted ahead of a low-energy one, we have constructed a scheme for the γ transitions of Nd^{144}. The proposed scheme of transitions and levels is shown in Fig. 2.

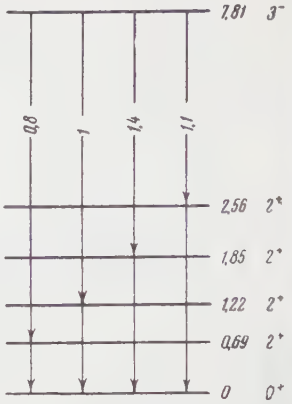

FIG. 2. Proposed scheme of levels and two-cascade γ transitions of Nd^{144}. The numbers on the arrows indicate the relative intensities (the energies of the corresponding levels are in Mev).

Starting with the fact that the relative intensities of the cascades are close to each other, we assume that all the γ-ray cascades have a similar character. The spin and parity of the initial state of Nd^{144}, formed after capture of thermal neutrons, have been determined as 3^- (reference 4), and the characteristics of the 0.69-Mev level are known to be 2^+, so that the transition between these states will be of type E1, while the 0.69-Mev transition to the ground state will be of type E2. Analogously, all the remaining two-cascade transitions from the initial state, shown in the figure, should also be of the E1 → E2 type, so that the states of all the intermediate levels are uniquely determined as 2^+. It is natural to assume that all these levels are identical in nature.

A few words concerning the levels 1.22 and 1.85. Firsov and Bashilov[6] have noted a $1.1 - 1.7$ Mev γ-ray cascade accompanying the β decay of Pr^{144}. We have also indicated[2] the possibility of a cascade of γ rays with close energies, namely $1.2 - 1.8$ Mev. Searches for these cascades by Porter and Day[7] were not successful. As can be seen from the present investigation, 1.22 and 1.85 Mev levels appear in Nd^{144}, and these may be responsible for the possible $1.2 - 1.8$ or $1.8 - 1.2$ Mev cascade from the ~3-Mev level in the β decay of Pr^{144}.

Note added in proof (August 4, 1960). It is possible that the 6.8–1.2 Mev cascade is partly due to an impurity of gadolinium in the investigated material, since a similar two-cascade transition was observed in gadolinium, as indicated in a paper by Bartholomew, Campion, and Knowles, presented to the Second All-Union Conference on Nuclear Reactions (Moscow, 1960).

[1] A. M. Hoogenboom, Nucl. Instr. **3**, 57 (1958).
[2] V. R. Burmistrov, Izv. Akad. Nauk SSSR, Ser. Fiz. **23**, 898 (1959), Columbia Tech. Transl. p. 886.
[3] H. J. Hay, J. Nucl. Energy **7**, 199 (1958).
[4] Campion, Knowles, and Bartholomew, Bull. Am. Phys. Soc. **4**, 247 (1959).
[5] W. H. Johnson and A. O. Nier, Phys. Rev. **105**, 1014 (1957).
[6] E. I. Firsov and A. A. Bashilov, Izv. Akad. Nauk SSSR, Ser. Fiz. **21**, 1633 (1957), Columbia Tech. Transl. p. 1619.
[7] E. T. Porter and P. P. Day, Phys. Rev. **114**, 1286 (1959).

Translated by J. G. Adashko
114

LONGITUDINAL POLARIZATION OF β ELECTRONS FROM Au^{198}

A. I. ALIKHANOV, G. P. ELISEEV, and V. A. LYUBIMOV

Submitted to JETP editor April 30, 1960

J. Exptl. Theoret. Phys. (U.S.S.R.) 39, 587-588 (September, 1960)

The ratio of the polarization of electrons from Au^{198} and Tm^{170} has been measured for energies of 145 kev and 390 kev. This ratio is equal to 0.8 ± 0.05 at 145 kev; a value 1.07 ± 0.08 has been obtained at 390 kev.

MEASUREMENTS of the longitudinal polarization of β electrons from different elements carried out during the last few years show that in a region in which the β-electron energies are not too low the longitudinal polarization is close to $-v/c$ for all elements investigated. An exception is RaE, for which a deviation from the above value[1,2] of the longitudinal polarization was expected, in view of the fact that its β spectrum differs from the Fermi shape. This deviation was observed shortly afterwards and studied in detail in several experiments.

In the case of Au^{198}, some authors observed complete polarization of electrons ($P = -v/c$ chiefly at medium and high energies,[3,4] and other authors, a considerably smaller polarization, at medium and low energies.[5] We have repeatedly obtained (in reference 4 and earlier) values appreciably less than $-v/c$ for the polarization of low-energy electrons from Au^{198}. But since the apparatus employed was not sufficiently adapted to the strong γ background accompanying the Au^{198} β decay, we were obliged to restrict the measurement of the polarization of electrons from Au^{198} only to energies higher than the maximum energy of the electrons efficiently generated in the apparatus by γ rays from the source. Otherwise, it would have been very difficult in principle to take into account the distortion of the results by the electron background from γ rays.

In the present work, in order to determine the value of the polarization of low-energy electrons from Au^{198}, we used an apparatus constructed on the same principle as that in reference 4, but considerably improved and adapted to work with β sources having a strong γ background.

The polarization was measured in two energy regions — in the low-energy region (145 kev) of interest to us and, for comparison, in the high-energy region (390 kev), where, according to our previous measurements,[4] the polarization is equal to $-v/c$.

The measurements were carried out by the relative method used earlier.[2] Identical samples of Au^{198} and Tm^{170} served, in turn, as the source in the apparatus. The corrections which had to be applied to the measured values were mainly the same for Au^{198} and Tm^{170} samples. Therefore, they compensated each other and were practically eliminated from the relative value of the longitudinal polarization of electrons from Au^{198}.

For β electrons from Au^{198} with mean energy of 145 kev (interval width about ±60 kev), the value of the longitudinal polarization relative to Tm^{170} was $P_{Au}/P_{Tm} = 0.80 \pm 0.05$. In this value, the azimuthal asymmetry of Au^{198} was increased by + 1.8% to compensate for the action of 76, 126, 145, 147 kev unpolarized conversion electrons emitted by Au^{199}, which is formed during the preparation of the source in the reactor from Au^{197} through Au^{198} as a result of the capture of two neutrons.[6] The amount of Au^{199} was determined by a calculation based on the irradiation time of the Au^{197} sample in the reactor, the thermal neutron flux density, and the respective capture cross sections.

The relative longitudinal polarization of 390 kev electrons (interval width of the order of ±100 kev) from Au^{198} turned out to be $P_{Au}/P_{Tm} = 1.07 \pm 0.08$, in agreement with the previous measurements. Here, a correction of + 8% was introduced into the azimuthal asymmetry of Au^{198} in connection with the presence of conversion electrons from the 411-kev γ line of Au^{198}. The contamination from internal conversion electrons in the stream of β electrons which experienced scattering by 90° on the scatterer—transformer was determined by direct measurement on a β spectrometer.

Recent measurements of Spivak and Mikaélyan[7] gave for 240-kev electrons from Au^{198} a polarization equal to $-(0.89 \pm 0.025)\ v/c$.

Analysis of the possible reasons for the devia-

tion of the value of the longitudinal polarization of Au^{198} from $-v/c$ was given by Geshkenbeĭn and Rudik.[8] They showed that in heavy nuclei, one should expect, for the first-forbidden transitions in the β spectrum regions which differ from the Fermi shape, a deviation of the value of the longitudinal polarization of electrons from $-v/c$, since the shape of the β spectrum and the value of the longitudinal polarization are determined by the same combinations of the same parameters. The β-electron spectrum of Au^{198}, according to the data presented in the survey in reference 9, has a Fermi shape for electrons of energy greater than 300 kev and appreciably differs from a Fermi shape for electrons of lower energy.

[1] Alikhanov, Eliseev, and Lyubimov, JETP **35**, 1061 (1958), Soviet Phys. JETP **8**, 740 (1959).

[2] Alikhanov, Eliseev, and Lyubimov, Nuclear Phys. **13**, 541 (1959).

[3] Benczer-Koller, Schwarzschild, Vise, and Wu, Phys. Rev. **109**, 85 (1958); Lipkin, Cuperman, Rothen, and de-Shalit, Phys. Rev. 109, 223 (1958); Geiger, Ewan, Graham, and Mackenzie, Bull. Am. Phys. Soc. **3**, 51 (1958).

[4] Alikhanov, Eliseev, and Lyubimov, JETP **34**, 1045 (1958), Soviet Phys. JETP 7, 723 (1958).

[5] Vishnevskiĭ, Grigor'ev, Ergakov, Nikitin, Pushkin, and Trebukhovskiĭ, Сб. Ядерные реакции при малых и средних энергиях (Collection: Nuclear Reactions at Low and Medium Energies), U.S.S.R. Acad. Sci. Press 1958, p. 363; Turner, Gard, and Cavanaugh, Bull. Am. Phys. Soc. 4, 77 (1959).

[6] R. D. Hill and J. W. Mihelich, Phys. Rev. 79, 275 (1950).

[7] P. E. Spivak and L. A.Mikaélyan, Материалы X Ежегодного совещания по ядерной спектроскопии (Materials of the Tenth Annual Conference on Nuclear Spectroscopy) Moscow, 1960; JETP **39**, 574 (1960), Soviet Phys. JETP **12**, 000 (1961).

[8] B. V. Geshkenbeĭn and A. P. Rudik, JETP **38**, 1894 (1960), Soviet Phys. JETP **11**, 1361 (1960).

[9] R. M. Steffen, Proc. Rehovoth Conf. Nucl. Structure, 1957, North-Holland Publishing Co., Amsterdam, 1958, p. 426.

Translated by E. Marquit
115

ELECTROMAGNETIC SCATTERING OF PARTICLES OF SPIN ½

L. G. MOROZ

Physics Institute, Academy of Sciences, Belorussian S.S.R.

Submitted to JETP editor November 2, 1959

J. Exptl. Theoret. Phys. (U.S.S.R.) **39**, 589-590 (September, 1960)

A general formula has been obtained for the electromagnetic scattering of two different longitudinally polarized particles of spin ½.

ONE of the consequences of parity nonconservation in weak interactions is the longitudinal polarization of the fermions produced in the process, in particular of μ mesons formed in the decay of π mesons. Therefore, it is useful to generalize Nikishov's formula[1] for the cross section for the scattering of a μ meson by a nucleon to the case of longitudinally polarized particles.

The calculation has been carried out on the basis of the scattering matrix including the Pauli interaction,[2] taking the internal structure of the particles into account by means of the form-factors $F_\mu(k^2)$, $l_\mu(k^2)$ and $F_N(k^2)$, $l_N(k^2)$, for the meson and the nucleon respectively (k is the transferred momentum). The square of the matrix element containing the initial spin states of definite polarization and summed over the final states was found by means of the method of projection operators.[2,3] The calculations were carried out in the laboratory system, and because of this the spin projection operator of the incident meson was taken for the spin projection operator of the nucleon at rest.

As a result of this calculation the following expression was obtained for the differential scattering cross section

$$\frac{d\sigma}{d\Omega} = \frac{e^4 \rho}{(2\pi)^2 v_{rel}} \{|\mathfrak{M}|^2 \pm |R|^2\}.$$

In this expression

$$e^2/4\pi = 1/137, \quad v_{rel} = |\mathbf{p}_0|/E_0,$$

$$\rho = \mathbf{p}_\mu^2 WE/[|\mathbf{p}_\mu|(M+E_0) - E|\mathbf{p}_0|\cos\vartheta],$$

the + and − signs refer to the case of parallel and antiparallel spins respectively; $|\mathfrak{M}|^2$ is the square of the matrix element for the scattering of unpolarized particles which coincides with the expression obtained by Nikishov[1] if we take it in the laboratory system and assume that $\Phi = l/2$, while $|R|^2$ has the following form

$$|R|^2 = \frac{1}{MWE_0Ek^4}\Big\{F_\mu^2\left[\tfrac{1}{4}F_N^2\left(\tfrac{1}{2}k^4 + 2ME_0\mathbf{p}_\mu^2\sin^2\vartheta\right) + l_N F_N M\left(\tfrac{1}{2}k^4 + ME_0\mathbf{p}_\mu^2\sin^2\vartheta\right) + \tfrac{1}{2}l_N^2 M^2 k^4\right]$$
$$+ \mu l_\mu F_\mu\left[F_N^2\left(\tfrac{1}{2}k^4 + ME_0\mathbf{p}_\mu^2\sin^2\vartheta\right) + l_N F_N M\left(4k^4 - k^2\mathbf{p}_\mu^2\sin^2\vartheta + 2ME_0\mathbf{p}_\mu^2\sin^2\vartheta\right) + l_N^2 M^2 k^2\left(2k^2 - \mathbf{p}_\mu^2\sin^2\vartheta\right)\right] + \tfrac{1}{2}\mu^2 l_\mu^2 k^4 (F_N + 2l_N M)^2\Big\},$$

where the notation of reference 1 has been used, i.e., M and μ are the nucleon and meson masses; E_0, $\mathbf{p}_0$ and E, $\mathbf{p}_\mu$ are the initial and final energy and momentum of the meson; W is the final nucleon energy.

In the case when the particles are point particles and the incident particle has no anomalous magnetic moment, i.e., for $F_\mu = F_N = 1$, $l_\mu = 0$ the expression for the differential cross section becomes simplified:

$$\frac{d\sigma}{d\Omega} = \frac{e^4}{(2\pi)^2}\frac{\rho}{v_{rel}MWE_0Ek^4}\{M(ME_0^2 - \tfrac{1}{2}E_0k^2 - \tfrac{1}{4}Mk^2)\times(1 + l_N^2k^2) + \tfrac{1}{4}k^2(\tfrac{1}{2}k^2 - \mu^2)(1 + 2l_NM^2) \pm \pm \tfrac{1}{2}[\tfrac{1}{4}k^2(1 + 2l_NM) + ME_0\mathbf{p}_\mu^2\sin^2\vartheta](1 + 2l_NM)\}.$$

After transition to the laboratory system the formula for the scattering of an electron by a proton given in Bincer's paper[4] assumes the same form.

In conclusion I express my gratitude to F. I. Fedorov for the method of calculation suggested by him.

[1] A. I. Nikishov, JETP **36**, 1604 (1959), Soviet Phys. JETP **9**, 1140 (1959).

[2] L. G. Moroz and F. I. Fedorov, JETP **39**, 293 (1960), Soviet Phys. JETP **12**, 209 (1961).

[4] A. Bincer, Phys. Rev. **107**, 1467 (1957).

Translated by G. Volkoff
116

*HIGHER BORN APPROXIMATIONS IN PAIR CONVERSION**

V. A. KRUTOV and V. G. GORSHKOV

Leningrad Physico-Technical Institute, Academy of Sciences, U.S.S.R.

Submitted to JETP editor March 1, 1960

J. Exptl. Theoret. Phys. (U.S.S.R.) **39**, 591-599 (September, 1960)

Higher Born approximations with respect to the nuclear Coulomb field are considered in pair creation processes. The integrals of the first Born approximation can be computed exactly and lead to a simple analytic result.

IN a number of quantum-mechanical problems one neglects the nuclear Coulomb field in the so-called Born approximation [we shall call this the zeroth Born approximation (z. B. a.)]. The computation of the higher approximations with respect to the Coulomb field is connected with considerable mathematical difficulties (see, for example, references 1 and 2). These difficulties are particularly great in the discussion of nuclear conversion with formation of electron-positron pairs,[2] so that up to now expressions for the probability of this process have only been obtained in the z. B. a.[3] At the same time, the calculations with exact wave functions in the field of the nucleus for the pair conversion are exceedingly cumbersome, so that it is very desirable to develop approximate methods.

In the present paper we consider the higher Born approximations. As the perturbing potential we choose a potential of the Yukawa type. In the final formulas the limit of a pure Coulomb potential is taken. In Sec. 1 we give the general expressions which can be applied to other problems (e.g., the photoeffect) besides the pair conversion. Section 2 is devoted to the discussion of the higher Born approximations for pair conversion. In Sec. 3 and the Appendices the calculations for the pair conversion are carried out to the end in the first Born approximation.

1. GENERAL RELATIONS

The matrix element describing quantum transitions of the electron (positron) due to the action of an electromagnetic field with frequency ω has the form (reference 4)†

$$S_{1\to 2} = -2\pi i e W \delta(E_2 - E_1 - \omega),$$
$$W = \int \overline{\Psi}_2(\mathbf{r}) B(\mathbf{r}) \Psi_1(\mathbf{r}) d^3r,$$
$$B = \gamma \mathbf{B} + \gamma_4 B_4, \qquad \gamma_j = -i\beta\alpha_j, \qquad \gamma_4 = \beta, \qquad \overline{\Psi} = \Psi^+\gamma_4, \tag{1}$$

where α_j, β are the Dirac matrices. $B(\mathbf{r})$ corresponds to the electromagnetic field, as for example, the photon (photoeffect, bremsstrahlung) or the potential of the nuclear current (conversion).

The functions Ψ_i in (1) are the wave functions of the free or bound electron (positron) in the static field of the nucleus. If we regard the latter as a perturbation for one or both of the functions Ψ_i and proceeding as in reference 4 (see Sec. 29), we obtain

$$\Psi_i(\mathbf{r}) = \sum_{k=0}^{\infty} \psi_i^{(k)}(\mathbf{r}),$$
$$\psi_i^{(k)}(\mathbf{r}) = -\frac{ie}{(2\pi)^3}\int d^3f e^{i\mathbf{f}\mathbf{r}} \frac{i\hat{f} - m}{f^2 + m^2 - i\varepsilon} \int d^3r' e^{-i\mathbf{f}\mathbf{r}'} A^{(e)}(\mathbf{r}') \psi_i^{(k-1)}(\mathbf{r}'),$$
$$\psi_i^{(0)}(\mathbf{r}) = u(\mathbf{p}_i) e^{i\mathbf{p}_i\mathbf{r}}. \tag{2}$$

For the field of the nucleus we take

$$A^{(e)}(\mathbf{r}) = A_4^{(e)}(\mathbf{r}) = -i\frac{eZe^{-\lambda r}}{4\pi r}. \tag{3}$$

In the momentum representation these formulas take the form

$$\Psi(\mathbf{r}) = \int \varphi(\mathbf{f}) e^{i\mathbf{f}\mathbf{r}} d^3f, \tag{4a}$$
$$\varphi(\mathbf{f}) = \left\{\sum_{n=0}^{\infty} \beta^n \varphi^{(n)}(\mathbf{f})\right\} u(\mathbf{p}), \qquad \beta = \frac{\alpha Z}{2\pi^2}, \tag{4b}$$
$$\varphi^{(n)}(\mathbf{f}) = \frac{m - i\hat{f}}{f^2 + m^2 - i\varepsilon} \int \frac{\gamma_4}{(\mathbf{f} - \mathbf{s})^2 + \lambda^2} \varphi^{(n-1)}(\mathbf{s}) d^3s,$$
$$f^0 = E, \qquad \varphi^0(\mathbf{f}) = \delta(\mathbf{f} - \mathbf{p}). \tag{4c}$$

The matrix element (1) is in the momentum representation

$$W = i\int d^3f_1 d^3f_2 \bar{\varphi}_2(\mathbf{f}_2) \hat{b}(\mathbf{f}_2 - \mathbf{f}_1) \varphi_1(\mathbf{f}_1), \tag{5}$$

*This paper was presented at the Ninth All-Union Conference on Nuclear Spectroscopy (Khar'kov, January 1959).

†If not noted otherwise, the notation is the same as in the book of Akhiezer and Berestetskii.[4] Heaviside units are used throughout.

where

$$b(\mathbf{k}) = -i\int e^{-i\mathbf{kr}} B(\mathbf{r})\, d^3r.$$

Using (4c), we can write W in the form

$$W = i\bar{u}(p_2)\, w u(\mathbf{p}_1), \tag{6a}$$

$$w = w(0\,|\,0) + \beta[w(0\,|\,1) + w(1\,|\,0)] + \beta^2[w(0\,|\,2) + w(1\,|\,1) + w(2\,|\,0)] + \ldots, \tag{6b}$$

$$w(k\,|\,n) = \int d^3f_1 d^3f_2\, \bar{\varphi}_2^{(k)}(\mathbf{f}_2)\, \hat{b}(\mathbf{f}_2 - \mathbf{f}_1)\, \varphi_1^{(n)}(\mathbf{f}_1). \tag{6c}$$

2. PAIR CONVERSION

For the description of nuclear conversion processes with formation of pairs we must make the following changes in the expressions of Sec. 1:* $\mathbf{p}_1 \to -\mathbf{p}_1$, $\mathbf{f}_1 \to -\mathbf{f}_1$, $E_1 \to -E_1$, and $\hat{B}$ must be replaced by the singular multipole potentials $\hat{B}^{(\lambda)}_{lm}$. Using the explicit expressions for the $\hat{B}^{(\lambda)}_{lm}$ of reference 4, we obtain in the momentum representation

$$b^{(0)}_{lm}(\mathbf{k}) = J_l(k)\, \mathbf{Y}_{l,l,m}(\mathbf{k}/k)\, \boldsymbol{\gamma}, \tag{7a}$$

$$\hat{b}^{(1)}_{lm}(\mathbf{k}) = \frac{1}{\sqrt{l+1}}\left[\sqrt{2l+1}\, J_{l-1}(k)\, \mathbf{Y}_{l,l-1,m}(\mathbf{k}/k)\, \boldsymbol{\gamma} - i\sqrt{l}\, J_l(k)\, Y_{lm}(\mathbf{k}/k)\, \gamma_4\right], \tag{7b}$$

$$J_l(k) = -i\int G_l(\omega r)\, g_l^*(kr)\, r^2\, dr. \tag{8}$$

The spherical vectors $\mathbf{Y}_{l,l+\lambda,m}$ and the functions G_l and g_l, which are proportional to the spherical Hankel and Bessel functions, respectively, are defined in reference 4 (pp. 33 and 426).

The integral $J_l(k)$ will be discussed in Appendix B.

The expression for the differential conversion coefficient for pair creation is, of course, of the same form as in the z. B. a.:

$$d\beta_{l\lambda} = \frac{\alpha\omega}{4}\frac{d^3p_1 d^3p_2}{(2\pi)^6}\, \sigma\delta(E_2 + E_1 - \omega),$$

$$\sigma = \sum_{\mu_1\mu_2} |W^{(\lambda)}_{lm}|^2, \tag{9}$$

where the summation goes over the spin states of the electron and the positron.

Using (6), we obtain

$$\sigma = \frac{1}{E_1 E_2}\frac{1}{4}\,\mathrm{Sp}\,[w(i\hat{p}_1 + m)\bar{w}(i\hat{p}_2 - m)] = \frac{1}{E_1 E_2}\sum_{s=0}^{\infty}\beta^s \sigma_s, \tag{10a}$$

$$\sigma_s = \sum_{k+n+k'+n'=s} \sigma\begin{pmatrix} k & n \\ k' & n' \end{pmatrix}, \qquad \bar{w} = \gamma_4 w^+ \gamma_4, \tag{10b}$$

$$\sigma\begin{pmatrix} k & n \\ k' & n' \end{pmatrix} = \frac{1}{4}\,\mathrm{Sp}\,[w(k\,|\,n)(i\hat{p}_1 + m)\bar{w}(k'\,|\,n')(i\hat{p}_2 - m)]. \tag{10c}$$

*Below the index 1 will thus refer to the positron and the index 2 to the electron.

Using the properties of traces and the relation of charge conjugation

$$\varphi_1(\mathbf{f}) = \{C\bar{\varphi}_2^T(\mathbf{f})\}_{(2\rightleftarrows 1)}$$

[$(2\rightleftarrows 1)$ signifies the interchange of 1 and 2, the index T denotes the transpose, and C is the matrix of charge conjugation], we easily derive the following properties of the symbols (10c):

$$\sigma\begin{pmatrix} k & n \\ k' & n' \end{pmatrix} = \left[\sigma\begin{pmatrix} k' & n' \\ k & n \end{pmatrix}\right]^*, \quad \sigma\begin{pmatrix} k & n \\ k' & n' \end{pmatrix} = (-1)^s\, \sigma\begin{pmatrix} n & k \\ n' & k' \end{pmatrix}_{(2\rightleftarrows 1)},$$

$$s = n + n' + k + k'. \tag{11}$$

3. CALCULATION OF THE PROBABILITY OF CONVERSION WITH FORMATION OF PAIRS IN THE FIRST APPROXIMATION

In the present paper we restrict ourselves to the calculation of σ_1.* With the help of (11) we can write

$$\sigma_1 = 2\,\mathrm{Re}\,\sigma\begin{pmatrix} 1 & 0 \\ 0 & 0 \end{pmatrix} - (2\rightleftarrows 1),$$

$$\sigma\begin{pmatrix} 1 & 0 \\ 0 & 0 \end{pmatrix} = \frac{1}{4}\,\mathrm{Sp}\,[w(1\,|\,0)(i\hat{p}_1 + m)\bar{w}(0\,|\,0)(i\hat{p}_2 - m)],$$

$$w(1\,|\,0) = -\int d^3f_2\, \gamma_4 (i\hat{f}_2 - m)\, b^{(\lambda)}_{lm}(\mathbf{f}_2 + \mathbf{p}_1)/[(\mathbf{f}_2 - \mathbf{p}_2)^2 + \lambda^2](\mathbf{f}_2^2 - \mathbf{p}_2^2 - i\varepsilon),$$

$$\bar{w}(0\,|\,0) = \bar{\hat{b}}^{(\lambda)}_{lm}(\mathbf{p}_1 + \mathbf{p}_2) = -\hat{b}^{(\lambda)*}_{lm}(\mathbf{p}_1 + \mathbf{p}_2). \tag{12}$$

Here we have used the identity

$$f_2^2 + m^2 = \mathbf{f}_2^2 + m^2 - E_2^2 = \mathbf{f}_2^2 - \mathbf{p}_2^2.$$

To simplify the subsequent calculations we introduce the following notation:

$$\mathbf{p}_1 + \mathbf{p}_2 = \mathbf{v}, \qquad \mathbf{f}_2 + \mathbf{p}_1 = \mathbf{k}, \qquad \mathbf{f}_2 - \mathbf{p}_2 = \mathbf{q} = \mathbf{k} - \mathbf{v},$$

$$\hat{b}_1 = \hat{b}^{(\lambda)}_{lm}(1\,|\,0) = \int d^3k \hat{b}^{(\lambda)}_{lm}(\mathbf{k})/(\mathbf{q}^2 + \lambda^2)(\mathbf{f}_2^2 - \mathbf{p}_2^2 - i\varepsilon),$$

$$\hat{b}_0 = \hat{b}^{(\lambda)}_{lm}(0\,|\,0) = \hat{b}^{(\lambda)}_{lm}(\mathbf{v}) \tag{13}$$

Then the expression for σ_1 has the form

$$\sigma_1 = 2\mathrm{Re}\,[\tfrac{1}{4}\,\mathrm{Sp}\,\{\gamma_4(i\hat{f}_2 - m)\hat{b}_1(i\hat{p}_1 + m)\hat{b}_0^*(i\hat{p}_2 - m)\}] - (2\rightleftarrows 1). \tag{14}$$

It should be recalled that b_1 is an integral operator which acts on functions of $\mathbf{k}$ both to the left and to the right.

First we calculate the traces and then the integrals, because in this case the expressions for the integrals assume a simpler form.

Let us rewrite (14) in the form

*The calculation of the correction $\sim(\alpha Z)^2$ will be published in a later paper.

$$\sigma_1 = 2\mathrm{Re}\,[\tfrac{1}{4}\,\mathrm{Sp}\,\{\hat{b}_1(i\hat{p}_1+m)\hat{b}_0^*(i\hat{p}_2-m)\gamma_4(i\hat{f}_2-m)\}] - (2\rightleftarrows 1). \quad (15)$$

Using the notation (13), we obtain

$$(i\hat{p}_2-m)\gamma_4(i\hat{f}_2-m) = -2E_2(i\hat{p}_2-m) + (i\hat{p}_2-m)\gamma_4 i\hat{q}. \quad (16)$$

We now split σ_1 into two parts, one containing $\mathbf{q}$, the other not containing $\mathbf{q}$:

$$\sigma_1 = \sigma_1(0) + \sigma_1(\mathbf{q}),$$

$$\sigma_1(0) = \{-4E_2\,\mathrm{Re}\,\tfrac{1}{4}\,\mathrm{Sp}\,[\hat{b}_1(i\hat{p}_1+m)\hat{b}_0^*(i\hat{p}_2-m)]\} - (2\rightleftarrows 1),$$

$$\sigma_1(\mathbf{q}) = 2\mathrm{Re}\,\tfrac{1}{4}\,\mathrm{Sp}\,\{\hat{b}_1(i\hat{p}_1+m)\hat{b}_0^*(i\hat{p}_2-m)\gamma_4 i\hat{q}\} - (2\rightleftarrows 1).$$

After evaluating the traces we find

$$\sigma_1(0) = 4E_2\,\mathrm{Re}\,\{(m^2+E_1E_2-\mathbf{p}_1\mathbf{p}_2)(b_1b_0^*) + (b_1p_1)(b_0^*p_2) + (b_1p_2)(b_0^*p_1)\} - (2\rightleftarrows 1),$$

$$\begin{aligned}\sigma_1(\mathbf{q}) = 2\mathrm{Re}\,\{&(\mathbf{b}_1\mathbf{q})[E_1(b_0^*p_2) + E_2(b_0^*p_1) - (m^2+E_1E_2-\mathbf{p}_1\mathbf{p}_2)b_0^*] \\ &+ (b_1b_0^*)[E_1(\mathbf{p}_2\mathbf{q}) - E_2(\mathbf{p}_1\mathbf{q})] + (b_1p_1)[E_2(\mathbf{b}_0^*\mathbf{q}) - b_0^*(\mathbf{p}_2\mathbf{q})] + (b_1p_2)[b_0^*(\mathbf{p}_1\mathbf{q}) \\ &- E_1(\mathbf{b}_0^*\mathbf{q})] - b_1[(p_1b_0^*)(\mathbf{p}_2\mathbf{q}) + (\mathbf{p}_1\mathbf{q})(p_2b_0^*) + (m^2+E_1E_2-\mathbf{p}_1\mathbf{p}_2)(\mathbf{b}_0^*\mathbf{q})]\} - (2\rightleftarrows 1). \end{aligned} \quad (17)$$

Using the definitions of b_0 and b_1 [formulas (13) and (7)], we average the scalar products of the spherical vectors and the products of the spherical harmonics in the numerators of the integrands over the magnetic quantum numbers. The averaged expressions must, of course, be invariant under spatial rotations, i.e., they must be expressed in terms of functions of scalar products of ordinary vectors. These invariants are calculated in Appendix A for all occurring combinations of spherical vectors of the electric or magnetic type. It follows from the formulas of Appendix A and (13) that the numerators of all integrals are proportional to functions of the form

$$(1, \mathbf{k})P_l\left(\frac{\mathbf{kv}}{kv}\right), \qquad (1, \mathbf{k})\frac{k_\alpha}{k}P_l'\left(\frac{\mathbf{kv}}{kv}\right),$$

$$(1, \mathbf{k})\frac{k_\alpha k_\beta}{k^2}P_l''\left(\frac{\mathbf{kv}}{kv}\right),$$

where P_l is the Legendre polynomial. The required real parts of these integrals are calculated in Appendix C.

It is seen from the final expressions (C.6) to (C.9) that the infinities arising in the limit of the pure Coulomb field drop out and that the result of the integration can be formally obtained in the following fashion: replace the integral sign by $\pi^3/2$, change the denominator of the integral (13) to p_2, and replace $\mathbf{k}$ by $\mathbf{v}$ everywhere in the remaining part of the function under the integral.

After the general proof of the necessity of performing these operations we can change the order of application and first perform the alterations in the expressions which formally correspond to the integration and then average over the magnetic quantum numbers.

Making the above-mentioned changes, we find that $\sigma_1(\mathbf{q}) = 0$.

For $\sigma_1(0)$ we obtain

$$\sigma_1(0) = 2\pi^2\cdot\pi(E_2/p_2 - E_1/p_1)\sigma_0,$$

$$\sigma_0 = \sigma\begin{pmatrix}0 & 0\\ 0 & 0\end{pmatrix} = (m^2+E_1E_2-\mathbf{p}_1\mathbf{p}_2)(b_0b_0^*) + (b_0p_1)(b_0^*p_2) + (b_0p_2)(b_0^*p_1). \quad (18)$$

Using (18), (10a), and (9), we have finally

$$d\beta_{l\lambda} = d\beta^0_{l\lambda}M(Z; E_1, E_2),$$

$$M(Z; E_1, E_2) = 1 - \pi\alpha Z(E_1/p_1 - E_2/p_2),$$

$$d\beta^0_{l\lambda} = \frac{\alpha\omega}{4}\frac{d^3p_1d^3p_2}{(2\pi)^6}\sigma_0\delta(E_2+E_1-\omega), \quad (19)$$

i.e., $d\beta^0_{l\lambda}$ is the differential conversion coefficient for pair formation in the z. B. a.*

The first Born approximation result is therefore obtained by multiplying the differential conversion coefficient for pair formation in the z. B. a. by the factor $M(Z; E_1, E_2)$.

Since $M(Z; E_1, E_2)$ is antisymmetric in the indices 1 and 2, the term proportional to αZ drops out in the integration over E_1 or E_2, i.e., it does not appear in the expressions for the angular distribution and the total conversion coefficient for pair formation. This is a consequence of the charge symmetry of the theory which requires that only even powers appear in the expansions of the total conversion coefficient for pair formation and of the angular distribution in powers of αZ.

The authors are grateful to B. S. Dzhelepov and L. A. Sliv for a discussion of the results of this paper and for valuable comments.

APPENDIX

A. FORMULAS FOR THE SCALARS FORMED OUT OF THE SPHERICAL VECTORS

To derive the formula for the probability we must write down the explicit covariant form of the

*Formula (19) is, of course, not valid near the limits of the energy spectrum, where the parameter $\alpha ZE/p$ is not small.

expressions*

$$S^{(1)}_{l\lambda}=\sum_{m=-l}^{l}(\mathbf{Y}_{l,l+\lambda,m}(\mathbf{k}/k)\ \mathbf{Y}^{*}_{l,l+\lambda,m}(\mathbf{v}/v)),$$

$$S^{(2)}_{l\lambda}=\sum_{m=-l}^{l}(\mathbf{p}\mathbf{Y}_{l,l+\lambda,m}(\mathbf{k}/k)(\mathbf{q}\mathbf{Y}_{l,l+\lambda,m}(\mathbf{v}/v))^{*},$$

$$S^{(3)}_{l}=\sum_{m=-l}^{l}Y_{lm}(\mathbf{k}/k)(\mathbf{q}\mathbf{Y}_{l,l-1,m}(\mathbf{v}/v))^{*}.$$

We are interested in the form of these expressions for $\lambda = 0$ and $\lambda = -1$.

Choosing the z axis in the direction of $\mathbf{v}$ and using the addition theorem for spherical functions, we obtain

$$S^{(1)}_{l,0}=\frac{2l+1}{4\pi}P_l\left(\frac{\mathbf{kv}}{kv}\right), \tag{A.1}$$

$$S^{(1)}_{l,-1}=\frac{2l+1}{2l-1}\frac{2l+1}{4\pi}P_l\left(\frac{\mathbf{kv}}{kv}\right). \tag{A.2}$$

To derive the remaining formulas we make use of the covariant differential representation of the spherical vectors (see, for example, reference 4, p. 34):

$$\mathbf{Y}_{l,l,m}\left(\frac{\mathbf{k}}{k}\right)=\mathbf{Y}^{(0)}_{l,m}\left(\frac{\mathbf{k}}{k}\right)=\frac{1}{\sqrt{l(l+1)}}\mathbf{L}Y_{lm}\left(\frac{\mathbf{k}}{k}\right)$$
$$=\frac{-i}{\sqrt{l(l+1)}}[\mathbf{k}\times\nabla_k]Y_{lm}\left(\frac{\mathbf{k}}{k}\right),$$

$$\mathbf{Y}_{l,l-1,m}\left(\frac{\mathbf{k}}{k}\right)=\sqrt{\frac{l}{2l+1}}\ \mathbf{Y}^{(-1)}_{lm}+\sqrt{\frac{l+1}{2l+1}}\ \mathbf{Y}^{(1)}_{lm}$$
$$=\frac{1}{k\sqrt{2l+1}}\left\{\sqrt{l}\,\mathbf{k}-\frac{1}{\sqrt{l}}[\mathbf{k}\times[\mathbf{k}\times\nabla_k]]\right\}Y_{lm}\left(\frac{\mathbf{k}}{k}\right).$$

After some transformations we then find

$$S^{(2)}_{l0}=\frac{2l+1}{4\pi l(l+1)}\left\{P'_l\frac{[\mathbf{p}\times\mathbf{k}][\mathbf{q}\times\mathbf{v}]}{kv}-P''_l\frac{([\mathbf{q}\times\mathbf{v}]\mathbf{k})([\mathbf{p}\times\mathbf{k}]\mathbf{v})}{k^2v^2}\right\}, \tag{A.3}$$

$$S^{(2)}_{l,-1}=\frac{1}{4\pi kv}\{lP_l(\mathbf{kp})(\mathbf{vq})+P'_l(kv)^{-1}\{(\mathbf{kp})([\mathbf{v}\times\mathbf{q}][\mathbf{v}\times\mathbf{k}])$$
$$+(\mathbf{vq})([\mathbf{k}\times\mathbf{p}][\mathbf{k}\times\mathbf{v}])+l^{-1}([[\mathbf{k}\times\mathbf{p}]\times\mathbf{k}][[\mathbf{v}\times\mathbf{q}]\times\mathbf{v}])\}$$
$$+l^{-1}P''_l(kv)^{-2}([\mathbf{k}\times\mathbf{p}][\mathbf{k}\times\mathbf{v}])([\mathbf{v}\times\mathbf{q}][\mathbf{v}\times\mathbf{k}])], \tag{A.4}$$

$$S^{(3)}_{l}=\frac{\sqrt{2l+1}}{4\pi v}\left\{\sqrt{l}\,P_l(\mathbf{qv})+\frac{1}{\sqrt{l}}P'_l\frac{[\mathbf{v}\times\mathbf{q}][\mathbf{v}\times\mathbf{k}]}{kv}\right\},$$
$$P^{(n)}_l\equiv P^{(n)}_l(\mathbf{kv}/kv). \tag{A.5}$$

B. CALCULATION OF THE INTEGRALS $J_l(k)$

To compute the integrals entering in the formula for the probability, we must know the singular points of the "radial" part of the Fourier transform of the nuclear potential $J_l(k)$.

*The first and second sums were computed by Berestetskiĭ, Dolginov, and Ter-Martirosyan[5] for the particular case $\mathbf{k} = \mathbf{v}$ and $\mathbf{p} = \mathbf{q}$.

By definition

$$J_l(k)=\frac{(2\pi)^3}{i\sqrt{\omega k}}\int_0^\infty H^{(1)}_{l+\frac12}(\omega r)I_{l+\frac12}(kr)\,rdr$$
$$=\frac{(2\pi)^3}{i\sqrt{\omega k}}\lim_{\lambda\to\infty}\int_0^\lambda H_{l+\frac12}(\omega r)\,I_{l+\frac12}(kr)\,rdr.$$

Using the antiderivative and the identity

$$\lim_{\lambda\to\infty}\frac{1-e^{i\lambda x}}{x}=\frac{\mathrm{P}}{x}-i\pi\delta(x),$$

where P designates the principal value, we obtain

$$J_l(k)=-\frac{(4\pi)^2}{\omega^{l+1}}k^l\left\{\frac{\mathrm{P}}{k^2-\omega^2}+i\pi\delta(k^2-\omega^2)\right\}$$
$$=-\frac{(4\pi)^2}{\omega^{l+1}}\frac{k^l}{k^2-\omega^2-i\varepsilon}.$$

C. CALCULATION OF THE BASIC INTEGRALS

The formula for the probability contains integrals of the form

$$(K^{(n)},\mathbf{K}^{(n)})=\mathrm{Re}\int\frac{J_l(k)\,P^{(n)}_l\left(\frac{\mathbf{kv}}{kv}\right)(1,\mathbf{k})\,d^3k}{[(\mathbf{k}-\mathbf{v})^2+\lambda^2][(\mathbf{k}-\mathbf{v}+\mathbf{p}_s)^2-\mathbf{p}^2-i\varepsilon]}\qquad(s=1,2). \tag{C.1}$$

Using the Feynman identity

$$\frac{1}{ab}=\int_0^1 dz/[az+b(1-z)]^2,$$

we find

$$(K,\mathbf{K})=\mathrm{Re}\int_0^1 dz\left\{(1,\mathbf{V})\frac{\partial}{\partial\Lambda^2}+(0,1)\,\mathbf{V}\,\frac{\partial}{\partial V^2}\right\}R, \tag{C.2}$$

$$R=\int\frac{J_l(k)\,P_l\left(\frac{\mathbf{kv}}{kv}\right)d^3k}{(\mathbf{k}-\mathbf{V})^2-\Lambda^2},\qquad \mathbf{V}=\mathbf{v}-\mathbf{p}z,$$
$$\Lambda^2=\mathbf{p}^2z^2-\lambda^2(1-z)+i\varepsilon z. \tag{C.3}$$

Choosing the z axis in the direction of $\mathbf{V}$ and integrating over the angles in (C.3), we obtain

$$R=P_l\left(\frac{\mathbf{Vv}}{Vv}\right)\frac{2\pi}{V}\int_0^\infty J_l(k)\,Q_l\left(\frac{k^2+V^2-\Lambda^2}{2kV}\right)kdk,$$

$$Q_l(x)=\frac12\int_0^1\frac{P_l(t)}{x-t}\,dt,$$

where Q_l are the Legendre functions of the second kind.

Since the integrand is an even function, we can extend the integration from $-\infty$ to $+\infty$ and consider the contour in the upper half plane. Calculating the residues with the help of Appendix B and using the identity

$$\ln\frac{(k+V)^2-\Lambda^2}{(k-V)^2-\Lambda^2}=\int_{-V+\Lambda}^{V+\Lambda}\frac{dt}{k-t}+\ln\frac{k+V+\Lambda}{k-V+\Lambda}$$

[the second term is regular in the upper half-plane,

see formula (C.3)], we obtain

$$R = P_l\left(\frac{\mathbf{Vv}}{Vv}\right)\frac{\pi^2 i}{V}\left\{\int_{-V+\Lambda}^{V+\Lambda} J_l(k)\,P_l\left(\frac{k^2+V^2-\Lambda^2}{2kV}\right)kdk + \frac{(4\pi)^2}{\omega}Q_l\left(\frac{\omega^2+V^2-\Lambda^2}{2\omega V}\right)\right. \tag{C.4}$$

Substituting (C.4) in (C.2) and separating out the term which contains Λ in the denominator and diverges for $\lambda \to 0$, we integrate this term by parts over z with dU = dz/Λ and obtain

$$(K, \mathbf{K}) = \mathrm{Re}\,\pi^2 i\left\{-(1, \mathbf{V})\,F\Big|_{z=0}\frac{1}{p}\ln\left[i\frac{\lambda}{p}+\frac{\lambda^2}{2p^2}\right] + (K,\mathbf{K})_0\right\},$$

$$(K, \mathbf{K})_0 = (1, \mathbf{V})\,F|_{z=1}\frac{1}{p}\ln\left[2+\frac{\lambda^2}{2p^2}\right] - \int_0^1 dz\,[(1, \mathbf{V})\,F]'\ln\left(\sqrt{z^2-\frac{\lambda^2}{p^2}(1-z)}\right.$$

$$+ z + \frac{\lambda^2}{2p^2} + \int_0^1 dz\left\{(1, \mathbf{V})\frac{P_l}{V}\left[\frac{1}{2}J_l(k)\,P_l(x)\Big|_{-V+\Lambda}^{V+\Lambda} - \frac{1}{2V}\int_{-V+\Lambda}^{V+\Lambda} J_l(k)\,P_l'(x)\,dk + \frac{\partial}{\partial\Lambda^2}\frac{(4\pi)^2}{\omega^2}Q_l(y)\right]\right.$$

$$\left.\left. + (0,1)\,\mathbf{V}\,\frac{\partial}{\partial V^2}\left[\frac{P_l}{V}\left(\int_{-V+\Lambda}^{V+\Lambda} J_l(k)\,P_l(x)\,kdk + \frac{(4\pi)^2}{\omega}Q_l(y)\right)\right]\right\}. \tag{C.5}$$

Here

$$P_l \equiv P_l\left(\frac{\mathbf{Vv}}{Vv}\right), \qquad x \equiv \frac{k^2-V^2-\Lambda^2}{2kV}, \qquad y \equiv \frac{\omega^2+V^2-\Lambda^2}{2\omega V},$$

$$F = \tfrac{1}{2}P_l\,(J_l(k)\,P_l(k)|_{V+\Lambda} - J_l(k)\,P_l(x)|_{-V+\Lambda}).$$

$(K, \mathbf{K})_0$ does not contain divergent parts and converges uniformly with respect to λ. The singularities of the type

$$\frac{1}{(V+\Lambda)^2-\omega^2}, \qquad \frac{1}{(V-\Lambda)^2-\omega^2},$$

$$\ln\frac{(V+\Lambda)^2-\omega^2}{(V-\Lambda)^2-\omega^2}, \qquad \ln\frac{(V+\omega)^2-\Lambda^2}{(\omega-V)^2-\Lambda^2}$$

under the integral do not give any imaginary contributions on account of the relations

$$(V-\Lambda)^2 < (V+\Lambda)^2 < (p_1+p_2)^2 < \omega^2,$$

$$(\omega+V)^2 > (\omega-V)^2 > p^2z^2 > \Lambda^2 \qquad (\lambda\to 0).$$

$(K, \mathbf{K})_0$ is therefore real for $\lambda \to 0$.

Finally we have

$$(K,\mathbf{K}) = \frac{\pi^3}{2p}J_l(v)(1, \mathbf{v}). \tag{C.6}$$

It is easily seen that replacing **v** in the argument of the Legendre polynomial in (C.1) by an arbitrary vector **u** leads to

$$\mathrm{Re}\int\frac{J_l(k)\,P_l\left(\frac{\mathbf{ku}}{ku}\right)(1, \mathbf{k})\,d^3k}{[(\mathbf{k}-\mathbf{v})^2+\lambda^2][(\mathbf{k}-\mathbf{v}+\mathbf{p})^2-p^2-i\varepsilon]} = \frac{\pi^3}{2p}J_l(v)P_l\left(\frac{\mathbf{vu}}{vu}\right)(1, \mathbf{v}). \tag{C.7}$$

Differentiating both sides of this equation once and twice with respect to u_α/u and setting $\mathbf{u} = \mathbf{v}$, we obtain

$$\mathrm{Re}\int\frac{J_l(k)P_l'\left(\frac{\mathbf{kv}}{kv}\right)(1, \mathbf{k})}{[1]\,[2]}\frac{k_\alpha}{k}d^3k = \frac{\pi^3}{2p}J_l(v)(1, \mathbf{v})\frac{v_\alpha}{v}, \tag{C.8}$$

$$\mathrm{Re}\int\frac{J_l(k)P_l''\left(\frac{\mathbf{kv}}{kv}\right)(1, \mathbf{k})}{[1]\,[2]}\frac{k_\alpha}{k}\frac{k_\beta}{k}d^3k = \frac{\pi^3}{2p}J_l(v)(1, \mathbf{v})\frac{v_\alpha}{v}\frac{v_\beta}{v}. \tag{C.9}$$

It follows from formulas (C.1), (C.6), (C.8), and (C.9) that the value of the integral just calculated can be formally obtained from the function under the integral by replacing the integral sign by $\pi^3/2$, changing the denominator of the expression under the integral to p, and replacing **k** by **v** in the numerator of all functions.

By this method one can also compute an arbitrary tensor $K^{\alpha\beta\ldots\sigma}$ with a rank which is conformity with the convergence of the integral

$$K^{\alpha,\beta\ldots\sigma} = \mathrm{Re}\int\frac{J_l(k)\,P_l(\mathbf{kv}/kv)\,k_\alpha k_\beta\ldots k_\sigma}{[1]\,[2]}d^3k. \tag{C.10}$$

In the calculation of $K^{\alpha\beta\ldots\sigma}$ we must use the identity

$$\frac{\overbrace{k_\alpha k_\beta\ldots k_\sigma}^{m}}{[(\mathbf{k}-\mathbf{V})^2-\Lambda^2]^2} = \overbrace{V_\alpha V_\beta\ldots V_\sigma}^{m}\left[\left(\frac{\partial}{\partial V^2}+\frac{\partial}{\partial\Lambda^2}\right)\int d\Lambda^2\right]^{m-1} \times\left(\frac{\partial}{\partial V^2}+\frac{\partial}{\partial\Lambda^2}\right)\frac{1}{(\mathbf{k}-\mathbf{V})^2-\Lambda^2}.$$

As a result we obtain

$$K^{\alpha,\beta\ldots\sigma} = \frac{\pi^3}{2p}J_l(v)\,v_\alpha v_\beta\ldots v_\sigma. \tag{C.11}$$

[1] R. H. Dalitz, Proc. Roy. Soc. **A206**, 509 (1951). M. Gavrila, Phys. Rev. **113**, 514 (1959). C. Kacser, Proc. Roy. Soc. **A253**, 103 (1959).

[2] G. H. Horton and E. Phibbs, Phys. Rev. **96**, 1066 (1954).

[3] V. B. Berestetskiĭ and I. M. Shmushkevich, JETP **19**, 591 (1949). I. S. Shapiro, JETP **19**, 597 (1949). M. E. Rose, Phys. Rev. **76**, 678 (1949).

[4] A. I. Akhiezer and V. B. Berestetskiĭ, Квантовая электродинамика (Quantum Electrodynamics), Fizmatgiz, 1959.

[5] Berestetskiĭ, Dolginov, and Ter-Martirosyan, JETP **20**, 527 (1950).

Translated by R. Lipperheide
117

ON THE DECAYS $K^+ \to \pi^+ + e^+ + e^-$ AND $K^+ \to \pi^+ + \mu^+ + \mu^-$

L. B. OKUN' and A. P. RUDIK

Submitted to JETP editor March 2, 1960

J. Exptl. Theoret. Phys. (U.S.S.R.) 39, 600-604 (September, 1960)

The hitherto unobserved decays $K^+ \to \pi^+ + e^+ + e^-$ and $K^+ \to \pi^+ + \mu^+ + \mu^-$, which may be due to combined electromagnetic and weak interactions, are examined. The absolute values of the probabilities of these decays are determined by the magnitude of the monopole moment of the transition $K \to \pi$, which cannot be calculated at present. The ratio of the probabilities can be computed and has been found to be $W_\mu/W_e = 0.2$. The π meson, electron, and muon spectra have been calculated, and some convenient methods for the treatment of the experimental results are indicated.

IT is known that, unlike the decays

$$K \to \pi + e + \nu, \qquad K \to \pi + \mu + \nu, \tag{1}$$

the decays

$$K \to \pi^+ + e^+ + e^-, \tag{2}$$

$$K \to \pi^+ + \mu^+ + \mu^-, \tag{3}$$

which have not as yet been observed experimentally, cannot be due to the weak interaction alone. This has to do with the fact that, according to the hypothesis of the universal weak interaction, the interaction contains only charged lepton pairs ($e^+\nu$, $\mu^+\nu$, $\times e^-\bar{\nu}$, $\mu^-\bar{\nu}$) and no neutral pairs (e^+e^-, $\mu^+\mu^-$, $\times \mu^+e^-$, $\nu\bar{\nu}$).

It is easily seen, however, that the decays (2) and (3) are not strictly forbidden even in the present theory and can come about through the combined effect of the weak non-leptonic and electromagnetic interactions. The Feynman graph corresponding to this process is shown in Fig. 1. Here the dotted line represents a virtual photon; the circle represents symbolically the totality of graphs corresponding to the decay of a K meson into a π meson and a γ quantum. One of these graphs is shown in Fig. 2. The decays (2) and (3) are analogous to the well-known 0-0 conversion transitions in nuclei.

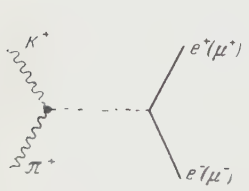

FIG. 1

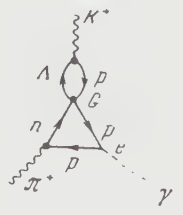

FIG. 2

In order to show how to write down the matrix element corresponding to the graph of Fig. 1, we recall that, in analogy to the 0-0 transition with emission of a real photon, the decay $K^+ \to \pi^+ + \gamma$ with emission of a real photon is forbidden by gauge invariance. Indeed, the only tensor which can be constructed from the four-momenta of the K meson, p, and of the π meson, q, must be proportional to $p_\mu q_\nu$, and thus gives zero when it is multiplied by the tensor of the electromagnetic field $F_{\mu\nu} = k_\nu \epsilon_\mu - k_\mu \epsilon_\nu$ (ϵ is the photon polarization four-vector, and k is the photon four-momentum):

$$p_\mu q_\nu F_{\mu\nu} = (pk)(k\varepsilon) - k^2(p\varepsilon) = 0.$$

The first term vanishes on account of the transversality of the photon, and the second, because $k^2 = 0$. However, for a virtual photon $k^2 \neq 0$, and the term $k^2(p\epsilon)$ is different from zero.

Keeping these remarks in mind, we write down the matrix element corresponding to the graph of Fig. 1 in the form*

$$M = efGk^2 p_\mu \frac{\varphi_K \varphi_\pi}{k^2} \sqrt{4\pi}\, e\bar{u}\gamma_\mu u = \sqrt{4\pi}\,\alpha G f \bar{u}\hat{p}\,u\varphi_K\varphi_\pi. \tag{4}$$

Here $\alpha = e^2 = 1/137$ ($\hbar = c = 1$); u is the spinor of the leptonic field (e or μ); φ_K and φ_π are the wave functions of the K meson and π meson field, respectively, and G is the weak interaction constant ($G = 10^{-5} m_p^{-2}$, where m_p is the proton mass). The vertex part represented in the graph of Fig. 1 by a circle is given by the expression $\varphi_K\varphi_\pi efGk^2p_\mu$ in formula (4), where f is a dimensionless function of k^2 or, what amounts to the same, of the energy

*We note that the decay described by the matrix element (4) conserves parity in contrast to the case of the direct (without participation of a virtual photon) weak interaction of a lepton pair with strongly interacting particles.

of the π meson: $k^2 = m_K^2 + m_\pi^2 - 2E_\pi m_K$. It can be expected that this function changes little in the interval $0 < k^2 < (m_K - m_\pi)^2$. Unless the contrary is specifically indicated, we shall therefore assume in the following that this function is constant. The quantity f does not contain the weak and electromagnetic coupling constants G and e, which appear as separate factors in expression (4); in this sense the constant f is therefore of "order unity." Numerically, however, it can be considerably less than unity. Unfortunately, we cannot calculate the value of f owing to the absence of a theory of strong interactions.

If, in analogy to the vertex $K \to \pi + \gamma$, we describe the vertex $K \to 2\pi$ phenomenologically by the amplitude $f_\theta G m_K^2 \varphi_K \varphi_{\pi_1} \varphi_{\pi_2}$ and determine f_θ by comparing the probability calculated with the help of this amplitude with the experimentally observed probability of the θ_1^0 decay, we obtain $f_\theta^2 \sim 10^{-4}$. This estimate gives us an idea of the possible value of f, although it is not excluded that f can differ from f_θ by several orders of magnitude. If we neglect the unknown dependence of f on k^2, we can calculate the total probabilities of the decays (2) and (3) with the help of the amplitude (4). We find

$$W_e = 0.56\ \overline{W}_0, \tag{5}$$

$$W_\mu = 0.11\ \overline{W}_0. \tag{6}$$

Here $\overline{W}_0 = (1/48)\,\alpha^2 G^2 m_K^5 f^2 \approx 5 \times 10^6 f^2\ \text{sec}^{-1} \approx W_\tau f^2$, where W_τ is the probability of the τ^+ decay. If f were of order unity, the decays (2) and (3), which should look like anomalous τ decays in the photoemulsions, would therefore be about as frequent as the normal τ decays. Up to now about 2000 normal τ decays have been investigated, but not a single occurrence of the decays (2) or (3) has been observed. This implies that $f^2 < 5 \times 10^{-4}$. The impossibility of a reliable calculation of the absolute probability of the decay (2) has been pointed out earlier by Dalitz,[1] who made an estimate of the order of magnitude of this probability.

It is seen from formulas (5) and (6) that, in contrast to the absolute probability, the relative probability of the decays (2) and (3) does not depend on f^2 and is uniquely determined as

$$W_\mu / W_e = 0.2. \tag{7}$$

We note that the numbers 0.56 and 0.11 in formulas (5) and (6) are obtained by integrating expressions (10) and (9). In the case of the electronic decay the integration is elementary and gives

$$1 - 8x^2 + 8x^6 - x^8 - 24\,x^4 \ln x = 0.56, \tag{8}$$

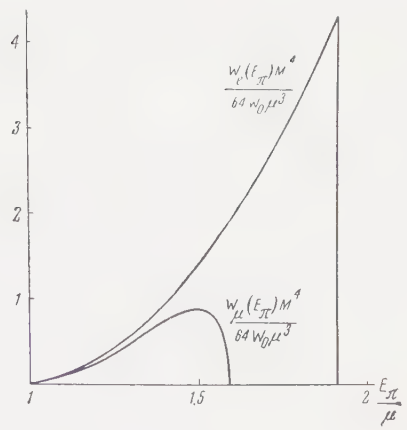

FIG. 3

where $x = \mu/M$ (μ is the π meson mass, and M is the mass of the K meson). In the case of the mesonic decay the integration is done numerically (see Fig. 3).

Let us now consider the spectra of the particles created in the decays (2) and (3). For the decay (3) the spectrum of the π mesons has the form

$$W_\mu(E_\pi)dE_\pi = \frac{64\,W_0(E_\pi)}{M^4}\left[1 + \frac{2m^2}{M^2 + \mu^2 - 2E_\pi M}\right] \times \left[\frac{M^2 + \mu^2 - 4m^2 - 2E_\pi M}{M^2 + \mu^2 - 2E_\pi M}\right]^{1/2} (E_\pi^2 - \mu^2)^{3/2} dE_\pi, \tag{9}$$

where the energy of the π mesons varies within the limits

$$\mu \leqslant E_\pi \leqslant (M^2 + \mu^2 - 4m^2)/2M,$$

where m is the mass of the μ meson. For the decay (2) the spectrum of the π mesons is obtained from (9) by going to the limit m = 0:

$$W_e(E_\pi)\,dE_\pi = 64 M^{-4} W_0(E_\pi)\,(E_\pi^2 - \mu^2)^{3/2} dE_\pi. \tag{10}$$

In this case the energy of the π mesons varies within the limits

$$\mu \leqslant E_\pi \leqslant (M^2 + \mu^2)/2M.$$

The spectra (9) and (10) are shown in Fig. 3. Each of the spectra (9) and (10) contains the unknown function $W_0(E_\pi)$, which can be determined only experimentally.* However, the ratio of the spectra (9) and (10) does not depend on this unknown function and is determined only by quantum electrodynamics. This can be used for the verification of the electromagnetic properties of the muons and electrons up to energies $M - \mu \approx 350$ Mev in the center of mass system of the leptons. It is of special interest to study the ratio of the spectra (9) and (10) in the region of small kinetic energies T of the π meson. In this case the energy of the leptons is close to its largest possible value. Then

*We note that the constant $\overline{W}_0$ which appears in the probabilities (5) and (6) is some average value of the function $W_0(E_\pi)$.

$$\frac{W_\mu(T)}{W_e(T)} = \left(1+\frac{2m^2}{(M-\mu)^2}\right)\left(1-\frac{4m^2}{(M-\mu)^2}\right)^{1/2} + O\left(\frac{T}{\mu}\right) \approx 0.95 \quad (11)$$

(m is the mass of the muon). Unfortunately, the number of π mesons with small energies is exceedingly small, as can be seen from Fig. 3.

The spectra of the muons and electrons in the decays (3) and (2) can be obtained in an explicit form only if it is assumed that f = const, in which case the spectra contain the constant $\overline{W}_0$. Then the spectrum of the muons has the form

$$W_\mu(E_\mu)\,dE_\mu = \frac{96\overline{W}_0}{M^4}\left\{\left[1+\frac{m^2-\mu^2}{Q^2}\right](ME_\mu - 2E_\mu^2 + m^2) - 2m^2\right\}\times\left[\frac{Q^2-2m^2-2\mu^2+(m^2-\mu^2)^2/Q^2}{Q^2}\right]^{1/2} \times (E_\mu^2-m^2)^{1/2}\,dE_\mu, \quad (12)$$

where $Q^2 = M^2 + m^2 - 2ME_\mu$, and the energy of the muon varies within the limits $m \le E_\mu \le [M^2 + m^2 - (m+\mu)^2]/2M$. The spectrum of the electrons in the decay (2) is obtained from (12) by going to the limit m = 0:

$$W_e(E_e)\,dE_e = \frac{96\overline{W}_0}{M^4}\,\frac{E_e^2(M^2-2ME_e-\mu^2)^2}{M^2(M-2E_e)}\,dE_e. \quad (13)$$

The shape of the electron and muon spectra is shown in Fig. 4.

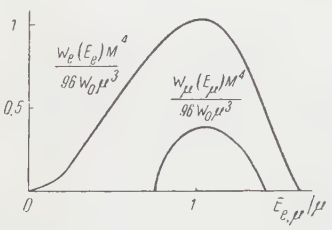

FIG. 4

It is also of interest to consider the simultaneous dependence of the probability on the two variables: the energy of the π mesons E_π and the absolute value of the energy difference between the leptons $\Delta = |E_1 - E_2|$. In this consideration we can use the experimental data for different π meson energies simultaneously. For the electronic decay (2) we then obtain the following spectrum

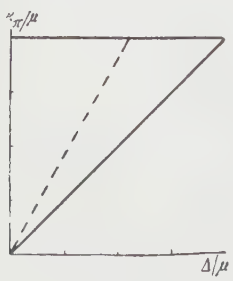

FIG. 5

$$W_e(\Delta,\ E_\pi)\,d\Delta\,dE_\pi = \frac{96W_0(E_\pi)}{M^4}\,[k_\pi^2-\Delta^2]\,d\Delta\,dE_\pi, \quad (14)$$

where $k_\pi^2 = E_\pi^2 - \mu^2$, and the variables are restricted to the region

$$0 \le \Delta \le k_\pi, \qquad 0 \le k_\pi \le (M^2-\mu^2)/2M,$$

as shown in Fig. 5.

FIG. 6

The spectrum (14) contains the unknown function $W_0(E_\pi)$. However, the determination of this function can be avoided by using the "sliding ray method," which has been proposed earlier[2] for the analysis of the K_{e3} decay. For this purpose we must draw the ray $\Delta = ak_\pi$ in Fig. 5, with a < 1. Then the ratio of the number of experimental points lying to the left of the ray over the total number of experimental points does not depend on the unknown function $W_0(E_\pi)$, but only on the quantity a:

$$\int_0^{ak_\pi} W_e(\Delta,\ E_\pi)\,d\Delta \Big/ \int_0^{k_\pi} W_e(\Delta,\ E_\pi)\,d\Delta = \frac{3}{2}\left[a-\frac{a^3}{3}\right]. \quad (15)$$

For the muonic decay (3) we also obtain the spectrum

$$W_\mu(\Delta,\ E_\pi)\,d\Delta\,dE_\pi = 96M^{-4}W_0(E_\pi)\,[k_\pi^2-\Delta^2]\,d\Delta\,dE_\pi. \quad (16)$$

The variables in the spectrum (16) are restricted to the region

$$0 \le \Delta \le k_\pi\left[1-\frac{4m^2}{M^2-2ME_\pi+\mu^2}\right]^{1/2},$$

$$0 \le k_\pi \le \frac{[(M+\mu)^2-4m^2]^{1/2}[(M-\mu)^2-4m^2]^{1/2}}{2M}$$

as shown in Fig. 6. This region differs essentially from the region shown in Fig. 5: for $k_\pi = k_{\pi\max}$ we have $\Delta = 0$. The "sliding ray method," therefore, cannot be directly applied to the spectrum (16).

In conclusion the authors express their deep gratitude to L. D. Landau and I. Yu. Kobzarev for comments, to S. A. Nemirovskaya for carrying out

the numerical calculations and to E. D. Zhizhin for pointing out an error in the initial calculations.

[1] R. H. Dalitz, Phys. Rev. **99**, 915 (1955).

[2] I. Yu. Kobzarev, Dissertation, ITÉF AN SSSR (Institute of Theoretical and Experimental Physics, Academy of Sciences, U.S.S.R.) (1959). L. B. Okun', Usp. Fiz. Nauk **68**, 449 (1959), Ann. Rev. Nuc. Sci. **9**, 61 (1959).

Translated by R. Lipperheide
118

WHICH IS HEAVIER, THE K_1^0 MESON OR THE K_2^0 MESON?

I. Yu. KOBZAREV and L. B. OKUN'

Submitted to JETP editor March 12, 1960

J. Exptl. Theoret. Phys. (U.S.S.R.) 39, 605-609 (September, 1960)

A method for determining the mass difference of the K_1^0 and K_2^0 mesons is proposed which makes it possible to find not only the absolute value of this difference but also its sign. The method is based on the observation of the interference of the K_1^0 mesons produced in plates of various substances by a beam of K_2^0 mesons.

IT is well known that in vacuum the K^0 meson and the $\bar{K}^0$ meson behave like coherent superpositions of time-even (K_1^0) and time-odd (K_2^0) mesons[1,2]:

$$K^0 = (K_1^0 + K_2^0)/\sqrt{2}, \qquad \bar{K}^0 = (K_1^0 - K_2^0)/\sqrt{2},$$
$$K_1^0 = (K^0 + \bar{K}^0)/\sqrt{2}, \qquad K_2^0 = (K^0 - \bar{K}^0)/\sqrt{2}. \tag{1}$$

The K_1^0 and K_2^0 mesons have different properties in relation to weak interactions; the result is that these two mesons have different decay modes and different lifetimes. The time-even meson K_1^0 is short-lived ($\tau_{K_1^0} = (1.00 \pm 0.04) \times 10^{-10}$ sec*) and decays mainly into two mesons (K_{π_2} decay). The time-odd meson K_2^0 is long-lived ($\tau_{K_2^0} = (6.1 \pm 1.6/1.1) \times 10^{-8}$ sec), and its main decay modes are K_{π_3}, K_{μ_3}, and K_{e_3}.

As was pointed out in the original paper by Gell-Mann and Pais,[1] the K_1^0 and K_2^0 mesons must have slightly different masses, because of the difference between their weak interactions. If the only transitions permitted in weak interactions are those with $\Delta S = \pm 1$, where S is the strangeness, then this mass difference must be of the order (cf. e.g., the paper by Zel'dovich[4])

$$\Delta m \sim g^2 m_K \sim 1/\tau_{K_1^0} \approx 10^{10}\,\text{sec}^{-1} \approx 10^{-5}\ \text{ev}, \tag{2}$$

where $g^2 \approx 10^{-13}$ is the square of the weak-interaction constant and m_K is the mass of the K meson ($\hbar = c = 1$). If transitions with $\Delta S = \pm 2$ were permitted, the mass difference would be[5]

$$\Delta m \sim g m_K \sim 10^{16}\,\text{sec}^{-1}. \tag{3}$$

Experiment[6] evidently indicates that $\Delta m \sim 10^{10}$ sec^{-1}, and consequently that transitions with $\Delta S = \pm 2$ are forbidden.

Unfortunately, because of the lack of a consistent theory of the strong interactions, even if we assume that transitions with $\Delta S = \pm 2$ are forbidden, we can predict only the order of magnitude of the absolute value of the mass difference Δm. At present we can say nothing definite about the sign of Δm, i. e., about which is heavier, the K_1^0 meson or the K_2^0 meson.

The experiments considered so far by a number of authors also cannot answer this question. For example, there is much discussion of an experiment for the determination of Δm in which one measures the number of $\bar{K}^0$ mesons that appear in a beam originally composed of K^0 mesons only. One can measure the number of $\bar{K}^0$ particles, for example, by placing in the path of the beam plates in which the $\bar{K}^0$ mesons will be captured with the production of hyperons. It is easy to see that in such an experiment one cannot measure the sign of Δm, since the number of $\bar{K}^0$ mesons produced in the time t is an even function of Δm:

$$w(\bar{K}^0) \sim e^{-\lambda_1 t} + e^{-\lambda_2 t} - 2e^{-(\lambda_1+\lambda_2)t/2}\cos(\Delta m t), \tag{4}$$
$$\lambda_1 = 1/\tau_{K_1^0}, \qquad \lambda_2 = 1/\tau_{K_2^0},$$

t is the characteristic time of the K meson. (sic)

In the present paper we suggest a method for experimentally determining the sign of Δm.

The proposed experiment uses interference phenomena which must occur in a beam of neutral K_2^0 mesons, and will be possible only if $\Delta m \sim 10^{10}$ sec^{-1}.

Let us consider a monochromatic beam of K_2^0 mesons which strikes a target consisting of two thin plates (a and b), which are in general made of different materials and are separated by a certain distance l (see diagram).

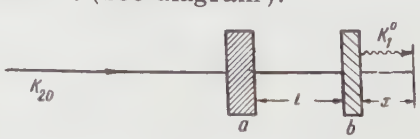

It is well known, that K^0 and $\bar{K}^0$ mesons have different interactions with atomic nuclei. We can

*These data are taken from the report by Alvarez at the Kiev Conference of 1959.[3]

describe the passage of the K-meson wave through plate a by introducing indices of refraction n_a for K^0 mesons and $\bar{n}_a$ for $\bar{K}^0$ mesons:

$$n_a = 1 + 2\pi k^{-2} N_a f_a(0), \qquad \bar{n}_a = 1 + 2\pi k^{-2} N_a \bar{f}_a(0). \quad (5)$$

Here k is the momentum of the incident K_2^0 mesons, $f_a(0)$ is the coherent scattering amplitude for K^0 mesons scattered at angle 0^0 by the nuclei of plate a, and $\bar{f}_a(0)$ is the corresponding quantity for $\bar{K}^0$ mesons; N_a is the number of atoms in 1 cm^3. Analogous formulas hold for plate b. After passage of a beam of K_2^0 mesons through a thin plate there is an admixture of K_1^0 mesons in the transmitted wave:

$$K_2^0 = (K^0 - \bar{K}^0)/\sqrt{2} \xrightarrow{a} (1 + ikd_a n_a) K^0/\sqrt{2}$$
$$- (1 + ikd_a \bar{n}_a) \bar{K}^0/\sqrt{2} = [1 + ikd_a (n_a + \bar{n}_a)/2] K_2^0$$
$$+ ikd_a (n_a - \bar{n}_a) K_1^0/2, \quad (6)$$

where d_a is the thickness of plate a. If we introduce the notation

$$\tfrac{1}{2} kd_a (n_a - \bar{n}_a) = r_a e^{i\varphi_a}, \quad (7)$$

$$\tan\varphi_a = \mathrm{Im}(f_a(0) - \bar{f}_a(0)/\mathrm{Re}(f_a(0) - \bar{f}_a(0)), \quad (8)$$

$$r_a = \pi N d_a k^{-1} \{[\mathrm{Im}(f_a - \bar{f}_a)]^2 + [\mathrm{Re}(f_a - \bar{f}_a)]^2\}^{1/2} \quad (9)$$

the amplitude of the K_1^0 wave after plate a is of the form

$$K_1^0 \sim i r_a \exp\{i\varphi_a + ik_1 x - \lambda_1' x/2\},$$
$$\lambda_1' = \lambda_1/v_1\gamma_1, \qquad k_1 = \sqrt{\omega^2 - m_1^2},$$
$$v_1 = k_1/\omega, \qquad \gamma_1 = \omega/m_1. \quad (10)$$

It follows from Eq. (6) that in first approximation we can neglect the weakening of the K_2^0 wave in the thin plate a; similarly, we can neglect the weakening of the K_1^0 wave in plate b. Then the total amplitude of the wave of K_1^0 mesons produced in plates a and b, evaluated at distance x from plate b (see diagram) can be written in the form

$$K_1^0 \sim i[r_a \exp\{i(\varphi_a + k_1 l) - \lambda_1' l/2\}$$
$$+ r_b \exp\{i(\varphi_b + k_2 l) - \lambda_2' l/2\}] \times \exp\{ik_1 x - \lambda_1' x/2\}, \quad (11)$$

where φ_b and r_b are quantities analogous to φ_a and r_a, and the factor $\exp\{ik_2 l - \lambda_2' l/2\}$ [where $k_2 = (\omega^2 - m_2^2)^{1/2}$] in the second term is due to the fact that in the interval between plates a and b part of the K_1^0 wave goes over into the form of a K_2^0 wave. In the derivation of the formula (11) we have used the condition $d_a, d_b \ll l$.

For the total probability of K_1^0 decays to the right of plate b we have

$$w(K_{\pi_2}) = r_a^2 e^{-\lambda_1 t_0} + r_b^2 e^{-\lambda_2 t_0} + 2 r_a r_b e^{-(\lambda_1+\lambda_2)t_0/2} \cos(\Delta\varphi - \Delta m t_0),$$
$$\Delta\varphi = \varphi_a - \varphi_b, \qquad \Delta m = m_1 - m_2, \quad t_0 = l/v\gamma. \quad (12)$$

It can be seen from Eq. (12) that by measuring the number of K_{π_2} decays (in particular, of decays $\theta_1^0 \to \pi^+ + \pi^-$) to the right of plate b for various distances between plates a and b (different values of t_0) one can determine the magnitude and sign of Δm. It is easy to see that the sign of Δm can be determined only if the plates a and b are made of different materials. In fact, if the plates are made of the same substance, then it follows from Eq. (8) that $\Delta\varphi = 0$ and $w(K_{\pi_2})$ is an even function of Δm.

It can be seen from Eq. (12) that it is advantageous for $\Delta\varphi$ to be close to $\pi/2$. It is obvious that in order for $\Delta\varphi$ to have the optimal value the nuclear properties of plates a and b must be very different. Evidently it is desirable to make one plate of a substance with a small atomic number and the other of a substance with a large atomic number.

The formula (12) shows that to determine the sign of Δm from this experiment we must know the sign of $\Delta\varphi$. For this, in turn, we must know the signs and magnitudes of $\mathrm{Re}\, f(0)$ and $\mathrm{Re}\, \bar{f}(0)$ for the plates a and b and the magnitudes of $\mathrm{Im}\, f(0)$ and $\mathrm{Im}\, \bar{f}(0)$ (as is well known, the signs of these latter quantities are always positive). For light nuclei the information we want can be obtained from data on the interactions of K^+ and K^- mesons with these nuclei, if we use the isotopic invariance of the strong interactions.

An analysis of the experimental data on the interaction of K^- mesons with protons indicates that the interaction of K^- mesons with nuclei at energies $\lesssim 100$ Mev must evidently be of the nature of an attraction, i.e., $\mathrm{Re}\, \bar{f}(0) > 0$. This follows from the fact that the real part of the amplitude for the scattering of a K^- meson by a nucleon is positive both in the state with T = 1 and also in the state with T = 0 (T is the isotopic spin).

For K^+ mesons the situation is less definite: it is known that the amplitude for the scattering of K^+ by a nucleon in the state with T = 1 is negative (repulsion), but the data on the interaction of the K^+ meson with the neutron is so incomplete that no definite conclusion can be drawn about the sign and magnitude of the amplitude with T = 0. Therefore so far we can say nothing about the sign of $\mathrm{Re}\, f(0)$.*

*If the amplitude with T = 0 is small, as the experiments evidently indicate, we may suppose that $\mathrm{Re} f(0) < 0$.

It follows from Eq. (12) that the number of K_2^0 mesons that must be sent through the pair of plates a and b in order to observe one K_1^0 decay to the right of plate b is of the order of magnitude of r_b^{-2}.

If in the expression (9) for r we neglect f(0) in comparison with $\bar{f}(0)$, we get

$$r_b^2 \approx d^2\pi^2 N^2 k^{-2} |f_{\bar{K}^0}(0)|^2. \qquad (13)$$

Assuming that plate b is made of copper and is of thickness d = 2 mm, and taking

$$\sigma_{\bar{K}^0}(\mathrm{Cu}) = \pi r_0^2 A^{2/3} \approx 10^{-24}\mathrm{cm}^2, \qquad 4\pi |f_{\bar{K}_0}(0)|^2 \sim \sigma_{\bar{K}_0}$$

for K mesons of energy 40 Mev, we get $r_b^{-2} = 4 \times 10^5$. If we use the fact that the decay $\theta_1^0 \to \pi^+ + \pi^-$ comprises two thirds of all decays of K_1^0 mesons, we find that to observe one decay $\theta_1^0 \to \pi^+ + \pi^-$ one must send about 600,000 K_2^0 mesons through the plates.

The proposed experiment can also be made with a nonmonochromatic beam of K_2^0 mesons, if from the kinematics of the decay $\theta_1^0 \to \pi^+ + \pi^-$ we determine the momentum of the incident K_1^0 meson and thus determine the time t_0 for each case of decay.

The experiment considered above is of course not the only possible one. For example, instead of observing decays $\theta_1^0 \to \pi^+ + \pi^-$ to the right of plate b, one can register the production of hyperons in this plate. The number of hyperons produced in plate b is proportional to the density of $\bar{K}^0$ mesons in the plate, and this quantity is in turn proportional to

$$\tfrac{1}{2} + \exp\{-\lambda_1 t_0/2\}\, r_a \sin(\varphi_a - \Delta m t_0) \qquad (14)$$

(in this formula we have neglected terms of order r^2 and terms of order $\lambda_2 t_0$).

This version of the experiment has the important disadvantage that the effect in which we are interested is in this case a small correction of order r added to the term ½ (the presence of the plate a causes a slight change of the number of hyperons that are produced in plate b). Therefore we think that the version of the experiment considered before is better.

We note that the sign of Δm can be obtained if we study the interference effects in the decay $K_{1,2}^0 \to \pi^+ + \pi^- + \pi^0$ that have been considered recently by Weinberg and Treiman.[7] The experimental study of these effects is, however, evidently much more complicated than the experiment we are suggesting.

The writers are grateful to V. I. Veksler, Ya. B. Zel'dovich, I. Ya. Pomeranchuk, and B. M. Pontecorvo for their interest in this work and for helpful discussions.

Note added in proof (July 19, 1960). In the actual experiment it is advantageous to use thick plates, since this increases the yield of K_1^0 mesons. The calculation for the case of thick plates has been made by S. G. Matinyan. For ~1 cm of copper the yield of K_1^0 mesons is 10^{-4}.

[1] M. Gell-Mann and A. Pais, Phys. Rev. **97**, 1387 (1955).

[2] Ioffe, Okun', and Rudik, JETP **32**, 396 (1957), Soviet Phys. JETP **5**, 328 (1957). L. D. Landau, JETP **32**, 405 (1957), Soviet Phys. JETP **5**, 336 (1957). Lee, Oehme, and Yang, Phys. Rev. **106**, 340 (1957).

[3] L. Alvarez, Тр. Киевской конференции по физике высоких энергий (Proceedings of Kiev Conference on High-Energy Physics) (in press).

[4] Ya. B. Zel'dovich, JETP **30**, 1168 (1956), Soviet Phys. JETP **3**, 989 (1956).

[5] L. Okun' and B. Pontecorvo, JETP **32**, 1587 (1957), Soviet Phys. JETP **5**, 1297 (1957).

[6] Boldt, Caldwell, and Pal, Phys. Rev. Letters **1**, 150 (1958).

[7] S. B. Treiman and S. Weinberg, Phys. Rev. **116**, 239 (1959).

Translated by W. H. Furry
119

CONCERNING THE THEORY OF THE EXCITON STATE IN SEMICONDUCTORS

I. P. DZYUB

Mathematics Institute, Academy of Sciences, U.S.S.R.

Submitted to JETP editor March 12, 1960

J. Exptl. Theoret. Phys. (U.S.S.R.) 39, 610-615 (Sept., 1960)

Exciton states are treated by the Green's function method. The spectra of Frenkel and Mott excitons are determined for an arbitrary temperature.

INTRODUCTION

THE investigation of exciton states in semiconductors can provide certain information concerning the band spectrum of electrons. The presence of exciton states to some degree provides a measure of the deviation of the energy spectrum of a system of electrons from the spectrum described by the band approximation, which in the majority of cases is sufficient to explain the available experimental data. The existence of excitons is related to correlation effects in a system of electrons which are located in the crystal lattice.

There are many experimental works confirming the exciton structure of the electron energy spectra near the bottom of the conduction band.[1-9] The majority of them are concerned with investigations of polar crystals, and only two investigations[8, 9] relate to the atomic semiconductor Ge. In the latter case the exciton level lies very close to the bottom of the conduction band and is thus quite difficult to detect experimentally. Investigations of the internal[10, 11] and external[12, 13] photoeffects in semiconductors also point to the existence of excitons. Of the theoretical works, which have appeared in recent years, we may mention references 14—19. There is considerable interest in works concerning diffusion of excitons,[20-22] and concerning their contribution to the dielectric constant[23-25] and to the coefficient of heat conduction, etc.

This wide variety of questions concerning excitons might usefully be considered from a single viewpoint. We wish to show that this is apparently possible by using the Green's function method. The superiority of this method over the others usually employed is that the treatment is carried out for an arbitrary temperature from the very outset. On the other hand the exciton energy spectrum (including the problem of damping), the absorption of light, the dielectric constant, the diffusion coefficient, and the thermal conductivity can be obtained by investigating the two-particle Green's function.[26]

In the present article we consider only the problem of excitons in an undeformed lattice.

EXCITON STATES IN AN UNDEFORMED LATTICE

Let us consider a system of valence electrons placed in the crystal lattice. The lattice sites are assumed stationary. In the general case the system of valence electrons is described by the Hamiltonian[27]

$$H = \sum_{f_1 f_2} L(f_1 f_2)\, a^+_{f_1} a^-_{f_2} + \frac{1}{2} \sum_{f_1 f_2 f_3 f_4} F(f_1 f_2 f_4 f_3)\, a^+_{f_1} a^+_{f_2} a_{f_3} a_{f_4}, \quad (1)$$

which takes into account the interaction between the electrons and the lattice site and between the electrons themselves. The index f defines the coordinate of the site and the state of the electron at this site. In particular, if the electron state is described by means of the Wannier function, then f defines the number of the site and of the band.

The band spectrum of the electrons can be obtained from the Hamiltonian (1) in the self-consistent field approximation. The problem is to calculate the correlation effects in the system of electrons; these effects have a considerable influence on the character of the energy spectrum close to the bottom of the conduction band. We shall investigate these correlation effects by making use of the two-particle (and double-time) retarded and advanced Green's functions determined by Bogolyubov and Tyablikov[28] (for convenience these functions are multiplied by the factor $-i$, cf. reference 26):

$$\langle\langle a_{f'}(\tau)\, a_{f''}(\tau) | a^+_{g'}(\tau')\, a_{g''}(\tau')\rangle\rangle_{ret} = -i\theta(\tau-\tau')\langle [a^+_{f'}(\tau)\, a_{f''}(\tau), a^+_{g'}(\tau')\, a_{g''}(\tau')]_-\rangle, \quad (2)$$

$$\langle a_{f'}^{+}(\tau)\,a_{f''}(\tau)\,|\,a_{g'}^{+}(\tau')\,a_{g''}(\tau')\rangle^{add}$$
$$= i^{0}(\tau'-\tau)\,\langle[a_{f'}^{+}(\tau)\,a_{f''}(\tau),\ a_{g'}^{+}(\tau')\,a_{g''}(\tau')]\rangle, \qquad (3)$$

where we denote

$$\ldots\rangle = Q^{-1}\,\mathrm{Sp}\,(\ldots e^{-H/\Theta}), \qquad Q = \mathrm{Sp}\,e^{-H/\Theta}.$$

The Fourier transforms of the functions (2) and (3) can be analytically continued in the upper and lower half-planes respectively and are to all intents and purposes a single analytic function throughout the whole of the E plane, which has a linear cut along the real axis.[28]

This situation enables us to determine the double-time correlation function $\langle a_{f'}^{+}(\tau)\,a_{f''}(\tau)\,a_{g'}^{+}(\tau')\,a_{g''}(\tau')\rangle$, by means of which we calculate the majority of the physical quantities relating to the electron system.[26]

The equations for the Fourier transforms of (2) and (3) coincide. They are easily obtained by using the equation of motion for the operators in the Heisenberg representation. By simple calculations we obtain

$$E\langle\langle a_{f'}^{+}a_{f''}\,|\,a_{g'}^{+}a_{g''}\rangle\rangle = \langle a_{g'}^{+}a_{f''}\rangle\,\delta_{g''f'} - \langle a_{f'}^{+}a_{g''}\rangle\,\delta_{g'f''}$$
$$+\sum_{f} L_{eff}(ff')\langle\langle a_{f}^{+}a_{f''}\,|\,a_{g'}^{+}a_{g''}\rangle\rangle - \sum_{f} L_{eff}(f''f)\langle\langle a_{f'}^{+}a_{f}\,|\,a_{g'}^{+}a_{g''}\rangle$$
$$+\sum_{f_1f_2f}(F(ff_1f'f_2) - F(ff_1f_2f'))\langle a_{f}^{+}a_{f''}\rangle\langle\langle a_{f_1}^{+}a_{f_2}\,|\,a_{g'}^{+}a_{g''}\rangle\rangle$$
$$-\sum_{f_1f_2f}(F(f''f_1ff_2) - F(f''f_1f_2f))\langle a_{f'}^{+}a_{f}\rangle\langle\langle a_{f_1}^{+}a_{f_2}\,|\,a_{g'}^{+}a_{g''}\rangle\rangle;$$

$$L_{\mathrm{eff}}(f_1f_2) = L(f_1f_2) + \sum_{f'f''}\{F(f_1f'f_2f'') - F(f_1f'f''f_2)\}\langle a_{f'}^{+}a_{f''}\rangle. \qquad (4)$$

In the derivation of this equation we used the following approximation to the three-particle Green's function:

$$\langle\langle a_{f_1}^{+}a_{f_2}^{+}a_{f_3}a_{f_4}\,|\,a_{g'}^{+}a_{g''}\rangle\rangle = \langle a_{f_2}^{+}a_{f_3}\rangle\langle\langle a_{f_1}^{+}a_{f_4}\,|\,a_{g'}^{+}a_{g''}\rangle\rangle$$
$$-\langle a_{f_2}^{+}a_{f_4}\rangle\langle\langle a_{f_1}^{+}a_{f_3}\,|\,a_{g'}^{+}a_{g''}\rangle\rangle + \langle a_{f_1}^{+}a_{f_4}\rangle\langle\langle a_{f_2}^{+}a_{f_3}\,|\,a_{g'}^{+}a_{g''}\rangle\rangle$$
$$-\langle a_{f_1}^{+}a_{f_3}\rangle\langle\langle a_{f_2}^{+}a_{f_4}\,|\,a_{g'}^{+}a_{g''}\rangle\rangle. \qquad (5)$$

Physically this approximation implies allowance for the interaction of the excited electron with the hole, which is formed in the background of filled single-electron states.

Equation (4) is easily solved by using the following subsidiary problem:

$$E_\gamma u_\gamma(f'f'') = \sum_{f} L_{\mathrm{eff}}(ff')\,u_\gamma(ff'') - \sum_{f} L_{eff}(f''f)\,u_\gamma(f'f)$$
$$+\sum_{f_1f_2f}\{(F(ff_1f'f_2) - F(ff_1f_2f'))\langle a_{f}^{+}a_{f''}\rangle$$
$$-(F(f''f_1ff_2) - F(f''f_1f_2f))\langle a_{f'}^{+}a_{f}\rangle\}\,u_\gamma(f_1f_2), \qquad (6)$$

with the normalizing condition

$$\sum_{f'f''} u_\gamma(f'f'')\,u_{\gamma'}^{*}(f'f'') = \delta_{\gamma\gamma'}.$$

The solution of (4) will have the form

$$\langle\langle a_{f'}^{+}a_{f''}\,|\,a_{g'}^{+}a_{g''}\rangle\rangle = \sum_{\alpha\alpha'}(E - E_\alpha)^{-1}\,c_{\alpha\alpha'}u_\alpha(f'f'')\,u_{\alpha'}^{*}(g'g''),$$

$$c_{\alpha\alpha'} = \sum_{g_1g_2f_1f_2}\{\langle a_{g_1}^{+}a_{f_2}\rangle\,\delta_{g_2f_1} - \langle a_{f_1}^{+}a_{g_2}\rangle\,\delta_{g_1f_2}\}\,u_\alpha^{*}(f_1f_2)\,u_{\alpha'}(g_1g_2). \qquad (7)$$

From the result obtained we conclude that in the electron system there are possible collective oscillations (called excitons), the spectra of which are determined by the eigenvalues of (6). This deduction is based on the fact that the Green's function (7) has a pole on the real axis. We note that the eigenvalues of (6) depend on the temperature through the mean value $\langle a_{f_1}^{+}a_{f_2}\rangle$

Let us consider two concrete cases.

Frenkel Exciton. Let us suppose that the excited electron remains at that site, at which it existed in the ground state. Conditionally we will define: **0g**-ground state of the electron at the site **g**; **1g** excited state of the electron at the same site **g**. For simplicity we neglect the degeneracy of the excited state. In this case Eq. (6) takes the form

$$E_\gamma u_\gamma(1g,\ 0g) = (L_{\mathrm{eff}}(1g,\ 1g) - L_{eff}(0g,\ 0g))\,u_\gamma(1g,\ 0g)$$
$$+\sum_{g',\,g'',\,\nu=0,\,1}\{[F(\nu g'',\ 1g';\ 1g,\ 0g')$$
$$-F(\nu g'',\ 1g';\ 0g',\ 1g)]\langle a_{\nu g''}^{+}a_{0g}\rangle - [F(0g,\ 1g';\ \nu g'',\ 0g')$$
$$-F(0g,\ 1g';\ 0g',\ \nu g'')]\langle a_{1g}^{+}a_{\nu g''}\rangle\}\,u_\gamma(1g',\ 0g')$$
$$+\sum_{g',\,g'',\,\nu=0,\,1}\{[F(\nu g'',\ 0g';\ 1g,\ 1g')$$
$$-F(\nu g'',\ 0g';\ 1g',\ 1g)]\langle a_{\nu g''}^{+}a_{0g}\rangle - [F(0g,\ 0g';\ \nu g'',\ 1g')$$
$$-F(0g,\ 0g';\ 1g';\ \nu g'')]\langle a_{1g}^{+}a_{\nu g''}\rangle\}\,u_\gamma(0g',\ 1g'). \qquad (8)$$

By analogy we can also write the equation for $u_\gamma(0g,\ 1g)$. From the translational invariance of the crystal lattice we find that $u_\gamma(1g,\ 0g)$ and $u_\gamma(0g,\ 1g)$ are proportional to $\exp(ikg)$, where **k** is the quasi-momentum vector. Equation (8) and the analogous equation for $u_\gamma(0g,\ 1g)$ are easily solved. Retaining only the two-center integrals and neglecting the exchange integrals, we obtain the energy spectrum of the exciton

$$E_\gamma \equiv E(k) = \{\,|\,\Delta E + \tilde{F}_1(k)\,|^2 - |\,\tilde{F}_2(k)\,|^2\}^{1/2}, \qquad (9)$$

where $\Delta E = L_{\mathrm{eff}}(1g,\ 1g) - L_{\mathrm{eff}}(0g,\ 0g)$ is the width of the gap, while $\tilde{F}_1(k)$ and $\tilde{F}_2(k)$ are respec-

tively the Fourier transforms of the functions

$$F_1(|\mathbf{g}-\mathbf{g}'|) = (n_0 - n_1) F(1\mathbf{g},\ 0\mathbf{g}';\ 0\mathbf{g},\ 1\mathbf{g}'),$$

$$F_2(|\mathbf{g}-\mathbf{g}'|) = (n_0 - n_1) F(1\mathbf{g},\ 1\mathbf{g}';\ 0\mathbf{g},\ 0\mathbf{g}'),$$

$$n_0 = \langle a^+_{0\mathbf{g}} a_{0\mathbf{g}} \rangle, \qquad n_1 = \langle a^+_{1\mathbf{g}} a_{1\mathbf{g}} \rangle.$$

The integrals $\mathbf{F_1}(|\mathbf{g}-\mathbf{g}'|)$ and $\mathbf{F_2}(|\mathbf{g}-\mathbf{g}'|)$ have the character of a Coulomb dipole interaction.[29] The difference between the spectrum (9) and that obtained by Heller and Marcus[29] by a variational method lies in the presence of the term $\mathbf{F_2(k)}$ in (9). We note that this difference is insignificant for small k, i.e., when

$$|\tilde{F}_1(\mathbf{k})| < \Delta E, \qquad |\tilde{F}_2(\mathbf{k})| < \Delta E,$$

for in this case $\mathbf{E(k)} = \Delta E + \tilde{\mathbf{F}}_1(\mathbf{k})$.

Mott Exciton. Let an electron, located at the site **g** in state 0, be transferred by excitation to site **h** in state 1 (for example in the S state, as in Cu_2O). In this case Eq. (5) is rewritten

$$\begin{aligned} E_\gamma u_\gamma(1\mathbf{h},\ 0\mathbf{g}) &= \sum_{\mathbf{h}'} L_{eff}(1\mathbf{h}',\ 1\mathbf{h})\, u_\gamma(1\mathbf{h}',\ 0\mathbf{g}) \\ &- \sum_{\mathbf{g}'} L_{eff}(0\mathbf{g},\ 0\mathbf{g}')\, u_\gamma(1\mathbf{h},\ 0\mathbf{g}') \\ &+ \sum_{\mathbf{g}',\ \mathbf{h}',\ \sigma=0\mathbf{g}'',\ 1\mathbf{h}''} \{[F(\sigma,\ 1\mathbf{h}';\ 1\mathbf{h},\ 0\mathbf{g}') \\ &- F(\sigma,\ 1\mathbf{h}';\ 0\mathbf{g}',\ 1\mathbf{h})]\langle a^+_\sigma a_{0\mathbf{g}}\rangle - [F(0\mathbf{g},\ 1\mathbf{h}';\ \sigma,\ 0\mathbf{g}') \\ &- F(0\mathbf{g},\ 1\mathbf{h}';\ 0\mathbf{g}',\ \sigma)]\langle a^+_{1\mathbf{h}} a_\sigma\rangle\}\, u_\gamma(1\mathbf{h}', 0\mathbf{g}') \\ &+ \sum_{\mathbf{g}',\ \mathbf{h}',\ \sigma=0\mathbf{g}'',\ 1\mathbf{h}''} \{[F(\sigma,\ 0\mathbf{g}',\ 1\mathbf{h},\ 1\mathbf{h}') \\ &- F(\sigma,\ 0\mathbf{g}';\ 1\mathbf{h}',\ 1\mathbf{h})]\langle a^+_\sigma a_{0\mathbf{g}}\rangle - [F(0\mathbf{g},\ 0\mathbf{g}';\ \sigma,\ 1\mathbf{h}') \\ &- F(0\mathbf{g},\ 0\mathbf{g}';\ 1\mathbf{h}',\ \sigma)]\langle a^+_{1\mathbf{h}} a_\sigma\rangle\}\, u_\gamma(0\mathbf{g}',\ 1\mathbf{h}'). \end{aligned} \tag{10}$$

An analogous equation can be written for $\mathbf{u_\gamma(0g,\ 1h)}$.

Retaining only the two-center integrals, we rewrite (10) in the form

$$\begin{aligned} E_\gamma u_\gamma(1\mathbf{h},\ 0\mathbf{g}) &= \sum_{\mathbf{h}'} L_{eff}(1\mathbf{h}',\ 1\mathbf{h})\, u\ (1\mathbf{h}',\ 0\mathbf{g}) \\ &- \sum_{\mathbf{g}'} L_{eff}(0\mathbf{g},\ 0\mathbf{g}')\, u_\gamma(1\mathbf{h},\ 0\mathbf{g}') + [F(0\mathbf{g},\ 1\mathbf{h};\ 1\mathbf{h},\ 0\mathbf{g}) \\ &- F(0\mathbf{g},\ 1\mathbf{h};\ 0\mathbf{g},\ 1\mathbf{h})](n_0 - n_1)\, u_\gamma(1\mathbf{h},\ 0\mathbf{g}), \end{aligned} \tag{11}$$

where

$$n_0 = \langle a^+_{0\mathbf{g}} a_{0\mathbf{g}}\rangle, \qquad n_1 = \langle a^+_{1\mathbf{h}} a_{1\mathbf{h}}\rangle.$$

In such an approximation the equations for the functions $\mathbf{u_\gamma(1h,\ 0g)}$ and $\mathbf{u_\gamma(0g,\ 1h)}$ are not coupled to each other. For excitons of large radii the difference equation (11) can be replaced by a differential equation. This can be done in the following way. We first separate the motion of the center of gravity, putting

$$u_\gamma(1\mathbf{h},\ 0\mathbf{g}) = \exp\{i\mathbf{k}(\alpha\mathbf{g} + \beta\mathbf{h})\}\, \overline{u_\gamma}(\mathbf{g}-\mathbf{h}),$$

where **k** is the exciton momentum. In the momentum representation we obtain for the function $\bar{u}_\gamma$ the equation

$$\begin{aligned} E_\gamma \overline{u_\gamma}(\mathbf{p}) &= (\varepsilon^{(1)}(\mathbf{p} - \beta\mathbf{k}) - \varepsilon^{(0)}(\mathbf{p} + \alpha\mathbf{k}))\, \overline{u_\gamma}(\mathbf{p}) \\ &- \sum_{\mathbf{p}'} \bar{V}(\mathbf{p} - \mathbf{p}')\overline{u_\gamma}(\mathbf{p}'), \end{aligned} \tag{12}$$

and the dispersion laws for an electron have the following form in the conduction and valence band respectively.

$$\varepsilon^{(1)}(\mathbf{p}) = \sum_{\mathbf{h}-\mathbf{h}'} L_{eff}(1\mathbf{h},\ 1\mathbf{h}')\, e^{-i\mathbf{p}(\mathbf{h}-\mathbf{h}')},$$

$$\varepsilon^{(0)}(\mathbf{p}) = \sum_{\mathbf{g}-\mathbf{g}'} L_{eff}(0\mathbf{g},\ 0\mathbf{g}')\, e^{-i\mathbf{p}(\mathbf{g}-\mathbf{g}')}.$$

In (12) we denote by $\bar{\mathbf{V}}(\mathbf{p})$ the Fourier transform of the function

$$\begin{aligned} V(\mathbf{g}-\mathbf{h}) &= (n_0 - n_1)[F(0\mathbf{g},\ 1\mathbf{h};\ 0\mathbf{g},\ 1\mathbf{h}) \\ &- F(0\mathbf{g},\ 1\mathbf{h};\ 1\mathbf{h},\ 0\mathbf{g})]. \end{aligned}$$

In the effective-mass approximation

$$\varepsilon^{(1)}(\mathbf{p}) = \Delta E + \mathbf{p}^2/2\mu_1, \qquad \varepsilon^{(0)}(\mathbf{p}) = -\mathbf{p}^2/2\mu_0,$$

where ΔE is the energy gap and μ_0, μ_1 are the effective masses.

Putting $\alpha = \mu_0/(\mu_0 + \mu_1)$ and $\beta = \mu_1/(\mu_0 + \mu_1)$, we write down Eq. (12) in the coordinate representation in the form

$$E_\gamma \overline{u_\gamma}(\mathbf{r}) = \left[\Delta E + \frac{\mathbf{k}^2}{2(\mu_0+\mu_1)} - \frac{\hbar^2}{2\mu}\Delta_{\mathbf{r}}\right]\overline{u_\gamma}(\mathbf{r}) - V(\mathbf{r})\,\overline{u_\gamma}(\mathbf{r}),$$

where μ is the reduced mass.

We thus arrive at an equation that defines the discrete structure of the exciton spectrum. The approximation adopted in going from Eq. (10) to Eq. (11), which consists in neglecting configurational integrals above the second order, means that the resonance mechanism of transferring the exciton excitation is disregarded. An account of these integrals alters the dependence of E_γ on **k**.[30] We shall remark only that a correct account of the resonance transfer of exciton excitation must be accomplished by using Eq. (10).

We note now that the exciton spectrum depends on the temperature factor $n_0 - n_1$, indicating a decrease of the degree of population of the ground level with increasing temperature. In the case of the Mott exciton the presence of this factor leads to a decrease of the effective Coulomb interaction

between the electron and the hole. Furthermore, from a comparison of the results obtained here with those which Heller and Marcus[29] obtained by a variational method, it follows that for small **k** the use of the variational method is justified.

The approximation (5) does not permit the finding of the attenuation for the exciton level. To find that attenuation it would be necessary to consider more accurately the three-particle Green's function, which is a cumbersome matter. This is all the more so, because there is no attenuation at small **k**, for, as perturbation theory shows, the attenuation is due to the transition of the exciton to two electron-hole pairs, which is impossible when $E_\gamma(\mathbf{k}) < 2\Delta E$. For small **k** the attenuation is largely determined by the interaction of the excitons with the lattice vibrations and with impurity centers.

The author thanks N. N. Bogolyubov, S. V. Tyablikov, and D. N. Zubarev for valuable advice and a discussion of the present work.

[1]M. Hayashi and K. Katsuki, J. Phys. Soc. Japan, **5**, 381 (1950); **7**, 599 (1952).

[2]E. F. Gross, N. A. Karryev, Doklady Akad. Nauk. S.S.S.R. **84**, 261 (1952).

[3]Gross, Zakharchenya, and Reinov, Doklady Akad. Nauk. S.S.S.R. **92**, 265 (1953); **99**, 231 (1954).

[4]E. F. Gross and A. A. Kaplyanskiĭ, Физика твердого тела **2**, 379 (1960), Soviet Phys.—Solid State, **2**, 353 (1960).

[5]Nikitine, Perny, and Sieskind, J. phys. et radium **15**, 18 (1954).

[6]G. Perny and S. Nikitine, Compt. rend **244**, 278 (1957).

[7]J. Appel and L. N. Hadley, Phys. Rev. **100**, 1689 (1955).

[8]Zwerdling, Roth, and Lax, Phys. Rev. **109**, 2207 (1958).

[9]Zwerdling, Lax, Roth, and Button, Phys. Rev. **114**, 80 (1959)

[10]V. P. Zhuze and S. M. Ryvkin, Izv. Akad. Nauk S.S.S.R., Ser. Fiz **6**, 93 (1952)

[11]Lashkarev, Sal'kov, Fedorus, and Sheĭnkman, Doklady Akad. Nauk S.S.S.R. **114**, 1203 (1957), Soviet Phys.—Doklady **2**, 291 (1958).

[12]L. Apker and E. Taft, Phys. Rev. **81**, 698 (1951); **82**, 814 (1951).

[13]Taft, Philipp, and Apker, Phys. Rev. **113**, 157 (1957).

[14]A. Overhauser, Phys. Rev. **101**, 1073 (1956).

[15]G. Dresselhaus, J. Phys. Chem. Solids **1**, 14 (1956).

[16]Y. Takeuti, Progr. Theor. Phys. **18**, 421 (1957).

[17]Y. Toyozawa, Progr. Theor. Phys. **20**, 53 (1958).

[18]S. A. Moskalenko and K. B. Tolpygo, JETP **36**, 149 (1959), Soviet Phys. JETP **9**, 103 (1959).

[19]C. Horie, Prog. Theor. Phys. **21**, 113 (1959).

[20]V. E. Lashkarev and Iu. I. Korkhinin, Doklady Akad. Nauk S.S.S.R. **101**, 829 (1955).

[21]Z. S. Gribnikov and E. I. Rashba, J. Tech. Phys. (U.S.S.R.) **28**, 1948 (1958), Soviet Phys.—Tech. Phys. **3**, 1790 (1959).

[22]A. N. Ansel'm and Yu. A. Firsov, JETP **28**, 151 (1955) and **30**, 719 (1956), Soviet Phys. JETP **1**, 139 (1955) and **3**, 564 (1956).

[23]V. M. Agronovich, JETP **37**, 430 (1959), Soviet Phys. JETP **10**, 307 (1960).

[24]J. J. Hopfield, Phys. Rev. **112**, 1555 (1958).

[25]S. I. Pekar and B. E. Tsekvava, Физика твердого тела **2**, 261 (1960), Soviet Phys.—Solid State **2**, 242 (1960).

[26]D. N. Zubarev, Usp. Fiz. Nauk **71**, 71 (1960), Soviet Phys.—Uspekhi **3**, 320 (1960).

[27]N. N. Bogolyubov, Лекции по квантовой статистике (Lectures on quantum statistics), Kiev, (1949).

[28]N. N. Bogolyubov and S. V. Tyablikov, Doklady Akad. Nauk..S.S.S.R. **126**, 53 (1959), Soviet Phys.—Doklady **4**, 589 (1959).

[29]W. Heller and A. Marcus, Phys. Rev. **84**, 809 (1951).

[30]É. I. Rashba, JETP **36**, 1703 (1959), Soviet Phys. JETP **9**, 1213 (1959).

Translated by K. J. S. Cave
120

ANALYSIS OF NUCLEAR INTERACTIONS OF NUCLEONS WITH $E \geq 10^{11}$ ev IN PHOTOGRAPHIC EMULSIONS

É. G. BOOS

Nuclear Physics Institute, Academy of Sciences, Kazakh S.S.R.

Submitted to JETP editor March 17, 1960

J. Exptl. Theoret. Phys. (U.S.S.R.) **39**, 616-623 (September, 1960)

The experimental data on collisions between nucleons and emulsion nuclei are compared with the various theories of multiple production of mesons, in which the tunnel model has been employed.

1. METHODS OF ANALYSIS OF THE INTERACTIONS

In the following discussion, a comparison is made between the experimental data and the various theories of multiple meson production using the tunnel model. By "tunnel" we understand a cylinder of nuclear matter with the base equal to the geometrical cross section of the nucleon. The idea of such a comparison consists of the following: if we take into account[1-3] the experimental data indicating that, at energies $E \geq 10^{11}$ ev, the cross section for meson production coincides sufficiently with the geometrical cross section of the target nuclei[4-7] and varies very little with the energy of the producing particles, then we can calculate the corresponding tunnel length distribution, from the composition of the nuclei of the detector medium. If we take into account that the matter density inside the nucleus is constant, it is easy to calculate the effective mass of the tunnel n in units of the rest mass of the nucleon. In the present experiment, the Ilford G-5 emulsion served as the shower detector. The distribution of the differential probability $\Delta N/N\Delta n$ of observing a tunnel with mass n for this emulsion is shown in Figs. 3 and 4.

On the other hand, generalizing the theory of multiple production for the case of a collision between a nucleon and a nucleus, one can find the variation of an expected multiplicity n_s with the primary energy and the number of nucleons in the tunnel. If we now consider the showers observed in the emulsion, we can estimate the energy independently of n_s for each individual case, using the theoretical relation between them to calculate the corresponding number of nucleons n in the tunnel for each theory. If a sufficiently large number of showers are available, one can construct the distribution of the relative number of showers with respect to the values of n calculated in such a way, and then compare it with the expected distribution for the emulsion. From such a comparison, one can draw conclusions about the applicability of various theories of multiple meson production to nucleon-nucleus collisions within the framework of the assumed model.

In the present paper, data of other laboratories[8-10] were used* in addition to the showers detected in our laboratory.[1] Only the events with $n_s \geq 5$ shower particles, produced by neutral or singly-charged particles, were selected. Secondary showers observed in the emulsion were not taken into consideration. Since the emulsion was exposed in the majority of cases at a high altitude, one can assume that the showers selected in such a way were primarily produced by nucleons. No limitations on the number of grey and black tracks in the stars were imposed. The Lorenz factor γ_c of the nucleon-tunnel center-of-mass system (c.m.s.t.) was found assuming a symmetrical emission of shower particles and the equality of their velocities in the c.m.s.t. to the velocity of the system itself. The latter leads to a systematical overestimate of γ_c.[1,3,11] However, the possible effects of such an overestimate will be discussed below. We then selected showers with $\gamma_c \geq 7$, which corresponds in the laboratory system (l. s.) to energies of $E \geq 10^{11}$ ev. The total number of such showers was equal to 154.

We shall now discuss the various theories.

a) The hydrodynamical theory of Landau was generalized for the nucleon-nucleus collision in the article of Belen'kiĭ and Milekhin[12] where, in par-

*Unpublished data sent to us from the Moscow and Leningrad laboratories were also used.

ticular, a small infraction of the emission symmetry of produced mesons in the c.m.s.t. is shown to exist. Generalizing the relation between the total number of produced particles N and the energy in nucleon-nucleon (NN) collisions, we can write for the nucleon-nucleus collision

$$N = (n+1)\gamma_c^{1/2} \text{ for } n \leqslant 3{,}7, \quad (1)$$

$$N = 1{,}84\,(n - {}^1/_4)^{3/4}\gamma_c^{1/2} \text{ for } n > 3{,}7. \quad (2)$$

Assuming, furthermore, that only π mesons and nucleons are among the shower particles taking part in the collision, we find

$$n_s = 0{,}67\,\gamma_c^{1/2}(n+1) - (n+1)/6 \text{ for } n \leqslant 3{,}7, \quad (3)$$

$$n_s = 1{,}23\,\gamma_c^{1/2}(n - {}^1/_4)^{3/4} - (n+1)/6 \text{ for } n > 3{,}7. \quad (4)$$

b) The energy spectrum of the produced mesons as derived from the Heisenberg theory[13] has been widely confirmed experimentally in showers produced on light and heavy nuclei.[7,8,14-16] It will therefore be useful to consider the application of this theory to nucleon-nucleus collisions within the framework of the assumed model. In order to explain the observed multiplicity in NN collisions, Heisenberg considered the inelasticity factor K, which he connected with the impact parameter of nucleons. In spite of the fact that, as a result, it is possible to explain the observed multiplicity, and that, moreover, the experimental data confirm the character of the variation of the average value of K with the energy of colliding particles,[10,11,17] there is also considerable discrepancy between theory and experimental data, e.g., the absence of a logarithmic increase of the meson-production cross section with the energy.[18,19]

We shall therefore consider an essentially different scheme, in which we postulate the possibility of an inelastic collision of the primary nucleon with a nucleon or a nucleus, without relating it to the impact parameter. The kinematics of such collisions within the framework of the accepted model is as follows (see Fig. 1): before the collision (Fig. 1a), the primary nucleon and the tunnel

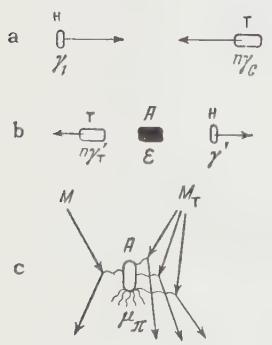

FIG. 1. Scheme of the inelastic nucleon-nucleus collision according to the tunnel model. a – before collision, b – after collision, c – corresponding Feynman diagram.

have equal and opposite momenta in the c.m.s.t. After the collision (Fig. 1b), a strongly excited volume of meson field A is produced in the c.m.s.t., from which the produced mesons are emitted. If the symmetry of emission of these mesons in the c.m.s.t. is conserved, the momenta of the tunnel and of a nucleon after the collision will again be equal. Moreover, the energy ϵ transferred to the meson field is determined as the difference in the total energy of the system nucleon-tunnel before and after the collision. The inelasticity factor K for $\gamma_c^2 \gg 1$ can, in analogy to an NN collision, be determined from the equation*

$$\varepsilon = KM(2n\gamma_c - n - 1) \approx 2KMn\gamma_c. \quad (5)$$

The scheme under consideration may be represented by the Feynman diagram (Fig. 1c), which describes the whole process as an interaction between a virtual π meson from the cloud of the incident nucleon with virtual π mesons of the nucleons of the tunnel, leading to the production of a single excited volume A. Moreover, the nucleons are not excited, or only weakly excited.[20] It is essential to note that, for large energies ($\gamma_c^2 \gg 1$), consecutive peripheral interactions of the primary nucleon with each of the nucleons of the tunnel ($\pi\pi$ collisions with a production of real mesons), clearly are impossible. This follows from the fact that, in c.m.s.t., the time of existence of a virtual π meson belonging to the cloud of the primary nucleon $\gamma_1 \sim \gamma_c/\mu_\pi$ is much greater than the time $\tau_2 \sim 1/\mu_\pi\gamma_c$ necessary for traversing the distance between the two neighboring nucleons in the nucleus.† The Heisenberg theory is fully applicable to the description of the meson-production mechanism from the excited volume A. An unimportant difference, as compared with the usual theory, consists only in the determination of the maximum energy ϵ_M of produced particles, which, in the given case, is determined from the minimum dimensions of the nucleon-tunnel system.

$$\varepsilon_M \approx \mu_\pi^{''} n\gamma_c/(1+n^2). \quad (6)$$

Using the relation (6) and the expression for the energy spectrum of produced mesons of the i-th type,[13] we calculate the number of mesons N_i and the energy ϵ_i carried away by them:‡

*Here and in the following, we used a system of units in which $\hbar = c = 1$.

†The author is thankful to D. S. Chernavskiĭ for a number of useful comments concerning the physical interpretation of the discussed scheme.

‡μ_i is the rest mass of the i-th type of mesons.

$$N_i = A_i \varphi_1(\alpha_i)/\mu_i, \qquad (7)$$

$$\varepsilon_i = A_i \varphi_2(\alpha_i) \qquad (\alpha_i = \mu_i/\varepsilon_M), \qquad (8)$$

$$\varphi_1(\alpha_i) = \frac{2\alpha_i^2+1}{2}\tan^{-1}\frac{\sqrt{1-\alpha_i^2}}{\alpha_i} - \alpha_i\sqrt{1-\alpha_i^2}\tan^{-1}\left(\frac{1-\alpha_i^2}{1+\alpha_i^2}\right)^{1/2} - \frac{\alpha_i}{2}\sqrt{1-\alpha_i^2}, \qquad (9)$$

$$\varphi_2(\alpha_i) = \frac{1}{2}\sqrt{1+\alpha_i^2}\ln\frac{\sqrt{1+\alpha_i^2}+\sqrt{1-\alpha_i^2}}{\sqrt{1+\alpha_i^2}-\sqrt{1-\alpha_i^2}} - \sqrt{1-\alpha_i^2}. \qquad (10)$$

Following Heisenberg,[13] we put $A_i = g_i A$, where g_i is the number of possible charge states of the i-th type of mesons (taking strangeness into account), and A is a constant. In the case of multiple production of π and K mesons, $g_\pi = 3$ and $g_K = 4$. The ratio of the number of $K^\pm$ mesons to the total number of charged K and π mesons can be obtained, assuming charge symmetry, by means of Eqs. (7) and (9):

$$\frac{N_K^\pm}{(N_K^\pm + N_\pi^\pm)} = \frac{3\mu_\pi g_K \varphi_1(\alpha_K)}{3\mu_\pi g_K \varphi_1(\alpha_K) + 4\mu_K g_\pi \varphi_1(\alpha_\pi)}. \qquad (11)$$

In Fig. 2, this ratio is shown as a function of γ_c for NN collisions (curve 1), and for the collision between a nucleon and a tunnel containing seven nucleons (curve 2). The contribution of heavier particles is small and has been neglected. The ratio $N_K^\pm/(N_K^\pm + N_\pi^\pm)$ for high energies ($\gamma_c > 30$) tends towards the value 0.2. This is in satisfactory agreement with experimental estimates[10,16,21] of the fraction of heavy charged particles in showers.

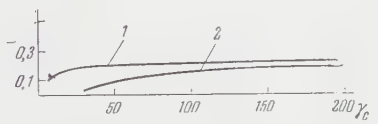

FIG. 2. Ratio between the number of charged K mesons to the total number of charged mesons according to the Heisenberg theory. Curve 1 – for a NN collision, curve 2 – for a collision between a nucleon and a nucleus consisting of seven nucleons.

In order to obtain the variation of multiplicity with the energy, we shall use the equations (5), (8), (9), and (10), from which we shall determine the constant A. Substituting its value into (7), and assuming that $n_s = N_\pi^\pm + N_K^\pm$, we obtain

$$n_s = \frac{KM(2n\gamma_c - n - 1)}{g_\pi \varphi_2(\alpha_\pi) + g_K \varphi_2(\alpha_K)}\left[\frac{2}{3}\frac{g_\pi}{\mu_\pi}\varphi_1(\alpha_\pi) + \frac{1}{2}\frac{g}{\mu_K}\varphi_1(\alpha_K)\right]. \qquad (12)$$

An additional unknown parameter in Eq. (12) is the quantity K, which may be different in each shower. In order to give an estimate of this quantity to a roughest approximation, let us assume that it is constant for all showers with energy higher than 100 Bev. The order of magnitude of the quantity K can be estimated from the condition that the distribution of showers with respect to the tunnel length corresponds to the distribution of the relative differential probability of collision with the tunnel for the detector medium.

The value of n for each shower has been calculated from the hydrodynamical theory [(3) and (4)] and the Heisenberg theory (12), for various K = 0.1, 0.2, 0.3, and 0.5. The histograms of the distribution of the relative number of showers with respect to the values of n calculated in such a way are shown in Figs. 3 and 4.

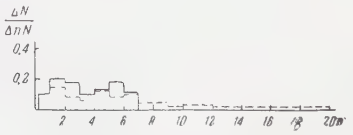

FIG. 3. Distribution of the relative differential density of the number of showers $\Delta N/N\Delta n$ with respect to n according to the Landau theory (dotted line). Density of the probability of distribution of tunnels with respect to n for the Ilford G-5 emulsion is shown by the solid line.

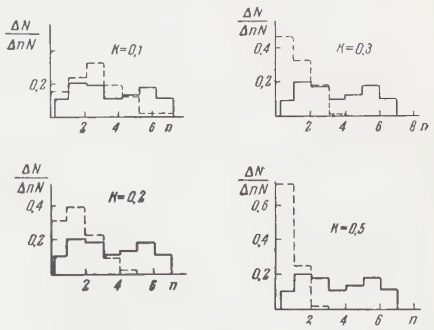

FIG. 4. Distributions of the relative differential density of the number of showers $\Delta N/N\Delta n$ with respect to n (dashed line) obtained from Heisenberg's theory for inelasticity factor K = 0.5, 0.3, 0.2, and 0.1 respectively. The solid line represents the probable distribution of tunnels with respect to n for the Ilford G-5 emulsion.

2. DISCUSSION OF RESULTS

1. The histogram of shower distribution with respect to the tunnel length obtained from the hydrodynamical theory of Landau (Fig. 3) generally follows the distribution expected for emulsions. However, a considerable shift towards greater tunnel lengths is observed. The fraction of showers to which one has to ascribe a fictitious tunnel length $n > 7$ in order to explain the observed multiplicity amounts to 30%. This is also reflected in the ratio of the number of showers N_1 produced only on heavy nuclei ($n > 3.7$) to the number of showers N_2 produced both on heavy and light nuclei (n

≤ 3.7). For the emulsion, this ratio is equal to 0.9, while, according to the hydrodynamical theory of Landau, it equals 1.8. The multiplicity of showers to which, according to the theory, it was necessary to ascribe a fictitious tunnel length ($n > 7$) is great ($n_s > 15$), and the taking into account of the fluctuations in the angular distribution of shower particles will therefore not lead to considerable corrections in γ_c. Since the values of γ_c used[3,11] were systematically overestimated, one can conclude that the disagreement between the theory and the actual conditions cannot be ascribed to experimental errors.*

2. The modified Heisenberg theory leads, within the framework of the accepted model, to a sharp discrepancy between the tunnel-length distribution of the showers and the expected distribution for emulsion for values $K \geq 0.5$ (Fig. 4). For values $K = 0.1$ and 0.2, the ratio N_1/N_2 is equal to 0.3 and 0.1. The value $N_1/N_2 = 0.9$ could have been obtained for $K < 0.1$. However, such a value of inelasticity cannot be accepted, since it lies outside the limits of estimates carried out directly for showers with a known energy distribution of secondary particles.[1,7,11,17] It should, however, be noted that a systematical overestimate of γ_c leads to a worse agreement between the histograms shown in Fig. 4 (γ_c is found[3] to be overestimated by roughly a factor of 1.5). Taking this into account, one can expect an agreement between the present model and the experiment for values of the inelasticity factor substantially smaller than unity ($K \approx 0.1 - 0.2$). The value of K corresponding to the Feynman diagram (Fig. 1c) is approximately equal to $\mu_\pi/M = 0.15$.[20] For the analysis of high-energy showers ($E \geq 10^{11}$ ev) with a known energy distribution of secondary particles and a small number of grey and black tracks ($N_h \leq 3$, i.e., mainly NN interactions), the mean value of the inelasticity factor K was found to equal $0.2 - 0.3$ (references 7, 11, 17), which is not very different from the estimate obtained above. Analogous measurements on showers produced in interactions of nucleons with heavy nuclei ($N_h > 7$) are of great interest.

For two showers with $N_h > 10$ (of type 20 + 12 p and 18 + 11 p), it was found possible in our laboratory to measure the energies of shower particles† (reference 15).

For high energy ($\gamma_c^2 \gg 1$) we can write*

$$Kn \approx \frac{1.5\,\mu_\pi}{2M\gamma_c} \sum_{i=1}^{n_s} E_i'. \qquad (13)$$

In columns 1 and 2 of the table, the type of the shower and the corresponding mean value of the transverse momentum of shower particles are given. In the columns 3, 4, and 5, the values of γ_c, Kn and the shower energy in the l.s. E_0 are given. If we assume that, in these showers, a collision of a primary nucleon occurred with a tunnel of at least average length ($n \approx 3.5$), then the value K is found to be substantially smaller than unity ($K \approx 0.1 - 0.2$). For $K \approx 1$, the quantity Kn should amount to several units, which does not correspond to the table. These data are a very tentative indication that the inelasticity coefficient should be considerably less than unity in showers produced in the collision between a nucleon and a heavy nucleus. The final solution of this problem depends on a marked increase in the number of similar showers observed.

1	2	3	4	5
Type of shower	$\bar{p}_\perp/\mu_\pi$	γ_c	Kn	E_0, Bev
20+12(p)	0.9	5—6	0.8—0.6	$\geqslant$100
18+11(p)	1.1	8—14	0.3—0.2	$>$100

An interesting consequence of the discussed model of multiple meson production in nucleon-nucleus collisions is the possibility of explaining the appearance of a large number of grey and black tracks in high-energy showers. According to the usual hydrodynamical theory, the appearance of such tracks cannot be explained without additional assumptions, since such a large momentum is transferred to the tunnel as a whole (for $K \approx 1$) that it manages to leave the nucleus before disintegrating into separate particles, and the excitation energy equal to the variation of the surface energy of the nucleus is insufficient to explain the observed number of grey and black tracks.

In the case where $K \ll 1$, the nucleons of the tunnel conserve high velocity in their original direction after the collision with a primary nucleon. In the l.s., their velocity β_l relative to the nucleus is small, and they can therefore initiate intranuclear cascades. Such cascades can, in prin-

*Transformation to the system of equal velocities does not lead to a greater similarity between the histograms shown in Fig. 3.[2]

†The energy of all particles was measured in the shower 20 + 12 p. In the shower 18 + 11 p, the energy of three shower particles emitted at the greatest angle could not be measured because of the small length of the track in the emulsion layer. The energy of these particles was found by assuming that their transverse momentum $p_\perp$ is equal to the value $\overline{p_\perp}$ of all remaining particles.

*The energy of shower particles in the c.m.s.t. E_i' is measured in units of rest mass of the π meson.

ciple, be calculated according to the scheme of Goldberger.[22] Since the initial velocity of nucleons of the tunnel is, in the l.s., mainly in the same direction as the primary particle, one should expect the appearance of anisotropy in the angular distribution of recoil nucleons with the maximum in the same direction.

A simple kinematic calculation shows that, if we take the time of flight τ of the primary nucleon (without interaction) through a distance equal to the tunnel length ($\tau \sim n/\mu_\pi$) as the time scale in the l.s., then the fraction of nucleons $\Delta n/n$ in the tunnel remaining during that time inside the nucleus amounts to $\Delta n/n \approx (1 - \beta_l)$. For a high energy ($\gamma_c^2 \gg 1$), $\beta_l \approx K$ and $\Delta n/n \approx (1 - K)$. The mean energy of these nucleons in the l.s. is $\gamma_l \approx M(1 - K^2)^{-1/2}$. For $K \lesssim 0.5$, the kinetic energy of the tunnel nucleons is ~ 1000 Mev, which is wholly sufficient for the ejection of recoil nucleons from the nucleus. If we assume that the mean transverse momentum of the tunnel nucleons $p_\perp \approx M$, we can estimate the opening angle ϑ of the cone in which they are collimated as $\tan \vartheta \approx \sqrt{1 - K^2}/K$. The formulas presented are only estimates. However, it already follows from them that, for $K \approx 1$, the development of the internuclear cascades is impossible, since the fraction of nucleons remaining in the nucleus and also the angle of their collimation are very small. This practically coincides with the ideas of the hydrodynamical theory.

c) The statistical Fermi theory[23] is not applicable in the energy range $E \geq 10^{11}$ ev, since, by means of it, it is impossible to explain the anisotropy in the angular distribution of the produced mesons[24] without using the law of conservation of moment of momentum. In that case, however, the theory becomes self-contradictory even when using it for NN collisions,[25] and all the more so for the tunnel model.

CONCLUSIONS

1. An analysis of different theories of multiple meson productions carried out on the basis of the tunnel model shows that none of the discussed theories in the energy range $E \geq 10^{11}$ ev leads to a good agreement between the tunnel-length distribution of showers and the distribution expected for photographic emulsion.

2. The comparison shows that the hydrodynamical theory of Landau, and the theory of Heisenberg extended for the case of nucleon-nucleus collisions, lead to diametrically opposite effects. Using the first theory, one obtains too great a number of collisions with long tunnels ($N_1/N_2 = 1.8$), while the second theory results in an excess of collisions with short tunnels ($N_1/N_2 = 0.3$) as compared with the number expected for emulsion ($N_1/N_2 = 0.9$). This difference is mainly determined by the value of the inelasticity factor. The hydrodynamical theory is applicable under the assumption that only head-on collisions ($K \sim 1$) occur, while, for the field theory, one has to expect an agreement with the experiment assuming that only peripheral interactions of a primary nucleon with nucleons of the nucleus (leading to the production of a small number of mesons, $K \sim 0.1$) occur. At the present time, the ideas on the multiple meson production in nucleon-nucleus collisions with a small energy transfer to the particles produced ($K \ll 1$) should be regarded as a model whose experimental confirmation requires that many more showers produced on heavy nuclei ($N_h > 10$) be analyzed in detail. Within the framework of this model, it is possible to explain, at least qualitatively, the appearance of a great number of grey and black tracks in corresponding stars.

In conclusion, the author wishes to express his deep gratitude to Prof. Zh. S. Takibaev for proposing the subject, and for his constant attention to the present research.

[1] Zh. S. Takibaev, Тр. ИЯФ АН КазССР Proceedings of the Nuclear Physics Institute, Academy of Sciences Kazakh S.S.R. **1**, 114 (1958).

[2] San'ko, Takibaev, and Shakhova, JETP **35**, 574 (1958), Soviet Phys. JETP **8**, 396 (1959).

[3] É. G. Boos and Zh. S. Takibaev, op. cit. ref. 1 S.S.R. **3**, 46 (1960).

[4] N. A. Dobrotin, Космические лучи (Cosmic Rays) Gostekhizdat, 1954, p. 122.

[5] Grigorov, Murzin, and Rappoport, JETP **36**, 1068 (1959), Soviet Phys. JETP **9**, 759 (1960).

[6] A. A. Alekseeva and N. L. Grigorov, JETP **35**, 599 (1958), Soviet Phys. JETP **8**, 416 (1959).

[7] S. Powell, Proceedings of the Second International Conference on the Peaceful Applications of Atomic Energy, Geneva 1958; Proceedings of the 9th Conference on High-Energy Physics, Kiev 1959.

[8] Fenyves, Gombosi, and Syranyi, Nuovo cimento **11**, 21 (1959).

[9] C.B.A. McCusker and F. C. Roesler, Nuovo cimento **5**, 1141 (1957); Gurevich, Mishakova, Nikol'skiĭ, and Surkova, JETP **34**, 265 (1958), Soviet Phys. JETP **7**, 185 (1958); G. Bertolino, Nuovo cimento **3**, 141 (1956).

[10] Edwards, Losty, Perkins, Pinkau, and Reynolds, Phil Mag. **3**, 237 (1958).

[11] É. G. Boos and Zh. S. Takibaev, Тр. Международной конференции по космическим лучам (Proceedings of the International Conference on Cosmic Rays), Vol I, Moscow 1960.

[12] S. Z. Belen'kiĭ and G. A. Milekhin, JETP **29**, 20 (1955), Soviet Phys. JETP **2**, 14 (1956); S. Z. Belen'kiĭ and L. D. Landau, Usp. Fiz. Nauk **56**, 309 (1955); G. A. Milekhin, JETP **35**, 978 (1958), Soviet Phys. JETP **8**, 682 (1959).

[13] W. Heisenberg, Z. Naturforsch, **133**, 65 (1952); Kosmische Strahlung, Berlin 1953, p. 149.

[14] M. Schein, op. cit. ref. 11, Vol I, Moscow 1960.

[15] Vinitskiĭ, Takibaev, Golyak, and Chasnikov, op. cit. ref. 11, Vol. I, Moscow 1960.

[16] S. Hasegawa, Nuovo cimento **14**, 909 (1959).

[17] W. Fretter and J. Hansen, op. cit. ref. 11, Vol. I, Moscow 1960.

[18] E. L. Feĭnberg and D. S. Chernavskiĭ, Dokl. Akad. Nauk SSSR **91**, 511 (1953).

[19] I. L. Rozental' and D. S. Chernavskiĭ, Usp. Fiz. Nauk **52**, 185 (1954).

[20] D. S. Chernavskiĭ, Postepy Fizyki **9**, 653 (1958).

[21] E. Lohrmann and M. W. Teucher, Phys. Rev. **112**, 587 (1958).

[22] M. L. Goldberger, Phys. Rev. **74**, 1269 (1948); Metropolis, Bivins, Strom, Miller, Friedlander, and Turkevich, Phys. Rev. **110**, 185 (1958); Phys. Rev. **110**, 204 (1958).

[23] E. Fermi, Nuclear Processes at High Energies, Russ. Transl. in Usp. Fiz. Nauk **46**, 71 (1952).

[24] Bartke, Ciok, Gierula, Holynski, Miesowicz, and Saniewska, Nuovo cimento **15**, 18 (1960); G. Bozoki and E. Gombosi, Nuclear Phys. **9**, 400 (1959).

[25] E. L. Feĭnberg and D. S. Chernavskiĭ, Dokl. Akad. Nauk SSSR **81**, 795 (1951).

Translated by H. Kasha
121

POLARIZATION OF INTERNAL-CONVERSION ELECTRONS EMITTED AFTER BETA DECAY OF ORIENTED NUCLEI

I. S. BAĬKOV

Submitted to JETP editor March 4, 1960

J. Exptl. Theoret. Phys. (U.S.S.R.) 39, 624-632 (September, 1960)

The correlation of the polarization of conversion electrons and β particles emitted in the decay of oriented nuclei is considered. The calculation is carried out with allowance for the electric field of the nucleus. Formulas are derived for the angular distribution, and longitudinal and transverse polarization of conversion electrons from any shell with an arbitrary multipole mixture. The numerical results for the L_I, L_{II}, and L_{III} shells refer to M1 and E2 multipoles or their mixture, and are presented in the form of tables of the b^R_{kq} coefficients. These coefficients also determine the polarization of conversion electrons emitted after β decay of nonoriented nuclei. The correlation of the β and conversion electrons can be employed to verify the invariance of the β interaction under time inversion.

UNLIKE the β decay of nonoriented nuclei, the daughter nucleus obtained after the β decay of an oriented nucleus would be polarized even if parity in β decay were conserved. The presence of an initial orientation of the nucleus leads to an anisotropy of the angular distribution of the internal-conversion electrons. The polarization of internal-conversion electrons following the β decay of nonpolarized nuclei was considered in a number of works.[1-3] The present article supplements the results of these papers by considering mixed conversion transitions from three L subshells, and pure transitions from the L_{III} subshell.

The investigation of the polarization correlation of β particles and the following conversion electrons in the β decay of oriented nuclei can furnish more complete information on the β-interaction constants.

We consider the

$$I_i \xrightarrow{\beta} I_1 \xrightarrow{\text{c. e.}} I_2$$

cascade (c.e. is a conversion electron). We choose the direction of the spin $\mathbf{I}_i$ of the oriented nucleus as the z axis, we denote the momentum of the emitted β particle with $\mathbf{p}$, and the unit vector along the direction of emission of the conversion electron with $\mathbf{n}$. The correlation function of the two successive nuclear emissions, when the intermediate state is not perturbed, can be written in the form

$$P_{\xi\xi'} = \sum{}' \rho_{M_i} \langle I_1 M_1 \mathbf{p}\sigma | H_\beta | I_i M_i \nu \rangle \times \langle I_1 M_1' \mathbf{p}\sigma' | H_\beta | I_i M_i \nu \rangle^* \, \mathfrak{M}^{\xi}_{I_1 M_1 I_2 M_2} \mathfrak{M}^{\xi'}_{I_1 M_1' I_2 M_2}, \quad (1)$$

where the summation is over all magnetic quantum numbers, and the prime denotes averaging over all unobserved quantities. $\mathfrak{M}_{\ldots}$ is the matrix element of the conversion process, ξ and ξ' characterize the polarization of the conversion electron in its c.m.s., and ρ_{M_i} is the density matrix of the initial state. The Hamiltonian of the β interaction is the same as in reference 4, represented in the multipole form analogous to that in reference 5. The electron is described in (1) by its momentum $\mathbf{p}$, and its spin component along $\mathbf{p}$. The wave function of the emitted electron is a solution of the Dirac equation which represents at infinity a superposition of a plane and converging spherical wave:

$$|\mathbf{p}\sigma\rangle = (4\pi)^{1/2} \sum_{\varkappa m} i^{l_2} (2l+1)^{1/2} C(l_2 {}^1\!/_2 0\sigma;\ j\sigma) D^j_{m\sigma}(z \to p) \times \exp[-i\Delta(\varkappa)] |\varkappa m\rangle, \quad (2)$$

$$|\varkappa m\rangle = \begin{pmatrix} -if_\varkappa(r)\, \chi^m_{-\varkappa}(\mathbf{r}) \\ g_\varkappa(r)\, \chi^m_\varkappa(\mathbf{r}) \end{pmatrix}. \quad (3)$$

The state of the electron is characterized by the magnetic quantum number m, and by the eigenvalue κ of the operator $\beta(\boldsymbol{\sigma}\mathbf{L} + 1)$.

The conversion matrix element can be written in the form

$$\mathfrak{M} = \sum_{LM} \int \Psi_2^* Q^*(\pi LM)\, \Psi_1 d\tau \int \psi_2 B(\pi LM)\, \psi_1 d\tau \quad (4)$$

where Ψ_2 and Ψ_1 are the wave functions of the nucleus after and until conversion, ψ_2 and ψ_1 are the corresponding wave functions of the electron, and π indicates the transition parity which is

$(-1)^L$ for electric and $(-1)^{L+1}$ for magnetic multipoles. The electromagnetic interaction is invarient under time inversion; the nuclear matrix elements can, therefore, be considered real without loss of generality.

For an electric multipole we have

$$B(ELM) = \left[\frac{L}{L+1}\right]^{1/2} h_L(\omega r) i Y_{LM}(\mathbf{n}) + \left[\frac{2L+1}{L+1}\right]^{1/2} h_{L-1}(\omega r)\, \boldsymbol{\alpha} \mathbf{Y}_{L,\, L-1,\, M}(\mathbf{n}),$$

and for a magnetic multipole

$$B(MLM) = h_L(\omega r) \boldsymbol{\alpha} \mathbf{Y}_{LLM}(\mathbf{n}),$$

where $\omega = E_1 - E_2$ is the energy of the conversion transition, α is the Dirac matrix, and h_L is a spherical Hankel function of the first kind. The initial wave function of the electron is normalized to unity in configuration space, and the final to a δ function of the energy. We can then write

$$\psi_2 = 4\pi \sum_{\varkappa_2 M_2} \sqrt{\frac{E_2}{p_2}} [\chi^{M_2}_{\varkappa_2}(\mathbf{n})]^*_\xi \begin{pmatrix} i f_{\varkappa_2} \chi^{M_2}_{-\varkappa_2}(\mathbf{n}) \\ g_{\varkappa_2} \chi^{M_2}_{\varkappa_2}(\mathbf{n}) \end{pmatrix} i^{l_2} \exp[-i\Delta(\varkappa_2)]. \tag{5}$$

The electron matrix elements in (4), after integration over the angular variables, take on the form

$$B^\xi_{21}(\pi L m) = \int \psi_2^* B \psi_1 d\tau = \sum_{\varkappa_2 M_2 \mu_2} (-1)^L \left[\frac{E_2}{p_2}(2L+1)(2j_2+1)\right]^{1/2} \times \begin{pmatrix} j_2 & L & j_1 \\ -M_2 & m & M_1 \end{pmatrix} \begin{pmatrix} l_2 & 1/2 & j_2 \\ \mu_2 & \xi & -M_2 \end{pmatrix} \times \begin{pmatrix} j_1 & j_2 & L \\ -1/2 & 1/2 & 0 \end{pmatrix} Y_{l_2\mu_2}(\mathbf{n})\, \mathscr{E}_{\varkappa_2}(\pi L),$$

$$\mathscr{E}_{\varkappa_2}(ML) = [L(L+1)]^{-1/2} \exp(i\delta_{\varkappa_2})(\varkappa_1 + \varkappa_2)(R_1 + R_2),$$

$$\mathscr{E}_{\varkappa_2}(EL) = [L(L+1)]^{-1/2} \exp(i\delta_{\varkappa_2})[(R_3 + R_4 - R_5 + R_6)L - (\varkappa_2 - \varkappa_1)(R_5 + R_6)],$$

$$\delta_{\varkappa_2} = \Delta(\varkappa_2) - \pi(l_2 - 1)/2, \tag{6}$$

The radial integrals R_n are defined in the book by Rose,[6] j_1 is the angular momentum of the electron before the conversion, and L is the multipolarity of the transition.

The polarization of the conversion electrons is determined by

$$\langle \boldsymbol{\sigma} \rangle = \mathrm{Sp}\, P\boldsymbol{\sigma} / \mathrm{Sp}\, P, \tag{7}$$

where $\frac{1}{2}\langle\sigma\rangle$ is the mean value of the electron spin in the rest system. The Pauli matrices are conveniently expressed in terms of the coefficients of the vector sum:

$$\sigma^m_{\xi\xi'} = \sqrt{6}(-1)^{1/2-\xi} \begin{pmatrix} 1/2 & 1/2 & 1 \\ -\xi' & \xi & -m \end{pmatrix}. \tag{8}$$

Employing formulas (1) — (8), and averaging over the direction of emission of the neutrino and the polarization of the β particle, we obtain

$$\zeta = \mathrm{Sp}\, P\sigma = \sum_{\substack{\nu k R \pi\pi' \\ L,\, L_1 \leqslant L',\, L_1'}} (-)^{L_1' + R + \nu} f_\nu(I_i) \left[\frac{2\nu+1}{2R+1}\right]^{1/2} X \begin{vmatrix} I_i & I_1 & L_1 \\ I_i & I_1 & L_1' \\ \nu & k & R \end{vmatrix} \times b^R(L_1 L_1') [F_{R\nu k}(\mathbf{p}, \mathbf{n})]^q (2 - \delta_{\pi\pi'}\delta_{LL'}) N(\pi L) N(\pi L') \times [I_0^{\varkappa_1}(\pi L) I_0^{\varkappa_1}(\pi L')]^{1/2} F_k(LL' I_2 I_1) b^{\varkappa_1}_{kq}(\pi L \pi' L') + \mathrm{c.c.} \tag{9}$$

$$\mathrm{Sp}\, P = \sum_{\substack{\nu k R \pi\pi' \\ L,\, L_1 \leqslant L',\, L_1'}} (-)^{L_1' + R + \nu} \left[\frac{1 + (-1)^k}{2}\right] f_\nu(I_i) \left[\frac{2\nu+1}{2R+1}\right]^{1/2} \times X \begin{vmatrix} I_i & I_1 & L_1 \\ I_i & I_1 & L_1' \\ \nu & k & R \end{vmatrix} b^R(L_1 L_1')\, F_{R\nu k}(\mathbf{p}, \mathbf{n}) \times (2 - \delta_{\pi\pi'}\delta_{LL'})\, N(\pi L)\, N(\pi L') \times [I_0^{\varkappa_1}(\pi L)\, I_0^{\varkappa_1}(\pi L')]^{1/2} F_k(LL' I_2 I_1)\, b^{\varkappa_1}_{kq}(\pi L \pi' L') + \mathrm{c.c.} \tag{10}$$

Here F_k are the "geometric factors" that characterize the electromagnetic radiation; they are tabulated in reference 7. We note that

$$F_0(LL' I_2 I_1) = \delta_{LL'}.$$

We describe the initial orientation of the nucleus by means of the statistical tensors

$$f_\nu(I_i) = \sum_{M_i} (-1)^{I_i - M_i} C(I_i I_i \nu;\ M_i - M_i)\, \rho_{M_i}.$$

bk and b_{kq} are parameters of the conversion electron for the correlation of the directions and for the polarization, respectively:

$$b^{\varkappa_1}_k(\pi L \pi' L') = (-1)^{L+L'} \left[\frac{L(L+1)L'(L'+1)}{(2L+1)(2L'+1)}\right]^{1/2} \frac{M^{\varkappa_1}_k(\pi L \pi' L')}{[D_0^{\varkappa_1}(\pi L)\, D_0^{\varkappa_1}(\pi' L')]^{1/2}},$$

$$b^{\varkappa_1}_{kq}(\pi L \pi' L') = (-1)^{L+L'+1} \left[\frac{L(L+1)L'(L'+1)}{(2L+1)(2L'+1)}\right]^{1/2} \times \frac{M^{\varkappa_1}_{kq}(\pi L \pi' L')}{[D_0^{\varkappa_1}(\pi L)\, D_0^{\varkappa_1}(\pi' L')]^{1/2}}, \tag{11}$$

$$M^{\varkappa_1}_{kq}(\pi L \pi' L') = \left[\frac{L(L+1)L'(L'+1)}{(2L+1)(2L'+1)}\right]^{-1/2} \begin{pmatrix} L & L' & k \\ 1 & -1 & 0 \end{pmatrix}^{-1} \times \sum_{\varkappa_2 \varkappa_3} (-1)^{L+L'+j_1+1/2} (2j_2+1)(2j_3+1) \times (2K+1)^{-1/2} \mathscr{E}_{\varkappa_2}(\pi L)\, \mathscr{E}^*_{\varkappa_3}(\pi' L') \times C(j_2 j_1 L;\ 1/2 - 1/2)\, C(j_3 j_1 L';\ 1/2 - 1/2)\, C(j_2 j_3 K;\ 1/2 - 1/2) \times A_q(\varkappa_2 \varkappa_3)\, W(j_2 L j_3 L';\ j_1 K);$$

$$A_q(\varkappa_2 \varkappa_3) = \begin{cases} -1 & q = -1, \\ \varkappa_2 + \varkappa_3 & q = 1, \\ i(\varkappa_2 - \varkappa_3) & q = 0. \end{cases} \tag{12}$$

The expression for $M_k^{\varkappa_1}$ is obtained from (12) if it is assumed that $A_q = 1$. Furthermore

$$D_0^{\varkappa_1}(\pi L) = \frac{L(L+1)}{2L+1} M_0^{\varkappa_1}(\pi L)$$

$$= \sum_{\varkappa_2} (2j_2+1) |\mathcal{E}_{\varkappa_2}(\pi L)|^2 C^2(j_2 j_1 L;\ 1/2 - 1/2)$$

$$I_0^{\varkappa_1}(\pi L) = \frac{E_2}{p_2} \frac{D_0^{\varkappa_1}(\pi L)}{2L+1};$$

the latter value is proportional to the conversion coefficient up to a nonessential factor.

$N(\pi L)$ are the reduced nuclear matrix elements, and b^R are parameters characterizing the β decay. For allowed transitions $b^R(L_1 L_1')$ has the form [for $L_1 \neq L_1'$ the values $b^R(L_1 L_1') + b^R(L_1' L_1)$ are given]:

$$b^0(00) = [|C_S|^2 + |C_S'|^2 + |C_V|^2 + |C_V'|^2 \pm 2\,\mathrm{Re}(C_S^* C_V + C_S'^* C_V')\gamma/\varepsilon]\,|M_F|^2,$$

$$b^0(1,1) = -\sqrt{3}[|C_T|^2 + |C_T'|^2 + |C_A|^2 + |C_A'|^2 \pm 2\,\mathrm{Re}(C_T^* C_A + C_T'^* C_A')\gamma/\varepsilon]\,|M_{GT}|^2,$$

$$b^1(0,1) = [2(C_T^* C_S' + C_T'^* C_S - C_A^* C_V' - C_A'^* C_V) \pm 2(-i) \times (C_A^* C_S' + C_A'^* C_S - C_T^* C_V' - C_T'^* C_V)\,\alpha Z/p]\,M_{GT}^* M_F\, p/\varepsilon;$$

$$b^1(1,1) = \pm\sqrt{2}[2(C_T^* C_T' - C_A^* C_A') \mp (-i)\,2(C_T^* C_A' + C_T'^* C_A)\,\alpha Z/p]\,|M_{GT}|^2 p/\varepsilon.$$

Here the upper sign refers to the electron decay, the lower to positron decay, and ϵ is the energy of the electron. The value $M_{GT}^* M_F$ is assumed real. For first-forbidden transitions one can use the most complete results of Morita.[8]

The function $F_{R\nu k}$ determines the angular dependence

$$F_{R\nu k}(\mathbf{p}, \mathbf{n}) = 4\pi \sum_{\mu} C(\nu k R;\ 0\mu)\, Y_{R\mu}(\mathbf{p})\, Y_{k\mu}^*(\mathbf{n}). \quad (13)$$

The function $[F_{R\nu k}]^q$ is obtained from $F_{R\nu k}$ by substituting $(-1)^\mu Y_{k-\mu}$ for $Y_{k\mu}^*$, where

$$\mathbf{Y}_{k-\mu}^q(\mathbf{n}) = \begin{cases} Y_{k-\mu}^{(-1)}(\mathbf{n}) & q = -1 \\ [k(k+1)]^{-1/2} \mathbf{Y}_{k-\mu}^{(1)}(\mathbf{n}) & q = 1 \\ -i\,[k(k+1)]^{-1/2} \mathbf{Y}_{k-\mu}^{(0)}(\mathbf{n}) & q = 0 \end{cases}$$

On the right we have the spherical vectors[9] which are conveniently represented in a spherical coordinate system:

$$[\mathbf{Y}_{k-\mu}^{(-1)}]_n = Y_{k-\mu},$$

$$[\mathbf{Y}_{k-\mu}^{(+1)}]_\theta = i[\mathbf{Y}_{k-\mu}^{(0)}]_\varphi = [k(k+1)]^{-1/2} \frac{\partial}{\partial\theta} Y_{k-\mu}(\mathbf{n}),$$

$$[\mathbf{Y}_{k-\mu}^{(+1)}]_\varphi = -i[\mathbf{Y}_{k-\mu}^{(0)}]_\theta = [k(k+1)]^{-1/2} \frac{1}{\sin\theta} \frac{\partial}{\partial\varphi} Y_{k-\mu}(\mathbf{n}). \quad (14)$$

Hence it is seen that it is sufficient to know the $F_{R\nu k}$ in order to obtain the values of $[F_{R\nu k}]^q$ by simple differentiation.

The mixing coefficient of the multipoles L and L′ for γ rays is determined in the following manner:

$$\delta(\pi L \pi' L') = N(\pi' L')/N(\pi L) = \pm[I_\gamma(\pi' L')/I_\gamma(\pi L)]^{1/2},$$

where $I_\gamma(\pi L)$ is the intensity of the pure πL-pole γ radiation. For conversion electrons one can introduce the corresponding mixing parameters

$$\bar{\delta}(\pi L \pi' L') = \left[\frac{c(\pi' L')}{c(\pi L)}\right]^{1/2} \delta(\pi L \pi' L') = \left[\frac{I_0(\pi' L')}{I_0(\pi L)}\right]^{1/2} \delta(\pi L \pi' L'),$$

where $c(\pi L)$ is the conversion coefficient for a πL multipole. Selecting an arbitrary multipole $\pi_0 L_0$ as the standard, we can write the polarization of the conversion electrons for an arbitrary multipole mixture in the form

$$\langle \sigma \rangle = \sum_{\substack{\nu k R \pi\pi'; \\ L L_1 \leqslant L' L_1'}} (-)^{L_1' + R + \nu} f_\nu(I_i) \left[\frac{2\nu+1}{2R+1}\right]^{1/2} X \begin{vmatrix} I_i I_1 L_1 \\ I_i I_1 L_1' \\ \nu\ k\ R \end{vmatrix} \times b^R(L_1 L_1')\,[F_{R\nu k}(\mathbf{p}, \mathbf{n})]^q (2 - \delta_{\pi\pi'}\delta_{LL'}) \times \delta(\pi_0 L_0;\ \pi L)\,\bar{\delta}(\pi_0 L_0 \pi L) \times F_k(LL' I_2 I_1)\, b_{kq}^{\varkappa_1}(\pi L \pi' L') + \mathrm{c.c.}\Big\} W^{-1}; \quad (15)$$

$$W = \sum_{\substack{\nu k R \pi\pi'; \\ L, L_1 \leqslant L', L_1'}} (-)^{L_1' + R + \nu} \left[\frac{1 + (-1)^k}{2}\right] \times f_\nu(I_i) \left[\frac{2\nu+1}{2R+1}\right]^{1/2} X \begin{vmatrix} I_i I_1 L_1 \\ I_i I_1 L_1' \\ \nu\ k\ R \end{vmatrix} \times b^R(L_1 L_1')\, F_{R\nu k}(\mathbf{p}, \mathbf{n})\,(2 - \delta_{\pi\pi'}\delta_{LL'})\,\bar{\delta}(\pi_0 L_0 \pi L) \times \bar{\delta}(\pi_0 L_0 \pi' L')\ F_k(LL' I_2 I_1)\, b_k^{\varkappa_1}(\pi L \pi' L') + \mathrm{c.c.} \quad (16)$$

The quantity W determines the angular distribution of the conversion electrons following the β decay of oriented nuclei.

The angular correlation of the conversion electron from the β decay of an oriented nucleus can be used to verify the invariance of the β interaction under time inversion. One of the methods of verification consists in measuring the upward-downward asymmetry of the β intensities for the correlation of the β particle and the conversion electron (with regard to both direction and polarization) in the decay of oriented nuclei with respect to the plane containing $\mathbf{I}_i$ and $\mathbf{n}$.

If it is assumed that there occurs an AV and TS interaction (the assumption that there is no interference between the AV and STP interactions is in agreement with present-day data on β decay), it follows from (15) and (16) that the asymmetry

arises from terms with odd $\nu + R + k$ corresponding to the interference between β-decay matrix elements of various rank (this follows from the properties of the Fano coefficients for odd $\nu + R + k$). All these terms contain the factor

$$\mathrm{Im}\,(C_T^* C_S' + C_T'^* C_S - C_A^* C_V' - C_A'^* C_V).$$

To observe the contribution of such terms to the polarization of the conversion electrons, it is sufficient to know the dipole polarization of the initial nucleus (the term which contains $F_{111} \sim I[p \times n]$). The absence of such terms in the experiment could serve as a proof of the invariance of the β interaction under time inversion. However, if another combination of the interaction variants occurs (interference of the AV and STP interactions is present), then terms proportional to $\alpha Z/p$ will enter into the correlation of β particles and conversion electrons. These terms may cause an upward-downward asymmetry of the β intensities with respect to the plane containing $\mathbf{I_i}$ and $\mathbf{n}$, even when time parity is conserved; an example is the term

$$\mathrm{Re}\,(C_A^* C_S' + C_A'^* C_S - C_T^* C_V' - C_T'^* C_V)\,\alpha Z/p.$$

Hence it is clear that in this case both terms which do not conserve time parity, and Coulomb terms which do conserve time parity will contribute to the same phenomenon. It must be noted that in this case (interference between the AV and STP interactions) it is possible to check time parity by investigating the correlation between the polarization of the β particle and the conversion electron without employing oriented nuclei.

We denote the pseudovector of the β-particle polarization in the rest system by $\zeta_1(\chi, \omega)$. The angles χ and ω are taken in a coordinate system whose z axis is along the direction of $\mathbf{p}$. The following expression for the longitudinal polarization of the conversion electrons, when the β electron and its polarization are observed and the initial nucleus is not oriented, can then be obtained:

$$\begin{aligned}\langle\sigma\rangle_{\mathbf{n}} = \sum_{\pi\pi' L \leqslant L'} \{&[2p\,\mathrm{Re}\,Q_m + 2\alpha Z\,\mathrm{Im}\,Q_n - \lambda_{I_1 I_i}(p\,\mathrm{Re}\,Q_1 \\ &+ \alpha Z\,\mathrm{Im}\,Q_1)]\,E^{-1}\cos\theta_n - \tfrac{1}{3}(2\,\mathrm{Re}\,D + \lambda I_1 I_2 G) \\ &\times(\cos\theta_n\cos\chi + \sin\chi\sin\theta_n\cos\omega) \\ &+ [-2p\,\mathrm{Im}\,Q_n + 2\alpha Z\,\mathrm{Re}\,Q_m + \lambda_{I_1 I_i}(p\,\mathrm{Im}\,Q_1 \\ &- \alpha Z\,\mathrm{Re}\,Q_1)]\,E^{-1}\sin\theta_n\sin\chi\sin\omega \\ &+ \tfrac{1}{3}(1-\gamma/E)[-2\,\mathrm{Re}\,(D_0 + D_1) \\ &+ \lambda_{I_1 I_i}(M_1 + N_1)](2\cos\theta_n\cos\chi - \sin\theta_n\sin\chi\cos\omega)\} \\ &\times(2-\delta_{\pi\pi'}\delta_{LL'})\,\bar{\delta}(\pi_0 L_0 \pi L)\,\bar{\delta}(\pi_0 L_0 \pi' L') \\ &\times F_1(LL' I_2 I_1)\, b_{11(-1)}^{\varkappa_1}(\pi L \pi' L') \\ &\times\Big\{\sum_{\pi L}\bar{\delta}^2(\pi_0 L_0 \pi L)\sqrt{3}\Big[b^0(0,0) + M_1 - \frac{\gamma}{E}N_1 \\ &+ E^{-1}[p\,\mathrm{Re}\,(Q_0+Q_1) + \alpha Z\,\mathrm{Im}\,(Q_0+Q_1)]\cos\chi\Big]\Big\}^{-1}. \qquad (17)\end{aligned}$$

The transverse polarization is obtained from the same formula by substituting $b_{11}^{\varkappa_1}$ for $b_{1(-1)}^{\varkappa_1}$, and by using relations (14). Formula (17) is written in a coordinate system whose z axis is directed along $\mathbf{p}$, and in which $\mathbf{n}$ lies in the zx plane. In (17) we have put

$$\lambda_{I_1 I_i} = [I_1(I_1+1) - I_i(I_i+1) + 2]/2[I_1(I_1+1)]^{1/2}.$$

The remaining quantities in (17) are defined as follows (cf. reference 10):

$$\begin{aligned}&Q_m = -(\beta_{ST} - \beta_{VA})\,M_F M_{GT}, \quad Q_n = (\beta_{VT} - \beta_{SA})\,M_F M_{GT}^*, \\ &D_0 = -(\alpha_{ST} + \alpha_{VA})\,M_F M_{GT}^*, \quad D_1 = (\alpha_{VT} + \alpha_{SA})\,M_F M_{GT}^*, \\ &\mathrm{Re}\,Q_1 = (\beta_{TT} - \beta_{AA})\,|M_{GT}|^2, \quad \mathrm{Im}\,Q_1 = -2\,\mathrm{Im}\,\beta_{AT}\,|M_{GT}|^2, \\ &\mathrm{Re}\,Q_0 = (\beta_{SS} - \beta_{VV})\,|M_F|^2, \quad \mathrm{Im}\,Q_0 = -2\,\mathrm{Im}\,\beta_{VS}\,|M_F|^2, \\ &M_1 = (\alpha_{TT} + \alpha_{AA})\,|M_{GT}|^2, \quad N_1 = -2\,\mathrm{Re}\,\alpha_{TA}\,|M_{GT}|^2, \\ &D = (D_0 - \gamma D_1/E) - 2(D_1 - \gamma D_0/E), \\ &G = (M_1 - \gamma N_1/E) - 2(N_1 - \gamma M_1/E),\end{aligned}$$

where

$$\alpha_{xy} = C_x C_y^* + C_x' C_y'^*, \qquad \beta_{xy} = C_x C_y'^* + C_x' C_y^*.$$

Formula (17) describes electron decay. To obtain positron decay, the following substitutions have to be made:

$$Z \to -Z, \qquad C_i \to -C_i'^*, \qquad C_i' \to C_i'^* \qquad (i = A, S)$$

and

$$C_j \to C_j'^*, \qquad C_j'^* \to -C_j'^* \qquad (j = V, T).$$

Finally, we bring the expression for the polarization of the conversion electrons for the case when an M1—E2 multipole mixture is considered, the initial nucleus is not polarized, and the β transition is allowed (no polarization of β particles is observed). From (15) or (17) we obtain

$$\begin{aligned}\langle\sigma\rangle = \frac{\alpha}{(1+\bar{\delta}^2)\sqrt{3}}\Big\{&\mathbf{n}\Big(\frac{\mathbf{p}}{p}\,\mathbf{n}\Big)[F_1(11 I_2 I_1)\, b_{1(-1)}^{\varkappa_1}(M1) \\ &+ 2\bar{\delta}F_1(12 I_2 I_1)\, b_{1(-1)}^{\varkappa_1}(M1E2) + \bar{\delta}^2 F_1(22 I_2 I_1)\, b_{1(-1)}^{\varkappa_1}(E2)] \\ &+ \frac{1}{2p}[\mathbf{p} - (\mathbf{pn})\,\mathbf{n}]\,[F_1(11 I_2 I_1)\, b_{11}^{\varkappa_1}(M1) + 2\bar{\delta}F_1(12 I_2 I_1) \\ &\times b_{11}^{\varkappa_1}(M1E2) + \bar{\delta}^2 F_1(22 I_2 I_1)\, b_{11}^{\varkappa_1}(E2)]\Big\}.\end{aligned}$$

Here $\bar{\delta} = \bar{\delta}$ (M1E2) and α differ by a factor $-[(I_1+1)/I_1]^{1/2}$ from the expression employed by Geshkenbeĭn.[2] For reference we list the values of F_1:

$$F_1(LLI_2I_1) = \frac{\sqrt{3}\,[L(L+1)+I_1(I_1+1)-I_2(I_2+1)]}{2L(L+1)[I_1(I_1+1)]^{1/2}},$$

$$F_1(12I_2I_1) = \frac{[3(I_2+I_1-1)(I_2+I_1+3)(I_1-I_2+2)(I_2-I_1+2)]^{1/2}}{4[5I_1(I_1+1)]^{1/2}}$$

Our consideration of the β-e correlation is applicable when the nucleus is free in the intermediate state. If the nucleus is acted upon in the intermediate state by a torque, arising as a result of the interaction of the magnetic dipole moment μ with the external magnetic field **B**, or from the interaction of the electrical quadrupole moment Q with the gradients of the electric fields $\partial^2V/\partial z^2$, then the β-e correlation, generally speaking, decreases. The magnitude of this perturbation depends mainly on the average lifetime τ_{I_1} of the nucleus in the intermediate state. If the perturbation is described by the precession frequency ω, then for magnetic interactions ω is equal to the Larmor frequency, and for the quadrupole interaction $\omega \sim Q$ and $\partial^2V/\partial z^2$. A rough criterion of the applicability of our considerations can be obtained from the condition $\omega\tau_{I_1} < 0.1$. Hence $\tau_{I_1} < 10^{-10}$ sec.

In conclusion, I express my deep gratitude to B. V. Geshkenbeĭn and I. S. Shapiro for their interest in the work and its discussion.

APPENDIX

Below we list the values of the polarization parameters calculated with the aid of tables of radial integrals compiled by L. A. Sliv (private

TABLE I. Polarization parameter $b^{L_I}_{1(-1)}$ (M1E2) for the longitudinal polarization for an M1—E2 mixture and conversion from the L_I shell.

Z	k					
	0.10	0.15	0.2	0.3	0.5	0.7
57	0.045	0,18	0.25		0.45	0.54
65	—0.047	0.047	0.14	0.26	0.36	0.47
73	0.11	—0.046	0.02	0.14	0.29	0.39
81	0.41	0.075	—0.47	0.031	0.19	0.31

TABLE II. Polarization parameter $b^{L_I}_{1(1)}$ (M1E2) for the transverse polarization for an M1—E2 mixture and conversion from the L_I shell.

Z	k				
	0.10	0.2	0.3	0.5	0.7
57	—0.098	—0.35	—0.49	—0.63	—0.68
65	0.008	—0.23	—0.37	—0.50	—0.61
73	—0.13	—0.081	—0.23	—0.40	—0.51
81	—0.42	—0.001	—0.094	—0.28	—0.41

TABLE III. Polarization parameter $b^{L_{II}}_{1(-1)}$ (M1E2) for the longitudinal polarization for an M1—E2 mixture and conversion from the L_{II} shell.

Z	k		
	0.1	0.3	0.7
57	—1.0	—0.99	—0.97
65	—1.0	—0.99	—0.97
73	—1.0	—0.98	—0.95
81	—0.97	—0.95	—0.92

TABLE IV. Polarization parameter $b^{L_{II}}_{1(-1)}$ (M1E2) for the transverse polarization for an M1—E2 mixture and conversion from the L_{II} shell.

Z	k			
	0.1	0.15	0.3	0.7
57	—0.94	—0.83	—0.81	—0.76
65	—0.92	—0.87	—0.84	—0.79
73	—0.93	—0.88	—0.85	—0.81
81	—0.91	—0.88	—0.86	—0.80

TABLE V. Polarization parameter $b^{L_{III}}_{1(-1)}$ (M1) for longitudinal polarization in the case of a pure conversion transition from the L_{III} shell.

Z	k				
	0.1	0.2	0.3	0.5	0.7
57	—0.06	—0.21	—0.32	—0.43	—0.49
65	0.006	—0.14	—0.27	—0.41	—0.48
73	0.08	—0.12	—0.24	—0.38	—0.46
81	0.13	—0.08	—0.19	—0.34	—0.44

TABLE VI. Polarization parameter $b^{L_{III}}_{1(1)}$ (M1) for transverse polarization in the case of a pure conversion transition from the L_{III} shell.

Z	k				
	0.1	0.2	0.3	0.5	0.7
57	0.19	0.29	0.38	0.41	0.40
65	0.05	0.23	0.31	0.37	0.38
73	—0.03	0.16	0.23	0.32	0.34
81	—0.09	0.08	0.16	0.24	0.27

TABLE VII. Polarization parameter $b^{L_{III}}_{1(-1)}$ (M1E2) for longitudinal polarization for an M1—E2 mixture and conversion from the L_{III} shell.

Z	k					
	0.1	0.15	0.2	0.3	0.5	0.7
57	0.55	0.58	0.56	0.48	0.28	—0.011
65	0.51	0.56	0.52	0.45	0.26	0.011
73	0.44	0.49	0.48	0.43	0.24	0.046
81	0.38	0.45	0.43	0.38	0.24	0.12

TABLE VIII. Polarization parameter $b^{L_{III}}_{1(1)}$ (M1E2) for transverse polarization for an M1—E2 mixture and conversion from the L_{III} shell.

Z	k					
	0.1	0.15	0.2	0.3	0.5	0.7
57	0.68	0.62	0.61	0.56	0.65	0.69
65	0.82	0.74	0.68	0.66	0.69	0.75
73	0.89	0.82	0.72	0.71	0.74	0.81
81	0.89	0.83	0.77	0.72	0.79	0.91

TABLE IX. Polarization parameter $b^{L_{III}}_{1(-1)}$ (E2) for longitudinal polarization in the case of a pure conversion transition from the L_{III} shell.

Z	k				
	0.1	0.2	0.3	0.5	0.7
57	0.35	0.35	0.34	0.28	0.082
65	0.32	0.33	0.33	0.23	0.1
73	0.27	0.29	0.29	0.21	0.12
81	0.21	0.24	0.23	0.19	0.115

TABLE X. Polarization parameter $b_{1(1)}^{L_{III}}$ (E2) for the transverse polarization in the case of a pure conversion transition from the L_{III} shell.

Z	k				
	0.1	0.2	0.3	0.5	0.7
57	0.83	0.59	0.37	0.006	−0.42
65	0.97	0.71	0.47	0.14	−0.27
73	1.15	0.87	0.64	0.27	−0.062
81	1.29	0.98	0.79	0.43	0.15

communication). The calculations are carried out for nuclei with Z = 57, 65, 73, and 81, and transition energies from 0.1 to 0.7 in units of $m_e c^2$ for conversion from the L_I, L_{II}, and L_{III} shells.

[1] B. V. Berestetskiĭ and A. P. Rudik, JETP **35**, 159 (1958), Soviet Phys. JETP **8**, 111 (1959).

[2] B. V. Geshkenbeĭn, JETP **35**, 1235 (1958), Soviet Phys. JETP **8**, 865 (1959).

[3] R. L. Becker and M. E. Rose, Nuovo cimento **13**, 1182 (1959).

[4] T. D. Lee and C. N. Yang, Phys. Rev. **104**, 254 (1956).

[5] L. C. Biedenharn and M. E. Rose, Revs. Modern Phys. **25**, 729 (1953).

[6] M. E. Rose, Multipole Fields, New York, Wiley, 1955.

[7] Alder, Stech, and Winther, Phys. Rev. **107**, 728 (1957).

[8] M. Morita and R. S. Morita, Phys. Rev. **109**, 2048 (1957).

[9] A. I. Akhiezer and V. B. Berestetskiĭ, Квантовая электродинамика (Quantum Electrodynamics) Fizmatgiz, 1959.

[10] A. Z. Dolginov, JETP **35**, 178 (1958), Soviet Phys. JETP **8**, 123 (1959).

Translated by Z. Barnea
122

A RELATIVISTIC GENERAL THEORY OF REACTIONS

M. I. SHIROKOV

Submitted to JETP editor March 18, 1960

J. Exptl. Theoret. Phys. (U.S.S.R.) 39, 633-638 (September, 1960)

The formulas of a relativistic general theory of reactions for the cross section and the polarization in terms of phase shifts may assume a different form for different definitions of the relativistic spin operator. However, in the rest system of the particle the spin operators coincide. This allows one to express the general theory in a form which is the same for all equivalent definitions of the spin.

INTRODUCTION

FOR the relativistic generalization of the formulas expressing the differential cross section and the polarization in terms of phases it is necessary to define the relativistic spin operator for the particle and to find the transformation functions for the transformation from a representation in terms of the momenta and the projections of the spins to a representation which is diagonal in the conserved total angular momentum of the system of interacting particles. In the papers of Chou Kuang-Chao and the author[1] and Yu. Shirokov[2] the Foldy—Yu. Shirokov representation[3] was used for the description of particles with spin. Chou Kuang-Chao and the author[1] arrived at this representation starting from a definition of the spin as the internal angular momentum of the particle with respect to its center of inertia.

However, other relativistic definitions of the coordinates of the center of inertia (see, for example, the papers of Pryce[4] and Yu. Shirokov[5]) are possible, for which the operator of the internal angular momentum is different from the spin of Pryce-Foldy-Shirokov (there is, for example, the possibility of a spin operator whose components do not commute, as the Pauli matrices; see references 4). Moreover, the Dirac spinors transform in a different way in going from one Lorentz frame to another than the spinor functions in the Foldy-Shirokov representation.* There exist still other possibilities of defining the relativistic spin operator (see, for example, references 5 and 6).

*It can be shown that these possibilities of a relativistic description of particles with spin correspond, mathematically, to non-unitary representations of the inhomogeneous Lorentz group (whereas the Foldy-Shirokov representation, which is particularly convenient for the general theory of reactions, is a unitary representation of this group).

Different definitions of the spin may give rise to different transformation functions and, correspondingly, to different expressions for the cross section and the polarization.* In the present paper we show that there exists a form of the general theory in which the transformation functions and formulas for the cross section and polarization are the same for all equivalent representations of the inhomogeneous Lorentz group (abbreviated ILG). We assume that the rest masses of all particles are different from zero and the spins are arbitrary.

We note that the wave functions describing the states of the interacting particles must transform according to representations of the ILG. The theory of representations of the ILG gives a description of systems all the states of which can be obtained from any arbitrary given state by translations, rotations, and Lorentz transformations (and superpositions of such states). There is thus no relativistically invariant difference between different states of the system.[7] The homogeneous Lorentz group does not contain translations and, therefore, cannot describe all states of the free particles.

THE SPIN IN THE REST SYSTEM OF THE PARTICLE AND THE GENERAL THEORY OF REACTIONS

1. The state of a free particle with spin is defined in the following way: 1) we give the momentum of the particle, p, (for example, in the c.m. system of the reaction), and 2) we give the spin

*It can, nevertheless, be shown that the angular correlations (for example, the azimuthal asymmetries in experiments on double and triple scattering) are the same, although they are expanded in terms of different complete systems of angular functions.

state of the particle in the Lorentz system in which it is at rest.

The spin operator of the particle in the rest system, $\mathbf{s}^0$, is equal to its total angular momentum M (since the orbital angular momentum in this system vanishes); hence all spin operators coincide in the rest system of the particle. The projection of the spin is defined as the eigenvalue of the operator $\Sigma = \mathbf{s}^0\mathbf{n} = \mathbf{M}\mathbf{n}$, where $\mathbf{n}$ is a unit vector in the direction of $\mathbf{p}$ (with respect to the rest system).

2. The general principles of the formal theory of reactions have been given in a paper by the author[8] (Sec. 1) and in the paper of Jacob and Wick[9] (Introduction). The elements of the S matrix for a reaction of the type $a + b \to c + d$,

$$(m_c m_d \mathbf{p}' \mid S \mid m_a m_b \mathbf{p}) \tag{1}$$

must be expressed in terms of the phases* (more precisely, in terms of the elements of this matrix in the representation which is diagonal in the total angular momentum). The conservation of the total momentum is assumed to be already accounted for; $\mathbf{p}'$ and $\mathbf{p}$ are the relative momenta of the particles; the m's are the eigenvalues of the operators Σ of the separate particles. In contrast to reference 9, the spin functions which enter in the element (1) of the S matrix are referred to the c.m.s. of the particles (besides this, m_d in reference 9 is the eigenvalue of $\mathbf{M}_d(-\mathbf{n}')$, whereas here m_d denotes the eigenvalue of the operator $\mathbf{M}_d\mathbf{n}'$). However, the total angular momentum (being a quantity which is common to the initial and final states) must be referred to the same Lorentz frame (conveniently, the c.m.s. of the reaction) and, of course, to the same axis of quantization z.

The expression for the matrix element (1) in terms of the elements $(\lambda_c\lambda_d\mathbf{p}' \mid S_0 \mid \lambda_a\lambda_b\mathbf{p})$, which are referred to the c.m.s. of the reaction, must have the form

$$(m_c m_d \mathbf{p}' \mid S \mid m_a m_b \mathbf{p}) = q^*(m_c, m_d, p') \times (m_c m_d \mathbf{p}' \mid S_0 \mid m_a\, m_b\, \mathbf{p})\, q(m_a, m_b, p), \tag{2}$$

because we are dealing with Lorentz transformations with velocities parallel to the momenta of the particles (see the Appendix).

The elements of the matrix S_0 appearing in (2) can now be expressed in terms of the elements of S_0 in the representation determined by the squares and the z projections of the operator $\mathbf{J} = \mathbf{M}_1 + \mathbf{M}_2$, the total angular momentum (which is the spin of the system of interacting particles in the c.m.s. of the reaction), the operators Σ_1 and Σ_2, and the total energy E. The corresponding transformation function was obtained in the papers of Chou Kuang-Chao[10] and Jacob and Wick.[9] Its derivation (see reference 10, Sec. 2) does not rest on any assumptions about the particular representation in which the particles are described (in particular, even representations with vanishing rest mass are allowed). Using the fact that S_0 is diagonal with respect to the square, $J(J+1)$, and the projection, M, of the total angular momentum, we have (with the normalization of Jacob and Wick[9])

$$(m_c m_d \mathbf{p}' \mid S \mid m_a m_b \mathbf{p}) = \frac{2J+1}{4\pi} \sum_{JM} D^J_{m_c+m_d,M}(-\pi, \vartheta', \pi-\varphi')\, q^*(m_c, m_d, p') \times (m_c m_d p' JM \mid S_0 \mid m_a m_b p JM)\, q(m_a, m_b, p) \times D^J_{M,m_a+m_b}(\varphi, \vartheta, 0). \tag{3}$$

If we now introduce the matrix $\widetilde{S}$,

$$(m_c \mid \widetilde{S}^{JE} \mid m_a) = q^*(m_c, p')\,(m_c \mid S_0{}^{JE} \mid m_a)\, q(m_a, p), \tag{4}$$

we have completed the inverse transformation of (2), i.e., $\widetilde{S} = S$. We note that in the phase analysis we can only determine the product of all the factors on the right-hand side of (4), but not each factor separately.

The expression for the polarization tensors of the reaction products in terms of the elements (1) and the tensors of the beam and the target are determined by the nonrelativistic formulas (see, for example, reference 11). The elements $(m_c m_d \mid S^J \mid m_a m_b)$ can be introduced in these formulas. In particular, they appear in the expressions for the angular distribution and the polarization vector of reference 9. Of course, the polarization vector, for example, must be defined as the average value of the spin vector of the particle in its rest system. If it is initially known in some other Lorentz system, for example, in the laboratory system (polarized beam), one must find the corresponding expression in the rest system of the particle. To do this one may need a specific representation. In the remaining part of the paper we present a form of the general theory which is not significantly different from that discussed in detail by Jacob and Wick[9] and which is the same for different representations of particles with spin.

3. In this general theory of reactions still another problem comes up, the formulation and

*The invariance under four-dimensional rotations can also be expressed in the manner adopted by Stapp,[6] but only in terms of the phases can the unitarity of the S matrix be simply accounted for.

solution of which we shall demonstrate on the example of the double scattering of the proton.

Let us assume that we have found the polarization of the proton from the azimuthal asymmetry of the angular distribution of scattering II and that we want to use it for the phase analysis of scattering I. From the asymmetry of II one can find the components P_{z_2}, P_{y_2}, and P_{x_2} of the polarization vector in the direction of the proton momentum p_2 in the c.m.s. of II (or in the laboratory system, since the target II is at rest), of the normal y_2 to the plane of scattering I, etc, as referred to the rest system of the proton K_2. For the phase analysis of scattering I we need the components P_{z_1}, P_{y_1}, and P_{x_1} (z_1 is parallel to the proton momentum p_1 in the c.m.s. of I, $y_1 \parallel y_2$, etc.), referred to the rest system of the proton K_1, which differs from the rest system of the proton K_2 in the way explained below.

By rotating the components P_{z_2}, P_{y_2}, P_{x_2} about the angle between p_2 and p_1 we obtain the components P'_{z_1}, P'_{y_1}, P'_{x_1} referring to z_1, y_1, x_1 (for details see reference 11, Sec. 3), but expressed in the system K_2. In order to go from K_2 to K_1, we must carry out the following Lorentz transformations: 1) from K_2 to the laboratory system K_l by the velocity $\beta_2 \parallel p_2$, 2) from K_l to the c.m.s. of I by the velocity β parallel to the scattered beam I, and 3) from the c.m.s. of I to K_1. The corresponding velocity β_1 is computed as the relativistic sum of the velocities β_2 and β. The product of these three transformations is a three-dimensional rotation (see reference 12, Sec. 22; reference 6; and also reference 1, footnote 5).

Thus the system of axes $z_1y_1x_1$ is oriented differently with respect to the spatial axes of K_2 than with respect to the axes of K_1. In other words, the vector p_1 has different spherical angles with respect to K_2 than with respect to K_1.

The determination of the axis and the angle Ω of the above-mentioned rotation is a purely kinematical problem. In particular, Ω is the angle between the velocities ω and ω'' of Møller (reference 12, Sec. 22, formulas (59) and (59′), and to find $\sin\Omega$ it suffices to take the vector product of the expressions for ω and ω''.

The results are given in reference 1 in terms of the rotation of the spin vector with respect to the fixed spatial axes, which is equivalent to the above-mentioned rotation of the axes of K_1 with respect to the axes of K_2.

4. The general theory of reactions can thus be expressed in a form whose basic formula is (3), the same for different but equivalent representations of the inhomogeneous Lorentz group describing a particle with spin. Formula (3) agrees in form with the corresponding non-relativistic formula. In contrast to the non-relativistic case, the polarization tensors must be subjected to a certain rotation of relativistic origin in the phase analysis or in the determination of the angular correlations. The axis and the angle of this rotation are the same for different representations of particles with spin.

In conclusion I express my gratitude to Yu. M. Shirokov and I. V. Polubarinov for valuable comments.

APPENDIX

We presuppose the knowledge of the fundamentals of the theory of representations of the inhomogeneous Lorentz group (see, for example, references 13 and 14). The following considerations are valid for arbitrary representations of this group (not only for the unitary representations).

1. Since $\mathbf{s}^0$ is equal to $\mathbf{M}$ in the rest system, $[s_i^0, s_j^0] = i\epsilon_{ijk}s_k^0$. These commutation rules determine a representation of the three-dimensional rotation group, which can be assumed to be unitary.[15] Hence, s_k^0 can be assumed to be a Hermitian matrix.

2. We introduce the four-dimensional vector

$$\Gamma_\mu = \frac{1}{2i}\sum_{\nu,\sigma,\lambda} \varepsilon_{\mu\nu\sigma\lambda} M_{\nu\sigma} p_\lambda$$

($\epsilon_{\mu\nu\sigma\lambda}$ is the completely antisymmetric unit tensor of fourth rank), whose length Γ^2 is an invariant of the inhomogeneous Lorentz group.[13] In the rest system $\mathbf{\Gamma} = \kappa\mathbf{M}$, $\Gamma_4 = 0$ (κ is the rest mass of the particle), i.e., $\mathbf{s}^0 = \mathbf{\Gamma}/\kappa$. It follows from this that the square of the spin in the rest system, $(\mathbf{s}^0)^2$, is equal to the Lorentz invariant Γ^2/κ^2, which characterizes (together with the mass κ) a definite irreducible representation of the ILG (Γ^2 determines, in particular, the number of components of the wave function of the particle).

3. Without using a definite representation we cannot determine the transformation properties of the spinor functions under changes of the Lorentz frame. But in our form of the general theory we need only know how the spinor functions transform under Lorentz transformations Λ with a velocity β parallel to the momentum $\mathbf{p}$ of the particle. The operator $\Sigma = \mathbf{s}^0\mathbf{n} = \Gamma_4/i\kappa|\mathbf{p}|$ is invariant under such transformations. Indeed, if

$\beta = \alpha p/p_0$ $(0 < \alpha < 1)$, then

$$\frac{\Gamma_4'}{|p'|} = \frac{\gamma\{\Gamma_4 - i\beta\Gamma\}}{|p + \beta[\beta p(\gamma - 1)/\beta^2 - p_0\gamma]|} = \frac{\Gamma_4}{|p|}, \qquad \gamma = \frac{1}{\sqrt{1-\beta^2}}$$

(we made use of the equation $\sum_\mu \Gamma_\mu p_\mu = 0$).

Let us denote the representation of the group of transformations Λ by U_Λ, so that $\psi = U_\Lambda \psi'$. We have shown that $\Sigma' = U_\Lambda^{-1}\Sigma U_\Lambda = \Sigma$, i.e., $[\Sigma, U_\Lambda] = 0$. This implies that the matrix U_Λ is diagonal with respect to the eigenvalues of Σ, and the state $|p, m\rangle$ goes over into

$$U_\Lambda |pm\rangle = \sum_{m'} |\Lambda p, m'\rangle Q_{m',m}(p, \Lambda) = |\Lambda p, m\rangle q(m, p) \tag{A.1}$$

for transformations Λ.

We now show that the diagonal elements $q(m, p)$ of the spinor part of the transformation U_Λ depend only on $|p|$.

The generator of U_Λ is an operator proportional to pN, so that

$$U_\Lambda = \exp i\{-\tanh^{-1}\beta(pN)/|p|\}.$$

The operator $p \cdot N$ is a three-dimensional scalar and, therefore, commutes with the three-dimensional rotation operators U_R. Hence

$$U_R U_\Lambda |pm\rangle = U_\Lambda U_R |pm\rangle$$

or*

$$R\Lambda p, m\rangle q(m, p) = |\Lambda Rp, m\rangle q(m, Rp), \tag{A.2}$$

from where we conclude

$$q(m, p) = q(m, Rp) \equiv q(m, |p|).$$

4. In conclusion we show that the proof of the equivalence of the irreducible representations of the ILG with the same values of κ^2 and Γ^2, given by Wigner,[14] can apparently be assumed to be valid for non-unitary representations as well. Wigner showed that an arbitrary representation is equivalent to the representation U_0, which is the product of the representation of some rotation within the "little group" (for particles with finite mass this group consists of the three-dimensional rotations in the space of wave functions with $p_0 = 0$) and a representation of the Lorentz transformation of the class Λ which acts only on the momentum variables [see formulas (67) and (67a) in reference 14]. More precisely, we have $Q^0_{m,m'} \times (p, \Lambda(p)) = \delta_{m,m'}$ for transformations $\Lambda(p)$ from the rest system to a system where the momentum of the particle is equal to p. If a given representation does not satisfy this requirement, then an equivalent representation which is obtained by a transformation which takes the function $\varphi(p, m)$ into

$$\sum_{m'} Q_{m,m'}(p_0, \Lambda^{-1}(p))\varphi(p, m')$$

does.

We emphasize that this transformation is among those generated by the operators (representing the transformations Λ) of the given representation.

For an arbitrary representation of the ILG one can thus find a transformation (not necessarily unitary) by which this representation is brought into the form (67a) of reference 14, which is identical for all representations.

*We fix the phases of states $|pm\rangle$ with different m by defining $|pm\rangle$ as

$$|pm\rangle = \sum_n |pn\rangle D_{n,m}(p),$$

with D(p) being the spinor part of U_R which depends on the Eulerian angles of rotation $\{-\pi, \vartheta, \pi - \varphi\}$, where ϑ and φ are the spherical angles of the momentum p in some fixed reference system, to which the projections n are also referred.[8] Then

$$U_R |pm\rangle = \sum_{n',n} |Rp, n'\rangle D_{n',n}(R) D_{n,m}(p)$$

$$= \sum_{n'} |Rp, n'\rangle D_{n',m}(Rp) = |Rp, m\rangle.$$

[1] Chou Kuang-Chao and M. I. Shirokov, JETP **34**, 1230 (1958), Soviet Phys. JETP 7, 851 (1958).
[2] Yu. M. Shirokov, JETP **35**, 1005 (1958), Soviet Phys. JETP **8**, 703 (1959).
[3] L. L. Foldy, Phys. Rev. **102**, 568 (1959). Yu. M. Shirokov, Dokl. Akad. Nauk SSSR **94**, 857 (1954).
[4] M. H. L. Pryce, Proc. Roy. Soc. **A195**, 62 (1948).
[5] Yu. M. Shirokov, JETP **21**, 748 (1951).
[6] H. P. Stapp, Phys. Rev. **103**, 425 (1957).
[7] T. D. Newton and E. P. Wigner, Revs. Modern Phys. **21**, 400 (1949).
[8] M. I. Shirokov, JETP **32**, 1022 (1957), Soviet Phys. JETP **5**, 835 (1957).
[9] M. Jacob and G. C. Wick, Ann. of Phys. **7**, 404 (1959).
[10] Chou Kuang-Chao, JETP **36**, 909 (1959), Soviet Phys. JETP **9**, 642 (1959).
[11] M. I. Shirokov, JETP **36**, 1524 (1959), Soviet Phys. JETP **9**, 1081 (1959).
[12] C. Møller, The Theory of Relativity, Oxford (1952).
[13] Yu. M. Shirokov, JETP **33**, 861 (1957), Soviet Phys. JETP **6**, 664 (1958).
[14] E. P. Wigner, Ann. Math. **40**, 149 (1939), Sec. 6C.
[15] Gel'fand, Minlos, and Shapiro, Представления группы вращений и группы Лоренца (Representations of the Rotation and Lorentz Groups), Gostekhizdat (1958).

Translated by R. Lipperheide
123

ON THE GROUND STATES OF ATOMIC NUCLEI. I

M. Ya. AMUS'YA

Leningrad Physico-Technical Institute, Academy of Sciences, U.S.S.R.

Submitted to JETP editor March 22, 1960

J. Exptl. Theoret. Phys. (U.S.S.R.) **39**, 639-650 (September, 1960)

A variational principle is formulated and applied to a many-particle system with two-particle interaction. The wave function is chosen in a form which permits exact account to be taken of pair correlation. Equations are obtained for one- and two-particle functions in the first approximation in the correlation. It is shown that these can easily be extended to the case of strong correlations and three-particle interactions. The results are applied to the case of the so-called nuclear matter. The equations obtained are compared with those of Brueckner.

1. FORMULATION OF THE VARIATIONAL PRINCIPLE

GREAT mathematical difficulties limit the solution of the many-body problem in its application to atomic nuclei, in particular, in the study of infinitely extended nuclear matter. In this case, it is always assumed that the methods developed for spatially infinite systems (see, for example, reference 1) can easily be extended to the case of finite systems.

Inasmuch as such an assumption is not self-evident, we shall from the beginning consider a system of finite volume, consisting of N interacting particles, and attempt to ascertain for what equilibrium density this system will be stable relative to spontaneous decrease in the volume. If we assume the interactions among the particles of the system to be given, then the total energy E will depend upon the particle density distribution $\rho(\mathbf{r})$ and the condition for stability is written as

$$\delta E/\delta\rho(\mathbf{r}) = 0 \tag{1}$$

or

$$\frac{\delta\left((\psi|\hat{H}|\psi) - E(\psi|\psi)\right)}{\delta\psi^*\psi} = 0, \tag{2}$$

where E is the total energy of the system.

It is evident that such a system, as for example a stable nucleus, can exist for an infinitely long time in the ground state, and consequently (1) and (2) are satisfied for it. Similar relations are not valid for excited states.

We shall now so particularize (2) that there is a possibility of taking into account the presence of two-particle correlations in the system. In this case we shall assume that the total energy depends not only on the single-particle wave functions φ_i (Hartree-Fock), but also on the pair correlation functions χ_{ik}, and requires that

$$\delta E/\delta\varphi_i = 0, \qquad \delta E/\delta\chi_{ik} = 0. \tag{3}$$

The first of these equations leads to an equation of the Hartree-Fock type, while the second permits us to consider direct interaction of pairs of particles and to make the Hartree-Fock method more precise.

If many-particle forces act in the system and it is necessary to take into account the effect of many-particle correlations, then (1) must be written in the form*

$$\sum_{i\leqslant F}\frac{\delta E}{\delta\varphi_i}\frac{\delta\varphi_i}{\delta\rho} + \sum_{i,k\leqslant F}\frac{\delta E}{\delta\chi_{ik}}\frac{\delta\chi_{ik}}{\delta\rho} + \sum_{i,k,l\leqslant F}\frac{\delta E}{\delta\eta_{ikl}}\frac{\delta\eta_{ikl}}{\delta\rho} + \ldots = 0. \tag{4}$$

Detailed consideration of (4) leads to a system of functional equations of the type (3), which represent interlocking equations for quasi-particles, pairs, etc.

However, we note that only the relations (1) and (2) follow from general considerations of the existence of a state which is stable relative to spontaneous decrease in the volume. The system (3) imposes a set of additional restrictions in comparison with (1) and (2).

2. EQUATIONS OF THE TYPE OF THE FOCK EQUATIONS

Let us consider a system consisting of N identical fermions and limit ourselves to the case in which the Hamiltonian of the system is described in the following fashion:

*$\leq F$ denotes summation over all occupied states and $>F$ over all free states.

$$\hat{H} = -\sum_{i=1}^{N} \Delta_i + \frac{1}{2} \sum_{i,k=1}^{N} V_{ik}, \qquad V_{ik} \equiv V(\mathbf{r}_i - \mathbf{r}_k). \tag{5}$$

We choose the wave function in the form

$$\psi = (N!)^{-1/2} A \prod_{i=1}^{N} \varphi_i(\mathbf{r}_i) \prod_{i<k}^{N} \chi_{ik}(\mathbf{r}_i, \mathbf{r}_k), \tag{6}$$

where A is the operator of anti-symmetrization.

Improvement of the Fock method is necessary only in the investigation of systems in which forces appear which are large in size and small in radius.

We assume that the presence of pair correlations in the motion of the particles χ_{ik} does not lead to the formation of bound complexes inside the system. Inasmuch as we shall be interested primarily in the explanation of the consequences following from the relations (1) and (2), we limit ourselves to the case of weak correlations. Representing χ_{ik} in the form[2] $1 + f_{ik}$, we keep in (6) only the terms of first order in f_{ik}:*

$$\psi = (N!)^{-1/2} A \prod_{i=1}^{N} \varphi_i(\mathbf{r}_i) \left(1 + \sum_{k<l} f_{kl}(\mathbf{r}_k, \mathbf{r}_l)\right). \tag{7}$$

In what follows we shall write down some qualitative considerations in favor of a similar approximation. We note that although terms like $f_{kl}f_{ij}$ possibly do not play a role in the calculation of the binding energy of such a system as an atomic nucleus, they are evidently important for the determination of the wave functions of the quasi-particles φ_i.

In the variation, the following additional conditions are imposed:

$$\int \varphi_i^*(\mathbf{r}) \varphi_k(\mathbf{r}) \, d\tau = \delta_{ik},$$

$$\int \varphi_k^*(\mathbf{r}) \varphi_l^*(\mathbf{r}') \varphi_f(\mathbf{r}) \varphi_n(\mathbf{r}') (1 + f_{fn}(\mathbf{r}, \mathbf{r}')) (1 + f_{kl}^*(\mathbf{r}, \mathbf{r}')) \, d\tau \, d\tau'$$
$$= C\delta_{kf}\delta_{ln}, \tag{8}$$

where i, l, f, k, $n \leq F$, and C is a normalization factor.

The second of the conditions (8) follows from the fact that all the levels in the ground state up to the boundary are filled. Therefore, distortion of the wave function of the pair $\psi_{ik} = \varphi_i\varphi_k(1 + f_{ik})$, due to the account of the two-particle interaction, can lead only to the appearance of components pertaining to the free states in the expansion of ψ_{ik} in φ_1, and consequently,

$$\int \varphi_k^*(\mathbf{r}) \varphi_l^*(\mathbf{r}') \varphi_f(\mathbf{r}) \varphi_n(\mathbf{r}') f_{fn}(\mathbf{r}, \mathbf{r}') \, d\tau d\tau' = 0, \tag{9}$$

where k, l, f, $n \leq F$, which also leads to the relation (8).

We introduce the notation

$$\psi^{(0)} = (N!)^{-1/2} A \Pi \varphi_k(\mathbf{r}_k), \tag{10}$$

$$\psi^{(1)} = (N!)^{-1/2} A \Pi \varphi_k(\mathbf{r}_k) \sum_{p<l} f_{pl}(\mathbf{r}_p, \mathbf{r}_l), \tag{11}$$

$$\psi^{(2)} = {}^1/_2 (N!)^{-1/2} A \Pi \varphi_k(\mathbf{r}_k) \sum_{\substack{p<l,\, i<j \\ ij \neq pl}} f_{pl}(\mathbf{r}_p, \mathbf{r}_l) f_{ij}(\mathbf{r}_i, \mathbf{r}_j). \tag{12}$$

Then the energy of the system, in first order in f_{ik}, is equal to

$$E = (\psi^{(0)} | \hat{H} | \psi^{(0)}) + (\psi^{(1)} | \hat{H} | \psi^{(0)}) + (\psi^{(0)} | \hat{H} | \psi^{(1)}). \tag{13}$$

However, the equations for the correlation functions can be obtained only by taking into account in the energy expression terms of second order in f and the change of the normalization of the wave function of the system:

$$E = \frac{(\psi^{(0)} | \hat{H} | \psi^{(0)}) + (\psi^{(1)} | \hat{H} | \psi^{(0)}) + (\psi^{(0)} | \hat{H} | \psi^{(1)})}{1 + (\psi^{(1)} | \psi^{(1)}) + (\psi^{(0)} | \psi^{(2)}) + (\psi^{(2)} | \psi^{(0)})}$$
$$+ \frac{(\psi^{(0)} | \hat{H} | \psi^{(2)}) + (\psi^{(2)} | \hat{H} | \psi^{(0)}) + (\psi^{(1)} | \hat{H} | \psi^{(1)})}{1 + (\psi^{(1)} | \psi^{(1)}) + (\psi^{(0)} | \psi^{(2)}) + (\psi^{(2)} | \psi^{(0)})}. \tag{14}$$

Denoting $\varphi_k(\mathbf{r})\varphi_l(\mathbf{r}')f_{kl}(\mathbf{r}, \mathbf{r}')$ and $\varphi_k(\mathbf{r})\varphi_p \times (\mathbf{r}')\varphi_l f_{kl}(\mathbf{r}, \mathbf{r}'')$ by $\overline{kl}$ and $\overline{kpl}$, respectively, we write down the matrix elements of first order in f in the form

$$(\psi^{(0)} | \hat{H} | \psi^{(0)}) = -\sum_{k=1}^{N} (k | \Delta_k | k) + \tfrac{1}{2} \sum_{i,k} (ik | V_{ik} | Aik), \tag{15}$$

$$(\psi^{(0)} | \hat{H} | \psi^{(1)}) = \sum_{k<l} (kl | -\Delta_k - \Delta_l + Q_{kl} V_{kl} | A\overline{kl})$$
$$+ \sum_{k;p<l} (kpl | V_{pk} + V_{kl} | Ak\overline{pl}), \tag{16}$$

$$(\psi^{(1)} | \hat{H} | \psi^{(0)}) = (\psi^{(0)} | \hat{H} | \psi^{(1)})^*, \tag{17}$$

where A is as before the anti-symmetrization operator, and Q_{kl} is a projection operator with the following property:

$$Q_{kl} U(\mathbf{r}\mathbf{r}') = \varphi_k(\mathbf{r}) \varphi_l(\mathbf{r}') (kl | U) + \sum_{i<F} \varphi_k(\mathbf{r}) \varphi_i(\mathbf{r}') (ki | U)$$
$$+ \sum_{j>F} \varphi_j(\mathbf{r}) \varphi_l(\mathbf{r}') (jl | U) + \sum_{i,j>F} \varphi_j(\mathbf{r}) \varphi_i(\mathbf{r}') (ji | U). \tag{18}$$

In the expression for the energy the operator Q_{kl} is unimportant, since the matrix element in (16) does not depend on the presence of Q. The latter appears by virtue of the anti-symmetry of the initial wave function and the symmetry of $\sum_{i,k} V_{ik}$. Actually,

*Investigation of the properties of pair correlations in the case of nuclear matter, carried out by the Brueckner method in the work of Gomes et al.,[3] has shown that for pair interaction with repulsive cores of radius 0.4×10^{-13} cm χ_{ik} depends only on $\mathbf{r}_i - \mathbf{r}_k$ and differs essentially from unity for $\mathbf{r}_i - \mathbf{r}_k \approx (1 \text{ to } 1.5) \times 10^{-13}$ cm.

$$\frac{1}{2}\sum_{i,k}^{N} V_{ik}\,\psi^{(1)} = A\prod_{k=1}^{N}\varphi_k(\mathbf{r}_k)\sum_{p<q}^{N} V_{pq} f_{pq}(\mathbf{r}_p, \mathbf{r}_q)$$
$$+ A\prod_{k=1}^{N}\varphi_k(\mathbf{r}_k)\sum_{\substack{i<k,\ p<q,\\ ik\neq pq}} V_{ik} f_{pq}(\mathbf{r}_p, \mathbf{r}_q). \qquad (19)$$

The presence of the operator A permits us to rewrite the first term of (19) in the form

$$A\Pi\varphi_k(\mathbf{r}_k)\sum_{p<q}^{N} Q_{pq} V_{pq} f_{pq}(\mathbf{r}_p, \mathbf{r}_q),$$

which also leads to the appearance of Q_{kl} in (19). The remaining matrix elements are computed and listed in the Appendix.

Varying (14) with respect to φ^* and f*, a system of interlocking equations can be obtained which permits us to find φ and f.

We introduce the following notation: the Hartree-Fock Hamiltonian

$$H_p^{HF} = -\Delta_p + \sum_k \int d\mathbf{r}'\,\varphi_k^*(\mathbf{r}')\,V(\mathbf{r}-\mathbf{r}')\,A\varphi_k(\mathbf{r}'),$$

the Hamiltonian of Bethe-Goldstone[4]

$$H_{pq}^{BG} = -\Delta_p - \Delta_q + Q_{pq}V(\mathbf{r}-\mathbf{r}')$$
$$+ \sum_k \int d\mathbf{r}''\,\varphi_k^*(\mathbf{r}'')\,(V(\mathbf{r}-\mathbf{r}'') + V(\mathbf{r}'-\mathbf{r}''))\,A\varphi_k(\mathbf{r}'')$$

and the Hamiltonian

$$H_{kpq} = -\Delta_k - \Delta_p - \Delta_q + Q_{kpq}(V(\mathbf{r}-\mathbf{r}') + V(\mathbf{r}-\mathbf{r}'')$$
$$+ V(\mathbf{r}'-\mathbf{r}'')) + \sum_l \int d\mathbf{r}'''\,\varphi_l^*(\mathbf{r}''')\,(V(\mathbf{r}-\mathbf{r}''')$$
$$+ V(\mathbf{r}'-\mathbf{r}''') + V(\mathbf{r}''-\mathbf{r}'''))\,A\varphi_l(\mathbf{r}'''),$$

where Q_{kpq} is the operator which projects the function of three variables on the level k, p, q and on the level lying outside the Fermi sphere F. For ψ_{pq} we obtain*

$$H_{pq}^{BG}\psi_{pq} + \Big\{\sum_k (k\,|\,H_{kpq}\,|\,A(\overline{kpq} + \overline{kpq}))\Big\} + \text{compl. conj.}\Big\}$$
$$+ \Big[\sum_{k<l}(kl\,|\,V_{lq} + V_{pk}\,|\,A\,\overline{kl}\,pq)$$
$$+ \text{compl. conj.}\Big] = \varepsilon_{pq}\,\psi_{pq}. \qquad (20)$$

The meaning of the different terms entering into the equation is easily understood. The first term is the left side of the Bethe-Goldstone equation;[4] it describes the direct action of the pair pq moving in a self-consistent field created by the remaining particles of the system. The term in the curly brackets takes into account the effect of the direct interaction of the pairs pk and qk, moving in the self-consistent field generated by the remaining particles, on the pair pq under consideration. It is significant that this effect is described by the functions f_{pk} and f_{kq}. The last term describes the action of the remaining pairs k*l* on the isolated pair pq.

If all $f_{ik} = 0$ except f_{pq}, then we obtain from (20) the Bethe-Goldstone equation:[4]

$$H_{pq}^{BG}\,\psi_{pq} = \varepsilon_{pq}\psi_{pq}. \qquad (21)$$

This corresponds to the fact[3] that the Bethe-Goldstone equation* can be obtained if the interaction of the pair under discussion is considered exactly and it is assumed that the remaining particles move independently (in the sense of an absence of correlation). Their effect on the pair is reduced to the formation of a self-consistent potential.

We now consider the equation for φ obtained by variation of (13) with respect to φ_p^*:

$$H_p^{HF}\varphi_p + \Big[\sum_k (k\,|\,H_{kp}^{BG} - \varepsilon_{kp}\,|\,A\overline{kp}) + \text{compl. conj.}\Big]$$
$$+ \Big\{\sum_{k<l}(kl\,|\,V_{pk} + V_{pl}\,|\,Ap\overline{kl})$$
$$+ \text{compl. conj.}\Big\} = E_p\varphi_p. \qquad (22)$$

The first term in (22) is the left hand side of the usual Hartree-Fock equation, since the term in the square brackets takes into account the effect of direct interaction of the particles p and k moving in a self-consistent field created by the remaining particles. We note that, as in (20) for three particles, the effect of direct interaction in (22) for two particles is determined by the function f_{kp}. Finally, the last term describes the action of the pair correlations of any two particles on the considered third particle p.

An important advantage of these equations is the comparative ease of their generalization to the case of the presence of three-particle forces or considerable pair correlations, when it is necessary to take into account some higher power of f. Actually, it is easy to write down Eq. (20) in a form in which generalization to the case of three-particle potentials is trivial. In our approximation, the three-particle function has the form

$$\psi_{ikl} = \varphi_i\varphi_k\varphi_l(1 + f_{ik} + f_{il} + f_{kl}). \qquad (23)$$

With account of this formula, we can write down (20) in the form

*The complex-conjugate terms differ from those written out by the fact that the correlation functions enter at the left; for example, compl. conj. in the square brackets in (20) means

$$(\overline{kl}\,|\,V_{lq} + V_{pk}\,|\,Aklpq).$$

*It is equivalent to the equation for the t-matrix of Brueckner [see (29) in reference 4].

$$H_{pq}^{BG}\psi_{pq}+\sum_k(\varphi_k\,|\,H_{kpq}\,|\,A(\psi_{kpq}-\varphi_k\psi_{pq}))$$
$$+\sum_{k<l}[(\varphi_k\varphi_l\,|\,V_{ql}+V_{pk}\,|\,A\varphi_p\varphi_q(\psi_{kl}-\varphi_k\varphi_l))$$
$$+\text{compl. conj.}]=\varepsilon_{pq}\psi_{pq}$$
$$+(1/\varphi_p^*\varphi_q^*)\sum_k(\psi_{pq}\varphi_k-\psi_{kpq}\,|\,H_{kpq}\,|\,A\varphi_k\varphi_p\varphi_q). \qquad (24)$$

Introduction of three-particle interaction leads to an evident change in the Hamiltonian H_p^{HF}, H_{pq}^{BG}, H_{kpq}. The following equation, which is necessary for the determination of ψ_{kpq}, can be written down by analogy with (24).

Just as for (20), we write Eq. (22) in the form

$$H_p^{HF}\varphi_p+\sum_k(\varphi_k\,|\,H_{kp}^{BG}-\varepsilon_{kp}\,|\,A(\psi_{kp}-\varphi_k\varphi_p))$$
$$+\sum_{k<l}[(\varphi_k\varphi_l\,|\,V_{pk}+V_{pl}\,|\,A\varphi_p(\psi_{kl}-\varphi_k\varphi_l))$$
$$+\text{compl. conj.}]=E_p\varphi_p$$
$$+(1/\varphi_p^*)\sum_k(\varphi_k\varphi_p-\psi_{kp}\,|\,H_{kp}^{BG}-\varepsilon_{kp}\,|\,A\varphi_k\varphi_p). \qquad (25)$$

In conclusion we note that in this section we have actually dealt with quasi-single-particle functions. Actually, in accord with (22), account of correlations in first order leads to the appearance of terms which depend on momentum (of the type of the effective mass M_{eff}), and to the replacement of the two-particle interaction V by V_{eff}. We shall assume that $f_{ik}=f_{ik}^*$. Then (22) takes the form

$$\Big\{-\frac{1}{2}\Big(\Delta\,\frac{1}{\mu_p^{eff}}+\frac{1}{\mu_p^{eff}}\,\Delta\Big)$$
$$+\sum_k\int d\mathbf{r}'\,\varphi_k^*(\mathbf{r}')\,V_{kp}^{eff}(\mathbf{r}\mathbf{r}')\,\varphi_k(\mathbf{r}')-E_p\Big]\varphi_p(\mathbf{r})=0,$$

$$\frac{1}{\mu_p^{eff}}=\frac{M}{M_p^{eff}}=1+2\sum_k\int|\varphi_k(\mathbf{r}')|^2 f_{kp}(\mathbf{r}'\mathbf{r})\,d\mathbf{r}',$$

$$V_{kp}^{eff}=V_{kp}\Big\{A+f_{kp}A+Af_{kp}+\sum_l[(\varphi_l f_{lp}\,|\,\varphi_l)A$$
$$+(\varphi_l\,|\,\varphi_l Af_{lp})+(\varphi_l\,|\,\varphi_l f_{kl})A+(\varphi_l\,|\,\varphi_l Af_{kl})]\Big\}$$
$$-f_{kp}(\Delta_k+\varepsilon_{pk})A-(\Delta_k+\varepsilon_{pk})Af_{kp}$$
$$+\sum_l[(\varphi_l\,|\,V_{lk}\,|\,f_{kp}A\varphi_l)+(\varphi_l\,|\,V_{lk}\,|\,Af_{kp}\varphi_l)]. \qquad (22a)$$

Hence it is clear that account of pair correlations in finite systems leads simultaneously to mass "renormalization" and two-particle interaction, while, roughly speaking, $V_{eff}/V\approx M/M_{eff}$, in accord with the fact that introduction of the effective mass requires a change in the depth of the potential well in the relation written down, as is well known.

3. NUCLEAR MATTER

An approach was developed by a number of authors to the solution of the many-body problem which is known as the Brueckner approximation, which takes pair interactions between the particles into account, in more exact fashion than in the Hartree-Fock method. Let us consider the problem of the relationship of the Brueckner method to our variational principle (22) and compare the equations of reference 1 with those obtained in the present work.

According to Brueckner, the expression for the energy of a system of particles with the Hamiltonian (5) can be described,[1] after some simplification, in the form

$$E=-\sum_{i=1}^{N}(i\,|\,\Delta\,|\,i)+\frac{1}{2}\sum_{i,k=1}^{N}(ik\,|\,t\,|\,Aik),$$
$$(ik\,|\,t\,|\,lq)=(ik\,|\,V\,|\,lq)+\sum_{s,\,p>F}\frac{(ik\,|\,V\,|\,sp)\,(sp\,|\,t\,|\,lq)}{E_t+E_q-E_s-E_p},$$
$$E_l=-(l\,|\,\Delta\,|\,l)+\sum_{q\leqslant F}(lq\,|\,t\,|\,Alq). \qquad (26)$$

In the process of constructing the Brueckner equation for finite nuclei, it is assumed that solutions of the equation

$$\Delta\varphi_i+\int(\mathbf{r}\,|\,U\,|\,\mathbf{r}')\,\varphi_i(\mathbf{r}')\,d\tau'=E_i\varphi_i(\mathbf{r}) \qquad (27)$$

form a complete set of basis functions and the self-consistent nonlocal potential is chosen from the condition of vanishing of the contribution of terms of second order in the expansion of the energy of the system in t:

$$(\varphi_i\,|\,U\,|\,\varphi_i)=\sum_{k\leqslant F}(ik\,|\,t\,|\,Aik). \qquad (28)$$

We introduce the operator R, for which t = VR, and denote $R\varphi_i\varphi_k=\psi_{ik}$. Then, inasmuch as

$$\int(\mathbf{r}\,|\,U\,|\,\mathbf{r}')\,\varphi_k(\mathbf{r}')\,d\tau'=\sum_{i\leqslant F}\int\varphi_i^*(\mathbf{r}')\,(\mathbf{r}',\,\mathbf{r}\,|\,t\,|\,Aik)\,d\tau',$$
$$(\mathbf{r},\,\mathbf{r}'\,|\,t\,|\,Aik)=V(\mathbf{r}-\mathbf{r}')\,\psi_{ik}(\mathbf{r},\,\mathbf{r}'), \qquad (28a)$$

we find a set of interlocking equations [by transforming in (26) to a mixed representation] which connect the one- and two-particle functions.*

$$-\Delta\varphi_i+\sum_{k\leqslant F}\int d\tau'\varphi_k^*(\mathbf{r}')\,V(\mathbf{r}-\mathbf{r}')\,\psi_{ik}(\mathbf{r},\,\mathbf{r}')=E_i\varphi_i,$$
$$\psi_{ik}(\mathbf{r},\,\mathbf{r}')=A\varphi_i(\mathbf{r})\,\varphi_k(\mathbf{r}')+\sum_{q,\,l>F}\int d\tau''d\tau'''$$
$$\times\frac{\varphi_q(\mathbf{r})\,\varphi_l(\mathbf{r}')\,\varphi_q^*(\mathbf{r}'')\,\varphi_l^*(\mathbf{r}''')}{E_i+E_k-E_q-E_l}\,V(\mathbf{r}''-\mathbf{r}''')\,\psi_{ik}(\mathbf{r}'',\,\mathbf{r}'''). \qquad (29)$$

*It can be shown that the second equation of (29) coincides with the Bethe-Goldstone equation.[4]

The first equation of the set (29) is similar to the Hartree-Fock equation, but it cannot be obtained by the Fock variational principle from the equation for the energy of the system.

Actually, by varying E with respect to φ_i^*, we would have obtained the equation

$$-\Delta\varphi_i + \sum_{k\leqslant F}\int d\tau'\,\varphi_k^*(\mathbf{r}')\,V(\mathbf{r}-\mathbf{r}')\,\psi_{ik}(\mathbf{r},\mathbf{r}') + \tfrac{1}{2}\sum_{k,\,q\leqslant F}\int d\tau' d\tau''\varphi_k^*(\mathbf{r}')\,\varphi_q^*(\mathbf{r}'')\,V(\mathbf{r}'-\mathbf{r}'') \times \frac{\delta\psi_{ik}(\mathbf{r}',\mathbf{r}'')}{\delta\rho(\mathbf{r})}\frac{\delta\rho(\mathbf{r})}{\delta\varphi_i(\mathbf{r})} = E_i\varphi_i, \tag{30}$$

which differs from (29) by a term which has been given the name "rearrangement potential" in the literature.

If the wave function is determined from (30), then the initial assumption (28) is generally violated; according to this assumption one can neglect terms of second order in t and in place of (26) there would be introduced another expression for the total energy. Estimates of the term arising because of the dependence of the t-matrix on the density of nuclear matter, carried out by Brueckner,[5] show that it is approximately equal to 10-15 Mev, and consequently it cannot be neglected.

We shall now consider to what the variational principle (2) leads for the case of nuclear matter, where, as follows from general considerations connected with the absence of a singularity in the system with the Hamiltonian (5), the correlation functions $f_{ik}(\mathbf{r}_i, \mathbf{r}_k)$ depend only on the difference $\mathbf{r}_i - \mathbf{r}_k$, while the quasi-single-particle functions are plane waves. In this case, as is not difficult to show, we have in place of (9),

$$\int \varphi_k^*(\mathbf{r})\,\varphi_i(\mathbf{r})\,f_{il}(\mathbf{r},\mathbf{r}')\,d\tau = 0, \tag{31}$$

and the action of the projection operator on a function depending on the difference in the coordinates is now determined by the relation

$$Q_{kl}W(\mathbf{r}-\mathbf{r}') = \varphi_k(\mathbf{r})\,\varphi_l(\mathbf{r}')\,(kl\,|\,W) + \sum_{i,\,j>F}\varphi_i(\mathbf{r})\,\varphi_j(\mathbf{r}')\,(ij\,|\,W), \tag{32}$$

which takes the place of (18).

The relation (31)shows that the matrix element corresponding to graphs of the type of Fig. 1 with free ends, corresponding to correlation functions,* do not make a contribution, in the case of nuclear matter, to the expression for the total energy of the system. The latter, in accord with (15), (16), and (17), is equal to

*A description of graphical techniques is given in the Appendix.

$$E = -\sum(k\,|\,\Delta\,|\,k) + \sum_{i<k}[(ik\,|\,V_{ik}\,|\,Aik) + (ik\,|\,V_{ik}\,|\,\overline{ik}) + \text{c. c.}]. \tag{33}$$

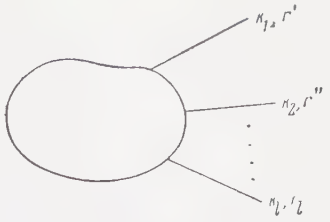

FIG. 1

This expression is essentially in agreement with (26) if we take into account (28a).

From (15), (16), (17), and (33) we find equations for φ_i and ψ_{ik} which we write in a form suitable for comparison with (29):

$$-\Delta\varphi_i + \sum_{k\leqslant F}(\varphi_k(\mathbf{r}')\,|\,V(\mathbf{r}-\mathbf{r}')(1+f_{ik}^*(\mathbf{r},\mathbf{r}'))\,|\,A\psi_{ik}(\mathbf{r},\mathbf{r}')) = E_i\varphi_i, \tag{34}$$

$$H_{ik}^{BG}\psi_{ik} = \varepsilon_{ik}\psi_{ik} - \sum_p\{(p\,|\,V_{ip}\,|\,A\overline{pik}) + (p\,|\,V_{kp}\,|\,A\overline{pik}) + \text{c. c.}\}. \tag{35}$$

Hugenholtz[6] has shown that the Brueckner method is valid in the approximation of small particle distribution density in the system if a number of assumptions are made whose validity is questionable. We have made use of the assumption of the smallness of the correlation functions. This is obviously equivalent to the approximation of low density,* inasmuch as the latter reduces to elimination of the possibility of simultaneous direct action of more than two particles.

However, it is seen that even in the approximation under consideration for wave functions of pairs an equation is obtained which differs somewhat from (21) [it can be shown that (21) is equivalent to (29)]. The complementary terms in (35), in comparison with (21), have a very clear physical meaning; for example, the first term in the curly brackets describes the change of the self-consistent field acting on the particle i as a result of correlations between the moving particles k and p.

It seems to us that the form of Eq. (35) strengthens the validity of the doubts raised by Hugenholtz,[6,7] inasmuch as there are no very weighty arguments for the elimination of the additional terms in (35), except for, in our view, not very convincing general remarks which reduce

*If we denote the momentum of the Fermi system by k_F and the effective radius of the two-particle interaction by r_0, then by the approximation of low density is understood an approximation which is valid for $k_F r_0 \ll 1$.

to the fact that, inasmuch as the wave function of the pair ψ_{ik} differs markedly from the product of one-particle functions only at small values of $\mathbf{r} - \mathbf{r}'$ (see reference 3), the remaining particles act on the given pair as free particles and, consequently, the term in the curly brackets in (35) should be thrown out.

Comparison of (35), (20), and (21) shows that the method developed by Brueckner is valid only for spatially infinite systems and the application of it to finite systems requires not only the replacement of quasi-one-particle functions by functions of finite systems (oscillator and so forth, as was done, for example by Banerjee and Roy,[8] and by Eden and Emery[9]) but also an important change in the fundamental equations — the substitution of (34) and (35) for (20) and (22).

4. SATURATION OF NUCLEAR FORCES AND THE VARIATIONAL PRINCIPLE (2)

It is known from experiment that the energy entering into a single nucleon in the nucleus E_{av} and the mean density of nuclear matter ρ_{av} do not depend on the number of nucleons in the nucleus N and are equal to 8 Mev and 2×10^{38} cm^{-3}, respectively. For nuclear matter, by virtue of the infinite volume of the system Ω, we have as $\Omega \to \infty$*

$$\frac{\partial E_{av}}{\partial N} = \frac{1}{\Omega}\frac{\partial E_{av}}{\partial \rho} \to 0, \qquad \frac{\partial \rho_{av}}{\partial N} = \frac{1}{\Omega} - \frac{\rho}{\Omega}\frac{\partial \Omega}{\partial N} \to 0,$$
$$(\rho = \rho_{av} = N/\Omega). \tag{36}$$

If the interaction between the particles is given, then $E = E(\rho)$ and for a fixed number of particles we have for the ground state

$$\left.\frac{\partial E}{\partial \rho}\right|_N = 0,$$

that is, $\partial E_{av}/\partial \rho = 0$ and $\partial E_{av}/\partial N = 0$ not only when $\Omega \to \infty$. It is thus seen that the requirement $\partial E_{av}/\partial \rho = 0$, which usually figures in researches on nuclear matter, follows from the condition for the existence of a stable configuration of nuclear matter which is distributed over all space with the same density. This requirement for nuclear matter coincides with the experimental observed independence of E_{av} on the number of nucleons in the nucleus.

We note that the variational principle (2) does not guarantee saturation of nuclear forces and density, for finite systems, in the sense of independence of E_{av} and ρ_{av} of the number of nucleons in the nucleus. The satisfaction of (2) speaks only of the existence of a stable state of the system with a finite number of particles in a spatially limited volume.

For example, (2) can be valid also for forces entering into the "collapse" (contraction) of nuclei. Satisfaction of the same conditions $\partial E_{av}/\partial N \approx 0$ and $\partial \rho_{av}/\partial N \approx 0$ depends on the specific character of the nuclear forces.

CONCLUSION

The reliability of the approximation of weak correlation used by us depends on how the forces act between the nucleons in the nucleus. Data on nucleon-nucleon scattering in the range from 2 to 300 Mev can be interpreted with the aid of various potentials: the potentials of Signel and Marshak, of Gammel-Christian-Teller, of Gammel-Teller. The latter is widely used in the researches of Brueckner and his co-workers. The characteristic of this potential lies in the introduction of infinitely strong repulsions at small distances ($r \leq 0.5 \times 10^{-13}$ cm). In the present research, we have essentially limited ourselves to the qualitative side of the problem, not touching on the possibility of the use of Eqs. (21), (22), (33), and (34) for calculation of the ground state of a system of nucleons interacting, for example, through a Gammel-Teller potential. A more detailed investigation of the resultant equations, and also a concrete calculation will be given in a subsequent paper.

Moreover, we have assumed from the beginning that pair correlations do not lead to the formation of bound states. Bound states, for example, in infinite nuclear matter, are characterized by the fact that not $f(\mathbf{r}_1 - \mathbf{r}_2)$, but $\chi(\mathbf{r}_1 - \mathbf{r}_2) \to 0$ for $\mathbf{r}_1 - \mathbf{r}_2 \to \infty$. Therefore, account of bound pairs, say in the region of the Fermi surface, would have required for the model under consideration the use of the correlation functions χ and not f.

The impression can be created that the superposition of a large number of conditions $\delta E/\delta \chi_{ik} = 0$ makes the system redefined. However, if we assume approximately that all correlation functions are identical, then in place of $N(N-1)$ there will be only a single additional condition, and the equations (21), (22), (33), (34) are essentially unchanged. One of the achievements of the method considered is the ease of generalization to the case of strong correlations, many-particle interactions (24) and (25) of systems composed of particles of several sorts, α, β, . . . , etc.

In the latter case, it is necessary to require

$$\delta E/\delta \rho_\alpha = \delta E/\delta \rho_\beta = \ldots = 0, \qquad \delta E/\delta \varphi_i^{(\alpha)} = \delta E/\delta \varphi_i^{(\beta)} = \ldots = 0,$$
$$\delta E/\delta \chi_{ik}^{\alpha)} = \delta E/\delta \chi_{ik}^{(\beta)} = \ldots = 0. \tag{37}$$

*The density of nuclear matter is equal to the mean density of finite nuclei.

in place of (1) and (3). Violation of (37) in the ground state of atomic nuclei leads to spontaneous conversion $-\beta^{\pm}$, α decays, and fission.

In conclusion we note that the application of the variational principle (2) to boson systems with two- and many-particle interactions makes it possible to obtain equations for them of the type (20), (22), (24) and (25).

I take it my pleasant duty to express my deep gratitude to Professor L. A. Sliv for numerous discussions and valuable remarks, and also to G. M. Sklyarevskiĭ and B. L. Birbrair for discussion of the results.

APPENDIX

For the matrix element $(\psi^{(1)} | H | \psi^{(1)})$, we find

$$(\psi^1|\hat{H}|\psi^{(1)}) = -\sum_{p<q}(\overline{pq}|\Delta_p+\Delta_q|A\overline{pq})$$

$$-\sum_{\substack{p<q\\k\neq p,q}}(k|\Delta|k)(\overline{pq}|A\overline{pq})$$

$$-\sum_{p<q,k}(k\overline{pq}|\Delta_k+\Delta_p+\Delta_q|A\overline{kp}\,q)$$

$$-\sum_{k,p<q}(k\overline{pq}|\Delta_k+\Delta_p+\Delta_q|A\overline{kpq})$$

$$-\sum_{\substack{i\neq p,q,k\\p<q,k}}(i|\Delta|i)(k\overline{pq}|A\overline{kpq})-\sum_{\substack{i\neq p,q,k\\k,p<q}}(i|\Delta|i)(k\overline{pq}|A\overline{kpq})$$

$$+\sum_{p<q}(\overline{pq}|V_{pq}|A\overline{pq})+\sum_{\substack{i<k;\ p<q\\ik\neq pq}}(ik|V_{ik}|Aik)(\overline{pq}|A\overline{pq})$$

$$+\sum_{k,p<q}(k\overline{pq}|V_{kp}+V_{kq}|Ak\overline{pq})$$

$$+\sum_{\substack{i<k;\ p<q,l\\ik\neq p,q,l}}(ik|V_{ik}|Aik)(l\overline{pq}|A\overline{lp}\,q)$$

$$+\sum_{\substack{i<k;l,p<q\\i,k\neq p,q,l}}(ik|V_{ik}|Aik)(l\overline{pq}|A\overline{lpq})$$

$$+\sum_{k,\ p<q}(k\overline{pq}|V_{kp}+V_{pq}+V_{qk}|A\overline{kpq})$$

$$+\sum_{p<q,\,k}(k\overline{pq}|V_{kp}+V_{pq}+V_{qk}|A\overline{kp}\,q)$$

$$+\sum_{p<q,\,k<l}(k\overline{pq}\,l|V_{kl}+V_{pl}+V_{ql}|A\overline{kp}\,ql)$$

$$+\sum_{k,p<q<l}(k\overline{pq}\,l|V_{kl}+V_{pl}+V_{ql}|A\overline{kpq}l)$$

$$+\sum_{q<p,\,k<l}(\overline{kpq}\,l|V_{kl}+V_{pq}|Ak\overline{pql}).$$

It is convenient to associate a graph with each matrix element, introducing the corresponding graphical form for the different functions and corresponding operators entering into the expression for the matrix element. We shall denote the correlation function $f_{pl}(\mathbf{r}, \mathbf{r}')$ by a solid line directed from $\mathbf{r}'$ to $\mathbf{r}$ (see Fig. 2), the complex conjugate function $f^*_{pl}(\mathbf{r}, \mathbf{r}')$ by a solid line directed from $\mathbf{r}$ to $\mathbf{r}'$. The potential $V(\mathbf{r}-\mathbf{r}')$ will be expressed by a wavy line, and the Laplace operator Δ by a dashed line.

The matrix element

$$(k\overline{pq}|\Delta_k+\Delta_p+\Delta_q|A\overline{kpq})$$

is described by the graph of Fig. 3a, and the matrix element

$$(k\overline{pq}|V_{kp}+V_{pq}+V_{qk}|A\overline{kpq})$$

by the graph of Fig. 3b. The matrix element $(ik \mid V_{ik} \mid A_{ik})\,(\overline{pq} \mid A \mid \overline{pq})$ corresponds to the unconnected graph of Fig. 4.

Consideration of the matrix elements makes it possible to formulate a number of rules with whose help it is possible to construct the expression for the energy of the system of N particles with account of corrections of second, third and higher degrees in the correlation functions.

1. Graphs determining the energy of the system contain not more than $2(N-1)$ straight lines, the vertex index p and its coordinate $\mathbf{r}$ are the same for all lines entering the vertex.

2. In each graph there is not more than one wavy or dashed line.

3. Graphs with disconnected straight lines are equal to zero.

4. Summation in the expression of the energy is carried out over all indices encountered in the diagram, and integration over the coordinates of the end lines.

5. Closed loops of solid lines are possible only in those cases in which it is possible with account

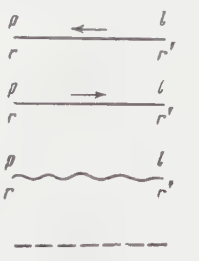

FIG. 2

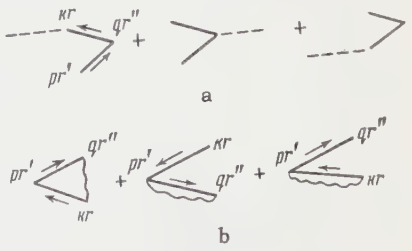

FIG. 3

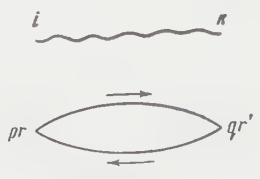

FIG. 4

FIG. 5

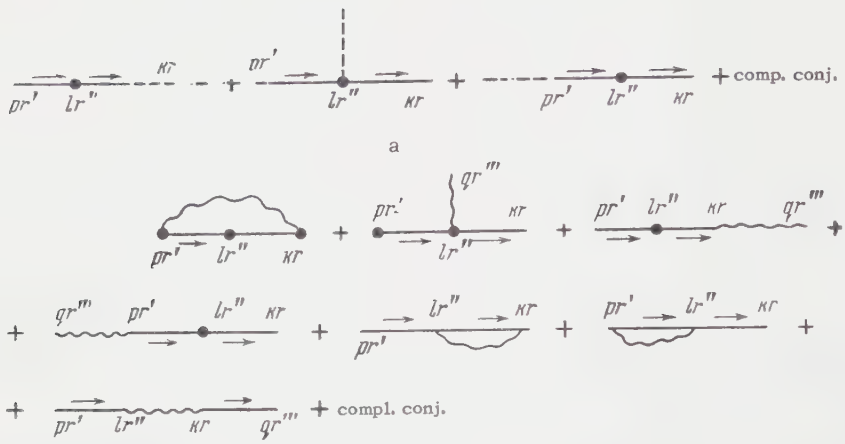

FIG. 6

of the direction of the lines to form a closed contour with a definite direction of rotation — in the clockwise direction or the reverse.

6. To each index k and coordinate **r** of the end of the line there corresponds $\varphi_k(\mathbf{r})$ and $\varphi_k^*(\mathbf{r})$. The correlation functions directed to the right and the product of all functions φ corresponding to a given graph are anti-symmetrized.

7. Graphs with unconnected wavy and dashed lines do not, in any case for large systems, make any contribution to the expression for the energy since they correspond to normalization of the complete wave function of the system.

8. If the graph consists of several disconnected parts, then summation in each part is carried out independently; however, in each term of the sum the disconnected parts do not keep the same indices.

Making use of rules 1 — 8, it is possible to establish the fact that graphs containing disconnected correlation parts of the type of Fig. 5 do not have to be taken into account in the computation of the energy since they correspond to normalization of the wave function of the ground state.

Thus, the situation here is similar to quantum field theory where the vacuum-vacuum transitions do not change the propagation function.

Higher degrees of correlation functions f take into account the change of the energy of the system as the result of finding three or more particles close to one another.

The matrix element $(\psi^{(2)}|\hat{H}|\psi^{(0)}) + (\psi^{(0)}|\hat{H}|\psi^{(2)}) = T^{(2)} + U^{(2)}$ is represented by the graph of Fig. 6 ($T^{(2)}$ corresponds to the graph of Fig. 6a; $U^{(2)}$ to the graph of Fig. 6b; we have omitted the disconnected graphs). Making use of rules 1 — 8, it is easy to write down the analytic expressions for $T^{(2)}$ and $U^{(2)}$.

[1] K. A. Brueckner and J. L. Gammel, Phys. Rev. **109**, 1023 (1958).

[2] A. De-Shalit and V. F. Weisskopf, Ann of Phys. **5**, 282 (1958).

[3] Gomes, Waleska, and Weisskopf, Ann of Phys. **3**, 241 (1958).

[4] H. A. Bethe and G. Goldstone, Proc. Roy. Soc. (London) **A238**, 551 (1956).

[5] K. A. Brueckner, Phys. Rev. **110**, 597 (1958).

[6] N. M. Hugenholtz, Physica **23**, 533 (1957).

[7] N. M. Hugenholtz, Physica **23**, 481 (1957).

[8] M. Banerjee and B. Roy, Ann of Phys. **7**, 484 (1959).

[9] R. Eden and V. Emery, Proc. Roy. Soc. (London) **A248**, 266 (1958); **A253**, 177, 186 (1959).

Translated by R. T. Beyer
124

THEORY OF RELAXATION OF THE MAGNETIC MOMENT IN FERROMAGNETIC MATERIALS

V. G. BAR'YAKHTAR and S. V. PELETMINSKIĬ

Physico-Technical Institute, Academy of Sciences, Ukrainian S.S.R.

Submitted to JETP editor March 23, 1960

J. Exptl. Theoret. Phys. (U.S.S.R.) 39, 651-656 (September, 1960)

The relaxation of the magnetic moment of a ferromagnetic material is considered. It is shown that because of sd-exchange interaction between spin waves and conduction electrons, there is first established a quasi-equilibrium distribution of spin waves and conduction electrons with a definite nonequilibrium value of the projection of the magnetic moment along the axis of easiest magnetization. Then because of weak relativistic spin-orbit interaction, there is gradually established an equilibrium value of this quantity. The relaxation time of the projection of the magnetic moment along the axis of easiest magnetization is independent of temperature and of order of magnitude 10^{-8} to 10^{-9} sec.

1. Kinetic and relaxation phenomena in ferromagnetic materials are determined by various processes of interaction of spin waves with conduction electrons and with one another. In the temperature range

$$\Theta_c \gg T \gg 4\Theta_c (Ja/\hbar v_0)^2$$

(Θ_c is a quantity of the order of magnitude of the Curie temperature, J is the sd-exchange integral, a is the lattice constant, and v_0 is the limiting Fermi velocity), the strongest interaction is the sd-exchange interaction of spin waves and conduction electrons; because of it, there is established a quasi-equilibrium distribution of conduction electrons and spin waves, corresponding to a definite value of the magnetic moment of the body.

The transition to the equilibrium value of the magnetic moment is caused by a relativistic spin-orbit interaction of spin waves and conduction electrons. This interaction is weak in comparison with the sd-exchange interaction, and therefore the relaxation of the magnetic moment proceeds slowly in comparison with the process of establishment of the quasi-equilibrium distribution functions.

2. We shall use a model of a ferromagnet that starts with the concept of two groups of electrons — the conduction electrons (s electrons) and the ferromagnetic d electrons.[1] The s and d electron interaction energy operator is the sum of a Hamiltonian $\mathcal{H}_1$, which describes the exchange interaction between s and d electrons, and a Hamiltonian $\mathcal{H}_2$, which describes the interaction of the magnetic moment $\mathbf{M}(\mathbf{r}, t)$ of the d electrons with the conduction-electron current $\mathbf{j}(\mathbf{r}, t)$.

The Hamiltonian $\mathcal{H}_1$ has the form

$$\mathcal{H}_1 = \mu \int \varphi^+(\mathbf{r}, t)\, \sigma\, \varphi(\mathbf{r}, t)\, \mathbf{H}^{(e)}(\mathbf{r}, t)\, d\mathbf{r}, \qquad (1)$$

where μ is the Bohr magneton, σ is the spin operator of a conduction electron, φ^+ and φ are the creation and absorption operators of a conduction electron, and $\mathbf{H}^{(e)}$ is the exchange magnetic field, equal to

$$\mathbf{H}^{(e)}(\mathbf{r}, t) = \int J(\mathbf{r} - \mathbf{r}')\, \mathbf{M}(\mathbf{r}', t)\, d\mathbf{r}'.$$

The Hamiltonian $\mathcal{H}_2$ has the form

$$\mathcal{H}_2 = \int \mathbf{M}(\mathbf{r}, t)\, \mathbf{H}(\mathbf{r}, t)\, d\mathbf{r}, \qquad (2)$$

where $\mathbf{H}(\mathbf{r}, t)$ is the magnetic field produced by the conduction-electron current:[2]

$$\mathbf{H}(\mathbf{r}, t) = \frac{1}{c} \int \frac{[\mathbf{j}(\mathbf{r}', t), \mathbf{r} - \mathbf{r}']}{|\mathbf{r} - \mathbf{r}'|^3} e^{-q|\mathbf{r}-\mathbf{r}'|} d\mathbf{r}',$$

$$q = \left(\frac{4\pi n e^2}{mc^2}\right)^{1/2}$$

(q^{-1} is the shielding radius; e, m, and n are respectively the charge, mass, and density of the electrons; c is the speed of light).

The current operator $\mathbf{j}$ is connected with φ^+ and φ by the relation

$$\mathbf{j} = (ie\hbar/2m)\{\varphi \nabla \varphi^+ - (\nabla\varphi)\varphi^+\}.$$

The operators φ^+ and φ can be expanded as series of Bloch wave functions $u_{\mathbf{k}}(\mathbf{r})\, e^{i\mathbf{k}\cdot\mathbf{r}}$:

$$\varphi_\sigma(\mathbf{r}) = \frac{1}{\sqrt{V}} \sum_{\mathbf{k}} c_{\mathbf{k}\sigma} u_{\mathbf{k}}(\mathbf{r})\, e^{i\mathbf{k}\mathbf{r}}, \quad \varphi_\sigma^+(\mathbf{r}) = \frac{1}{\sqrt{V}} \sum_{\mathbf{k}} c_{\mathbf{k}\sigma}^+ u_{\mathbf{k}}^*(\mathbf{r})\, e^{-i\mathbf{k}\mathbf{r}},$$

where $c^+_{k\sigma}$ and $c_{k\sigma}$ are the creation and annihilation operators of an electron with wave vector k and spin projection σ.

On further expressing $\mathbf{M}(\mathbf{r}, t)$ in terms of the creation and annihilation operators a^+_f, a_f of the spin waves, we finally express the Hamiltonian of the ferromagnet in the form

$$\mathcal{H} = \mathcal{H}_0 + \mathcal{H}_{1\,int} + \mathcal{H}_{2\,int}; \tag{3}$$

$$\mathcal{H}_0 = \sum_{k,\sigma} E_{k\sigma} c^+_{k\sigma} c_{k\sigma} + \sum_f \varepsilon_f a^+_f a_f, \tag{4}$$

$$\mathcal{H}_{1\,int} = \mu \left(\frac{4\mu M_0}{V}\right)^{1/2} \sum_{k,k',f} J_f \Lambda_{kk'} \{a^+_f c^+_{k'_-} c_{k_+} + a_{-f} c^+_{k'_+} c_{k_-}\} \Delta(k' - k + f), \tag{5}$$

$$\mathcal{H}_{2\,int} = \frac{\pi i e}{c} \left(\frac{4\mu M_0}{V}\right)^{1/2} \sum_{k,k',f,\sigma} \Lambda_{kk'} f^{-2} \left(1 - \frac{q}{f} \tan^{-1} \frac{f}{q}\right) \times c_{k\sigma} c^+_{k'_\sigma} \{a^+_f f \times [v_k + v_{k'}]^- + a_{-f} f \times [v_k + v_{k'}]^+\} \Delta(k' - k + f). \tag{6}$$

Here $\epsilon_f = \Theta_c (af)^2 + \epsilon_0$ is the energy of a spin wave; $E_{k\sigma} = E_k + 2\mu M_0 J_0 \sigma$ is the energy of an electron with wave vector k and spin projection σ ($\sigma = \pm 1/2$); $v_k = \hbar^{-1} \partial E_k / \partial k$ is the velocity of the conduction electrons; $A^\pm = A_x \pm iA_y$;

$$\Lambda_{kk'} = \frac{1}{\Omega} \int_\Omega u^*_k u_{k'} dr, \quad J_f = \int J(r) e^{ifr} dr, \quad \Delta(k) = \begin{cases} 1, & k = 0 \\ 0, & k \neq 0 \end{cases} \tag{7}$$

(Ω is the volume of the elementary cell).

The operator $\mathcal{H}_{1\,int}$ describes the creation and annihilation of a spin wave with change of the projection of the electron spin (sd-exchange interaction), and the operator $\mathcal{H}_{2\,int}$ describes the creation and annihilation of a spin wave without change of the projection of the electron spin.

3. The change in unit time of the number of spin waves with wave vector f, caused by the sd-exchange interaction $\mathcal{H}_{1\,int}$ and the spin-orbit interaction $\mathcal{H}_{2\,int}$, is determined by the formulas

$$n_f = \dot{n}^{col}_f \equiv \mathcal{L}_f \{n, N\},$$
$$\mathcal{L}_f \{n, N\} = \mathcal{L}^{(e)}_f \{n, N\} + \mathcal{L}^{(r)}_f \{n, N\}, \tag{8}$$

where the collision integrals $\mathcal{L}^{(e)}_f$ and $\mathcal{L}^{(r)}_f$, connected respectively with the Hamiltonians $\mathcal{H}_{1\,int}$ and $\mathcal{H}_{2\,int}$, are equal to

$$\mathcal{L}^{(e)}_f \{n, N\} = \frac{2\pi}{\hbar} \frac{4\mu^3 M_0}{V} \sum_{k,k'} |J_f \Lambda_{k'k}|^2 \{(n_f + 1) N_{k_+} (1 - N_{k'_-}) - n_f N_{k'_-} (1 - N_{k_+})\} \Delta(k' - k + f) \delta(\varepsilon_f - E_{k_+} + E_{k'_-}). \tag{9}$$

$$\mathcal{L}^{(r)}_f \{n, N\} = \frac{2\pi}{\hbar} \frac{\pi^2 e^2}{c^2} \frac{4\mu M_0}{V} \sum_{k,k',\sigma} \left|\frac{\Lambda_{kk'}}{f^2}\right|^2 \left(1 - \frac{q}{f} \tan^{-1} \frac{f}{q}\right)^2 \times |f \times [v_k + v_{k'}]^+|^2 \{(n_f + 1)(1 - N_{k'\sigma}) N_{k\sigma} - n_f (1 - N_{k\sigma}) N_{k'\sigma}\} \Delta(k - k' - f) \delta(\varepsilon_f + E_k - E_k). \tag{10}$$

Here n_f and $N_{k\sigma}$ are the distribution functions of the spin waves and of the electrons, respectively.

The change in unit time of the number of electrons in the state k, σ is determined by the following kinetic equation:

$$\dot{N}_{k\sigma} = (\dot{N}_{k\sigma})^{col} \equiv L^{(e)}_{k\sigma} \{n, N\} + L^{(r)}_{k\sigma} \{n, N\}, \tag{11}$$

where the collision integrals $L^{(e)}_{k\sigma}$ and $L^{(r)}_{k\sigma}$ are connected with the Hamiltonians $\mathcal{H}_{1\,int}$ and $\mathcal{H}_{2\,int}$ and are equal to

$$L^{(e)}_{k_+} \{n, N\} = \frac{8\pi\mu^3 M_0}{\hbar V} \sum_{f,k'} |J_f \Lambda_{kk'}|^2 \{n_f (1 - N_{k_+}) N_{k'_-} - (n_f + 1)(1 - N_{k'_-}) N_{k_+}\} \Delta(k' - k + f) \delta(E_{k'_-} - E_{k_+} + \varepsilon_f), \tag{12}$$

$$L^{(r)}_{k_+} \{n, N\} = \frac{8\pi^2 e^2}{\hbar c^2} \frac{\mu M_0}{V} \sum_{f,k'} \left|\frac{\Lambda_{kk'}}{f^2}\right|^2 \left(1 - \frac{q}{f} \tan^{-1} \frac{f}{q}\right)^2 \times |f \times [v_k + v_{k'}]^+|^2 \{[(n_f + 1)(1 - N_{k_+}) N_{k'_+} - n_f N_{k_+} (1 - N_{k'_+})] \Delta(k - k' + f) \times \delta(E^+_{k'} - E^+_k - \varepsilon_f) - [(n_f + 1) N_{k_+} (1 - N_{k'_+}) - n_f (1 - N_{k_+}) N_{k'_+}] \Delta(k - k' - f) \delta(E^+_{k'} - E^+_k + \varepsilon_f)\}. \tag{13}$$

The collision operators $L^{(e)}_{k_-}$ and $L^{(r)}_{k_-}$ have a similar form.

By use of the expressions for the collision operators, one can find the mean rate for the various processes of collision of spin waves with electrons. This rate is determined in accordance with the formula

$$W = \frac{1}{\tau} = -\sum \left(\frac{\delta \mathcal{L}}{\delta n}\right)_0 n^0 / \sum n^0, \tag{14}$$

where $(\delta \mathcal{L} / \delta n)_0$ is the variational derivative of the collision integral with respect to the distribution function, evaluated at the equilibrium values of the distribution functions of the spin waves, n^0_f, and of the electrons $N^0_{k\sigma}$.

By use of the expression (9) for $\mathcal{L}^{(e)}_f$ and of formula (14), one can calculate the mean rate of emission or absorption of a spin wave by an electron, as a result of exchange interaction:

$$\frac{1}{\tau^{(e)}_s} = \frac{(ak_0)^2}{\pi^{3/2} \zeta(3/2)} \frac{\Theta_0}{\hbar} \left(\frac{T}{\Theta_c}\right)^{1/2} \Psi(e^{-\Theta_0/T}), \tag{15}$$

where T is the temperature; $\Theta_0 = 4\Theta_c (J/E^*)^2$; $E^* = hv_0/a$; v_0 and $\hbar k_0$ are the limiting Fermi velocity and momentum of an electron; and

$$\Psi(x) = \frac{1}{2} \ln(1 - x) \ln \frac{x^2}{1 - x} + \int_0^{x/(1-x)} \frac{\ln(1 + t)}{t} dt.$$

The expression for $1/\tau^{(e)}_s$ simplifies considerably in the limiting cases of high and low temperatures:

$$\frac{1}{\tau_s^{(e)}} \approx \frac{\sqrt{\pi}}{6\zeta(3/2)}(ak_0)^2 \frac{\Theta_0}{\hbar}\left(\frac{T}{\Theta_c}\right)^{1/2} \quad \text{for } \Theta_c \gg T \gg \Theta_0,$$

$$\frac{1}{\tau_s^{(e)}} \approx \frac{(ak_0)^2}{\pi^{3/2}\zeta(3/2)} \frac{\Theta_0}{\hbar}\left(\frac{\Theta_0}{\Theta_c}\right)^{1/2}\left(\frac{\Theta_0}{T}\right)^{1/2} e^{-\Theta_0/T} \text{ for } \Theta_0 \gg T. \quad (16)$$

We note that for $T = \Theta_0$, both limiting expressions in formula (16) have the same order of magnitude.

In a similar way one can calculate the mean rate of emission or absorption of a spin wave by an electron, as a result of the relativistic interaction $\mathcal{H}_2$ int:

$$\frac{1}{\tau_s^{(r)}} \approx \frac{512\sqrt{\pi}}{3\zeta(3/2)} \frac{\Theta_c}{\hbar}\left(\frac{\Theta_c}{T}\right)^{1/2}(ak_0)^2\left(\frac{\mu M_0 m a^2}{\hbar^2}\right)^2 \ln y_0^{-1},$$

$$y_0 = (\Theta_c/T)^{1/2} aq \qquad (\Theta_c \gg T \gg \Theta_c(aq)^2). \quad (17)$$

On putting $\Theta_c = 10^3$ °K, $ak_0 \sim 1$, $a \sim 10^{-8}$ cm, $m \sim 10^{-27}$ g, and $T \sim \Theta_0 \sim 10$°K, we get $\tau_s^{(e)} \approx 10^{-11}$ sec, $\tau_s^{(2)} \approx 10^{-8}$ sec; that is, $\tau_s^{(e)} \ll \tau_s^{(r)}$ for $T \geq \Theta_0 \approx 10$°K. This means that in the temperature range $T \gtrsim \Theta_0$, the inequality $\mathcal{L}^{(e)} \gg \mathcal{L}^{(r)}$ holds.

The mean rate of scattering of electrons by a spin wave, as a result of exchange interaction, can be calculated by use of the expression (12) for $L_k^{(e)}$. We give here the final answer for $1/\tau_e^{(e)}$ in the limiting cases of low and high temperatures:[3]

$$\frac{1}{\tau_e^{(e)}} \approx \frac{3}{8\pi}\frac{E^*}{\hbar}\left(\frac{T}{\Theta_c}\right)^2 e^{-\Theta_0/T} \text{ for } T \ll \Theta_0,$$

$$\frac{1}{\tau_e^{(e)}} \approx \frac{3}{8\pi}\frac{E^*}{\hbar}\frac{\Theta_0}{\Theta_c}\frac{T}{\Theta_c}\left(\ln\frac{T}{\Theta_c} - 1\right) \text{for } \Theta_c \gg T \gg \Theta_0. \quad (18)$$

By use of the expression (13) for $L^{(r)}$, one can calculate the mean rate of scattering of an electron by a spin wave, as a result of the relativistic interaction $\mathcal{H}_2$ int:

$$\frac{1}{\tau_e^{(r)}} \approx \frac{\mu M_0}{\hbar}\left(\frac{e^2 k_0}{mc^2}\right)\left(\frac{1}{aq}\right)^2 \frac{T}{\Theta_c}. \quad (19)$$

By comparison of the expressions (18) and (19), it is easily verified that in the temperature range $T \gtrsim \Theta_0$, the inequality $\tau_e^{(e)} \ll \tau_e^{(r)}$ holds.

4. Thus, in the temperature range $T \gtrsim \Theta_0$, the strongest interaction is the exchange. Consequently, in determining the quasistationary distribution functions n and N one can start from the equations[4]

$$L^{(e)}\{n, N\} = 0, \qquad \mathcal{L}^{(e)}\{n, N\} = 0. \quad (20)$$

It is easily seen that the general solution of these equations has the form

$$n_f = \left[\exp\left(\frac{\varepsilon_f - \gamma}{T}\right) - 1\right]^{-1}, \quad N_{k\pm} = \left[\exp\left(\frac{E_{k\pm} - \zeta_\pm}{T}\right) - 1\right]^{-1}, \quad (21)$$

where $\zeta_+ = \gamma + \zeta_-$.

By use of the conservation law for the number of electrons,

$$\sum_{k\sigma} N_{k\sigma} = \text{const},$$

we get

$$\zeta_+ = E_0 + \gamma/2, \qquad \zeta_- = E_0 - \gamma/2.$$

The arbitrary γ can be related to the size of the projection of the magnetic moment along the axis of easiest magnetization (the z axis):

$$\mathfrak{M}_z = -\mu\int \varphi^+\sigma_z\varphi\, d\mathbf{r} + \int M_z dr$$

$$= M_0 V - 2\mu\sum_f n_f + \mu\sum_k (N_{k-} - N_{k+}). \quad (22)$$

The possibility of the existence of solutions of equations (20) with an arbitrary value of the chemical potential γ is connected with the fact that the magnetic moment of the body commutes with the exchange-interaction Hamiltonian $\mathcal{H}_1$ int. We note that in formula (22) we have not included the contribution of the orbital magnetic moment of the s electrons; this is permissible if the length of the free path of the electrons is much smaller than the Larmor radius in a field M_0.

We now take into consideration the relativistic interaction $\mathcal{H}_2$ int. Then the distribution (21), since it satisfies (20), will no longer satisfy the equations

$$\mathcal{L}^{(e)}\{n, N\} + \mathcal{L}^{(r)}\{n, N\} = 0, \quad L^{(e)}\{n, N\} + L^{(r)}\{n, N\} = 0.$$

Since, however, $L^{(e)} \gg L^{(r)}$ and $\mathcal{L}^{(e)} \gg \mathcal{L}^{(r)}$, the distribution (21) with a slowly varying parameter γ can satisfy approximately the kinetic equations

$$\dot{n}_f = \mathcal{L}_f^{(e)} + \mathcal{L}_f^{(r)}, \qquad \dot{N}_{k\sigma} = L_{k\sigma}^{(e)} + L_{k\sigma}^{(r)}.$$

Since the size of the projection of the magnetic moment, $\mathfrak{M}_Z$, is determined by the occupancy numbers of the spin waves and of the electrons, it is possible, by use of the kinetic equations (8) and (11) and of the quasi-equilibrium distribution functions (21), to determine the change of magnetic moment with time caused by the relativistic spin-orbit interaction. On differentiating equation (22) for $\mathfrak{M}_Z$ with respect to time, we get

$$\dot{M}_z \equiv \frac{\dot{\mathfrak{M}}_z}{V} = -\frac{\mu}{2\pi^2}\left\{\frac{k_0^2}{\hbar v_0} + \frac{\pi T}{2a^3\Theta_c}\frac{1}{\sqrt{\varepsilon_0\Theta_c}}\right\}\dot{\gamma}$$

$$= \frac{\mu}{V}\sum_k \{(\dot{N}_{k-})^{col} - (\dot{N}_{k+})^{col}\} - \frac{2\mu}{V}\sum_f \dot{n}_f^{col}$$

Since the relativistic interaction $\mathcal{H}_2$ int does not change the number of electrons with a given spin projection,

$$\sum_k (\dot{N}_{k\pm})^{col} = 0.$$

By using the expression (10) for $\mathcal{L}_k^{(r)}$, one easily gets the following equation for the change of the quantity γ with time:

$$\dot{\gamma} = -\gamma/\tau, \tag{23}$$

$$\frac{1}{\tau} \approx \frac{8(\pi^2-8)}{3\cdot 137}\left(\frac{v_0 k_0}{cq}\right)^2 \frac{c}{v_0}\left(\frac{\varepsilon_0 \Theta_c}{E^{*2}}\right)^{1/2} \frac{\mu M_0}{\hbar}. \tag{24}$$

The change of the projection of the magnetic moment, $\mathfrak{M}_z$, with time is determined by the formula

$$(\mathfrak{M}_z - \bar{\mathfrak{M}}_z) = (\mathfrak{M}_{z0} - \bar{\mathfrak{M}}_z)\, e^{-t/\tau}, \tag{25}$$

where $\bar{\mathfrak{M}}_z$ is the equilibrium value of the magnetic moment at the given temperature. On setting $v_0 \sim 10^8$ cm/sec, $\epsilon_0 \sim 1°K$, $n \sim 10^{22}$ cm^{-3}, $M_0 \sim 10^3$ gauss, $a \sim 10^{-8}$ cm, and $\Theta_c \sim 10^3 °K$, we get $1/\tau \sim 10^8$ to 10^9 sec^{-1}. We emphasize that the relaxation time of the magnetic moment is independent of temperature.

The authors express their gratitude to A. I. Akhiezer for proposing the problem and for valuable discussions, and to M. I. Kaganov for discussions of the work.

[1] S. V. Vonsovskiĭ, JETP **16**, 981 (1946).
[2] E. Abrahams, Phys. Rev. **98**, 387 (1955).
[3] E. A. Turov, Izv. Akad. Nauk SSSR, Ser. Fiz., **19**, 474 (1955), Columbia Tech. Transl. p. 426.
[4] Akhiezer, Bar'yakhtar, and Peletminskiĭ, JETP **36**, 216 (1959), Soviet Phys. JETP **9**, 146 (1959).

Translated by W. F. Brown, Jr.
125

FLOW OF A PLASMA INTO VACUUM IN THE PRESENCE OF A MAGNETIC FIELD

R. V. POLOVIN

Physico-Mathematical Institute, Academy of Sciences, Ukranian S.S.R.

Submitted to JETP editor March 23, 1960

J. Exptl. Theoret. Phys. (U.S.S.R.) **39**, 657-661 (September, 1960)

Hydromagnetic waves excited by disintegration of the boundary between the plasma and vacuum are investigated. The boundary velocity (escape velocity) is determined. The amplitude of the electromagnetic wave radiated into the vacuum during the disintegration of the discontinuity is determined.

1. In the present article we investigate the flow of plasma into vacuum in the presence of a magnetic field. This problem has many applications in astrophysics and plasma physics. The formulation of the problem is as follows. A stationary plasma of infinite conductivity fills the half-space $x > 0$ at the initial instant of time $t = 0$. The state of the plasma is characterized by a pressure p_1, a density ρ_1, and magnetic-field components H_x and H_{1y} (to be specific, we put $H_x > 0$, $H_{1y} > 0$, $H_{1z} = 0$). A constant magnetic field with components H_x and H_{0y} and a constant electric field $E_{0z} \ll H_{0y}$ are produced in the vacuum. The necessary boundary conditions are not satisfied on such a discontinuity (when $H_x \neq 0$),* which therefore breaks up into several shock waves and self-similar waves. In the plasma there will propagate a rapid wave (shock or self-similar), followed by an Alfvén discontinuity, and finally by a slow wave. An electromagnetic wave propagates in the vacuum.† Some of the aforementioned waves may be missing. The problem is to determine the character of these waves, their amplitudes, and the velocity of the plasma on the boundary with the vacuum.

This problem was solved by Golitsyn[4] for the case when the normal magnetic-field component H_x vanishes. In the solution, Golitsyn used the fact that when $H_x = 0$ the equations of magnetohydrodynamics assume the same form as the equations or ordinary hydrodynamics,[5,6] provided the pressure p and the energy per unit mass ϵ are replaced by the total pressure $p^* = p + H^2/8\pi$ and the total energy $\epsilon^* = \epsilon + H^2/8\pi\rho$.

The presence of a longitudinal magnetic-field component H_x leads to a qualitatively different picture of the flow of plasma to the vacuum.

As already noted, three waves travel in the plasma (instead of one in the case $H_x = 0$). After the departure of these waves, the following conditions should be satisfied on the boundary between the plasma and the vacuum:

$$p = 0, \qquad \{H_y\} = 0, \qquad \{E_z\} = 0. \tag{1}$$

The first of these conditions means that the pressure vanishes behind the waves that go into the plasma, i.e., cavitation takes place. Since cavitation is impossible on a fast rarefaction wave,[7] the cavitation takes place on the slow wave, which is thus self-similar. The fast wave can be either self-similar or a shock wave, depending on the initial conditions.

The discontinuities of the electric and magnetic field in the electromagnetic wave propagating in the vacuum are connected by the relation $\Delta H_y = \Delta E_z$. If the velocity of the flowing plasma becomes nonrelativistic, then the discontinuity of the magnetic field in the electromagnetic wave will be considerably smaller than the magnitude of the magnetic field. Therefore, to solve the problem of the flow of a plasma into a vacuum it is necessary to satisfy only the first two boundary conditions in (1). The concomitant discontinuity of the electric field E_z determines the amplitude of the electromagnetic wave radiated into the vacuum.

Thus, the amplitudes of the fast and the slow waves are obtained from the equation

$$p_1 + \Delta_+ p + \Delta_- p = 0, \tag{2}$$

$$H_{1y} + \Delta_+ H_y + \Delta_A H_y + \Delta_- H_y = H_{0y}, \tag{3}$$

where Δ_+, Δ_-, and Δ_A denote the jumps in the

*If the vacuum is considered as a limiting case of a magnetohydrodynamic medium of zero density, the relativistic equations must be used.[1,2]

†The emission of an electromagnetic wave from a discontinuity with a conductivity jump was first noted by Kulikovskiĭ and Lyubimov.[3]

magnetohydrodynamic quantities on the fast wave, the slow wave, and Alfvén discontinuity. Since the fast and the slow waves are plane (the magnetic field inside the wave and behind the wave are in the same plane that passes through the x axis, in our case the xy plane), the Alfvén discontinuity, if it does exist at all, can rotate the magnetic field only through 180°. Therefore the jump of the magnetic field in the Alfvén discontinuity is equal to $\Delta_A H_y = -2H_y$, where H_y is the transverse magnetic field ahead of the discontinuity. The velocity jump in the Alfvén discontinuity is

$$\Delta_A v_y = 2H_y/\sqrt{4\pi\rho}.$$

Since the transverse magnetic field does not reverse sign in shock and self-similar waves,[8] there is no Alfvén discontinuity when $H_{0y} > 0$, and a 180° Alfvén discontinuity occurs when $H_{0y} < 0$.

In order to find the amplitudes of the fast and slow waves, we must express $\Delta_+ H_y$ in terms of $\Delta_+ p$ and $\Delta_- H_y$ in terms $\Delta_- p$. Equations (2) and (3) then determine the amplitudes $\Delta_+ p$ and $\Delta_- p$.

2. To obtain the dependence of $\Delta_+ H_y$ on $\Delta_+ p$ and of $\Delta_- H_y$ on $\Delta_- p$, we use the fact that the solution of the equations of simple waves reduces to the integration of the differential equation[9]

$$dq_\pm/dr = q_\pm^2 (q_\pm - 1)/\theta (rq_\pm^2 - 1), \tag{4}$$

where

$$r = c^2/U_x^2 \equiv 4\pi\gamma p/H_x^2, \qquad c(r) = \text{const} \cdot r^{(\gamma-1)/2\gamma},$$
$$\mathbf{U} = \mathbf{H}/\sqrt{4\pi\rho}, \qquad \theta = \gamma/(2-\gamma), \qquad q_\pm = U_\pm^2/c^2,$$
$$U_\pm = \{U^2 + c^2 \pm [(U^2+c^2)^2 - 4c^2U_x^2]^{1/2}\}^{1/2}/\sqrt{2},$$

the upper sign pertains to the fast wave and the lower one to the slow wave; γ is the Poisson-adiabat exponent (c is the velocity of sound and r is the dimensionless pressure).

The quantities q_{1+} and r_1 ahead of the fast simple wave are specified. Consequently Eq. (4) determines the function $q_+(r)$, and the jumps in the velocity are then determined from the well-known formulas[10,11]

$$\Delta_+ v_x = -\frac{1}{\gamma}\int_{r_2}^{r_1} c(r)\sqrt{q_+(r)}\,\frac{dr}{r} \tag{5}$$

$$\Delta_+ v_y = \frac{1}{\gamma}\int_{r_2}^{r_1} \frac{c(r)}{r}\left[\frac{q_+(r)-1}{rq_+(r)-1}\right]^{1/2} dr. \tag{6}$$

The subscript 2 refers to the region behind the fast wave and ahead of the slow wave.

The quantities $r_0 = 0$ and $q_0 = H_X^2/H_0^2$ are specified behind the slow wave. Therefore Eq. (4) determines the function $q_-(r)$, after which the jump in the velocity is determined from the formulas

$$\Delta_- v_x = -\frac{1}{\gamma}\int_0^{r_2} c(r)\sqrt{q_-(r)}\,\frac{dr}{r}, \tag{7}$$

$$\Delta_- v_y = -\frac{1}{\gamma}\int_0^{r_2} \frac{c(r)}{r}\left[\frac{1-q_-(r)}{1-rq_-(r)}\right]^{1/2} dr. \tag{8}$$

The magnetic field in the region contained between the two waves is defined by the relation

$$H_{2y}^2/H_x^2 = Q_+(r_2) = Q_-(r_2),$$
$$Q_\pm(r) = [q_\pm(r) - 1)][rq_\pm(r) - 1]/q_\pm(r). \tag{9}$$

The pressure jump in the fast shock wave is connected with the jump in the magnetic field $h \equiv (H_{2y} - H_{1y})/H_1$ by the equation[12]

$$\frac{r_2 - r_1}{r_1} = \frac{\gamma}{r_1}\left\{-\frac{h^2}{2} + h\left[\frac{(\gamma h/2)\sin\theta_1 + r_1 - 1 \pm \sqrt{R(h)}}{2\sin\theta_1 - (\gamma-1)h}\right]\right\}, \tag{10}$$

where

$$R(h) = h^2[\tfrac{1}{4}\gamma^2\sin^2\theta_1 - (\gamma-1)] + (2-\gamma)(1+r_1)h\sin\theta_1$$
$$+ [4r_1\sin^2\theta_1 + (1-r_1)^2],$$
$$\sin\theta_1 = H_{1y}/H_1.$$

The sign ahead of the root in formula (10) is chosen to satisfy the condition $r_2 > r_1$. The jumps in the velocity in the fast shock wave are determined from the relations

$$\Delta_+ v_x = U_{1x}\bar{\eta}(1 - \bar{\eta}h^{-1}\sin\theta_1)^{-1/2}, \tag{11}$$

$$\Delta_+ v_y = U_{1x}h(1 - \bar{\eta}h^{-1}\sin\theta_1)^{1/2}/\cos\theta_1, \tag{12}$$

where

$$\bar{\eta} = h\left[\frac{-(\gamma h/2)\sin\theta_1 + r_1 - 1 \pm \sqrt{R(h)}}{2r_1\sin\theta_1 - (\gamma-1)h}\right]. \tag{13}$$

The sign ahead of the root in (13) is chosen in the same way as in (10).

If $H_{1y}^2/H_X^2 \equiv Q_+(r_1) > Q_-(r_1)$, then the equation $Q_+(r) = Q_-(r)$ determines the root $r_2 < r_1$, after which the values of $\Delta_\pm v$ are determined. In this case the fast wave will be self-similar.

If $H_{1y}^2/H_X^2 < Q_-(r_1)$, then the fast wave will be a shock wave, and the value of $r_2 > r_1$ is determined from (13) and from $H_{2y}^2/H_X^2 = Q_-(r_2)$.

The escape velocities v_x and v_y in the absence of an Alfvén discontinuity are given by

$$v_x = \Delta_+ v_x + \Delta_- v_x, \qquad v_y = \Delta_+ v_y + \Delta_- v_y, \tag{14}$$

where the quantities $\Delta_+ v_x$ and $\Delta_+ v_y$ are determined from (5) and (6) if the fast wave is self-similar, and from (11) and (12) if the fast wave is a shock wave. The quantities $\Delta_- v_x$ and $\Delta_- v_y$ are given by (7) and (8).

The escape velocity in the presence of an Alfvén discontinuity is given by

$$v_x = \Delta_+ v_x + \Delta_- v_x, \qquad v_y = \Delta_+ v_y + 2U_{2y} - \Delta_- v_y, \qquad (15)$$

where $\Delta_\pm v$ have the same meaning as in (14).

The electric field on the boundary between the plasma and the vacuum is determined by

$$E_z = v_y H_x - v_x H_y \qquad (16)$$

(the velocity of light is set equal to unity). The amplitude of the electromagnetic wave ΔE_Z radiated into the vacuum is $\Delta E_Z = E_Z - E_{0Z}$, where E_Z is given by (16).

3. The foregoing relations become much simpler when the Alfvén velocity $U_1 = H_1/\sqrt{4\pi\rho_1}$ is considerably smaller than the velocity of sound. In this case the fast shock wave will be the same as in the absence of the magnetic field, and the jump in the magnetohydrodynamic quantities in the self-similar waves can be obtained in explicit form[10]. In this approximation, the character of the waves that travel into the plasma is determined by the quantity $\mu \equiv H_{0y}/\sqrt{8\pi\rho_1}$. The Alfvén discontinuity will exist only when $\mu < 0$. The fast wave will be a shock wave if $|\mu| > 1$ and self-similar if $|\mu| < 1$.

The escape velocities v_x and v_y and the electric field E_z on the plasma—vacuum boundary are determined by the following formulas (see the figure)

1) In the case when

$$|\mu| \ll (U_{1x}/c_1)\,\xi_m^{(\gamma-1)/\gamma}, \quad \xi_m = \xi_1 [\xi_1 (\gamma-1) r_1]^{1/(\theta-1)}, \quad \xi_1 = q_{1+}^{-1}$$

(the subscript 1 refers to the unperturbed region in the plasma), we have

$$v_x/c_1 = -2/(\gamma-1),$$

$$v_y/c_1 = (U_{1y}/c_1)(U_{1x}/c_1)^{1/\gamma} h(\gamma) - \sqrt{2/\gamma}\,\xi_m^{1/\gamma} r_1^{1/2\gamma}\mu,$$

$$E_z/H_x c_1 = (U_{1y}/c_1)(U_{1x}/c_1)^{1/\gamma} h(\gamma) + 2\sqrt{2}\,c_1\mu/(\gamma-1)\sqrt{\gamma}\,U_{1x}.$$

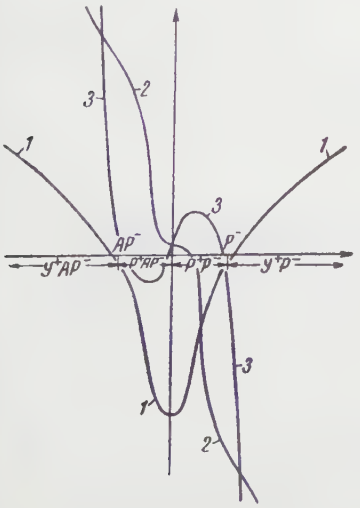

1 – longitudinal escape velocity v_x/c_1, 2 – transverse escape velocity v_y/c_1, 3 – electric field $E_z/H_x c_1$ on the plasma–vacuum boundary. The abscissas represent the quantity $\mu \equiv H_{0y}\sqrt{8\pi p_1}$. The x axis is directed into the plasma. The letters Y^+, P^+, P^-, and A denote the presence of a fast shock wave, of a fast and slow rarefaction wave, and of an Alfvén discontinuity.

Here

$$h(\gamma) = \Gamma[(\gamma-1)/2\gamma]\,\Gamma(1/\gamma)/\gamma\Gamma[(\gamma+1)/2\gamma], \qquad h(5/3) = 3.52.$$

2) In the case when $U_{1X}/c_1 \ll |\mu| \leq 1$, we have

$$v_x/c_1 = -2/(\gamma-1) + 2|\mu|^{(\gamma-1)/\gamma}/(\gamma-1) - U_{1x} f(\gamma)/c_1 |\mu|^{1/\gamma},$$

$$v_y/c_1 = -\mu g(\gamma)\,|\mu|^{-1/\gamma},$$

$$E_z/H_x c_1 = -(g - \sqrt{2/\gamma}\,f)\,\mu\,|\mu|^{-1/\gamma} + 2\sqrt{2}\,c_1\mu\,(1 - |\mu|^{(\gamma-1)/\gamma})/(\gamma-1)\sqrt{\gamma}\,U_{1x}.$$

Here

$$f(\gamma) = \frac{1}{\sqrt{2\gamma}} \int_0^1 \frac{\sigma^{-(\gamma+1)/2\gamma}}{\sqrt{1 - \sigma(\theta+1)^{-1}}}\, d\sigma,$$

$$g(\gamma) = \frac{1}{\gamma} \int_0^1 \sqrt{\frac{1 - \sigma(\theta+1)^{-1}}{1-\sigma}}\, \sigma^{-(\gamma+1)/2\gamma}\, d\sigma,$$

$$f(5/3) = 2.78, \qquad g(5/3) = 3.67.$$

3) In the case when $|\mu| \gg 1$, we have

$$v_x/c_1 = |\mu|\sqrt{2/\gamma(\gamma+1)},$$

$$v_y/c_1 = -\sqrt{(\gamma-1)/(\gamma+1)}\,g(\gamma)\,\mu,$$

$$E_z/H_x c_1 = -2c_1\mu\,|\mu|/\gamma\sqrt{\gamma+1}\,U_{1x}.$$

The author thanks L. I. Sedov for a general formulation of the problem, and A. I. Akhiezer and G. Ya. Lyubarskiĭ for variable discussions.

[1] I. M. Khalatnikov, JETP **32**, 1102 (1957), Soviet Phys. JETP **5**, 901 (1957).

[2] A. I. Akhiezer and R. V. Polovin, JETP **36**, 1845 (1959), Soviet Phys. JETP **9**, 1316 (1959).

[3] A. G. Kulikovskiĭ and G. A. Lyubimov, Doklady Akad. Nauk SSSR **129**, 52 (1959), Soviet Phys.-Doklady **4**, 1185 (1960).

[4] S. G. Golitsyn, JETP **37**, 1062 (1959), Soviet Phys. JETP **10**, 756 (1960).

[5] F. Hoffmann and E. Teller, Phys. Rev. **80**, 692 (1950).

[6] S. A. Kaplan and K. P. Stanyukovich, Doklady Akad. Nauk SSSR **95**, 769 (1954).

[7] A. I. Akhiezer and R. V. Polovin, JETP **38**, 529 (1960), Soviet Phys. JETP **11**, 383 (1960).

[8] R. V. Polovin and G. Ya. Lyubarskiĭ, Ukr. Phys. J. **3**, 571 (1958).

[9] J. Bazer. Astroph. J. **128**, 686 (1958).

[10] R. V. Polovin, JETP **39**, 463 (1960), Soviet Phys. JETP **12**, 326 (1961).

[11] N. H. Kemp and H. E. Petschek. Phys. Fluids **2**, 599 (1959).

[12] J. Bazer and W. B. Ericson. Astroph. J. **129**, 758 (1959).

Translated by J. G. Adashko
126

DECAY OF A PLASMON AT ABSOLUTE ZERO

Yu. A. ROMANOV

Gor'kiĭ Institute of Physics and Technology

Submitted to JETP editor March 24, 1960

J. Exptl. Theoret. Phys. (U.S.S.R.) **39**, 662-665 (September, 1960)

We discuss the effect of phonon interactions between electrons on the decay of a plasmon in a solid (in the isotropic model).

1. Although plasmon oscillations in a solid have been considered in a number of papers (for example, references 1-3), processes involving phonons have not been discussed up to the present. In this paper it will be shown that the phonon interaction between electrons changes the frequency and relaxation time of a plasmon. The methods of quantum field theory[3-5] provide tools for examining this question. As is shown in references 3 — 5, the poles of the single particle Green's function give the energy and relaxation time of the quasi-particles. The Green's function of interest is that for the photon, and is given by

$$D_{\mu\nu}(x-x') = i\langle T(A_\mu(x)A_\nu(x'))\rangle \tag{1}$$

where the indices μ and ν run from 1 to 4 and the $A_\mu(x)$ are the electromagnetic field operators in the Heisenberg representation. The average is taken over the ground state of the system. This function describes the interaction between the photon and the surrounding medium, and satisfies the equation

$$(\Box + P)D(x) = -\delta(x) \tag{2}$$

(see reference 5, for example). Here P is the polarization operator, which is related to the compact photon self-energy part Π through $P = i\Pi$.

The homogeneous equation

$$(\Box + P)\langle 0|A_\mu|r\rangle = 0 \tag{3}$$

is satisfied by the wave function corresponding to the given excitation (or, more precisely, by the matrix element $\langle 0 \mid A_\mu \mid r\rangle$ for the transition from the ground state to a single-particle excited state).

Since we are interested only in longitudinal waves, we neglect retardation effects and write these equations as

$$(\Delta + P)D(x) = -\delta(x), \tag{2'}$$

$$(\Delta + P)\langle 0|A_0|r\rangle = 0, \tag{3'}$$

or, in the momentum representation,

$$[k^2 - P(k, \omega)]D(k, \omega) = 1. \tag{2''}$$

The dispersion relation in which we are interested takes on the form

$$k^2 - P(k, \omega) = 0. \tag{4}$$

2. Feynman's well known rules can be used to write the polarization operator as

$$P(k, \omega) = \frac{e^2}{i(2\pi)^4}\mathrm{Sp}\int G\left(p+\frac{k}{2}\right)\Gamma(p, k)\,G\left(p-\frac{k}{2}\right)d^4p, \tag{5}$$

Here, $\Gamma(p, k)$ is the vertex part, while $G(p)$ is the electron Green's function; in the absence of interactions[4], it is given by

$$G_0(p) = \frac{1}{\varepsilon_p^0 - \varepsilon - i\Delta(p)}, \qquad \Delta(p) \to \begin{cases} +0, & p > p_0 \\ -0, & p < p_0. \end{cases} \tag{6}$$

Carrying out the calculation to first order in e^2, we obtain for $v_0 k \ll \omega_0$:

$$P_0(k, \omega) = \frac{e^2}{i(2\pi)^4}\mathrm{Sp}\int G_0\left(p+\frac{k}{2}\right)G_0\left(p-\frac{k}{2}\right)d^4p$$
$$= -\frac{4e^2}{(2\pi)^3}\int\limits_{p<p_0}\frac{(\varepsilon^0_{p+k} - \varepsilon^0_p)\,d^3p}{(\varepsilon^0_{p+k} - \varepsilon^0_p)^2 - \omega^2 - i0} \approx \frac{\omega_0^2}{\omega^2}k^2\left[1 + \left(\frac{v_0 k}{\omega_0}\right)^2\right], \tag{7}$$

where ω_0 is the plasma frequency, $v_0^2 = \frac{3}{5}p_0^2$, $m_e = \hbar = 1$.

Substitution of (7) into (4) leads to the well known dispersion relation

$$\omega^2 = \omega_0^2 + v_0^2 k^2. \tag{8}$$

The frequency ω is real, with the consequence that for small k the plasmon does not decay, which is a well known result (see, for example, references 3 and 6). In this approximation, the plasmon decays for $k = k_m$, as determined by the poles of the expression under the integral sign in (7),

$$\omega(k_m) = \tfrac{1}{2}k_m^2 + k_m p_0. \tag{9}$$

If higher order diagrams were to be taken into ac-

count, the qualitative picture would not be changed.

3. Phonon interactions between electrons can lead to decay of the plasmon. This interaction would be described by the Hamiltonian

$$H_{int} = \sum_{q<q_m} \alpha_q a^+_{p+q} a_p (b_q + b^+_{-q}), \qquad (10)$$

where the $a^+_p(a_p)$ and $b^+_q(b_q)$ are creation (annihilation) operators for electrons and phonons; $\alpha_q^2 = \lambda_0 \pi^2 \omega_q^0 / p_0$; $\omega_q^0 = c_0 q$; $\lambda_0 \leq 1$; q_m is the maximal phonon momentum and c_0 is the speed of sound.

The Green's function for a free phonon is (see, for example, reference 7),

$$K_0(q) = \alpha_q^2 \left\{ \frac{1}{\omega_q^0 - \omega - i0} + \frac{1}{\omega_q^0 + \omega - i0} \right\}. \qquad (11)$$

It is not difficult to find the effect of phonons on the dispersion relation for the plasmon. We calculate the polarization operator only to first order in e^2. Then the function $G(p)$ in (5) should be taken as the propagation function for an electron interacting with phonons; the difference between $\Gamma(p, k)$ and 1 will also be due to phonon interactions.

Migdal has shown[7] that when phonon interactions are included, $G(p)$ differs from $G_0(p)$ only for $|\epsilon - \epsilon_0| \sim c_0 q_m$ and $|p - p_0| \ll p_0$. On the other hand, it is easy to see that $G(p)$ contributes to the polarization operator of the plasmon only for $|p - p_0| \sim k \ll p_0$ and $|\epsilon - \epsilon_0| \sim \omega_0 \gg c_0 q_m$. Hence in calculating $P(\mathbf{k}, \omega)$ we can use perturbation theory, i.e., we can expand in powers of the photon interaction constant and keep only the first order terms, which are those corresponding to the diagrams shown in Fig. 1.

FIG. 1

The first two terms give small contributions to the imaginary part and affect only the frequency of the plasmon; the principal contribution comes from the third diagram. The imaginary part can be written

$$\operatorname{Im} P_1(\mathbf{k}, \omega) = \frac{e^2}{i(2\pi)^4} \operatorname{Re} \operatorname{Sp} \int G_0\left(p + \frac{k}{2}\right) \Gamma_1(p, k)\, G_0\left(p - \frac{k}{2}\right) d^4p, \qquad (12)$$

where the vertex part $\Gamma_1(p, k)$ is given by Fig. 2.

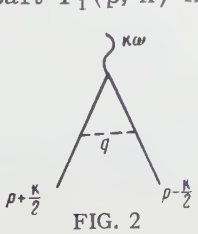

FIG. 2

Assuming that $\Gamma_1(p, k)$ has no poles, we find that

$$\operatorname{Im} P_1(\mathbf{k}, \omega) = -\frac{2e^2}{(2\pi)^3} \left[\int\limits_{\substack{p<p_0 \\ |p+k|>p_0}} \frac{\operatorname{Im} \Gamma_1\left(p + \frac{k}{2}, \varepsilon_p^0 + \frac{\omega}{2}; k, \omega\right)}{\varepsilon^0_{p+k} - \varepsilon^0_p - \omega} d^3p \right.$$

$$\left. + \int\limits_{\substack{p<p_0 \\ |p+k|>p_0}} \frac{\operatorname{Im} \Gamma_1\left(-p - \frac{k}{2}, \varepsilon_p^0 - \frac{\omega}{2}; k, \omega\right)}{\varepsilon^0_p - \varepsilon^0_{p+k} + \omega} d^3p \right]$$

$$= \frac{2e^2}{(2\pi)^6} \int\limits_{\substack{p<p_0 \\ |p+k|>p_0}} d^3p \int\limits_{\substack{p_1<p_0 \\ |p_1-p|<q_m}} d^3p_1 \alpha^2_{p-p_1} \{[(\varepsilon^0_{p+k} - \varepsilon^0_p - \omega)$$

$$\times (\varepsilon^0_{p_1} - \varepsilon^0_p - \omega^0_{p-p_1} + i0)\,(\varepsilon^0_{p_1+k} - \varepsilon^0_p - \omega^0_{p-p_1} - \omega)]^{-1}$$

$$+ [(\varepsilon^0_p - \varepsilon^0_{p+k} + \omega)(\varepsilon^0_{p_1} - \varepsilon^0_p - \omega^0_{p-p_1} + i0)$$

$$\cdot (\varepsilon^0_{p_1+k} - \varepsilon^0_p - \omega^0_{p-p_1} + \omega)]^{-1}\}$$

$$\approx -i \begin{cases} \dfrac{\lambda_0 \pi}{80 c_0^2} k^4, & k < 2c_0 \\ \lambda_0 \pi c_0 \left(\dfrac{\kappa}{2p_0}\right)^3 k, & 2c_0 \ll k \ll p_0, \end{cases}$$

where $\kappa = \min\{q_m, 2p_0\}$.

Upon substituting the polarization operator $P = P_0 + P_1$ in (4), we find that the decay constant is

$$\gamma \approx \begin{cases} \omega_0 \dfrac{\pi \lambda_0}{40} \left(\dfrac{k}{2c_0}\right)^2, & k < 2c_0 \\ \omega_0 \dfrac{\pi \lambda_0}{4} \left(\dfrac{\kappa}{2p_0}\right)^3 \dfrac{2c_0}{k}, & 2c_0 \ll k \ll p_0, \end{cases} \qquad (13)$$

which is fairly large. From the third diagram in Fig. 1, it is clear that this decay constant may be considered to be due to the decay of a plasmon into an electron and a hole, with the emission of a phonon. This differs from the decay described by Landau and which may be considered as the inverse of the Vavilov-Cerenkov effect.

In conclusion, I should like to express my deep gratitude to D. S. Chernavskiĭ for suggesting this problem and to E. S. Fradkin for valuable discussions and for communicating his own results to me.

[1] D. Pines, Revs. Modern Phys. **28**, 184 (1956).

[2] E. L. Feĭnberg, JETP **34**, 1125 (1958), Soviet Phys. JETP **7**, 780 (1958).

[3] V. L. Bonch-Bruevich, Физика металлов и металловедение (Phys. of Metals and Metallography **4**, 546 (1957).

[4] V. M. Galitskiĭ and A. B. Migdal, JETP **34**, 139 (1958), Soviet Phys. JETP **7**, 96 (1958).

[5] A. I. Akhiezer and V. B. Berestetskiĭ, Квантовая электродинамика (Quantum Electrodynamics), Second edition, 1959, Sec. 43.

[6] Sawada, Brueckner, Fukuda, and Brout, Phys. Rev. **108**, 507 (1957).

[7] A. B. Migdal, JETP **34**, 1438 (1958), Soviet Phys. JETP **7**, 996 (1958).

Translated by R. Krotkov
127

RESONANCE SCATTERING OF GAMMA QUANTA BY Li^7

I. Sh. VASHAKIDZE, T. I. KOPALEĬSHVILI, V. I. MAMASAKHLISOV, and G. A. CHILASHVILI

Tbilisi State University and Institute of Physics, Academy of Sciences, Georgian S.S.R.

Submitted to JETP editor March 31, 1960

J. Exptl. Theoret. Phys. (U.S.S.R.) **39**, 666-668 (September, 1960)

Correlation functions are found for resonance scattering of γ quanta with excitation of the $^5/_2^-$ (7.46 Mev) level in Li^7 for two cases of excitation: single-particle and rotational. In addition, the lifetime of the $^1/_2^-$ (0.477 Mev) state of this nucleus was determined.

THE present work concerns the investigation of resonance scattering of γ quanta by the Li^7 nucleus with excitation of the $^1/_2^-$ (0.477 Mev) and $^5/_2^-$ (7.46 Mev) levels.

Let us first consider the resonance scattering of γ quanta by the $^5/_2^-$ (7.46 Mev) level. It is clear that this level can be obtained in general either by single-particle or by collective excitation. We may expect that the correlation function relating the directions of the emitted and absorbed γ quanta in the process of resonance scattering will have different forms, depending on which of the mechanisms of excitation is assumed in the calculation. Comparison with the experimental data will then enable us to answer the question as to which of these mechanisms should be preferred.

In Fig. 1 we show the first few excited states of Li^7.[1] Let us assume that the $^5/_2^-$ (7.46 Mev) level is a $3f_{5/2}$ single-particle level. It can then be shown that to obtain energy values for all the lower lying levels which agree with the experimental data, one must assign to these levels the respective states $1p_{1/2}$, $2d_{3/2}$, $3f_{7/2}$, $3p_{3/2}$, starting from the ground level, if the calculation is made on the oscillator potential model, including spin orbit coupling and for an oscillator parameter with the value

$$r_0 = (\hbar / 2\mu\omega_0)^{1/2} = 1.8 \cdot 10^{-13} \text{ cm}.$$

On the other hand, as has been shown,[2] this level can be considered as a rotational level if we treat the Li^7 as a rigid rotator consisting of an α particle and a triton, $Li^7 = (\alpha + t)$.

It is easy to see that in both cases of excitation the transition from the $^5/_2^-$ level to the ground $^3/_2^-$ level can in general occur by a radiative transition of type E2 + M1. However, according to the selection rules for the orbital angular momentum, in the case of a single-particle excitation the M1 transition is forbidden, whereas there is no such forbiddenness for collective excitation. Therefore, in the latter case the correlation function will differ from that which corresponds to a pure quadrupole transition of type E2. In order to find the form of this function we use the expression for the quadrupole moment operator of the Li^7 nucleus given in reference 2,

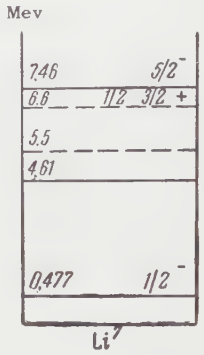

FIG. 1

$$Q_0 = \tfrac{68}{49} \overline{r^2}, \tag{1}$$

where $\overline{r^2}$ is the mean-squared separation of the α particle and the triton. In addition, we must determine the operator for the magnetic moment of the rigid rotator $(\alpha + t)$.

For this purpose we construct an ellipsoid of revolution which is equivalent to this rotator, so that its quadrupole moment, computed in the hydrodynamic approximation, coincides with the quadrupole moment (1), i.e.,

$$3ZR^2\beta/\sqrt{5\pi} = \tfrac{68}{49}\overline{r^2}, \tag{2}$$

where Z = 3, R is the equilibrium radius of the sphere, and β is a parameter determining the deformation of the Li^7 nucleus.

On the other hand, the operator for the magnetic moment of a nucleus which is deformed to the shape of an ellipsoid of revolution with defor-

mation parameter β has the form (cf. the paper of Davydov and Filippov[3]):

$$\mathfrak{M}_p = \frac{e\hbar}{2MC} g \left\{ \frac{1}{2} \sqrt{\frac{3}{\pi}} J_p + \beta \frac{5\sqrt{6}}{7\pi} \sum_{\nu} (21p - \nu, \nu \mid 1p) D^2_{p-\nu,0}(\theta_i) J_\nu \right\}, \quad (3)$$

where J_p is the spherical part of the total angular momentum vector of the nucleus, g is the gyromagnetic ratio, equal to $\sim Z/A$, $D^2_{p-\nu,0}(\theta_i)$ is the well-known matrix of transformation of the spherical functions, $\theta_i = (\theta_1, \theta_2, \theta_3)$ are the Euler angles.

Using formulas (1) and (3), we can find the correlation function for the case where the $^5/_2^-$ (7.46 Mev) level is assumed to be a rotational level. It is easy to see that this function will depend on R^2. Substituting the value $\beta = 0.56$ which was found in the paper of Gonchar, Inopin, and Tsytko[4] in formula (3), we obtain $R^2 = 1.1\overline{r^2}$.

If we take for $(\overline{r^2})^{1/2}$ the value 2.71×10^{-13} cm, which was used in reference 2, we finally obtain for the correlation function

$$I(\theta) \sim [1 + 1.22P_2(\cos\theta) + 2.77P_4(\cos\theta)], \quad (4)$$

where θ is the angle between the absorbed and emitted γ quanta.

Curves showing the correlation functions obtained on the assumptions of single-particle and collective excitation are shown in Fig. 2. As one sees, these curves are symmetric around 90°, but their shapes differ essentially from one another. Therefore, experimental investigation of the correlation of γ quanta can make possible a solution of the question as to which assumption is closer to reality.

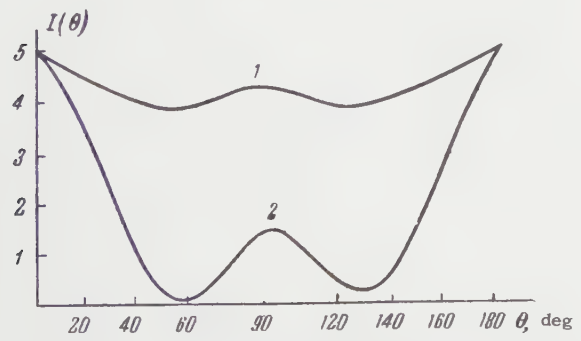

FIG. 2. Curve 1 corresponds to single-particle excitation, curve 2 to collective excitation.

We note that the sequence of levels shown in Fig. 1 can be obtained also on the assumption that the excitation of the nucleus occurs because of a change in the relative motion of the triton and the α particle. In this case, the correlation function turns out to be the same as for the case of single-particle excitation. Therefore, on the basis of an analysis of data concerning resonance scattering of γ quanta by the 7.56 Mev level, one cannot obtain information as to whether we have a single nucleon or a single triton excitation in the nucleus. But, as we shall show below, such information concerning the structure of the Li^7 nucleus can be obtained if we consider the resonance scattering in the first excited state $^1/_2^-$ (0.47 Mev) of this nucleus. This level corresponds to $l = 1$, $j = {}^1/_2$ both on the single particle and the α-triton model. Then, since the ground state has $l = 1$, $j = {}^3/_2$, we may conclude that the excited $p_{1/2}$ level is obtained on the first model as a result of a rotation of the spin of the nucleon, and on the second model by a rotation of the triton spin with respect to the corresponding orbital angular momentum. This assumption is the more likely to be valid if the excitation energy corresponding to the $p_{1/2}$ level is sufficiently small.

The lifetime of the $p_{1/2}$ state, from experiments on resonance scattering of γ quanta by this level of Li^7, is $(1.09 \pm 0.07) \times 10^{-13}$ sec.[5] It is easy to see that, on both models for the Li^7 nucleus, both E2 and M1 transitions are permissible, but, as the calculation shows, the probability for E2 transition is two orders of magnitude lower than the probability for M1 transition. In addition, the M1 transition contains both orbital and spin magnetic terms. However, the contribution of the orbital term to the transition probability is very small, since the spin term plays the major role in an M1 transition. Here it is assumed that only those nucleons participate in the process which are outside the closed shell in Li^7.

On the basis of the assumption of single-nucleon excitation, we obtained for the lifetime of the $^1/_2^-$ (0.49 Mev) state of Li^7 the value 1.5×10^{-13} sec, whereas the α-triton model gives 0.96×10^{-13} sec. The latter value is in good agreement with the experimental value 1.09×10^{-13} sec. Thus we see that the assumption that the $^1/_2^-$ (0.47 Mev) level of Li^7 is the result of a rotation of the triton spin and not of a nucleon is in better agreement with the experimental data.

As for the correlation function, it is almost constant, not dependent on the angle between the γ quanta, because of the fact that this transition is basically a pure spin transition.

[1] F. Ajzenberg and T. Lauritsen, Revs. Modern Phys. **27**, 77 (1955).

[2] V. I. Mamasakhlisov and G. I. Kopaleĭshvili, JETP **37**, 1134 (1959), Soviet Phys. JETP **10**, 807 (1960).

[3] A. S. Davydov and G. F. Filippov, JETP **35**, 703 (1958), Soviet Phys. JETP **8**, 488 (1959).

[4] Gonchar, Inopin, and Tsytko, Легкие ядра и обобщенная модель (Light Nuclei and the Uniform Model). Press, Physico-Technical Institute, Academy of Sciences, Ukrainian S.S.R., 1959.

[5] Swann, Rasmussen, and Metzger, Phys. Rev. **114**, 862 (1959).

Translated by M. Hamermesh
128

NATURAL OSCILLATIONS OF A BOUND PLASMA

D. A. FRANK-KAMENETSKIĬ

Submitted to JETP editor April 2, 1960

J. Exptl. Theoret Phys. 39, 669-679 (September, 1960)

The general properties of cylindrical waves in a cold plasma are examined. The results are applied to low-frequency natural oscillations of a plasma cylinder surrounded by conductive walls. The conditions of magneto-acoustic resonances that ensure effective penetration of the oscillations inside the plasma have been found. The nature of the resonance phenomena depends on the linear density of the electrons. Approximate formulas are given for the natural oscillations of a long plasma cylinder. It is shown that purely radial oscillations are not feasible in a region close to the geometric mean of the electron and ion cyclotron frequencies for even slight deviations from it sharply change the resonance frequency.

WHILE the propagation of waves in a plasma has been adequately treated in the literature (see, for example, references 1-4) natural oscillations of a bound plasma have been studied mainly in the high frequency regions,[5,6] where the ion motion can be neglected. Low-frequency (magnetohydrodynamic and magnetoacoustic) oscillations of a bound plasma have been examined only for special cases.[7-10]

In this paper we investigate oscillations of a plasma cylinder surrounded by conducting walls in a homogeneous static longitudinal magnetic field. The main problem is to find the natural oscillations, but we study first the general properties of cylindrical waves in a cold plasma. Attention is directed particularly to the case when the oscillation frequency is low compared with the plasma frequency (magnetohydrodynamic and magnetoacoustic oscillations).

The entire examination is carried out in a linear approximation by neglecting collisions and other dissipative processes (an ideal plasma) and thermal motion (cold plasma). The plasma is assumed to consist of two components (electrons and homogeneous ions) and its density is constant over the entire area of the examined cylinder.

BASIC EQUATIONS

By assuming that the electron mass is small compared with the ion mass, we can write equations for the motion of charged particles in a plasma in the form of equations for the mass-velocity:

$$\mathbf{v} = (n_i M \mathbf{V}_i + n_e m \mathbf{v}_e)/(n_i M + n_e m) \qquad (1)$$

and for the current density

$$\mathbf{j} = e(Zn_i \mathbf{V}_i - n_e \mathbf{v}_e) \approx en(\mathbf{V}_i - \mathbf{v}_e). \qquad (2)$$

In the linear approximation for a cold plasma without collisions these equations have the form

$$\frac{\partial \mathbf{v}}{\partial t} = \frac{1}{\rho c}[\mathbf{j} \times \mathbf{H}_0], \qquad (3)$$

$$\frac{\partial \mathbf{j}}{\partial t} = \frac{\omega_0^2}{4\pi}\left(\mathfrak{E} + \frac{1}{c}[\mathbf{v} \times \mathbf{H}_0]\right) - \frac{e}{mc}[\mathbf{j} \times \mathbf{H}_0]. \qquad (4)$$

Here

$$\rho = Mn_i + mn_e \approx Mn_i, \qquad (5)$$

$\mathbf{H}_0$ is the static magnetic field, which is assumed to be homogeneous and, according to the linearity condition, is large compared with the alternating magnetic field $\mathfrak{H}$.

Setting the time dependence in the form $e^{-i\omega t}$, we can write (3) in the form of

$$\mathbf{v} = (i/\rho c\omega)[\mathbf{j} \times \mathbf{H}_0]. \qquad (6)$$

Substituting in (4) and expanding the triple vector product we finally get:

$$\omega^2 \mathbf{j} = i\frac{\omega_0^2 \omega}{4\pi}\mathfrak{E} + \omega_i \omega_e [\mathbf{j} - \mathbf{h}(\mathbf{j}\mathbf{h})] - i\omega\omega_e [\mathbf{j} \times \mathbf{h}], \qquad (7)$$

where $\mathbf{h}$ is a unit vector along the static magnetic field $\mathbf{H}_0$, ω_0 is the electron plasma frequency, while ω_i and ω_e are the ion and electron cyclotron frequencies.

If the electron mass is not neglected compared with the ion mass, but the quasi-neutrality condition is retained, then the form of the equations can be preserved by changing only the definitions of the characteristic frequencies:

$$\omega_0^2 = \frac{4\pi n e^2}{m}\left(1 + \frac{Zm}{M}\right) \approx \frac{4\pi n e^2}{m}, \quad \omega_e = \frac{eH_0}{mc}\left(1 - \frac{Zm}{M}\right) \approx \frac{eH_0}{mc},$$

$$\omega_i = \frac{ZeH_0}{Mc(1 - Zm/M)} \approx \frac{ZeH_0}{Mc}.$$

Obviously, Zm/M can almost always be neglected compared with unity.

To analyze the oscillations, it is more convenient to rewrite Maxwell's equations in the form:

$$\nabla^2\mathfrak{E} - \operatorname{grad}\operatorname{div}\mathfrak{E} + \frac{\omega^2}{c^2}\mathfrak{E} = -i\frac{4\pi\omega}{c^2}\mathfrak{j}. \tag{9}$$

SIMPLE CYLINDRICAL WAVES

We locate two coordinates q_1 and q_2 of the locally orthogonal coordinate system in a plane perpendicular to the magnetic field, and align the coordinate q_3 with the static magnetic field $\mathbf{H}_0$. The electric field and the current density are best represented in the form

$$\begin{aligned}
&\mathfrak{E}_\pm = \mathfrak{E}_1 \pm i\mathfrak{E}_2 = (E_1 \pm iE_2)\,F_\pm(q_1, q_2, q_3;\ t),\\
&\mathfrak{E}_3 = E_3F_3(q_1, q_2, q_3, t),\\
&\mathfrak{j}_\pm = \mathfrak{j}_1 \pm i\mathfrak{j}_2 = (j_1 \pm ij_2)\,F_\pm(q_1, q_2, q_3, t),\\
&\mathfrak{j}_3 = j_3F_3(q_1, q_2, q_3, t).
\end{aligned} \tag{10}$$

The Gothic letters indicate the variable quantities to distinguish them from the constant amplitudes.

Equation (7) can be written in the variables (10) as:

$$(\omega_0^2\omega/4\pi)\,\mathfrak{E}_\pm = i\,(\omega_i\omega_e - \omega^2 \pm \omega\omega_e)\,\mathfrak{j}_\pm, \tag{11}$$

$$\mathfrak{j}_3 = i\,(\omega_0^2/4\pi\omega)\,\mathfrak{E}_3. \tag{12}$$

We shall use henceforth a cylindrical system of coordinates: $q_1 = \mathbf{r}$; $q_2 = \varphi$; $q_3 = z$. The function F is sought in the form:

$$F = Z(k_1r)\,e^{i\psi}, \qquad \psi = k_3z + m\varphi - \omega t. \tag{13}$$

Here m is the azimuthal number, k_1 and k_3 are the components of the wave vector and Z designates a cylindrical function. The solution that remains finite on the cylinder axis has the form

$$Z_\pm = J_{m\pm1}(k_1r), \qquad Z_3 = J_m(k_1r), \tag{14}$$

where J is the Bessel function of the first kind. For a coaxial gap they are replaced by general cylindrical functions, i.e., linear combinations from the Bessel and Neumann functions with the same indices. Substitution of (11)–(13) into the expression for the differential operators and use of the properties of the Bessel function gives:

$$\operatorname{div}\mathfrak{E} = i\,(k_1E_2 + k_3E_3)\,J_m(k_1r)\,e^{i\psi}, \tag{15}$$

$$\nabla^2\mathfrak{E} = -(k_1^2 + k_3^2)\,\mathfrak{E} = -k^2\mathfrak{E}, \tag{16}$$

$$(\operatorname{grad}\operatorname{div}\mathfrak{E})_\pm = \mp ik_1\,(k_1E_2 + k_3E_3)\,J_{m\pm1}(k_1r)\,e^{i\psi}, \tag{17}$$

$$(\operatorname{grad}\operatorname{div}\mathfrak{E})_3 = -k_3\,(k_1E_2 + k_3E_3)\,J_m(k_1r)\,e^{i\psi}. \tag{18}$$

We see from this that Eq. (9) is satisfied for the selected form of the functions. Substitution of (10)–(18) into (9) yields a characteristic system of linear homogeneous equations connecting the integration constants E and j, while the determinant of this system yields the dispersion equation.

We shall first examine the components along the magnetic field. Substituting (14) in (10) and taking (10), (16), and (18) into account, we get

$$E_3 = E_2k_1k_3c^2/(k_1^2c^2 + \omega_0^2 - \omega^2). \tag{19}$$

It is seen directly that in the two special cases $k_1 = 0$ and $k_3 = 0$ (axial and purely-radial oscillations) the equation for E_3 separates. In these cases there are two independent oscillation modes. The mode with $E_3 = 0$ constitutes for $k_3 = 0$ purely radial magnetoacoustic oscillations and for $k_1 = 0$ magnetohydrodynamic waves propagated along the field. The mode with $E_3 \neq 0$ constitutes in the second case longitudinal plasma waves and in the first a transverse electromagnetic wave. The dispersion equation for this mode is obtained by equating to zero the denominator of the left portion of (19), and is independent of the presence of the magnetic field.

In the general case of oblique propagation, the equation for E_3 does not separate and (19) gives only the connection between E_3 and E_2. Inserting (19) in (15), (16), (17), and (9), we get

$$k_1E_2 + k_3E_3 = \frac{k^2c^2 + \omega_0^2 - \omega^2}{k_1^2c^2 + \omega_0^2 - \omega^2}\,k_1E_2, \tag{20}$$

$$\begin{aligned}
&(-k^2 + \omega^2/c^2)\,(E_1 \pm iE_2) \pm ik_1\,(k_1E_2 + k_3E_3)\\
&\quad = -i4\pi\omega c^{-2}\,(j_1 \pm ij_2).
\end{aligned} \tag{21}$$

From (21) we can get the connection between the amplitudes of the electric field and current in the form

$$(k^2c^2 - \omega^2)\,E_1 = i4\pi\omega j_1, \qquad (k_3^2c^2q - \omega^2)\,E_2 = i4\pi\omega j_2, \tag{22}$$

where

$$q = (\omega_0^2 - \omega^2)/(k_1^2c^2 + \omega_0^2 - \omega^2). \tag{23}$$

From (11) we get for the same amplitudes

$$\begin{aligned}
(\omega_0^2\omega/4\pi)\,E_1 &= i\,(\omega_i\omega_e - \omega^2)\,j_1 + \omega\omega_e j_2,\\
(\omega_0^2\omega/4\pi)\,E_2 &= i\,(\omega_i\omega_e - \omega^2)\,j_2 - \omega\omega_e j_1.
\end{aligned} \tag{24}$$

The system of characteristic equations (22)–(24) yields the dispersion equation

$$\left(\frac{\omega_0^2\omega^2}{k^2c^2 - \omega^2} - \omega_i\omega_e + \omega^2\right)\left(\frac{\omega_0^2\omega^2}{k_3^2c^2q - \omega^2} - \omega_i\omega_e + \omega^2\right) - \omega^2\omega_e^2 = 0. \tag{25}$$

We note that the parameter q contains $k_1^2c^2$ in

the denominator, so that the dispersion equation is the second degree in k_1^2 (or k^2) if k_3^2 and ω^2 are given, or in k_3^2 if k_1^2 and ω^2 are given. The dispersion equation does not contain m and is identical with the equation for plane waves,[1] if the direction of the propagation is assumed to lie in the r, z plane.

Maxwell's equation:

$$(i\omega/c)\,\tilde{\mathbf{H}} = \operatorname{curl} \mathfrak{E} \tag{26}$$

makes it possible to find the alternating magnetic field $\tilde{\mathbf{H}}$. We can then write the complete solution with the azimuthal number m:

$$\mathfrak{E}_r = i\frac{E_2}{2}[(1-p)J_{m+1}(k_1 r) - (1+p)J_{m-1}(k_1 r)]\,e^{i\psi}, \tag{27}$$

$$\mathfrak{E}_\varphi = \frac{E_2}{2}[(1-p)J_{m+1}(k_1 r) + (1+p)J_{m-1}(k_1 r)]\,e^{i\psi}, \tag{28}$$

$$\mathfrak{E}_z = E_3 J_m(k_1 r)\,e^{i\psi}, \tag{29}$$

$$\mathfrak{j}_r = \frac{j_2}{2}[(1-s)J_{m+1}(k_1 r) - (1+s)J_{m-1}(k_1 r)]\,e^{i\psi}, \tag{30}$$

$$\mathfrak{j}_\varphi = -i\frac{j_2}{2}[(1-s)J_{m+1}(k_1 r) + (1-s)J_{m-1}(k_1 r)]\,e^{i\psi}. \tag{31}$$

Here

$$p = i\frac{E_1}{E_2} = \frac{\omega^2{}_0\frac{w}{w_e} - \left(\frac{w_i}{w} - \frac{w}{w_e}\right)\left(k^2{}_3\,c^2 q - w^2\right)}{k^2\,c^2 - w^2},$$

$$s = \frac{k^2c^2 - \omega^2}{k_3^2 c^2 q - \omega^2}\,p; \tag{32}$$

j_2 is related to E_2 by formula (22). Furthermore,

$$\mathfrak{j}_z = i\frac{\omega_0^2}{4\pi\omega}E_3 J_m(k_1 r)e^{i\psi}, \tag{33}$$

$$\tilde{H}_r = -\frac{E_2}{2}\frac{k_3 c}{\omega}[(q-p)J_{m+1}(k_1 r) + (q+p)J_{m-1}(k_1 r)]\,e^{i\psi}, \tag{34}$$

$$\tilde{H}_\varphi = i\frac{E_2}{2}\frac{k_3 c}{\omega}[(q-p)J_{m+1}(k_1 r) + (q-p-2)J_{m-1}(k_1 r)]\,e^{i\psi}, \tag{35}$$

$$\tilde{H}_z = ipE_2\frac{k_1 c}{\omega}J_m(k_1 r)\,e^{i\psi}. \tag{36}$$

Here $k_1 = k_r$ and $k_3 = k_z$ are the radial and axial wave numbers.

We note that the radial magnetic field $\tilde{H}_r$ is expressed in terms of the electric field components $\mathfrak{E}_z$ and $\mathfrak{E}_\varphi$ in the form

$$i\frac{\omega}{c}\tilde{H}_r = i\frac{m}{r}\mathfrak{E}_z - ik_z\mathfrak{E}_\varphi. \tag{37}$$

We shall call the complex solutions of type (27)–(36) simple cylindrical waves. The real part of such a solution directly gives directly a helical traveling wave. Because of the gyrotropic plasma properties, the natural oscillations have the form of standing waves along the axis but are traveling waves in azimuth.

Natural oscillation with given k_3^2 can be expressed as the sum or difference of the two simple cylindrical waves with axial wave numbers $+k_3$ and $-k_3$. It is convenient to set the origin at a node of the standing wave and to express the natural oscillation as a difference of simple cylindrical waves. In this case, since the first power of k_3 enters only into formulas (19) (35) and (36), we have

$$\mathfrak{E}_r,\ \mathfrak{E}_\varphi,\ \mathfrak{j}_r,\ \mathfrak{j}_\varphi,\ \tilde{H}_z \sim i\sin k_3 z; \quad \mathfrak{E}_z,\ \mathfrak{j}_z,\ \tilde{H}_r,\ \tilde{H}_\varphi \sim \cos k_3 z. \tag{38}$$

From such formulas (27)–(36) it is apparent that the radial distributions of the amplitudes are different in oscillations with azimuthal numbers +m and −m. This discloses the gyrotropic properties of the plasma; this is precisely why the natural oscillations of the plasma should be represented by azimuthal traveling waves.

In deriving all the previous formulas we have neglected only the non-linearity, thermal motion and collisions. Otherwise, the formulas are general and applicable for arbitrary frequencies. In what follows we shall examine a number of very simple cases, with special attention being directed to low frequencies, where the ion motion is significant, i.e., to magnetoacoustic and magnetohydrodynamic oscillations.

All the results cited can be also obtained from the general theory of propagation of electromagnetic waves in gyrotropic media[8-11] by substituting the dielectric tensor of the plasma. However, it is necessary in this case to express not the field in terms of the current, but the current in terms of the field, which results in a rather cumbersome derivation. For the cases of specific interest to us, the method given above is the simplest and clearest.

EXACT BOUNDARY CONDITIONS

The natural oscillations of a bounded plasma are described by the obtained solutions of the equations if they satisfy the boundary conditions. The electromagnetic fields as well as the plasma motion are relevant in this respect and, therefore, the boundary conditions may generally be both electrodynamic and hydrodynamic.

The hydrodynamic boundary condition must be imposed when the plasma comes into direct contact with the solid walls. Then the normal component of the mass velocity must vanish at the wall surface. In a cold plasma, according to formula (6), the velocity along the magnetic field is also equal to zero. Therefore, the hydrodynamic boundary condition is imposed only on the lateral surface of the plasma cylinder. It appears

from (6) that if this surface comes into direct contact with the solid walls, then the following condition must be in effect on it:

$$j_\varphi(k_1 R_0) = 0, \tag{39}$$

where R_0 is the radius of the plasma cylinder.

The electrodynamic boundary conditions are that the normal component of the alternating magnetic and the tangential components of the electric field at the plasma surface have at all times the same values as in the surrounding medium. At the ends of the cylinder the conditions are imposed on $\tilde{H}_z$, $\mathfrak{E}_r$ and $\mathfrak{E}_\varphi$. For solutions of type (38), values of k_3 satisfying such conditions can always be found. In particular, if the plasma cylinder of length L is bounded on the ends by ideally conducting walls, then the boundary conditions at the ends give

$$k_3 = l\pi / L, \tag{40}$$

where l is an integer.

It is apparent from (38) that the solution with $l = 0$ contains only $\mathfrak{E}_z$, j_z, $\tilde{H}_r$ and $\tilde{H}_\varphi$. This special solution, with $k_3 = 0$ and $E_3 \neq 0$ constitutes, as we have already pointed out, a transverse electromagnetic wave polarized along the magnetic field and propagated in the same manner as without a field. For the oscillations of interest to us, which depend on the magnetic field, and especially for all the low-frequency oscillations, the eigenvalues k_3 correspond to values of l from 1 to ∞ in (40).

Considerably more complex are the electrodynamic boundary conditions on the lateral surface of the cylinder. Here, they are imposed on $\tilde{H}_r$, $\mathfrak{E}_z$, and $\mathfrak{E}_\varphi$. The connection (37) between these values makes it possible in the simplest cases to reduce the three conditions to two.

It is seen from (27) and (28) that the radial dependences of $\mathfrak{E}_z$ and $\mathfrak{E}_\varphi$ are expressed by various combinations of Bessel functions. Therefore, one simple cylindrical wave, generally speaking, cannot satisfy the boundary conditions; a linear combination of two simple cylindrical waves with different k_1 is required for this.

Since the dispersion equation is of the second degree in k_1^2, two such cylindrical waves can always be constructed for given ω^2 and k_3^2. If k_1 is imaginary for one of these solutions, their linear combination can still satisfy the boundary conditions for the natural oscillations. In a region where both values of k_1 are imaginary, however, only forced oscillations are possible.

APPROXIMATE BOUNDARY CONDITIONS

The problem of natural oscillations makes sense if the plasma is located inside a closed cavity with ideally conducting walls, for example, coaxially inside a metallic cylinder. Then an exact condition for the lateral surface will require matching to the oscillations of a coaxial dielectric gap.

The radial functions for a coaxial gap are combinations of Bessel and Neumann functions of the argument $k_e r$. Here k_e is the external radial wave number, determined from the relationship

$$k_e^2 = \lambda_0^{-2} - \lambda_3^{-2}, \tag{41}$$

$\lambda_0 = c/\omega$ is the vacuum wavelength and $\lambda_3 = 1/k_3$ is the longitudinal wavelength. If the thickness of the gap is small compared with λ_0 and λ_3, the variation of the fields in it may be neglected. Then the boundary condition on the plasma surface can be assumed given in the following form:

$$\mathfrak{E}_\varphi(k_1 R_0) = 0, \qquad \mathfrak{E}_z(k_1 R_0) = 0, \tag{42}$$

where R_0 is the radius of the plasma cylinder. It is apparent from (37) that the boundary condition for $\tilde{H}_r$ is thus satisfied automatically. On the other hand, for small k_3 and low frequencies, $\mathfrak{E}_z$ may, according to (19), be neglected. Then the conditions at the lateral surface of the plasma cylinder will have the form

$$\mathfrak{E}_\varphi(k_1 R_0) = 0, \qquad j_\varphi(k_1 R_0) = 0. \tag{43}$$

The second condition pertains only to cases when the plasma surface is in direct contact with the solid walls. In case of a free plasma surface the approximate boundary condition reduces to

$$k_1 R_0 = \alpha_n, \tag{44}$$

where α_n are the roots of the right half of (28). One can speak of oscillations of a plasma confined by a free surface only to the extent that the periods of the considered oscillations are small compared with the skin times.

MAGNETOACOUSTIC REGION

For frequencies which are low compared with ionic cyclotron ones, the gyrotropic properties of the plasma do not affect the oscillations. We shall call this frequency region the magnetoacoustic region. From Eqs. (26)–(30) two independent oscillation branches are obtained for it. For the first:

$$E_2 = 0, \quad k^2 c^2/\omega^2 \approx \omega_0^2/\omega_i\omega_e; \tag{45}$$

for the second:

$$E_1 = 0, \quad k_3^2c^2/\omega^2 \approx \omega_0^2/\omega_i\omega_e. \tag{46}$$

This approximation is valid when

$$k_1^2c^2 \ll \omega_0^2, \tag{47}$$

$$k_3^2c^2 \ll \omega_0^2. \tag{48}$$

Newcomb[12] calls the first branch the TE mode, and the second the TEM mode.

LINEAR DENSITY OF THE ELECTRONS

For small k_3, the magnetoacoustic region is determined by inequality (47). We substitute the plasma frequency and express k_1 from the boundary condition, written in the form of (44). Then (47) will have the form

$$\omega_0^2/k_1^2c^2 = 4\alpha_n^{-2}(e^2/mc^2)\pi R_0^2 n_e \gg 1. \tag{49}$$

The quantity

$$(e/mc^2)\pi R_0^2 n_e = \Pi \tag{50}$$

contained in (50) has a simple meaning. This is the total number of electrons along the length of a cylinder equal to the classical electron radius. At the suggestion of S. É. Braginskiĭ, we call Π the linear density of the electrons.

We shall call the following quantity,

$$\omega_0^2/k_1^2c^2 = 4\alpha_n^{-2}\Pi = \Pi^* \tag{51}$$

which depends on the boundary conditions, the effective linear density of the electrons.

Now inequality (49) acquires the following meaning: the magnetoacoustic region is realized when the effective linear density of the electrons is large.

DISPERSION EQUATION IN DIMENSIONLESS VARIABLES

In going over to dimensionless quantities, the dispersion equation (25) can be given in a form containing two dimensionless parameters:

$$A = \omega_0^2/\omega_i\omega_e = c^2/u_A^2, \qquad B = \omega_e/\omega_i$$

and the dimensionless variables

$$x = (k_1^2c^2 + \omega_0^2 + \omega^2)/\omega_0^2, \qquad y = k_3^2c^2/\omega_0^2, \qquad \Omega = \omega^2/\omega_i\omega_e.$$

The parameter A depends only on the velocity u_A; it is equal to the square of the index of refraction of the plasma in the magnetoacoustic region. The parameter B depends only on the nature of the gas, and is always large ($B \geq M/m$).

Expanding the left side of the dispersion equation (25) in powers of X and Y, we can set it in the symmetric form:

$$a_{20}x^2 + a_{10}x + a_{11}xy + a_{01}y + a_{02}y^2 = 0,$$

$$a_{20} = (1-\Omega)(A+1-\Omega) - B\Omega, \quad a_{10} = B\Omega - A - 1 + \Omega,$$

$$a_{11} = A(1-\Omega) + (A-2\Omega)[B\Omega - (1-\Omega)^2]/\Omega,$$

$$a_{01} = (A-\Omega)(1-\Omega-B\Omega)/\Omega,$$

$$a_{02} = (A-\Omega)[B\Omega - (1-\Omega)^2]/\Omega. \tag{52}$$

The index of refraction of the plasma tends to infinity when the highest-order coefficients a_{20} or a_{02} vanish. The coefficient a_{02} vanishes at frequencies close to the electron and ion cyclotron frequencies. a_{20} vanishes at two frequencies which, after Hurwitz,[8] are called hybrid. The higher one is close to the plasma frequency and the lower one is determined by the relationship:

$$\omega_h^2 = \omega_i\omega_e/[1 + (\omega_e/\omega_0)^2]. \tag{53}$$

LOW-FREQUENCY OSCILLATIONS OF A LONG CYLINDER

We shall examine a case when an approximate expression for the lower natural frequencies can be obtained in explicit form. We set in (25)

$$\omega_0^2\omega^2/(k_3^2c^2q - \omega^2) \gg \omega_i\omega_e - \omega^2. \tag{54}$$

Obviously, this approximation is suitable for not too high k_3; we shall therefore call it the long-cylinder approximation. A special case where approximation (54) is inapplicable is the TEM mode in a magnetoacoustic region. Otherwise, its applicability region is rather extensive: in particular, it is always applicable when $k_3^2c^2q$ is close to ω^2 or when ω^2 is close to $\omega_i\omega_e$. Moreover, by setting:

$$\omega^2 \ll k^2c^2, \qquad \omega^2 \ll \omega_0^2, \tag{55}$$

we get from (25)

$$\omega^2 \approx \omega_i\omega_e \frac{1 + (\omega_e/\omega_i)\,k_3^2c^2/(\omega_0^2 + k_1^2c^2)}{1 + (\omega_0/kc)^2 + (\omega_e/\omega_0)^2}. \tag{56}$$

If $k_3 \ll k_1$, we can introduce the effective linear density of the electrons Π according to (51) and write (56) in the form

$$\omega^2 \approx \omega_i\omega_e \frac{1 + (\Pi^*+1)^{-1}(\omega_e/\omega_i)(k_3/k_1)^2}{\Pi^* + 1 + \omega_e^2/\omega_0^2}. \tag{57}$$

In the limit of a very large linear electron density, (57) goes into expression (45) for the magnetoacoustic region. But this limit is attained only when

$$\Pi^* \gg (\omega_e/\omega_i)(k_3/k_1)^2, \tag{58}$$

which, for not too small k_3, is a very stringent requirement. If the less stringent condition is imposed:

$$\Pi^* \gg 1, \quad \Pi^* \gg (\omega_e/\omega_0)^2,$$

then (57) will give:

$$\omega^2 \approx (k_1^2 + k_3^2\omega_e/\Pi^*\omega_i)\, u_A^2. \tag{59}$$

Here the natural frequency is almost as if the propagation had an Alfvén velocity across the field and a velocity $u_e/\sqrt{\Pi^*}$ along the field, where u_e is the "electron Alfvén velocity" which is $\sqrt{M/Zm}$ times larger than the Alfvén velocity.

$$u_e^2 = \omega_e^2 c^2/\omega_0^2 = H_0^2/4\pi n_e m. \tag{60}$$

When $k_1^2/k_3^2\,\Pi^* \ll \omega_e/\omega_i$ the natural frequency no longer depends on the ion mass and becomes inversely proportional to the length of the cylinder. This region can be called pseudo-magnetohydrodynamic.

EXCITATION OF THE OSCILLATIONS

The forced plasma-cylinder oscillations are best analyzed by expansion in a series of natural oscillations. When the forcing frequency approximates one of the natural frequencies of the cylinder, the corresponding term of the expansion sharply increases and resonance occurs.

We consider the simplest case of excitation. Let the plasma be surrounded by an ideally-conducting metallic cylinder, the lateral surface of which has a dielectric cut along the generatrix. A sinusoidal external voltage of given frequency ω is applied to this cut. By assuming the cut to be infinitesimally thin we may write the boundary condition in the form:

$$\mathfrak{E}_\varphi = (V/R_1)\,\delta(\varphi), \quad \text{for } r = R_1, \tag{61}$$

where V is the voltage on the cut. We assume

$$V = V_0 e^{-i\omega t} \tag{62}$$

and expand the δ function in a Fourier series

$$\delta(\varphi) = \frac{1}{2\pi}\sum_{-\infty}^{\infty} e^{im\varphi}. \tag{63}$$

Because of the gyrotropic properties of the plasma, waves with positive as well as negative azimuthal numbers must be independently present in the expansion.

The solution for the forced oscillation is found in the form:

$$\mathfrak{E}_\varphi = \sum_{-\infty}^{\infty} C_m Z_m(k_1 r)\, e^{i\psi}, \tag{64}$$

where Z_m is a function of the form (28) or a linear combination of two such functions; k_1 satisfies the dispersion equation for given ω and k_3, but does not satisfy the boundary conditions for $\mathfrak{E}_\varphi$. For low-frequency oscillations, an approximate boundary condition can be used by considering that (61) is given not at the inner radius R_1 of the metallic housing, but at the radius R_0 of the plasma cylinder. Then

$$C_m = V/2\pi R_1 Z_m(k_1 R_0). \tag{65}$$

When k_1R_0 approaches one of the roots of the right side of (28), one of the terms of the series in (73) sharply increases. Under these conditions resonances should be observed, accompanied by an effective penetration of the alternating field into the plasma.

Other excitation schemes are considerably more difficult to calculate, since it is necessary to expand not only in azimuthal, but in radial functions. The qualitative conclusion that resonance phenomena are present is general.

MAGNETOACOUSTIC RESONANCE IN A PLASMA

The dispersion equation (25) or (52) for a cold plasma is of the fifth power with respect to the square of the frequency. Therefore, generally speaking, up to five different resonance frequencies correspond to given values of k_1, k_3 and m, but these frequencies differ in character.

For a cold unbounded plasma there are also five characteristic frequencies: 2 cyclotron, 2 hybrid, and 1 plasma. Often these frequencies are called natural or resonant. In this case the term resonance is not always unambiguously defined.

Near cyclotron and hybrid frequencies, one of the indices of refraction of the plasma tends to become infinite on passing from positive to negative values. This phenomenon is similar to anomalous dispersion in optics.

The tendency for the index of refraction to become infinite indicates that the phase velocity vanishes. Near this point, thermal motion can no longer be neglected. If the phase velocity is small and there is even a slight thermal motion in the direction of propagation, there will always be particles for which the thermal velocity component in this direction will be close to the phase velocity. These particles move in phase with the wave and irreversibly draw energy from it. In other words, it can be said that these particles are in resonance with the wave. Examples of such a single-

particle resonance are ion and electron cyclotron resonances.

Single-particle resonance is associated with the conversion of oscillation energy into energy of other degrees of freedom of the plasma motion (for example, cyclotron rotation). Therefore, single-particle resonance results in a unique energy absorption not associated with collisions and oscillation damping. It can be stated that if account is taken of even the slightest thermal motion, then the imaginary part of the index of refraction must tend to infinity together with the real part.

For a bounded plasma, a phenomenon of a completely different nature takes place — collective resonance at the natural frequencies of the plasma volume. These natural frequencies have been examined above; they depend on the plasma concentration and on the boundary conditions. Resonance at the natural frequencies of a bounded plasma results, generally speaking, in the penetration of alternating fields inside the plasma.

However, if the geometric dimensions of the plasma volume are small compared with the vacuum wavelength, then high indices of refraction are required for resonance at the natural frequencies. Therefore, certain of the natural frequencies of a plasma volume are in many cases close to the anomalous dispersion frequencies, i.e., the collective resonance practically coincides with the single-particle resonance.[6]

If the natural frequency of a plasma volume coincides with the single-particle resonance, then the plasma cannot be made to oscillate at this frequency, because of specific absorption; i.e., it is impossible to produce in the plasma large alternating field amplitudes. We call such resonances absorption resonances; they include the ion and electron cyclotron resonances. They result only in surface heating of the plasma, i.e., the latter is opaque to the corresponding frequencies.

Anomalous dispersion type resonances constitute a larger group and include all the resonances close to frequencies where the index of refraction tends to infinity, i.e., resonances at hybrid as well as at cyclotron frequencies. All these resonances may be called trivial, since their frequencies are close to the natural frequencies of an unbounded plasma.

Natural-frequency resonances that depend on the boundary conditions, i.e., on the geometry and the plasma volume dimensions, are characteristic of a bounded plasma. These resonances are not due to specific absorption; the phase velocity is sufficiently large and assures effective penetration of the alternating fields inside the plasma. We shall call such resonances build-up resonances. The most important of them is the magnetoacoustic resonance, which is produced when the linear density of the electrons is large.

The use of build-up resonances and, particularly, of magnetoacoustic resonances, in contrast to the ordinary surface effect of high frequency fields (skin-effect), makes possible a deep penetration of the alternating field inside the plasma.

I thank V. P. Demidov for valuable consultations.

[1] E. Aström, Arkiv Fysik, **2**, 443, 1950.

[2] V. L. Ginzburg, JETP, **21**, 788 (1951).

[3] Gershman, Ginzburg and Denisov, Usp. Fiz. Nauk, **61**, 561 (1957).

[4] T. Bernstein, Phys. Rev. **109**, 10 (1950).

[5] S. Braun, Радиотехника и электроника (Radio Engineering and Electronics) **4**, 1244 (1959).

[6] T. Stix, Phys. Rev. **106**, 1146 (1957).

[7] K. Korper, Z. Naturforsch **12a**, 815 (1957).

[8] Auer, Hurwitz, and Miller, Phys. Fluids **1**, 501 (1958).

[9] Ya. B. Faĭnberg and M. F. Gorbatenko, J. Tech Phys. (U.S.S.R.) **29**, 549 (1959).

[10] G. Suhl and L. Walker, Problems of Waveguide Propagation of Electromagnetic Waves in Gyrotropic Media, (Russ. Transl.) IIL, Moscow, 1955.

[11] M. A. Ginsberg, Doklady Akad. Nauk SSSR **95**, 489 (1954).

[12] V. Newcomb, Magnetohydrodynamics, Materials of a Symposium edited by Landshoff [Russ. Transl.] M., Atomizdat, 1958.

Translation furnished by the Atomic Energy Commission
129

RELAXATION OF THE MAGNETIC MOMENT IN AN ANTIFERROMAGNETIC DIELECTRIC

G. I. URUSHADZE

Physico-Technical Institute, Academy of Sciences, Ukrainian S.S.R.

Submitted to JETP editor April 2, 1960

J. Exptl. Theoret. Phys. (U.S.S.R.) 39, 680-683 (September, 1960)

The relaxation time of the magnetic moment of an antiferromagnetic dielectric is calculated in the case in which the nonequilibrium magnetic moment is perpendicular to the axis of the crystal. It is shown that at temperatures satisfying condition (17), the relaxation time is inversely proportional to the first power of the temperature.

THE present work deals with the problem of relaxation of the magnetic moment in an antiferromagnetic dielectric in the case in which the external magnetic field and the magnetic moment of the body are perpendicular to the crystal axis z. After switching off of the magnetic field, the magnetic moments of the sublattices begin to relax, turning toward the crystal axis; that is, the magnetic moment induced by application of the field disappears. Since the nonequilibrium value of this magnetic moment is determined by the number of spin waves with momentum $\mathbf{k} = 0$, the magnetic-moment relaxation time found here determines, in order of magnitude, the line width in uniform antiferromagnetic resonance.

As is known, the exchange-interaction Hamiltonian commutes with the total magnetic moment of the body, and therefore it cannot change the previously induced nonequilibrium magnetic moment. The change of the magnetic moment of the body will occur because of weak relativistic interaction.

1. We write the Hamiltonian of an antiferromagnetic dielectric in the following form:

$$\mathcal{H} = \int dV \left[\frac{\alpha}{2} \left(\frac{\partial \mathbf{M}_1}{\partial x_i} \right)^2 + \frac{\alpha}{2} \left(\frac{\partial \mathbf{M}_2}{\partial x_i} \right)^2 + \alpha_{12} \frac{\partial M_{1k}}{\partial x_i} \frac{\partial M_{2k}}{\partial x_i} + \gamma \mathbf{M}_1 \mathbf{M}_2 + \frac{\beta}{2} (M_{1x}^2 + M_{1y}^2 + M_{2x}^2 + M_{2y}^2) + \frac{\mathbf{h}^2}{8\pi} \right], \tag{1}$$

where $\mathbf{M}_1$ and $\mathbf{M}_2$ are the magnetic moments of the sublattices; $\mathbf{h}$ is the magnetic field produced by the oscillations of the magnetic moment; α, α_{12}, and γ are constants related to the exchange interaction; and β is the magnetic anisotropy constant.

By analogy with the work of Holstein and Primakoff,[1] we introduce the spin-wave creation and annihilation operators a_j^+ and a_j ($j = 1, 2$), connected with the sublattice magnetic moments $\mathbf{M}_1$ and $\mathbf{M}_2$ by the relations

$$\begin{aligned} m_j^- &= M_{jx} - iM_{jy} \approx (2\mu M)^{1/2} [a_j - (\mu / 4M) a_j^+ a_j a_j], \\ m_j^+ &= M_{jx} + iM_{jy} \approx (2\mu M)^{1/2} [a_j^+ - (\mu / 4M) a_j^+ a_j^+ a_j], \\ m_j^z &= M_{jz} - M = -\mu a_j^+ a_j. \end{aligned} \tag{2}$$

Here μ is the Bohr magneton and M is the saturation magnetic moment of a sublattice. The operators a_j^+ and a_j are subject to the usual commutation rule

$$[a_i(\mathbf{r}), a_j^+(\mathbf{r}')] = \delta_{ij} \delta(\mathbf{r} - \mathbf{r}'). \tag{3}$$

By using formulas (2) and expanding the operators $a_j^+(\mathbf{r})$ and $a_j(\mathbf{r})$ in Fourier series, one can write the Hamiltonian (1) in the form

$$\mathcal{H} = \mathcal{H}_0 + \mathcal{H}_{int}; \tag{4}$$

$$\mathcal{H}_0 = \sum_{\mathbf{k}} \{ \tfrac{1}{2} A_{\mathbf{k}} a_{1\mathbf{k}}^+ a_{1\mathbf{k}} + \tfrac{1}{2} A_{\mathbf{k}} a_{2\mathbf{k}}^+ a_{2\mathbf{k}} + B_{\mathbf{k}} a_{1\mathbf{k}} a_{2-\mathbf{k}} + C_{\mathbf{k}} a_{1\mathbf{k}}^+ a_{1-\mathbf{k}}^+ + C_{\mathbf{k}} a_{2\mathbf{k}} a_{2-\mathbf{k}} + 2C_{\mathbf{k}} a_{1\mathbf{k}}^+ a_{2\mathbf{k}} \} + \text{Herm. adj.} \tag{5}$$

$$\mathcal{H}_{int} = -\frac{\beta\mu^2}{2V} \sum_{\mathbf{k}_1 \mathbf{k}_2 \mathbf{k}_3 \mathbf{k}_4} (a_{1\mathbf{k}_1}^+ a_{1\mathbf{k}_2}^+ a_{1\mathbf{k}_3} a_{1\mathbf{k}_4} + a_{2\mathbf{k}_1}^+ a_{2\mathbf{k}_2}^+ a_{2\mathbf{k}_3} a_{2\mathbf{k}_4}) \Delta(\mathbf{k}_1 + \mathbf{k}_2 - \mathbf{k}_3 - \mathbf{k}_4). \tag{6}$$

Here the following symbols have been introduced:

$$\begin{aligned} A_{\mathbf{k}} &= \mu M (\alpha k^2 + 2\pi \sin^2 \theta_{\mathbf{k}} + \gamma + \beta), \\ B_{\mathbf{k}} &= \mu M (\alpha_{12} k^2 + 2\pi \sin^2 \theta_{\mathbf{k}} + \gamma), \\ C_{\mathbf{k}} &= \pi\mu M \sin^2 \theta_{\mathbf{k}} \exp(-2i\varphi_{\mathbf{k}}), \end{aligned} \tag{7}$$

where $\theta_{\mathbf{k}}$ and $\varphi_{\mathbf{k}}$ are the azimuthal and polar angles of the wave vector $\mathbf{k}$; $\Delta(\mathbf{k}) = 1$ for $\mathbf{k} = 0$, $= 0$ for $\mathbf{k} \neq 0$. In $\mathcal{H}_{\text{int}}$ we have not included terms containing products of three operators $a_{j\mathbf{k}}^+ a_{j\mathbf{k}}$; as will become clear later, these will not interest us.

2. To find the spin-wave spectrum of the antiferromagnetic dielectric, we diagonalize the Hamiltonian (4). To this end, we go over from the operators $a_{j\mathbf{k}}$ and $a_{j\mathbf{k}}^+$ to the operators $c_{j\mathbf{k}}$ and $c_{j\mathbf{k}}^+$[2,3]:

$$a_{1\mathbf{k}} = U_{11}c_{1\mathbf{k}}e^{-i\varepsilon_1 t/\hbar} + U_{12}c_{2\mathbf{k}}e^{-i\varepsilon_2 t/\hbar} + V_{11}^{+}c_{1-\mathbf{k}}^{+}e^{i\varepsilon_1 t/\hbar} + V_{12}^{+}c_{2-\mathbf{k}}^{+}e^{i\varepsilon_2 t/\hbar},$$
$$a_{2\mathbf{k}} = U_{22}c_{2\mathbf{k}}e^{-i\varepsilon_2 t/\hbar} + U_{21}c_{1\mathbf{k}}e^{-i\varepsilon_1 t/\hbar} + V_{22}^{+}c_{2-\mathbf{k}}^{+}e^{i\varepsilon_2 t/\hbar} + V_{21}^{+}c_{1-\mathbf{k}}^{+}e^{i\varepsilon_1 t/\hbar}. \quad (8)$$

The amplitudes U_{ij} and V_{ij} in (8) are found with the aid of the equation of motion of the operators $a_{j\mathbf{k}}$,

$$\dot{a}_{j\mathbf{k}} = (i/\hbar)\,[\mathcal{H}_0, a_{j\mathbf{k}}]. \quad (9)$$

On substituting formula (8) in Eq. (9) and equating coefficients of $c_{j\mathbf{k}}$ and $c_{j\mathbf{k}}^{+}$, we get the system of linear homogeneous equations

$$\begin{aligned}
&(A_{\mathbf{k}} - \varepsilon_{\mathbf{k}})\,U_{11} + B_{\mathbf{k}}V_{21} + 2C_{\mathbf{k}}V_{11} + 2C_{\mathbf{k}}^{+}U_{21} = 0,\\
&2C_{\mathbf{k}}U_{11} + 2C_{\mathbf{k}}V_{21} + (A_{\mathbf{k}} + \varepsilon_{\mathbf{k}})\,V_{11} + B_{\mathbf{k}}U_{21} = 0,\\
&B_{\mathbf{k}}U_{11} + (A_{\mathbf{k}} + \varepsilon_{\mathbf{k}})\,V_{21} + 2C_{\mathbf{k}}^{+}V_{11} + 2C_{\mathbf{k}}^{+}U_{21} = 0,\\
&2C_{\mathbf{k}}U_{11} + 2C_{\mathbf{k}}V_{21} + B_{\mathbf{k}}V_{11} + (A_{\mathbf{k}} - \varepsilon_{\mathbf{k}})\,U_{21} = 0,
\end{aligned} \quad (10)$$

and similar equations in which, instead of the quantities U_{11}, U_{21}, V_{11}, and V_{21}, there enter the quantities U_{22}^{+}, U_{12}^{+}, V_{22}^{+}, and V_{12}^{+}.

On solving (10), we find the dispersion law for spin waves in an antiferromagnetic dielectric:

$$\varepsilon_{1,2}(\mathbf{k}) = \mu M\sqrt{2\gamma\,[\beta + (\alpha - \alpha_{12})\,k^2]\,[1 \pm (\pi/\gamma)\sin^2\theta_{\mathbf{k}}]}. \quad (11)$$

Here $\theta_{\mathbf{k}}$ is the angle between the z axis and the direction of the wave vector $\mathbf{k}$. The upper and lower signs correspond to two energy branches, the difference between which is $\Delta\epsilon \sim \mu M$.

For the amplitudes, from (8), we get the following expressions:

$$U_{11} = U_{22} = U_{12} = U_{21} \equiv U_{\mathbf{k}} \approx -\frac{B_{\mathbf{k}}}{2\varepsilon_{\mathbf{k}}}\left(\frac{2\varepsilon_{\mathbf{k}}}{\varepsilon_{\mathbf{k}} + A_{\mathbf{k}}}\right)^{1/2},$$
$$V_{11} = V_{22} = V_{12} = V_{21} \equiv V_{\mathbf{k}} \approx -\left(\frac{\varepsilon_{\mathbf{k}} + A_{\mathbf{k}}}{2\varepsilon_{\mathbf{k}}}\right)^{1/2}. \quad (12)$$

By use of formulas (8) and (12), one can express the Hamiltonian for the interaction of spin waves with one another in terms of the operators $c_{i\mathbf{k}}$ and $c_{i\mathbf{k}}^{+}$:

$$\mathcal{H}_{int} = \mathcal{H}_{int}^{(1)} + \mathcal{H}_{int}^{(2)};$$
$$\mathcal{H}_{int}^{(1)} = -\frac{\beta\mu^2}{2V}\sum_{\mathbf{k}_1\mathbf{k}_2\mathbf{k}_3\mathbf{k}_4}\{[\Phi_{\mathbf{k}_1\mathbf{k}_2\mathbf{k}_3\mathbf{k}_4}^{(1)}c_{1\mathbf{k}_1}^{+}c_{1\mathbf{k}_2}^{+}c_{1\mathbf{k}_3}c_{1\mathbf{k}_4} + \Phi_{\mathbf{k}_1\mathbf{k}_2\mathbf{k}_3\mathbf{k}_4}^{(2)}c_{1\mathbf{k}_1}^{+}c_{2\mathbf{k}_2}^{+}c_{1\mathbf{k}_3}c_{2\mathbf{k}_4}]\,\Delta(\mathbf{k}_1 + \mathbf{k}_2 - \mathbf{k}_3 - \mathbf{k}_4)$$
$$+ [\Psi_{\mathbf{k}_1\mathbf{k}_2\mathbf{k}_3\mathbf{k}_4}^{(1)}c_{1\mathbf{k}_1}^{+}c_{1\mathbf{k}_2}^{+}c_{1\mathbf{k}_3}^{+}c_{1\mathbf{k}_4} + \Psi_{\mathbf{k}_1\mathbf{k}_2\mathbf{k}_3\mathbf{k}_4}^{(2)}c_{1\mathbf{k}_1}^{+}c_{2\mathbf{k}_2}c_{2\mathbf{k}_3}c_{2\mathbf{k}_4}]$$
$$\times\,\Delta(\mathbf{k}_1 + \mathbf{k}_2 + \mathbf{k}_3 - \mathbf{k}_4) + \text{Herm. adj.}\}, \quad (13)$$

where

$$\Phi_{\mathbf{k}_1\mathbf{k}_2\mathbf{k}_3\mathbf{k}_4}^{(1)} = \tfrac{1}{2}(U_{\mathbf{k}_1}U_{\mathbf{k}_2}U_{\mathbf{k}_3}U_{\mathbf{k}_4} + V_{\mathbf{k}_1}V_{\mathbf{k}_2}V_{\mathbf{k}_3}V_{\mathbf{k}_4}),$$
$$\Phi_{\mathbf{k}_1\mathbf{k}_2\mathbf{k}_3\mathbf{k}_4}^{(2)} = 2U_{\mathbf{k}_1}V_{\mathbf{k}_2}U_{\mathbf{k}_3}V_{\mathbf{k}_4},$$
$$\Psi_{\mathbf{k}_1\mathbf{k}_2\mathbf{k}_3\mathbf{k}_4}^{(1)} = 2U_{\mathbf{k}_1}V_{\mathbf{k}_2}U_{\mathbf{k}_3}V_{\mathbf{k}_4}, \quad \Psi_{\mathbf{k}_1\mathbf{k}_2\mathbf{k}_3\mathbf{k}_4}^{(2)} = 2V_{\mathbf{k}_1}V_{\mathbf{k}_2}U_{\mathbf{k}_3}V_{\mathbf{k}_4}.$$

$\mathcal{H}_{\text{int}}^{(2)}$ is obtained from $\mathcal{H}_{\text{int}}^{(1)}$ by the substitution $c_{1\mathbf{k}} \leftrightarrow c_{2\mathbf{k}}$.

We now calculate the mean value of the square of the magnetic moment and of the square of its component perpendicular to the crystal axis:

$$\langle\mathfrak{M}^2\rangle = \left\langle\left[\int(\mathbf{M}_1 + \mathbf{M}_2)\,dV\right]^2\right\rangle,$$
$$\langle\mathfrak{M}_{\perp}^2\rangle = \left\langle\left[\int(M_{1\perp} + M_{2\perp})\,dV\right]^2\right\rangle. \quad (14)$$

With the aid of formulas (2), (8), and (11), the quantities $\langle\mathfrak{M}^2\rangle$ and $\langle\mathfrak{M}_{\perp}^2\rangle$ can be expressed in terms of the occupancy numbers n_{10} and n_{20} of spin waves with momentum $\mathbf{k} = 0$.

The averaged quantities $\mathfrak{M}^2$ and $\mathfrak{M}_{\perp}^2$ have the following form:

$$\langle\mathfrak{M}^2\rangle = \langle\mathfrak{M}_{\perp}^2\rangle = 2\mu_{\text{eff}}\,MV\,[(1 + \cos 2\varphi_0)\,n_{10} + (1 - \cos 2\varphi_0)\,n_{20}],$$

where φ_0 is the polar angle of the spin wave vector with $\mathbf{k} = 0$, and

$$\mu_{\text{eff}} = \mu\frac{(\varepsilon_0 + A_0)^2 + B_0^2}{(\varepsilon_0 + A_0)^2 - B_0^2} \approx \mu\left(\frac{\gamma}{2\beta}\right)^{1/2}.$$

To determine φ_0, it is necessary to take into account the boundary conditions on the vectors $\mathbf{M}$ and $\mathbf{H}$. In the case in which the antiferromagnet fills the half-space $x > 0$ and the crystal axis is directed parallel to its surface, the value of φ_0 is zero. Suppressing the index 1 on n_{10}, we get

$$\langle\mathfrak{M}^2\rangle = \langle\mathfrak{M}_{\perp}^2\rangle = 4\mu_{\text{eff}}\,MVn_0. \quad (15)$$

Thus we see that the relaxation of the magnetic moment of an antiferromagnetic dielectric is determined by the number of spin waves with momentum $\mathbf{k} = 0$. From knowledge of the interaction Hamiltonian $\mathcal{H}_{\text{int}}$, one can find the change of the number of spin waves with momentum $\mathbf{k} = 0$. We remark that a change of n_0 cannot cause processes of union of two spin waves into one, or of splitting of one spin wave into two, since in these processes it is impossible to satisfy simultaneously the laws of conservation of energy and of momentum. Therefore for determination of the change of n_0 with time, as has already been indicated, it is necessary to take into account, in the Hamiltonian $\mathcal{H}_{\text{int}}$, the later terms of the expansion, describing processes that involve participation of four spin waves.

On using expression (13) for the interaction Hamiltonian that describes these processes, we get the following kinetic equation:

$$\dot{n}_0 = \mathcal{L}_0\{n\},$$

$$\mathcal{L}_0\{n\} = \frac{32\pi}{\hbar}\frac{\beta^2\mu^4}{V^2}U_0^2\sum_{1,2,3}\{5U_1^2U_2^2U_3^2[(n_0+1)(n_1+1)n_2n_3 - n_0n_1(n_2+1)(n_3+1)]\Delta(\mathbf{k}_1-\mathbf{k}_2-\mathbf{k}_3)\delta(\varepsilon_0+\varepsilon_1-\varepsilon_2-\varepsilon_3) + 2U_1^2U_2^2U_3^2[(n_0+1)(n_1+1)(n_2+1)n_3 - n_0n_1n_2(n_3+1)]\Delta(\mathbf{k}_1+\mathbf{k}_2-\mathbf{k}_3)\delta(\varepsilon_0+\varepsilon_1+\varepsilon_2-\varepsilon_3)\}.$$

In writing $\mathcal{L}_0\{n\}$ we have assumed that $\epsilon_{1\mathbf{k}} \approx \epsilon_{2\mathbf{k}}$ and $U_{\mathbf{k}} \approx V_{\mathbf{k}}$; this is correct at sufficiently low temperatures, $\mu M \ll T \ll \Theta_C$. Since the occupation numbers n_0 are large ($n_0 \gg 1$), the collision operator $\mathcal{L}_0$ can be expressed approximately in the form

$$\mathcal{L}_0\{n\} = -n_0/\tau_0.$$

The kinetic equation then takes the form

$$\dot{n}_0 = -n_0/\tau_0,$$

where the relaxation time τ_0 is determined by the formula

$$\frac{1}{\tau_0} = \frac{\beta^2U_0^2\mu^4}{4\pi^5\gamma^3\sigma^6\hbar(\alpha-\alpha_{12})^3T}(e^{\xi}-1)J(T),$$

$$J(T) = \int\frac{d\mathbf{x}_1\,d\mathbf{x}_2\,d\mathbf{x}_3}{x_1x_2x_3}[(x_1^2-\xi^2)(x_2^2-\xi^2)(x_3^2-\xi^2)]^{1/2} \times U_1^2U_2^2U_3^2n_1^0n_2^0n_3^0e^{x_2}[5\delta(\xi+x_1-x_2-x_3) + 2\delta(\xi+x_1+x_2-x_3)]\delta[(x_1^2-\xi^2)^{1/2}\mathbf{n}_1 + (x_2^2-\xi^2)^{1/2}\mathbf{n}_2 - (x_3^2-\xi^2)^{1/2}\mathbf{n}_3]. \quad (16)$$

Here $n_{\mathbf{k}}^0 = (e^{\epsilon\mathbf{k}/T}-1)^{-1}$ is the Bose equilibrium distribution function, $\xi = \epsilon_0/T$, $\sigma = \mu M/T$, and $\mathbf{n}_1$, $\mathbf{n}_2$, and $\mathbf{n}_3$ are unit vectors in the directions $\mathbf{x}_1$, $\mathbf{x}_2$, and $\mathbf{x}_3$.

At temperatures

$$T \gg (\beta\mu M\Theta_c)^{1/2}. \quad (17)$$

(which corresponds to $\xi \ll 1$), the expression for $J(T)$ simplifies considerably, and except for a numerical factor of order unity we get the following expression for $1/\tau_0$:

$$\frac{1}{\tau_0} \sim \beta^2\frac{\mu M}{\hbar}\frac{\mu M}{\Theta_c}\frac{T}{\Theta_c}. \quad (18)$$

In conclusion, the author considers it a pleasant duty to express his profound gratitude to A. I. Akhiezer and V. G. Bar'yakhtar for proposing the problem and for discussion.

[1] T. Holstein and H. Primakoff, Phys. Rev. 58, 1098 (1940).

[2] N. Bogolyubov, Лекции по квантовой статистике (Lectures on Quantum Statistics), Kiev, 1947.

[3] V. Tsukernik, Dissertation, Khar'kov State University, 1957.

Translated by W. F. Brown, Jr.
130

POLARIZATION OF INTERNAL-CONVERSION ELECTRONS AND POSITRONS EMITTED AFTER BETA DECAY OF THE NUCLEUS

G. A. LOBOV

Submitted to JETP editor April 26, 1960

J. Exptl. Theoret. Phys. (U.S.S.R.) 39, 684-688 (September, 1960)

We consider the correlation between the direction of emission of internal-conversion electrons and positrons and the direction of emission of β electrons from the preceding β-decaying nucleus. The calculation is conducted for allowed β transitions without taking into account the Coulomb field of the nucleus (in the Born approximation) under some very general assumptions regarding the β-interaction Hamiltonian. The expressions obtained refer to arbitrary 2^j-pole electric and magnetic types of nuclear conversion transitions. The case of VA types of β coupling (with conservation of time parity) is considered as well as the case of β transitions involving a change by unity of the nuclear spin, $\Delta I = \pm 1$ ($\Delta T = \pm 1$). A numerical computation is carried out on the polarization of internal conversion electrons emitted after β decay of the Na^{24} nucleus.

PARITY nonconservation in β decay processes makes the nucleus obtained as a result of β decay polarized in the direction of emitted β electron. It is assumed that the initial nucleus is unpolarized and the direction of emission of the neutrino is not registered. Consequently, if the β decay is followed by conversion with production of electron-positron pairs, the pair particles should be polarized in a definite manner. Let us consider the polarization of the internal-conversion electrons and positrons.

Let I_1 be the angular momentum of the parent nucleus, I_2 and m_2 the momentum and the projection of the momentum of the nucleus produced as a result of the β decay, with I_3 and m_3 the same for the final nucleus.

We are thus considering a process comprised of the $I_1 \to I_2$ (β decay) transition followed by I_2, $m_2 \to I_3$, m_3 (internal conversion with pair production). The β-decay stage of this process is described by a density matrix that characterizes the polarization state of the nucleus due to the β decay.

An expression for the density matrix was obtained by Berestetskiĭ and Rudik.[1] For an allowed β transition in the case of the S, T, A, and V variants of the interaction without allowance for the Coulomb field of the nucleus, the matrix has the form

$$\rho_{m_2 m_2'} = \frac{1}{2I_2+1}\left\{\delta_{m_2 m_2'} + \left(\frac{I_2+1}{I_2}\right)^{1/2} \xi \sum_{\mu} C^{I_2 m_2}_{I_2 m_2'; 1\mu} v^{\mu}\right\}, \qquad (1)$$

where v^{μ} are the spherical components of the β-electron velocity vector

$$v^0 = v_z, \qquad v^{\pm 1} = \mp (v_x \mp i v_y)/\sqrt{2};$$

$C^{a\alpha}_{b\beta;d\delta}$ is the Clebsch-Gordan coefficient; ξ is a constant that determines the angular distribution of the β electrons when a polarized nucleus with momentum I_2 and with an average momentum projection $\langle I_{2Z} \rangle$ decays to a state with momentum I_1:

$$\xi = 2\,\mathrm{Re}\,\{(c_T c_S'^{*} + c_T' c_S^{*} - c_A c_V'^{*} - c_A' c_V^{*})[I_2/(I_2+1)]^{1/2}\delta_{I_1 I_2} M_F M_{GT}^{*} + (c_T c_T'^{*} - c_A c_A'^{*})|M_{GT}|^2 \Lambda_{I_1 I_2}\}\{(|c_S|^2 + |c_S'|^2 + |c_V|^2 + |c_V'|^2)|M_F|^2 + (|c_T|^2 + |c_T'|^2 + |c_A|^2 + |c_A'|^2)|M_{GT}|^2\}^{-1}, \qquad (2)$$

$$\Lambda_{I_1 I_2} = [I_2(I_2+1) - I_1(I_1+1) + 2]/2I_2(I_2+1),$$

$$M_F = \left(\int 1\right), \qquad M_{GT} = \left(\int \sigma\right).$$

The probability of conversion with production of electron-positron pairs, for a nucleus which has previously experienced a β decay, is[1]

$$W = \sum_{\substack{m_2 m_2' m_3 \\ MM'}} \rho_{m_2 m_2'} (I_2 m_2 | Q^{(\lambda)}_{jM} | I_3 m_3)^{*} (I_2 m_2' | Q^{(\lambda)}_{jM'} | I_3 m_3) \times (B^{(\lambda)}_{jM})_{21} (B^{(\lambda)}_{jM'})^{*}_{21}. \qquad (3)$$

Here $(I_2 m_2 | Q^{(\lambda)}_{jM} | I_3 m_3)$ is the nuclear matrix element of the conversion transition; $Q^{(\lambda)}_{jM}$ or the operator of the 2^j-pole electric ($\lambda = 1$) are magnetic ($\lambda = 0$) moments of the nucleus, corresponding to the given type of conversion transition; $B^{(\lambda)}_{jM}$ is the operator of the interaction between the electron and positron of internal conversion with the field of the multipole;

$$(B_{jM}^{(\lambda)})_{21} = \int \psi_2^* B_{jM}^{(\lambda)} \psi_1 \, dr$$

is the matrix element of this operator while ψ_1, and ψ_2 are the wave functions of the positron and electron respectively.

The matrix element of the multipole moment of the nucleus can be represented in the form

$$(I_2 m_2 | Q_{jM}^{(\lambda)} | I_3 m_3)^* = Q^{(\lambda)} C_{I_3 m_3; jM}^{I_2 m_2}, \qquad (4)$$

where $Q^{(\lambda)}$ is independent of the quantum numbers m_2, m_3, and M. Substituting (4) in (3) and taking into account the properties of the Clebsch-Gordan coefficients

$$\sum_{m_2 m_3'} \delta_{m_2 m_2'} C_{I_3 m_3; jM}^{I_2 m_2} C_{I_3 m_3; jM'}^{I_2 m_2'} = \frac{2I_2 + 1}{2j + 1} \delta_{MM'},$$

$$\sum_{m_2 m_2' m_3} C_{I_3 m_3; jM}^{I_2 m_2} C_{I_3 m_2'; 1\mu}^{I_2 m_2'} C_{I_3 m_3; jM'}^{I_2 m_3}$$

$$= \frac{2I_2 + 1}{2j + 1} \frac{j(j+1) + I_2(I_2+1) - I_3(I_3+1)}{2\sqrt{j(j+1)\, I_2(I_2+1)}} C_{jM'; 1\mu}^{jM},$$

we transform the expression into

$$W = \sum_{MM'} \left\{ \delta_{MM'} + \frac{j(j+1) + I_2(I_2+1) - I_3(I_3+1)}{2I_2\sqrt{j(j+1)}} \xi \sum_{\mu} C_{jM'; 1\mu}^{jM} v^{\mu} \right\}$$

$$\times (B_{jM}^{(\lambda)})_{21} (B_{jM'}^{(\lambda)})_{21}^* = \sum_{MM'} A_{MM'} (B_{jM}^{(\lambda)})_{21} (B_{jM'}^{(\lambda)})_{21}^*. \qquad (5)$$

The wave functions of the internal-conversion electron and positron will be taken in the form of plane waves

$$\psi_1 = v \exp(i\mathbf{p}_+ \mathbf{r}), \qquad \psi_2 = u \exp(-i\mathbf{p}_- \mathbf{r}),$$

where $\mathbf{p}_+$ and $\mathbf{p}_-$ are the momenta of the positron and the electron, while v and u are unit Dirac bispinors for the positron and electron respectively. With these wave functions, the expression for the probability of pair conversion following β decay has the form (accurate to inessential multipliers)

$$W = \sum_{MM'} A_{MM'} \mathrm{Sp}\{(i\hat{p}_- - m) V_{jM}^{(\lambda)} (i\hat{p}_+ + m) \overline{V_{jM'}^{(\lambda)}}\},$$

where $\hat{p}_\pm = p_\pm^i \gamma_i$; the form of the expressions $V_{jM}^{(\lambda)}$, $\overline{V_{jM'}^{(\lambda)}} = \gamma_4 V_{jM'}^{(\lambda)+} \gamma_4$ will be given below.

The states of the polarization of the conversion electrons and positrons will be described with the aid of density matrices, which can be introduced in the usual manner. The normalized density matrix that determines the polarization of the conversion electrons in this process has the form

$$P_{(-)} = -\frac{1}{2\varepsilon_- W} \left\{ \sum_{MM'} A_{MM'} (i\hat{p}_- - m) V_{jM}^{(\lambda)} (i\hat{p}_+ + m) \overline{V_{jM'}^{(\lambda)}} (i\hat{p}_- - m) \gamma_4 \right\}, \qquad (6)$$

and analogously for positrons

$$P_{(+)} = -\frac{1}{2\varepsilon_+ W} \left\{ \sum_{MM'} A_{MM'} (i\hat{p}_+ + m) \overline{V_{jM'}^{(\lambda)}} (i\hat{p}_- - m) V_{jM}^{(\lambda)} (i\hat{p}_+ + m) \gamma_4 \right\}. \qquad (7)$$

If we do not register the angle θ between the momenta of the internal-conversion electron and positron, then the numerator and the denominator of the expressions (6) and (7) must be integrated with respect to θ.

The electron (positron) polarization 4-vector $\zeta_\mu = \{\boldsymbol{\zeta}; \zeta_0\}$ satisfies the condition $\zeta_\mu p_\mu = 0$. Therefore, in a reference frame where the electron (positron) is at rest, we have $\mathbf{p} = 0$ and $\zeta_0 = 0$, i.e., $\zeta_\mu^0 = \{\boldsymbol{\zeta}^0; 0\}$.

Consequently, the polarization properties of the electron (positron) can be determined, as is customarily done, with the aid of the three-dimensional vector $\boldsymbol{\zeta}^0$, connected with $\boldsymbol{\zeta}$,

$$\boldsymbol{\zeta}^0 = \boldsymbol{\zeta}_\perp + m\varepsilon^{-1} \boldsymbol{\zeta}_\parallel, \qquad (8)$$

where $\boldsymbol{\zeta}_\perp$ and $\boldsymbol{\zeta}_\parallel$ are the transverse and longitudinal components of the vector $\boldsymbol{\zeta}$, expressed in terms of the electron (positron) density matrix in the following manner:

$$\boldsymbol{\zeta} = i\varepsilon m^{-1} \mathrm{Sp}\{P\gamma_4\gamma_5\boldsymbol{\gamma}\}. \qquad (9)$$

Magnetic type of transition ($\lambda = 0$). The matrix element of the interaction operator of the internal-conversion electron and positron with the multipole field has the form[2]

$$(B_{jM}^{(0)})_{21} = u^* V_{jM}^{(0)} v = q^j (\omega^2 - q^2)^{-1} u^* \boldsymbol{\alpha} \mathbf{Y}_{jjM}(\mathbf{q}/q)\, v,$$

where $\mathbf{q} = \mathbf{p}_+ + \mathbf{p}_-$ and $\omega = \epsilon_+ + \epsilon_-$ are the momentum and the energy of the conversion transition, $\boldsymbol{\alpha}$ is the Dirac velocity matrix, and $Y_{jjM}(\mathbf{q}/q)$ is a transverse spherical vector.

Substituting the expressions for $V_{jM}^{(0)}$ and $V_{jM'}^{(0)}$ in (6), then (6) in (9), and then calculating the trace, summing over the magnetic quantum numbers M and M' (a method for summing similar expressions is developed in papers by Berestetskiĭ et al.[1,3]), and integrating over the angle θ, we obtain for the polarization vector of the internal-conversion electron the expression

$$\boldsymbol{\zeta}_{(-)}^0 = N_0 \{m^2\omega J_{2j-2}\mathbf{q}(\mathbf{vq}) + \tfrac{1}{2}(\varepsilon_+ - \varepsilon_-)(J_{2j} - \omega^2 J_{2j-2})\mathbf{p}_-(\mathbf{vq})\}$$
$$\times \{\varepsilon_- [(\varepsilon_+\varepsilon_- + m^2) J_{2j} - \tfrac{1}{4} J_{2j+2} - \tfrac{1}{4}\omega^2 (\varepsilon_+ - \varepsilon_-)^2 J_{2j-2}]\}^{-1},$$
$$N_0 = \xi [j(j+1) + I_2(I_2+1) - I_3(I_3+1)]/2I_2 j(j+1). \qquad (10)$$

The form of the expressions J_{2j+k} is given in the appendix.

It is obvious that all the results obtained are symmetrical under a substitution of the electrons

symbols (−) for the positron symbols (+) and vice versa, inasmuch as the calculation did not account for the Coulomb field of the nucleus. Therefore the corresponding expression $\zeta^0_{(+)}$ for positrons can be obtained directly from (10), by making everywhere in (10) the interchange $\epsilon_+ \rightleftarrows \epsilon_-$, $p_+ \rightleftarrows p_-$.

Electric type transition ($\lambda = 1$). In this case the matrix element of the operator $B^{(1)}_{jM}$ has the form[2]

$$(B^{(1)}_{jM})_{21} = u^* V^{(1)}_{jM} v = \frac{q^j}{\omega^2 - q^2} u^* \left\{ Y_{jM}(\mathbf{q}/q) - \sqrt{\frac{2j+1}{j}} \frac{\omega}{q} \mathbf{Y}_{j,\, j-1,\, M}(\mathbf{q}/q)\, \boldsymbol{\alpha} \right\} v,$$

where $Y_{jM}(\mathbf{q}/q)$ is the Laplace spherical function and $Y_{j,\, j-1,\, M}(\mathbf{q}/q)$ is a spherical vector. We use everywhere the system of mutually-orthogonal spherical vectors described in detail in reference 2.

After performing the same operations with $V^{(1)}_{jM}$ as in the case of magnetic transition, we obtain for the polarization vector of the internal-conversion electron

$$\zeta^0_{(-)} = N_1 \frac{\omega}{m} \left\{ m^2 J_{2j}(\mathbf{v} - \mathbf{n}(\mathbf{vn})) - \frac{m}{\epsilon_-} J_{2j} \mathbf{p}_-(\mathbf{v}(\mathbf{p}_+ - \mathbf{p}_-)) - \frac{m^3\omega^2}{j\epsilon_-} J_{2j-2}\, \mathbf{n}(\mathbf{vn}) + \frac{m\omega(\epsilon_+ - \epsilon_-)}{2j\epsilon_-} (\omega^2 J_{2j-4} + (2j-1) J_{2j-2})\, \mathbf{p}_-(\mathbf{vq}) \right\} \times \left\{ \frac{1}{2} J_{2j+2} - \frac{1}{2} J_{2j} \left[\omega^2 \frac{5j+1}{2j} + (\epsilon_+ - \epsilon_-)^2 \right] + \omega^2 J_{2j-2} \left(\frac{\omega^2}{2} + 2\epsilon_+\epsilon_- + 2m^2 + (\epsilon_- - \epsilon_+)^2 \right) + \frac{j-1}{4j} \omega^2 (\epsilon_+ - \epsilon_-)^2 J_{2j-4} \right\}^{-1}, \quad (11)$$

where $N_1 = N_0(j+1)$ and $\mathbf{n} = \mathbf{q}/q$ is a unit vector in the direction of the total momentum of the pair. By corresponding substitution, we can obtain directly from (11) an expression for the polarization vector of the positron $\zeta^0_{(+)}$.

In the case of the V − A variants of the β interaction (with conservation of time parity) the constant ξ, which enters into the expression of the density matrix $\rho_{m_1 m_2'}$, assumes the following form.

$$\xi = \{c_A^2 |M_{GT}|^2 \Lambda_{I_1 I_2} - 2c_V c_A [I_2/(I_2+1)]^{1/2} \delta_{I_1 I_2} M_F M^*_{GT}\} \times \{c_V^2 |M_F'|^2 + c_A^2 |M_{GT}|^2\}^{-1}.$$

In the case of a Gamow-Teller transition where the spin (or isotopic spin) changes by unity, $\Delta I = \pm 1$ ($\Delta T = \pm 1$), this constant is independent of the nuclear matrix elements and of the constants of the β interaction

$$\xi = \Lambda_{I_1 I_2} = [I_2(I_2+1) - I_1(I_1+1) + 2]/2I_2(I_2+1),$$

and depends only on the spins of the initial and final states of the nucleus (I_1 and I_2).

The expression (11) obtained in the present paper for $\zeta^0_{(-)}$ has been used for a numerical calculation of the polarization of the internal-conversion electrons that follow the β decay of the nucleus $Na^{24}[4^+(\beta^-)4^+(E2)2^+(E2)0^+]$. The transition $4^+(\beta^-)4^+$ is a Gamow-Teller transition in the isotopic spin.[4] Since, disregarding the Coulomb field of the nucleus, emission of conversion electrons and positrons with equal momenta is the most probable, we assume in the calculations $\epsilon_+ = \epsilon_- = \omega/2$ [for the conversion transition $4^+ \rightarrow 2^+(E2)$].

The calculation for the polarization of the pair-conversion electrons yielded in this transition

$$\zeta^0_{(-)} = 10^{-2}\{3(\mathbf{n}_\beta - \mathbf{n}(\mathbf{n}_\beta \mathbf{n})) - 0{,}7(\mathbf{n}_\beta \mathbf{n})\mathbf{n}\}.$$

It is clear therefore that in the conversion transition considered here the transverse polarization is one order of magnitude greater than the longitudinal polarization.

It must be noted that an account of the Coulomb field of the nucleus is apparently inessential in the conversion parts of the calculations, since the internal conversion is the most effective for nuclei with small charge Z, for which the Born approximation gives good results. On the other hand, the Coulomb field of the nucleus, for the β-decay stage of the considered process, can be readily accounted for by using the density matrix $\rho_{m_2 m_2'}$, obtained by Geshkenbeĭn.[5]

The author is deeply grateful to I. S. Shapiro for suggesting the topic and for constant interest in the work.

APPENDIX

The quantities J_{2j+k} ($k = 0, \pm 2, -4$) which arise upon integration over the angle of emission of the pair, are determined in the following manner

$$J_{2j-2} = p_+ p_- \int_0^\pi \frac{q^{2j-2}}{(q^2 - \omega^2)^2} \sin\theta\, d\theta = \frac{1}{4(j-2)} \{(p_+ + p_-)^{2(j-2)} (m^2 - p_+p_- - \epsilon_+\epsilon_-) - (p_+ - p_-)^{2(j-2)} (m^2 + p_+p_- - \epsilon_+\epsilon_-) + 4\omega^2 (j-1) J_{2j-4}\} \qquad (j \neq 2). \quad (A1)$$

When $j = 2$, we obtain by direct integration

$$J_2 = \ln \frac{m\omega}{p_+p_- + \epsilon_+\epsilon_- + m^2} + \frac{p_+p_-}{2m^2}. \quad (A2)$$

Analogously,

$$J_{2j} = p_+p_- \int_0^\pi \frac{q^{2j}}{(q^2-\omega^2)^2} \sin\theta\, d\theta$$

$$= \frac{1}{4(j-1)} \{(p_+ + p_-)^{2(j-1)} (m^2 - p_+p_- - \varepsilon_+\varepsilon_-)$$

$$- (p_+ - p_-)^{2(j-1)} (m^2 + p_+p_- - \varepsilon_+\varepsilon_-) + 4\omega^2 j J_{2j-2}\} (j \neq 1); \quad \text{(A3)}$$

when j = 1 we have the already obtained expression (A2).

[1] V. B. Berestetskiĭ and A. P. Rudik, JETP **35**, 159 (1958), Soviet Phys. JETP **8**, 111 (1959).

[2] A. I. Akhiezer and V. B. Berestetskiĭ, Квантовая электродинамика (Quantum Electrodynamics), 2d Ed. Fizmatgiz, 1959.

[3] Berestetskiĭ, Dolginov, and Ter-Martirosyan, JETP **20**, 527 (1950).

[4] N. A. Burgov and Yu. V. Terekhov, JETP **35**, 932 (1958), Soviet Phys. JETP **8**, 651 (1959).

[5] B. V. Geshkenbeĭn, JETP **35**, 1235 (1958), Soviet Phys. JETP **8**, 865 (1959).

Translated by J. G. Adashko
131

THE QUANTUM THEORY OF THE ELECTRICAL CONDUCTIVITY OF METALS IN STRONG MAGNETIC FIELDS

Yu. A. BYCHKOV

Institute for Physics Problems, Academy of Sciences, U.S.S.R.

Submitted to JETP editor April 8, 1960

J. Exptl. Theoret. Phys. (U.S.S.R.) 39, 689-702 (September, 1960)

We consider quantum mechanically galvanomagnetic phenomena in strong magnetic fields at very low temperatures in the limit where the lifetime of an electron is much larger than the period of its revolution in the magnetic field. We investigate metals with a quadratic dispersion law. We obtain formulae for the scattering of an electron by an impurity when a magnetic field is present.

I. M. Lifshitz and co-workers[1,2] have recently constructed in a number of papers a semiclassical theory of galvanomagnetic phenomena in metals in strong magnetic fields, taking the complicated character of the dispersion law for the elementary excitations into account. Also, a number of authors[3-5] obtained the quantum corrections to the resistivity tensor (the Shubnikov—de Haas effect). The results of different papers are, however, not in agreement with one another. A clarification of this problem is essentially connected with the paper by Adams and Holstein,[6] in which the transverse part of the conductivity tensor $\sigma_{\alpha\alpha}$ ($\alpha = x, y$; H is parallel to the z axis) was evaluated for a dispersion law $\epsilon = p^2/2m$ and in which the calculations of other authors were analyzed.

We obtain in the present paper expressions for σ_{ik} for metals with a small number of carriers, the dispersion law of which we know with assurance to be very close to quadratic. The energy surface can then be split up into several mutually nonintersecting ellipsoids. Bismuth is a typical example of such a metal.

One of the basic problems which arise also in the quantum case is that of taking into account the specific character of the scattering of an electron by impurities when a strong magnetic field is present. It will be shown in the following that in several cases an account of this fact determines in an essential way how the different quantities depend on the magnetic field.

1. FREE ELECTRON IN A MAGNETIC FIELD

We consider the motion of an electron with an arbitrary quadratic dispersion law

$$\varepsilon = \tfrac{1}{2}\mu_{ik}p_i p_k \qquad (1)$$

in a strong magnetic field. We find the wave functions and energy eigenvalues from the Schrödinger equation (here and henceforth $\hbar = c = 1$)

$$\hat{H}\psi_n = \tfrac{1}{2}\mu_{ik}(\hat{p}_i - eA_i)(\hat{p}_k - eA_k)\psi_n = E_n\psi_n, \qquad (2)$$

where μ_{ik} is the symmetrical inverse mass tensor and A_i the components of the vector potential of the magnetic field.

It is well known that the state of an electron in a magnetic field is characterized by the following quantities: the momentum p_z along the z axis, the momentum p_y which is connected with the x component x_0 of the center of the orbit along the x axis by the relation

$$x_0 = p_y/eH$$

and the magnetic quantum number M. In the following the index n denotes the set of all these quantities.

The energy eigenvalue of the n-th state is

$$E_n = \omega(M + 1/2) + p_z^2/2m_{zz},$$

where $\omega = eH\sqrt{m_{zz}/|m|}$, m_{ik} are the components of the mass tensor ($m_{ik} = \mu_{ik}^{-1}$) and $|m|$ is the determinant of the mass tensor.

We need in this paper the quantity

$$\int (x - x_0)^2 |\psi_n(x)|^2 dx.$$

If we use the well-known solutions of Eq. (2) we get easily

$$\int (x - x_0)^2 |\psi_n(x)|^2 dx = (M + 1/2)\frac{\mu_{xx}}{\omega}. \qquad (3)$$

2. SCATTERING OF AN ELECTRON IN A MAGNETIC FIELD BY AN IMPURITY

We need to know in the following the scattering amplitude for the scattering of an electron in a strong magnetic field by an impurity. Finding this amplitude is made much easier by the fact that for the metals with a small number of carriers, which we are considering, the electron wavelength is large compared with the range of the potential. It is well known that in that case we can use a δ-function potential to evaluate the transition amplitude

$$U(r) = f\delta(\mathbf{r}), \tag{4}$$

where f is the scattering amplitude for a zero-energy electron, when there is no magnetic field and where we have assumed for the sake of simplicity that the impurity is at the origin. We have then for the amplitude for the transition from the state n to the state m:

$$F_{mn} = \int \psi_m^*(\mathbf{r})\, U(\mathbf{r})\, \psi_n(\mathbf{r})\, d\mathbf{r} = f\psi_m^*(0)\,\psi_n(0). \tag{5}$$

Using this expression for the transition amplitude we can obtain the total probability for a transition from the state n to any state m ($E_m = E_n$):

$$W_n = 2\pi f^2 \sum_m |\psi_m(0)|^2 |\psi_n(0)|^2 \delta(E_n - E_m)$$
$$= \sqrt{2}\pi^{-1} f^2 |\psi_n(0)|^2 \omega |m|^{1/2} \sum_M [E_n - \omega(M + 1/2)]^{-1/2}. \tag{6}$$

The summation is over those values of M for which the expression under the radical sign is positive. It is clear from the expression given here for W_n that one can choose a value of the magnetic field in such a way that $E_n = \omega(N + 1/2) + \Delta$, $|\Delta| \ll \omega$. If $\Delta > 0$ and sufficiently small,

$$W_n = f^2 |\psi_n(0)|^2 \frac{\sqrt{2}\omega |m|^{1/2}}{\pi \sqrt{\Delta}}, \tag{7}$$

i.e., when $\Delta \to 0$ the total transition probability tends to infinity. The result obtained indicates that if one takes the influence of the magnetic field on the scattering into account only through Eq. (5), this will, as is well known, be insufficient in the neighborhood of some values of the magnetic field.

We try to find those corrections to F_{mn} in the higher approximations in U which are due only to the presence of the magnetic field. Generally speaking, one can only use the potential in the form (4) when looking for the transition amplitude in the first Born approximation. We retain (4), however, also when looking for the next approximations in the scattering amplitude, but keep in the different terms only expressions which are essentially connected with the magnetic field.

The exact transition amplitude is in the form of a series

$$F_{mn} = U_{mn} - \sum_k \frac{U_{mk}U_{kn}}{E_k - E - i\delta} + \sum_{k,l} \frac{U_{mk}U_{kl}U_{ln}}{(E_k - E - i\delta)(E_l - E - i\delta)} \cdots \tag{8}$$

We consider the second term in that series in more detail

$$-\sum_k \frac{U_{mk}U_{kn}}{E_k - E - i\delta} = -f^2\psi_m^*(0)\,\psi_n(0) \sum_k \frac{|\psi_k(0)|^2}{E_k - E - i\delta}$$
$$= -f^2\psi_m^*(0)\,\psi_n(0)\,\frac{\omega |m|^{1/2}}{2^{3/2}\pi}\left\{ i\sum_M [E - \omega(M + 1/2)]^{-1/2} \right.$$
$$\left. + \sum_M [\omega(M + 1/2) - E]^{-1/2} \right\}. \tag{9}$$

Here and henceforth the summation over M is only over those values of M for which the respective expressions under the square root sign are positive. The second sum within the curly brackets diverges. This divergence is caused by the fact that we have used a δ-function potential. If we take f to mean the total amplitude for $E = 0$ when there is no magnetic field, we must simply drop the divergent terms. The correction to the scattering amplitude in the second Born approximation will be small except when the energy is very near a odd-half-integral multiple of ω, i.e., $\Delta \to 0$. If the absolute magnitude of Δ is sufficiently small the expression within the braces is equal to

$$\frac{i}{\sqrt{\Delta}} = \begin{cases} \dfrac{i}{\sqrt{\Delta}}, & \Delta > 0 \\ \dfrac{1}{\sqrt{|\Delta|}}, & \Delta < 0 \end{cases}$$

and we get for (9) as $\Delta \to 0$

$$-f^2\psi_m^*(0)\,\psi_n(0)\,\frac{i\omega |m|^{1/2}}{2^{3/2}\pi\sqrt{\Delta}}.$$

We note easily that if we retain only the terms that tend to infinity in the series (8) near $\Delta = 0$, we get the simple geometric series

$$F_{mn} = f\psi_m^*(0)\,\psi_n(0)\{1 - fG_1 + f^2G_1^2 - \ldots\}$$
$$= f\psi_m^*(0)\,\psi_n(0)(1 + fG_1)^{-1},$$

$$G_1 = \frac{\omega |m|^{1/2}}{2^{3/2}\pi\sqrt{\Delta}}. \tag{10}$$

From the relation just obtained it is clear that as $\Delta \to 0$

$$|F_{mn}|^2 = |\psi_m(0)|^2 |\psi_n(0)|^2 8\pi^2 |\Delta|/\omega^2 |m|.$$

In some cases the amplitude has still another singularity. Let $\Delta < 0$. Then

$$F_{mn} = f\psi_m^*(0)\,\psi_n(0)\left\{1 + \frac{f\omega\,|m|^{1/2}}{2^{3/2}\pi\sqrt{|\Delta|}}\right\}^{-1}.$$

If f < 0 then for some value of $|\Delta_0|$ such that

$$|\Delta_0|^{1/2} = -f\omega\,|m|^{1/2}/2^{3/2}\pi \ll \omega,$$

Fmn will tend formally to infinity. It is clear that when $\Delta = -|\Delta_0|$ and $\Delta = 0$ Eq. (10) for the transition amplitude becomes incorrect, for in fact the amplitude will tend neither to zero nor to infinity.

It is easiest to correct Eq. (10) near $\Delta = -|\Delta_0|$. Near this point it is no longer possible to discard the finite imaginary part in Eq. (9). Taking this fact into account, we get the following expression for the amplitude near the resonance*

$$F_{mn} = f\psi_m^*(0)\,\psi_n(0)\left\{1 + \frac{f\omega\,|m|^{1/2}}{2^{3/2}\pi\sqrt{-\Delta}} + i\frac{f\omega\,|m|^{1/2}}{2^{3/2}\pi}\sum_M [E - \omega(M + 1/2)]^{-1/2}\right\}^{-1}. \quad (11)$$

We note here that the resonance width $(\Delta E)_{res}$ is much smaller than the width of the interval ΔE in which the amplitude is less than its classical value, namely

$$(\Delta E)_{res} \sim \Delta E\sqrt{\sigma}/\lambda,$$

where σ is the scattering cross section for H = 0, and $1/\lambda \sim \sqrt{mE}$. The presence of such a resonance is connected with the existence of a bound state of the electron in the attractive potential when a magnetic field is present. To find the energy and the wave function of this bound state we turn to the integral equation for the wave function

$$\psi(\mathbf{r}) = -\int G(\mathbf{r}, \mathbf{r}'; E)\,U(\mathbf{r}')\,\psi(\mathbf{r}')\,d\mathbf{r}', \quad (12)$$

where

$$G(\mathbf{r}, \mathbf{r}'; E) = \sum_n \frac{\psi_n(\mathbf{r})\,\psi_n^*(\mathbf{r}')}{E_n - E - i\delta} \qquad (\delta \to 0), \quad (13)$$

is the electron Green function. It is necessary for us to find the wave function in the region where the attractive force is acting, i.e., for very small values of $\mathbf{r}$ and $\mathbf{r}'$. In that region, however,

$$G(\mathbf{r}, \mathbf{r}'; E) = G_0(\mathbf{r}, \mathbf{r}') + G_1(E),$$

where $G_0(\mathbf{r}, \mathbf{r}')$ is the electron Green function for E = 0 when there is no magnetic field. To obtain $G_1(E)$ we take it into account that when there is no impurity the electron is in the ground state with M = 0. The attraction of the impurity causes the energy to become equal to

$$E = \omega/2 - \delta_1, \qquad 0 < \delta_1 \ll \omega.$$

There is then in the sum (13) a large term corresponding to M = 0, which is equal to

$$G_1(E) = \frac{\omega\,|m|^{1/2}}{2^{3/2}\pi\sqrt{\omega/2 - E}},$$

so that

$$\psi(\mathbf{r}) = -\int [G_0(\mathbf{r}, \mathbf{r}') + G_1(E)]\,U(\mathbf{r}')\,\psi(\mathbf{r}')\,d\mathbf{r}'$$

$$= G_1(E)\,\alpha - \int G_0(\mathbf{r}, \mathbf{r}')\,U(\mathbf{r}')\,\psi(\mathbf{r}')\,d\mathbf{r}',$$

$$\alpha = -\int U(\mathbf{r}')\,\psi(\mathbf{r}')\,d\mathbf{r}'.$$

One obtains easily from this equation the fact that $\psi(\mathbf{r}) = G_1(E)\,\alpha\psi_0(\mathbf{r})$, where $\psi_0(\mathbf{r})$ is the electron wave function for E = 0 in the field of the impurity when there is no magnetic field. It is clear that

$$f = \int U(\mathbf{r})\,\psi_0(\mathbf{r})\,d\mathbf{r},$$

from which one obtains easily a condition for finding the energy

$$1 = -fG_1(E) = -f\omega\,|m|^{1/2}/2^{3/2}\pi\sqrt{\omega/2 - E},$$

$$E = \omega/2 - f^2\omega^2\,|m|/8\pi^2. \quad (14)$$

This is indeed the energy of the bound state.

Using (12) one obtains easily an expression for the wave function of the bound state far from the impurity (for the sake of simplicity we have written down here the expression for the cose $\epsilon = p^2/2m$)

$$\psi(\mathbf{r}) = A\exp\left\{-|z|\sqrt{2m(\omega/2 - E)} - \frac{1}{4}(x^2 + y^2)eH\right\}, \quad (15)$$

where A is a normalizing factor. It is clear that there can only be a bound state if the magnitude of the reciprocal volume occupied by the electron is much larger than the impurity concentration, i.e., the condition

$$N_{imp} \ll (eH)^2 mf$$

must be satisfied.

It is clear that the resonance found in the foregoing for the scattering of electrons when M > 0 is caused by the virtual transition to the bound state. In the following we discuss the problem of the possibility to observe this resonance by investigating the behavior of the resistivity in a magnetic field.

We now turn to an investigation of the behavior

*Skobov obtained this result independently of the dispersion law $\epsilon = p^2/2m$. I use this opportunity to thank Skobov for sending me his manuscript prior to its publication.

of F_{mn} near $\Delta = 0$, i.e., near the point where it tends to zero, according to (10). To do this we turn to the integral equation for the wave function $\psi(\mathbf{r})$

$$\psi_n(\mathbf{r}) = \psi_{n_0}(\mathbf{r}) - \int G(\mathbf{r}, \mathbf{r}'; E)\, U(\mathbf{r}')\, \psi_n(\mathbf{r})\, d\mathbf{r}'. \quad (16)$$

When $\Delta \approx 0$ Eq. (13) for $G(\mathbf{r}, \mathbf{r}'; E)$ can be written as the sum of two terms

$$G(\mathbf{r}, \mathbf{r}'; E) = G'(\mathbf{r}, \mathbf{r}'; E) + \Delta^{-1/2} g_N(\rho, \rho'),\ \Delta \to 0.$$

In the expression for $G'(\mathbf{r}, \mathbf{r}'; E)$ the summation is over all magnetic quantum numbers $M \neq N$ ($E = \omega(N + \frac{1}{2})$) and we can thus put $\Delta = 0$ in $G'(\mathbf{r}, \mathbf{r}'; E)$ and $g_N(\rho, \rho')$. It is clear that $g_N(\rho, \rho')$ is independent of z and z', i.e., the z component of the vector ρ is equal to zero.

The function $\psi_n(\mathbf{r})$ satisfies in the point $\Delta = 0$ two equations

$$\int g_N(\rho, \rho')\, U(\mathbf{r}')\, \psi_n(\mathbf{r}')\, d\mathbf{r}' = 0, \quad (17)$$

$$\psi_n(\mathbf{r}) = \psi_{n_0}(\mathbf{r}) + A(\rho) - \int G'(\mathbf{r}, \mathbf{r}'; E)\, U(\mathbf{r}')\, \psi_n(\mathbf{r}')\, d\mathbf{r}', \quad (17')$$

where $A(\rho)$ is some function which is independent of z and which is determined by (17). Because (17) must be satisfied for any ρ, Eq. (17') is equivalent to the condition

$$\int U(\rho, z)\, \psi_n(\rho, z)\, dz = 0. \quad (17'')$$

If the potential $U(\mathbf{r})$ is sufficiently weak it is clear from (17') that

$$\frac{\partial \psi_n}{\partial z} = \frac{\partial \psi_{n_0}}{\partial z} = i p_z^n\, \psi_{n_0}, \qquad \frac{\partial^2 \psi_n}{\partial z^2} = \frac{\partial^2 \psi_{n_0}}{\partial z^2} = -(p_z^n)^2\, \psi_{n_0},$$

$$p_z^n \neq 0.$$

We put $\psi_{n_0}(\mathbf{r}) = \exp(i p_z^n z)\, \varphi_n(\rho)$. We have then from (17'')

$$\psi_n(\rho, 0) \int U(\rho, z)\, dz + i p_z^n\, \varphi_n(\rho) \int z U(\rho, z)\, dz$$

$$- \frac{(p_z^n)^2}{2} \varphi_n(\rho) \int z^2 U(\rho, z)\, dz = 0,$$

$$\psi_n(\rho, 0) = -i p_z^n \varphi_n(\rho) \frac{\int z U(\rho, z)\, dz}{\int U(\rho, z)\, dz}$$

$$+ \frac{(p_z^n)^2}{2} \varphi_n(\rho) \frac{\int z^2 U(\rho, z)\, dz}{\int U(\rho, z)\, dz}.$$

We now get easily the amplitude for the transition from the state n to the state m

$$F_{mn} = \int \psi_{m_0}^*(\mathbf{r})\, U(\mathbf{r})\, \psi_n(\mathbf{r})\, d\mathbf{r} = p_z^n\, p_z^m \int d\rho\, \varphi_m^*(\rho)\, \varphi_n(\rho)$$

$$\times \left\{ \int z^2 U(\rho, z)\, dz - \left[\int U(\rho, z)\, z\, dz \right]^2 \Big/ \int U(\rho, z)\, dz \right\},$$

$$p_z^n \neq 0,\ p_z^m \neq 0, \quad (18)$$

i.e., we get for $\Delta = 0$ a transition amplitude which though very small is different from zero.

We considered the case where there was one group of electrons. In practice, however, the energy surface in metals splits up into several ellipsoids and to each of these there corresponds a well defined group of electrons. In the scattering field of the impurity there are now possible not only transitions within a given group, but also a transition from one group into another one. In the following we shall give a qualitative analysis of this case.

We can now write the wave function in the following form

$$\psi(\mathbf{r}) = \psi_n^l(\mathbf{r})\, e^{i \mathbf{p}_l \mathbf{r}},$$

where $\psi_n^l(\mathbf{r})$ is the solution of Eq. (2) with the inverse mass tensor μ_{ik}^l corresponding to the ellipsoid with index 1, while the phase factor $e^{i\mathbf{p}_l \mathbf{r}}$ is due to the fact that the center of the ellipsoid in quasi-momentum space is not the same as the origin.

It is now no longer possible to assume the potential to have a δ-function shape, since when an electron goes from one group to another there occurs an appreciable transfer of quasi-momentum. At the same time, we shall assume that when $H = 0$ the potential is a Born potential. We have then in first approximation

$$F_{mn}^{l'l} = \int e^{-\mathbf{p}_{l'} \mathbf{r}}\, \psi_m^{*l'}(\mathbf{r})\, U(\mathbf{r})\, e^{i \mathbf{p}_l \mathbf{r}}\, \psi_n^l(\mathbf{r})\, d\mathbf{r}$$

$$\approx \psi_m^{l'*}(0)\, \psi_n^l(0) \int e^{-i(\mathbf{p}_{l'} - \mathbf{p}_l)\mathbf{r}}\, U(\mathbf{r})\, d\mathbf{r}$$

$$= f_{l'l}\, \psi_m^{l'*}(0)\, \psi_n^l(0) = U_{mn}^{l'l}.$$

We assume now that in the group l_0 there is for given H a state with $v_z \sim 0$, i.e., $\Delta l_0 \sim 0$. It is now no longer possible to restrict ourselves to the first Born approximation, so that

$$F_{mn}^{l'l} = U_{mn}^{l'l} - \sum_{l_i, k} \frac{U_{mk}^{l'l_i}\, U_{kn}^{l_i l}}{E_k - E - i\delta} + \dots$$

It is clear that in the sum over intermediate states we must retain only the term with $l_i = l_0$. The term in the second order in U is then of the form

$$- f_{l'l_0} f_{l_0 l}\, \psi_m^{l'*}(0)\, \psi_n^l(0)\, G_{l_0}(E), \quad (19)$$

where

$$G_{l_0}(E) = i\omega_{l_0} |m^{l_0}|^{1/2} / 2^{3/2} \pi \sqrt{\Delta_{l_0}}. \quad (19')$$

When we consider the terms in the next approximations in U we find easily that near $\Delta l_0 = 0$

$$F_{mn}^{l'l} = \psi_m^{l'*}(0)\, \psi_n^l(0) \left[f_{l'l} - \frac{f_{l'l_0} f_{l_0 l}\, G_{l_0}}{1 + G_{l_0} f_{l_0 l_0}} \right]$$

and that as

$$\Delta_{l_0} \to 0, \quad G_{l_0} \to \infty$$

we have

$$F_{mn}^{l'l} = \psi_m^{l'*}(0)\,\psi_n^{l}(0)\,[f_{l'l} - f_{l'l_0} f_{l_0 l}/f_{l_0 l_0}]. \qquad (20)$$

From this formula it is clear that if either l or l' is equal to l_0 the corresponding amplitude tends to zero. When $l \neq l_0$, $l' \neq l_0$ it is always different from zero.

It is easy to investigate the case when for two or more electrons there occur states with $v_z = 0$. To do this we turn to the integral equation for $\psi(\mathbf{r})$

$$\psi_n(\mathbf{r}) = \psi_{n0}^{l}(\mathbf{r})\,e^{i\mathbf{p}_l\mathbf{r}} - \int G(\mathbf{r}, \mathbf{r}'; E)\,U(\mathbf{r}')\,\psi_n(\mathbf{r}')\,d\mathbf{r}'. \qquad (21)$$

One can write the function $G(\mathbf{r}, \mathbf{r}'; E)$ in the form

$$G(\mathbf{r}, \mathbf{r}'; E) = \sum_j e^{i\mathbf{p}_j(\mathbf{r}-\mathbf{r}')}\,G_j(E) + G_0(\mathbf{r}, \mathbf{r}'),$$

where G_j is described by Eq. (19′) and where $G_0(\mathbf{r}, \mathbf{r}')$ is the Green function when there is no magnetic field.

As we assume the potential to be a Born one, we can neglect on the right hand side of (21) the term with G_0. We have then

$$\psi_n(\mathbf{r}) = \psi_{n0}^{l}(\mathbf{r})\,e^{i\mathbf{p}_l\mathbf{r}} - \sum_j e^{i\mathbf{p}_j\mathbf{r}}\,G_j(E)\int e^{-i\mathbf{p}_j\mathbf{r}'}\,U(\mathbf{r}')\,\psi_n(\mathbf{r}')\,d\mathbf{r}'. \qquad (22)$$

Here $\psi_{n_0}^{l}(\mathbf{r})$ is the electron wave function when there are no impurities. By definition the amplitude of the transition from a state described by the wave function $\psi_{n_0}^{l}(\mathbf{r})$ to a state $\psi_{m_0}^{l'}(\mathbf{r})$ is

$$F_{mn}^{l'l} = \int e^{-i\mathbf{p}_{l'}\mathbf{r}}\,\psi_{m0}^{l'*}(\mathbf{r})\,U(\mathbf{r})\,\psi_n(\mathbf{r})\,d\mathbf{r},$$

where $\psi_n(\mathbf{r})$ is a solution of Eq. (22). It is thus necessary to know $\psi_n(\mathbf{r})$ within the range of the potential. Assuming as before that the potential is a short-range one we can put in (22) $\psi_{n_0}^{l}(\mathbf{r})$ constant within the range of the impurity field.

It is, however, not possible to replace the exponential by unity since when we go from a state corresponding to the group l to a state corresponding to the group l', a large momentum transfer takes place. If we take this fact into account we can write the solution of (22) in the form

$$\psi_n(\mathbf{r}) = \psi_{n0}^{l}(0)\,\{e^{i\mathbf{p}_l\mathbf{r}} - \sum_j e^{i\mathbf{p}_j\mathbf{r}}\,G_j(E)\,\alpha_j\}.$$

It is clear from Eq. (22) that the quantities α_j can be found from the equation

$$\alpha_j = f_{jl} - \sum_k G_k\,\alpha_k\,f_{jk}. \qquad (23)$$

The final expression for the amplitude $F_{mn}^{l'l}$ will be of the form

$$F_{mn}^{l'l} = \psi_{m0}^{l'*}(0)\,\psi_{n0}^{l}(0)\,[f_{l'l} - \sum_k G_k\,f_{l'k}\,\alpha_k]. \qquad (24)$$

We easily get from Eqs. (23) and (24), for instance, the expression for $F_{mn}^{l'l}$ when G_α and $G_\beta \to \infty$. In that case

$$F_{mn}^{l'l} = \psi_{m0}^{l'*}(0)\,\psi_{n0}^{l}(0)\left[f_{l'l} - \frac{f_{l'\alpha}\,G_\alpha\,f_{\alpha l}\,(1+G_\beta\,f_{\beta\beta}) + f_{l'\beta}\,G_\beta\,f_{\beta l}\,(1+G_\alpha\,f_{\alpha\alpha}) - f_{l'\alpha}\,G_\alpha\,f_{\alpha\beta}\,G_\beta\,f_{\beta l}}{(1+f_{\alpha\alpha}\,G_\alpha)\,(1+f_{\beta\beta}\,G_\beta) - G_\alpha\,f_{\alpha\beta}\,G_\beta\,f_{\beta\alpha}}\right.$$

$$\left. - \frac{f_{l'\beta}\,G_\beta\,f_{\beta\alpha}\,G_\alpha\,f_{\alpha l}}{(1+f_{\alpha\alpha}\,G_\alpha)\,(1+f_{\beta\beta}\,G_\beta) - G_\alpha\,f_{\alpha\beta}\,G_\beta\,f_{\beta\alpha}}\right],$$

and as $G_\alpha = G_\beta = \infty$ we get

$$F_{mn}^{l'l} = \psi_{m0}^{l'*}(0)\,\psi_{n0}^{l}(0)\left[f_{l'l} - \frac{f_{l'\alpha}\,f_{\alpha l}\,f_{\beta\beta} + f_{l'\beta}\,f_{\beta l}\,f_{\alpha\alpha} - f_{l'\alpha}\,f_{\alpha\beta}\,f_{\beta l} - f_{l'\beta}\,f_{\beta\alpha}\,f_{\alpha l}}{f_{\alpha\alpha}\,f_{\beta\beta} - f_{\alpha\beta}\,f_{\beta\alpha}}\right]. \qquad (25)$$

From this formula it is at once clear that if either l or l' is equal to α or β, the corresponding amplitude tends to zero. If, however, $l \neq \alpha, \beta$; $l' \neq \alpha, \beta$ the amplitude differs from zero. This result has a general character and can be formulated as follows: If $l^{(1)}, l^{(2)}, \ldots$ are the numbers of the groups of electrons which possess for a given H a state with $v_z = 0$, then $F_{mn}^{l'l} = 0$ if either l or l' is equal to $l^{(1)}, l^{(2)}, \ldots$, and $F_{mn}^{l'l}$ is different from zero if $l \neq l^{(1)}, l^{(2)}, \ldots, l' \neq l^{(1)}, l^{(2)}, \ldots$

3. GALVANOMAGNETIC PHENOMENA

We turn to a direct investigation of the dependence of the electrical conductivity on the magnetic field. We shall in the following be interested only in the case where the period of revolution of the electron in the magnetic field is appreciably less than the time of mean free flight, i.e., where the relation $1/\omega\tau \ll 1$ is satisfied. Since the scattering is elastic the total current of the system of electrons is simply the sum of the currents caused by the different electrons. It is also necessary to

take into account the fact that the scattering is by a random distribution of impurities the average distance between which is larger than the electron wave length and the scattering amplitude. The waves scattered by different impurities do therefore not interfere with one another.

It is well known that the conductivity σ in a magnetic field is a tensor quantity whose components σ_{ik} satisfy the symmetry relations[8] $\sigma_{ik}(\mathbf{H}) = \sigma_{ki}(-\mathbf{H})$. It is convenient to write σ_{ik} as a sum of two terms

$$\sigma_{ik} = s_{ik} + a_{ik},$$
$$s_{ik}(\mathbf{H}) = s_{ki}(\mathbf{H}), \quad a_{ik}(\mathbf{H}) = -a_{ki}(\mathbf{H}).$$

When we change over from the components of the conductivity tensor to the components of the resistivity tensor, we must take it into account that in pure metals with a quadratic dispersion law the condition that there be as many electrons as holes must be satisfied. Applied to a real metal this means that a_{xy} though different from zero is appreciably less than s_{xy} in spite of the fact that the first one is proportional to H^{-1} and the second one to H^{-2}. Account of this leads to the following equations expressing the resistivity tensor in terms of the conductivity tensor

$$\sigma_{ik}^{-1} = \rho_{ik} + b_{ik}, \qquad \rho_{ik}(\mathbf{H}) = \rho_{ki}(\mathbf{H}),$$
$$b_{ik}(\mathbf{H}) = -b_{ki}(\mathbf{H}).$$

If we now introduce a vector $\mathbf{a}$ which is the dual of the tensor a_{ik} and a vector $\mathbf{b}$ which is dual to b_{ik} we get for the most important components of the tensor σ_{ik}^{-1}[8]

$$\rho_{xx} = |\sigma|^{-1}(a_x^2 + s_{yy}s_{zz}), \qquad \rho_{xy} = |\sigma|^{-1}(a_x a_y - s_{xy}s_{zz}),$$
$$\rho_{yy} = |\sigma|^{-1}(a_y^2 + s_{xx}s_{zz}), \qquad \rho_{zz} = |\sigma|^{-1}(s_{xx}s_{yy} - s_{xy}^2) \quad (26)$$

for the symmetric part and

$$b_x = -|\sigma|^{-1}(a_x s_{xx} + a_y s_{xy}), \quad b_y = -|\sigma|^{-1}(a_x s_{xy} + a_y s_{yy}),$$
$$b_z = -|\sigma|^{-1}(a_x s_{xz} + a_y s_{yz} + a_z s_{zz}) \quad (27)$$

for the antisymmetric part of the resistivity tensor. Here $|\sigma|$ is the determinant of the tensor σ_{ik}:

$$|\sigma| = (s_{xx}s_{yy} - s_{xy}^2)s_{zz} + \sum_{\alpha,\beta} a_\alpha a_\beta s_{\alpha\beta} \qquad (\alpha, \beta = x, y).$$

We must find the tensor s_{ik} and the vector $\mathbf{a}$. The simplest to find are the components a_x and a_y, and we now proceed to evaluate these.

In the approximation considered ($1/\omega\tau \ll 1$) these components are independent of τ and can thus be found using the classical equations of motion for an electron when there are no impurities

$$\frac{d\mathbf{p}}{dt} = e\mathbf{E} + e[\mathbf{v}\times\mathbf{H}].$$

We take the magnetic field strength vector $\mathbf{H}$ in the direction of the z axis and the electrical field strength vector in the direction of the x axis.

Then

$$\frac{dp_x}{dt} = eE + ev_y H, \qquad \frac{dp_y}{dt} = -ev_x H, \qquad \frac{dp_z}{dt} = 0.$$

Using these equations for quantities averaged over a period of the motion in the magnetic field, we get

$$\bar{v}_y = -E/H, \qquad \bar{v}_x = 0, \qquad p_z = \text{const.} \quad (28)$$

From the relation $\epsilon = \frac{1}{2}\mu_{ik}p_i p_k$ we get $\bar{p}_i = m_{ik}\bar{v}_k$.

It is clear that the average drift velocity along the z axis is independent of p_z when the dispersion law is quadratic. For $p_z = 0$ we have thus

$$0 = m_{zx}\bar{v}_x + m_{zy}\bar{v}_y + m_{zz}\bar{v}_z,$$

or, if we take (28) into account

$$\bar{v}_z = Em_{zy}/Hm_{zz}.$$

For the components a_i we get, however, at once

$$a_l = \frac{E}{H}\sum_l \frac{m_{lz}^l}{m_{zz}^l} n_l. \quad (29)$$

The summation over l is here over all ellipsoids and for the groups corresponding to electrons $n_l > 0$ and for holes $n_l < 0$. In practice only the components a_x and a_y are different from zero since

$$a_z = (E/H)(n_e - n_h) = 0$$

in the approximation considered.

We find now the symmetric part s_{ik} (except the component s_{zz}). We use the Einstein relation according to which the current along the x axis ($\mathbf{H}$ is parallel to the z axis and $\mathbf{E}$ parallel to the x axis) is connected with the mean square displacement of the center of the electron orbit per unit time due to collisions:

$$\overline{(\Delta x)^2} = 2D, \quad (30)$$

where D is the diffusion coefficient. Then

$$j_x = -e^2E\int d\varepsilon \frac{\partial f_0}{\partial \varepsilon}\sum_l D_l(\varepsilon)\frac{dn_l}{d\varepsilon}. \quad (31)$$

Here f_0 is the electron Fermi distribution function

$$f_0 = \left\{1 + \exp\left(\frac{\varepsilon - \zeta}{kT}\right)\right\}^{-1}$$

(ζ has clearly different values for the electrons and the holes) $dn_l/d\epsilon$ is the density of states with the given energy which is well known to be equal to

$$\frac{dn_l}{d\varepsilon} = \frac{\omega_l |m^l|^{1/2}}{\sqrt{2}\,\pi^2}\sum_M \frac{1}{\sqrt{\varepsilon - \omega_l(M + \frac{1}{2})}} \quad (32)$$

in a magnetic field.

The problem of evaluating $s_{xx} = j_x/E$ is reduced to calculating the average value $(\Delta x)^2$.

It is clear that

$$\langle(\Delta x)^2\rangle = \Big\langle \sum_{l',\,m} (x_m - x_n)^2\, 2\pi\, |F^{l'l}_{mn}|^2\, \delta(E_m - E_n)\Big\rangle.$$

The symbol $\langle \ldots \rangle$ indicates averaging over all initial states n with energy ϵ; x_n and x_m are the centers of the electron orbits in the initial and final states.

If we now take it into account that according to the results obtained in Sec. 2

$$|F^{l'l}_{mn}|^2 = |f_{l'l}|^2\, |\psi^{l'}_m(0)|^2\, |\psi^{l}_n(0)|^2,$$

then

$$\langle(\Delta x)^2\rangle = 4\pi \sum_{l,'m} x_m^2\, |\psi^{l'}_m(0)|^2 \delta(E_m - \varepsilon)\, |f_{l'l}|^2\, N_{\text{imp}}$$

$$= \frac{\sqrt{2}}{\pi^2} \sum_{l'} |m^{l'}|^{1/2} \mu^{l'}_{xx} \sum_M \frac{M + 1/2}{\sqrt{\varepsilon - \omega_{l'}(M+1/2)}}\, 2\pi N_{\text{imp}}\, |f_{l'l}|^2. \tag{33}$$

We used Eq. (3) in deriving (33).

Substituting the expression obtained for $\langle(\Delta x)^2\rangle$ into (31) we get finally*

$$s_{xx} = -\frac{\sqrt{2}\, e^2 N \text{imp}}{\pi} \int d\varepsilon\, \frac{\partial f_0}{\partial \varepsilon} \sum_{l',\,l} |m^{l'}|^{1/2} \mu^{l'}_{xx}\, |f_{l'l}|^2\, \frac{dn_l}{d\varepsilon}$$

$$\times \sum_M \frac{M + 1/2}{\sqrt{\varepsilon - \omega_{l'}(M + 1/2)}}. \tag{34}$$

Expressions for the other components of S_{ik} (except S_{zz}) are obtained from Eq. (34) by substituting there μ_{ik} for μ_{xx}.

We consider now the component s_{zz}. To evaluate this we can use a transport equation which in this special case has a very simple form (we write the distribution function f as $f = f_0 + f^1$)

$$-eE\, \frac{p_z}{m^l_{zz}} \frac{\partial f_0}{\partial E_n} + \sum_{l',\,m} 2\pi\, |F^{l'l}_{mn}|^2 (f^1_m - f^1_n)\, \delta(E_m - E_n) = 0. \tag{35}$$

It is clear from (35) that $f^1 \sim p_z$ so that the term with f^1_m drops out as f^1_m is an odd function of p_z while $|F^{l'l}_{mn}|^2$ is an even one. Taking this into account we get

$$f^1_n \sum_{l',\,m} 2\pi\, |\psi^{l'}_m(0)|^2\, |\psi^{l}_n(0)|^2\, |f_{l'l}|^2\, \delta(E_m - E_n)$$

$$= -eE\, \frac{p_z}{m^l_{zz}} \frac{\partial f_0}{\partial E_n}.$$

Summing over all m and l' and averaging over the position of the center of the electron orbit in the initial state we find

$$f^1_n\, N_{\text{imp}} \sum_{l'} \frac{dn_{l'}}{d\varepsilon}\, 2\pi\, |f_{l'l}|^2 = -eE\, \frac{p_z}{m^l_{zz}} \frac{\partial f_0}{\partial \varepsilon},$$

$$s_{zz} = -\frac{e^2\pi}{\sqrt{2}} \int \frac{\partial f_0}{\partial \varepsilon}\, d\varepsilon \sum_l n_l \Big\{ N_{\text{imp}} \sum_{l'} |f_{l'l}|^2\, m^l_{zz}\, \omega_{l'}\, |m^{l'}|^{1/2}$$

$$\times \sum_M \frac{1}{\sqrt{\varepsilon - \omega_{l'}(M + 1/2)}} \Big\}^{-1}. \tag{36}$$

It is clear from the equations obtained for σ_{ik} that $a, a_y \sim H^{-1}$; $a_z \sim H^{-3}$; s_{ik} $(i \neq z, k \neq z)$ $\sim H^{-2}$; $s_{zz} \sim 1$. As far as σ^{-1}_{ik} is concerned, the components $\sigma^{-1}_{\alpha\beta}$ $(\alpha, \beta = x, y)$ and ρ_{zz} are the most important ones.

It follows from (25) and (26) that

$$\rho_{\alpha\beta} \sim H^2, \qquad b_z \sim H,$$

so that we shall only be interested in the following in $\rho_{\alpha\beta}$ and ρ_{zz}.

We start our investigation of the conductivity with the semi-classical region where the relation $\omega/\zeta \ll 1$ is satisfied. We can then represent the sums over the magnetic quantum number occurring within the braces in Eqs. (34) and (36), with sufficient accuracy, as follows

$$\sum_M \frac{1}{\sqrt{\varepsilon - \omega(M + 1/2)}} \approx 2\, \frac{\varepsilon^{1/2}}{\omega} + \frac{1}{\sqrt{\Delta}},$$

$$\sum_M \frac{M + 1/2}{\sqrt{\varepsilon - \omega(M + 1/2)}} \approx \frac{4}{3}\, \frac{\varepsilon^{3/2}}{\omega^2} + \frac{\varepsilon}{\omega\sqrt{\Delta}}, \tag{37}$$

where Δ is defined as before by the equation

$$\varepsilon = \omega(N + 1/2) + \Delta, \quad \Delta \ll \omega.$$

In (37), $\Delta > 0$.

For the range of values of the magnetic field considered it is convenient to introduce quantities $s^{l'l}_{\alpha\beta}(\text{cl})$ defined by means of the relations

$$s_{\alpha\beta}(\text{cl}) = \sum_{l',\,l} s^{l'l}_{\alpha\beta}(\text{cl}).$$

Then

$$s^{l'l}_{\alpha\beta}(\text{cl}) = N_{\text{imp}} \frac{4e^2}{3\pi^4} |m^{l'}|\, \mu^{l'}_{\alpha\beta} \frac{\zeta^2}{\omega^2_{l'}}\, 2\pi\, |f_{l'l}|^2. \tag{38}$$

If we use the results obtained we shall get for $s_{\alpha\beta}$ and s_{zz}

$$s_{\alpha\beta} = s_{\alpha\beta}(\text{cl})$$

$$- \sum_{l',\,l} s^{l'l}_{\alpha\beta}(\text{cl}) \int \frac{\partial f_0}{\partial \varepsilon}\, d\varepsilon \left[\frac{3\omega_{l'}}{4\zeta^{1/2}\sqrt{\Delta_{l'}}} + \frac{\omega_l}{2\zeta^{1/2}\sqrt{\Delta_l}} + \frac{3\omega_l\omega_{l'}}{8\zeta\sqrt{\Delta_l \Delta_{l'}}} \right]$$

$$s_{zz} = -\frac{e^2\pi}{2^{3/2} N_{\text{imp}}}$$

$$\times \int \frac{\partial f_0}{\partial \varepsilon}\, d\varepsilon \sum_l n_l \left\{ \sum_{l'} \left| f_{l'l} \right|^2 m_{zz} \left| m^{l'} \right|^{1/2} \zeta \left(1 + \frac{\omega_{l'}}{2\zeta^{1/2}\sqrt{\Delta_{l'}}} \right) \right\}^{-1} \tag{39}$$

It is necessary to emphasize here that the $f_{l'l}$ are different from zero only when the indices l' and l

*A similar equation for s_{xx} was obtained by B. Davydov and I. Pomeranchuk.[4]

refer either only to electron or only to hole states, i.e., when the electrons do not go over into holes, or vice versa, in the scattering by the impurity.

The terms containing $\Delta^{-1/2}$ in the expressions which we have written down describe the usual semi-classical oscillations of the conductivity in a magnetic field.

If we substitute the quantities $s_{\alpha\beta}$ and s_{zz} which we have found into (26) we obtain the final equations for the ρ_{ik}. These formulae are very cumbersome, for when the magnetic field has an arbitrary orientation with respect to the crystallographic directions, all the electron groups connected with the various ellipsoids will give contributions of the same order. We note that the formulae for the conductivity for the case when the magnetic field is perpendicular to the three-fold axis of bismuth were investigated in detail by I. Pomeranchuk and B. Davydov.[4] We shall therefore in the following investigate $\rho_{\alpha\beta}$ and ρ_{zz} only in the region where their behavior is anomalous.

1. By changing the magnitude of the magnetic field we can get $\Delta \ll \omega^2\zeta^{-1}$ for one or several electron groups. In practice this can apparently only be obtained for electrons corresponding to some given ellipsoids, which we denote by l_0. When we change over to the resistivity tensor we note that for sufficiently small Δl_0

$$\rho_{xx} = s_{yy}(s_{xx}s_{yy} - s_{xy}^2)^{-1}, \qquad \rho_{yy} = s_{xx}(s_{xx}s_{yy} - s_{xy}^2)^{-1},$$
$$\rho_{xy} = -s_{xy}(s_{xx}s_{yy} - s_{xy}^2)^{-1}, \qquad \rho_{zz} = s_{zz}^{-1}. \quad (40)$$

As far as s_{zz} is concerned in terms of which ρ_{zz} in (40) is expressed, if the group l_0 refers to electrons, only the term corresponding to holes remains in Eq. (39) for s_{zz}.

If Δl_0 is so small that we can retain in (39) just the term with Δ, then

$$s_{\alpha\beta} = -\frac{3}{8} s_{\alpha\beta}^{l_0 l_0}(\mathrm{cl}) \frac{\omega_{l_0}^2}{\zeta} \int \frac{\partial f_0}{\partial \varepsilon} \frac{d\varepsilon}{\Delta_{l_0}}, \quad (41)$$

$$\rho_{xx} = -\frac{8}{3} \rho_{xx}^{l_0 l_0}(\mathrm{cl}) \frac{\zeta}{\omega_{l_0}^2} \left[\int \frac{\partial f_0}{\partial \varepsilon} \frac{d\varepsilon}{\Delta_{l_0}}\right]^{-1}$$
$$= -\frac{\pi^3 \mu_{yy}^{l_0}}{e^2\zeta N_{\mathrm{imp}} |f_{l_0 l_0}|^2 m_{zz}^{l_0}} \left[\int \frac{\partial f_0}{\partial \varepsilon} \frac{d\varepsilon}{\Delta_{l_0}}\right]^{-1}. \quad (42)$$

One obtains similar expressions for ρ_{xy} and ρ_{yy}.

If $T = 0$ we have $\int \frac{\partial f_0}{\partial \epsilon} \frac{d\epsilon}{\Delta l_0} = -\frac{1}{\Delta l_0(\zeta)}$. When $T \ll \omega^2\zeta^{-1}$ (but $T \neq 0$) we must take into account the behavior of $|F_{mn}^{l' l}|^2$ as $\Delta l_0 \to 0$ when integrating. This leads to the following integral

$$\int \frac{\partial f_0}{\partial \varepsilon} \frac{d\varepsilon}{\Delta_{l_0} + a} = -\left[\frac{1}{\Delta_{l_0}(\zeta)} + \frac{\partial f_0(-\Delta_{l_0}(\zeta))}{\partial \zeta} \ln a\right],$$

where

$$a = |f_{l_0 l_0}|^2 \omega_{l_0}^2 |m^{l_0}| / 8\pi^2.$$

It is clear from Eq. (42) that $\rho_{\alpha\beta} \sim \Delta l_0$, i.e., that $\rho_{\alpha\beta}$ is appreciably decreased when Δl_0 is sufficiently small. The steep decrease of $\rho_{\alpha\beta}$ which we have obtained when $\Delta l_0 \to 0$ can in practice be observed only when the following conditions are satisfied:

$$kT \ll \omega_{l_0}^2 \zeta^{-1}, \qquad (\omega_{l_0}\tau)^{-1} \ll \omega_{l_0}\zeta^{-1}$$

and when the magnetic field is stabilized $\Delta H/H \ll \omega_{l_0}^2 \zeta^{-2}$. We note that this effect takes place not only in the semi-classical region but everywhere, so long as $\zeta = \omega(N + \frac{1}{2}) + \Delta$ and $\Delta \to 0$.

When the field is sufficiently strong ζ is not equal to its value when there is no field and must be determined from two conditions: the fact that the number of electrons must be equal to the number of holes $n_e = n_h$, and the condition that $\zeta_1 + \zeta_2 = E_0$ where $\zeta_1 \to \zeta_e$, $\zeta_2 \to \zeta_h$ and E_0 is a constant which is independent of H_0.

2. The expressions for $\rho_{\alpha\beta}$ and ρ_{zz} which we wrote down in the foregoing are valid for sufficiently small, but not too small values of Δl_0. If Δl_0 is very small it is essential to take into account the dependence of the scattering amplitude $F^{l' l}$ on the magnetic field H. For the sake of simplicity we restrict ourselves to the case $T = 0$. We note now immediately that it is apparently practically impossible to observe the anomaly in the resistivity near the resonance for scattering by impurities with an attractive potential because of the too stringent limitations as to the purity of the metal and the temperature. We shall therefore not investigate ρ_{ik} near this resonance.

When $\Delta l_0 \to 0$

$$s_{\alpha\beta} = \pi^{-3} e^2 N_{\mathrm{imp}} |m^{l_0}| \mu_{\alpha\beta}^{l_0} |f_{l_0 l_0}|^2 \zeta$$
$$\times \left[\Delta_{l_0} + \frac{1}{8}\pi^{-2} |f_{l_0 l_0}|^2 \omega_{l_0}^2 |m^{l_0}|\right]^{-1} \quad (43)$$

and we have, for instance, for ρ_{xx}

$$\rho_{xx} = \frac{\pi^3 \mu_{yy}^{l_0}}{e^2 N_{\mathrm{imp}} |f_{l_0 l_0}|^2 m_{zz}^{l_0} \zeta} \left[\Delta_{l_0} + \frac{|f_{l_0 l_0}|^2 \omega_{l_0}^2 |m^{l_0}|}{8\pi^2}\right].$$

It is clear from this formula that as $\Delta l_0 \to 0$, $\rho_{\alpha\beta}$ tends to some very small though finite limit.

We investigate now the behavior of ρ_{zz} for very small Δl_0. As before we have then $\rho_{zz} = s_{zz}^{-1}$. If we take the results of Sec. 2 into account we are led to the conclusion that for $\Delta l_0 = 0$ all amplitudes for which either l' or l is equal to l_0 tend to zero and that there remain only terms with $l \neq l_0$ and $l' \neq l_0$. At the same time these amplitudes $F^{l' l}$

are changed according to the results of Sec. 2. Finally, s_{zz} is given by Eq. (36) where $l' \neq l_0$ and $l \neq l_0$ and where we have instead of $|f_{l'l}|^2$

$$|f_{l'l} - f_{l'l_0} f_{l_0 l} / f_{l_0 l_0}|^2.$$

This result can be summarized as follows: for some values of **H** the group l_0 does not make any contribution to the conductivity s_{zz}. Up to now we considered the case where Δl_0 tended to zero from the positive side. However, the opposite case is, of course, also possible. The equation for s_{zz} is then not changed. $s_{\alpha\beta}$ will be given by Eq. (34) with $l \neq l_0$ and $l' \neq l_0$ if in that equation we replace

$$f_{l'l} \text{ by } f_{l'l} - f_{l'l_0} f_{l_0 l} / f_{l_0 l_0}.$$

The transition from the s_{ik} to the ρ_{ik} is then performed by means of Eqs. (26).

The final results about the behavior of the tensor ρ_{ik} near $\Delta l_0 = 0$ can be summarized as follows: when $\Delta l_0 \to 0$, $\rho_{\alpha\beta} \sim \Delta l_0$ and tends to a finite though very small limit; in a narrow region near $\Delta l_0 = 0$ $\rho_{\alpha\beta}$ changes quickly and the limits of $\rho_{\alpha\beta}$ when $\Delta l_0 \to +0$ and when $\Delta l_0 \to -0$ are essentially different from one another.

In conclusion I express my gratitude to Academician L. D. Landau and to I. M. Khalatnikov for valuable discussions when this research was done.

[1] Lifshitz, Azbel', and Kaganov, JETP **31**, 63 (1956), Soviet Phys. JETP **4**, 41 (1957).

[2] I. M. Lifshitz and V. G. Peschanskiĭ, JETP **35**, 1251 (1958), Soviet Phys. JETP **8**, 875 (1959).

[3] I. M. Lifshitz and L. M. Kosevich, JETP **33**, 88 (1957), Soviet Phys. JETP **6**, 67 (1958).

[4] B. Davydov and I. Pomeranchuk, JETP **9**, 1294 (1939).

[5] P. N. Argyres and E. N. Adams, Phys. Rev. **104**, 900 (1956); P. N. Argyres, Phys. Rev. **109**, 1115 (1958).

[6] E. N. Adams and T. D. Holstein, J. Phys. Chem. Solids **10**, 254 (1959).

[7] V. G. Skobov, JETP **37**, 1467 (1959), Soviet Phys. JETP **10**, 1039 (1960).

[8] L. D. Landau and E. M. Lifshitz, Электродинамика сплошных сред (Electrodynamics of Continuous Media) Gostekhizdat, 1957.

Translated by D. ter Haar
132

ON THE PSEUDOVECTOR CURRENT AND LEPTON DECAYS OF BARYONS AND MESONS

CHOU KUANG-CHAO

Joint Institute for Nuclear Research

Submitted to JETP editor April 7, 1960

J. Exptl. Theoret. Phys. (U.S.S.R.) **39**, 703-712,(September, 1960)

By the use of the analytic properties of a certain matrix element it is shown that the result of Goldberger and Treiman regarding the decay $\pi \to \mu + \nu$ is valid for wider classes of strong interactions than those found by Feynman, Gell-Mann, and Levy, and in particular for the ordinary pseudoscalar theory with pseudoscalar coupling. A formula is obtained which can be used for an experimental test of the assumptions that are made. Lepton decays of hyperons and K mesons are also discussed.

1. INTRODUCTION

AT the present time the theory of the universal V − A interaction given by Feynman and Gell-Mann and by Sudarshan and Marshak is in good agreement with all the experimental data on β decay and the decay of the μ meson.[1] The experimental ratio of the probabilities for the two types of π-meson decay, $R(\pi \to e + \nu)/R(\pi \to \mu + \nu)$, also agrees with the theoretical prediction. It may therefore be supposed that the universal V − A theory is also valid for processes of capture of μ mesons in nuclei.

One of the most important problems is the calculation of the probability of the decay $\pi \to \mu + \nu$ according to the universal V − A theory. This problem has been studied in detail in a paper by Goldberger and Treiman (G. T.)[2] by means of the technique of dispersion theory. Despite the fact that G. T. made many crude approximations, the numerical result of their work agrees almost exactly with the experimental result.

Quite recently Feynman, Gell-Mann, and Levy (F.G.L.) have reexamined this problem in a very interesting paper.[3] They have shown that the G.T. result can be obtained rigorously in certain models. Namely, let us write the Hamiltonian for β decay and μ-meson capture in the form

$$H = (g_0/\sqrt{2})(P_\alpha + V_\alpha) L_\alpha + \text{Herm. adj.} \qquad (1)$$

where

$$L_\alpha = \bar{\nu}\gamma_\alpha (1 + \gamma_5) e + \bar{\nu}\gamma_\alpha (1 + \gamma_5)\mu. \qquad (2)$$

P_α and V_α are the pseudovector and vector currents for the weak interactions. F.G.L. succeeded in finding three models of the strong interactions in which the following equation holds:

$$\partial_\alpha P_\alpha(x) = ia\pi(x)/\sqrt{2},$$

where a is a constant parameter and $\pi(x)$ is the pion-field operator. By using the equation (3), F.G.L. obtained the G.T. result in a simple and elegant way.

F.G.L. stated that their results would be extended later to any theory of the strong interactions. In their new theory, it is said in reference 3, there appears a form factor $\varphi(s)$, which is very complicated in the usual theory. In the opinion of F.G.L. it is only in the case of their models that it is reasonable to assume that $\varphi(s)$ is slowly varying.

After studying reference 3 we have come to the conclusion that the G.T. result is a good approximation for a wider class of strong interactions. In the present paper this conclusion is examined under the following assumptions:

1. The matrix element $\langle n | \partial_\alpha P_\alpha(0) | p \rangle$ is an analytic function of the variable $s = -(p_n - p_p)^2$.

2. If the matrix element of the commutator for equal times is equal to zero, then we can write a dispersion relation without subtraction.

3. The contribution of the nearest singularities predominates in the dispersion relation.

From our point of view the form factor $\varphi(s)$ actually is slowly varying in any theory in which there is a dispersion relation without subtraction for a certain matrix element.

In Secs. 2 and 3 a derivation of the G.T. result is presented in the most general form. It is shown that the G.T. result is also a good approximation for the ordinary pseudoscalar theory with pseudoscalar coupling. A relation is obtained between the pseudovector constant g_A for μ capture, g_A for β decay, and the pseudoscalar coupling constant f for μ capture. Since we can measure $g_{A\mu}$,

$g_{A\beta}$, and f separately, a test of this relation between the constants gives a sensitive criterion for the correctness of the assumptions made about the universality of the pseudovector coupling in the weak interaction and the analyticity of a certain matrix element.

In Sec. 4 the lepton decays of hyperons and K mesons are treated in an analogous way. From the data on the lifetime of K mesons the result is obtained that the pseudovector coupling constant g_{AY} for the β decay of hyperons is smaller than the coupling constant g_A for the β decay of neutrons.[9]

2. THE RESULT OF GOLDBERGER AND TREIMAN

Let us write

$$i\partial_\alpha P_\alpha(x) \equiv O(x). \tag{4}$$

Applying this equation to the decay $\pi \to \mu + \nu$, we get

$$\langle 0|O(0)|\pi\rangle = -q_\alpha \langle 0|P_\alpha(0)|\pi\rangle, \tag{5}$$

where q_α is the four-momentum of the pion. The matrix element $\langle 0|P_\alpha(0)|\pi\rangle$ can be expressed in the form

$$\langle 0|P_\alpha(0)|\pi\rangle = -q_\alpha F(m^2)/\sqrt{2q_0}, \tag{6}$$

where m is the mass of the pion and $F(m^2)$ is a constant parameter, which is determined by the lifetime of the pion.

Substituting Eq. (6) in Eq. (5), we get

$$\langle 0|O(0)|\pi\rangle = -m^2 F/\sqrt{2q_0}. \tag{7}$$

Let us now turn to the consideration of β decay and μ capture. In the general case the matrix element $\langle n|P_\alpha(0)|p\rangle$ is of the form

$$\langle n|P_\alpha(0)|p\rangle = \bar{u}_n\{g_A\gamma_\alpha\gamma_5 + if(p_p - p_n)_\alpha\gamma_5\}u_p, \tag{8}$$

where g_A and f are invariant functions of $s = -(p_p - p_n)^2$.

Applying the relation (4) to β decay and μ capture, we get

$$\langle n|O(0)|p\rangle = -(p_p - p_n)_\alpha \langle n|P_\alpha(0)|p\rangle. \tag{9}$$

Substituting Eq. (8) in Eq. (9), we have

$$\langle n|O(0)|p\rangle = i[2Mg_A + fs]\bar{u}_n\gamma_5 u_p. \tag{10}$$

The central problem is to find the connection between the matrix elements $\langle n|O(0)|p\rangle$ and $\langle 0|O(0)|\pi\rangle$. This can be done if we use the analyticity properties of the matrix element

$$\langle n|O(0)|p\rangle = i\bar{u}_n\gamma_5 u_p T(s), \tag{11}$$

$$T(s) = -\sqrt{2}GFm^2/(-s+m^2) + T'(s), \tag{12}$$

where G is the renormalized constant of the strong interactions of pions with nucleons, and $T'(s)$ is a function analytic in the region

$$|s| < 9m^2. \tag{13}$$

The derivation of (11) — (14) is given later, in Sec. 3. It is also shown there that $T'(s)$ is in fact a slowly varying function for small s.

In the region $|s| < m^2$ the function $T'(s)$ is approximated with good accuracy by a constant.

Let us rewrite (12) in the form

$$T(s) = -\sqrt{2}GF\varphi(s)m^2/(-s+m^2). \tag{14}$$

where

$$\varphi(s) = 1 + \alpha(s - m^2)/m^2. \tag{15}$$

Comparing (11) with (10), we get

$$2Mg_A + fs = -\sqrt{2}GF\varphi(s)m^2/(-s+m^2). \tag{16}$$

A very important fact is that the relation (16) holds for all s. Setting s = 0, we get

$$F = -2Mg_{A\beta}/\sqrt{2}G\varphi(0), \qquad g_{A\beta} = g_A(0). \tag{17}$$

This is the fundamental result of F.G.L., which was first obtained in the paper of Goldberger and Treiman.[2]

For μ capture

$$s_\mu = -Mm_\mu^3/(M+m_\mu) = -0.9\,m_\mu^2.$$

From (15), (16), and (17) we get*

$$2Mg_{A\mu} + f_\mu s_\mu = m^2 2Mg_{A\beta}/(-s_\mu + m^2). \tag{18}$$

Equation (18) is an exact relation between g_A, f for μ capture and g_A for β decay, which can be tested experimentally. It must be pointed out that the derivation of (18) has been carried out in the most general way, for an arbitrary value of α. As will be shown in Sec. 3, this holds for almost any theory in which the matrix element $\langle n|\partial_\alpha P_\alpha \times (0)|p\rangle$ is analytic.

Substituting the experimental values of G, $g_{A\beta}$ and F in (17), we get

$$\varphi(0) = 0.8. \tag{19}$$

From this and Eq. (15) we find

$$\alpha = 0.2. \tag{20}$$

We emphasize that the G.T. result is valid only for those theories in which the condition $\alpha \ll 1$ holds. This question is discussed in the following section.

*This relation is contained implicitly in a formula of Goldberger and Treiman.[4]

3. THE ANALYTICITY OF THE MATRIX ELEMENTS

Let us now turn to the calculation of the matrix element $\langle n|O(0)|p\rangle$. Using the standard method,[5] we write

$$\langle n|O(0)|p\rangle = -i\bar{u}_n \int d^4z e^{-ip_n z}\langle 0|T(\eta(z)O(0))|p\rangle$$

$$-u_n^{\cdot}\int d^4z e^{-ip_n z}\delta(z_0)\langle 0|[\psi_n(z), O(0)]|p\rangle, \qquad (21)$$

where $\eta(z) = iS^{+}\delta S/\delta\bar{\psi}_n(z)$ is the current operator for the neutron field. Hereafter the equal-time commutator will be omitted; it would give an additive constant in the final expression and would not affect the analytic structure of the matrix element, for example, the locations of the poles and their residues, the branch points, and so on.

We note that

$$T(\eta(z)O(0)) = \theta(-z)[O(0), \eta(z)] + \eta(z)O(0),$$

where $\theta(z) = 1$ for $z_0 > 0$ and $\theta(z) = 0$ for $z_0 < 0$. The second term makes no contribution to the matrix element. Thus we have

$$\langle n|O(0)|p\rangle = -i\bar{u}_n\int d^4z e^{-ip_n z}\theta(-z)\langle 0|[O(0), \eta(z)]|p\rangle. \qquad (22)$$

In the coordinate system $p_p = 0$ it is easy to show by the method of Bogolyubov[6] that the function $T(s)$ in Eq. (11) has a pole at $s = m^2$ and a cut that begins at the point $s = 9m^2$. At other points it is analytic, if the following inequality holds:

$$|\operatorname{Im} p_{n0}| > |\operatorname{Im}\sqrt{p_{n0}^2 - M^2}| \qquad (p_{n0} = M - s/2M). \qquad (23)$$

Unfortunately, the inequality (23) is satisfied only in the case of imaginary nucleon mass. We assume in what follows that the analyticity of the matrix element in the variable s does not change on analytic continuation with respect to the mass variable.

The residue at the pole $s = m^2$ is easily calculated and is equal to $2^{1/2}G\langle 0|O(0)|\pi\rangle(2q_0)^{1/2}$. Thus we have

$$T(s) = \frac{\sqrt{2}G}{-s+m^2}\langle 0|O(0)|\pi\rangle\sqrt{2q_0}$$

$$+ T'(s) = -\frac{\sqrt{2}GFm^2}{-s+m^2} + T'(s). \qquad (24)$$

The corresponding Feynman diagram for the term with the pole is shown in the drawing.

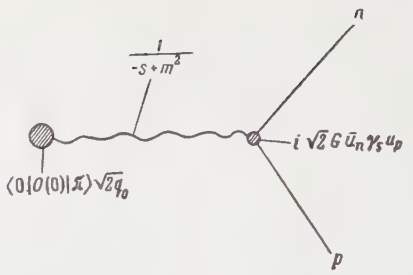

In Eq. (24), $T'(s)$ is an analytic function with a branch point at $s = 9m^2$. The spectral resolution of the function $T'(s)$ if of the form

$$T'(s) = a_0 + \frac{s}{\pi}\int_{9m^2}^{\infty}\frac{\rho(s')}{s'(s'-s)}ds', \qquad (25)$$

where $\rho(s')$ is the spectral function. For small s we can expand $T'(s)$ in a power series in s, which has the radius of convergence $9m^2$.

Setting

$$T'(s) = \sum_n a_n s^n, \qquad (26)$$

one can easily show that for large n

$$\lim_{n\to\infty}\left|\frac{a_{n+1}s}{a_n}\right| \leqslant \frac{|s|}{9m^2}. \qquad (27)$$

Therefore the series (26) converges rapidly in the region $|s| < m^2$.

If the spectral function does not change sign, the inequality (27) holds also for small n. In this case, for arbitrary $n > 1$ we have

$$|a_{n+1}| = \frac{1}{\pi}\left|\int_{9m^2}^{\infty}\frac{\rho(s')}{s'^{n+2}}ds'\right| \leqslant \frac{1}{9m^2}\frac{1}{\pi}\left|\int_{9m^2}^{\infty}\frac{\rho(s')}{s'^{n+1}}ds'\right| = \frac{|a_n|}{9m^2}.$$

We note that for β decay and μ capture the distance between the points $s = 0$ and $s_\mu = -0.9m_\mu^2$ is much smaller than the radius of convergence $9m^2$. Therefore with good accuracy we can replace $T'(s)$ by a single constant both for β decay and for μ capture (the error is of the order of $0.9m_\mu^2/9m^2 \approx 1/20$).

Thus we get the final result given by the formulas (14) and (15).

Let us now go on to the consideration of the quantity α. If the matrix element of the equal-time commutator is not zero, then in general one must use a dispersion relation with a subtraction. In this case the quantity α is proportional to the subtraction constant a_0, which can be very large.

If, on the other hand, the matrix element of the commutator is zero, than there is a dispersion relation without a subtraction. Then it is reasonable to suppose that the contribution of the nearest singularity predominates and the quantity α is small ($\alpha \approx 0.2 \ll 1$).

Thus it is reasonable to assume that $\varphi(s)$ is slowly varying for any theory in which there is a dispersion relation without subtraction.

Let us consider the ordinary pseudoscalar theory, with the Lagrangian

$$L = -\bar{N}(\hat{\partial} + M_0 - iG_0(\tau\pi)\gamma_5)$$
$$\times N - m_0^2\pi^2/2 - (\partial_\alpha\pi)^2/2 - \lambda_0\pi^4. \quad (28)$$

By means of the gauge transformation

$$N \to (1 + i(\tau v)\gamma_5)N, \qquad \pi \to \pi + v(4M_0 + 2M)/3G_0$$

we get by the standard method, explained in reference 3,

$$\mathbf{P}_\alpha = \bar{N}\tau\gamma_\alpha\gamma_5 N - i\partial_\alpha\pi(4M_0 + 2M)/3G_0, \quad (29)$$

$$\mathbf{O}(x) = i\partial_\alpha\mathbf{P}_\alpha = 2G_0\bar{N}N\pi + i\tfrac{2}{3}(M_0 - M)\bar{N}\tau\gamma_5 N$$
$$+ (m_0^2\pi + 4\lambda_0\pi^2\pi)(4M_0 + 2M)/3G_0. \quad (30)$$

We shall show in this case that the equal-time commutator for the operator O makes no contribution to the matrix element $\langle n|O(0)|p\rangle$. Let us examine the matrix element of the commutator

$$\mathbf{I} = \langle 0|2G_0N\pi + i\tfrac{2}{3}(M_0 - M)\tau\gamma_5 N|N\rangle.$$

From symmetry properties we have

$$\mathbf{I} = iA\tau\gamma_5 u_N. \quad (31)$$

Multiplying Eq. (31) on the left by the matrix $\tau\gamma_5$, we get

$$i3Au_N = -2i\langle 0|\eta(0)|N\rangle,$$

where

$$\eta(0) = iG_0(\tau\pi)\gamma_5 N + (M - M_0)N$$

is the current of the nucleon field. It is known that the matrix element $\langle 0|\eta(0)|N\rangle$ is equal to zero, and therefore $\mathbf{I} = 0$.

Thus we have shown that in the ordinary pseudoscalar theory there exists the pseudovector current (29), which satisfies all the necessary requirements.

If the pseudovector current is of the ordinary form

$$\mathbf{P}_\alpha = \bar{N}\tau\gamma_\alpha\gamma_5 N,$$

then the matrix element of the commutator is not zero, and in general there is no dispersion relation without subtraction. Even in this case there is hope that the G.T. result is valid. This question will be discussed in the Appendix.

4. LEPTON DECAYS OF HYPERONS AND K MESONS

The experimental limit for the probabilities of lepton decays of Λ and Σ hyperons is an order of magnitude smaller than the theoretical value calculated on the hypothesis that the effective coupling constants in hyperon decays are equal to those in β decays.[7] Many authors have expressed the opinion that the universality of the weak interactions evidently does not extend to strange-particle decays. Nevertheless, it is reasonable to assume the existence of a limited universality [a lepton current in the form (2)[8]].

In what follows we assume that the K meson is pseudoscalar and the V and A interactions exist for the lepton decays of strange particles. In this case the Hamiltonian for the weak decays of strange particles is of the form (1). Following the example given in Sec. 2 for the pseudoscalar theory with pseudoscalar coupling, we can construct the pseudovector current in such a form that a dispersion relation without subtraction holds for the matrix element $\langle N|\partial_\alpha P_\alpha|Y\rangle$.

Generally speaking, the matrix element for hyperon decay consists of three terms:

$$\langle N|P_\alpha(0)|Y\rangle = \bar{u}_N\{g_{AY}\gamma_\alpha\gamma_5 + i\xi_{5Y}[(\hat{p}_N - \hat{p}_Y)$$
$$\times\gamma_\alpha - \gamma_\alpha(\hat{p}_N - \hat{p}_Y)]\gamma_5 + if_Y(p_Y - p_N)_\alpha\gamma_5\}u_Y, \quad (32)$$

from which we have

$$\langle N|O(0)|Y\rangle = i\langle N|\partial_\alpha P_\alpha|Y\rangle$$
$$= i[(M_N + M_Y)g_{AY} + f_{Ys}]\bar{u}_N\gamma_5 u_Y, \quad (33)$$

where $s = -(p_Y - p_N)^2$. Repeating one after another the arguments presented in Secs. 2 and 3, we easily get the following equation:

$$[(M_N + M_Y)g_{AY} + f_{Ys}]$$
$$= -G_{KY}F_K m_K^2/(-s + m_K^2) + T_Y(s), \quad (34)$$

where G_{KY} is the renormalized coupling constant for the KYN interaction, and F_K is a constant parameter associated with the decay of K mesons. We have further

$$\langle 0|P_\alpha(0)|K\rangle = -q_\alpha F_K/\sqrt{2q_0}. \quad (35)$$

We can determine F_K from data on the lifetime for the decay $K \to \mu + \nu$. In Eq. (34) $T_Y(s)$ is a function that is analytic in the region

$$|s| < (m_K + 2m)^2. \quad (36)$$

Let us denote by T_N the kinetic energy of the nucleon recoil in the rest system of the hyperon. Expressing s in terms of T_N, we get

$$s = (M_Y - M_N)^2 - 2M_Y T_N. \quad (37)$$

In the present case the values of s that correspond to β and μ decays are very close together, as compared with the distance between the s given by Eq. (37) and $s = (m_K + 2m)^2$. Therefore with good accuracy we can replace $T_Y(s)$ by a constant a_Y.

Thus we have

$$[(M_N + M_Y) g_{AY} + f_Y s] = -G_{KY} F_K m_K^2 / (-s + m_K^2) + a_Y. \quad (38)$$

The relation (38) can be used to test the universality of the pseudovector current in lepton decays of strange particles.

Applying the dispersion theory of Goldberger and Treiman, we find for the function f_Y:

$$f_Y = -G_{KY} F_K / (-s + m_K^2) + T'_Y(s), \quad (39)$$

where $T'_Y(s)$ is a function analytic in the region (36), which with good accuracy can be replaced by a constant a'_Y.

Substituting Eq. (39) in Eq. (38), we get

$$(M_N + M_Y) g_{AY} = -G_{KY} F_K + a_Y - s a'_Y. \quad (40)$$

The relation (40) is a generalization of the formula of Goldberger and Treiman for the decay of strange particles.

The experimental data on the lifetimes of K and π mesons show that $F_K^2 \ll F_\pi^2$. Therefore it can be seen from a comparison of Eqs. (40) and (16) that to accuracy $a_Y - s a'_Y$

$$g_{AY}^2 \ll g_{A\beta}^2, \quad (41)$$

even for the case in which G_{KY} and G are of the same order of magnitude. This fact was first pointed out by Sakita.[9]

We emphasize that our method can also be easily extended to the case of a scalar K meson and to other types of weak interactions (for example, S + P).

In the case in which the relative parity of K and YN is positive, we have to deal with the divergence of a vector current

$$i\partial_\alpha V_\alpha = O(x). \quad (42)$$

The matrix element $\langle N | V_\alpha(0) | Y \rangle$ is of the form

$$\langle N | V_\alpha(0) | Y \rangle = \bar{u}_N \{ g_{VY} \gamma_\alpha + iC_Y [(\hat{p}_N - \hat{p}_Y) \gamma_\alpha - \gamma_\alpha (\hat{p}_N - \hat{p}_Y)] + i d_Y (p_Y - p_N)_\alpha \} u_Y. \quad (43)$$

From this we have

$$\langle N | O(0) | Y \rangle = i [(M_N - M_Y) g_{VY} + d_Y s] \bar{u}_N u_Y. \quad (44)$$

It is easy to repeat the remaining arguments, and the final formula will be of the form

$$(M_N - M_Y) g_{VY} + d_Y s = -G_{KY} F_K m_K^2 / (-s + m_K^2) + a_Y. \quad (45)$$

Applying the dispersion theory for the function d_Y, we find

$$d_Y = -G_{KY} F_K / (-s + m_K^2) + a'_Y. \quad (46)$$

Substituting (46) in (45), we get

$$(M_N - M_Y) g_{VY} = -G_{KY} F_K + a_Y - a'_Y s. \quad (47)$$

Comparing (47) and (16), one sees that to accuracy $a_Y - s a'_Y$

$$\left(\frac{g_{VY}}{g_{A\beta}}\right)^2 \approx \left(\frac{2M_N}{M_N - M_Y} \frac{F_K G_{KY}}{F_\pi G_\pi}\right)^2 \approx 5C \left(\frac{G_{KY}}{G_\pi}\right)^2,$$

where C is of the order of unity. Therefore in the case of the scalar K meson the small probability of lepton decay of hyperons could be explained only by having the coupling constant G_{KY} for the KYN interaction be smaller than the pion-nucleon constant G_π.

We note that Λ and Σ can have different relative parities. Let us consider this case. For simplicity we call the K particle a scalar, if the relative parity of K and Λ N is positive, and a pseudoscalar if it is negative. In the case of the pseudoscalar K meson, Eq. (40) holds for the decay of Λ particles, and Eq. (47) holds for the decay of Σ particles, if we write $\langle N | P_\alpha | \Sigma \rangle$ in the form (43). In the case of the scalar K meson, conversely, Eq. (47) holds for the decay of Λ particles and Eq. (40) for Σ particles, if we write $\langle N | V_\alpha | \Sigma \rangle$ in the form (32).

We note that the relations (38) and (45) can be used for the determination of the renormalized coupling constants G_{KY}, if precise experiments are made on the decays of strange particles.

The writer expresses his hearty gratitude to Professor M. A. Markov, Ya. A. Smorodinskiĭ, and Chu Hung-Yüang, and also to Ho Tso-Hsiu and V. I Ogievetskiĭ for their interest in this work and a discussion of the results.

APPENDIX

In the usual theory the pseudovector current has the form

$$P_\alpha = \bar{N} \tau \gamma_\alpha \gamma_5 N, \quad (A.1)$$

for which the divergence has been calculated in reference 3 and is given by

$$\partial_\alpha P_\alpha = 2M_0 \bar{N} \tau \gamma_5 N - 2iG_0 \bar{N} N \pi. \quad (A.2)$$

In order to calculate the matrix element $\langle 0 | \partial_\alpha P_\alpha | \pi \rangle$, we write Eq. (A.2) in the form

$$\partial_\alpha P_\alpha = -i \frac{2M_0}{G_0} j + i \frac{2M_0}{G_0} [(m_0^2 - m^2) \pi - 4\lambda_0 \pi^2 \pi] - 2iG_0 \bar{N} N \pi, \quad (A.3)$$

where j is the meson-field current. Using the

fact that the matrix element $\langle 0|\mathbf{j}(0)|\pi\rangle$ is equal to zero, we get

$$\langle 0|\partial_\alpha P_\alpha(0)|\pi\rangle = i2M_0G_0^{-1}\delta m^2\sqrt{Z_3}/\sqrt{2q_0} - 8M_0\lambda_0G_0^{-1}\langle 0|\pi^2\pi\ \pi\rangle - 2iG_0\langle 0|\bar{N}N\pi\ \pi\rangle, \quad (A.4)$$

where Z_3 is the renormalization constant for the pion wave function.

We now go on to the consideration of $\langle n|\partial_\alpha P_\alpha|p\rangle$. We rewrite Eq. (A.4) in the form

$$\partial_\alpha \mathbf{P}_\alpha = -i\frac{4M_0+2M}{3G_0}\mathbf{j} + \mathbf{O}(x), \quad (A.5)$$

where the operator O is that of Eq. (30).

In the present case we can write a dispersion relation without subtraction for the matrix element $\langle n|O(0)|p\rangle$, with the term with the pole defined by Eq. (12). Thus we have

$$i\langle n|\partial_\alpha P_\alpha(0)|p\rangle = \tfrac{1}{3}(4M_0+2M)GG_0^{-1}d(s)F(s)\sqrt{Z_3}i\bar{u}_n\gamma_5 u_p + \langle n|O(0)|p\rangle, \quad (A.6)$$

where d(s) and F(s) are the respective form factors for the π-meson propagation function and the vertex part. If the first term in Eq. (A.6) is small in comparison with the term with the pole, then the G.T. result would hold also for the usual theory.

We assume that the first term in Eq. (A.5) predominates. Comparing Eqs. (A.5) and (A.6), we get

$$F_7 \approx \frac{2M_0}{G_0}\frac{\delta m^2}{m^2}\sqrt{Z_3}. \quad (A.7)$$

By means of Eq. (A.7) the first term in Eq. (A.6) can be expressed in the form

$$i\frac{2M_0+M}{3M_0}G\frac{Fm^2}{\delta m^2}\bar{u}_n\gamma_5 u_p\, d(s)F(s). \quad (A.8)$$

Since in perturbation theory the quantity δm^2 diverges quadratically, it is very probable that

$$\frac{2M_0+M}{3M_0}\frac{m^2}{\delta m^2} \ll 1. \quad (A.9)$$

In this case the first term in Eq. (A.6) is actually small in comparison with the term that has the pole. Therefore it seems to us that the G.T. result is also valid for the usual theory.

It is interesting to note one more example, in which the pseudovector current has the form

$$i\mathbf{P}_\alpha(x) = \partial_\alpha\pi(x). \quad (A.10)$$

It is easy to show directly from Eq. (A.10) that the matrix element $\langle n|P_\alpha(0)|p\rangle$ for β decay is equal to zero.

In this case the divergence of the pseudovector current is

$$i\partial_\alpha \mathbf{P}_\alpha = m_0^2\pi - iG_0\bar{N}\tau\gamma_5 N - 4\lambda_0\pi^2\pi = m^2\pi(x) - \mathbf{j}(x) = \mathbf{O}(x) - \mathbf{j}(x). \quad (A.11)$$

From this we get

$$\langle 0|O(0)|\pi\rangle = i\langle 0|\partial_\alpha P_\alpha(0)|\pi\rangle = m^2\sqrt{Z_3}/\sqrt{2q_0}, \quad (A.12)$$

$$i\langle n|\partial_\alpha P_\alpha|p\rangle = \langle n|O(0)|p\rangle - i\sqrt{2}Gd(s)F(s)\sqrt{Z_3}\bar{u}_n\gamma_5 u_p. \quad (A.13)$$

The term with the pole is of the form

$$\sqrt{2}G\sqrt{Z_3}m^2/(-s+m^2). \quad (A.14)$$

Comparing the expression (A.14) with the second term in Eq. (A.13), we verify that they are of the same order and cancel each other.

From this example it can be seen that for those theories in which a dispersion relation without subtraction does not hold for the matrix element $\langle n|\partial_\alpha P_\alpha(0)|p\rangle$ the G.T. result is in general not a good approximation.

[1] R. P. Feynman and M. Gell-Mann, Phys. Rev. **109**, 193 (1958). E. C. G. Sudarshan and R. E. Marshak, Phys. Rev. **109**, 1860 (1958).

[2] M. L. Goldberger and S. B. Treiman, Phys. Rev. **110**, 1178 (1958).

[3] Feynman, Gell-Mann, and Levy, The Axial Vector Current in β Decay (preprint, 1960).

[4] L. Wolfenstein, Nuovo cimento **8**, 882 (1958). M. L. Goldberger and S. B. Treiman, Phys. Rev. **111**, 354 (1958).

[5] N. N. Bogolyubov and D. V. Shirkov, Введение в теорию квантованных полей (Introduction to the Theory of Quantized Fields), GITTL, 1957. [Interscience, 1959] Lehmann, Symanzik, and Zimmerman, Nuovo cimento **1**, 205 (1955).

[6] Bogolyubov, Medvedev, and Polivanov, Вопросы теории дисперсионных соотношений (Problems of the Theory of Dispersion Relations) Fizmatgiz, 1958.

[7] F. S. Crawford, Jr., et al., Phys. Rev. Letters **1**, 377 (1958). P. Nordin et al., Phys. Rev. Letters **1**, 380 (1958).

[8] Chou Kuang-Chao and V. Maevskiĭ, JETP **35**, 1581 (1958), Soviet Phys. JETP **8**, 1106 (1959). R. H. Dalitz, Revs. Modern Phys. **31**, 823 (1959).

[9] B. Sakita, Phys. Rev. **114**, 1650 (1959).

Translated by W. H. Furry
133

ON THE NUCLEON-NUCLEON POTENTIAL

A. F. GRASHIN and Yu. P. NIKITIN

Submitted to JETP editor April 8, 1960

J. Exptl. Theoret. Phys. (U.S.S.R.) 39, 713-719 (September, 1960)

A convenient method is proposed for setting up a potential in the form of the series $U(x) = \Sigma U^{(n)}(x)$, where $U^{(n)} \sim e^{-nx}$ for $x \to \infty$, starting from the relativistic meson-theoretical scattering amplitude expressed as an expansion in the number of exchange mesons (x is the distance in the units $1/\mu$, where μ is the meson mass). In the case of peripheral nucleon interaction this method yields a two-meson potential with a broad locality region $p^2/m^2 \ll 1$ (nonrelativistic region). The two-meson potential consists essentially of attractive tensor and central forces which depend weakly on the isotopic state.

In reference 1 a nucleon-nucleon potential was found for large distances $x > 1$ (in the units $1/\mu$, where μ is the mass of the π meson), which in first Born approximation is equivalent to the two-meson scattering amplitudes.[1-3] This potential (which we shall call the pseudopotential) is convenient for practical applications, since it permits us to make again use of the first Born approximation in various problems. A characteristic feature of the pseudopotential is its strong dependence on the energy in the region $E_{lab} \gtrsim 40$ Mev, $p^2/\mu^2 \gtrsim 1$ (p is the momentum in the system of the center of inertia). This "anomalous" energy dependence (nonlocality) is due to the infinite discontinuity in the absorptive part of the two-meson amplitude $\Delta M^{(2)}(q^2)$ at the point* $q^2 = -4\mu^2(1 + \mu^2/4p^2)$ (the so-called Karplus singularity) and also to the terms of the type $1/(p^2 + \mu^2)$. The anomalous nonlocality has a particularly marked effect in states with the isotopic spin $T = 0$; this must be taken into account in the analysis of the experimental data with the help of phenomenological potentials.†

The strong nonlocality of the pseudopotential, however, deprives it of its theoretical value, and it is still an open question whether it is possible to construct a "genuine" (local) potential with a broad region of locality $p^2 \ll m$ (nonrelativistic region), i.e., a potential which would, with the help of nonrelativistic techniques (Schrödinger equation), lead to the relativistic meson-theoretical scattering amplitude with an accuracy up to the "normal" corrections $\sim p^2/m^2$ (m is the nucleon mass).

*We use the notation of reference 1; in particular $q^2 = (p' - p)^2$ is the square of the momentum transfer.

†In the analysis of the experimental data with the help of phenomenological models one uses practically only the first Born approximation. Therefore, the majority of authors are dealing with pseudopotentials.

Charap and Fubini[4] showed on the example of scalar particles that an equivalent local potential for a given scattering amplitude can be constructed in the energy region $p^2 \ll m\mu + \mu^2/4$. In the construction of one- and two-meson potentials (i.e., potentials with the asymptotic behavior e^{-x} and e^{-2x}) this method is equivalent to the use of the Born approximation as in reference 1, if in addition one includes the second iteration of the one-meson potential.

In the present paper we show that a local potential in the form of the expansion

$$U(x) = \sum_{n=1}^{\infty} U^{(n)}(x), \qquad U^{(n)}(x) \sim e^{-nx} \quad \text{as } x \to \infty, \quad (1)$$

corresponding to an expansion of the amplitude in the number of exchange mesons,[5,2] can be constructed correctly from a given scattering amplitude, using the Born expansion. In this method we retain the possibility of making concrete estimates of the accuracy with which the potential reproduces the relativistic scattering matrix. Application of the method in the case of the two-meson interaction of the nucleons leads to a local potential with a wide locality region $p^2 \ll m^2$. This indicates that the anomalous nonlocality of the pseudopotential is equivalent to the description of the higher Born approximations by a "genuine" potential and has, therefore, no physical meaning.

1. GENERAL METHOD

In setting up the potential we start from the sequence of relativistic amplitudes* $M^{(n)}(q^2)$

*If spin and isospin variables are included, the amplitudes and the potential are to be replaced by the corresponding operators in spin and isospin space. We then investigate the analytic properties of the scalar functions which multiply certain spinor invariants (which, themselves, still depend on the direction of the vector $\mathbf{q}$).

which are obtained from meson theory by an expansion in the number of exchange mesons, or, more precisely, by successive separation of the contributions with the nearest singularity in q^2 (with fixed energy) in the points $q^2 = -\mu^2, -4\mu^2, \ldots, -(n\mu)^2, \ldots$ We restrict the discussion to the interaction of identical particles (of mass m) due to the exchange of mesons with mass μ only. In this case only the exchange graphs appearing as a consequence of the symmetrization of the amplitude have singularities on the right semi-axis. Therefore, these can in general be left out of the discussion. Moreover, we assume that we do not encounter any anomalous graphs with nearest singularities $q^2 \neq (n\mu)^2$, as, for example, the "square" in Fig. 1 with the condition $m^2 > \mu_1^2 + \mu_2^2$ at the vertex.

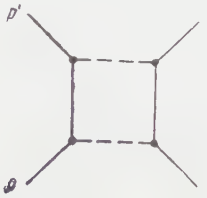

FIG. 1

To find the equations connecting the potential (1) with the sequence $M^{(n)}$ we consider the iteration solution of the Schrödinger equation with the potential (1). Denoting the nonrelativistic scattering amplitude in the j-th Born approximation by T_j, we find

$$T_1 = -\frac{m}{4\pi} U(\mathbf{q}), \qquad U(\mathbf{q}) = \int e^{-i\mathbf{q}\mathbf{r}} U(\mathbf{r})\, d\mathbf{r},$$

$$T_j = -\frac{m}{(2\pi)^3} \int \frac{U(\mathbf{p}' - \mathbf{k})\, T_{j-1}(\mathbf{k} - \mathbf{p}, p^2)}{p^2 - k^2 + i0} d\mathbf{k} \text{ for } j \geqslant 2. \quad (2)$$

The Born expansion (2) can be used for separating from the nonrelativistic amplitude the contributions $T^{(n)}$ with the nearest singularity at $q^2 = -\mu^2$, $-4\mu^2$, etc. Considering that the nearest singularity of the Fourier component of the n-meson potential lies at $q^2 = -(n\mu)^2$, we obtain for the first iteration

$$T_1^{(n)} = -(m/4\pi)\, U^{(n)}(\mathbf{q}). \quad (3)$$

For the classification of the contributions from the following iterations we use the "displacement theorem" for the singularities: the nearest singularity of a function of the form

$$f(q^2, p^2) = \int \frac{f^{(n_1)}[(\mathbf{p}' - \mathbf{k})^2]\, f^{(n_2)}[(\mathbf{k} - \mathbf{p})^2]}{p^2 - k^2 + i0} d\mathbf{k}$$

is located at $q^2 = -(n_1 + n_2)^2\mu^2$, where $-(n_1\mu)^2$ and $-(n_2\mu)^2$ are the locations of the nearest singularities for $f^{(n_1)}(q^2)$ and $f^{(n_2)}(q^2)$. For the proof of this theorem it suffices to write the functions in the form of spectral integrals

$$f^{(n)}(q^2) = \int_{(n\mu)^2}^{\infty} \frac{\rho(\varkappa^2)\, d\varkappa^2}{q^2 + \varkappa^2}$$

and, after changing the order of integration, to find the nearest singularity of the function

$$\int [(\mathbf{p}' - \mathbf{k})^2 + \varkappa_1^2]^{-1} [(\mathbf{p} - \mathbf{k})^2 + \varkappa_2^2]^{-1} [p^2 - k^2 + i0]^{-1} d\mathbf{k}.$$

With the help of the methods proposed by Landau for relativistically invariant integrals[6] we easily find the value

$$q^2 = -(\varkappa_1 + \varkappa_2)^2\mu^2 \leqslant -(n_1 + n_2)^2\mu^2.$$

In particular, it follows from this theorem that the amplitude T_j has the nearest singularity* at $q^2 = -(j\mu)^2$, i.e., the contributions $T_j^{(n)}$ are different from zero only for $j \leq n$.

We now require that the non-relativistic techniques reproduce the sequence of meson-theoretical amplitudes $M^{(n)}$ with an accuracy up to relativistic corrections. Comparing consecutively the contributions $T^{(n)}$ and $M^{(n)}$ for n = 1, 2, 3, ..., we obtain a system of recurrence relations for the stepwise construction of the sequence $U^{(n)}$:

$$\begin{aligned} U^{(1)}(\mathbf{q}) &= -4\pi m^{-1} M^{(1)}(\mathbf{q}, p^2), \\ U^{(2)}(\mathbf{q}) &= -4\pi m^{-1} [M^{(2)}(\mathbf{q}, p^2) - T_2^{(2)}(\mathbf{q}, p^2)], \\ U^{(3)}(\mathbf{q}) &= -4\pi m^{-1} [M^{(3)}(\mathbf{q}, p^2) - T_2^{(3)}(\mathbf{q}, p^2) - T_3^3(\mathbf{q}, p^2)], \end{aligned} \quad (4)$$

The left-hand sides of Eqs. (4) are independent of p^2 by definition, so that one can set $p^2 = 0$ in the right-hand sides, i.e., retain only the basic terms of the expansions in p^2. If, on the other hand, we retain the corrections $\sim p^2$ on the right-hand sides, we also obtain nonlocal corrections to the potential and can in this way estimate the accuracy of the local potential.

Going over to the coordinate representation, we can write $U^{(n)}$ as the residue of the pole $q^2 = -\mu^2$ (for n = 1) or as an integral of the discontinuity $\Delta M^{(n)}(q, 0) - \Delta T^{(n)}(q, 0)$ across the cut $q^2 \leq -(n\mu)^2$ for $n \geq 2$ (reference 1); for the construction of the potential it therefore suffices practically to know only the absorptive parts of the amplitudes in q^2. This leads us to certain conditions which have to be fulfilled in order that the potential can be expanded into the series (1). Indeed, the two-meson potential is expressed in the form of an integral over $q^2 \leq -4\mu^2$, but the region of integration $q^2 \leq -9\mu^2$ gives a contribution of the same

*This result was obtained earlier by Bowcock and Martin[7] using a Yukawa potential.

type as the three-meson potential $U^{(3)}$, etc. On the other hand, it is obvious that this method enables us to set up a unique potential without expanding it into a series at all. For this purpose we must consider successively the regions of integration

$$-4\mu^2 \geqslant q^2 > -9\mu^2, \qquad -9\mu^2 \geqslant q^2 > -16\mu^2, \ldots,$$

collecting all non-vanishing contributions of the absorptive part of $\Delta M - \Delta T$. This shows that the system of equations (4) is equivalent to the Charap-Fubini method, slightly modified and generalized to the case of particles with spin.

Our method is formally analogous to that used earlier (see, for example, the paper of Klein and McCormick[8]) in the construction of an adiabatic potential in the form of an expansion in the number of exchange mesons, but differs by the parallel use of the nonrelativistic formalism and the relativistic scattering amplitude (the importance of this difference was noted in reference 4). We emphasize that in our method the Born approximation is only used as a means of classification of the nonrelativistic amplitudes according to the extent of the region of analyticity, and corresponds to the expansion in the number of exchange mesons in meson theory. In other words, the series (1) represents an expansion in the "degree of peripheralness" and not in the coupling constant, which can have an arbitrary value.

2. PERIPHERAL NUCLEON-NUCLEON POTENTIAL

Substituting the one-meson nucleon-nucleon amplitude (see, for example, reference 9) in (4) and going to the x representation, we obtain the well-known static one-meson potential

$$U^{(1)}(x) = \tfrac{1}{4}\mu g^2 \varepsilon^2 (\tau^{(1)}\tau^{(2)})(\sigma^{(1)}\nabla)(\sigma^{(2)}\nabla)\, e^{-x}/x,$$
$$\varepsilon^2 = \mu^2/m^2. \qquad (5)$$

The inclusion of the nonlocal corrections to the one-meson potential introduces the factor $(1 + p^2/m^2)^{-1/2}$; the static potential (5) can therefore be used in the energy region $p^2/m^2 \ll 1$.

To find the two-meson potential we must calculate the second iteration

$$T_2^{(2)}(q, p^2) = \frac{m^2}{2(2\pi)^4}\int \frac{U^{(1)}(p' - k)\, U^{(1)}(k - p)}{p^2 - k^2 + iO}\, dk, \qquad (6)$$

or more precisely, the discontinuity $\Delta T_2^{(2)}$ on the cut $q^2 \leq -4\mu^2$. Substituting (5) in (6) and integrating over dk, we obtain for $q^2 \leq -4\mu^2$

$$\Delta T_2^{(2)} = i\pi g^4 \frac{(3 - 2\lambda_\tau)\varepsilon}{32 m \sqrt{1 - s^2}} \left\{ \frac{(1 - 2s^2)^2}{v} \right.$$
$$+ i\mathrm{Sn}p^2 \sin\theta \frac{1 - 2s^2}{p^2 + \mu^2(1 - s^2)} \left(\frac{1 - 2s^2}{v} - 1 \right)$$
$$+ [(\sigma^{(1)}q)(\sigma^{(2)}q) - q^2\sigma^{(1)}\sigma^{(2)}] \frac{1 - 2s^2 - v}{4(p^2 + \mu^2(1 - s^2))}$$
$$+ (\sigma^{(1)}n)(\sigma^{(2)}n) \frac{\varepsilon^2(1 - s^2)m^2}{p^2 + \mu^2(1 - s^2)}$$
$$\left. \times \left[v + \frac{(1 - 2s^2)^2}{v} - 2(1 - 2s^2) \right] \right\};$$
$$s^2 = 1 + q^2/4\mu^2, \qquad v = \sqrt{4s^2p^2 + \mu^2}/\mu,$$
$$S = \tfrac{1}{2}(\sigma^{(1)} + \sigma^{(2)}), \qquad n = [p' \times p]/|[p' \times p]|.$$

$\lambda_T = 1$ or -3 for the isotopic spin $T = 1$ or 0, respectively. The further calculations consist in the integration of the absorptive part of the potential

$$\Delta M^{(2)}(q, p^2) - \Delta T_2^{(2)}(q, p^2) \qquad (7)$$

along the cut $q^2 \leq -4\mu^2$ for $p^2 = 0$, which presents no essential difficulties.

Let us now examine to which extent the adiabatic absorptive part ($p^2 = 0$) is equivalent to the exact meson-theoretical amplitudes in the non-relativistic approximation $p^2 \ll m^2$, i.e., which corrections to $\Delta M^{(2)}(q, p^2)$ must be discarded in order that the absorptive part (7) cease to depend on the energy. Starting from the expansion of the meson-nucleon amplitude in powers of the invariant ν for a given q^2 (see reference 2), one can show that, at least for $-4\mu^2 \geq q^2 > -9\mu^2$, only the fourth-order contribution of perturbation theory, $\Delta M_4^{(2)}$, corresponding to Fig. 1, has a significant energy dependence.

Neglecting corrections $\sim p^2/m^2$ to $\Delta M_4^{(2)}$, we can convince ourselves that the subtraction of $\Delta T_2^{(2)}$ leads to the cancellation of all terms having an appreciable energy dependence in the region $\mu^2 \lesssim p^2 \ll m^2$, and, in particular, to the disappearance of the discontinuity in the Karplus point $q^2 = -4\mu^2 \times (1 + \mu^2/4p^2)$. If we assume that the two-meson potential is determined only by the region $-4\mu^2 \geq q^2 > -9\mu^2$, this means that the potential $U^{(1)}(x) + U^{(2)}(x)$ is equivalent to the one- and two-meson amplitudes with an accuracy up to terms of order $\sim p^2/m^2$.

In the foregoing discussion we have also assumed that besides the Karplus singularity from the graph of Fig. 1, there are no other singularities in the region $-4\mu^2 \geq q^2 > -9\mu^2$. The nearest omitted singularity is given by the graph shown in Fig. 2, which has a singularity at infinity for p^2

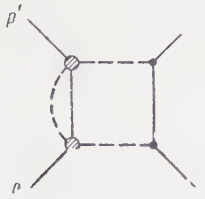

FIG. 2

$= m\mu + \mu^2/4$ (threshold for π meson creation) which quickly approaches $-4\mu^2$ as the energy increases. As long as this singularity lies beyond $-9\mu^2$ ($p^2/m^2 < 0.5$), it gives rise to the same type of effects as the three-meson amplitude. For higher energies the effects from this singularity must be included in the two-meson approximation; they can only be described with the help of a nonlocal two-meson potential. The condition $p^2/m^2 < 0.5$ ($E_{lab} < 900$ Mev) is, however, comprised in the non-relativistic approximation and does not lead to additional restrictions.

For the explicit calculation of the two-meson potential we use the approximation used in the determination of the pseudopotential[1] (expansion in terms of $1/x$, ϵ^2, and $\epsilon\sqrt{x}/2$). We find

$$U^{(2)}(x) = U_S^{(2)}(x) + \mathrm{LS}U_{LS}^{(2)}(x) + [(\sigma^{(1)}\mathbf{n}_x)(\sigma^{(2)}\mathbf{n}_x) - \sigma^{(1)}\sigma^{(2)}]\,U_T^{(2)}(x), \tag{8}$$

where

$$U_S^{(2)}(x) = -\frac{3g^4\epsilon^2\mu}{4\sqrt{\pi}}\frac{e^{-2x}}{x^{5/2}}\left\{(\alpha-1)^2 + \epsilon\sqrt{\pi x}(\alpha-1) + \epsilon^2 x\left(1-\alpha+\frac{\lambda_\tau}{3}\right)\right\};$$

$$U_{LS}^{(2)}(x) = -\frac{3g^4\epsilon^4\mu}{4\sqrt{\pi}}\frac{e^{-2x}}{x^{7/2}}\left\{(\alpha-1)^2 - \frac{4\lambda_\tau}{3}\left(\beta_2 - \frac{\beta}{2}\right) + \epsilon\sqrt{\pi x}\alpha - \frac{4\lambda_\tau}{3}\frac{\beta\sqrt{\pi}}{\epsilon\sqrt{x}}\right\};$$

$$U_T^{(2)}(x) = -\frac{3g^4\epsilon^4\mu}{4\sqrt{\pi}}\frac{e^{-2x}}{x^{5/2}}\left\{1 + \frac{2\lambda_\tau}{3}\beta_1\left(\frac{\sqrt{\pi}}{\epsilon\sqrt{x}} - 1\right) - \epsilon\sqrt{\pi x}\,\frac{9+2\lambda_\tau}{24}\right\},$$

$$\alpha = 1.2\,(\Delta|\alpha| \leqslant 10\%), \qquad \beta_1 = 0.025, \qquad \beta_2 = -0.029,$$

$$(\Delta|\beta_1|, \Delta|\beta_2| \leqslant 20\%), \qquad \beta = -\beta_1 - \beta_2.$$

Expression (8) is the principal term of the asymtotic expansion in $1/x$ and gives the two-meson potential in the peripheral region $x > 1$ with an accuracy $\sim 1/x$. For relatively low energies, $E_{lab} \lesssim 100$ Mev, the region $x \gtrsim 1$ gives the main contribution for all orbital angular momenta $l \geq 1$. The potential (8) enables us therefore, at least qualitatively, to study the most important properties of the two-meson interaction. The expansion in $\epsilon^2 x/4$ practically leads to no further restrictions, since the region $\epsilon^2 x/4 \gtrsim 1$ ($x \gtrsim 180$) is of no practical interest. However, the presence of the parameter $\epsilon^2 x/4$ has theoretical significance, since it seems to indicate that the static approximation in meson theory is not correct (see also reference 4).

The interaction obtained above takes account of virtual scattering processes (rescattering corrections) with the help of the parameters α, β_1, and β_2, which have a very definite theoretical meaning,[2] and is thus a rigorous consequence of the pseudoscalar, symmetric meson theory. However, in obtaining the numerical values of these parameters we have used the experimental data on meson-nucleon scattering, so that the potential (8), with the indicated values of the parameters, is, in a certain sense, semi-phenomenological.

Let us consider briefly the properties of the two-meson interaction. The characteristic feature of the potential (8) which distinguishes it from the pseudopotential[1] is its weak dependence on the isotopic state. The scalar and spin-orbit forces are very different from those calculated by perturbation theory on account of the combination $\alpha - 1 \ll \alpha, 1$ which enters in the basic terms. The tensor forces and the forces of the type $\sigma^{(1)}\sigma^{(2)}$ have the additional smallness ϵ^2 in comparison with $U_S^{(2)}$, but their relative contribution is strongly increased on account of the additional compensation in $U_S^{(2)}$. In the complete expression for the potential these forces, however, play a minor role owing to the presence of large contributions of the same type from the one-meson potential. The forces of the type $(\sigma^{(1)}\mathbf{L})(\sigma^{(2)}\mathbf{L})$ have the additional smallness $\epsilon^4 x/4$ and have been omitted completely in the computations.

Of particular interest are the spin-orbit forces, for which several different expressions have been found,[10-13] and whose role in the interpretation of the experimental data is also not sufficiently clear (see references 14 to 16). The two-meson interaction $U_{LS}^{(2)}$ is considerably weaker than the strong phenomenological spin-orbit forces of Gammel and Thaler[14] and Signell and Marshak,[15] and can be neglected in the region $x \gtrsim 1$.* Calculations on the basis of the non-relativistic meson theory[10,11] lead to the same result, although the two-meson potential (8) differs quantitatively from the potentials obtained earlier (more precisely, their peripheral parts).

*In the paper of Grashin and Kobzarev presented at the Ninth Conference on High Energy Physics at Kiev, 1959, a spin-orbit interaction was given which was too strong by an order of magnitude, due to an error in the calculations. This error has been corrected in the published article.[1]

We note that for comparatively low energies the semi-phenomenological potentials without spin-orbit forces have been successfully employed by a number of authors for the interpretation of the experimental scattering data[16] and of certain properties of the nuclear interactions.[17] We believe, however, that it is difficult to explain the experimental data for energies of several hundred Mev without introducing strong spin-orbit forces; apparently, these must therefore be connected with potentials of shorter range corresponding to effective masses $m_{eff} = |q|_{eff} \geq 3\mu$.

Our calculations show that the only correction to the one-meson potential in the region $x \gtrsim 1$ is given by attractive central forces which are independent of the spin and isotopic spin states. The other types of forces give only small contributions and can be neglected. The interaction obtained in this way is in qualitative agreement with the phenomenological potentials used earlier,[16,17] even extrapolating into the region $x < 1$. One may assume that the addition of some phenomenological core at distances $x \lesssim \mu/m$ to the potential $U^{(1)} + U^{(2)}$ [formulas (5) and (8)] enables us to use it for the description of the interaction of a pair of nucleons at comparatively low energies.

It appears that the best method of introducing a phenomenological core is that of imposing a boundary condition on the logarithmic derivative, as proposed by Moszkowski and Scott.[18] The boundary condition must be chosen in such a way that the potential gives the correct S phases. To obtain better agreement with experiment one can also try to vary the parameters α, β_1, and β_2 within the limits of error $\Delta|\alpha|$, $\Delta|\beta_1|$, and $\Delta|\beta_2|$ with which they were determined from the experimental data on meson-nucleon scattering.

The authors are grateful to V. N. Gribov, I. Yu. Kobzarev, L. D. Landau, L. B. Okun', I. Ya. Pomeranchuk, and K. A. Ter-Martirosyan for discussions and useful comments.

[1] A. F. Grashin and I. Yu. Kobzarev, JETP **38**, 863 (1960), Soviet Phys. JETP **11**, 624 (1960).

[2] Galanin, Grashin, Ioffe, and Pomeranchuk, JETP **37**, 1663 (1959), Soviet Phys. JETP **10**, 1179 (1960).

[3] Galanin, Grashin, Ioffe, and Pomeranchuk, JETP **38**, 475 (1960), Soviet Phys. JETP **11**, 347 (1960).

[4] J. M. Charap and S. P. Fubini, Nuovo cimento **14**, 540 (1959).

[5] L. B. Okun' and I. Ya. Pomeranchuk, JETP **36**, 300 (1959), Soviet Phys. JETP **9**, 207 (1959).

[6] L. D. Landau, JETP **37**, 62 (1959), Soviet Phys. JETP **10**, 45 (1960).

[7] J. Bowcock and A. Martin, Nuovo cimento **14**, 516 (1959).

[8] A. Klein and B. H. McCormick, Phys. Rev. **104**, 1747 (1956).

[9] A. F. Grashin, JETP **36**, 1717 (1959), Soviet Phys. JETP **9**, 1223 (1959).

[10] Yu. V. Novozhilov and I. A. Terent'ev, JETP **36**, 129 (1959), Soviet Phys. JETP **9**, 89 (1959).

[11] S. Okubo and S. Sato, Progr. Theor. Phys. **21**, 383 (1959).

[12] Tzoar, Raphael, and Klein, Phys. Rev. Lett. **2**, 433 and **3**, 145 (1959).

[13] E. Butkov, Nuovo cimento **13**, 809 (1959).

[14] J. C. Gammel and R. M. Thaler, Phys. Rev. **107**, 291 and 1337 (1957).

[15] P. C. Signell and R. E. Marshak, Phys. Rev. **106**, 832 (1957) and **109**, 1229 (1958). Signell, Zinn, and Marshak, Phys. Rev. Lett. **1**, 416 (1959).

[16] Hamada, Iwadare, Otsuki, Tamagaki, and Watari, Progr. Theor. Phys. **22**, 566 (1959) and **23**, 366 (1960).

[17] Nagata, Sasakawa, Sawada, and Tamagaki, Progr. Theor. Phys. **22**, 274 (1959). Takagi, Watari, and Yasuno, Progr. Theor. Phys. **22**, 549 (1959).

[18] S. A. Moszkowski and B. L. Scott, Phys. Rev. Lett. **1**, 298 (1958).

Translated by R. Lipperheide
134

THE DECAY OF ACOUSTIC EXCITATIONS IN CRYSTALS

V. L. POKROVSKIĬ and A. M. DYKHNE

Institute of Radio Physics and Electronics, Siberian Branch, Academy of Sciences, U.S.S.R.

Submitted to JETP editor April 5, 1960

J. Exptl. Theoret. Phys. (U.S.S.R.) **39**, 720-725 (September, 1960)

The properties of the acoustic excitation spectra in crystals near the decay threshold are considered. The longitudinal-phonon attenuation due to the decay of the longitudinal phonon into transverse phonons, is shown to be proportional to k^5. The effect of anisotropy on the phonon decay of transverse excitations is investigated. The weak coupling between acoustic vibrations causes a characteristic splitting of the spectrum near the decay threshold into two excitations with non-zero momenta. This can show up in neutron scattering experiments, where it causes the simultaneous existence of two peaks in the energy distribution of neutrons scattered at an angle close to critical.

THE singularities of the spectrum of elementary excitations near their decay threshold have been recently considered by Pitaevskiĭ[1]. He treated mainly the case of a Bose liquid. Although the qualitative picture also remains in force for acoustic excitations in crystals, there are in this case a number of particular circumstances, such as the existence of three branches of vibrations, anisotropy, and weak interaction (due to anharmonic effects) between the elementary excitations.

We write the phonon-interaction Hamiltonian in the form

$$H_{int} = \frac{\gamma}{V\overline{V}} \sum_{\mathbf{p}_1+\mathbf{p}_2=\mathbf{p}_3} \sqrt{\omega_{p_1}\omega_{p_2}\omega_{p_3}}\, a^+_{p_1} a^+_{p_2} a_{p_3} + \text{Herm. adj.} \quad (1)$$

where the interaction constant $\gamma = \hbar^{3/2}(\rho c^2)^{-1/2}$, ρ is the density, c is the velocity of sound. The summation over the polarizations is omitted.

1. THE DECAY OF A LONGITUDINAL PHONON INTO TWO TRANSVERSE PHONONS

It is apparent that the decay of a fast phonon into phonons with smaller propagation velocities is possible kinematically. The polarization selection rules do not forbid such a decay, because along the crystallographic axes the velocity of longitudinal sound is greater than that of transverse sound. Such a decay causes the attenuation of longitudinal sound from the very beginning.

To calculate this attenuation or decay we will find the correction to the frequency $\omega_{\parallel}(q)$, which is described by the diagram in Fig. 1. We have

$$\Sigma(p) = G^{-1}(p) - G_0^{-1}(p) = \frac{i\gamma^2\omega^2_{\parallel}(p)}{(2\pi)^4\hbar^2}\int \frac{\omega^2_{\perp}(q)\,\omega^2_{\perp}(\mathbf{p}-\mathbf{q})\,d^3q\,d\omega}{[\omega^2-\omega^2_{\perp}(q)-i\delta]\,[(\omega-\varepsilon)^2-\omega^2_{\perp}(\mathbf{p}-\mathbf{q})-i\delta]}, \quad (3)$$

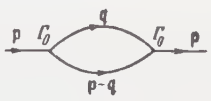

FIG. 1

where $\omega_{\parallel}(p)$ and $\omega_{\perp}(p)$ are respectively the frequencies of the longitudinal and transverse branches. After integrating with respect to ω and changing the variables, (3) can be brought to the form

$$\Sigma(p) = -\frac{\gamma^2\omega^2_{\parallel}(p)}{p\pi^2\hbar^2}\int_0^{q_m} \omega_{\perp}(q)\,q\,dq \times \int_{|p-q|}^{p+q} \frac{\omega_{\perp}(u)\,(\omega_{\perp}(u)+\omega_{\perp}(q))\,u\,du}{(\omega_{\perp}(u)+\omega_{\perp}(q)+\varepsilon)\,(\omega_{\perp}(u)+\omega_{\perp}(q)-\varepsilon-i\delta)}. \quad (4)$$

To calculate the attenuation in the phonon part of the spectrum, we put

$$\omega_{\parallel}(p) = c_{\parallel}p, \qquad \omega_{\perp}(p) = c_{\perp}p. \quad (5)$$

The results thus obtained will also give the correct order of magnitude when dispersion is present. By substituting (5) in (4), and calculating the imaginary part as half the residue during the integration over u, we obtain

$$\operatorname{Im}\Sigma(p) = -2iAc_{\parallel}p^6,$$

$$A = \frac{\gamma^2 c_{\parallel}c_{\perp}}{4\hbar^2}\left(\frac{1}{80} - \frac{1}{24}\left(\frac{c_{\parallel}}{c_{\perp}}\right)^2 + \frac{1}{16}\left(\frac{c_{\parallel}}{c_{\perp}}\right)^4\right). \quad (6)$$

Hence, we have for the spectrum of elementary excitations

$$\omega_{\parallel}(p) = c_{\parallel}p - iAp^5. \quad (7)$$

The attenuation is everywhere small. For $p \sim 1/a$ (a is the lattice constant) we have Im ω

$\times (p)/\omega(p) \sim \alpha = \hbar/\rho c a^4$. The parameter α has the value 10^{-1} to 10^{-2} for light elements and 10^{-3} to 10^{-4} for heavy elements. It is not difficult to see that anisotropy does not introduce important changes in the result obtained.

2. ALLOWANCE FOR ANISOTROPY IN THE PHONON DECAY OF EXCITATIONS

The transverse acoustic branches, which are stable at the start, can split up into two excitations, one of which is a phonon. We will find the kinematic conditions for such a decay in the anisotropic case. The laws of conservation of energy and momentum give

$$\Phi_{\mathbf{p}}(\mathbf{q}) = \varepsilon(\mathbf{q}) + \varepsilon(\mathbf{p}-\mathbf{q}) - \varepsilon(\mathbf{p}) = 0, \qquad \varepsilon(\mathbf{p}) = \hbar\omega(\mathbf{p}). \tag{8}$$

For small values of q we obtain

$$\Phi_{\mathbf{p}}(\mathbf{q}) = (c(\mathbf{n}) - \mathbf{v}_{\mathbf{p}}\mathbf{n})\, q,$$

where $\mathbf{c}(\mathbf{n})$ is the velocity of sound along the direction $\mathbf{n}$; $\mathbf{q} = \mathbf{n}q$: $\mathbf{v}_{\mathbf{p}} = \partial\epsilon/\partial\mathbf{p}$. If $c(\mathbf{n}) > \mathbf{v}_{\mathbf{p}}\mathbf{n}$ for all $\mathbf{n}$, (8) has only the trivial solution $q = 0$. If p is increased along some direction, decay starts at the value of p for which the equation $c(\mathbf{n}) = \mathbf{v}_{\mathbf{p}} \cdot \mathbf{n}$ is first satisfied, at least for one direction of $\mathbf{n}$.

We introduce the function $\varphi(\mathbf{p})$ as follows:

$$\varphi(\mathbf{p}) = \min \frac{c(\mathbf{n})}{\mathbf{v}_{\mathbf{p}}\mathbf{n}},$$

i.e. $\varphi(\mathbf{p})$ is the minimum value of the ratio given, considered as a function of $\mathbf{n}$ for a given $\mathbf{p}$. The equation of the threshold surface then takes the form $\varphi(\mathbf{p}) = 1$.

We investigate the attenuation of excitations close to the threshold of phonon creation. Taking into account, as in the preceding case, only the contribution from the diagram in Fig. 1, we obtain after integration over ω:

$$\Sigma(p) \sim \gamma^2 \int \frac{q^3 dq\, d\cos\theta\, d\varphi}{x + (c(\mathbf{n}) - \mathbf{v}_c\mathbf{n})\, q - 2\beta_{ik}\Delta p_i q_k + \beta_{ik} q_i q_k - i\delta},$$

$$\beta_{ik} = \frac{1}{2}\frac{\partial^2\varepsilon}{\partial p_i \partial p_k}\bigg|_{\mathbf{p}=\mathbf{p}_c}, \qquad x = \mathbf{v}_c\Delta\mathbf{p} + \beta_{ik}\Delta p_i \Delta p_k - \Delta\varepsilon. \tag{9}$$

Attenuation occurs in cases where the denominator of the expression under the integral in (9) has zeros in the region of integration and is determined by half the residue at the corresponding pole. Close to a pole we always have $x \ll \Delta p$. This means that the correction to $\Delta\epsilon$ due to the decay is smaller than $(\Delta p)^2$, which will be confirmed by the result.

For the denominator in (9) to tend to zero requires apparently (for $\beta_i = \beta_{ik}n_k$):

$$c(\mathbf{n}) - \mathbf{v}_c\mathbf{n} \sim \beta_i \Delta p_i$$

(here the sign $\sim$ means agreement in order of magnitude). But the function $c(\mathbf{n}) - \mathbf{v}_c\mathbf{n}$ by hypothesis has a minimum at $\mathbf{n} = \mathbf{n}_c$ and close to the latter $c(\mathbf{n}) - \mathbf{v}_c\mathbf{n}$ takes the form

$$c(\mathbf{n}) - \mathbf{v}_c\mathbf{n} = Q(\Delta\theta, \Delta\varphi),$$

where $Q(x, y)$ is some positive determinate quadratic form. Hence, the important range of integration over θ and φ is found to be $\Delta\theta, \Delta\varphi \sim \sqrt{\beta_i \Delta p_i}$.

Having calculated the residue in (9), we obtain near the threshold

$$\varepsilon(p) = \varepsilon(p_c) + \mathbf{v}_c\Delta\mathbf{p} + \beta_{ik}\Delta p_i \Delta p_k - iB(\beta_i \Delta p_i)^3. \tag{10}$$

We note that in the isotropic case for a threshold for decay into phonons to appear on the $\epsilon(\mathbf{p})$ curve, at least a point of inflection must exist. In the anisotropic case it is much easier to satisfy the conditions of decay. In particular, the presence of a point of inflection on the $\epsilon(\mathbf{p})$ curves along a given direction is not required.

3. THE SPECTRUM CLOSE TO THE THRESHOLD OF DECAY INTO EXCITATION WITH NONZERO MOMENTA

Pitaevskiĭ has shown[1] that the decay of elementary excitations into two excitations with momenta not equal to zero is also possible. In this case the spectrum of elementary excitations breaks up at the decay point (p_c, ϵ_c). Its behavior beyond the decay point cannot be clarified without resorting to perturbation theory.

In the case we are considering the treatment can be complete because the interaction of the elementary excitations is weak, which allows perturbation theory to be used, We will limit ourselves to the contribution to Σ of the lowest order in the coupling constant given by the same diagram (see Fig. 1). The Green's function in the approximation taken agrees with that found by Pitaevskiĭ[1] and has the form

$$G^{-1}(p) \approx v_0\Delta p - \Delta\varepsilon + 2\alpha\sqrt{\varepsilon_c(v_c\Delta p - \Delta\varepsilon)}, \tag{11}$$

where v_0 is the velocity of the elementary excitation at the threshold point without taking interaction into account; v_c is the velocity of the excitations at which decay occurs; $\Delta\mathbf{p}$ and $\Delta\epsilon$ are the momenta and energy referred to the threshold point;* $\alpha \sim \hbar/\rho c a^4 > 0$. We choose in (11) that the branch of the root which is positive on the positive axis and which has a cut along the negative axis.

*In (11) only the singular part of $\Sigma(p)$ is taken into account. The inclusion of the regular part causes an unimportant displacement of the threshold point.

We shall show that $v_0 > v_c$. The function $F(p)$ is introduced as follows:

$$F(p) = \varepsilon(q_c) + \varepsilon(p - q_c) - \varepsilon(p). \quad (12)$$

Of course, $F(q_c) = 0$. The decay threshold p_c is that zero of the functions $F(p)$, which is closest to q_c (for $p_c > q_c$), where the condition below must be satisfied;

$$\varepsilon'(q_c) = \varepsilon'(p_c - q_c) \equiv v_c < c, \quad (13)$$

where c is the velocity of sound. The latter inequality is necessary to make decay with phonon creation impossible. It is seen that, by virtue of (13), $F(p) > 0$ in the range $q_c < p < p_c$. Since $F(p_c) = 0$, we have $F'(p_c) < 0$ and, consequently, $v_0 > v_c$.

The energy of the elementary excitations is determined by the poles of the Green's function, i.e., by the zeros of the double-valued function (11), which lie either on the real ϵ axis on the first sheet of the Riemann surface to the left of the cut, or in the lower half-plane of the second sheet close to the cut.

It is convenient to introduce new variables

$$x = (v_0 - v_c)\Delta p / \varepsilon_c, \qquad y = (\Delta\varepsilon - v_c\Delta p)/\varepsilon_c, \quad (14)$$

in which the equation $G^{-1}(p, \epsilon) = 0$ has the form

$$x - y - 2i\alpha\sqrt{y} = 0. \quad (15)$$

Here $\arg\sqrt{y} = \frac{1}{2}\arg y$, where in the first sheet we take $0 < \arg y < 2\pi$. Putting $y = re^{i\varphi}$, we obtain from (15)

$$x - r\cos\varphi + 2\alpha\sqrt{r}\sin(\varphi/2) = 0, \quad (16)$$

$$r\sin\varphi + 2\alpha\sqrt{r}\cos(\varphi/2) = 0. \quad (17)$$

Equation (17) has solutions: $\varphi = \pm\pi$ and $\sin(\varphi/2) = -\alpha/\sqrt{r}$. Substituting $\varphi = +\pi$ in (16), we obtain

$$x + r + 2\alpha\sqrt{r} = 0, \quad (18)$$

which is only possible for negative values of x. It is not difficult to verify that this is the only solution on the first sheet and that for $x > 0$ there is no solution of (15) on the first sheet. We note that $r \to 0$ as $x \to 0$, so that near p_c the dispersion law has the form $\Delta\epsilon = v_c\Delta p + 0(\Delta p^2)$, the same as that of Pitaevskiĭ.[1]

Further, putting $\varphi = -\pi$, we obtain real solutions on the second sheet:

$$\sqrt{r} = \alpha \pm \sqrt{\alpha^2 - x}. \quad (19)$$

The solution with the positive sign has a meaning when $-\infty \le x \le \alpha/\sqrt{r}$; the solution with the minus sign has a meaning only when $0 \le x \le \alpha^2$.

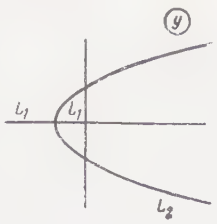

FIG. 2

We consider finally the case when $\sin(\varphi/2) = -\alpha/\sqrt{r}$. In this case all the roots of (15) lie on the second sheet and satisfy the equality $r = x$. It is necessary, apparently, to satisfy the condition $x \ge \alpha^2$, for which real solutions of (15) do not exist. The lines on which the poles of the Green's function are situated are shown in Fig. 2. The energies of the elementary excitations coincide with the poles situated on the line L_1 and the branch L_2 in the lower half-plane.

Transforming again to Δp, $\Delta\epsilon$, we obtain for $\Delta p < 0$

$$\Delta\varepsilon = v_0\Delta p + 2\alpha\varepsilon_c\left(\sqrt{\alpha^2 - (v_0 - v_c)\Delta p/\varepsilon_c} - \alpha\right). \quad (20)$$

Equation (20) shows that $\Delta\epsilon = v_0\Delta p$ for $|\Delta p| \gg \alpha^2\epsilon_c/(v_0 - v_c)$ and $\Delta\epsilon = v_c\Delta p$ for $|\Delta p| \ll \alpha^2\epsilon_c/(v_0 - v_c)$. We note, however, that as $\Delta p \to 0$ the residue of the Green's function diminishes as Δp, which causes excitations with dispersions $\Delta\epsilon = v_c\Delta p$ to have diminishing weight.

For $\Delta p \gtrsim \alpha^2\epsilon_c/(v_0 - v_c)$ the energy of the elementary excitations is given by the equation

$$\Delta\varepsilon = v_0\Delta p - 2\alpha^2\varepsilon_c - 2i\alpha\varepsilon_c\sqrt{[(v_0 - v_c)\Delta p/\varepsilon_c] - \alpha^2}. \quad (21)$$

For $\Delta p \gg \alpha^2\epsilon_c/(v_0 - v_c)$ formula (21) determines the energy and attenuation of the elementary excitations. The latter is proportional to $\sqrt{\Delta p}$.

In the region $(v_0 - v_c)\Delta p \sim \alpha^2\epsilon_c$ the poles of the Green's function are close to the branch point and both formulae (20) and (21) lose their meaning. To clarify the situation in this region we use a representation of the wave function of the excited system with the aid of the Green's function, which has been given by Galitskiĭ and Migdal:[2]

$$\langle\psi_p(t)\,\psi_p(0)\rangle = -iG(p, t) = i\int_0^\infty \operatorname{Im} G(p, \varepsilon)\, e^{-i\varepsilon t}\, d\varepsilon. \quad (22)$$

The integral (22) reduces to half the residue of $G(p, \epsilon)$ relative to the pole situated on the real axis [this pole is determined by Eq. (20)] and to the integral along the upper side of the cut.

In the variables x, y we have (for $\Delta p < 0$):

$$\langle\psi_p(t)\,\psi_p(0)\rangle = -i\pi\frac{xe^{-i\epsilon(p)t}}{\sqrt{\alpha^2 - x}\,(\alpha + \sqrt{\alpha^2 - x})} + 2i\alpha\exp\{-i(\varepsilon_c + v_c\Delta p)t\}\int_0^\infty \frac{\sqrt{y}\,e^{-iy\varepsilon_0 t}\,dy}{(x - y)^2 + 4\alpha^2 y}. \quad (23)$$

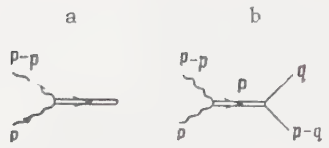

FIG. 3

The integral in (23) essentially diminishes in the time $\Delta t = 1/\alpha^2\epsilon_c$. In the course of this interval both terms in (23) play an equal role for $x \sim \alpha^2$. For $x \ll \alpha^2$ the second term is the most important and describes an excitation with energy ϵ_c and decay time $\sim 1/\alpha^2\epsilon_c$.

When $\Delta p > 0$, the first term in (23) disappears. The second term, for $\Delta p \gg \alpha^2\epsilon_c/(v_0 - v_c)$, as can be seen without difficulty, reduces to the residue with respect to the pole of the Green's function lying in the second sheet and determined by (21). When the coupling constant α becomes of the order of unity, the picture given above reduces to the case considered by Pitaevskiĭ.

In the case of weak coupling, the threshold effect gives a peculiar result in the neutron scattering spectrum. We will consider the scattering of neutrons by phonons in crystals of light elements (where anharmonic effects are comparatively large) at a temperature $T < \alpha^2 T_D$ (T_D is the Debye temperature).

Close to the threshold, the principal contribution to the scattering cross section is given by the diagrams in Fig. 3 (a, b). The diagram of Fig. 3,a contributes a sharp line, the intensity of which is given by the formulae

$$I \sim \begin{cases} 1-(1-(v_0-v_c)\,\Delta p/\alpha^2)^{-1/2}, & \Delta p = p - p_c < 0, \\ 0, & \Delta p > 0, \end{cases} \quad (24)$$

and the position of ϵ is given by formula (20).

The diagram of Fig. 3,b makes a contribution to the neutron scattering cross section of the form

$$|G(p)|^2\,\delta(\varepsilon_P - \varepsilon_{\mathbf{P}-\mathbf{p}} - \varepsilon_q - \varepsilon_{\mathbf{p}-\mathbf{q}})\,d^3p\,d^3q, \quad (25)$$

Here **P** is the momentum of the neutron before scattering. After integrating the cross section (25) with respect to q, we obtain a formula for the distribution of scattered neutrons in energy for a given loss of momentum p:

$$F(p) = \begin{cases} dw = \dfrac{BF(p)\,d\varepsilon}{(v_0\Delta p - \Delta\varepsilon)^2 + 4\alpha^2(\Delta\varepsilon - v_c\Delta p)}, & (26) \\ \left(\dfrac{P^2}{2M} - \dfrac{(\mathbf{P}-\mathbf{p})^2}{2M} - \varepsilon_c - v_c\Delta p\right)\dfrac{1}{(ca)^2} \text{ for } \dfrac{P^2}{2M} - \dfrac{(\mathbf{P}-\mathbf{p})^2}{2M} > \varepsilon_c + v_c\Delta p \\ 0 \qquad \text{for } \dfrac{P^2}{2M} - \dfrac{(\mathbf{P}-\mathbf{p})^2}{2M} < \varepsilon_c + v_c\Delta p. & (27) \end{cases}$$

Formula (26) corresponds to a line of width $\sim \alpha^2\epsilon_c$, which appears for $|v_c\Delta p| \sim \alpha^2\epsilon_c$ ($\Delta p < 0$).

Formulae (24) to (27) can be used to obtain the angular distribution and the distribution over energy of the scattered neutrons. Without giving the results, we will describe qualitatively the picture thus obtained.

For angles of scattering smaller than some φ_c, there is a sharp line in the energy distribution of neutrons at the energy $\epsilon_0(\varphi)$, the width of which depends on temperature and not on the angle of scattering. When the angle of scattering tends to φ_c, the intensity of this line diminishes as $\varphi_c - \varphi$. Apart from this line there is in the neutron energy distribution a background at energies greater than $\epsilon_0(\varphi)$. For $\varphi_c - \varphi \sim \alpha^2$ this background gradually gathers up into a line of width $\sim \alpha^2\epsilon_c$, while the intensity of the line increases as $\varphi - \varphi_c \to 0$. The center of this line lies at the energy $\epsilon_1(\varphi) > \epsilon_0(\varphi)$, where $\epsilon_1(\varphi) - \epsilon_0(\varphi) \sim \varphi_c - \varphi$. For $\varphi > \varphi_c$ there is only a smeared-out line.

We take this opportunity of expressing our gratitude to L. P. Pitaevskiĭ and L. P. Gor'kov for valuable discussions.

[1] L. P. Pitaevskiĭ, JETP **36**, 1168 (1959), Soviet Phys. JETP **9**, 830 (1959).

[2] V. M. Galitskiĭ and A. B. Migdal, JETP **34**, 139 (1958), Soviet Phys. JETP **7**, 96 (1958).

Translated by K. F. Hulme
135

MAGNETIC RELAXATION IN FERROMAGNETIC METALS

L. I. BUISHVILI, G. R. KHUTSISHVILI, and O. D. CHEISHVILI

Institute of Physics, Academy of Sciences, Georgian S. S. R.

Submitted to JETP editor April 7, 1960

J. Exptl. Theoret. Phys. (U.S.S.R.) **39**, 726-736 (September, 1960)

A microscopic calculation of magnetic relaxation in ferromagnets, due to sd exchange interaction, is carried out. Expressions are derived for the corresponding kinetic coefficients. A general phenomenological analysis of the problem is made with allowance for the so-called indirect relaxations.

1. A theoretical analysis of magnetic relaxation in ferrodielectrics has been the subject of many papers.[1-5] An additional relaxation, due to the sd interaction, should be observed in the case of a ferromagnetic metal.

The purpose of the present investigation was an analysis of magnetic relaxation in ferromagnetic metals. We use the simplified model of a ferromagnetic metal, which starts out with the existence of two groups of electrons (cf., e.g., Akhiezer and Pomeranchuk[6]), the conduction (s) and ferromagnetic (d) electrons, and proceed to calculate the relaxation terms due to the sd exchange interaction, in the spin-wave approximation.

We note that Turov[7] and Mitchell[8] carried out microscopic calculations of the relaxation due to sd interaction. They have assumed, however, that the conduction electrons are also in equilibrium relative to the spin direction.

2. The model we use for the ferromagnetic metal is quite crude. We therefore confine ourselves to a consideration of the simplest case of a cubic crystal (iron, nickel). We assume furthermore that the external field **H** (which is aligned with the z axis) is so large that the sample consists of a single domain.

We denote by **S** and $\mathbf{S}_d$ the respective spin operators of the conduction electron and of the electron shell of the ferromagnetic ion, by g_s and g_d the absolute values of their g factors, and by N the concentration of the ferromagnetic atoms. We have

$$Na^3 = \nu, \tag{1}$$

where a is the edge of the elementary cube and ν is the number of atoms per elementary cube.

We denote furthermore by **M** the magnetic moment (due to the d electrons) per unit volume of the ferromagnet, and by $\mathbf{M}_\sigma$ the value of **M** in absolute saturation (i.e., at 0° K). We have

$$\mathbf{M}_\sigma = -Ng_d\beta\mathbf{S}_d = -\nu a^{-3}g_d\beta\mathbf{S}_d, \tag{2}$$

where β is the Bohr magneton.

The energy operator of the exchange-interaction of the conduction electron with the ferromagnetic electrons will be written in the following form:[6]

$$V(\mathbf{r}) = (A/Ng_d\beta)\,\mathbf{SM}(\mathbf{r}), \tag{3}$$

where A is the constant of the sd exchange interaction.

In the expression

$$\mathbf{SM} = \tfrac{1}{2}(S_+M_- + S_-M_+) + S_zM_z$$

$$(S_\pm = S_x \pm iS_y, \quad M_\pm = M_x \pm iM_y)$$

the last term near the ground state is much greater than the others. Therefore, if we confine ourselves to states close to the ground state (i.e., if we consider the case of temperatures which are much lower than the Curie temperature Θ), the operator S_z will commute with the exchange energy and its eigenvalue will be a good quantum number.

It is well known that for states close to the ground state, the operators M_x and M_y are small quantities of first order of smallness, and M_z differs from M_σ by a quantity of second order of smallness. Therefore, when finding the energy levels (states close to the ground state), we can replace **M** in (3) by $\mathbf{M}_\sigma$. This yields (see reference 9)

$$V = -A\mathbf{S}\mathbf{S}_d. \tag{4}$$

We denote by H_s the effective magnetic field due to the sd exchange interaction, which acts on the spin of the conduction electron. Analogously, let H_d represent the effective field due to the sd exchange and acting on the spin of the ferromagnetic ion. Using formula (4), we find

$$H_s = -A\langle S_{dz}\rangle/g_s\beta, \qquad H_d = -A\langle S_z\rangle\rho/g_d\beta, \tag{5}$$

where the brackets $\langle\,\rangle$ denote averaging, and ρ

is the number of conduction electrons per atom. Considering that in states close to the ground state almost all the d spins are directed opposite to the field, we have

$$H_s = AS_d / g_s\beta. \tag{6}$$

The spin of the conduction electron is in a field $H + H_S$. Recalling the expression for the Pauli paramagnetic susceptibility, we obtain

$$\langle S_z \rangle = -3g_s\beta(H + H_s)/8\mu_0,$$

where μ_0 is the chemical potential of the conduction-electron gas. Consequently

$$H_d = (3g_sA\rho / 8g_d\mu_0)H + 3A^2S_d\rho / 8g_d\beta\mu_0. \tag{7}$$

However, the question of the second term in H_d calls for a detailed analysis. The point is that when we substitute the value of A, taken for the free ion (~ 0.3 ev), the resultant second term is of the order of 100 koe, which sharply contradicts the experiment (this would cause a very strong shift of the resonant frequency). In this connection, Kittel and Mitchell believe that in a ferromagnet the constant A is reduced by screening by a factor of several times. However, so strong a screening appears little likely to us.

We adhere to a second explanation. The second term (7) is due to the part of the conduction-electron polarization caused by the field H_S. Therefore the second term in (7) coincides in direction with the magnetization due to the d electrons. It follows therefore that the second term in H_d does not give a rotational moment that acts on **M**, and consequently does not change the resonant frequency (in this connection, see the papers by Yosida and Hasegawa[10]). In quantum language, we can say that the Zeeman energy of the vector **M** in the additional field is independent of the orientation of **M**, and therefore drops out in the energy difference. Thus, instead of (7) it would be more correct to write

$$H_d = (3g_sA\rho / 8g_d\mu_0)H. \tag{8}$$

3. The spin Hamiltonian of the conduction electron can be written in the following form

$$\mathcal{H}(\mathbf{r}) = g_s\beta HS_z + (Aa^3 / vg\ \beta)\mathbf{SM}(\mathbf{r}). \tag{9}$$

In the ground state, all the ferromagnetic spins are directed opposite to the z direction. The operator M_+ increases the overall d-electron spin projection by unity, while M_- decreases it. In other words, the operator M_+ causes the production of a ferromagnon, while the operator M_- causes its annihilation. According to the commutation rule (see, for example, reference 2)

$$[M_+(\mathbf{r}),\ M_-(\mathbf{r}')] = -2g_d\beta M_\sigma\delta(\mathbf{r} - \mathbf{r}'). \tag{10}$$

Let the volume of the sample be unity. Then

$$M_+(\mathbf{r}) = -\sqrt{2g_d\beta M_\sigma}\sum_{\mathbf{f}} a_{\mathbf{f}}^+ e^{-i\,\mathbf{fr}},$$

$$M_-(\mathbf{r}) = -\sqrt{2g_d\beta M_\sigma}\sum_{\mathbf{f}} a_{\mathbf{f}} e^{i\mathbf{fr}}, \tag{11}$$

where $a_{\mathbf{f}}^+$ and $a_{\mathbf{f}}^-$ are the operators of production and annihilation of a ferromagnon with wave vector **f**, respectively. Substitution in (9) yields

$$\mathcal{H}(\mathbf{r}) = (g_s\beta H + AS_d)S_z$$

$$- AS_d\sqrt{g_d\beta / 2M_\sigma}\sum_{\mathbf{f}}[a_{\mathbf{f}}^+ S_- e^{-i\mathbf{fr}} + a_{\mathbf{f}}S_+ e^{i\mathbf{fr}}]. \tag{12}$$

In the derivation of (12), we substitute M_σ for M_Z in the term S_ZM_Z.

Let us carry out second quantization over the conduction electrons. We readily obtain for the second-quantized Hamiltonian

$$\mathcal{H} = \tfrac{1}{2}(g_s\beta H + AS_d)\sum_{\mathbf{k}}(b_{\mathbf{k}}^+ b_{\mathbf{k}} - d_{\mathbf{k}}^+ d_{\mathbf{k}})$$

$$- AS_d\sqrt{g_d\beta / 2M_\sigma}\sum_{\mathbf{kf}}[a_{\mathbf{f}}^+ d_{\mathbf{k}-\mathbf{f}}^+ b_{\mathbf{k}} + a_{\mathbf{f}} b_{\mathbf{k}}^+ d_{\mathbf{k}-\mathbf{f}}], \tag{13}$$

where $b_{\mathbf{k}}^+$ and $b_{\mathbf{k}}$ are respectively the operators of production and annihilation of a conduction electron with a wave vector **k** and a spin projection $\frac{1}{2}$ on the z axis. The operators $d_{\mathbf{k}}^+$ and $d_{\mathbf{k}}$ are analogously defined for an electron with a spin projection $-\frac{1}{2}$.

It follows from (12) that the energy spectrum of the conduction electron in the ferromagnet has the form

$$\varepsilon(\mathbf{k}, m_s) = \varepsilon_0(\mathbf{k}) + (g_s\beta H + AS_d)m_s, \tag{14}$$

where m_S is the eigenvalue of the operator S_Z and $\epsilon_0(\mathbf{k})$ is the energy of the conduction electron in the absence of an external field and of sd exchange interaction. In further calculations we assume that

$$\varepsilon_0(k) = \hbar^2k^2 / 2m \tag{15}$$

(m is the effective mass of the conduction electron).

For the energy of the ferromagnon we use the expression[11]

$$\varepsilon(\mathbf{f}) = 2JS_d(af)^2 + g_d\beta H_{\mathbf{eff}}, \tag{16}$$

where J is the dd exchange integral, and $H_{\mathbf{eff}}$ is the total field acting on the spin of the ferromagnetic ion. It is given by the formula

$$H_{\mathbf{eff}} = H + H_a + H_d,$$

where H_a is the anisotropy field. Considering that A is considerably smaller than μ_0, we can neglect H_d compared with H [see Eq. (8)]. Next, since we consider the case of large H (compared with H_a), we can put $H_{eff} = H$ (we note that in the final result H_{eff} is contained only under the logarithm sign).

The dispersion law, given by (16), is valid only for values of f that are not too small. Accordingly, on the one hand, as indicated in references 3 and 12, formula (16) can be used for temperatures higher than about 2 or 3° K; on the other hand, the spin-wave picture can be used for temperatures lower than approximately one-tenth the Curie temperature.

4. The second term in (13) causes transitions between the stationary states of the system. For example, the term $a^+_{\mathbf{f}} d^+_{\mathbf{k}-\mathbf{f}} b_{\mathbf{k}}$ causes a process in which an electron with wave vector **k** and a spin projection $1/2$ is annihilated, and an electron with a wave vector **k − f** and a spin projection $-1/2$ appears together with a ferromagnon with wave vector **f**. The overall projection of the spin is conserved here (the projection of the ferromagnon spin is equal to +1) since this an exchange interaction.

Using standard perturbation theory, we readily obtain

$$dn(\mathbf{f})/dt = C \sum_{\mathbf{k}} \delta[\varepsilon(\mathbf{k}, +1/2) - \varepsilon(\mathbf{k}-\mathbf{f}, -1/2) - \varepsilon(\mathbf{f})]$$
$$\times \{[n(\mathbf{f})+1][1-g(\mathbf{k}-\mathbf{f}, \mu_-)]\, g(\mathbf{k}, \mu_+)$$
$$- n(\mathbf{f})[1-g(\mathbf{k}, \mu_+)]\, g(\mathbf{k}-\mathbf{f}, \mu_-)\}. \qquad (17)$$

In this formula $n(\mathbf{f})$ denotes the distribution function of the ferromagnons; $g(\mathbf{k}, \mu_+)$ and $g(\mathbf{k}, \mu_-)$ are the distribution functions of the conduction electrons with spin projections $1/2$ and $-1/2$, respectively; μ_+ and μ_- are the corresponding chemical potentials; C is a constant given by the formula

$$C = (AS_d)^2 \pi g_d \beta / \hbar)\, M_\sigma. \qquad (18)$$

We assume that the totality of conduction electrons with given spin direction is both in internal equilibrium and in equilibrium with the lattice (therefore each of these totalities is described by a Fermi distribution with a temperature equal to the lattice temperature). This assumption is correct, since the corresponding relaxation time is exceedingly small (the process is not connected with spin flip). However, these two electron gases are generally speaking not in equilibrium with each other, and therefore $\mu_+ \neq \mu_-$. On the other hand, the ferromagnon gas is not in equilibrium with the lattice.

Our problem is to calculate the relaxation terms due to the sd exchange interaction. In addition, there are other relaxation mechanisms present, namely: a) the mechanism connected with the direct interaction between the conduction electrons and the lattice,[13,14] without account of the sd exchange, b) the mechanism connected with the interaction between the ferromagnetic spins and the lattice, c) internal relaxation in the ferromagnon gas. Neither the lattice nor the conduction electron participates in the latter case. In this relaxation, therefore, the total ferromagnon-gas energy and the z component of the magnetization remain constant. A Planck distribution is established with a certain temperature which, in general, is different from the lattice temperature.

Processes b) and c) are not connected with the conduction electrons, and must therefore proceed in the same manner in a ferromagnetic metal as in a ferrodielectric.[1-5]

In accordance with the foregoing, we represent $n(\mathbf{f})$ in the following form:

$$n(\mathbf{f}) = n^0(\mathbf{f}) + \Delta n(\mathbf{f}), \qquad n^0(\mathbf{f}) = (e^{\varepsilon(\mathbf{f})/T} - 1)^{-1}; \qquad (19)$$

$\Delta n(\mathbf{f})$ is a small addition. The temperature is measured everywhere in energy units.

Taking into consideration the form of the functions $n^0(\mathbf{f})$ and $g(\mathbf{k}, \mu)$, and also the conservation of energy (which is taken into account by the δ function), we can readily bring (17) to the form

$$dn(\mathbf{f})/dt = C \sum_{\mathbf{k}} \delta[\varepsilon(\mathbf{k}, 1/2) - \varepsilon(\mathbf{k}-\mathbf{f}, -1/2) - \varepsilon(\mathbf{f})]$$
$$\times \{n^0(\mathbf{f})[1-g(\mathbf{k}, \mu_+)]\, g(\mathbf{k}-\mathbf{f}, \mu_-)$$
$$\times [\exp\{(\mu_+ - \mu_-)/T\} - 1]$$
$$- [g(\mathbf{k}-\mathbf{f}, \mu_-) - g(\mathbf{k}, \mu_+)]\, \Delta n(\mathbf{f})\}. \qquad (20)$$

5. We denote by L/2 the absolute value of the overall projection of all the d spins, and by L_0 the equilibrium value of L. We have

$$L = 2[NS_d - \sum_{\mathbf{f}} n(\mathbf{f})], \qquad L_0 = 2[NS_d - \sum_{\mathbf{f}} n^0(\mathbf{f})],$$
$$L - L_0 = -2 \sum_{\mathbf{f}} \Delta n(\mathbf{f}). \qquad (21)$$

When $S_d = 1/2$, L represents the excess of the d spins directed against the field.

We denote further by D the excess of the conduction electrons with spins directed opposite the field, and by D_0 the equilibrium value of D. It is easy to see that the z components of the magnetic moments of the sample, caused by the d and s electrons, are to $(1/2) g_d \beta L$ and $(1/2) g_s \beta D$ respectively. According to Overhauser,[15] we have

$$\mu_+ - \mu_- = 4\mu_0 (D_0 - D)/3N\rho. \qquad (22)$$

We confine ourselves henceforth to the case of linear relaxation. For this purpose it is necessary to satisfy the rather stringent condition

$$|\mu_+ - \mu_-| / T = 4\mu_0 |D_0 - D| / 3N\rho T \ll 1. \quad (23)$$

Considering that

$$D_0 = 3N\rho (AS_d + g_s\beta H) / 4\mu_0,$$

the last condition becomes

$$\frac{|D_0 - D|}{D_0} \frac{AS_d + g_s\beta H}{T} \ll 1. \quad (24)$$

In addition, in all the foregoing derivations we have assumed that the condition

$$|L_0 - L| / L_0 \ll 1 \quad (25)$$

is satisfied. Actually, the usual spin-wave picture is not applicable otherwise.

Taking all the foregoing into account, we now readily obtain

$$dL/dt = -2C \sum_{\mathbf{kf}} \delta [\varepsilon(\mathbf{k}, +1/2) - \varepsilon(\mathbf{k} - \mathbf{f}, -1/2) - \varepsilon(\mathbf{f})]$$
$$\times \{(\mu_+ - \mu_-) T^{-1} n^0(\mathbf{f}) [1 - g(\mathbf{k}, \mu_0)] g(\mathbf{k} - \mathbf{f}, \mu_0)$$
$$- [g(\mathbf{k} - \mathbf{f}, \mu_0) - g(\mathbf{k}, \mu_0)] \Delta n(\mathbf{f})\}. \quad (26)$$

The calculation of the second term in the case of arbitrary $\Delta n(\mathbf{f})$ is impossible. We shall assume that the ferromagnon gas is in internal equilibrium, i.e., $n(\mathbf{f})$ is in the form of a Planck function with a temperature different from the lattice temperature. Then, taking (21) into account, we obtain

$$\Delta n(\mathbf{f}) = \frac{\partial n^0(\mathbf{f})}{\partial T} \Delta T = \left[2 \sum_{\mathbf{f}} \frac{\partial n^0(\mathbf{f})}{\partial T} \right]^{-1} \frac{\partial n^0(f)}{\partial T} (L_0 - L),$$

which can be reduced to the form

$$\Delta n(\mathbf{f}) = \frac{(8\pi JS_d)^{3/2} a^3}{3\zeta(3/2) T^{3/2}} [n^0(\mathbf{f})]^2 \varepsilon(\mathbf{f}) e^{\varepsilon(\mathbf{f})/T} (L_0 - L), \quad (27)$$

where ζ is the Riemann zeta function. Taking (22) and (27) into account, (26) becomes

$$dL/dt = -(D_0 - D)/T_{sd} + (L_0 - L)/T_{ds}, \quad (28)$$

and after rather lengthy calculations we obtain

$$\frac{1}{T_{sd}} = \frac{maA^2T}{8 \cdot 3^{1/2} \pi^{5/2} \hbar^3 (N\rho)^{1/2} \nu J} I_{sd}, \qquad \frac{1}{T_{ds}} = \frac{2^{1/2} m^2 J^{1/2} S_d^{3/2} a A^2 T^{1/2}}{3\pi^{3/2} \zeta(3/2) \hbar^5 N} I_{ds}, \quad (29)$$

where

$$I_{sd} = \frac{ze^z}{e^z - 1} - \ln(e^z - 1), \qquad I_{ds} = 2 \int_z^\infty \frac{zdz}{e^z - 1} + \frac{z^2}{e^z - 1},$$
$$z = \frac{1}{T} \left[\frac{(AS_d)^2}{B\mu_0} + g_d \beta H \right], \qquad B = \hbar^2 / ma^2 JS_d. \quad (30)$$

In the extreme cases we have

$$I_{sd} = \ln z^{-1}, \qquad I_{ds} = \pi^2/3 \text{ for } z \ll 1; \quad (30a)$$

$$I_{sd} = ze^{-z}, \qquad I_{ds} = z^2 e^{-z} \text{ for } z \gg 1. \quad (30b)$$

We have calculated the relaxation terms due to the sd exchange interaction. Since the quantity L + D is conserved in exchange interaction, dD/dt is given by (28) but with the opposite sign.

6. Let us now take into account the fact that the spins of the conduction electrons, and also the ferromagnetic spins, interact not only with each other, but also with the lattice directly. The relaxation times of the direct interaction with the lattice will be denoted by T_{sl} and T_{dl} respectively. Then the relaxation equations assume the form

$$\dot{D} = \frac{D_0 - D}{T_s} - \frac{L_0 - L}{T_{ds}}, \qquad \dot{L} = \frac{L_0 - L}{T_d} - \frac{D_0 - D}{T_{sd}}, \quad (31)$$

where

$$1/T_s = 1/T_{sl} + 1/T_{sd}, \qquad 1/T_d = 1/T_{dl} + 1/T_{ds}. \quad (32)$$

The solution of the system (31) has the form

$$D(t) = D_0 + d_+ \exp(-\lambda_+ t) + d_- \exp(-\lambda_- t),$$
$$L(t) = L_0 + l_+ \exp(-\lambda_+ t) + l_- \exp(-\lambda_- t), \quad (33)$$

with

$$\lambda_\pm = \frac{1}{2} \left(\frac{1}{T_s} + \frac{1}{T_d} \right) \pm \frac{1}{2} \left[\left(\frac{1}{T_s} - \frac{1}{T_d} \right)^2 + \frac{4}{T_{sd} T_{ds}} \right]^{1/2}. \quad (34)$$

Further, the quantities l_+ and l_- are expressed in terms of d_+ and d_- by formulas such as

$$\frac{d}{l} = \frac{1/T_{ds}}{1/T_s - \lambda} = \frac{1/T_d - \lambda}{1/T_{sd}}.$$

The coefficients d_+ and d_- are determined from the initial conditions.

Thus, D and L in general are sums of two exponentials.

7. Let us consider two particular cases.

Case 1 (see reference 9). Assume that the following conditions are satisfied

$$T_{sl} \ll T_{sd}, T_{ds}. \quad (35)$$

The condition $T_{sl} \ll T_{sd}$ denotes that the direct coupling between the conduction electrons and the lattice is considerably stronger than the couplings between these electrons and the d spins. We shall have here $T_s \approx T_{sl}$. In the equation for $\dot{D}$ we can neglect the term $(L_0 - L)/T_{ds}$. We then obtain $\dot{D} = (D_0 - D)/T_s$. It follows therefore that D approaches an equilibrium value with a relaxation time T_s. For times much longer than T_s we can neglect the term $(D_0 - D)/T_{sd}$ in the equation for $\dot{L}$, and therefore $L = (L_0 - L)/T_d$.

As a result we obtain the solutions

$$D(t) = D_0 + [D(0) - D_0] e^{-t/T_s},$$
$$L(t) = L_0 + [L(0) - L_0] e^{-t/T_d}. \quad (36)$$

We thus have in this case independent relaxation of D and L.

Case 2. Assume that the conditions

$$T_{sd} \ll T_{sl}, \qquad T_{ds} \ll T_{dl}, \tag{37}$$

are satisfied; in other words, the s and d spins are coupled more strongly to each other than to the lattice. Here we have

$$T_s \approx T_{sd}, \qquad T_d \approx T_{ds}.$$

The sum D + L is conserved in the sd exchange interaction. Therefore in the case of total absence of direct coupling with the lattice, D and L cannot relax to the values D_0 and L_0 [provided the condition $D(0) + L(0) = D_0 + L_0$ is not satisfied]. It is easy to see that D and L will relax with a relaxation time equal to $T_S T_d/(T_S + T_d)$ to values D_S and L_S, which are determined from the condition that D + L is conserved and from the condition that they are stationary with respect to sd interactions.

$$(D_0 - D_s)/T_s = (L_0 - L_s)/T\ . \tag{38}$$

It is easy to get

$$\begin{aligned} D_s &= (T_d + T_s)^{-1}\{T_d D_0 - T_s L_0 + T_s[D(0) + L(0)]\}, \\ L_s &= (T_d + T_s)^{-1}\{T_s L_0 - T_d D_0 + T_d[D(0) + L(0)]\}. \end{aligned} \tag{39}$$

For complete relaxation we have

$$\begin{aligned} D(t) &= D_0 + (D_s - D_0)\exp(-\lambda_- t) + [D(0) \\ &\quad - D_s]\exp(-\lambda_+ t), \\ L(t) &= L_0 + (L_s - L_0)\exp(-\lambda_- t) + [L(0) \\ &\quad - L_s]\exp(-\lambda_+ t), \end{aligned} \tag{40}$$

where

$$\lambda_+ = \frac{1}{T_s} + \frac{1}{T_d}, \qquad \lambda_- = \frac{1}{T_s + T_d}\left(\frac{T_s}{T_{sl}} + \frac{T_d}{T_{dl}}\right) \ll \lambda_+. \tag{41}$$

Adding D and L and taking into consideration the fact that $D_S + L_S = D(0) + L(0)$, we obtain from (40)

$$\begin{aligned} D(t) + L(t) &= (D_0 + L_0) + \{[D(0) \\ &\quad - D_0] + [L(0) - L_0]\}\exp(-\lambda_- t). \end{aligned}$$

In other words, λ_-^{-1} is the relaxation time of the quantity D + L.

We introduce the quantities

$$D_s(t) = D_0 + (D_s - D_0)\exp(-\lambda_- t),$$

$$L_s(t) = L_0 + (L_s - L_0)\exp(-\lambda_- t).$$

Then (40) assumes the form

$$\begin{aligned} D(t) &= D_s(t) + [D(0) - D_s]\exp(-\lambda_+ t), \\ L(t) &= L_s(t) + [L(0) - L_s]\exp(-\lambda_+ t). \end{aligned} \tag{42}$$

It is easy to see that $D_S(t)$ and $L_S(t)$ satisfy the condition of stationarity with respect to sd exchange interaction, (38), and their sum is D(t) + L(t), i.e., $D_S(t)$ and $L_S(t)$ are the quasi-equilibrium values of D(t) and L(t), corresponding to equilibrium under sd exchange interaction for specified D(t) + L(t).

Thus, in our case we have the following final result: an equilibrium with respect to sd exchange interaction is established with a relaxation time λ_+^{-1}; this is followed by a slower establishment of complete equilibrium, with a relaxation time λ_-^{-1}, and the equilibrium relative to exchange interaction is maintained all the time during this process.*

Case 2a. Assume that the following condition is satisfied in addition to conditions (37):

$$T_s \ll T_d \quad (\text{i. e. } T_{sd} \ll T_{ds}), \tag{43}$$

Now Eqs. (41) and (39) yield

$$\lambda_+ = \frac{1}{T_s}, \qquad \lambda_- = \frac{T_s}{T_d}\frac{1}{T_{sl}} + \frac{1}{T_{dl}}; \tag{44}$$

$$\begin{aligned} D_s &= D_0 - [L_0 - L(0)]T_s/T_d - [D_0 - D(0)]T_s/T_d. \\ L_s &= L(0) + [L_0 - L(0)]T_s/T_d - (1 - T_s/T_d)[D_0 - D(0)]. \end{aligned} \tag{45}$$

Let us consider relaxation in ferromagnetic resonance after turning off the alternating field. Under ordinary ferromagnetic resonance, a reduction in L takes place (saturation). Since our analysis is suitable only for relatively small deviations of L from L_0 (i.e., for small values of the resonance saturation parameter), we confine ourselves to the case $L(0) \lesssim L_0$.

Let us consider furthermore that the magnetization due to the d spins is considerably higher than the magnetization due to the s spins [i.e., L_0 and L(0) are much greater than T_0 and D(0)]. Then (45) yields

$$D_s = D_0 - [L_0 - L(0)]T_s/T_d, \qquad L_s = L(0). \tag{46}$$

According to (40) we obtain

$$\begin{aligned} D(t) &= D_0 + [D(0) - D_0]\exp(-\lambda_+ t) \\ &\quad + [L(0) - L_0][\exp(-\lambda_- t) - \exp(-\lambda_+ t)]T_s/T_d, \\ L(t) &= L_0 + [L(0) - L_0]\exp(-\lambda_- t). \end{aligned} \tag{47}$$

Thus, in Case 2a, the fast relaxation drops out from L and only the slow relaxation remains. As regards D, it first deviates rapidly from its initial value (and at the same time an equilibrium is established relative to the exchange interaction†), after which it slowly relaxes to its equilibrium value.

*This means that when $\lambda_+ t \gg 1$ we have $D(t) = D_S(t)$ and $L(t) = L_S(t)$.

†The corresponding term in L can be neglected, in view of the large value of L(0).

8. Let us estimate the quantities T_{sd} and T_{ds}, given by (29), in the case of iron.

From a measurement of the magnetization of the absolute saturation it follows that the number of magnetons per atom of iron is 2.22 (reference 16). This leads to an average configuration* $3d^{7.78}4s^{0.22}$ for the iron atom, which yields $S_d = 1.1$ and $\rho = 0.22$. For the dd exchange integral we take the value† $J = 175\,k = 2.4 \times 10^{-14}$ erg. We substitute furthermore the value $\nu = 2$ (since the iron lattice is body-centered cubic), $a = 2.85 \times 10^{-8}$ cm, $N = 0.86 \times 10^{23}$ cm^{-3}, and $g_d = 2$. The effective mass of the conduction electron in iron is unknown, and we shall use for it a value equal to 0.3 of the true mass of the electron, obtaining $\mu_0 = 1.4 \times 10^{-11}$ erg. At the present time, there are no data on the numerical value of the sd interaction constant A in ferromagnetic metals. As was indicated in Sec. 3, it appears little likely to us that screening would reduce this constant by a factor several times ten compared with its value in the free atom; we put in (29) a value $A = 4.8 \times 10^{-13}$ erg. For the constant B we obtain from (30) $B = 190$. It then follows from (30) that

$$z = (0.8 + 1.3 \cdot 10^{-4}H) \cdot T,$$

where T is given in degrees Kelvin.

Since our analysis holds only for temperatures greater than 2 or 3° K, we confine ourselves to the case $z < 1$. Equations (29) and (30a) yield

$$\frac{1}{T_{sd}} = 2 \cdot 10^9 T \ln \frac{T}{0.8 + 1.3 \cdot 10^{-4}H}, \qquad \frac{1}{T_{ds}} = 10^9 \sqrt{T}. \quad (48)$$

These equations can be used from 2 or 3° K approximately to 100° K. The condition $T_{ds} \gg T_{sd}$ is satisfied over this entire temperature interval.

The expression for T_{dl} can be taken from the paper by Akhiezer, Bar'yakhtar, and Peletminskiĭ.[4] The condition $T_{dl} \gg T_{ds}$ is satisfied over the entire temperature interval of interest to us. For T_{sl} we use the expression obtained by Andreev and Gerasimenko.[14] Substituting the values of the constants for iron in the suitable formula, we obtain

$$T_{sl} \sim 10^{-11}/(\Delta g)^2 T, \quad (49)$$

where Δg is the deviation of the conduction-electron g factor from its value for the free electron (2.0023). If Δg is of the same order (10^{-4} to 10^{-3}) for iron as for alkaline metals, then $T_{sl} \gg T_{sd}$, and Case 2a will take place (see Sec. 7).

9. Kittel and Mitchell believe[9] that in metals of the transition group of iron (in particular, in ferromagnetic metals), Δg will be considerably greater than in the case of alkaline metals, in view of the overlap of the 3d and 4s bands. However, comparing (48) with (49) we see that in order for T_{sl} to become of the same order as T_{sd}, it is necessary that Δg in iron be on the order of 0.2.

The values of Δg for metals of the transition groups are still unknown. In addition, in the derivation of (48) we used the unscreened value of the sd interaction constant. We cannot therefore draw any final conclusions concerning the mechanism of magnetic relaxation in ferromagnetic metals.

We consider that $T_{sl} \gg T_{sd}$, and therefore Case 2a, considered above, takes place. The fact that the resultant value of T_{sd} is so small should not cause any surprise: actually, the sd exchange interaction is strong (provided the constant A is of the same order as in the free atom).

One might ask why the relaxation time T_{sd} does not cause a broadening of ferromagnetic resonance (then the line width would be greater than the width measured in experiment). The point is, as was shown in Sec. 7, that in Case 2a the rapid relaxation drops out from the magnetization relaxation due to the d spins, and only the slow relaxation with relaxation time λ_-^{-1} remains.

We assume that the width of the ferromagnetic resonance (corresponding to a relaxation time 10^{-10}—10^{-9} sec) is due to the establishment of internal equilibrium in the d-spin system. This is very probable also because, according to experiment, the width of ferromagnetic resonance is of the same order in ferromagnetic metals and in ferrodielectrics.

However, in this case our calculation of T_{ds} is inconsistent. Actually, in calculating the terms that contain $\Delta n(\mathbf{f})$ in expression (26), we assumed that internal equilibrium is established in the ferromagnon gas. Strictly speaking, such a consideration would be valid only if the time of internal relaxation in the ferromagnon gas is smaller than λ_+^{-1}, which, in our opinion, does not take place. However, we believe that our calculation still yields an approximately correct value* of T_{ds}.

*The question of the average configuration is not completely resolved. See the paper by Mott and Stevens[17] regarding another possibility.

†This value of J follows from the work by Fallot,[18] in which the coefficient preceding $T^{3/2}$ in the temperature dependence of the magnetization is determined. Here we took account of the fact that $S_d = 1.1$.

*We have also calculated the second term in the expression (26), using the method employed in references 1–5. In other words, we have used the formula

$$\sum_{\mathbf{f}} W(\mathbf{f})\,\Delta n(\mathbf{f}) = \Big[\sum_{\mathbf{f}} n^0(\mathbf{f})\Big]^{-1} \sum_{\mathbf{f}} W(\mathbf{f})\, n^0(\mathbf{f}) \sum_{\mathbf{f}} \Delta n(\mathbf{f}).$$

In the case $z < 1$ we obtain here for $1/T_{ds}$ an expression that differs from (29) only by a factor equal to 3/4. We note also

It would be quite interesting to carry out resonance experiments on the conduction electrons in a ferromagnet. However, if the constant A is not greatly reduced by screening, the resonance will be in the infrared region (the value A = 0.3 ev corresponds to a frequency 0.8×10^{14} cps). In particular, it would be quite interesting to investigate the effect of saturation of ferromagnetic resonance on the resonance of the conduction electrons and vice versa. It would be also interesting to investigate the Overhauser effect in ferromagnetic metals, i.e., to measure the polarization of the nuclei in saturation of ferromagnetic resonance or resonance of conduction electrons.

At high temperatures, near the Curie point, the field due to the ds spins acting on the conduction electrons will be considerably less than the value H_S given by (6). The conduction-electron resonance should therefore shift towards the centimeter waves. It must be considered, however, that in this case the eigenvalue of the conduction-electron spin projection on the direction of the field will not be a good quantum number, since S_Z does not commute with the sd exchange interaction Hamiltonian at high temperatures.

The authors are grateful to M. I. Kaganov and to V. G. Bar'yakhtar for useful discussions.

[1] A. I. Akhiezer, J. of Phys. U.S.S.R. **10**, 217 (1946).

[2] C. Kittel and E. Abrahams, Phys. Rev. **88**, 1200 (1953); Revs. Modern Phys. **25**, 233 (1953).

[3] M. I. Kaganov and V. M. Tsukernik, JETP **34**, 1610 (1958) and **36**, 224 (1959), Soviet Phys. JETP **7**, 1107 (1958) and **9**, 151 (1959).

[4] Akhiezer, Bar'yakhtar, and Peletminskiĭ, JETP **36**, 216 (1959), Soviet Phys. JETP **9**, 146 (1959).

[5] V. G. Bar'yakhtar, JETP **37**, 690 (1959), Soviet Phys. JETP **10**, 493 (1960).

[6] A. I. Akhiezer and I. Ya. Pomeranchuk, JETP **36**, 859 (1959), Soviet Phys. JETP **9**, 605 (1959).

[7] E. A. Turov, Izv. Akad. Nauk SSSR, Ser. Fiz. **19**, 462 (1955), Columbia Tech. Transl. p. 414.

[8] A. H. Mitchell, Phys. Rev. **105**, 1439 (1957).

[9] C. Kittel and A. H. Mitchell, Phys. Rev. **101**, 1611 (1956).

[10] K. Yosida, Phys. Rev. **106**, 893 (1957); H. Hasegawa, Progr. Theoret. Phys. **21**, 483 (1959).

[11] J. Van Kranendonk and J. H. Van Vleck, Revs. Modern Phys. **30**, 1 (1958).

[12] C. Herring and C. Kittel, Phys. Rev. **81**, 869 (1950).

[13] R. J. Elliot, Phys. Rev. **96**, 266 (1954).

[14] V. V. Andreev and V. I. Gerasimenko, JETP **35**, 1209 (1958), Soviet Phys. JETP **8**, 846 (1959).

[15] A. Overhauser, Phys. Rev. **92**, 311 (1953).

[16] S. V. Vonsovskiĭ, Современное учение о магнетизме (Modern Theories of Magnetism), Gostekhizdat, 1952.

[17] N. F. Mott and W. H. Stevens, Phil. Mag. **2**, 1364 (1957).

[18] M. Fallot, Ann. phys. **6**, 305 (1938).

that if the Case 2a considered above takes place, then only the slow relaxation, whose time is considerably greater than the time for establishment of internal equilibrium in the spin system, remains in ordinary ferromagnetic resonance.

Translated by J. G. Adashko
136

NORMALIZATION CONSTANTS OF STATE VECTORS IN FIELD THEORY

M. A. BRAUN

Leningrad State University

Submitted to JETP editor April 9, 1960

J. Exptl. Theoret. Phys. (U.S.S.R.) **39**, 737-740 (September, 1960)

By means of weak-convergence methods it is shown that the normalization constant introduced by Van Hove and De Witt[1,2] for an n-particle state in field theory is equal to the product of the so-called vacuum constant and a factor Z^n, where Z is the constant of wave-function renormalization in the usual formalism of field theory.

1. The study of the eigenstates of field theory in the Schrödinger representation[1-3] has led to the appearance in the theory of normalization constants N_α (in the notation of references 2 and 3). Without any sort of proof, De Witt[1] has identified these constants with products of certain numbers of wave-function renormalization constants Z in the usual formalism of field theory (Z_2 and Z_3 in quantum electrodynamics). Later, however, after a rather detailed analysis, Frazer and Van Hove[3] came to the conclusion that the constant N_α cannot be connected with the constants Z in such a simple way.

In the present paper we shall show, by using the methods of weak convergence, that the result of Frazer and Van Hove is untrue, and that the connection between N_α and Z is essentially that given by De Witt. This fact makes possible a rigorous justification of the usual procedure for renormalizing the external lines of S-matrix diagrams in the interaction representation, and thus also a proof of the renormalizability of the S matrix.

2. For simplicity let us consider a scalar field A(x) interacting with itself. The extension to more complicated cases is not difficult.

Let H be the Hamiltonian of the system, $H = H_0 + V$, where H_0 is the Hamiltonian of the noninteracting particles, with the eigenstates $|\alpha\rangle$ (α characterizes the number of particles n and their four-momenta $k_1, \ldots, k_n$, with $k_i^2 = m^2$, where m is the mass of the particles). Also let $H_0|\alpha\rangle = E_\alpha|\alpha\rangle$, and

$$\langle\alpha|\beta\rangle = \bar{\delta}_{\alpha\beta} \equiv \delta_{mn} 2k_1^0 \ldots 2k_n^0 S\,\delta(k_1' - k_1)\ldots\delta(k_n' - k_n). \quad (1)$$

Here $\alpha = (k_1 \ldots k_n)$, $\beta = (k_1' \ldots k_m')$, and S is the sign for symmetrization with respect to the arguments.

We put in correspondence with the state $|\alpha\rangle$ two eigenstates of the Hamiltonian H, denoted by $\Psi_\alpha^{(\pm)}$ and characterized by the equations:

$$\langle\Psi_\alpha^{(\pm)}|\Psi_\beta^{(\pm)}\rangle = \bar{\delta}_{\alpha\beta}, \quad (2)$$

$$\langle\alpha|\Psi_\beta^{(\pm)}\rangle = N_\beta^{1/2}[\bar{\delta}_{\alpha\beta} - B_{\alpha\beta}/(E_\alpha - E_\beta \mp i0)], \quad (3)$$

where $0 \le N_\beta \le 1$ and $B_{\alpha\beta}^{(\pm)}$ has no singularity at $E_\alpha = E_\beta$.

We assume that the renormalization of the vacuum energy and the mass of the particle has been carried out, so that

$$H\Psi_\alpha^{(\pm)} = E_\alpha\Psi_\alpha^{(\pm)}. \quad (4)$$

Equation (3) can be used as the definition of the normalization constants N_α. It has been shown by Hugenholtz[2] that

$$N_\alpha = \bar{N}_{k_1}\ldots\bar{N}_{k_n}N_0, \quad (5)$$

where N_0 is the vacuum constant defined in the following way:

$$\langle 0|\Psi_0\rangle = N_0^{1/2} \quad (6)$$

($|0\rangle$ and Ψ_0 are the mathematical and physical vacua). N_0 decreases exponentially with the volume of the system.

As for the renormalization constant Z of the wave function, it is well known that it can be defined by the equation

$$\langle\Psi_0|A(x)|\Psi_p\rangle = (2\pi)^{-3/2}e^{-ipx}Z^{1/2} \quad (7)$$

(Ψ_p is a one-particle state). It follows from Eq. (7) that the Green's function in the momentum representation for interacting particles has a pole at the point $p^2 = m^2$ with the residue Z/i.

It is shown in Sec. 5 that $\bar{N}_p = Z$.

3. The starting point for what follows is the following fundamental fact of weak convergence:

$$U(t)|\alpha\rangle \equiv e^{iHt}e^{-iH_0t}|\alpha\rangle \to N_\alpha^{1/2}\Psi_\alpha^{(\pm)} \text{ for } t \to \mp\infty. \quad (8)$$

This assertion is proved in the review article by Brenig and Haag[4] for the special case of a one-particle state in meson-field theory that interacts with bound nucleons. Here we shall present a brief general proof.

Let us consider the matrix element

$$\langle\Phi_1|U(t)|\Phi_2\rangle, \qquad \Phi_1=\sum_\beta c_1^{(\pm)}(\beta)\,\Psi_\beta^{(\pm)},$$

$$\Phi_2=\sum_\alpha c_2(\alpha)|\alpha\rangle,$$

where $<\Phi_1|\Phi_1><\infty$ and $<\Phi_2|\Phi_2><\infty$. On the basis of Eq. (3) we find:

$$\langle\Phi_1|U(t)|\Phi_2\rangle=\sum_\alpha c_1^{(\pm)*}(\alpha)\,c_2(\alpha)\,N_\alpha^{1/2}$$

$$-\sum_{\alpha\beta}c_1^{(\pm)*}(\beta)\,c_2(\alpha)\,B_{\alpha\beta}^{(\pm)*}$$

$$\times\exp\{-it(E_\alpha-E_\beta)\}/(E_\alpha-E_\beta\pm i0).$$

For $t\to\mp\infty$ the second term goes to zero, and we get*

$$\lim_{t\to\mp\infty}\langle\Phi_1|U(t)|\Phi_2\rangle=\sum_\alpha c_1^{(\pm)*}(\alpha)\,c_2(\alpha)\,N_\alpha^{1/2},$$

which was to be proved.

4. Let us now use weak convergence for the proof of the equation:

$$\langle\Psi_\alpha^{(-)}|T\{A(x_1)\dots A(x_n)\}|\Psi_\beta^{(+)}\rangle$$

$$=N_\alpha^{-1/2}N_\beta^{-1/2}\langle\alpha|T\{\overline{A}(x_1)\dots\overline{A}(x_n)S_1\}|\beta\rangle,$$

$$\overline{A}(x)=\exp(iH_0x^0)\,A(x,0)\exp(-iH_0x^0),$$

$$S_1=T\left\{\exp\left(-i\int_{-\infty}^{+\infty}\overline{V}(t)\,dt\right)\right\}. \tag{9}$$

In fact, as we have seen

$$\langle\Psi_\alpha^{(-)}|T\{A(x_1)\dots A(x_n)\}|\Psi_\beta^{(+)}\rangle=\lim_{\substack{t_2\to+\infty\\ t_1\to-\infty}}N_\alpha^{-1/2}N_\beta^{-1/2}$$

$$\times\langle\alpha|U^+(t_2)\,T\{A(x_1)\dots A(x_n)\}\,U(t_1)|\beta\rangle.$$

Let $x_1^0>x_2^0>\dots>x_n^0$. Then, defining

$$U(t_2,t_1)=U^+(t_2)\,U(t_1),$$

we find:

$$U^+(t_2)\,T\{A(x_1)\dots A(x_n)\}\,U(t_1)$$

$$=U(t_2,x_1^0)\,\overline{A}(x_1)\,U(x_1^0,x_2^0)\,\overline{A}(x_2)\dots\overline{A}(x_n)\,U(x_n^0,t_1)$$

$$=T\{\overline{A}(x_1)\dots\overline{A}(x_n)\,U(t_2,t_1)\}.$$

If we also use the fact that (cf. reference 4)

$$U(t_2,t_1)=T\left\{\exp\left(-i\int_{t_1}^{t_2}\overline{V}(t)\,dt\right)\right\},$$

we at once arrive at the formula (9), from which there follow in particular expressions for the S matrix

$$S_{\alpha\beta}=\langle\Psi_\alpha^{(-)}|\Psi_\beta^{(+)}\rangle=N_\alpha^{-1/2}N_\beta^{-1/2}\langle\alpha|S_1|\beta\rangle \tag{10}$$

and for the Green's function

$$\Delta_c'(x_1-x_2)=\langle\Psi_0|T\{A(x_1)\,A(x_2)\}|\Psi_0\rangle$$

$$=N_0^{-1}\langle0|T\{\overline{A}(x_1)\,\overline{A}(x_2)\,S_1\}|0\rangle. \tag{11}$$

5. We can now go on to our main problem of correlating the constants N_α and Z. Taking both states in Eq. (10) to be vacuum states, we find:

$$S_{00}=1=N_0^{-1}\langle0|S_1|0\rangle, \qquad N_0=\langle0|S_1|0\rangle. \tag{12}$$

We note that $<0|S_1|0>$ is real and decreases exponentially with the volume (this is of course due to the renormalization of the vacuum energy which we have carried out).

Taking into account (12) formula (11) takes on the usual form

$$\Delta_c'(x_1-x_2)=\langle0|T\{\overline{A}(x_1')\,\overline{A}(x_2)\,S_1\}|0\rangle/\langle0|S_1|0\rangle.$$

Let us now consider the expression

$$\langle\Psi_0|A(x)|\Psi_p\rangle=N_0^{-1/2}N_p^{-1/2}\langle0|T\{\overline{A}(x)\,S_1\}|p\rangle.$$

Calculating the matrix element in the right member, we get

$$\langle0|T\{\overline{A}(x)\,S_1\}|p\rangle=\frac{1}{(2\pi)^{3/2}}e^{-ipx}\langle0|S_1|0\rangle\,\Delta_c'(p)\,\Delta_c^{-1}(p),$$

where $\Delta_c(p)$ is the Green's function of free particles in the momentum representation. Since $p^2=m^2$, we have $\Delta_c'(p)\Delta_c^{-1}(p)=Z$. When we use Eqs. (5) and (12), we now have

$$\langle\Psi_0|A(x)|\Psi_p\rangle=(2\pi)^{-3/2}e^{-ipx}Z\overline{N}_p^{-1/2}.$$

Comparison of this result with Eq. (7) leads to the desired relation:

$$\overline{N}_p=Z. \tag{13}$$

6. In conclusion we shall make some remarks about the renormalization of external lines in the S matrix. According to Eq. (10)

$$\langle k_1\dots k_n|S|k_1'\dots k_m'\rangle$$

$$=(\overline{N}_{k_1}\dots\overline{N}_{k_n}\overline{N}_{k_1'}\dots\overline{N}_{k_m'})^{-1/2}$$

$$\langle k_1\dots k_n|S_1|k_1'\dots k_m'\rangle\,N_0^{-1},$$

or, if we use our formulas (12) and (13)

$$\langle k_1\dots k_n|S|k_1'\dots k_m'\rangle$$

$$=Z^{-(n+m)/2}\langle k_1\dots k_n|\overline{S}_1|k_1'\dots k_m'\rangle, \tag{14}$$

where the bar over S_1 means that vacuum diagrams need not be taken into account.

As is well known, in the renormalization process each line in a diagram, and also each external line, produces a factor Z. In a renormalized vertex part one includes a factor $Z^{1/2}$ from each line entering it. The remaining $(n+m)$ factors $Z^{1/2}$ from the external lines cancel against the factor

*Some care is required in the case $m=0$, but it turns out that in this case, too, the arguments given here are correct.

in the right member of Eq. (14). Thus the final expression for the S matrix, and consequently the expression for the transition probability, do not depend explicitly on the constants Z, and are expressed in terms of the renormalized interaction constant only.

The writer expresses his deep gratitude to Yu. V. Novozhilov for his constant interest in this work and for helpful comments, and to L. D. Faddeev for helpful discussions.

[1] B. De Witt, Phys. Rev. **100**, 905 (1955).

[2] L. Van Hove, Physica **21**, 901 (1955); **22**, 343 (1956). N. M. Hugenholtz, Physica **23**, 481 (1957).

[3] W. R. Frazer and L. Van Hove, Physica **24**, 137 (1958).

[4] W. Brenig and R. Haag, Fortschritte der Physik **7**, 183 (1959).

Translated by W. H. Furry
137

QUANTUM OSCILLATIONS OF THE THERMAL CONDUCTIVITY COEFFICIENT OF AN ELECTRON GAS IN A MAGNETIC FIELD

V. V. ANDREEV and A. M. KOSEVICH

Physico-Technical Institute, Academy of Sciences, Ukrainian S.S.R.

Submitted to JETP editor April 9, 1960

J. Exptl. Theoret. Phys. (U.S.S.R.) 39, 741-745 (September, 1960)

The quantum oscillations of the thermal conductivity coefficient of conduction electrons in a strong magnetic field H ($\omega\tau \gg 1$, $\omega = eH/mc$, τ is the relaxation time) are computed at low temperatures ($kT \ll \zeta$, ζ being the chemical potential of the electron gas) when scattering of the electrons on impurities is of decisive importance. It is shown that the oscillating part of the thermal conductivity coefficient can be expressed in a simple manner in terms of the oscillations of the specific electric conductivity.

1. The thermal conductivity of metals in a magnetic field at low temperatures exhibits a singularity similar to the Shubnikov—De Haas phenomenon: the thermal conductivity coefficient depends on the magnetic field in a non-monotonic, oscillating manner.[1] Since the presence of oscillations in a magnetic field is a common quantum property of the thermodynamic and kinetic characteristics of a degenerate electron gas, one can assume that the electronic part of the thermal conductivity of the metal is responsible for the observed effect. Therefore, theoretical consideration of the quantum oscillations of the electronic contribution to the thermal conductivity coefficient of metal is of interest.

In the present work, quantum corrections to the classical (smoothly dependent on the magnetic field) coefficient of thermal conductivity of a metal[2] are investigated within the framework of a free gas of conduction electrons. We consider the electron gas in a metal whose temperature T has a small constant gradient grad T perpendicular to an external homogeneous magnetic field H. The density of the electrons is assumed to be sufficiently great that the temperature and the magnetic field satisfy the conditions $\Theta \equiv kT \ll \zeta$ and $\hbar\omega \ll \zeta$, where ζ is the chemical potential of the electron gas and $\omega = eH/mc$. These conditions make it possible to use a quasi-classical approximation for the investigation of the behavior of an electron gas in a magnetic field.

In the calculation of kinetic coefficients, only the scattering of electrons on impurities present in metals at low temperatures is taken into account. It is assumed that the concentration of the impurities is small and the stationary state of the electron in the given magnetic field can be established in the time interval between collisions with impurities, i.e., it is assumed that if τ is the characteristic relaxation time, then $\omega\tau \gg 1$. The inequalities $\hbar\omega \ll \zeta$ and $\omega\tau \gg 1$ can easily be satisfied simultaneously in metals at low temperatures. $1/\omega t$ and $\hbar\omega/\zeta$ are small parameters, in powers of which the expansions will later be carried out.

The state of the electron gas with account of scattering of electrons on impurities is described by the single-particle statistical operator ρ, which is found from the quantum kinetic equation obtained in our previous work.[3] The "collision integral" of this equation was calculated by perturbation theory for the interaction potential of an electron with the impurity. Such an approximation suffices if we are interested only in the principal term of the expansion in powers of $1/\omega\tau$ and $\hbar\omega/\zeta$. Actually, comparison of the results of our work[3] with the calculation of Skobov,[4] carried out without perturbation theory in the case $\omega\tau \gg 1$ for point impurities, shows that the principal terms in the parameter $\hbar\omega/\zeta$ in the expansion of the smooth and oscillating parts of the conductivity of the electron gas, measured in terms of the classical characteristics of the conductivity, are correctly described by the solution of the given kinetic equation. The latter verifies the possibility of use of the quantum kinetic equation of reference 3 to find the chief terms of the expansion of other kinetic coefficients in powers of $1/\omega\tau$ and $\hbar\omega/\zeta$.

The method used in the present work makes it possible to study the thermal conductivity of an electron gas with an arbitrary dispersion law; however, for simplicity, the case of an isotropic quadratic dispersion law is considered.

2. The Hamiltonian $\mathcal{H}$ of an individual electron in an external field has the form

$$\mathcal{H} = \varepsilon(H) - e\mathbf{E}\mathbf{r}, \qquad \varepsilon(H) = \frac{1}{2m}\left(\mathbf{p} - \frac{e}{c}\mathbf{A}\right)^2,$$

where $\epsilon(H)$ is the Hamiltonian of the electron in a homogeneous magnetic field **H**, which is considered to be parallel to the z axis; $\mathbf{E}(E_1, E_2, 0)$ is the electric field derived from grad T. The remaining notation is standard.

If grad T is directed along the y axis, then the vector potential of the magnetic field **A** is conveniently chosen such $(A_x = -Hy, A_y = A_z = 0)$ that the operator $y_0 = -cp_x/eH$, which plays the role of the y coordinate of the center of the electronic charge in a stationary orbit in a magnetic field, commutes with the Hamiltonian $\epsilon(H)$.

In the stationary case, the single-particle statistical operator ρ, which describes the electron gas, is determined from the following equation $(\partial\rho/\partial t = 0)$:

$$(i/\hbar)[\mathcal{H}, \rho] + D\{\rho\} = 0, \tag{1}$$

where $[\mathcal{H}, \rho] = \mathcal{H}\rho - \rho\mathcal{H}$, and $D\{\rho\}$ is the quantum analog of the "collision integral," depending exclusively on the electric field.[3] In the case of elastic scattering by large impurities, $D\{\rho\}$ is a linear transformation of ρ.

If we limit ourselves to the quasi-classical approximation, it is natural to seek ρ (by analogy with the solution of the classical kinetic equation) in the form

$$\rho = f_0\left[\frac{\varepsilon - \zeta(y_0)}{\Theta(y_0)}\right] + F_0 + \rho_1. \tag{2}$$

Here f_0 is the Fermi distribution function, while $\zeta(y)$ and $T(y)$ are the chemical potential and the temperature, which depend on the coordinate y in classical fashion, in particular, $T(y) = T_0 + (\partial T/\partial y)y$ (T_0 is a certain mean temperature for the entire gas). By F_0 is meant a definite matrix (obtained in reference 3) which takes into account the shift in the energy levels of the electron in the field of the impurities and which leads to a small shift in the chemical potential, while ρ_1 is the small change that is sought, and is linear in $\partial T/\partial y$ and E.

Since the operator y_0 commutes with $\epsilon(H)$, the choice of the solution of (1) in the form (2) makes it possible to carry out a simplification of Eq. (1), linearizing it in the small quantities $\partial T/\partial y$ and E.

If we are not interested in the shift of the electron levels in the field of the impurities and if from the very beginning we take into account the small shift in the chemical potential, then we can neglect in (2) the matrix F_0, which makes no contribution to the current and the heat flow. Then the quantum kinetic equation, linearized in $\partial T/\partial y$ and E, takes the form[3]

$$\frac{i}{\hbar}[\varepsilon, \rho_1] + D_0\{\rho_1\} = \frac{i}{\hbar}[e\mathbf{E}\mathbf{r}, \rho_0] - \frac{\partial T}{\partial y} T D_0\left\{y_0 \rho_0' \frac{\partial}{\partial T}\left(\frac{\varepsilon - \zeta}{\Theta}\right)_0\right\} - e\mathbf{E} D_0\{\mathbf{r}g\},$$

$$\rho_0(\varepsilon) = f_0\left(\frac{\varepsilon - \zeta_0}{\Theta_0}\right), \tag{3}$$

where ζ_0 is the chemical potential corresponding to the temperature T_0. The matrix g in the representation of the Hamiltonian $\epsilon(H)$, the eigenvalues of which $\epsilon_\mu \equiv \epsilon_n(p_z)$, $(\mu = n, p_x, p_z)$, are determined by the formula

$$g^{\mu\mu'} = (\rho^0_\mu - \rho^0_{\mu'})/(\varepsilon_\mu - \varepsilon_{\mu'}), \qquad \rho^0_\mu = \rho_0(\varepsilon_\mu),$$

and the product rg can be understood as the direct product of the operators:

$$(\mathbf{r}g)^{\mu\mu'} = \mathbf{r}^{\mu\mu'} g^{\mu\mu'}.$$

The linear transformation D_0 appearing in (3) no longer contains the electric field and can be expressed in terms of the classical collision integral.[3]

The meaning of the first two terms on the right hand side of (3) is evident, while the third component describes the effect of the electric field on the "collision integral." Writing down of the last component is somewhat different from the corresponding expression in reference 3, since in the given case the field is not directed along the y axis but is located at a certain angle with respect to the y axis in the xy plane.

In the classical limiting case, in which the scattering of the electron on a short-range center takes place with the conservation of the coordinate **r** at the scattering point, $D_0\{\mathbf{r}g\} \to D_{cl}\{\mathbf{r}\rho_0'(\epsilon)\} = 0$, and Eq. (3) transforms into the classical kinetic equation for the correction to the distribution function of an electron gas.

3. The solution of Eq. (3) is found in the form of an expansion in powers of $1/\omega\tau$, where use is made of the fact that D_0 is proportional to $1/\tau$. In the expansion of ρ_1, just as in reference 3, the terms of zero and first approximation in $1/\omega\tau$ remain. With the help of the matrix ρ_1 determined in such fashion, and also with the help of the expression for the density of the electric current **j** and the energy flux **q**

$$\mathbf{j} = e\,\mathrm{Sp}\{\rho\mathbf{v}\}, \qquad \mathbf{q} = \tfrac{1}{2}\,\mathrm{Sp}\{\rho(\varepsilon\mathbf{v} + \mathbf{v}\varepsilon)\},$$

we establish a linear connection relating **j** and **q** with **E** and grad T:

$$j_\alpha = \sigma_{\alpha\alpha'}E_{\alpha'} + s_\alpha(\partial T/\partial y), \qquad q_y = \eta_\alpha E_\alpha + \beta(\partial T/\partial y)$$
$$(\alpha, \alpha' = 1, 2).$$

In the approximation under consideration,

$$\sigma_{xx} = \sigma_{yy} = (emc/H)\,\mathrm{Sp}\,\{D_0(y_0\rho_0')\,v_x\},\quad \sigma_{xy} = -\sigma_{yx} = ecn_0/H,$$
$$s_x = 0,\qquad s_y = (\Theta mc/H)\,\mathrm{Sp}\left\{D_0\left[y_0\rho_0'\frac{\partial}{\partial\Theta}\left(\frac{\varepsilon-\zeta}{\Theta}\right)_0\right]v_x\right\},$$
$$\eta_x = -\frac{5}{3}\bar{\varepsilon}cn_0/H,$$
$$\eta_y = (mc/2H)\,\mathrm{Sp}\,\{D_0(y_0\rho_0')(\varepsilon v_x + v\,\varepsilon)\},$$
$$\beta = (\Theta mc/2eH)\,\mathrm{Sp}\left\{D_0\left[y_0\rho_0'\frac{\partial}{\partial\Theta}\left(\frac{\varepsilon-\zeta}{\Theta}\right)\right]_0(\varepsilon v_x + v_x\varepsilon)\right\}, \qquad (4)$$

where n_0 is the electron number density corresponding to the chemical potential ζ_0, while $\bar{\epsilon}$ is the average energy of the electron.

Expressions of the type (4) for the tensors of the thermoelectric coefficients in a magnetic field are obtained in completely analogous fashion in the case of an arbitrary dispersion law. Similar to what was done for σ,[3] one can easily study its oscillating parts, expressing the latter in terms of the oscillation of the magnetic moment. However, calculation of the oscillating part of the thermal conductivity coefficient in the general case entails very great computational difficulties; therefore, the simplest case of a quadratic isotropic dispersion law is considered.

Any of the thermoelectric coefficients (4) is expressed by a formula of the type

$$\sigma = \mathrm{Sp}\,\{D_0(R)\,\varphi\},$$

in which R is the diagonal matrix of the form $R = \rho_0'\psi(y_0, \epsilon)$, while φ is a matrix which is diagonal in y_0 and p_z.

The linear transformation $D_0(R)$ is written in matrix form in the following way:

$$D_0(R)^{nm} = \sum D^{nm}_{n'm'}(y_0, p_z; y_0', p_z')\,R^{n'm'}(y_0', p_z')$$
$$= \sum W_{KK'}(\varepsilon_n, y_0, p_z; \varepsilon_n', y_0', p_z')\,R^K(\varepsilon_n', y_0', p_z')$$

(summation is carried out over all primed indices). Here $K = n - m$, $K' = n' - m'$, and for the matrix element $W_{KK'}$, we substitute the Fourier component of the kernel of the corresponding classical collision integral (this substitution of matrix elements is discussed in the work of I. M. Lifshitz[5] and is used in reference 3).

If we make use of the form of R given above and the Hermitian character of the operator φ, then we get the following expression for the coefficient σ:

$$\sigma = \sum \rho_0'(\varepsilon_{n'})\,\Phi_K^* W_{K0}\psi_0, \qquad (5)$$

in which summation is carried out over all indices, and which can be represented in a form similar to Eq. (19) of reference 3:

$$\sigma = -2\sum_{\varepsilon_n}\int \frac{df_0}{d\varepsilon_n}\,\chi m\Delta\varepsilon_n\,dp_z. \qquad (6)$$

The definition of the quantity χ entering into σ is evident from (5).

Writing down of an arbitrary thermoelectric coefficient in the form (6) makes it possible, directly or with a little alteration (brought about by an account of the higher powers of the expansion in Θ/ζ) to make use of Eqs. (20) — (24) of reference 3. These formulas make it possible to separate the basic classical parts of coefficients of the type σ and the corresponding oscillatory quantum contributions, and it is found that the essential dependence on H and Θ of the oscillating parts of the thermoelectric coefficients (4) is the same as for the oscillating magnetic moment, and is always taken into account either by a factor F* (see reference 6) of the form

$$F^* = \sum_{K=1}^{\infty}\frac{(-1)^K}{K^{3/2}}\frac{K\lambda}{\sinh(K\lambda)}\cos\left(\frac{2\pi K\zeta_0}{\hbar\omega} - \frac{3\pi}{4}\right), \qquad \lambda = \frac{2\pi^2\Theta}{\hbar\omega}, \qquad (7)$$

or by its derivatives with respect to H and Θ.

4. The coefficient of thermal conductivity κ is usually identified with the coefficient of proportionality (taken with reverse sign) between the component q along grad T and the gradient of the temperature at $j = 0$. In the case under consideration, it is composed of the coefficients (4) in the following fashion:

$$\varkappa = s_y(\eta_y\sigma_{xx} - \eta_x\sigma_{xy})/\Delta - \beta, \qquad \Delta = \sigma_{xx}^2 + \sigma_{xy}^2. \qquad (8)$$

Having the expressions given above for the smooth and oscillating portions of the coefficients (4) in the coefficient of thermal conductivity defined by Eq. (8), we can also separate the classical part κ_0, which is smoothly varying with the magnetic field, and a small oscillating quantum correction $\Delta\kappa$. The classical part κ_0 is connected in obvious fashion with the classical electrical conductivity in a magnetic field σ_0:

$$\varkappa_0 = (\pi^2/3)(k/e)^2\,T\sigma_0,$$

where k is the Boltzmann constant and the oscillating part $\Delta\kappa$ is expressed in terms of the oscillating part of the electrical conductivity $\Delta\sigma$, determined in references 3, 4, and 7.

It is convenient to write the connection of the principal term (for small parameters $\hbar\omega/\zeta$ and Θ/ζ) in $\Delta\kappa$ with $\Delta\sigma$ following from (8) and (4) in compact form, after a long series of calculations and estimates:

$$\pi^2H^2\frac{\partial^2}{\partial H^2}\left(\frac{\Delta\varkappa}{\varkappa_0}\right) = 3\zeta_0(0)^2\frac{\partial^2}{\partial\Theta^2}\left(\frac{\Delta\sigma}{\sigma_0}\right), \qquad (9)$$

where $\zeta_0(0)$ is the classical chemical potential at $T = 0^0K$, and the differentiation takes into account

only the very strong and important dependence on H and Θ, determined by the factor F*.

The quantity $\Delta\sigma$ entering into (9), as was emphasized above, can in turn be expressed through the oscillating part of the magnetic moment of the electron gas.[3] The latter indicates that the periods of oscillation of the thermal conductivity coefficient coincide with the periods of oscillation in the DeHaas—Van Alphen effect (this result naturally remains true even in the case of an arbitrary dispersion law). It is well known that experimental measurements of the period of oscillation of κ lead to the same conclusion.[1]

If we take into account only the fundamental dependence of $\Delta\kappa$ and $\Delta\sigma$ on H and Θ, given by a factor of the type (7), then we have a quantity of order of magnitude

$$H\frac{\partial}{\partial H}\Delta\varkappa\sim\frac{\zeta_0}{\hbar\omega}\Delta\varkappa,\qquad \zeta_0\frac{\partial}{\partial\Theta}\Delta\sigma\sim\frac{\zeta_0}{\hbar\omega}\Delta\sigma,$$

and therefore it follows from (9) that

$$\Delta\varkappa/\varkappa_0\sim\Delta\sigma/\sigma_0.$$

For not very low temperatures, when $\hbar\omega < \Theta$, we have the equality

$$\Delta\varkappa/\varkappa_0=3(\Delta\sigma/\sigma_0).$$

I take this opportunity to express my deep gratitude to I. M. Lifshitz and M. Ya. Azbel' for valuable discussions.

[1] M. S. Steele and J. Babiskin, Phys. Rev. **98**, 359 (1955). P. B. Alers, Phys. Rev. **107**, 959 (1957).

[2] Azbel', Kaganov, and Lifshitz, JETP **32**, 1188 (1957), Soviet Phys. JETP **5**, 967 (1957).

[3] A. M. Kosevich and V. V. Andreev, JETP **38**, 882 (1960), Soviet Phys. JETP **11**, 941 (1960).

[4] V. G. Skobov, JETP **38**, 1304 (1960), Soviet Phys. JETP **11**, 941 (1960).

[5] I. M. Lifshitz, JETP **32**, 1509 (1957), Soviet Phys. JETP **5**, 1227 (1957); J. Phys. Chem. Solids **4**, 11 (1958).

[6] I. M. Lifshitz and A. M. Kosevich, JETP **33**, 88 (1957), Soviet Phys. JETP **6**, 67 (1958).

[7] E. N. Adams and T. D. Holstein, J. Phys. Chem. Solids **10**, 254 (1959).

Translated by R. T. Beyer
138

STRUCTURE OF LOW INTENSITY SHOCK WAVES IN MAGNETOHYDRODYNAMICS

E. P. SIROTINA and S. I. SYROVAT-SKIĬ

Submitted to JETP editor April 13, 1960; re-submitted June 8, 1960

J. Exptl. Theoret. Phys. (U.S.S.R.) 39, 746-753 (September, 1960)

A general expression has been deduced for the width of low intensity shock waves in magnetohydrodynamics. The damping coefficient for small amplitude waves is determined and its relation to the discontinuity width is established.

THE problem of the determination of the structure of shock waves in magnetohydrodynamics is mathematically very cumbersome and can be solved in the general case only by numerical methods. At the present time the structure of perpendicular shock waves (i.e., traveling strictly perpendicular to the magnetic field) has been studied in sufficient detail.[1-4] However, such a wave is only one of the simplest types of shock waves in magnetohydrodynamics. So far as shock waves of the general types are concerned, the so-called oblique shocks, their structure has been considered only under certain simplifying assumptions, namely, under consideration of Joule dissipation only.[5] Even in this case, one has to resort to numerical integration, which complicates the investigation of the dependence of the solution on its parameters.

In this connection, it is interesting to investigate the structure of low intensity shock waves by a method developed by Landau and Lifshitz[6] for a shock wave in ordinary hydrodynamics, and by one of the present authors[4] for a perpendicular shock wave in magnetohydrodynamics. Although this method does not make it possible to include in the discussion such peculiarities characteristic of strong shocks as isothermal and isomagnetic discontinuities, it nevertheless does make it possible to solve the problem in the general case for waves of an arbitrary type with consideration of all dissipative processes. This is especially important in the study of the dependence of the solution on its parameters and on the special features arising therein.

1. THE EQUATION OF A LOW INTENSITY SHOCK WAVE

In what follows, it is convenient to select a set of coordinates[7] in which the lines of the magnetic field and the streamlines of the liquid are parallel at great distances from the discontinuity. This set of coordinates can be introduced for all shock waves with the exception of the strictly perpendicular, in which $\mathbf{v} \perp \mathbf{H}$. However, as we shall see below, the result does not depend on the choice of coordinates and therefore it will be useful for the perpendicular shock wave also.

Let us consider a plane shock in which all the quantities depend only on x. The general equation for stationary one-dimensional flow can be written in the following form:[4]

$$j = v_n / V = j_1, \tag{1}$$

$$H_n = H_{n1}, \tag{2}$$

$$jV\mathbf{H}_\tau - H_n\mathbf{v}_\tau - \beta\, d\mathbf{H}_\tau / dx = 0, \tag{3}$$

$$j\mathbf{v}_\tau - H_n\mathbf{H}_\tau - \eta\, d\mathbf{v}_\tau / dx = j\mathbf{v}_{\tau 1} - H_n\mathbf{H}_{\tau 1}, \tag{4}$$

$$p + j^2V + \tfrac{1}{2}H_\tau^2 - \left(\tfrac{4}{3}\eta + \zeta\right) j\, dV/dx = p_1 + j^2V_1 + \tfrac{1}{2}H_{\tau 1}^2, \tag{5}$$

$$\tfrac{1}{2}j^2V^2 + \tfrac{1}{2}v_\tau^2 + w - \left(\tfrac{4}{3}\eta + \zeta\right)jV\frac{dV}{dx} - \eta\frac{dv_\tau^2}{dx} - \frac{\kappa}{j}\frac{dT}{dx} = \tfrac{1}{2}j^2V_1^2 + \tfrac{1}{2}v_{\tau 1}^2 + w_1. \tag{6}$$

Here the following notation is introduced: w, p, T, and V are, respectively, the heat function of a unit mass of the substance, the pressure, the temperature and the specific volume of the medium; η and ζ are the first and second viscosity coefficients, κ is the coefficient of thermal conductivity of the medium, and $\beta = c_0^2/4\pi\sigma$ is the magnetic viscosity (σ is the electrical conductivity of the medium and c_0 is the speed of light). The rationalized system of units has been introduced for the intensity of the magnetic field. The index 1 denotes the value of the corresponding quantities at a large distance in front of the discontinuity. The indices n and τ respectively denote the components of the vector velocity v and the intensity of the magnetic field H normal and tangential to the surface of discontinuity.

Equations (5) and (6) contain only the squares of the tangential components $\mathbf{H}_\tau$ and $\mathbf{v}_\tau$. Since Eqs. (3) and (4) are linear in $\mathbf{v}_\tau$ and $\mathbf{H}_\tau$, then they

can be transformed into equations containing only the squares H_τ^2 and v_τ^2. This transformation makes it possible to consider as low intensity discontinuities not only discontinuities in which all the physical quantities change but slightly, but also discontinuities in which the absolute values of all physical quantities undergo little change while the directions of the vectors **v** and **H** can change appreciably.

The latter can be the case if the change of the vectors **v** and **H** inside the discontinuity are determined by their rotation about the normal to the discontinuity. For rotational discontinuities, the angle of rotation can be arbitrary. However, for shock waves, the boundary equations require that the vectors **v** and **H** in front of the discontinuity and behind it lie in a single plane. Therefore, in the case of a shock wave, the rotation of the vectors **v** and **H** inside the discontinuity can exist only at an angle which is a multiple of π.

So far as we know, this interesting case of shock waves has not been discussed to date. The difficulty here lies in the fact that the problem of the structure of shock waves ought to be solved for nonplanar motion. However, in the approximation of weak shock waves considered below, this problem does not differ from the problem for plane motion.

For low-intensity shock waves, the differences of the physical quantities

$$\delta p = p - p_1, \quad \delta V = V - V_1, \quad \delta T = T - T_1,$$

$$\delta H_\tau^2 = H_\tau^2 - H_{\tau 1}^2, \quad \delta v_\tau^2 = v_\tau^2 - v_{\tau 1}^2$$

are small and we can limit ourselves in the equation to terms of no higher than second order of smallness in δp, δV and so forth. Moreover, we make use of the fact that the inverse of the discontinuity width $1/l$, as will be seen from the results, has the same order of smallness as the discontinuities in the quantities δp, δV and so forth at the discontinuity, and consequently differentiation with respect to x increases the order of smallness by unity.

Making use of Eqs. (3) and (4), we express the discontinuities δH^2 and δv^2 under these assumptions in terms of δV, with accuracy up to terms of second order:

$$\delta H_\tau^2 = a_1 \delta V + b_1 (\delta V)^2 + c_1 dV/dx, \tag{7}$$

$$\delta v_\tau^2 = a \delta V + b (\delta V)^2 + c dV/dx; \tag{8}$$

$$a = V_1 a_1, \quad b = V_1 b_1 + a_1/2, \quad c = V_1 c_1 + (\eta/j) V_1 a_1,$$
$$a_1 = 2j^2 H_{\tau 1}^2/\Delta, \quad b_1 = 3j^4 H_{\tau 1}^2/\Delta^2,$$
$$c_1 = -2jH_{\tau 1}^3 \Delta^{-2} (j^2 \beta + H_n^2 \eta), \quad \Delta = H_n^2 - j^2 V_1. \tag{9}$$

We note here that in the solution of Eqs. (3), (4), (7), and (8) with respect to a, a_1, ..., division is carried out by the factor Δ which vanishes for rotational ($H_n^2 = \rho v_n^2$) discontinuities. The appearance of a singularity in Eqs. (7) — (9) for $\Delta = 0$ signifies the absence of a stationary structure in these discontinuities. In fact, for rotational discontinuities, the boundary equations require an equality of density, pressure and, consequently, entropy on both sides of the discontinuity. This requirement is in contradiction with the increase in entropy as the result of dissipation. Therefore, the rotational discontinuities cannot have a stationary character, and are smeared out with passage of time, as was shown by Landau and Lifshitz[8] for an incompressible fluid.

Equations (5) and (6), with account of (7) and (8), reduce to the form

$$\delta p + (j^2 + \tfrac{1}{2} a_1) \delta V + \tfrac{1}{2} b_1 (\delta V)^2 + [\tfrac{1}{2} c_1 - j(\tfrac{4}{3}\eta + \zeta)] dV/dx = 0, \tag{10}$$

$$\delta w + (j^2 V_1 + \tfrac{1}{2} a) \delta V + \tfrac{1}{2} (j^2 + b^2) (\delta V)^2 + [\tfrac{1}{2} c - jV(\tfrac{4}{3}\eta + \zeta)] dV/dx - (\eta a / 2j) dV/dx = (\varkappa / j) dT/dx. \tag{11}$$

It is convenient to solve the systems (10) and (11) for δp. For this purpose, multiplying (10) by V_1 and subtracting the result from (11) we get the following equation:

$$\delta w - V_1 \delta p + \tfrac{1}{2} (j^2 + \tfrac{1}{2} a_1) (\delta V)^2 = (\varkappa / j) dT/dx. \tag{12}$$

Further, taking the pressure p and the entropy of a unit mass s as independent variables, and representing δw, δV and δT in Eqs. (12) in the form of series in δp and δs, we get for the first two terms (the contributions are similar to those obtained by Landau and Lifshitz[6]):

$$\delta s = \frac{\varkappa}{jT} \left(\frac{\partial T}{\partial p}\right)_s \frac{dp}{dx}. \tag{13}$$

Equation (13) shows that for low intensity discontinuities in magnetohydrodynamics, with the exception of the vicinity of the singular point $\Delta = 0$, at which the expansions (7) and (8) are inappropriate, the change in entropy inside the discontinuity is small in comparison with the change in pressure. Therefore, it suffices in what follows to limit ourselves to the account of terms of first order in δs. In this approximation considering (13), we have

$$\delta V = \left(\frac{\partial V}{\partial p}\right)_s \delta p + \frac{1}{2} \left(\frac{\partial^2 V}{\partial p^2}\right)_s (\delta p)^2 + \frac{\varkappa}{jT} \left(\frac{\partial T}{\partial p}\right)_s \left(\frac{\partial V}{\partial s}\right)_p \frac{dp}{dx}. \tag{14}$$

Substituting this expression in (10), we obtain a differential equation for the pressure p(x):

$$\left[1+\left(j^2+\frac{a_1}{2}\right)\left(\frac{\partial V}{\partial p}\right)_s\right]\delta p+\frac{1}{2}\left[\left(j^2+\frac{a_1}{2}\right)\left(\frac{\partial^2 V}{\partial p^2}\right)_s + b_1\left(\frac{\partial V}{\partial p}\right)_s^2\right](\delta p)^2 = -\left\{\frac{j^2+a_1/2}{T}\frac{\varkappa}{j}\left(\frac{\partial T}{\partial p}\right)_s\left(\frac{\partial V}{\partial s}\right)_p + \left[\frac{c_1}{2}-j\left(\frac{4}{3}\eta+\zeta\right)\left(\frac{\partial V}{\partial p}\right)_s\right]\right\}\frac{dp}{dx}, \quad (15)$$

where $\delta p = p(x) - p_1$.

In the case of the absence of a magnetic field, Eq. (15) reduces to the equation for $p(x)$ in ordinary hydrodynamics, introduced by Landau and Lifshitz,[6] inasmuch as the coefficients a_1, b_1, c_1 tend to zero along with the intensity of the magnetic field.

2. DAMPING OF SMALL AMPLITUDE WAVES IN MAGNETOHYDRODYNAMICS

Equation (15) can be used directly for the determination of the damping coefficient of waves of small amplitude in magnetohydrodynamics. For this purpose, it will be sufficient to limit ourselves to the linear approximation, omitting from (15) the term with $(\delta p)^2$, and neglecting the difference between V and V_1 in the expression $j = v_n/V$. Moreover, taking into consideration the thermodynamic relations

$$\left(\frac{\partial V}{\partial p}\right)_s = -\frac{1}{\rho^2 c^2}, \qquad \left(\frac{\partial T}{\partial p}\right)_s\left(\frac{\partial V}{\partial s}\right)_p = \frac{T}{\rho^2 c^2}\left(\frac{1}{C_v}-\frac{1}{C_p}\right),$$

where c is the speed of sound and $\rho = 1/V$ is the density of the medium, and also Eq. (9) for the coefficients a_1 and b_1, we get as a result

$$\frac{v_n}{\rho c^2}\left[\left(1+\frac{H_{\tau 1}^2}{\Delta}\right)\varkappa\left(\frac{1}{C_v}-\frac{1}{C_p}\right)+\left(\frac{4}{3}\eta+\zeta\right)+\frac{H_{\tau 1}^2}{\Delta^2}(\rho^2 v_n^2\beta+H_n^2\eta)\right]\frac{dp}{dx} + \left[1-\frac{v_n^2}{c^2}\left(1+\frac{H_{\tau 1}^2}{\Delta}\right)\right]\delta p = 0. \quad (16)$$

In the process of deriving this equation, we have omitted terms with higher derivatives in addition to linearizing in the amplitude. In the initial equations (3) — (6), terms with first derivatives in x contain as a factor one of the dissipative coefficients η, ζ, κ, or β. Therefore, in neglecting the products of these terms and terms with higher derivatives, we actually neglect products of the dissipation coefficients. This is equivalent to an assumption on the smallness of damping, which will be considered in the present work.

For perturbations whose time dependence has the form e^{ikx}, Eq. (16) reduces to the well-known relation between v_n and k:

$$v_n^4 - v_n^2(c^2+u_n^2+u_\tau^2)+c^2u_n^2 + ik\frac{v_n}{\rho}\left\{\left[\varkappa\left(\frac{1}{C_v}-\frac{1}{C_p}\right)+\left(\frac{4}{3}\eta+\zeta\right)\right](u_n^2-v_n^2)+u_\tau^2\varkappa\left(\frac{1}{C_v}-\frac{1}{C_p}\right) + \frac{u_\tau^2}{u_n^2-v_n^2}(\rho v_n^2\beta+u_n^2\eta)\right\}=0, \quad (17)$$

$u_n = H_n/\sqrt{\rho}$ is the Alfvén velocity, $u_\tau = H_\tau/\sqrt{\rho}$.

Equation (17) for $v_n = \omega/k$ is equivalent to the dispersion equation for small amplitude waves in magnetohydrodynamics with consideration of weak damping. In fact, the time-independent equation (16) can be obtained from the general linearized system of equations of magnetohydrodynamics by a formal transformation of coordinates: $x = x' + v_n t$, and by a corresponding transformation of the desired functions $e^{i(kx-\omega t)} \to e^{ikx'}$ (if $v_n = \omega/k$). Therefore, in the determination of the damping coefficient, one can start out immediately from Eq. (17), setting the phase velocity of the excitation $v = k^{-1}\mathrm{Re}\ \omega = \mathrm{Re}\, v_n$ and the damping coefficient $\gamma = \mathrm{Im}\omega = k\,\mathrm{Im}\, v_n$.

Without consideration of dissipative terms, Eq. (17) is reduced to the dispersion equation for small perturbations:[9]

$$v^4 - v^2(c^2+u_n^2+u_\tau^2)+c^2u_n^2 = 0. \quad (18)$$

Solution of Eq. (17) in the case of weak damping can be represented in the form

$$v_n = v + iv_1 = v + i\gamma/k,$$

where $\gamma \ll kv$, and v satisfies Eq. (18). Substituting this solution in (17), we find the damping coefficient γ, which determines the decrease in the amplitude of the wave with time as $e^{-\gamma t}$,

$$\gamma = k^2 a, \quad (19)$$

$$a = \frac{1}{2(v^4-c^2u_n^2)}\left\{c^2(v^2-u_n^2)\left[\frac{\varkappa}{\rho}\left(\frac{1}{C_v}-\frac{1}{C_p}\right)+\frac{v^2}{\rho c^2}\left(\frac{4}{3}\eta+\zeta\right)\right]+(v^2-c^2)\left(v^2\beta+\frac{u_n^2}{\rho}\eta\right)\right\}. \quad (20)$$

For a parallel shock wave, the phase velocity of the wave $v = c$ and the coefficient a is given by

$$a = a_\parallel = \frac{1}{2\rho}\left[\varkappa\left(\frac{1}{C_v}-\frac{1}{C_p}\right)+\left(\frac{4}{3}\eta+\zeta\right)\right], \quad (21)$$

which coincides with the expression obtained by Landau and Lifshitz.[6]

For a weak rotational (Alfvén) discontinuity ($v = v_n$) we obtain

$$a = a_A = \tfrac{1}{2}(\beta+\eta/\rho). \quad (22)$$

As is seen from (22), the dissipation in this case, as in the case of an incompressible fluid,[8] is due only to the viscosity and the conductivity of the medium.

For a weak oblique wave, considered as the limit for $u_n^2 = c^2$, $u_\tau^2 \to 0$, we find from (18) and (20) that $v^2 = u_n^2 = c^2$, and

$$a_0 = \frac{1}{4}\left[\frac{\varkappa}{\rho}\left(\frac{1}{C_v}-\frac{1}{C_p}\right)+\frac{1}{\rho}\left(\frac{4}{3}\eta+\zeta\right)+\left(\beta+\frac{\eta}{\rho}\right)\right]. \quad (23)$$

We note that in this case the damping coefficient is equal to half the sum of the coefficients in the ordinary sound wave and in a weak rotational discontinuity.

For a perpendicular wave, in which $u_n^2 = 0$, but $u_\tau = H_\tau^2/\rho \neq 0$, we find $v^2 = u_\tau^2 + c^2$ and

$$a = a_\perp = \frac{1}{2(1+u_\tau^2/c^2)}\left[\frac{\varkappa}{\rho}\left(\frac{1}{C_v}-\frac{1}{C_p}\right) + \left(1+\frac{u_\tau^2}{c^2}\right)\frac{1}{\rho}\left(\frac{4}{3}\eta+\zeta\right)+\frac{u_\tau^2}{c^2}\beta\right]. \quad (24)$$

3. WIDTH OF THE DISCONTINUITY

The width of the discontinuity can be determined from Eq. (15). At large distances the pressure on the left and right of the discontinuity is equal to p_1 and p_2 respectively, while the right hand side of the equation vanishes along with dp/dx. Therefore, the roots of the quadratic three terms on the left hand side will be p_1 and p_2, and Eq. (15) is equivalent to the equation

$$\frac{dp}{dx} = -\frac{2}{A}(p-p_1)(p-p_2). \quad (25)$$

The coefficient A is equal to double the ratio of the coefficients for dp/dx and $(\delta p)^2$ in (15); with the aid of the relations used in the derivation of Eq. (16), this coefficient can be written in the form

$$A = 4\frac{c^2}{\rho v} \times \frac{(1+H_\tau^2/\Delta)\varkappa(1/C_v - 1/C_p)+(4\eta/3+\zeta)+(H_\tau/\Delta)^2(\rho^2v^2\beta+H_n^2\eta)}{\rho^2c^4(1+H_\tau^2/\Delta)(\partial^2V/\partial p^2)_s + 3v^2H_\tau^2/\Delta^2}. \quad (26)$$

The quantity $\Delta = H_n^2 - j^2V_1 = \rho(u_n^2 - v^2)$ appearing here depends on the velocity of the medium v relative to the surface of discontinuity. For this velocity we can substitute in Eq. (26) (in the approximation under discussion) the velocity of small excitations determined from the dispersion equation (18). Then A, with consideration of (20), takes the following form:

$$A = \frac{8c^2\rho}{v}\frac{(v^4-c^2u_n^2)\,a}{\rho^3c^6(v^2-u_n^2)(\partial^2V/\partial p^2)_s + 3(v^2-c^2)v^2}. \quad (27)$$

Integration of Eq. (25) shows (see, for example, reference 6) that the change in pressure takes place essentially in a layer of thickness

$$l \approx A/(p_2-p_1), \quad (28)$$

that is, l is the effective thickness of the discontinuity.

Let us consider in more detail the expressions (27) and (28) for the width of the discontinuity. For a parallel shock wave ($H_\tau^2 = 0$), Eq. (28) coincides with the width of the ordinary shock wave,[6] as it should, inasmuch as

$$A_\parallel = \frac{8V^2a_\parallel}{c^3}\left(\frac{\partial^2V}{\partial p^2}\right)_s^{-1} = \frac{4V^3}{c^3}\left(\frac{\partial^2V}{\partial p^2}\right)_s^{-1}\left[\varkappa\left(\frac{1}{C_v}-\frac{1}{C_p}\right) + \left(\frac{4}{3}\eta+\zeta\right)\right]. \quad (29)$$

The set of coordinates we have chosen is generally not suitable for consideration of a perpendicular wave. However, Eq. (28) also contains the perpendicular wave as a limiting case $H_n \to 0$ and $H_\tau \neq 0$. In this case,

$$A = \frac{4c\left[\varkappa(C_v^{-1}-C_p^{-1})+(4\eta/3+\zeta)(1+u_\tau^2/c^2)+\rho\beta u_\tau^2/c^2\right]}{\sqrt{1+u_\tau^2/c^2}\left[\rho^3c^4(\partial^2V/\partial p^2)_s + 3u_\tau^2/c^2\right]} \quad (30)$$

and the width of the discontinuity coincides with that obtained earlier.[4]

As is seen from the derivation of Eqs. (10) and (11), the singular case $\Delta = 0$ is, strictly speaking, excluded from our consideration. In addition to the rotational discontinuity and discontinuities close to it, a singular oblique wave,[9] in which $H_\tau = 0$ on one side of the discontinuity and $\Delta = 0$ on the other, also corresponds to this case.

So far as the rotational discontinuity is concerned, such a discontinuity (as has been noted above) cannot have a stationary width in the presence of a dissipation. Formally, this case corresponds to an infinite width because of the vanishing of the denominator of Eq. (28). For discontinuities close to rotational, we get from (26), for $\Delta = 0$,

$$A = \frac{4}{3}\frac{c^2}{v^3}\left(\rho v^2\beta + \frac{H_n^2}{\rho}\eta\right). \quad (31)$$

However, as can be seen from Eqs. (7) — (9), in such discontinuities (i.e., for $H_\tau \neq 0$) δV, and therefore δp also, must approach zero along with Δ, and therefore Eq. (28) does not give a finite value for the width of the discontinuity. Thus one can conclude that both the rotational discontinuity and discontinuities close to it cannot have a stationary width.*

For the singular oblique wave, considered as the limit of a shock wave for $u_n^2 = c^2$ and $u_\tau^2 \to 0$, the expression for A reduces to the following:

$$A = \frac{4c\left[\varkappa\left(C_v^{-1}-C_p^{-1}\right)+\left(4\eta/3+\zeta\right)+(\beta\rho+\eta)\right]}{\rho^3c^4(\partial^2V/\partial p^2)_s+3}. \quad (32)$$

For such a limiting transition, the coefficients of the expansions (7) and (8) remain finite and,

*Furthermore, we note that, in discontinuities close to rotational, the tangential component of the magnetic field changes sign. Such shock waves, as has been pointed out by Polovin and Lyubarskiĭ,[10] are unstable relative to splitting (non-evolutionary).

consequently, the peculiarities which are characteristic of rotational discontinuities do not appear here.

4. THE CONNECTION BETWEEN THE DAMPING COEFFICIENT AND THE WIDTH OF A LOW INTENSITY DISCONTINUITY

One can also arrive at Eqs. (27) and (28) for the width of the discontinuity by starting from the qualitative picture of shock wave formation. In fact, the stationary structure of the discontinuity is established as a result of the equilibrium of two opposing processes. The first of these consists in the smearing out of the jump under the action of viscosity, finite conductivity and thermal conductivity. The action of these dissipative processes can be described by a certain effective viscosity which for a wave of small amplitude is connected to the damping coefficient by the well-known relation $\gamma = ak^2$, and therefore is determined by Eq. (20) in magnetohydrodynamics. The smearing out of the discontinuity as the result of dissipation has a diffusion character and the velocity of such smearing out V_- can be estimated from the relation

$$l^2 \sim 4at, \qquad V_- \sim l/t \sim 4a/t, \tag{33}$$

where l is the width of the discontinuity and t is the time, measured from the moment of formation of the discontinuity.

As the opposing process, we have the "entanglement" of the discontinuity brought about by the different velocities of the excitation in front of the discontinuity and behind it. The "entanglement" tends to reduce the width of the shock which takes on a certain stationary value when both these processes are equal to one another, i.e., the rate of entanglement V_+ becomes equal to the rate of smearing out V_-. In this case the width of the discontinuity, in accord with (33), becomes equal in order of magnitude to

$$l \approx 4a/V_+. \tag{34}$$

The rate of "entanglement" V_+ is equal to the difference of the velocities of small disturbances in front of the discontinuity and behind it in a fixed system of coordinates:

$$V_+ = v' + \delta v_{\mathrm{av}} - v = \delta v + \delta v_{\mathrm{av}}, \tag{35}$$

where v' and v are the velocities of propagation of the waves of small amplitude under consideration relative to the medium on the two sides of the discontinuity, and δv_{av} is the jump in the normal component of the velocity of the medium in the shock wave.

In zero approximation (for magnetohydrodynamic "sound"), the velocities v' and v coincide and are equal to the velocity of the discontinuity. In the following approximation, one can determine $\delta v = v' - v$ from the dispersion equation (18), in which it is convenient to select as independent variables the density ρ and the tangential component H_τ:

$$v^4 - v^2 (c^2 + H_n^2/\rho + H_\tau^2/\rho) + c^2 H_n^2/\rho = 0. \tag{36}$$

Then

$$\delta v = \frac{\partial v}{\partial \rho}\delta\rho + \frac{\partial v}{\partial \mathbf{H}_\tau}\delta\mathbf{H}_\tau, \tag{37}$$

where we have taken it into consideration that H_n is continuous and the change in entropy is small in comparison with the change in the density. Therefore,

$$\delta c \approx \left(\frac{\partial c}{\partial \rho}\right)_s \delta\rho = \frac{c}{\rho}\left[\frac{\rho^3 c^4}{2}\left(\frac{\partial^2 V}{\partial p^2}\right)_s - 1\right]\delta\rho. \tag{38}$$

Computing the derivatives $\partial v/\partial\rho$ and $\partial v/\partial \mathbf{H}_\tau$ by means of (18), and taking it into account that in a wave of small amplitude [see reference 9, Eqs. (2.21) and (2.22)]

$$\delta \boldsymbol{H}_\tau = [(v^2 - c^2)/H_\tau^2]\,\mathbf{H}_\tau \delta\rho, \tag{39}$$

$$\delta v_{\mathbf{av}} = v\delta\rho/\rho, \tag{40}$$

we finally obtain:

$$V_+ = \delta v + \delta v_{\mathrm{cp}} = \frac{v^2\delta\rho}{2\rho v\,[v^4 - c^2 u_n^2]}\left[(v^2 - u_n^2)\,\rho^3 c^6\left(\frac{\partial^2 V}{\partial p^2}\right)_s + 3v^2(v^2 - c^3)\right]. \tag{41}$$

This expression for the rate of "entanglement," together with (34) again leads to Eqs. (27) and (28) for the width of the discontinuity.

From the qualitative considerations that have been given, it is clear that the rotational discontinuity for which "entanglement" is absent ($\delta\rho = 0$) cannot have a stationary width.

[1] W. Marshall, Proc. Roy. Soc. (London) **A233**, 367 (1955).

[2] G. S. Golitsyn and K. P. Stanyukovich, JETP **33**, 1417 (1957), JETP **6**, 1090 (1958).

[3] A. G. Kulikovskiĭ and G. A. Lyubimov, Журнал прикл. матем. и механ. (J. Appl. Math. and Mech.) **23**, 1146 (1959).

[4] S. I. Syrovatskiĭ, Труды ФИАН (Trans. Phys. Inst. Acad. Sci.) **8**, 13 (1956).

[5] M. I. Kiselev and V. I. Tseplyaev, JETP **34**, 1605 (1958), Soviet Phys. JETP **7**, 1104 (1958).

[6] L. D. Landau and E. M. Lifshitz, Механика сплошных сред Mechanics of Continuous Media (2nd edition), Gostekhizdat, 1954.

[7] F. Hoffman and E. Teller, Phys. Rev. 80, 692 (1950).

[8] L. D. Landau and E. M. Lifshitz, Электродинамика сплошных сред (Electrodynamics of Continuous Media), Gostekhizdat, 1959.

[9] S. I. Syrovat-skiĭ, Usp. Fiz. Nauk 62, 247 (1957).

[10] R. V. Polovin and G. Ya. Lyubarskiĭ, Ukr. Fiz. Zh. 3, 571 (1958).

Translated by R. T. Beyer
139

COVARIANT STATISTICAL THEORIES OF MULTIPLE PARTICLE PRODUCTION

V. M. MAKSIMENKO and I. L. ROZENTAL'

P. N. Lebedev Physics Institute, Academy of Sciences U.S.S.R.

Submitted to JETP editor April 13, 1960

J. Exptl. Theoret. Phys. (U.S.S.R.) **39**, 754-756 (September, 1960)

Possible covariant theories of multiple particle production are analyzed under the condition that the matrix element can be factorized. The multiplicity of the secondary particles is computed by assuming that the matrix element is a power function of the energy of the particles involved in the process.

1. The probability W_N that N particles with masses $m_1, m_2, \ldots m_N$ are produced in the collision of two particles is of the following form:

$$W_N = \int \cdots \int \Phi(K_0, k_1, \ldots, k_N)\,\delta^4 \times \Big(K_0 - \sum_{j=1}^{N} k_j\Big) \prod_{j=1}^{N} \delta(k_j^2 - m_j^2)\, d^4k_j, \quad (1)$$

where $K_0(i\mathbf{P}_0, E_0)$ is the four-momentum of the initial state, $k_j(i\mathbf{p}_j, \epsilon_j)$ is the momentum of the j-th particle, and $\Phi(K_0, k_1, \ldots k_j)$ is an invariant function depending on the character of interaction of the particles.

We shall consider the case where the interaction between the particles is sufficiently small so that we can neglect the correlations. The function $\Phi(K_0, k_1, \ldots k_N)$ can then be represented in the form of the product

$$\Phi(K_0, k_1, \ldots, k_N) = \prod_{j=1}^{N} \Phi_j(K_0, k_j). \quad (2)$$

In the following, we shall limit ourselves to invariant functions of $\Phi_j(K_0, k_j)$ of a special class, such that

$$\Phi_j(K_0, k_j) = C\,(K_{0\nu}k_{j\nu})^q / (\sqrt{K_{0\nu}K_{0\nu}})^s, \quad (3)$$

where C is independent of K_0 and k_j, and is determined by the coupling constants, masses,* spins, and isotopic spins of the particles; q and s are integers.

Taking Eq. (2) into account, the relation (1) can be converted into the form

$$W_N = \frac{C^N}{2^N} \int \cdots \int \delta^4\Big(K_0 - \sum_{j=1}^{N} k_j\Big) \prod_{j=1}^{N} \Phi_j(K_0, k_j)\, \varepsilon_j^{-1} d^3p_j. \quad (4)$$

We shall dwell in detail upon the important special cases:

$$\Phi_j(K_0, k_j) = C\,(K_{0\nu}k_{j\nu}) / (K_{0\nu}k_{0\nu}), \quad (5)$$

$$\Phi_j(K_0, k_j) = C. \quad (6)$$

The function (5) corresponds to the statistical Fermi theory,[1] and the function (6) to the theory of Shrivastava and Sudarshan[2] (SS theory).

The special cases based on the choice of Eq. (5) or Eq. (6) are of special interest because of the possibility of giving them a simple and clear interpretation. The physical interpretation of the Fermi theory is well known. The choice of $\Phi_j(K_0, k_j)$ in the form (6) can be treated in the following way: expanding the meson field of the nucleon (at sufficiently great distances from its center) in a Fourier integral, it is found[3,4] that the probability ω_j of a pseudoscalar meson having momentum in the interval $\mathbf{p}_j$, $\mathbf{p}_j + d\mathbf{p}_j$ is equal to

$$\omega_j = d^3p_j / \varepsilon_j. \quad (7)$$

If ω_j is independent of the remaining ω_k ($k \neq j$), which is equivalent to the assumption of statistical independence of the particles, then the probability of N mesons being in the states with momenta $\mathbf{p}_j \ldots \mathbf{p}_N$ is equal to the product of corresponding probabilities for separate particles. Furthermore, in line with the Lewis, Oppenheimer, and Wouthuysen theory[4,5] (LOW theory), the process of multiple particle production can be interpreted as the breaking up of a meson cloud without any change in its internal state (i.e., conserving the distribution $\prod_{j=1}^{N} d^3p_j/\epsilon_j$).

Such an interpretation leads to Eq. (4), under condition (6). It is, however, necessary to mention that the SS theory is then not fully equivalent to the LOW theory, since the role of nucleons in the collision process is treated differently in the two theories. While, according to the LOW theory, it is necessary to assume that the nucleons lose a

*Moreover, the mass dependence should be such that W_N is a dimensionless quantity.

relatively small energy fraction, and consequently, have to be treated as separate particles from the energy point of view, the nucleons are treated equally with other particles in the relations (4) and (6). In essence, the mathematical formulation of the LOW theory is reduced to the following relation

$$W_N \sim \int \delta^4\Big(K - \sum_{j=3}^{N} k_j\Big) A(K_1, K_2) \prod_{j=3}^{N} d^3p_j / \varepsilon_j, \qquad (8)$$

where $K = K_0 - K_1 - K_2$; K_1 and K_2 are the four-momenta of both nucleons determined by the mechanism of the process. The summation and multiplication is carried only over meson indices.

2. We shall calculate the probability W_N for the class of theories indicated in Sec. 1. We have previously developed a method of calculating the quantity (4) for the Fermi theory [assumption (5)].[6] Here, we shall apply this method for calculating Eq. (4) with Φ_j in the form (3) with arbitrary q and s; in particular, we shall obtain formulas for the SS and LOW variants.

In order to simplify the calculations, we shall consider the problem in the c.m.s. ($P_0 = 0$). Since the probability W_N depends only on the invariants $E_0^2 - P_0^2$ and m_j, it is necessary to make the substitution $E_c^2 \to E_0^2 - P_0^2$ in the final expressions in order to go over to the general case $P_0 \neq 0$. Using the Fourier transform of the δ function, we transform (4) to the form

$$W_N = C^N [2^N E_c^{(s-q)N} (2\pi)^4]^{-1} \int_{-\infty-i\delta}^{+\infty-i\delta} \exp[-i\tau_1 E_c]\, d\tau_1 \int_{-\infty-i\delta}^{+\infty-i\delta} d\tau \times \prod_{j=1}^{N} \int_{-\infty}^{+\infty} (p_j^2 + m_j^2)^{(q-1)/2} \exp[i(\tau_1 \sqrt{p_j^2 + m_j^2} + \tau \mathbf{p}_j)]\, d^3p_j. \qquad (9)$$

The integral over p_j can easily be transformed to the form

$$J_j = \frac{2\pi}{\tau i^q} \frac{d^q}{d\tau_1^q} \frac{d}{d\tau} \int_{-\infty}^{\infty} \exp[i(\tau_1 \sqrt{p_j^2 + m_j^2} + \tau p_j)] \times (p_j^2 + m_j^2)^{-1/2} dp_j = -\frac{2\pi}{\tau i^q} \frac{d^q}{d\tau_1^q} \frac{d}{d\tau} i\pi H_0^1(m_j \sqrt{\tau_1^2 - \tau^2}) \qquad (10)$$

[where $H_0^{(1)}(z)$ is the Hankel function]. The phase φ of argument $m_j\sqrt{\tau_1^2 - \tau^2}$ is chosen in the following way:

$$\varphi = 0 \text{ for } \tau_1 > \tau, \quad \varphi = i\pi/2 \text{ for } -\tau < \tau_1 < \tau, \quad \varphi = i\pi \text{ for } \tau_1 < -\tau. \qquad (11)$$

Carrying out the differentiation, and using the recurrent formula for the Hankel function, we obtain

$$J_j = \frac{2\pi^2}{i^{q+1}} \frac{m_j^{q+1} \tau_1^q}{(\tau_1^2 - \tau^2)^{(q+1)/2}} H_{q+1}^{(1)}(m_j \sqrt{\tau_1^2 - \tau^2}). \qquad (12)$$

For future calculations, similarly to what was done by us earlier,[6] we shall expand the product of the Hankel functions in a series and integrate it term by term. As a result, we obtain the expression for (9) in the form of a non-power series of a small parameter ν_j

$$\nu_j = m_j / E_c. \qquad (13)$$

In particular, the first term of this series, independent of ν_j, (which corresponds to ultra-relativistic particles), is of the form

$$W_N = \frac{C^N \pi^{N-1} (q!)^N}{2^{N(q+1)-1}} \times \frac{(2N(q+1)-4)!\, E_c^{N(2+2q-s)-4}}{[N(q+2)-4]!\, [N(q+1)-1]!\, [N(q+1)-2]!}. \qquad (14)$$

We shall estimate the variation of the most-probable value of $\bar{N}$ with energy. If N is sufficiently large so that we can use the Stirling formula, we obtain

$$\bar{N} \sim E_c^{(2q-s+2)/(q+3)}. \qquad (15)$$

In the case of the SS or LOW theory ($q = 0$, $s = 0$), we obtain the following expression for W_N

$$W_N = C^N \Big(\frac{\pi}{2}\Big)^{N-1} (E_c^2)^{N-2} \Big\{ \frac{1}{(N-1)!\,(N-2)!} - \frac{1}{(N-2)!\,(N-3)!} \times \Big[\sum_{j=1}^{N} \nu_j^2 \ln \frac{1}{\nu_j^1} - \Big(\sum_{m=1}^{N-2} \frac{1}{m} + \sum_{m=1}^{N-3} \frac{1}{m} - 1 \Big) \sum_{j=1}^{N} \nu_j^2 \Big] + \dots \Big\}. \qquad (16)$$

The first term of this series has been obtained earlier.[4,7] In addition to the first term, Yakovlev[7] has, by different methods, obtained the expressions for W_N for $N = 3, 4, 5$. However, in our opinion, errors were committed in the derivation, and the expressions are not correct.

In conclusion, the authors express their gratitude to E. L. Feĭnberg for helpful comments.

[1] E. Fermi, Progr. Theor. Phys. **5**, 570 (1950).
[2] P. P. Srivastava and G. Sudarshan, Phys. Rev. **110**, 781 (1958).
[3] Umezawa, Takahanshi, and Kamefuchi, Phys. Rev. **85**, 505 (1952).
[4] H. Lewis, Revs. Modern Phys. **24**, 241 (1952).
[5] Lewis, Oppenheimer, and Wouthuysen, Phys. Rev. 73, 127 (1948).
[6] V. M. Maksimenko and I. L. Rozental', JETP **32**, 658 (1957), Soviet Phys. JETP **5**, 546 (1957).
[7] L. G. Yakovlev, JETP **37**, 1041 (1959), Soviet Phys. JETP **10**, 741 (1960).

Translated by H. Kasha
140

RADIATIVE CORRECTIONS TO THE SCATTERING OF μ MESONS ON ELECTRONS

A. I. NIKISHOV

P. N. Lebedev Physics Institute, Academy of Sciences, U.S.S.R.

Submitted to JETP editor April 13, 1960; resubmitted June 9, 1960

J. Exptl. Theoret. Phys. (U.S.S.R.) **39**, 757-766 (September, 1960).

Formulas of the cross sections for the processes $\mu + e^{\pm} \to \mu + e^{\pm}$ and $e^+ + e^- \to \mu^+ + \mu^-$ are deduced with an accuracy to e^6.

INTRODUCTION

THE expected possibility of producing opposing beams of electrons and positrons in the near future, raises the question of an experimental investigation of the processes

$$e^- + e^- \to \mu^- + \mu^-, \qquad e^- + e^- \to \pi^- + \pi^-.$$

The cross section of the first process, without radiative corrections, was first obtained by Berestetskiĭ and Pomeranchuk.[1] The second process was considered by Aleksin (see the book by Akhiezer and Berestetskiĭ)[2] and by Afrikyan and Garibyan.[3] In the present article we give formulas for the radiative corrections to scattering and transformation processes, accurate to e^6. We show also that the exchange between two photons does not contribute to the total cross section (i.e., the cross section integrated over the angle) of the transformation $e^+ + e^- \to X + \bar{X}$, where X and $\bar{X}$ denote any particle and antiparticle.

1. ELASTIC SCATTERING OF NEGATIVE MUONS BY ELECTRONS

We shall calculate the scattering of a muon by an electron by a Feynman technique[4] similar to that used for the scattering of an electron by an electron.[5-6] We shall use a notation close to that of Redhead.[6]

Let p_1 and p_{1M} be the four-momenta of the colliding particles, and let p_2 and p_{2M} be the four momenta of the scattered particles with masses m = 1 and M respectively. We put:

$$q = p_2 - p_1, \qquad \xi = q^2 = 4\sinh^2 w = 4M^2\sinh^2 w_M,$$

$$\eta = (p_{1M} - p_1)^2, \qquad \zeta = (p_{2M} - p_1)^2 = \eta - \xi$$

$$(ab = \mathbf{ab} - a_0 b_0).$$

The square of the matrix element for the process under consideration, averaged over the initial spin states and summed over the final ones, is

$$|\mathfrak{M}|^2 = \frac{1}{E_1 E_2 E_{1M} E_{2M} \xi^2} \operatorname{Re}\{Q + \frac{\alpha}{\pi}[2Q(A + A_M + W) + B^{(1)} + B^{(2)} + Z\xi(\xi - 2M^2) + Z_M M\xi(\xi - 2)]\}, \quad (1)$$

where

$$Q = \tfrac{1}{8}[2\eta^2 + \xi^2 - 2\xi\eta + 4\eta(M^2+1) - 4\xi(M^2+1) + 2(M^2+1)^2]; \quad (2)$$

$$A_M = \left(\ln\frac{M}{\lambda} - 1\right)(1 - 2w_M \coth 2w_M) - \frac{w_M}{2}\tanh w_M - 2\coth 2w_M \int_0^{w_M} \beta\tanh\beta d\beta;$$

$$A = \left(\ln\frac{1}{\lambda} - 1\right)(1 - 2w\coth 2w) - \frac{w}{2}\tanh w - 2\coth 2w \int_0^{w} \beta\tanh\beta d\beta; \quad (3)$$

$$Z_M = w_M/4\sinh 2w_M, \qquad Z = w/4\sinh 2w; \quad (4)$$

$$W = \frac{1 - 2\sinh^2 w}{3\sinh^2 w}(1 - w\coth w) + \frac{1}{9}. \quad (5)$$

As usual, we have introduced the fictitious photon mass λ.

The terms $B^{(1)}$ and $B^{(2)}$ are due to the contribution from the exchange by two photons (interference of the main term with the terms from diagrams 1 and 2 of Fig. 1):

$$B^{(1)} = \tfrac{1}{8}\xi\{-8(\eta + M^2 + 1)Qb^{(1)} + (H^{(1)} - \tfrac{1}{2}\xi b^{(1)})\varphi_1^{(1)} + \bar{G}\varphi_2^{(1)} + G\varphi_3^{(1)} - \frac{\ln\xi}{2(\xi+4)}\varphi_4^{(1)} + \frac{\ln(\xi/M^2)}{2(\xi+4M^2)}\varphi_5^{(1)} + \tfrac{1}{2}N^{(1)}\varphi_6^{(1)} + \tfrac{1}{2}K^{(1)}\varphi_7^{(1)}\}, \quad (6)$$

$$B^{(2)} = \tfrac{1}{8}\xi\{-8(\zeta + M^2 + 1)Qb^{(2)} + (H^{(2)} - \tfrac{1}{2}\xi b^{(2)})\varphi_1^{(2)} + \bar{G}\varphi_2^{(2)} + G\varphi_3^{(2)} + \frac{\ln\xi}{2(\xi+4)}\varphi_4^{(2)} + \frac{\ln(\xi/M^2)}{2(\xi+4M^2)}\varphi_5^{(2)} + \tfrac{1}{2}N^{(2)}\varphi_6^{(2)} + \tfrac{1}{2}K^{(2)}\varphi_7^{(2)}\}. \quad (7)$$

Here

$$\varphi_1^{(1)} = 2\eta^2 - \eta\xi + 6\eta(M^2+1) - \xi(M^2+1) + 4(M^2+1)^2,$$

$$\varphi_2^{(1)} = -2\eta^2 + \eta\xi + 2\xi(M^2+1) - 2\eta(2M^2+3) - 2(M^2+1)(M^2+2) - \xi[\xi^2 + 2\xi + 4\eta + 4(M^2+1)]/2(\xi+4),$$

$$\varphi_3^{(1)} = -2\eta^2 + \eta\xi + 2\xi(M^2+1) - 2\eta(3M^2+2) - 2(M^2+1)(2M^2+1) - \xi[\xi^2 + 2M^2\xi + 4M^2\eta + 4M^2(M^2+1)]/2(\xi+4M^2),$$

$$\varphi_4^{(1)} = \xi^2 - \xi\eta + 4\eta - \xi(M^2+1) + 4(M^2+1),$$

$$\varphi_5^{(1)} = \xi^2 - \xi\eta + 4\eta M^2 - \xi(M^2+1) + 4M^2(M^2+1), \qquad \varphi_6^{(1)} = \eta^2 - \xi\eta + 2\eta - \xi(3M^2+1) + 1 - M^4,$$

$$\varphi_7^{(1)} = \eta^2 - \xi\eta + 2M^2\eta - \xi(M^2+3) + M^4 - 1, \qquad \varphi_1^{(2)} = -2\eta^2 - \xi^2 + 3\xi\eta - 2\eta(M^2+1) + \xi(M^2+1),$$

$$\varphi_2^{(2)} = 2\eta^2 - \tfrac{7}{2}\xi\eta + \tfrac{3}{2}\xi^2 + 2\eta(2M^2+1) - \tfrac{1}{2}\xi(9M^2+5) + 2M^2(M^2+1) + \xi^2(\eta + M^2 + 3)/2(\xi+4),$$

$$\varphi_3^{(2)} = 2\eta^2 - \tfrac{7}{2}\xi\eta + \tfrac{3}{2}\xi^2 + 2\eta(M^2+2) - \tfrac{1}{2}\xi(5M^2+9) + 2(M^2+1) + \xi^2(\eta + 3M^2 + 1)/2(\xi+4M^2),$$

$$\varphi_4^{(2)} = -\xi\eta - \xi(M^2+5) + 4\eta + 4(M^2+1), \qquad \varphi_5^{(2)} = -\xi\eta - \xi(5M^2+1) + 4M^2\eta + 4M^2(M^2+1),$$

$$\varphi_6^{(2)} = -\eta^2 + \xi\eta + \xi(5M^2+1) - 2\eta(2M^2+1) - (M^2+1)(3M^2+1),$$

$$\varphi_7^{(2)} = -\eta^2 + \xi\eta + \xi(M^2+5) - 2\eta(M^2+2) - (M^2+1)(M^2+3);$$

$$b^{(1,2)} = -(2\mu^{(1,2)}/\xi)\ln(\xi/\lambda^2), \qquad H^{(1,2)} - \tfrac{1}{2}\xi b^{(1,2)} = I^{(1,2)} + \mu^{(1,2)}\ln\xi. \tag{8}$$

We denote for brevity

$$\alpha_1 = (M^2-1)/(\eta + 2M^2 + 2), \qquad \alpha_2 = (M^2-1)/\zeta,$$

$$\beta_1 = [\alpha_1^2 + \eta/(\eta + 2M^2 + 2)]^{1/2},$$

$$\beta_2 = [\alpha_2^2 + (\zeta + 2M^2 + 2)/\zeta]^{1/2},$$

$$x_1 = \alpha_1 + \beta_1, \qquad y_1 = -\alpha_2 + \beta_2,$$

$$x_2 = \alpha_1 - \beta_1, \qquad y_2 = -\alpha_2 - \beta_2. \tag{9}$$

Then

$$\mu^{(1)} = \frac{-1}{(\eta + 2M^2 + 2)\,2\beta_1}\left\{\ln\left[\frac{1-x_1}{1-x_2}\,\frac{1+x_2}{1+x_1}\right] + 2\pi i\right\},$$

$$\mu^{(2)} = \frac{1}{\zeta 2\beta_2}\ln\left[\frac{y_1-1-y_2-1}{y_1+1-y_2+1}\right]; \tag{10}$$

$$K^{(1)} = \left(1 + \frac{M^2-1}{\eta + 2M^2 + 2}\right)\mu^{(1)} + \frac{1}{\eta + 2M^2 + 2}\ln M,$$

$$K^{(2)} = \left(1 - \frac{M^2-1}{\zeta}\right)\mu^{(2)} - \frac{1}{\zeta}\ln M; \tag{11}$$

$$N^{(1)} = \left(1 - \frac{M^2-1}{\eta + 2M^2 + 2}\right)\mu^{(1)} - \frac{1}{\eta + 2M^2 + 2}\ln M,$$

$$N^{(2)} = \left(1 + \frac{M^2-1}{\zeta}\right)\mu^{(2)} + \frac{1}{\zeta}\ln M. \tag{12}$$

The function $I^{(1)}$ is of the form

$$I^{(1)} = -\mu^{(1)}\ln\frac{\eta + 2M^2 + 2}{4} + \frac{1}{(\eta + 2M^2 + 2)\,\beta_1}\left\{u_2\ln\frac{\eta + 2M^2 + 2}{4} + u_1\ln\frac{\eta + 2M^2 + 2}{4M^2} - 2\int_0^{u_2}\beta\coth\beta d\beta - 2\int_0^{u_1}\beta\coth\beta d\beta + 2\pi i\ln 2\beta_1 + \pi^2\right\},$$

$$u_2 = \frac{1}{2}\ln\frac{1-x_2}{1-x_1}, \qquad u_1 = \frac{1}{2}\ln\frac{1+x_1}{1+x_2}. \tag{13}$$

$I^{(2)}$ has different forms for $\zeta > 0$ and $\zeta < 0$. When $\zeta > 0$

$$I^{(2)} = -\mu^{(2)}\ln\frac{\zeta}{4} + \frac{1}{\zeta\beta_2}\left\{-\varphi_2\ln\frac{\zeta}{4} - \varphi_1\ln\frac{\zeta}{4M^2} + 2\int_0^{\varphi_2}\beta\tanh\beta d\beta + 2\int_0^{\varphi_1}\beta\tanh\beta d\beta\right\},$$

$$\varphi_2 = \frac{1}{2}\ln\frac{1-y_2}{-1+y_1}, \qquad \varphi_1 = \frac{1}{2}\ln\frac{1+y_1}{-1-y_2}, \tag{14}$$

and when $\zeta < 0$

$$I^{(2)} = -\mu^{(2)}\ln\frac{|\zeta|}{4} + \frac{1}{|\zeta|\beta_2}\left\{-\Omega_2\ln\frac{|\zeta|}{4} + \Omega_1\ln\frac{|\zeta|}{4M^2} + 2\int_0^{\Omega_2}\beta\coth\beta d\beta - 2\int_0^{\Omega_1}\beta\coth\beta\,d\beta\right\},$$

$$\Omega_2 = \frac{1}{2}\ln\frac{-1+y_1}{-1+y_2}, \qquad \Omega_1 = \frac{1}{2}\ln\frac{1+y_1}{1+y_2}. \tag{15}$$

At the point $\zeta = 0$, the function $I^{(2)}$ is continuous: $I^{(2)}(\zeta) \to M^{-2}\ln^2 M$ as $\zeta \to \pm 0$.

Finally

$$\bar{G} = \frac{1}{2\sqrt{\xi(\xi+4)}}\left[\ln^2\frac{1-\beta}{\beta} - \ln^2\frac{\alpha-1}{\alpha} - 2\Phi\left(\frac{\beta}{\beta-1}\right) + 2\Phi\left(\frac{\alpha}{\alpha-1}\right) + \pi^2\right], \tag{16}$$

$$\alpha = \tfrac{1}{2}[\xi + 2 + \sqrt{\xi(\xi+4)}]; \quad \beta = \tfrac{1}{2}[\xi + 2 - \sqrt{\xi(\xi+4)}];$$

$$G = \frac{1}{2\sqrt{\xi(\xi+4M^2)}}\left[\ln^2\frac{1-\beta'}{\beta'} - \ln^2\frac{\alpha'-1}{\alpha'} - 2\Phi\left(\frac{\beta'}{\beta'-1}\right) + 2\Phi\left(\frac{\alpha'}{\alpha'-1}\right) + \pi^2\right], \tag{17}$$

$$\alpha' = \tfrac{1}{2}\left[2 + \frac{\xi}{M^2} + \sqrt{\frac{\xi}{M^2}\left(\frac{\xi}{M^2}+4\right)}\right],$$

$$\beta' = \tfrac{1}{2}\left[2 + \frac{\xi}{M^2} - \sqrt{\frac{\xi}{M^2}\left(\frac{\xi}{M^2}+4\right)}\right],$$

where

$$\Phi(x) = -\int_0^x \ln|1-y|\,y^{-1}dy$$

is the Spence function, tabulated in the paper by Mitchell.[7]

2. INELASTIC-SCATTERING CROSS SECTION

We now add to the elastic-scattering cross section the cross section of the scattering that is accompanied by the emission of soft quanta (with total energy $\Delta\epsilon$). Here, as is well known, the photon mass λ, which we have introduced, drops out. The inelastic scattering cross section is

$$d\sigma_{\text{inel}} = d\sigma_{\text{el}} \frac{\alpha}{\pi}\left[L - L_0 \ln\frac{2\Delta\varepsilon}{\lambda}\right]$$

$$(\lambda \ll \Delta\varepsilon \ll E_1,\ E_2, E_{1M},\ E_{2M}), \qquad (18)$$

where

$$L_0 = 4 + 2K_0(p_1, p_2) + 2K_0(p_{1M}, p_{2M}) - 4K_0(p_1, p_{1M}) + 4K_0(p_1, p_{2M}), \qquad (19)$$

$$L = K(p_1, p_1) + K(p_2, p_2) + K(p_{1M}, p_{1M}) + K(p_{2M}, p_{2M}) - 2K(p_1, p_2) - 2K(p_{1M}, p_{2M}) - 2K(p_1, p_{2M}) - 2K(p_2, p_{1M}) + 2K(p_1, p_{1M}) + 2K(p_2, p_{2M});$$

$$K_0(P_1, P_2) = -\tfrac{1}{2}(P_1P_2)\int_{-1}^{1} P_z^{-2}\,dz,$$

$$K(P_1, P_2) = \tfrac{1}{4}(P_1P_2)\int_{-1}^{1} P_z^{-2}\frac{E_z}{|\mathbf{P}_z|}\ln\frac{E_z + |\mathbf{P}_z|}{E_z - |\mathbf{P}_z|}\,dz, \qquad (20)$$

$$P_z = \tfrac{1}{2}P_1(1+z) + \tfrac{1}{2}P_2(1-z);$$

$$K_0(p_1, p_2) = -2w\coth 2w,$$

$$K_0(p_{1M}, p_{2M}) = -2w_M\coth 2w_M, \qquad (21)$$

$$K_0(p_1, p_{1M}) = -(\eta + M^2 + 1)\,\mathrm{Re}\,\mu^{(1)},$$

$$K_0(p_1, p_{2M}) = (\zeta + M^2 + 1)\,\mu^{(2)}.$$

(P stands for p_1, p_{1M}, . . .).

After adding the elastic and inelastic scattering cross sections, the term $L - L_0 \ln(2\Delta\epsilon/\lambda)$ in the inelastic-scattering cross section [see formula (18)] is replaced by $L - L_0 \ln(2\Delta\epsilon)$.

The overall cross section for elastic and inelastic scattering, is symmetrical in the variables M^2 and m^2, as it should be. When $M = 1$, it is identical with the corresponding expression for the case of equal masses [see the first curly bracket of Eq. (2.16) in the paper by Redhead[6]]. As $M \to \infty$ we obtain Schwinger's formula with $Z = -1$ (the charge of the scattering center coincides with the charge of the incoming particle).[8,9]

3. SCATTERING OF POSITIVE MUONS BY ELECTRONS

Let us consider now the scattering of particles of different sign

$$\mu^+ + e^- \to \mu^+ + e^-, \qquad \mu^- + e^+ \to \mu^- + e^+.$$

The matrix element of this process is obtained from the initial element (1) by making the substitution

$$p_1 \to -p_{2+}, \qquad p_2 \to -p_{1+},$$

$$\xi \to \xi, \qquad \eta \to -\zeta - 2M^2 - 2.$$

The new ξ, η, and ζ are defined as

$$\xi = (p_{2+} - p_{1+})^2 = 4\sinh^2 w = 4M^2\sinh^2 w_M,$$

$$\eta = (p_{1M} - p_{1+})^2, \qquad \zeta = (p_{2M} - p_{1+})^2 = \eta - \xi.$$

Under the aforementioned substitution, $B^{(1)}$ and $B^{(2)}$, are transformed into one another with signs reversed, as they should:

$$\varphi_i^{(1)} \rightleftarrows -\varphi_i^{(2)}, \qquad Q \to Q,$$

$$\mu^{(1)} \leftrightarrows \mu^{(2)}, \qquad H^{(1)} \rightleftarrows H^{(2)} \text{ etc.}$$

The reason for this is that the main term in the matrix element is proportional to ee_M, and the corrections due to diagrams 1 and 2 of Fig. 1 are

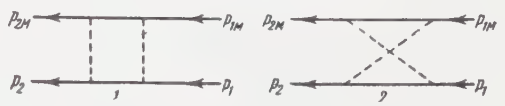

FIG. 1

proportional to $e^2e_M^2$. Their interference with the main term is proportional to $e^3e_M^3$, i.e., it reverses sign when one of the particles is replaced by an antiparticle. This property of the contribution from the two-photon exchange is also conserved when one of the particles is nuclear-active. For example, the total cross section of the processes $\mu^- + p \to \mu^- + p$ and $\mu^+ + p \to \mu^+ + p$ does not contain a contribution from the exchange of two photons (for more details see Appendix 1).

4. CONVERSION OF AN ELECTRON PAIR INTO A MESON PAIR

For the process $e^+ + e^- \to \mu^+ + \mu^-$ we must make the following substitution in the initial matrix element [formula (1)]

$$p_1 \to p_-, \qquad p_2 \to -p_+;$$

$$p_{1M} \to -p_{M+}, \qquad p_{2M} \to p_{M-},$$

or, what is the same,

$$\xi \to -(\eta + 4),$$

$$\eta \to \xi - (\eta + 4) = -\zeta - 2M^2 - 2, \qquad \zeta \to \xi,$$

where ξ, η, and ζ are defined as

$\xi = (p_{M-} - p_-)^2$, $\eta = (p_+ - p_-)^2 = 4\sinh^2 u$,

$\eta_M = (p_{M+} - p_{M-})$ $4M^2 \sinh^2 u_M$,

$\zeta = (p_{M+} - p_-)^2 = \eta - \xi - 2M^2 + 2$,

$\eta + 4 = \eta_M + 4M^2$.

For the real part of the function A_M we obtain instead of (3) (for more details see the paper by Redhead[6])

$$\mathrm{Re}\, A_M = \left(\ln\frac{M}{\lambda} - 1\right)(1 - 2u_M \coth 2u_M) - \frac{u_M}{2}\coth u_M + \frac{\pi^2}{2}\coth 2u_M - 2\coth 2u_M \int_0^{u_M} \beta \coth\beta d\beta.$$

The functions with index 1, which depend on η, become functions with index 2, which depend on ζ:

$$\mu^{(1)}(\eta) \to \mu^{(2)}(\zeta), \qquad H^{(1)}(\eta) \to H^{(2)}(\zeta), \ldots$$

Analogously

$$\mu^{(2)}(\zeta) \to \mu^{(2)}(\xi), \qquad H^{(2)}(\zeta) \to H^{(2)}(\xi), \ldots$$

L and L_0 of (18) now become

$$L = K(p_-, p_-) + K(p_+, p_+) + K(p_{M+}, p_{M+}) + K(p_{M-}, p_{M-}) - 2K(p_-, p_+) + 2K(p_-, p_{M+}) - 2K(p_-, p_{M-}) - 2K(p_+, p_{M+}) + 2K(p_+, p_{M-}) - 2K(p_{M+}, p_{M-}),$$

$$L_0 = 4 + 2K_0(p_-, p_+) + 2K_0(p_{M-}, p_{M+}) + 4K_0(p_-, p_{M-}) - 4K_0(p_-, p_{M+}).$$

$K(P_1, P_2)$ is defined in (20), and instead of (21) we have

$K_0(p_-, p_+) = -2u\coth 2u$,

$K_0(p_{M-}, p_{M+}) = -2u_M \coth 2u_M$,

$K_0(p_-, p_{M-}) = (\xi + M^2 + 1)\mu^{(2)}(\xi)$,

$K_0(p_-, p_{M+}) = (\zeta + M^2 + 1)\mu^{(2)}(\zeta)$.

If we consider the process in the c.m.s., then the substitution $\vartheta \to \pi - \vartheta$ will yield $\xi \rightleftarrows \zeta$ and $B^{(1)} \rightleftarrows -B^{(2)}$ (ϑ is the angle between $\mathbf{p}_-$ and $\mathbf{p}_{M-}$). Thus, the exchange of two photons not only does not change the total cross section for the conversion of the particles, but does not even change the angular distribution of the reaction products, if we disregard the sign of the particle charge. This property of the two-photon contribution is conserved also in a process with nuclear-active particles, for example, for $p + \bar{p} \to \mu^+ + \mu^-$ (see Appendix 1).

5. CASE OF HIGH ENERGIES. NUMERICAL RESULTS

Let us consider now the most interesting particular case, when $\xi \gg 1$ and η, $\zeta \geq -0.8\,M^2$. We make the following remark concerning $d\sigma_{\mathrm{inel}}$. The main contribution to terms of the type $K(P_1, P_2)$ [formula (20)] is made by the integration region near 1 and (or) -1, because the poles of the function $(P_Z^2 - E_Z^2)^{-1}$ are close to each other. If P_1 refers to a light particle and P_2 to a heavy one, only the region near one is significant in (20). If, however, the two momenta P_1 and P_2 refer to the light particle, both regions (near 1 and -1) become significant. If both P_1 and P_2 refer to the particle with mass M, then $K(P_1, P_2)$ is small. Naturally, when $\xi \gg m^2$ both regions are significant in any case, but we do not consider this circumstance since it will be apparently a long time before experiments can be performed on it.

The fact that the poles are close together makes it possible to obtain relatively simple approximate expressions for $K(P_1, P_2)$. By way of an example, let us give the value of $K(p, p_M)$ in the c.m.s.:

$$K(p, p_M) \approx \frac{E_M(1 - \beta_M \cos\vartheta)}{8[E_M - E + 2E\sin^2(\vartheta/2)]} \ln^2 4E^2.$$

Here β_M is the velocity of the particle M and ϑ is the angle between $\mathbf{p}$ and $\mathbf{p}_M$.

The most cumbersome expressions in the formula for the radiative corrections are due to the contribution of the irreducible diagrams [see Fig. 1 and formulas (6) and (7) for $B^{(1)}$ and $B^{(2)}$]. Allowance for the irreducible diagrams, and also for the emission of the soft quanta, does not entail much difficulty.

Let us pay principal attention now to $B^{(1)} + B^{(2)}$ and write out for the given particular case the expression for this sum without terms that depend on λ, assuming that the latter are included in $d\sigma_{\mathrm{inel}}$. This inclusion [together with the corresponding terms from A and A_M as given by (3)] eliminates the dependence on λ. The latter reduces to the substitution $\lambda \to 1$ in (18). Denoting by B the quantity

$$\frac{\alpha}{\pi}\frac{B^{(1)} + B^{(2)}}{Q},$$

in which the terms proportional to $\ln\lambda$ are left out, and retaining only the double-logarithmic terms, which make the principal contribution, we obtain for the scattering of a negative muon by an electron

$$B = \frac{\alpha}{\pi} 2\ln\xi \ln\frac{\eta + M^2}{\zeta + M^2} + \mathrm{Re}\,\frac{\alpha}{\pi}\frac{\xi}{8Q}\{(I^{(1)} + \mu^{(1)}\ln\xi)\varphi_1^{(1)} + (I^{(2)} + \mu^{(2)}\ln\xi)\varphi_1^{(2)} + \bar{G}(\varphi_2^{(1)} + \varphi_2^{(2)}) + G(\varphi_3^{(1)} + \varphi_3^{(2)})\};$$

$$Q = \tfrac{1}{8}(2\eta^2 + \xi^2 - 2\xi\eta + 4\eta M^2 - 4\xi M^2 + 2M^4), \qquad (22)$$

$$\varphi_1^{(1)} = -\xi\eta - \xi M^2 + 2(\eta^2 + 3\eta M^2 + 2M^4),$$

$$\varphi_1^{(2)} = -\xi^2 + \xi(3\eta + M^2) - 2\eta(\eta + M^2),$$

$$\varphi_2^{(1)} + \varphi_2^{(2)} = \xi^2 - 2\xi(\eta + M^2), \qquad \varphi_3^{(1)} + \varphi_3^{(2)} = \tfrac{3}{2}\xi^2 - \tfrac{1}{2}\xi(5\eta + M^2) - 4\eta M^2 - 4M^4 + [-\xi^3 + \xi(\xi - 4M^2)(\eta + M^2)]/2(\xi + 4M^2),$$

$$\mu^{(1)} = \frac{1}{\eta + M^2}\left\{\ln\frac{\eta + M^2}{M} - i\pi\right\}, \qquad \mu^{(2)} = \frac{1}{\zeta + M^2}\ln\frac{M}{\zeta + M^2}.$$

$I^{(1,2)}$ are determined by (13), (14), and (15), where we can now put

$$(\eta + 2M^2 + 2)\beta_1 \to \eta + M^2,$$

$$u_2 - \frac{1}{2}\ln\frac{(\eta + M^2)^2}{\eta + 2M^2}, \qquad u_1 = \frac{1}{2}\ln\frac{\eta + 2M^2}{M^2}$$

in (13) and

$$|\zeta|\beta_2 \to \zeta + M^2,$$

$$\varphi_2 = \Omega_2 = \frac{1}{2}\ln\frac{(\zeta + M^2)^2}{|\zeta|}, \qquad \varphi_1 = -\Omega_1 = \frac{1}{2}\ln\frac{|\zeta|}{M^2},$$

$$\overline{G} = \frac{1}{2\xi}\left[\ln^2\xi + \frac{4}{3}\pi^2\right]$$

in (14) and (15); G is defined in (17).

All these formulas can be readily obtained from the general equations if we write down (9) for this case in the form

$$x_1 = 1 - 2/(\eta + M^2), \qquad x_2 = -\eta/(\eta + 2M^2);$$

$$y_1 = 1 + 2/(\zeta + M^2), \qquad y_2 = -(\zeta + 2M^2)/\zeta \quad \text{for} \quad \zeta > 0,$$

$$y_1 = -(\zeta + 2M^2)/\zeta, \qquad y_2 = 1 + 2/(\zeta + M^2) \quad \text{for} \quad \zeta < 0.$$

We note, to avoid errors, that the changeover to other processes must be made in the complex matrix element, without first leaving out the imaginary parts in the individual terms.

We give now the numerical results for the c.m.s. The curves of Fig. 2 give the percentage contributions from the irreducible diagrams to the uncorrected cross section [i.e., the ordinates represent the quantity 100 B, see (22)]. For the scattering of particles of different signs, the values of B given on Fig. 2 must be taken with a minus sign. The corresponding corrections for the case of the conversion $e^+ + e^- \longleftrightarrow \mu^+ + \mu^-$ are given in Fig. 3.

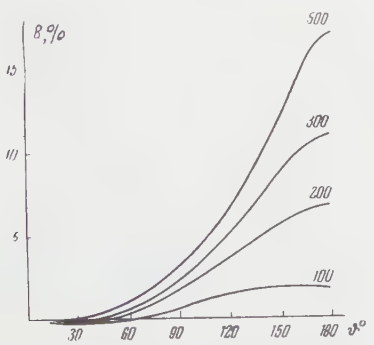

FIG. 2. Percentage of the contribution from the irreducible diagrams to the uncorrected cross section, for the scattering of particles of equal sign. ϑ – scattering angle in the c.m.s. The numbers on the curves indicate the energy of the incoming electron in the c.m.s. in mc^2 units.

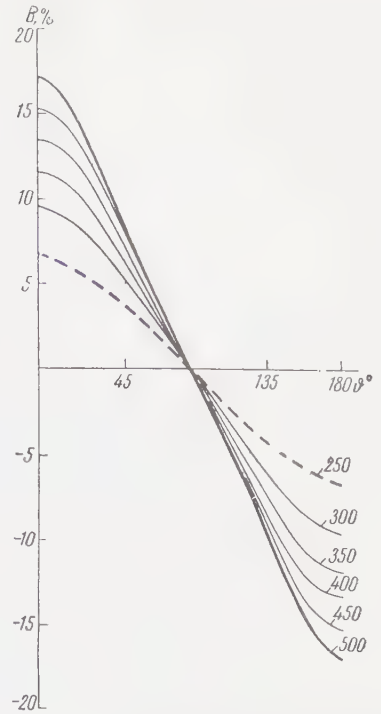

FIG. 3. Percentage contribution from irreducible diagrams to the uncorrected cross section, for the case $e^+ + e^- \leftrightarrow \mu^+ + \mu^-$. ϑ is the angle in the c.m.s. between the incoming electron and the outgoing μ^- meson. The numbers on the curves denote the energy of the incoming electron in mc^2 units.

Finally, Fig. 4 shows the total contribution, in percent, to the uncorrected cross section for the case when the c.m.s. electron energy is 300 mc^2 and the total loss to emission of soft quanta is $\leq 30\ mc^2 = \Delta\epsilon$.

In conclusion, I am grateful to I. L. Rozental' for interest in the work and to Z. S. Maksimova for making the numerical calculations.

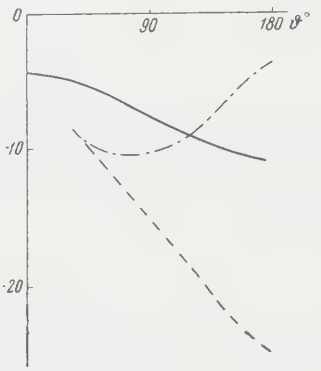

FIG. 4. Total percentage contribution to the uncorrected cross section, for an electron energy E = 300 mc^2 and $\Delta\varepsilon$ = 30 mc^2. Solid curves – corrections for the process $e^- + e^+ \leftrightarrow \mu^+ + \mu^-$; dashed curve – corrections for the process $e^- + \mu^+ \to e^- + \mu^+$; dash-dot curve – corrections for $e^- + \mu^- \to e^- + \mu^-$.

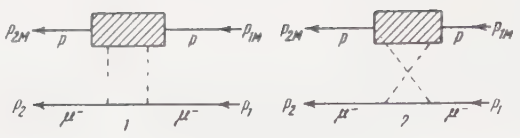

FIG. 5

APPENDIX 1

General Properties of Corrections Due to the Two-Photon Exchange

We denote the contributions to the scattering cross section from the irreducible diagrams 1 and 2 of Fig. 5 by $B^{(1)}$ and $B^{(2)}$. These functions are not independent. For example, the matrix element for the process $\mu^- + p \to \mu^- + p$ can be written in the form

$$|\mathfrak{M}|^2_{\mu-} = |\mathfrak{M}|^2_1 + B^{(1)}(\xi, \eta) + B^{(2)}(\xi, \eta),$$

where $B^{(1)}$ and $B^{(2)}$ corresponds to contributions from diagrams 1 and 2 of Fig. 5, and $|\mathfrak{M}_1|^2$ is the matrix element in the approximation of the one-photon exchange (see reference 10). Analogously, we have for $\mu^+ + p \to \mu^+ + p$ (see Fig. 6):

$$|\mathfrak{M}|^2_{\mu+} = |\mathfrak{M}|^2_1 - B^{(1)}(\xi, \eta) - B^{(2)}(\xi, \eta).$$

On the other hand, $|\mathfrak{M}|^2_{\mu+}$ can be obtained from $|\mathfrak{M}|^2_{\mu-}$ by the substitution

$$\xi \to \xi, \quad \eta \to -\zeta - 2M^2 - 2.$$

The diagrams 1 and 2 of Fig. 5 go in this case into the respective diagrams 2 and 1 of Fig. 6. Hence

$$B^{(1)}(\xi, \eta) = -B^{(2)}(\xi, -\zeta - 2M^2 - 2),$$

$$|\mathfrak{M}|^2_{\text{scat}} = |\mathfrak{M}|^2_{1\,\text{scat}} + B^{(2)}(\xi, \eta) - B^{(2)}(\xi, -\zeta - 2M^2 - 2).$$

For particle conversion we have

$$|\mathfrak{M}|^2_{\text{conv}} = |\mathfrak{M}|^2_{1\,\text{conv}} + B^{(2)}(-\eta - 4, -\zeta - 2M^2 - 2) - B^{(2)}(-\eta - 4, -\xi - 2M^2 - 2).$$

Thus, the contribution from the two-photon exchange is antisymmetrical in the variables ζ and ξ. This means that the charge acquires a tendency of retaining the direction of the initial motion after the particle conversion.

APPENDIX 2

We give here the results of the calculations of the principal integrals encountered in the matrix element for the scattering of muons by electrons. They can be used to calculate the polarization effects in μe interactions.

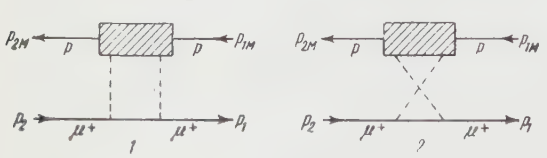

FIG. 6

These integrals have the following form (for notation see reference 6).

$$b^{(1)}_{1,\sigma,\sigma\tau} = \frac{1}{\pi^2 i}\int \frac{(1, K_\sigma, K_\sigma K_\tau)\, d^4K}{(0)\,(q)\,(1)\,(2)},$$

where we put for brevity

$$(0) = K^2 + 2Kp_1, \qquad (q) = (K - q)^2 + \lambda^2,$$
$$(1) = K^2 - 2Kp_{M1}, \qquad (2) = K^2 + \lambda^2.$$

We need also

$$H^{(1)}_{1,\sigma} = \frac{1}{\pi^2 i}\int \frac{(1, K_\sigma)}{(0)\,(1)\,(2)}\, d^4K, \qquad F^{(1)}_{1,\sigma} = \frac{1}{\pi^2 i}\int \frac{(1, K_\sigma)}{(0)\,(1)\,(q)}\, d^4K,$$

$$G^{(1)}_{1,\sigma} = \frac{1}{\pi^2 i}\int \frac{(1, K_\sigma)}{(1)\,(q)\,(2)}\, d^4K, \qquad \bar{G}_{1,\sigma} = \frac{1}{\pi^2 i}\int \frac{(1, K_\sigma)}{(0)\,(q)\,(2)}\, d^4K.$$

We have written out only the quantities with index 1. All the quantities with index 2 [for example, $b^{(2)}_{1\,\sigma,\sigma\tau}$] are obtained from the corresponding quantities with index 1 by the substitution $p_{1M} \to -p_{2M}$.

As a result of the calculation we obtain

$$H^{(1)}_1 = F^{(1)}_1 = H^{(1)} = I^{(1)} + \mu^{(1)} \ln \lambda^2,$$

where $I^{(1)}$ and $\mu^{(1)}$ are given by Eqs. (13) and (10) of the text. Furthermore

$$G^{(1)}_1 = G^{(2)}_1 = G$$

[See Eq. (17)].

The quantity G is given in (16), and

$$H^{(1)}_\sigma = K^{(1)}p_{1\sigma} - N^{(1)}p_{1\sigma M}, \quad F^{(1)}_\sigma = K^{(1)}p_{2\sigma} - N^{(1)}p_{2\sigma M} + q_\sigma H^{(1)},$$

where $K^{(1)}$ and $N^{(1)}$ are given in (11) and (12).

Finally

$$G^{(1)}_\sigma = \frac{1}{\xi + 4M^2}\left\{\xi G - 2\ln\frac{\xi}{M^2}\right\} p_{1\sigma M} + \left(2M^2 G + \ln\frac{\xi}{M^2}\right) q_\sigma,$$

$$\bar{G}^{(1)}_\sigma = -\frac{1}{\xi + 4}\{\xi\bar{G} - 2\ln\xi\}\, p_{1\sigma} + (2\bar{G} + \ln\xi)\, q_\sigma,$$

where $b^{(1)}_1 = b^{(1)}$ is given by (8).

The expressions for $b^{(1)}_\sigma$ and particularly for $b^{(1)}_{\sigma\tau}$ are quite cumbersome. We give therefore only their "projections," for they alone are used.

$$2p_{1\sigma}b^{(1)}_\sigma = G - F^{(1)}_1, \qquad 2p_{2\sigma M}b^{(1)}_\sigma = H^{(1)}_1 - \bar{G} - \xi b^{(1)}_1,$$
$$2p_{1\sigma}b^{(1)}_{\sigma\tau} = G^{(1)}_\tau - F^{(1)}_\tau, \qquad 2p_{2\sigma M}b^{(1)}_{\sigma\tau} = H^{(1)}_\tau - \bar{G}_\tau - \xi b^{(1)}_\tau,$$
$$2p_{1\sigma M}b^{(1)}_{\sigma\tau} = F^{(1)}_\tau - \bar{G}_\tau, \qquad 2p_{2\sigma}b^{(1)}_\sigma = G_1 - H^{(1)}_1 + \xi b^{(1)}_1,$$
$$2p_{1\sigma M}b^{(1)}_\sigma = F^{(1)}_1 - \bar{G}, \qquad 2p_{2\sigma}b^{(1)}_{\sigma\tau} = G^{(1)}_\tau - H^{(1)}_\tau + \xi b^{(1)}_\tau.$$

---

[1] V. B. Berestetskiĭ and I. Ya. Pomeranchuk, JETP **29**, 864 (1955), Soviet Phys. JETP **2**, 580 (1956).

[2] A. I. Akhiezer and V. B. Berestetskiĭ, Квантовая электродинамика (Quantum Electrody-

namics) 2d ed., Fizmatgiz, 1959, p. 644.

[3] L. M. Afrikyan and G. M. Garibyan, JETP **33**, 425 (1957), Soviet Phys. JETP **6**, 331 (1958).

[4] L. M. Brown and R. P. Feynman, Phys. Rev. **85**, 231 (1952).

[5] A. Akhiezer and R. Polovin, Doklady Akad. Nauk SSSR **90**, 55 (1953); R. Polovin, JETP **31**, 449 (1956), Soviet Phys. JETP **4**, 385 (1957).

[6] M. Redhead, Proc. Roy. Soc. **A220**, 219 (1953).

[7] K. Mitchell, Phil. Mag. **40**, 351 (1949).

[8] J. Schwinger, Phys. Rev. **76**, 790 (1949).

[9] L. Elton and H. Robertson, Proc. Phys. Soc. **A65**, 145 (1952).

[10] A. I. Nikishov, JETP **36**, 1604 (1959), Soviet Phys. JETP **9**, 1140 (1959).

Translated by J. G. Adashko
141

DEDUCTION OF THE RADIAL EQUATIONS OF THE THEORY OF COLLISIONS BETWEEN ELECTRONS AND ATOMS

L. A. VAĬNSHTEĬN and I. I. SOBEL'MAN

P. L. Lebedev Physics Institute, Academy of Sciences, U.S.S.R.

Submitted to JETP editor April 13, 1960

J. Exptl. Theoret. Phys. (U.S.S.R.) **39**, 767-775 (September, 1960)

Radial equations are derived for the excitation of an arbitrary level of a many-electron atom, with allowance for the nonorthogonality of the wave functions of the external and optical electrons. The well-known ambiguity which appears when approximate atomic wave functions are used is discussed. An approximate form of the equations is proposed, in which terms that contain simultaneously nonorthogonality integrals and higher multiple interactions are neglected. In this approximation the ambiguity disappears if semi-empirical wave functions are employed for the optical electron.

1 The various methods based on perturbation theory are as a rule insufficient in the calculation of the effective cross sections of the excitation of atoms by slow electrons. In the more general formulation, the problem reduces to the solution of a system of integro-differential equations for the radial wave functions of the external electron, analogous to the Hartree-Fock equations in the multiconfiguration approximation of electron theory. The present paper is devoted to a derivation of equations that describe the excitation of an arbitrary level of a multi-electron atom. The equations up to now are only for some particular cases (see, for example, reference 1).

Let us consider the following system: an atom with N electrons in state γLS and an outer electron with momentum l (γ is the totality of the remaining quantum numbers characterizing the LS term of the atom). The state of the system with specified values of total momenta $L_T S_T$ is defined by the set of quantum numbers $\Gamma = \gamma LS\tilde{l}L_T S_T$ (the quantum numbers M_{L_T} and M_{S_T}, which are of no importance in our problem, are omitted; the magnetic interactions are disregarded in this paper). The wave function of an arbitrary state of the system can be represented in the form

$$\Psi = \sum_{\Gamma} \Psi(\Gamma). \tag{1}$$

To separate the coordinate of the external electron it is necessary to change over to the incompletely antisymmetric functions

$$\Psi(\Gamma) \equiv \Psi(\gamma LS\tilde{l}L_T S_T) = \sum_i \frac{(-1)^{N+1-i}}{\sqrt{N+1}} \Psi(\gamma LS\tilde{l}_{(i)}L_T S_T). \tag{2}$$

The function $\Psi(\gamma LS\tilde{l}_{(i)}L_T S_T)$ is constructed in accordance with the general principle of addition of momenta, but unlike $\Psi(\gamma LS\tilde{l}L_T S_T)$ it is antisymmetric only in the electrons $1, 2, \ldots, i-1, i+1, \ldots, N+1$, while the i-th electron is assigned the state $\tilde{l}$. Using (2), we can separate the radial function of the external electron

$$\Psi(\Gamma) = \sum_i \frac{(-1)^{N+1-i}}{\sqrt{N+1}} \frac{F_\Gamma(r_i)}{r_i} \Phi(\gamma LS\tilde{l}_{(i)}L_T S_T). \tag{3}$$

The function $F_\Gamma(r)$ has an asymptotic value (Γ_0 is the initial state)

$$F_\Gamma(r) \sim \delta_{\Gamma\Gamma_0} \sin(kr - \tilde{l}\pi/2 + \eta \ln 2kr + \sigma_{\tilde{l}}) + T_{\Gamma\Gamma_0} \exp\{i(kr - \tilde{l}\pi/2 + \eta \ln 2kr + \sigma_{\tilde{l}})\},$$
$$\eta = (Z-N)/k, \qquad \sigma_{\tilde{l}} = \arg\Gamma(\tilde{l}+1-i\eta). \tag{4}$$

The total cross section of the atomic transitions $\gamma_0 L_0 S_0 \to \gamma LS$ is expressed in terms of $T_{\Gamma\Gamma_0}$:

$$Q^{\gamma_0 L_0 S_0}_{\gamma LS} = \frac{4\pi a_0^2 k}{k_0^3} \sum_{\tilde{l}\tilde{l}_0 L_T S_T} \frac{(2S_T+1)(2L_T+1)}{2(2S_0+1)(2L_0+1)} |T_{\Gamma\Gamma_0}|^2. \tag{5}$$

Thus, the cross section is determined by the asymptotic values of the functions $F_\Gamma(r)$. A system of equations for these functions can be obtained from the variational principle

$$\delta(F_\Gamma)\langle\Psi|H-E|\Psi\rangle = \sum_{\Gamma'} \delta(F_\Gamma)\langle\Psi(\Gamma)|H-E|\Psi(\Gamma')\rangle = 0. \tag{6}$$

The symbol $\delta(F_\Gamma)$ denotes variation over the function F_Γ in the left part of the matrix element. To carry out the variation in (6) in explicit form, it is necessary to express the matrix elements of $(H-E)$ in terms of the radial integrals.

2. We assume henceforth that the atomic functions are Hartree-Fock functions of single-configuration approximation. In the case of complicated atoms, the Hartree-Fock functions are the most exact functions that can be used in real calculations.

Generally speaking, the single-electron functions that enter into $\Psi(\Gamma)$ and $\Psi(\Gamma')$ may not be completely orthonormal. We shall consider only the nonorthogonality of the functions of the external and valence electrons, which plays the greatest role in the present problem. A full account of the nonorthogonality would lead to an excessive complication of the derivations and of the final expressions.

The energy of the system is made up of the energy of the atom E_a and the energy of the external electron $k^2/2$. For the energy of the atom it is necessary to use the same approximation as used for the wave functions in the calculation of the matrix elements, or else the contribution to E_a from the internal shells will not be compensated for by the corresponding terms in $\langle \Gamma | H | \Gamma \rangle$. It is physically obvious that the energy of the internal shells, which exceeds by many times the energy of the interaction of the external electron with the atom, should not enter into the equation for $F(r)$.

When using the approximate expression for the energy of the atom, the two representations

$$E = E_a + k^2/2, \qquad E = E_a' + k'^2/2 \tag{7}$$

are not equivalent. In the case of diagonal elements, the choice of the representation for E is dictated by the requirement of regular asymptotic behavior of the wave functions, viz., it is necessary to use the first representation in (7) for $\langle \Gamma | H - E' | \Gamma \rangle$ and the second for $\langle \Gamma' | H - E | \Gamma' \rangle$. As regards the nondiagonal matrix elements, either representation can be used with equal justification. This ambiguity, which arises in the use of approximate atomic functions, is known in literature as the prior—post divergence.[2]

3. If we disregard the excitation of the electrons of the internal shells, we can confine ourselves to matrix elements of three types

$$\langle T_c l_1^{n-1} \tau_1 \tilde{l} \tau l T | H - E | T_c l_1^{n-1} \tau_1 \tilde{l}' \tau' l' T \rangle, \tag{8}$$

$$\langle T_c l^n \tau \tilde{l} T | H - E | T_c l^{n-1} \tau_1' l' \tau' \tilde{l}' T \rangle, \tag{9}$$

$$\langle T_c l^n \tau \tilde{l} T | H - E | T_c l^n \tau' \tilde{l}' T \rangle. \tag{10}$$

Here and henceforth T will mean a pair of quantum numbers of the orbital and spin momenta of the system $T = (L_T S_T)$. Analogously, $\tau = (LS)$, $\tau_1 = (L_1 S_1)$, etc., while T_c includes all the closed shell of the atomic residue.* To shorten the notation, we shall denote the totality of the single-electron quantum numbers nl as simply l.

The Hamiltonian of the system H contains terms of two types:

$$H = F + Q = \sum_i f_i + \tfrac{1}{2} \sum_{ij}' q_{ij}. \tag{11}$$

The calculation of the matrix elements begins with a separation of the coordinates of the external electrons with the aid of formula (2). Some of the terms in the sum (2) will contain, in implicit form, nonorthogonality integrals of the type

$$\Delta(\tilde{l}l) = \delta_{\gamma_l} \int_0^\infty F_\Gamma(r) P_l(r)\, dr, \tag{12}$$

where $P_l(r)$ and $F_\Gamma(r)$ are the radial wave functions of the atomic (l) and external $(\tilde{l})$ electrons. To separate the nonorthogonality integrals it is necessary to separate the coordinates of one of the atomic electrons. Formula (2) cannot be applied to the equivalent electrons. For two groups of equivalent electrons, the relation needed has the form

$$\begin{aligned}\Psi(l'^n T', l''^m T'', T) &= \sqrt{\frac{n}{n+m}} (-1)^{n-i} \sum_{T_1}' G_{T_1}^{T'} \Psi(l'^{n-1} T_1' l'_{(i)} T', l''^m T'', T) \\ &+ \sqrt{\frac{m}{n+m}} (-1)^{n+m-i} \sum_{T_1''} G_{T_1''}^{T''} \Psi(l'^n T', l''^{m-1} T_1'' l''_{(i)} T'', T),\end{aligned} \tag{13}$$

where $G_{T_1}^{T}$ are the partial parentage coefficients introduced by Racah.[4] In Racah's notation

$$G_{T_1}^{T} \equiv G_{\alpha_1 L_1 S_1}^{\alpha L S}(l^n) \equiv (l^{n-1}[\alpha_1 L_1 S_1] l LS \,|\} l^n \alpha LS) \tag{14}$$

(see the preceding footnote concerning the quantum numbers α and α_1).

We shall also use the quantities

$$\bar{G}_{T_1}^{T} = \sqrt{n}\, G_{T_1}^{T}. \tag{15}$$

As above, the subscript (i) (in parentheses) following l will denote that the i-th electron is in the state l. The generalization of (13) to the case of three and more groups is obvious.

Let us consider a matrix element of the type (8). After all the transformations are made, it is represented in the form

*In order to specify the term of configuration $l^n (l \geq 2)$ it is necessary to introduce additional quantum numbers, for example, the seniority quantum number v for $l = 2$.[3] We shall omit these quantum numbers throughout. We note that the dependence on these quantum numbers is expressed in the following formulas only through the parentage coefficients.

$$\langle \Gamma | H - E | \Gamma' \rangle = \sum_{r=0}^{6} M_r(\Gamma\Gamma'), \tag{16}$$

$$M_0 = \delta_{\Gamma\Gamma'} \langle T_c \tilde{l}_{(N)} | H_N - k^2/2 | T_c \tilde{l}'_{(N)} \rangle, \tag{17}$$

$$M_1 = \delta_{nl,n'l'} \sum_{T_2} A_1 A_1' \langle l_1^{n-1} \tau_1 \tilde{l}_{(N)} T_2 | q_N | l_1^{n-1} \tau_1' \tilde{l}'_{(N)} T_2 \rangle, \tag{18}$$

$$M_2 = \delta_{\tau_1\tau_1'} \sum_{T_2} A_2 A_2' \langle l_{(1)} \tilde{l}_{(2)} T_2 | q_{12}(1 - P_{12}) | l'_{(1)} \tilde{l}'_{(2)} T_2 \rangle, \tag{19}$$

$$\begin{aligned} M_3 = & -\Delta(l\tilde{l}') A_3 [\langle T_c l_1^{n-1} \tau_1 \tilde{l}_{(N)} \tau' | H_N | T_c l_1^{n-1} \tau_1' l'_{(N)} \tau' \rangle \\ & - \tfrac{1}{2} \delta_{\tau_1\tau_1'} \Delta(\tilde{l} l') E_3] - \Delta(\tilde{l} l') \\ & \times A_3' [\langle T_c l_1^{n-1} \tau_1 l_{(N)} \tau | H_N | T_c l_1^{n-1} \tau_1' \tilde{l}'_{(N)} \tau \rangle \\ & - \tfrac{1}{2} \delta_{\tau_1\tau_1'} \Delta(l\tilde{l}') E_3], \end{aligned} \tag{20}$$

$$\begin{aligned} M_4 = & -\Delta(l_1\tilde{l}') \\ & \times \sum_{\tau_2\tau_2' T_2} A_4 [\langle T_c l_1^{n-2} \tau_2 \tilde{l}_{(N)} T_2 l \tau' | H_N | T_c l_1^{n-2} \tau_2' l_{1(N)} \tau_1' l' \tau' \rangle \\ & - \tfrac{1}{2} \delta_{\Gamma\Gamma'} \Delta(\tilde{l} l_1) E_4] - \Delta(\tilde{l} l_1) \\ & \times \sum_{\tau_2\tau_2' T_2} A_4' [\langle T_c l_1^{n-2} \tau_2 l_{1(N)} \tau_1 l \tau | H_N | T_c l_1^{n-2} \tau_2' \tilde{l}'_{(N)} T_2 l' \tau \rangle \\ & - \tfrac{1}{2} \delta_{\Gamma\Gamma'} \Delta(l_1\tilde{l}') E_4], \end{aligned} \tag{21}$$

$$\begin{aligned} M_5 = & -\delta_{\tau\tau'}(1 - \delta_{\Gamma\Gamma'}) \Delta(l_1\tilde{l}') \Delta(\tilde{l} l_1) \\ & \times \sum_{\tau_2\tau_2' T_2} A_5 A_5' \langle T_c l_1^{n-2} \tau_2 l_{(N)} T_2 | H_N | T_c l_1^{n-2} \tau_2' l'_{(N)} T_2 \rangle, \end{aligned} \tag{22}$$

$$\begin{aligned} M_6 = & \Delta(l_1\tilde{l}') \Delta(\tilde{l} l') \sum_{\tau_2\tau_2'} A_6 \langle T_c l_1^{n-2} \tau_2 l_{(N)} \tau_1' | H_N | T_c l_1^{n-2} \tau_2' l_{1(N)} \tau_1' \rangle \\ & + \Delta(l\tilde{l}') \Delta(\tilde{l} l_1) \sum_{\tau_2\tau_2'} A_6' \langle T_c l_1^{n-2} \tau_2 l_{1(N)} \tau_1 | H_N | T_c l_1^{n-2} \tau_2' l'_{(N)} \tau \rangle. \end{aligned} \tag{23}$$

In addition, another term arises, proportional to $\Delta(\tilde{l}\tilde{l}')$. We cannot account for this term and still use the asymptotic values of the radial functions. It is therefore omitted throughout. The following notation is used in (17) — (23)

$$H_N = f_N + q_N, \qquad q_N = \sum_i q_{Ni}(1 - P_{Ni}); \tag{24}$$

$$\begin{aligned} A_1 &= (\tau_1 l [\tau] \tilde{l} T | \tau_1 \tilde{l} [T_2] l T)(1 - \delta_{l_1 l})(1 - \delta_{l_1 l'}), \\ A_2 &= (\tau_1 l [\tau] \tilde{l} T | \tau_1, l\tilde{l} [T_2] T), \\ A_3 &= (\tau_1 l [\tau] \tilde{l} T | \tau_1 \tilde{l} [\tau'] l T), \\ A_4 &= \bar{G}^{\tau_1}_{\tau_2} \bar{G}^{\tau_1}_{\tau_2'} (\tau_2 l_1 [\tau_1] l [\tau] \tilde{l} T | \tau_2 \tilde{l} [T_2] l [\tau'] l_1 T), \\ A_5 &= \bar{G}^{\tau_1}_{\tau_2} (\tau_2 l_1 [\tau_1] l \tau | \tau_2 l [T_2] l_1 \tau), \\ A_6 &= \bar{G}^{\tau_1}_{\tau_2} \bar{G}^{\tau_1}_{\tau_2'} (\tau_2 l_1 [\tau_1] l \tau \tilde{l} T | \tau_2 l [\tau'] \tilde{l} [\tau'] l_1 T). \end{aligned} \tag{25}$$

The coefficients A'_r are obtained by means of the substitution $\tau_1 l \tau \tilde{l} \rightleftarrows \tau_1 l' \tau' \tilde{l}'$.

These formulas are valid for both diagonal and nondiagonal matrix elements. If we disregard the uninteresting transitions between terms of excited configurations, then the terms M_0 and M_1 contribute only to the diagonal matrix elements. We shall therefore write from now on $\delta_{\Gamma\Gamma'}$ in M_1 instead of $\delta_{nl,n'l'}$.

In the case of nondiagonal matrix elements, we can have two representations for E_2 and E_3:

$$\begin{aligned} E_2 &= \varepsilon_l + k^2/2, \qquad E_3 = \varepsilon_{l_1} + k^2/2; \\ E_2 &= \varepsilon'_{l'} + k'^2/2, \qquad E_3 = \varepsilon'_{l_1} + k'^2/2. \end{aligned} \tag{26}$$

ϵ_l and ϵ_{l_1} are the energy parameters of the Hartree-Fock equations for the l and l_1 electrons, corresponding to the atomic state τ; $\epsilon'_{l'}$ and ϵ'_{l_1} are the parameters of the l' and l_1 electrons, corresponding to the atomic state τ_1 (see Appendix).

The expression such as (9) for the matrix element can be obtained by replacing in the sum $\sum_r M_r$ [Eq. (16)] all the M_r except M_0 by $\sum_{\tau_1} \bar{G}^{\tau}_{\tau_1} M_r$, and by putting $l_1 = l$ and $M_1 = M_5 = 0$. In addition, E_2 is written in (26) in the form

$$E_2 = \varepsilon_l + \frac{k^2}{2} - \sum_{\tau_1} [\delta_{\tau_1\tau_1'} - (G^{\tau}_{\tau_1})^2] \langle l_1^{n-1} \tau_1 | Q | l_1^{n-1} \tau_1 \rangle. \tag{27}$$

The expression for the matrix element (10) can be obtained by replacing in the sum $\sum_r M_r$ all the M_r except M_0 by $\sum_{\tau_1\tau_1'} \bar{G}^{\tau}_{\tau_1} \bar{G}^{\tau'}_{\tau_1'} M_r$, and by putting $l_1 = l = l'$ and $M_1 = M_4 = M_5 = M_6 = 0$. In formula (24) it is necessary to leave out the exchange terms if the electrons $l_{(i)}$ and $l_{(N)}$ are equivalent.

If we start out directly with the expressions (16) — (23), we obtain exceedingly complicated equations for the functions $F(r)$. The use of such equations serves no purpose. We therefore confine ourselves to an approximate but much simpler representation. Assuming the nonorthogonality integrals to be small, we omit from (17) — (23) part of those terms that contain simultaneously nonorthogonality integrals and multipole interactions of second or higher order. It can be shown that this is equivalent to neglecting in the terms that contain the nonorthogonality integrals the difference in the terms of the considered configuration, compared with the average energy of the term. In this approximation, the matrix element of type (8) becomes

$$\langle\Gamma|H-E|\Gamma'\rangle=\delta_{\Gamma\Gamma'}\langle T_c\tilde{l}_{(N)}|H_N-\tfrac{1}{2}k^2|T_c\tilde{l}_{(N)}\rangle$$
$$+\delta_{\Gamma\Gamma'}\sum_{T_2}A_1A_1'\langle l_1^{n-1}\tau_1\tilde{l}_{(N)}T_2|q_{N'}|l_1'^{\,n}\tau_1'\tilde{l}'_{(N)}T_2\rangle$$
$$+\delta_{\tau_1\tau_1'}\sum_{T_2}A_2A_2'\langle l_{(1)}\tilde{l}_{(2)}T_2|q_{12}(1-P_{12})$$
$$+\lambda_{\Gamma\Gamma'}P_{12}|l'_{(1)}\tilde{l}'_{(2)}T_2\rangle, \tag{28}$$

$$\lambda_{\Gamma\Gamma'}=-\varepsilon'_{l'}+k^2/2 \quad \text{or} \quad \lambda_{\Gamma\Gamma'}=-\varepsilon+k'^2/2. \tag{29}$$

If Γ is the initial state and Γ' the final state, then the first expression corresponds to the "prior" approximation, while the second to the "post" approximation. Thus, the difference between these two approximation reduces to the difference between the multipliers of the nonorthogonality integrals in the nondiagonal matrix elements* (the two expressions coincide for the diagonal elements). Even this difference disappears, however, if we take for ϵ_l and $\epsilon'_{l'}$ the experimental values of the energies of the corresponding states. This way appears to us to be the most advantageous. Lack of space prevents us from giving many arguments in favor of this. We note only that the calculation of the energy parameters of the Hartree-Fock equations with complete self-consistency is a very laborious task.

Matrix elements of type (9) and (10) are obtained by averaging the ion terms, as was done above. In addition, the second term and the right half of (28) is equal to zero.

4. We proceed to separate the radial integrals from the matrix elements. The result can be represented in the following form

$$\langle\Gamma|H-E|\Gamma'\rangle=\delta_{\Gamma\Gamma'}[I_\Gamma+\sum_\varkappa a_\Gamma^\varkappa R_\varkappa(l_1\tilde{l},\ l_1\tilde{l})$$
$$-\sum_\varkappa b_\Gamma^\varkappa R_\varkappa(l_1\tilde{l},\ \tilde{l}l_1)]+\sum_\varkappa\alpha_{\Gamma\Gamma'}^\varkappa R_\varkappa(l\tilde{l},\ l'\tilde{l}')$$
$$-\sum_\varkappa\beta_{\Gamma\Gamma'}^\varkappa[R_\varkappa(l\tilde{l},\tilde{l}'l')-\delta_{\varkappa0}\frac{(-1)^{l+l'}\lambda_{\Gamma\Gamma'}}{(2l_0+1)^{1/2}(2l'+1)^{1/2}}$$
$$\times\Delta(l\tilde{l}')\Delta(\tilde{l}l')], \tag{30}$$

$$R_\varkappa(l\tilde{l},\ l'\tilde{l}')=\iint dr_1dr_2r_<^\varkappa r_>^{-\varkappa-1}P_l(r_1)P_{l'}(r_1)F_\Gamma(r_2)F_{\Gamma'}(r_2), \tag{31}$$

where $r_<$ ($r_>$) is the smaller (larger) of the r_1 or r_2.

We denote by I_Γ the first term in (28), which contains additive operators and the operator of interaction with the filled shell. The separation of the radial integral from this term entails no difficulty (see, for example, reference 5).

*Moreover, only in the exchange terms (see reference 2).

The coefficients a and b are expressed in terms of α and β of the preceding ion

$$a_\Gamma^\varkappa=\sum_{T_2}(A_1)^2\alpha^\varkappa_{\Gamma^*\Gamma^*},\qquad b_\Gamma^\varkappa=\sum_{T_2}(A_1)^2\beta^\varkappa_{\Gamma^*\Gamma^*},\qquad \Gamma^*=l_1^{n-1}\tau_1\tilde{l}T_2. \tag{32}$$

The coefficients α and β are of greatest interest, and we shall discuss them in greater detail. Using (25) and the general methods for calculating the matrix elements from the product of tensor operators,[3] we obtain

$$\alpha^\varkappa_{\Gamma\Gamma'}=\delta_{SS'}(-1)^{L_T+l+\tilde{l}'}(l\|C^\varkappa\|l')(\tilde{l}\|C^\varkappa\|\tilde{l}')\begin{Bmatrix}\varkappa & L & L'\\ L_T & \tilde{l}' & \tilde{l}\end{Bmatrix}\mu^\varkappa_{\Gamma\Gamma'}, \tag{33}$$

$$\beta^\varkappa_{\Gamma\Gamma'}=(-1)^{S_T+s/2-S+l+l'}(l\|C^\varkappa\|\tilde{l}')(\tilde{l}\|C^\varkappa\|l')\begin{Bmatrix}\varkappa & L & \tilde{l}'\\ L_T & L' & \tilde{l}\end{Bmatrix}\nu^\varkappa_{\Gamma\Gamma'}. \tag{34}$$

The reduced matrix elements $(l\|C^\kappa\|l')$ are expressed in terms of the 3-j symbols

$$(l\|C^\varkappa\|l')=(-1)^l(2l+1)^{1/2}(2l'+1)^{1/2}\begin{pmatrix}l & \varkappa & l'\\ 0 & 0 & 0\end{pmatrix}. \tag{35}$$

In the case when $L_1 = S_1 = 0$ (for example, one electron outside the filled shell) $\mu^\kappa = \nu^\kappa = 1$. In the more general case, we have for the matrix element of type (8)

$$\mu^\varkappa_{\Gamma\Gamma'}=\delta_{\tau_1\tau_1'}(-1)^{\varkappa+L+L'}(2L+1)^{1/2}(2L'+1)^{1/2}\begin{Bmatrix}\varkappa & L & L'\\ L_1 & l' & l\end{Bmatrix}, \tag{36}$$

$$\nu^\varkappa_{\Gamma\Gamma'}=\delta_{\tau_1\tau_1'}(-1)^{-S_T-1/2-S'}(2S+1)^{1/2}(2S'+1)^{1/2}\begin{Bmatrix}S_T & 1/2 & S'\\ S_1 & 1/2 & S\end{Bmatrix}$$
$$\times(2L+1)^{1/2}(2L'+1)^{1/2}\begin{Bmatrix}\varkappa & L & \tilde{l}'\\ L_T & L' & \tilde{l}\end{Bmatrix}^{-1}\sum_{L_2}(2L_2+1)$$
$$\times\begin{Bmatrix}\tilde{l} & l & L_2\\ L_1 & L_T & L\end{Bmatrix}\begin{Bmatrix}\tilde{l}' & l' & L_2\\ L_1 & L_T & L'\end{Bmatrix}\begin{Bmatrix}\tilde{l} & l & L_2\\ \tilde{l}' & l' & \varkappa\end{Bmatrix}. \tag{37}$$

For the matrix elements of type (9) and (10) it is necessary to average μ^κ and ν^κ over τ_1 or, respectively, over τ_1 and τ_1', i.e., we must take

$$\sum_{\tau_1}\bar{G}^\tau_{\tau_1}\begin{pmatrix}\mu^\varkappa_{\Gamma\Gamma'}\\ \nu^\varkappa_{\Gamma\Gamma'}\end{pmatrix}\text{ or }\sum_{\tau_1\tau_1'}\bar{G}^\tau_{\tau_1}\bar{G}^{\tau'}_{\tau_1'}\begin{pmatrix}\mu^\varkappa_{\Gamma\Gamma'}\\ \nu^\varkappa_{\Gamma\Gamma'}\end{pmatrix}. \tag{38}$$

Although the parentage coefficients for most configurations of interest were tabulated by Racah, the calculations become most complicated, particularly of matrix element of type (10). However, Racah[3,4] has developed special methods which greatly simplify the calculation in many cases.

5. We can now derive in explicit form the radial integro-differential equations from the variational principle (6). Inasmuch as all the matrix elements are diagonal in L_TS_T, we obtain an independent system of equations for each such pair L_TS_T. This system can be represented in the form

$$\left\{\frac{d^2}{dr^2}-\frac{l(l+1)}{r^2}-2U_\Gamma(r)+k^2\right\}F_\Gamma(r)=2\sum_{\Gamma'}{}'\delta_{T\Gamma'}U_{\Gamma\Gamma'}(r)F_{\Gamma'}(r), \tag{39}$$

$$U_\Gamma F_\Gamma = \frac{1}{r}\Big[-Z+\sum_{l_1\varkappa} a^\varkappa_\Gamma y^\varkappa_{l_1l_1}(r)\Big]F_\Gamma(r) - \frac{1}{r}\sum_{l_1\varkappa} b^\varkappa_\Gamma y^\varkappa_{l_1\tilde{l}}(r)\,P_{l_1}(r)$$
$$+\frac{1}{r}\sum_{\varkappa}\alpha^\varkappa_{\Gamma\Gamma}\,y^\varkappa_{ll}(r)\;F_\Gamma(r)$$
$$-\sum_{\varkappa}\beta^\varkappa_{\Gamma\Gamma}\Big[\frac{1}{r}\,y^\varkappa_{l\tilde{l}}\;(r)-\delta_{\varkappa 0}\,\frac{\lambda_\Gamma}{2l+1}\,\Delta(l\tilde{l})\Big]P_l(r), \qquad (40)$$

$$U_{\Gamma\Gamma'}F_{\Gamma'} = \frac{1}{r}\sum_{\varkappa}\alpha^\varkappa_{\Gamma\Gamma'}y^\varkappa_{ll'}(r)\,F_{\Gamma'}(r) - \sum_{\varkappa}\beta^\varkappa_{\Gamma\Gamma'}\Big[\frac{1}{r}\,y^\varkappa_{l\tilde{l}'}(r)$$
$$-\delta_{\varkappa 0}\,\frac{(-1)^{l+l'}\lambda_{\Gamma\Gamma'}}{(2l+1)^{1/2}(2l'+1)^{1/2}}\Big]P_{l'}(r). \qquad (41)$$

Here Z is the charge of the nucleus and $\sum_{l_1}$ denotes the summation over all the shells except the outer shell. For filled shells we have

$$a^\varkappa_\Gamma = n_1\delta_{\varkappa 0}, \qquad b^\varkappa_\Gamma = \frac{n_1}{2}\begin{pmatrix} l_1 & \varkappa & \tilde{l}\\ 0 & 0 & 0\end{pmatrix}, \qquad (42)$$

where n_1 is the number of electrons in the shell. For unfilled shells, $a^\varkappa_\Gamma$ and $b^\varkappa_\Gamma$ are determined in accordance with (32). The radial integrals $y^\varkappa(r)$ have the form

$$y^\varkappa_{l\tilde{l}}(r) = \int_0^r\Big(\frac{r_1}{r}\Big)^\varkappa P_l(r_1)\,F_\Gamma(r_1)\,dr_1 + \int_r^\infty\Big(\frac{r}{r_1}\Big)^{\varkappa+1}P_l(r_1)\,F_\Gamma(r_1)\,dr_1. \qquad (43)$$

Equations (39) represent an infinite system of coupled integro-differential equations. In practical calculations one frequently uses the approximation of distorted waves, in which only one term with $\Gamma = \Gamma_0$ is left in the right half of (39). In this case, the transition amplitude $T_{\Gamma\Gamma_0}$ can be represented in the form

$$T_{\Gamma\Gamma_0} = -e^{i(\delta_\Gamma+\delta_{\Gamma_0})}\,\frac{2}{k}\int\bar{F}_\Gamma U_{\Gamma\Gamma_0}\bar{F}_{\Gamma_0}dr$$
$$= -e^{i(\delta_\Gamma+\delta_{\Gamma_0})}\,\frac{2}{k}\Big\{\sum_\varkappa\alpha^\varkappa_{\Gamma\Gamma_0}\bar{R}_\varkappa(l_0\tilde{l}_0,l\tilde{l}) - \sum_\varkappa\Big[\beta^\varkappa_{\Gamma\Gamma_0}\bar{R}_\varkappa(l_0\tilde{l}_0,\;\tilde{l}\,l)$$
$$+\frac{(-1)^{l_0+l}\,\delta_{\varkappa 0}\,\lambda_{\Gamma\Gamma_0}}{(2l_0+1)^{1/2}(2l+1)^{1/2}}\,\bar{\Delta}(l_0\tilde{l})\,\Delta(\tilde{l}_0 l)\Big]\Big\}, \qquad (44)$$

where the functions $\bar{F}(r)$ are solutions of Eqs. (39) without the right halves, with use of the asymptotic expression

$$\bar{F}_\Gamma \sim \sin(kr - l\pi/2 + \eta\ln 2kr + \sigma_l + \delta_\Gamma). \qquad (45)$$

The bar over R and Δ denotes the use of $\bar{F}$ instead of F.

APPENDIX

The energy of the atom in the state $T_c l_1^{n-1}\tau_1 l\tau$ can be represented in the form

$$E_a = \langle T_c l_1^{n-1}\tau_1|H|T_c l_1^{n-1}\tau_1\rangle$$
$$+\langle T_c l_1^{n-1}\tau_1 l_{(N)}\tau|H_N|T_c l_1^{n-1}\tau_1 l_{(N)}\tau\rangle. \qquad (A1)$$

The Hartree-Fock equations are obtained by varying E_a with respect to P_l. It is easy to show that the second term in (A1) is equal to the energy parameter ϵ_l, since it is the only one that contains the function P_l.

In the case of the state $T_c l^n\tau$ we have

$$E = \sum_{\tau_1}(\bar{G}^\tau_{\tau_1})^2\langle T_c l^{n-1}\tau_1|H|T_c l^{n-1}\tau_1\rangle$$
$$+\sum_{\tau_1\tau_1'}\bar{G}^\tau_{\tau_1}\bar{G}^\tau_{\tau_1'}\langle T_c l^{n-1}\tau_1 l^\tau_{(N)}|H_N|T_c l^{n-1}\tau_1 l_{(N)}\tau\rangle. \qquad (A2)$$

To obtain the Hartree-Fock equation it is necessary to vary both terms. It can be shown, however, that the second term is equal to ϵ_l as before. Separating the radial integrals from (A2), we write E_a in the form

$$E_a = \Big[E(T_c) + (n-1)I(l) + \sum_\varkappa\alpha^\varkappa_1 R_\varkappa(ll)\Big]$$
$$+\Big[I(l) + \sum_\varkappa\alpha^\varkappa_2 R_\varkappa(ll)\Big] \qquad (A3)$$

On the other hand, the matrix element is

$$\langle T_c l^n\tau|H|T_c l^n\tau\rangle = E(T_c) + nI(l) + \sum_\varkappa\alpha^\varkappa R_\varkappa(ll). \qquad (A4)$$

Varying this expression, we obtain the Hartree-Fock equation for the l electron

$$\Big[\mathcal{H} + \frac{2}{n}\sum_\varkappa\alpha^\varkappa y^\varkappa(r)\Big]P_l(r) = \varepsilon_l P_l(r). \qquad (A5)$$

The operator $\mathcal{H}$ occurs when the matrix element $I(l)$ of the single-electron operator is varied. The diagonal matrix elements of the two-electron operator of the atom and the ion are connected by the simple relation

$$\alpha^\varkappa_1 = (n-2)\,\alpha^\varkappa/n, \qquad \text{i.e.} \quad \alpha^\varkappa_2 = 2\alpha^\varkappa/n, \qquad (A6)$$

therefore the second term in (A3) is

$$I(l) + \sum_\varkappa\alpha^\varkappa_2 R_\varkappa(ll) = \int_0^\infty dr P_l(r)\Big[\mathcal{H} + \sum_\varkappa\alpha^\varkappa_2 y^\varkappa(r)\Big]P_l(r) = \varepsilon_l,$$

and, consequently,

$$\sum_{\tau_1\tau_1'}\bar{G}^\tau_{\tau_1}\bar{G}^\tau_{\tau_1'}\langle T_c l^{n-1}\tau_1 l_{(N)}\tau|H_N|T_c l^{n-1}\tau_1 l_{(N)}\tau\rangle = \varepsilon_l. \qquad (A7)$$

Moreover, it is seen from the derivation that formula (A7) can be generalized by replacing the radial wave function of the l electron in the left half of the matrix element:

$$\sum_{\tau_1\tau_1'}\bar{G}^\tau_{\tau_1}\bar{G}^\tau_{\tau_1'}\langle T_c l^{n-1}\tau_1\tilde{l}_{(N)}\tau|H_N|T_c l^{n-1}\tau_1 l_{(N)}\tau\rangle = \varepsilon_l\Delta(\tilde{l}\,l), \qquad (A8)$$

provided the orbital quantum numbers $\tilde{l}$ and l are equal.

It is possible to obtain quite analogously an expression for the energy parameter of the internal electron ϵ_{l_1}.

[1] J. Percival, M. Seaton, Proc. Cambr. Phil. Soc. **53**, 654 (1957).

[2] Bates, Fundaminsky, Lech, and Massey, Phil. Trans. Roy. Soc. London **243**, 93 and 117 (1950).

[3] G. Racah, Phys. Rev. **62**, 438 (1942).

[4] G. Racah, Phys. Rev. **53**, 367 (1943).

[5] E. U. Condon and G. H. Shortley, The Theory of Atomic Spectra, Cambridge, 1951.

Translated by J. G. Adashko
142

ON THE THEORY OF UNSTABLE STATES

YA. B. ZEL'DOVICH

Submitted to JETP editor April 16, 1960

J. Exptl. Theoret. Phys. (U.S.S.R.) 39, 776—780 (September, 1960)

A perturbation theory is developed and an expression is given for the amplitude (corresponding to a given initial state) of a state that decays exponentially with time. A final expression is obtained which plays the role of the norm of such a state.

AN exponentially decaying state that describes, for example, the phenomenon of α decay, is characterized by a complex value of the energy, the imaginary part of the energy giving the decay probability. The wave function of this state increases exponentially in absolute value at large distances, and therefore the usual methods of normalization, of perturbation theory, and of expansion in terms of eigenfunctions do not apply to this state. We develop here a perturbation theory which gives an expression in terms of a quadrature for the changes of the mean energy and of the decay probability corresponding to an arbitrarily small change of the potential.

If the state is initially described by a certain wave function, then for a long time interval thereafter the wave function is close to an exponentially decaying function with a definite amplitude. This amplitude is also calculated in terms of quadratures.

The solutions of both problems—that of the energy and that of the amplitude of the exponentially decaying state—involve a quantity that plays the role of the norm of this state:

$$\lim_{\alpha\to 0}\int_0^\infty \chi^2 \exp(-\alpha r^2)\, r^2 dr.$$

For the calculation of this quantity we shall give a direct method which enables us to avoid the limiting process $\alpha \to 0$.

1. Let us consider a particle moving in a spherical potential with a barrier, i.e., moving like the α particle in the Gamow theory of α decay.

Let the corresponding Schrödinger equation have the formal solution

$$\psi(r, t) = e^{-iE't}\chi(r)$$

with the complex value $E' = E_0 - i\gamma$. The discrete value E' is obtained from the condition that at large distances $\chi(r)$ contains only an outgoing wave:

$$\chi(r) \approx Cr^{-1}e^{ikr}, \qquad r\to\infty,$$
$$k = +\sqrt{2E'}, \qquad \hbar = m = 1.$$

This solution is of interest not only as a description of an unstable state; the corresponding eigenvalue is a singular point—a pole—(in the complex plane) of the matrix for the scattering of a particle by the potential.

As is well known, $|\chi(r)|$ increases exponentially for $r \to \infty$; the function χ cannot be normalized, and in particular cannot be regarded as a wave function in the usual sense: it does not belong to the complete system of eigenfunctions ψ_n of the Hamiltonian operator. We cannot apply to χ the usual formulas of perturbation theory, for example

$$\delta E_n = \int \psi^* \delta H \cdot \psi_n d\tau \Big/ \int \psi_n^* \psi_n d\tau,$$

and the expansion of the function of an arbitrary state in terms of eigenfunctions:

$$\varphi(r) = A_n\psi_n, \qquad A_n = \int \psi_n^* \varphi\, d\tau \Big/ \int \psi_n^* \psi_n d\tau.$$

We shall find the expressions that replace these well known formulas in the case of the function χ.

Let us begin with the perturbation theory. In the simplest case of an S wave and a potential such that $V(r) = 0$ for $r > R$, by using the methods developed in references 1 and 2 we get without difficulty the expression

$$\delta E' = \int \chi^2(r)\,\delta V(r)\, d\tau \Big/ \Big\{\int [\chi^2(r) - (Cr^{-1}e^{ikr})^2]\, d\tau - C^2/2ik\Big\}, \qquad (1)$$

where C is the coefficient in the asymptotic formula for the unperturbed solution χ: $\chi(r) \approx Cr^{-1}e^{ikr}$ as $r \to \infty$. The two integrals—in the numerator and in the denominator—can be thought of as taken over all space: in the numerator the region of integration is fixed by the region of the perturbation $\delta V(r)$,

and in the denominator the integrand is zero for $r > R$.

We note that the integrands do not contain the square of the absolute value, but the complex quantity χ^2, and therefore $\delta E'$ is complex. The expression (1) gives not only the change of the energy E_0, but also the change of the decay probability $w = 2\gamma$.

To derive Eq. (1) we introduce the variable

$$y = d \ln \chi / dr; \qquad \chi(r) = \exp\left\{\int_0^r y(q)\, dq\right\}. \tag{2}$$

Schrödinger's equation then takes the form

$$dy/dr = -y^2 - 2[E' - V(r)], \tag{3}$$

and the equation for the perturbation of y is

$$d\,\delta y/dr = -2y\,\delta y + 2[\delta E' - \delta V(r)]. \tag{4}$$

The condition of regularity of χ at $r = 0$ uniquely determines $y(0)$, so that $\delta y(0) = 0$, and from this we have

$$\delta y(r) = \exp\left\{-2\int_0^r y\,dr\right\}\int_0^r [\delta V(q) - \delta E'] \exp\left\{2\int_0^q y\,dq\right\} dq$$

$$= \frac{2}{\chi^2(r)}\int_0^r [\delta V(q) - \delta E']\,\chi^2(q)\,dq. \tag{5}$$

The boundary condition for the perturbed problem for $r > R$ is

$$d \ln \chi'/dr = y + \delta y = i\sqrt{2(E' + \delta E')}$$

$$= i\sqrt{2E'} + i\delta E'/2E',$$

$$\delta y = i\delta E'/\sqrt{2E'} = i\delta E'/k. \tag{6}$$

Comparing Eqs. (6) and (5), we now get Eq. (1) by an elementary calculation.

If we prescribe $\delta V = \epsilon = \text{const}$ in the entire infinite volume, we must obviously get $\delta E' = \epsilon$; Therefore the finite expression in the denominator of Eq. (1) can be regarded as the definition of the diverging integral $\int \chi^2 dr$. This latter integral does have any unambiguous meaning because of the fact that

$$|\chi| \sim \exp(\gamma r/\sqrt{2E_0}) \to \infty \quad \text{for } r \to \infty$$

and does not become convergent if we multiply the integrand by $e^{-\alpha r}$ and subsequently take the limit $\alpha \to 0$. Convergence can be achieved by multiplication by $e^{-\alpha r^2}$:

$$\int \chi^2\, d\tau \equiv \lim_{\alpha \to 0} \int \chi^2 e^{-\alpha r^2} d\tau = J$$

$$= \int [\chi^2 - (Cr^{-1}e^{ikr})^2]\, d\tau - C^2/2ik. \tag{7}$$

Equation (1) can then be written in the form

$$\delta E' = \int \chi^2 \delta V\, d\tau \Big/ \int \chi^2\, d\tau. \tag{1a}$$

2. Let us now consider the nonstationary problem. Suppose that at the initial time the wave function

$$\psi(r, t = 0) = \varphi(r)$$

is prescribed. It is well known that the asymptotic form of the solution is

$$\psi(r, t) = Ae^{-iE't}\chi(r) + O(r, t), \tag{8}$$

where $O(r, t)$ falls off like $t^{-3/2}$ for small r [for further details about $O(r, t)$ see the paper of Khalfin[3]].

Despite the fact that the first term decreases exponentially as $e^{-\gamma t}$ and the second only by a power law, the separation of the first term is justified over a wide range of values of t for $\gamma \ll E_0$. Drukarev[4] has shown that the approach of $\psi(r, t)$ to the asymptotic expression (8) occurs nonuniformly at small r ($r < vt$, where v is the speed of the particle corresponding to the energy E_0). As has been shown by Fok and Krylov,[5] the coefficient A in the first term of Eq. (8) is proportional to the residue (at the pole $E = E'$) of the spectral density of the initial state $\varphi(r)$ when it is expanded in terms of the continuous-spectrum eigenfunctions $\psi(E, r)$ that correspond to real values of E.

The coefficient A can be expressed in terms of $\varphi(r)$ and $\chi(r)$ by a simple quadrature:

$$A = \int \varphi\chi\, d\tau \Big/ \int \chi^2\, d\tau, \tag{9}$$

where $\int \chi^2 d\tau$ is defined by Eq. (7).

To verify this we introduce, following N. A. Dmitriev, a function $\psi(r, s)$ defined by the formula

$$\psi(r, s) = -i\int_0^\infty \psi(r, t)\, e^{ist}\, dt, \tag{10}$$

for those values of s for which the integral converges. In the region where the integral diverges, we define $\psi(r, s)$ as the analytic continuation of the function defined by the integral (10).

The Schrödinger equation gives

$$-s\psi(r, s) - \tfrac{1}{2}\Delta\psi(r, s) + V(r)\,\psi(r, s) = -\varphi(r). \tag{11}$$

In the region $r > R$, where $V(r) = 0$ and $\varphi(r) = 0$, the solution is of the form

$$\psi(r, s) = [f(s)\exp(ir\sqrt{2s}) + f_1(s)\exp(ir\sqrt{2s})]\, r^{-1}, \tag{12}$$

where f and f_1 are arbitrary functions.

Considering the region $\operatorname{Im} s > 0$, where $\psi(r, s)$ is given by a convergent integral, we convince ourselves that $f_1(r, s) \equiv 0$, since $|\psi(r, s)|$ cannot increase for $r \to \infty$. The condition that $\psi(r, s)$ is a

diverging wave for large r is extended by the analytic continuation to arbitrary values of s.

The function $\chi(r)$ that describes the decaying state satisfies the same condition for $r \to \infty$ and an equation analogous to Eq. (11) but without the right member:

$$-E'\chi(r) - \tfrac{1}{2}\Delta\chi(r) + V(r)\chi(r) = 0 \qquad (13)$$

It follows from this that the solution of the equation (11) with the right member has a pole at $s = E'$ (with $\operatorname{Im} s = -\gamma < 0$):

$$\psi(r, s) = a\chi(r)/(s - E') + \psi_1(r, s), \qquad (14)$$

where $\psi_1(r, E')$ is regular.

To determine a we multiply Eq. (11) by $\chi(r)$ and Eq. (13) by $\psi(r, s)$ and subtract one equation from the other. We then integrate over the volume $0 < r < R$ and substitute the expression for $\psi(r, s)$ in the form (14). Then finally for $s \to E'$ we get an expression for a that coincides with the expression (9) for A.

Inverting the relation (1), we find that the pole term in Eq. (14) gives the exponential term in Eq. (8) with $A = a$, and this completes the derivation of (9).

3. The formulas are easily extended to the case of states with $l \neq 0$. In this case all formulas contain instead of χ^2 the product $\chi(\mathbf{r})\tilde{\chi}^*(\mathbf{r})$, where $\tilde{\chi}(\mathbf{r})$ is the solution of the adjoint equation (cf. reference 6). In the present case, since the operator H is Hermitian, the taking of the adjoint reduces to changing the sign of i in the boundary condition

$$\partial \ln r\chi/\partial r = +i\sqrt{2E'}, \qquad \partial \ln r\tilde{\chi}/\partial r = -i\sqrt{2E'^*}$$
$$(r \to \infty).$$

After separating off the angular factor in $\chi(\mathbf{r}) = P(\theta, \varphi)z(\mathbf{r})$, we get

$$\tilde{\chi} = \tilde{P}\tilde{z}, \qquad \tilde{P} = P, \qquad \tilde{z} = z^*,$$

so that finally

$$\delta E' = \int \tilde{\chi}^* \chi \delta V \, d\tau \Big/ \int \tilde{\chi}^* \chi \, d\tau, \qquad (15)$$

$$\psi(\mathbf{r}, t) = Ae^{-iE't}\chi(\mathbf{r}) + O(r, t), \qquad (16)$$

$$A = \int \tilde{\chi}^*(\mathbf{r})\varphi(\mathbf{r})\, d\tau \Big/ \int \tilde{\chi}^*(\mathbf{r})\chi(\mathbf{r})\, d\tau. \qquad (17)$$

In the equation for the radial function z(r) the effective potential U(r) includes the centrifugal potential:

$$U(r) = V(r) + r^{-2}l(l+1),$$

and therefore in the region $r > R$, where $V(r) = 0$, the function z(r) can be expressed in terms of a Hankel function of half-integral order of the complex argument kr (k is complex when E' is complex).

For $r \to \infty$ we also have $|\chi| \to \infty$, and therefore to give a definite meaning to the integral that plays the role of the normalization we must again either multiply the integrand by $e^{-\alpha r^2}$ and then let $\alpha \to 0$ or else use a finite expression of the type of (1), which does not require the passage to the limit:

$$\int_0^\infty z^2 r^2 dr = \int_0^r z^2 r^2 dr + r^2 z^2 \frac{\partial^2}{\partial E' \partial r} \ln(rz). \qquad (18)$$

For $r > R$ we get into the region where z(r) can be expressed in terms of a Hankel function, and the derivatives in the second term can be taken in an elementary way. Furthermore, it is easily verified that in virtue of the equation satisfied by z(r) the right member of (18) does not depend on r. The problem is solved in a similar way for the Coulomb potential, the only difference being that for $r > R$ the quantity z is expressed by a hypergeometric function.

Finally, in the case of a V(r) that contains, besides the Coulomb and centrifugal potentials, another part that is everywhere different from zero but that decreases sufficiently rapidly (exponentially), we must bring into the treatment, along with the solution z(r) of the complete equation, another function $z_1(r)$ that is a solution of the equation with $V(r) = 0$ and coincides with z(r) in the limit $r \to \infty$ [$z(\infty) = z_1(\infty)$]. The function z_1 can be expressed in terms of known (Hankel and hypergeometric) functions:

$$\int_0^\infty z^2 r^2 dr = \int_0^\rho z^2 r^2 dr + \int_0^\infty (z^2 - z_1^2) r^2 dr$$
$$+ z_1^2 \frac{\partial^2}{\partial E' \partial r} \ln(rz_1)\Big|_{r=\rho}. \qquad (19)$$

For $l \neq 0$ we must treat separately a neighborhood of the origin, $0 < r < \rho$, because of the fact that the Hankel function has a nonintegrable singularity at zero. It is assumed that after we have separated out from V(r) the terms of orders 1/r and $1/r^2$, V(r) falls off in such a way that $z^2 - z_1^2$ is a function that is integrable for $r \to \infty$.

In the case of a potential of complicated form, for which the integrals can only be calculated numerically, the advantage of the expression (19) as compared with (18) is that in Eq. (19) one takes the derivative of known functions.

I take occasion to note with gratitude that G. A. Drukarev, A. B. Migdal, V. A. Fok, and L. A. Khalfin have taken part in the discussion of this work. I must note particularly the important participa-

tion and assistance of N. A. Dmitriev, who provided formal proofs of a number of assertions contained in this paper.

[1] Ya. B. Zel'dovich, JETP **31**, 1101 (1956), Soviet Phys. JETP **4**, 942 (1957).

[2] F. S. Los', JETP **33**, 273 (1957), Soviet Phys. JETP **6**, 211 (1958).

[3] L. A. Khalfin, JETP **33**, 1371 (1957), Soviet Phys. JETP **6**, 1053 (1958).

[4] G. A. Drukarev, JETP **21**, 59 (1951).

[5] N. S. Krylov and V. A. Fok, JETP **17**, 93 (1947).

[6] P. L. Kapur and R. Peierls, Proc. Roy. Soc. **A166**, 277 (1938).

Translated by W. H. Furry

ANGULAR DISTRIBUTION OF FISSION FRAGMENTS PRODUCED BY LOW-ENERGY NEUTRONS

V. M. STRUTINSKIĬ

Submitted to JETP editor April 16, 1960

J. Exptl. Theoret. Phys. (U.S.S.R.) **39**, 781-793 (September, 1960)

The angular distribution of fission fragments produced in the capture of particles of low orbital angular momentum is considered. The spin of the target nucleus is taken into account. The effect of fluctuations in the distribution of the transition nucleus levels on the angular distribution of the fission fragments is also considered.

UNTIL recently, the available data on the angular distribution of fission fragments referred chiefly to fission induced by high-energy particles. Abundant experimental data for this energy region made it possible to establish the existence of not only qualitative but also quantitative agreement between the simple statistical theory of the angular anisotropy and experiment.[1-4]

The investigation of the low-energy excitation region of the transition nucleus* is of considerable interest. The study of the angular distribution of the fragments permits one to obtain information on the fission probability as a function of the value of the projection K of the spin of the transition nucleus on the direction of fission, and therefore on the K distribution of the transition nucleus levels for small excitation. When the transition nucleus is even — even, the fragment angular distribution also gives additional evidence of the existence of an energy gap in the spectrum of the transition nucleus levels and the existence of rotational levels inside the gap. However, there is need of a more accurate theory of the fragment angular distribution. Most important is the taking into account of the initial spin of the nucleus.

1. For a definite spin of the target nucleus, the probability amplitude for the emission of fragments in the direction $\mathbf{n}$ can be written in the form[5]

$$f_{lSJ}(\mathbf{n}) = \sqrt{\frac{4\pi}{2(2J_0+1)}} \sum_{m\mu M} C^{JM}_{S\mu lm} Y_{lm}(\boldsymbol{\nu}) \sum_{K=-J}^{J} \sqrt{p_J(K)}\, D^J_{MK}(\mathbf{n}), \quad (1)$$

where S is the spin of the channel; $S = J_0 \pm \frac{1}{2}$; J_0 is the spin of the target nucleus; J is the spin of the compound nucleus; l is the neutron orbital angular momentum; $\boldsymbol{\nu}$ is the direction of the neutron beam; m, μ, M are the projections of the vectors l, S, J on the axis of quantization; Y_{lm} and D^J_{MK} are the normalized spherical function and the matrix of the J-representation of the group of rotations; $C^{c\gamma}_{a\alpha b\beta}$ is the Clebsch — Gordan coefficient. Choosing in (1) the axis of quantization along the direction of fragment emission $\mathbf{n}$, one can obtain the following expression for the amplitude:

$$f_{lSJ} = \sqrt{(2J+1)/2(2J_0+1)} \sum_{m\mu} C^{JK}_{S\mu lm} \sqrt{p_J(K)}\, Y_{lm}(\boldsymbol{\nu}), \quad (2)$$

where use was made of the relation

$$D^J_{MK}(0) = \{(2J+1)/4\pi\}^{1/2} \delta_{MK}.$$

For the fragment angular distribution, we obtain

$$W_{lSJ}(\vartheta) = \{(2J+1)/2(2J_0+1)\} \times \sum_{m\mu} (C^{JK}_{S\mu lm})^2\, p_J(K) |Y_{lm}(\vartheta)|^2, \quad (3)$$

where ϑ is the angle between the direction of the neutron beam and the direction of fission. In formula (3) the interference terms have been discarded, as they are not important for a nucleus with a large density of levels.

The coefficients $p_J(K)$ are determined by the number of transition nucleus levels, for a given value of K, through which the fission takes place. They can be represented in the form

$$p_J(K) = \{\Gamma_f(0)\, a(K)/(2J+1)\} \times \left\{\Gamma_n + \Gamma_\gamma + \left[\Gamma_f(0) \sum_{K=-J}^{J} a(K)\right] \Big/ (2J+1)\right\}^{-1}, \quad (4)$$

where $a(K)$ is independent of J, and $\Gamma_f(0)$ is the fission width for $J = 0$. [It is assumed that $a(K)$ is normalized by the condition $a(0) = 1$]. With

*By transition nucleus we have in mind here a nucleus undergoing fission with a deformation corresponding approximately to a saddle point. The excitation energy of such a nucleus is approximately equal to the excitation energy of a compound nucleus minus the threshold energy for fission.

such a choice of $p_J(K)$, the angular distribution (3) turns out to be normalized in such a way that the integral of $W_{lSJ}(\vartheta)$ is equal to the probability of fission for the nuclear angular momentum J if the absorption coefficient is equal to unity:

$$\int W_{lSJ}(\vartheta)\, d\Omega = (2J+1)\Gamma_f/\Gamma; \tag{5}$$

$$\Gamma = \Gamma_n + \Gamma_\gamma + \Gamma_f(J), \quad \Gamma_f(J) = (2J+1)^{-1}\Gamma_f(0)\sum_{K=-J}^{J} a(K), \tag{6}$$

Γ_f is the fission width in the state J, M.* In formula (5), 2J + 1 is the statistical factor for the formation of a compound nucleus of angular momentum J and any allowed value of M for given l and S.

We now assume that the total width Γ of the excited state of the nucleus weakly depends on the angular momentum. This occurs, in particular, if $\Gamma_n + \Gamma_\gamma$ does not depend on J, and $\Gamma_f(J) < \Gamma_n + \Gamma_\gamma$ and also when $\sum_{K=-J}^{J} a(K) \approx 2J+1$, i.e., if $a(K)$ is very little different from unity. Taking this into account, we find the following expression for the angular distribution:

$$W_{lSJ}(\vartheta) = \sum_{\mu m K}^{l} (C^{JK}_{S\mu lm})^2\, a(K)\, |Y_{lm}(\vartheta)|^2. \tag{7}$$

In formula (7) we have omitted factors which are independent of l and J and which are not important for what follows.

The overall angular distribution of the fragments in the reaction has the form

$$W(\vartheta) = \sum_{lSJ} \zeta_{lSJ} W_{lSJ}(\vartheta), \tag{8}$$

where ζ_{lSJ} are the absorption coefficients. For the sake of simplicity, we assume that they do not depend on S and J. Setting $\zeta_{lSJ} \approx \zeta_l$ we find the following expression for the angular distribution of the fragments:

$$W(\vartheta) = \sum_l \zeta_l \sum_{S=J_0\pm 1/2} W_{lS}(\vartheta), \tag{9}$$

where $W_{lS}(\vartheta)$ is the angular distribution for the channel (l, S):

$$W_{lS}(\vartheta) = \sum_{J=|l-S|}^{l+S} W_{lSJ}(\vartheta) = \sum_{m=-l}^{l} |Y_{lm}(\vartheta)|^2 \sum_{K=m-S}^{m+S} a(K). \tag{10}$$

In the derivation of formula (10) we employed the relation

$$\sum_J (C^{JK}_{S\mu lm})^2 = \begin{cases} 1, & |K-m| \leqslant S \\ 0, & |K-m| > S \end{cases}.$$

In statistical theory the K distribution is given by the expression[1,7]

$$a(K) = \exp(-K^2/2K_0^2), \tag{11}$$

where $K_0^2 = \overline{\mathcal{J}}T/\hbar^2$; T is the transition nucleus temperature, $\overline{\mathcal{J}}^{-1} = \mathcal{J}_{\parallel}^{-1} - \mathcal{J}_{\perp}^{-1}$, $\mathcal{J}_{\parallel}$ and $\mathcal{J}_{\perp}$ are the moments of inertia of the transition nucleus with respect to the axis of symmetry (axis of fission) and the direction perpendicular to it. Taking into account the fact that for low angular momenta the inequality

$$J^2/2K_0^2 \ll 1, \tag{12}$$

holds, we expand a(K) into the series

$$a(K) \approx 1 - K^2/2K_0^2 + \ldots. \tag{13}$$

Inserting this expression into formulas (9) and (10), we obtain

$$W(\vartheta) \approx \sum_l \zeta_l \sum_{m=-l}^{l} |Y_{lm}(\vartheta)|^2 \sum_S (2S+1)$$
$$\{1 - (1/2K_0^2)[m^2 + S(S+1)/3]\}$$
$$= \frac{1}{4\pi}\sum_l (2l+1)\,\zeta_l \{1 - [l(l+1)/4K_0^2]\sin^2\vartheta\} + \text{const}, \tag{14}$$

which can also be represented in the form

$$W(\vartheta) \approx \text{const} \cdot \{1 - (\overline{l^2}/4K_0^2)\sin^2\vartheta\}, \tag{15}$$

where

$$\overline{l^2} = \Big\{\sum_l (2l+1)\,\zeta_l\, l(l+1)\Big\}\Big\{\sum_l (2l+1)\,\zeta_l\Big\}^{-1} \tag{16}$$

is the mean square of the orbital angular momentum imparted to the nucleus. For a black nucleus

$$\overline{l^2} = \tfrac{1}{2}\, l_{max}^2 = \tfrac{1}{2}(k_n R)^2. \tag{17}$$

For neutrons and nuclei with $A \sim 240$, the following expression is, in practice, more accurate:

$$\overline{l^2} \approx (2.5-3)\cdot E_n \ [\text{Mev}].$$

The small constant term dependent on the spin of the target nucleus and appearing in the braces in formula (14) has been omitted, since it obviously does not affect the shape of the angular distribution. It may therefore be said that for a small anisotropy, the statistical distribution of the fragments does not depend on the nuclear spin for any value of the orbital angular momentum of the neutron. The dependence of the angular distribution on the spin arises for the next term in the series (13). In the calculation of this term, the coefficient of $\sin^2\vartheta$ in formula (15) should be multiplied by

*Here the dependence of the fission width on the angular momentum of the nucleus, which is associated with the effect of rotation on the value of the fission threshold,[6] is not taken into account. This effect is important for very large angular momenta of the nucleus.

the spin-dependent factor $1 - S^2/2K_0^2$. The coefficient of $\sin^4\vartheta$ is independent of the spin. For a small anisotropy, the spin-dependent terms are negligibly small.

The reason for the weak dependence of the anisotropy on the value of the initial spin becomes more understandable if one considers the classical limit (l, $S \gg 1$). In this approximation, for a given distribution $a(K)$ the angular distribution of the fragments with respect to the spin direction of the compound nucleus can be represented in the form

$$W(\mathbf{n}) = \text{const} \cdot a(K)|_{K=\mathbf{Jn}}. \qquad (18)$$

We set $\mathbf{J} = \mathbf{l} + \mathbf{S}$ and average expression (18) over all possible directions of the vectors $\mathbf{l}$ and $\mathbf{S}$ (vector $\mathbf{l}$ lies in a plane perpendicular to the beam, vector $\mathbf{S}$ lies on a sphere). As a result, we obtain for the Gaussian distribution (13) an expression similar to formula (15) and, consequently, a weak dependence of the angular distribution on the initial spin. For another form of $a(K)$, the angular distribution, generally speaking, depends on the initial spin. In particular, a strong dependence on the magnitude of the initial spin occurs for the distribution used by Griffin:[4]

$$a(K) = \begin{cases} 1 - |K|/K_{max}, & |K| \leqslant K_{max} \\ 0, & |K| > K_{max} \end{cases}$$

(the anisotropy is less for a large value of S). If the series for $a(K)$ begins with the fourth power of K

$$a(K) \approx 1 - \varkappa K^4 \qquad (\varkappa > 0),$$

then the angular distribution has the form

$$W(\vartheta) = \text{const} \cdot \left\{1 - \varkappa\left(\tfrac{3}{8}\bar{l}^4 \sin^4\vartheta + S^2\bar{l}^2\sin^2\vartheta\right)\right\},$$

i.e., the anisotropy would even increase with an increase in the initial spin. The physical reason for this is the fact that along with the deterioration in the angular momentum of the compound nucleus for a definite initial spin, there is an effect leading to an increase in the anisotropy; this effect is connected with the fact that for a large initial spin there are, on the average, larger values of the angular momentum of the compound nucleus (see also reference 1). Therefore, the final result is determined by the degree of the dependence of the anisotropy on the magnitude of the angular momentum of the nucleus.

2. One can also set the task of determining the distribution $a(K)$ from the known angular distribution of the fragments. To do this, it is necessary to know the angular distribution for each K, separately.

We shall first consider the case $K = 0$. Since it is assumed that the transition nucleus has an axis of symmetry (coinciding with the direction of fission), there exists for the rotational states with $K = 0$ a selection rule, according to which only even values of angular momentum can occur for a compound nucleus of positive parity and odd values, for negative parity. Hence, for $K = 0$, the summation over J in the individual terms of formula (8) should be carried out in such a way that the parity of J is the same as the parity of l for a target nucleus of positive parity and of the opposite parity in the case of negative parity. This summation can be carried out in general form by means of the formula

$$\sum_J{}' (C^{J0}_{S\mu lm})^2 = \tfrac{1}{2}[1 + (-1)^{l+S+J}\delta_{m0}], \qquad (19)$$

where the primes on the summation sign indicate that the summation is carried out only over even or only over odd values of J. Employing (8) and (19), we find

$$W^{(K=0)}(\vartheta) = \sum_{lS} \zeta_l W^{(K=0)}_{lS}(\vartheta), \qquad (20)$$

$$W^{(K=0)}_{lS}(\vartheta) = \tfrac{1}{2}\left\{\sum_{|m|\leqslant S} |Y_{lm}(\vartheta)|^2 + (-1)^{l+S+J}|Y_{l0}(\vartheta)|^2\right\}. \qquad (21)$$

For each l the second term in formula (20) has opposite signs for the two values $S = J_0 \pm \tfrac{1}{2}$, and these terms cancel one another in the sum over S in formula (20). This also occurs in the case of a spin-orbit interaction between the neutron and nucleus when the absorption coefficient also depends on S and J. Therefore we shall omit this term everywhere below in the expressions for $W^{(K=0)}_{lS}(\vartheta)$.

For $l \leq S$

$$W^{(K=0)}_{lS}(\vartheta) = (2l + 1)/8\pi, \qquad (22)$$

i.e., for $K = 0$ the channels with $l \leq S$ give an isotropic contribution to the angular distribution. For the channels with $l > S$, the angular distribution for $K = 0$ can be written in the form

$$W^{(K=0)}_{lS}(\vartheta) = \tfrac{1}{2}\sum_{|m|\leqslant S} |Y_{lm}(\vartheta)|^2 = \frac{2l+1}{8\pi} F_{lS}(\vartheta), \qquad (23)$$

$$F_{l\lambda}(\theta) = \frac{4\pi}{2l+1}\sum_{m=-\lambda}^{\lambda} |Y_{lm}(\vartheta)|^2. \qquad (24)$$

A simple expression for the function $F_{l\lambda}$ is obtained in the quasi-classical approximation if, instead of the functions $|Y_{lm}|^2$, their classical analog

$$(1/2\pi^2)\{\sin^2\vartheta - (m^2/l^2)\}^{-1/2} \qquad (25)$$

is employed. Replacing in formula (24) the summation over m by an integration, we obtain

$$F_{l\lambda}(\vartheta) \approx \begin{cases} 1 & l \sin\vartheta \leqslant \lambda \\ (2/\pi)\ \sin^{-1}(\lambda/l \sin\vartheta), & l \sin\vartheta \geqslant \lambda. \end{cases} \quad (26)$$

For $\lambda \ll l$

$$F_{l\lambda}(\vartheta) \sim (2/\pi)(\lambda/l \sin\vartheta).$$

By means of formula (10), one can obtain expressions for the angular distribution for other fixed values of K. Noting that a(K) is an even function of K, we obtain the following resulting expression for the angular distribution of the fission fragments for a channel with a fixed value of |K|:

$$W_{lS}^{(|K|)}(\vartheta) = W_{lS}^{(K)}(\vartheta) + W_{lS}^{(-K)}(\vartheta),$$

where for $S \geq l$

$$W_{lS}^{(|K|)}(\vartheta) = \frac{2l+1}{4\pi} \begin{cases} 1 & |K| \leqslant S-l \\ 1 + F_{l,S-|K|}(\vartheta), & S-l < |K| \leqslant S, \\ 1 - F_{l,|K|-S-1}(\vartheta), & S < |K| \leqslant S+l, \end{cases} \quad (27)$$

and for $S < l$

$$W_{lS}^{(|K|)}(\vartheta) = \frac{2l+1}{4\pi} \begin{cases} F_{lS}(\vartheta), & K = 0 \\ F_{l,S-|K|}(\vartheta) + F_{l,S+|K|}(\vartheta), & 0 < |K| \leqslant S \\ 1 - F_{l,|K|-S-1}(\vartheta), & S < |K| \leqslant l+S. \end{cases} \quad (28)$$

Substituting (27) and (28) into formulas (9) and (10), we obtain the following expression for the angular distribution:

$$W(\vartheta) = \text{const} \cdot \sum_l (2l+1)\,\bar{\zeta}_l \cdot [a(S_1-\lambda) - a(S_1+\lambda)](F_{l,\lambda-1} + F_{l,\lambda}),$$

$$S_1 = J_0 + 1/2, \qquad a(-K) = a(K). \quad (29)$$

We introduce the quantity $A(\vartheta) = \{\sigma_f(\vartheta) - \sigma_f(90°)\}/\sigma_f(0°)$. For a small anisotropy, $A(\vartheta)$ practically coincides with the usually considered quantity $\cdot\{\sigma_f(\vartheta) - \sigma_f(90°)\}/\sigma_f(90°)$. The expression for $\sigma_f(0)$ can be obtained directly from formulas (9) and (10) if it is noted that

$$|Y_{lm}(0)|^2 = \{(2l+1)/4\pi\}\,\delta_{m0}.$$

Calculating $\sigma_f(0°)$ in this way, we find

$$A(\vartheta) = \sum_{\lambda=1} \beta_\lambda \Phi_\lambda(\vartheta), \quad (30)$$

where

$$\beta_\lambda = \frac{a(S_1-\lambda) - a(S_1+\lambda)}{2\{a(0) + a(S_1) + 2[a(1) + \ldots + a(S_1-1)]\}} \qquad (J_0 \neq 0); \quad (31)$$

$$\Phi_\lambda(\vartheta) = \left\{\sum_l (2l+1)\,\bar{\zeta}_l \Phi_{l\lambda}(\vartheta)\right\} \Big/ \sum_l (2l+1)\,\zeta_l,$$

$$\Phi_{l\lambda}(\vartheta) = F_{l,\lambda-1}(\vartheta) + F_{l,\lambda}(\vartheta) - F_{l,\lambda-1}(90°) - F_{l,\lambda}(90°). \quad (32)$$

For a small anisotropy, the denominator in formula (31) is approximately equal to $4S_1 = 2(2J_0 + 1)$. Some values of the functions $\Phi_{l\lambda}$ for $l \leq 3$ are shown in the table.

The functions $\Phi_\lambda(\vartheta)$ depend only on the incident neutron energy, since they are fully determined by the absorption coefficients. In the case of a black nucleus, they depend only on l_{max}. The index λ runs over the values from 1 to l_{max}. Thus, knowing the angular distribution of the fragments, one can, in principle, determine l_{max} independent differences of the coefficients a(K). Using the functions (26), we can obtain the following quasiclassical expression for $\Phi_\lambda(\vartheta)$ for a black nucleus:

$$\Phi_\lambda(\vartheta) = \sum_{n=\lambda-1}^{\lambda} \bar{F}_{ln}\Big|_{90°}^{\vartheta},$$

$$\bar{F}_{ln}(\vartheta) \approx \begin{cases} 2\pi^{-1}(\sin^{-1} x + x\sqrt{1-x^2}), & x = n/l_{max} \sin\vartheta \leqslant 1 \\ 1, & x > 1 \end{cases}.$$

The angular distribution of the fragments is readily calculated by means of formulas (30) — (32) if the distribution of a(K) is given. If, as happens in the statistical case, a(K) is a monotonically decreasing function of K, all the coefficients β_λ are positive, and $A(\vartheta)$ is a monotonically decreasing function of the angle ϑ. [Both functions $\Phi_\lambda(\vartheta)$ and $\Phi_{l\lambda}(\vartheta)$ decrease monotonically with an in-

Values of the function $\Phi_{l\lambda}$

ϑ, deg	l, λ					
	1,1	2,1	3,1	2,2	3,2	3,3
0	1.000	1.500	1.636	0.750	1.272	0.636
10	0.970	1.412	1.460	0.750	1.267	0.636
20	0.884	1.170	1.032	0.740	0.226	0.634
30	0.750	0.844	0.556	0.703	1.076	0.626
40	0.589	0.518	0.218	0.623	0.810	0.593
50	0.413	0.256	0.066	0.492	0.486	0.510
60	0.250	0.062	0.036	0.330	0.218	0.373
70	0.117	0.020	0.034	0.165	0.068	0.205
80	0.030	0.002	0.020	0.041	0.024	0.065
90	0.000	0.000	0.000	0.000	0.000	0.000

crease in ϑ.] In the statistical case, for a(K) not very different from unity, one can employ expansion (13), which gives

$$\beta_\lambda \approx \beta_\lambda^0 = \lambda / 2K_0^2. \quad (33)$$

The function $A(\vartheta)$, by (15), has the form

$$A(\vartheta) = (1/2K_0^2) \sum_\lambda \lambda \Phi_\lambda(\vartheta) = (\bar{l}^2/4K_0^2)\cos^2\vartheta. \quad (34)$$

In formulas (26)—(31), the above-mentioned selection rule for J was not taken into account for the states with K = 0. If this rule is taken into account, the coefficient a(0) decreases by one-half. This result is obvious in the classical limit: For a given orbital angular momentum and K = 0, fission is possible for only half the possible values of the angular momentum of the compound nucleus. As a result, formula (30) should be written in the form

$$A(\vartheta) \approx \sum_{\lambda=1} \beta_\lambda \Phi_\lambda(\vartheta) + \tfrac{1}{2}[2(2J_0+1)]^{-1}\Phi_{S_1}(\vartheta),$$
$$(S_1 \neq 1/2, \quad l_{\max} \geqslant S_1, \quad a(0) = 1). \quad (34')$$

For a Gaussian distribution of a(K) and a small anisotropy, the fragment angular distribution in which the selection rule for the states with K = 0 is taken into account has the form

$$A(\vartheta) \approx (\bar{l}^2/4K_0^2)\cos^2\vartheta - \tfrac{1}{2}[2(2J_0+1)]^{-1}\Phi_{S_1}(\vartheta). \quad (35)$$

For large l the integral contribution of the second term decreases as $l_{\max}^{-1}$. If the first term in formula (35) is independent of the initial spin, then the second term, other conditions being equal, leads to a certain decrease in the anisotropy for a smaller value of J_0.

3. In those cases for which the probability of fission in a channel of angular momentum J is determined not only by some statistical factors, as was assumed above, there may be need of expressions for the fragment angular distribution with a fixed value of J. In the classical limit, they can be obtained by replacing in formula (7) the square of the Clebsch-Gordan coefficient by its classical analog:

$$(C^{J0}_{S\mu lm})^2 \approx (1/\pi l)\{\sin^2\chi - (m^2/l^2)\}^{-1/2},$$
$$\cos\chi = (2lJ)^{-1}[l(l+1) - S(S+1) + J(J+1)], \quad (36)$$

and the functions $|Y_{lm}(\vartheta)|^2$ by expression (25). Replacing also the summation over m by integration, we obtain

$$W^{(K=0)}_{lSJ}(\vartheta) = \pi^{-3}\begin{cases}(\sin\chi)^{-1}K(z), & z = \sin^2\vartheta/\sin^2\chi < 1\\ (\sin\vartheta)^{-1}K(z^{-1}), & z \geqslant 1\end{cases}, \quad (37)$$

where K(z) is the complete elliptical integral of the first kind:

$$K(z) = \int_0^{\pi/2} (1 - z^2\sin^2\varphi)^{-1/2}\, d\varphi.$$

The quantum-mechanical expression for $W^{(K=0)}_{lSJ}$ has the form

$$\sum_\rho (-1)^S (2l+1)(2J+1)(C^{\rho 0}_{l0l0})^2 \times (C^{\rho 0}_{J0J0})^2 W(lJlJ|S\rho) P_\rho(\cos\vartheta), \quad (38)$$

where W(abcd|ef) are Racah coefficients.

Another classical expression for $W^{(K=0)}_{lSJ}(\vartheta)$ can be obtained by replacing the Racah coefficients in (38) and the squares of the Clebsch-Gordan coefficients by their classical analogs:

$$(C^{\rho 0}_{l0l0})^2 \approx (4/\pi)\{4l^2 - \lambda^2\}^{-1/2},$$
$$W(lJlJ|S\rho) \approx (-1)^{S-l-J}\{(2l+1)(2J+1)\}^{-1/2} P_\rho(\cos\chi).$$

As a result, we obtain

$$W^{(K=0)}_{lSJ}(\vartheta) \approx \frac{8}{\pi}\sum_\rho \{(2l+1)(2J+1)\}^{1/2}\{(4J^2 - \rho^2) \times (4l^2 - \rho^2)\}^{-1/4} P_\rho(\cos\chi) P_\rho(\cos\vartheta). \quad (39)$$

The last expression for $W^{(K=0)}_{lSJ}(\vartheta)$ is somewhat more accurate than (37).

4. In the presence of a spin-orbit interaction between the incident neutron and nucleus, the absorption coefficients ζ_{lSJ} depend on all the indices. Their explicit form can be found from a comparison of the expressions for the total wave function of the system in the representation used above for the spin of the channel and the ordinary j-representation ($j = l \pm 1/2$). Consideration of the spin-orbit interaction leads primarily to the replacement of ζ_l by the mean absorption coefficient

$$\bar{\zeta}_l = (2l+1)^{-1}\{(l+1)\zeta_{l,l+1/2} + l\zeta_{l,l-1/2}\},$$

where $\zeta_{l,j}$ are the absorption coefficients in the j-representation. In formulas (15), (34), and (35) there appears, moreover, the factor

$$[1 + 2(2l+1)^{-1}q_l],$$
$$q_l = (\zeta_{l,l+1/2} - \zeta_{l,l-1/2})/(\zeta_{l,l+1/2} + \zeta_{l,l-1/2})$$

in the coefficients of $\cos^2\vartheta$. This correction is not important. For $W^{(K=0)}(\vartheta)$, with allowance for the spin-orbit interaction, we obtain the expression

$$W^{(K=0)}(\vartheta) = \tfrac{1}{2}\Big\{\sum_{l,S}\bar{\zeta}_l \sum_{m=-S}^{S}|Y_{lm}(\vartheta)|^2 - \sum_{l,S_1}\bar{\zeta}_l[4q_lS_1/(2l+1)][1 + q_l/(2l+1)]|Y_{l,S_1}(\vartheta)|^2\Big\}. \quad (23')$$

The correction associated with the last term in (23') also proves to be small. We note the follow-

ing useful relations which are employed in calculations with spin-orbit coupling:

$$\sum_J J(J+1)(C^{JK}_{S\mu lm})^2 = \begin{cases} l(l+1)+S(S+1)+2m\mu, & |\mu|\leqslant S,\ |m|\leqslant l \\ 0, & |\mu|>S,\ |m|>l \end{cases},$$

$$\sum{}' J(J+1)(C^{J0}_{S\mu lm})^2 = \tfrac{1}{2}[1+(-1)^{S+l+J}\delta_{m0}][l(l+1)+S(S+1)]-m^2.$$

The validity of these relations, as well as formula (19), can be established by a comparison of the zero coefficients for ϑ^0, ϑ^2, $(\pi-\vartheta)^0$, and $(\pi-\vartheta)^2$ in the expansion in powers of ϑ and $(\pi-\vartheta)$ of the identity

$$D^S_{\mu\mu}D^l_{mm} - \sum_J (C^{JK}_{S\mu lm})^2 D^J_{KK} = 0.$$

5. If the values of the orbital angular momenta taking part in the reaction are not large, formula (30) can be used quite directly for the analysis of the experimental data. The "statistical" term of the angular distribution, which, for a small anisotropy, is given by formula (34), can be separated immediately. With the "fluctuational" part of the angular distribution separated in this way, it can readily be shown how the coefficients β_λ differ from their statistical values (33). To do this, it is necessary only to take into account the fact that the functions $\Phi_\lambda(\vartheta)$, which, although simple and similar in form, strongly differ as regards the width of the maxima (see Fig. 1). It is also important that the functions $\Phi_\lambda(\vartheta)$ very weakly depend on the assumptions concerning the absorption coefficients ζ_l. This can be seen in Fig. 1, where $\Phi_\lambda(\vartheta)$ calculated for two variants of $\overline{\zeta}_l$ are shown. The dotted curve denotes Φ_λ for a black nucleus with $l_{max} = 3$ ($\zeta_l = 1$, $l \leq l_{max}$). The solid curve represents the functions Φ_λ calculated with values of ζ_l computed by Nemirovskiĭ for a semi-transparent spherical nucleus with a diffuse boundary for KR = 11.5 and E_n = 1.5 Mev ($\overline{\zeta}_0 = 0.45$, $\overline{\zeta}_1 = 0.95$, $\overline{\zeta}_2 = 0.29$, $\overline{\zeta}_3 = 0.50$).* The nonmonotonic character of $\overline{\zeta}_l$ reflects the existence of a "resonance shape" for the p and f waves. The effect of the resonances decreases, owing to the deformation of the target nucleus, as a result of which the true values of the functions Φ_λ prove to be intermediate between the two curves shown in Fig. 1, which, however, are very close to each other.

The angular distribution of the fission fragments has been studied experimentally by Blumberg and Leachman[8] and by Henkel and Simmons.[9] Comparison of the angular distributions for U^{233} ($J_0 = 5/2$; fission threshold of 1.6 Mev), Pu^{239} ($J_0 = 1/2$, threshold of 1.6 Mev) and U^{235} ($J_0 = 7/2$, threshold of 0.6 Mev) indicates the absence of an appreciable influence of the spin of the target nucleus. Moreover, according to the experimental data of Henkel and Simmons,[9] the angular distributions for these targets are described, within the limits of experimental accuracy, by the expression $1 + A\cos^2\vartheta$, where $A \approx 0.1-0.15$. Both these circumstances are evidence in favor of a Gaussian distribution for a(K).* On the other hand, the

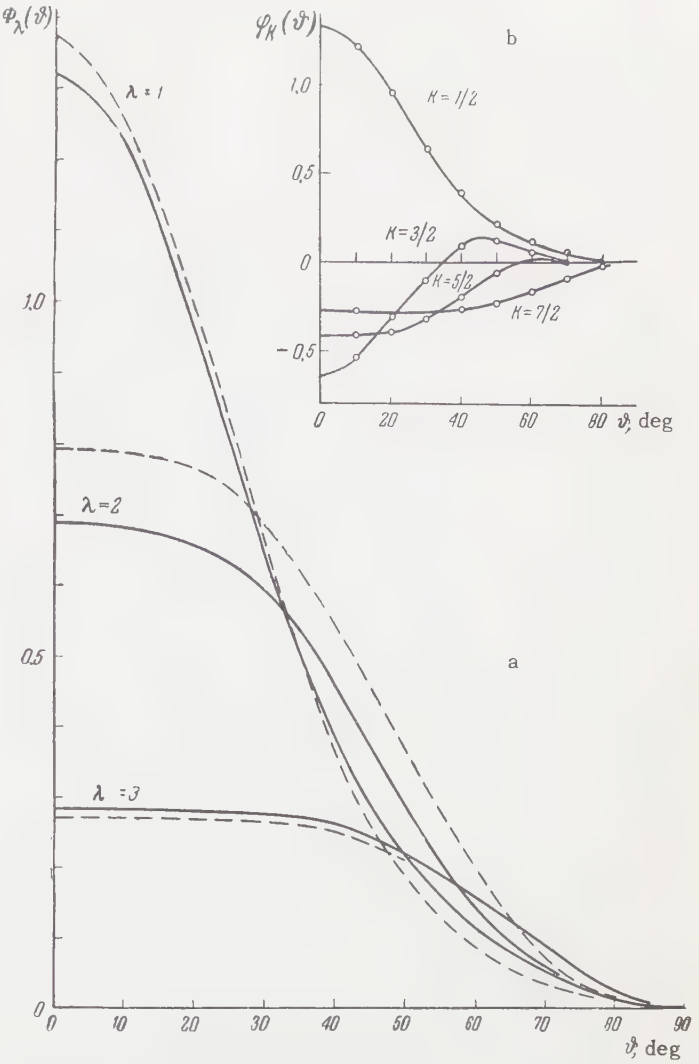

FIG. 1. a – functions $\Phi_\lambda(\vartheta)$ calculated for 1.5 Mev neutrons; solid curve corresponds to the optical model for a spherical nucleus with a diffuse boundary and with spin-orbit interaction (absorption coefficients are given in the text), dotted curve corresponds to the functions Φ_λ for a black nucleus and $l_{max} = 3$; b – functions $\varphi_K(\vartheta)$ calculated with formula (45) from the functions $\Phi_\lambda(\vartheta)$ for a semi-transparent nucleus (E_n = 1.5 Mev).

*The author expresses his indebtedness to P. É. Nemirovskiĭ for making available the results of his calculations of the absorption coefficients.

*For the determination of the value of K_0^2 from the experimental data, see references 8 and 9.

data of Blumberg and Leachman[8] for Pu^{239} and U^{233} apparently indicate the presence of substantial fluctuations in the distribution of a(K). Thus, on the basis of the angular distributions for $E_n = 1.5$, it has to be conceded that a(0) considerably exceeds the statistical value (it is 1.5 — 3 times as great).

The second term in formula (35) is associated with the selection rule for J in the state K = 0 for $J_0 = 5/2$ and $l_{max} = 3$-4, and does not exceed the value 0.02, which is within the limits of experimental error. For Pu^{239} ($J_0 = 1/2$), the amplitude of the second term is equal approximately to 0.15 — 0.20, i.e., larger than all values of the observed anisotropy. For the same values of the parameter $l^2/4K_0^2$ as for U^{233}, the presence of the second term in formula (35) should lead to the appearance of a relatively deep minimum at $\vartheta = 0°$ and a broad maximum at $\vartheta \approx 40°$, which is clearly contradicted by the experimental data.

Hence one may conclude that the interdiction on odd (or even) values of spin for an even (or odd) state of the nucleus does not occur, at least, for transition nucleus excitation energies $\gtrsim 3$ Mev. The absence of such an interdiction, well-known from weakly excited states of even-even deformed nuclei, may be associated with fluctuation deviations of the self-consistent field from axial symmetry. Such deviations may prove to be very important, since the criteria that the collective motion during fission be adiabatic are satisfied with only a small reserve[10] (see also reference 11). This would signify the impossibility of describing the nuclear state by means of a wave function of the rotational type. The quantum number K would have the meaning of a mean statistical constant of motion.

Comparison of the value of the anisotropy for U^{235}, U^{233}, and Pu^{239} (reference 9) indicates that there is a systematic tendency towards a small increase in the anisotropy for nuclei with larger values of J_0; the difference in the ratios $\sigma_f(0°)/\sigma_f(90°)$ is, in each case, approximately 0.03. This effect may be associated with the presence of the negative term proportional to K^4 in the expansion of a(K) in a series in K. Writing a(K) in the form

$$a(K) \approx 1 - (K^2/2K_0^2) - \varkappa K^4, \tag{40}$$

we obtain for the angular distribution

$$W(\vartheta) \approx 1 + (\bar{l}^2/4K_0^2)\cos^2\vartheta - \tfrac{3}{8}\varkappa \bar{l}^4 \sin^4\vartheta + \varkappa (J_0 + 1/2)^2 \bar{l}^2 \cos^2\vartheta. \tag{41}$$

Since the first three terms in formula (41) do not depend on J_0, comparison of the values of the anisotropy for different values of J_0 permits one to determine the parameter κ at once. For the indicated difference in the ratios $\sigma_f(0°)/\sigma_f(90°)$, we obtain $\kappa = (2-4) \times 10^{-4}$. For such κ, the last two terms in formula (41) have practically no influence on the shape of the angular distribution. The presence in the expansion of a(K) of a negative term proportional to K^4 gives a relative decrease in the contribution of large K in comparison with a Gaussian distribution.

6. In the case of neutron-induced fission of even-even nuclei ($J_0 = 0$), the angular distribution of the fragments is also described by formulas (30) — (32), where the coefficients β_λ are given by

$$\beta_\lambda = [a(1/2 - \lambda) - a(1/2 + \lambda)]/2a(1/2) \tag{42}$$

(for $S = 1/2$, σ_f is different from zero only for $K = 1/2$). If, now, the fission is characterized mainly by one value $K = K^*$, the coefficients a(K) in the numerator of formula (42) can be represented in the form

$$a(K) \approx a(K^*)\{\delta_{K,K^*} + \delta_{K,-K^*}\},$$

from which we obtain for the function $A(\vartheta)$

$$A(\vartheta) = [a(K^*)/2a(1/2)]\varphi_{K^*}(\vartheta), \tag{43}$$

$$\varphi_{K^*}(\vartheta) = \begin{cases} \Phi_1(\vartheta), & K^* = 1/2 \\ -\Phi_{K^*-1/2}(\vartheta), & K^* = l_{max} + 1/2 \\ \Phi_{K^*+1/2}(\vartheta) - \Phi_{K^*-1/2}(\vartheta), & K^* \neq 1/2,\ l_{max} + 1/2. \end{cases} \tag{43'}$$

The functions $\varphi_{K^*}(\vartheta)$ can also be represented in the form

$$\varphi_{K^*}(\vartheta) = 4\pi \sum_{l \geqslant K^* - 1/2} \zeta_l [\,|Y_{l,K^*-1/2}(\vartheta)|^2 + |Y_{l,K^*+1/2}(\vartheta)|^2] \Big/ \sum_l (2l+1)\zeta_l. \tag{43''}$$

For $K^* = 1/2$, we find

$$\sigma_f(\vartheta)/\sigma_f(90°) = 1 + \tfrac{1}{2}[\sigma_f(0°)/\sigma_f(90°)]\,\Phi_1(\vartheta), \tag{44}$$

where

$$\sigma_f(0°)/\sigma_f(90°) = \{1 - \tfrac{1}{2}\Phi_1(\vartheta)\}^{-1}.$$

The angular distribution for $K^* = 1/2$ is characterized by a sharp maximum for $\vartheta = 0°$ (the half-width of the maximum is of the order l_{max}^{-1}). For other values of K*, the function $\sigma_f(\vartheta)$ has a minimum at $\vartheta = 0°$. The width of the minimum increases, and its depth decreases, for larger K*. For small K* not equal to 1/2, there is also a small maximum at $\vartheta = 40 - 50°$. Figure 1 shows several functions $\varphi_K(\vartheta)$ calculated for a semi-transparent nucleus with $E_n = 1.5$ Mev. For another neutron energy (or other values of the absorption coefficients) the functions $\varphi_K(\vartheta)$, as is the case for the functions $\Phi_\lambda(\vartheta)$, can readily be calculated by formulas (32) — (43). For $E_n \lesssim 2$ Mev, the table can also be used.

For $K^* = 1/2$, the angular distribution of the fragments is determined single-valuedly if the function $\Phi_1(\vartheta)$ is known. For a neutron energy of 0.7 — 1.0 Mev, the value of $\Phi_1(0°)$ is 0.9 — 1.2, depending on the absorption coefficients. For E_n = 0.7 Mev, the optical model gives $\Phi_1(0°) = 1.05$ ($\overline{\xi}_0 = 0.35$, $\overline{\xi}_1 = 0.81$, $\overline{\xi}_2 = 0.12$, $\overline{\xi}_3 = 0.07$), from which, by formula (44), we find $\sigma_f(0°)/\sigma_f(90°) \simeq 2$. This value is close to the experimental value for Th^{230} (reference 12). Figure 2 shows the experimental data of Henkel and Brolley,[13] for fission of Th^{232} induced by 1.6-Mev neutrons. The solid and dotted curves represent the angular distributions calculated from formula (43) by means of the functions Φ_λ shown in Fig. 1 for a semi-transparent and a black nucleus, respectively, with $K^* = 3/2$. For the ratio of the coefficients, we have $a(3/2)/a(1/2) \approx 6 - 8$. The curve calculated with $\overline{\xi}_l$ for the optical model is in good agreement with the experimental data.

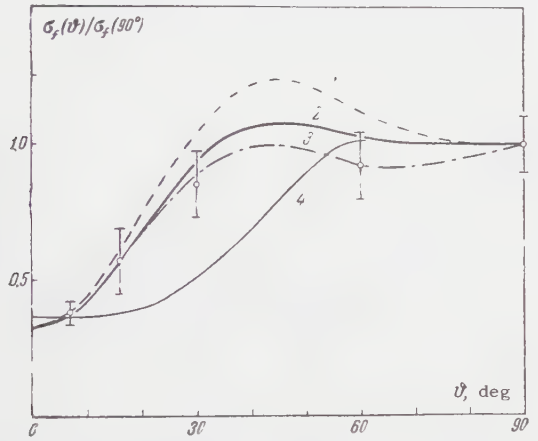

FIG. 2. Fragment angular distribution for fission of Th^{232} induced by 1.6-Mev neutrons, according to the data of Henkel and Brolley,[13] (experimental points). Curves 1 and 2 are the angular distributions for K = 3/2 for a semi-transparent and a black nucleus, respectively; Curve 3 is the "best" angular distribution for K = 3/2 determined by Wilets and Chase[14] by the method of least squares; Curve 4 was calculated from the optical model for K = 5/2.

The angular distribution of the fission fragments of Th^{232} was also analyzed by Wilets and Chase.[14] They represented the angular distribution in the form

$$\sum_{J=1/2}^{7/2} r(J) |D^J_{1/2\,1/2}(\vartheta)|^2 + \text{const},$$

where the coefficients r(J) were determined from the experimental points by the method of least squares. The curve obtained in this way is also shown in Fig. 2 (dash-dots). This curve differs little from the angular distribution calculated with the absorption coefficients for a semi-transparent nucleus. The difference between the solid and dotted curves in Fig. 2 is connected with the difference in the size of the contribution of $l = 2$ in the cases of black and semi-transparent nuclei. We note that in the case of a semi-transparent nucleus the choice of the parity of l, connected with the fact that the parity of the rotational states with respect to the same region should be the same, is not important, owing to the relatively small value of $\overline{\xi}_2$ in comparison with $\overline{\xi}_1$ and $\overline{\xi}_3$ in the optical model.

As shown by Henkel and Simmons,[9] there are many other cases of an "anomalous" angular distribution of fission fragments of even-even nuclei at neutron energies of the order 0.5 — 1.5 Mev. These distributions have the shape of the curves shown in Fig. 1b and may apparently be explained by the anomalously large contribution of fission with some particular value of K. Thus, for example, the angular distribution of the fission fragments of U^{236} for E_n = 0.85 Mev[9] is similar to the curve corresponding to $K^* = 3/2$ in Fig. 1b. In principle, the most complete information on the distribution of a(K) can be obtained from the experimental data directly from formula (30).

I express my sincere gratitude to B. T. Geĭlikman, D. P. Grechukhin and G. A. Pik-Pichak for valuable discussions on this work.

[1] I. Halpern and V. Strutinskiĭ, Second United Nations Intern. Conf. on the Peaceful Uses of Atomic Energy, Geneva, 1958, Vol. 15, p. 408.

[2] J. J. Griffin, Phys. Rev. **116**, 107 (1959).

[3] L. Wilets, op. cit. ref. 1, Vol. 15, p. 339.

[4] G. A. Pik-Pichak, JETP **36**, 961 (1959), Soviet Phys. JETP **9**, 679 (1959).

[5] V. M. Strutinskiĭ, JETP **30**, 606 (1956), Soviet Phys. JETP **3**, 638 (1956).

[6] G. A. Pik-Pichak, JETP **34**, 341 (1958), Soviet Phys. JETP **7**, 238 (1958).

[7] V. M. Strutinskiĭ, Атомная энергия (Atomic Energy) **2**, 508 (1957).

[8] L. Blumberg and R. B. Leachman, Phys. Rev. **116**, 102 (1959).

[9] R. H. Henkel and J. E. Simmons, Preprint.

[10] D. L. Hill and J. A. Wheeler, Phys. Rev. **89**, 1102 (1953).

[11] L. Wilets, Phys. Rev. **116**, 372 (1959).

[12] Gokhberg, Otroshchenko, and Shagin, Doklady Akad. Nauk SSSR **128**, 1157 (1959); Soviet Phys.-Doklady **4**, 1074 (1960).

[13] R. L. Henkel and J. E. Brolley, Jr., Phys. Rev. **103**, 1292 (1956).

[14] D. M. Chase and L. Wilets, Phys. Rev. **103**, 1296 (1956).

Translated by E. Marquit
144

MULTIPLE PROCESSES AND THE RELATIONS BETWEEN DIFFERENT TRANSITION MATRICES

B. T. VAVILOV and V. I. GRIGOR'EV

Moscow State University

Submitted to JETP editor April 18, 1960

J. Exptl. Theoret. Phys. (U.S.S.R.) **39**, 794-799 (September, 1960)

An infinite chain of equations relating the matrices of different transitions is constructed. After mass renormalization the equations are applied to multiple boson production in two-fermion collisions.

1. The transition from an initial state $|\ ink\ >$ with i bosons, n fermions and k antifermions to a final state $|\ jm\mathit{l}\ >$ may be represented by the matrix $V^{(ij,\ nm,\ k\mathit{l})}\ [\sigma, \sigma_0]$, which is related to the general transition matrix $V[\sigma, \sigma_0]$ (the S matrix for finite time intervals) by

$$\langle jml\,|\,V^{(ij,\ n,\ m,\ kl)}[\sigma, \sigma_0]\,|\,ink\rangle = \langle jml\,|\,V[\sigma, \sigma_0]\,|\,ink\rangle. \quad (1)$$

The general transition matrix $V[\sigma, \sigma_0]$ satisfies the Tomonaga-Schwinger equation with an interaction Hamiltonian $H(x)$ which in theories of the "electrodynamical type" is bilinear with respect to fermion (and antifermion) operators and linear with respect to boson operators.

In order to arrive at a system of equations linking the matrices of different transitions $V^{(\xi)}$ we proceed as follows:

a) We take the matrix element of the left-hand and right-hand sides of the equation for $V[\sigma, \sigma_0]$, for the initial state $|\ ink\ >$ and the final state $|\ jm\mathit{l}\ >$.* In accordance with (1), $V^{(\xi)}$ with different sets of indices ξ is obtained from different terms of the equation for $V[\sigma, \sigma_0]$.

b) For equality of the matrix elements obtained through a) it is sufficient to have equality of the operators whose matrix elements have been taken. This condition furnishes a system of linked equations relating different $V^{(\xi)}$.

c) The entire system must now be put into a form convenient for applications, wherein $V^{(ij,\ nm,\ k\mathit{l})}$ is given in terms of normal products of j boson-creation operators and i boson-destruction operators and, correspondingly, m and l creation operators together with n and k destruction operators for fermions and antifermions. For this purpose, from the equation obtained through b) for a given set of indices $(ij, nm, k\mathit{l})$ we subtract the equation for $(i-1, j-1; n-1, m-1; k-1, \mathit{l}-1)$.

The foregoing procedure results in the system

$$i\delta V^{(ij,\ nm,\ kl)}/\delta\sigma = \sum_{\substack{\alpha,\beta,\gamma\\ a,b,c\\ p,q,r}} \hat{H}^{(\alpha\beta\gamma)}_{(abc)} V^{(i-a+ap,\ j-\alpha+ap;\ n-b+bq,\ m-\beta+bq;\ k-c+cr,\ l-\gamma+cr)}_{(pqr)} \quad (2)$$

Here $\hat{H}^{(\alpha\beta\gamma)}_{(abc)}$ is the term of the interaction Hamiltonian containing α, β, γ creation operators for bosons, fermions and antifermions, respectively, and a, b, c corresponding destruction operators. The indices p, q, r indicate that of the creation operators in $V^{(\xi)}_{(pqr)}$ by definition p boson, q fermion and r antifermion operators contract with the corresponding destruction operators in the interaction Hamiltonian.*

The system of equations (2) requires considerable modification since it represents a system of "mathematical" particles. We shall perform a mass renormalization. When the masses of particles in the equations for field operators, in the Heisenberg representation, are taken to be the observed experimental masses, terms with pure electromagnetic (field) additions to the masses appear. When these terms are included in the interaction Hamiltonian, after passing to the interaction representation we obtain the familiar equation that includes counterterms. All field operators will now obey the equations for free physical particles with the experimentally observed masses. Performing operations a), b) and c) as above, we obtain (2) with its right-hand side increased by

*We may speak of operators on both mathematical and physical particles. These differ in their numerical factors, which are combinations of contractions and which will subsequently be canceled.

*We here sum over all possible combinations of contractions which are permissible for given values of α, β, and γ.

the counterterms

$$-\sum_{\gamma,\beta;\ b,c;\ q,r} \Delta\hat{M}^{(\beta\gamma)}_{(bc)} V^{(ij;\ n-b+bq,\ m-\beta+bq;\ k-c+cr,\ l-\gamma+cr)}_{(pqr)}$$

$$-\sum_{\alpha,a;\ p\leqslant a} \Delta\hat{m}^{(\alpha)}_{(a)} V^{(i-a+p,\ j-\alpha+p;\ nm,\ kl)}_{(p00)}, \qquad (3)$$

where the summations over γ, β, b, c, q and r are taken from 0 to 1, and over α, a and p from 0 to 2.

In (3) the quantity $\Delta\hat{M}^{(\beta\gamma)}_{(bc)}$ denotes the term of the operator for the electromagnetic mass of a fermion (or antifermion) which contains β fermion-emission operators and b fermion-absorption operators as well as γ and c corresponding antifermion operators. $\Delta\hat{m}^{(\alpha)}_{(a)}$ is the boson counterterm with α boson-creation operators and a boson-destruction operators.

Prior to the renormalization we must introduce additional conditions determining the constants in the counterterms, which we denote by the same symbols ΔM and Δm as the operators. We take these conditions to be*

$$V^{(11,\ 00,\ 00)}[\sigma,\ \sigma_0] = 0, \qquad V^{(00,\ 11,\ 00)}[\sigma,\ \sigma_0] = 0 \qquad (4)$$

The conditions (4) are favored by the following considerations:

1) If all terms contributing to the self-energy are excluded from the renormalized equations (2), then (4) follows directly from (2).

2) The usual result is obtained by means of (4) through the use of perturbation theory.

3) If only one particle, such as one boson, exists in the initial state, then from the condition that this is a physical particle it follows that the only operator which describes the temporal development of this system is $V^{(00,00,00)}[\sigma,\ \sigma_0]$, which is the amplitude of the probability that no particle creation or destruction occurs.

4) The conditions (4) lead to the cancellation of counterterms in the equations for any (ξ). This corresponds to the usual requirement of the renormalization method that neither the electromagnetic nor the bare mass should appear separately in transition amplitudes.

Our conditions (4) for mass renormalization differ in form from the usual conditions at least in so far as they do not require (although they do not exclude) the use of propagation functions other than those which correspond to the first perturbation approximation (but with the experimental masses).

*The vanishing of a number of other matrices such as $V^{(00,00,11)}$ follows from (4) and cross symmetry; this cannot be regarded as an independent auxiliary condition.

2. We shall now apply the foregoing method to the creation of N scalar (or pseudoscalar) bosons in two-fermion collisions. Several quantized field-theoretical studies of this problem have appeared (references 1—4 and others), but none of these can be regarded as sufficiently complete since they all remained within the bounds of perturbation theory.

The calculation that we present below does not of course solve (2) and (3) exactly, which we could hardly expect to do in general form. However, our simplifying assumptions do not represent the rejection of diagrams of sufficiently high orders, but rather the summation of an infinite number (not all) of the diagrams. We can regard this as a way of proceeding beyond the perturbation theory.

The simplifying assumptions may be formulated as follows:

a) The creation of fermion-antifermion pairs is excluded from consideration both in the final state and in intermediate states.* The indices k and l are always zero and need never be written.

b) Only central collisions of nucleons are assumed to occur.

c) The region of very high energies is considered, where many bosons are created.

d) It is assumed that the great majority of bosons have approximately the same energy (depending on the initial nucleon energy, of course). This approximates experimental results.†

On the basis of the foregoing assumptions we shall now write a system of linked equations for the matrix $V^{(0N,\ 22)}$ representing the production of N bosons in a two-fermion collision. We begin with the usual interaction Hamiltonian for scalar bosons in the case of scalar coupling:‡

$$H_I = g\bar{\psi}\psi\varphi(x), \qquad (5)$$

where, as usual,

$$\bar{\psi} = \bar{u} + v, \qquad \psi = u + \bar{v}, \qquad \varphi = \varphi^{(+)} + \varphi^{(-)}$$

In virtue of a), (5) is replaced by

*This assumption formally destroys the unitarity of the theory since the probability $|V^{(0)}|^2$ of the initial state is constant and equal to unity (see also reference 5). However, this can have only a small effect on the cross section since the exponentially diminishing factor that appears in $V^{(0)}$ in the exact treatment cancels the corresponding factor in $V^{(\xi)}$. This comment does not, of course, apply to processes whose very occurrence depends upon taking antifermions into account.

†The actual energy distribution is far from being δ-like. However, since we must sum over finite states, the integral over all finite energies is important rather than the detailed shape of the distribution.

‡In the case of pseudoscalar coupling for pseudoscalar mesons the same results are obtained for the multiplicity.

$$H_I = g\bar{u}u\{\varphi^{(+)} + \varphi^{(-)}\}. \quad (6)$$

Then, in accordance with (2), the equations for $V^{(0N,\ 22)}$ are

$$i\delta V^{(0N,\ 22)}/\delta\sigma = g\bar{u}u\varphi^{(+)}(x)\,V^{(0N-1,22)}_{(01)} + g\bar{u}u\varphi^{(-)}(x)\,V^{(0N+1,11)}_{(10)} + g\bar{u}u\varphi^{(-)}(x)\,V^{(0N+1,22)}_{(11)} - \Delta M\bar{u}u(x)\,V^{(0N,\ 22)}_{(01)}, \quad (7)$$

$$i\delta V^{(0N,\ 11)}/\delta\sigma = g\bar{u}u\ \varphi^{(+)}(x)\ V^{(0N-1,11)}_{(01)}\ g\bar{u}u\varphi^{(-)}(x)\,V^{(0N+1,11)}_{(11)} - \Delta M\bar{u}u(x)\,V^{(0N,\ 11)}_{(01)}. \quad (8)$$

Since we are considering central collisions (s states) it may be assumed that the existence of fermion spin cannot strongly affect the cross section. In our opinion, the matrix-type fermion propagation function can now be replaced with a numerical function which will correctly represent only the energy dependence of the exact propagation function. A similar procedure has been followed in the so-called Bloch-Nordsieck model.[6] A possible form of the approximate propagation function is*

$$S_c(p) = i(2\pi)^{-4}/E_p.$$

The employment of c-number propagation functions simplifies (7) and (8), which in virtue of (4) now appear as

$$iV^{(0N,\ 22)}[\sigma,\ \sigma_0] = g\int_{\sigma_0}^{\sigma} d^4x_1\,\bar{u}(x_1)\,u(x_1)\,\varphi^{(+)}(x_1)\,V^{(0N-1,22)}_{(01)}[\sigma_1,\ \sigma_0] + g\int_{\sigma_0}^{\sigma} d^4x_1\bar{u}(x_1)\,u(x_1)\,\varphi^{(-)}(x_1)\,V^{(0N+1,11)}_{(10)}[\sigma,\ \sigma_0] + \frac{g^2}{i}\int_{\sigma_0}^{\sigma} d^4x_1d^4x_2\,\bar{u}(x_1)\,u(x_1)\,\varphi^{(-)}(x_1)\varphi^{(+)} \times (x_2)\,\bar{u}(x_2)\,u(x_2)\,V^{(0N,\ 22)}_{(02)}[\sigma_2,\ \sigma_0], \quad (9)$$

$$iV^{(0N,\ 11)}[\sigma,\sigma_0] = g\int_{\sigma_0}^{\sigma} d^4x_1\,\bar{u}(x_1)\,u(x_1)\,\varphi^{(+)}(x_1)\,V^{(0N-1,11)}_{(01)}[\sigma_1,\ \sigma_0]. \quad (10)$$

The solutions of (9) and (10) will be sought in the forms

$$V^{(0N,\ 22)}[\sigma,\ \sigma_0] = \int_{\sigma_0}^{\sigma} d^4x\ \sum\bar{u}(p_1)\,\bar{u}(p_2)\,u(q_1)\,u(q_2) \times \prod_{i=1}^{N}\varphi^{(+)}(k_i)\,Q_N(\mathbf{p}_1,\ \mathbf{p}_2,\ \mathbf{q}_1,\ \mathbf{q}_2,\ \mathbf{k}_1\ldots\mathbf{k}_N) \times \exp\left\{ix\left(p_1+p_2-q_1-q_2+\sum_{\alpha=1}^{N}k_\alpha\right)\right\}, \quad (11)$$

*Other possible forms of this function, $i(2\pi)^{-4}|\mathbf{p}|/(p^2-m^2)$, $i(2\pi)^{-4}/|\mathbf{p}|$, $i(2\pi)^{-4}/(E_p-|\mathbf{p}|)$, yield identical results for the multiplicity. We shall everywhere neglect the rest masses of nucleons compared with their initial and final kinetic energies.

$$V^{(0N,\ 11)}[\sigma,\ \sigma_0] = \int_{\sigma_0}^{\sigma} d^4x\ \sum\bar{u}(p)\,u(q) \times \prod_{i=1}^{N}\varphi^{(+)}(k_i)\,B_N(\mathbf{p},\ \mathbf{q},\ \mathbf{k}_1\ldots\mathbf{k}_N) \times \exp\left\{ix\left(p-q+\sum_{\alpha=1}^{N}k_\alpha\right)\right\}, \quad (12)$$

where $\mathbf{q}_1(\mathbf{q}_1,\ E_{q_1})$, $\mathbf{q}_2(\mathbf{q}_2,\ E_{q_2})$ are the 4-momenta of fermions in the initial state, while $\mathbf{p}_1(\mathbf{p}_1,\ E_{p_1})$, $\mathbf{p}_2(\mathbf{p}_2,\ E_{p_2})$ and $\mathbf{k}_\alpha(\mathbf{k}_\alpha,\ \omega_\alpha)$ are the 4-momenta of fermions and of the α-th boson in the final state (in the laboratory system).

Substituting

$$Q_N = \tilde{Q}_N(\mathbf{q}_1,\ \mathbf{q}_2,\ \mathbf{k}_1\ldots\mathbf{k}_N)/|\mathbf{p}_2-\mathbf{p}_1|^2, \qquad B_N = \tilde{B}_N(\mathbf{q},\ \mathbf{k}_1\ldots\mathbf{k}_N)/|\mathbf{p}|^2 \quad (13)$$

and transforming to the center-of-mass system, where

$$\mathbf{q}_1 = -\mathbf{q}_2 = \mathbf{q}, \qquad \mathbf{p}_1 = -\mathbf{p}_2 = \mathbf{p}, \qquad E_{q_1} = E_{q_2} = E_q, \qquad E_{p_1} = E_{p_2} = E_p, \qquad |\mathbf{k}_\alpha| = k_E,$$

we obtain from (9) and (10):

$$\tilde{Q}_N\left(1+\frac{g^2}{8\pi^2}\right) = g\left[E_q - \frac{1}{2}\sum_{\alpha=1}^{N}\omega_\alpha\right]^{-1}\tilde{Q}_{N-1} - \frac{4g^{N+2}}{\mu^2}(N+1)\prod_{j=1}^{N}\left[E_q - \frac{1}{2}\sum_{\alpha=1}^{j}\omega_\alpha\right]^{-1}. \quad (14)$$

In arriving at (14) we have neglected $|\mathbf{k}_\alpha|$ compared with $|\mathbf{p}|$.

The solution of (14) is

$$\tilde{Q}_N = -\frac{4}{\mu^2}g^{N+2}\frac{1}{\lambda^N}\sum_{j=1}^{N}\lambda^{j-1}(j+1)\prod_{i=1}^{N}\frac{1}{E_q - i\omega_E/2}, \quad (15)$$

where

$$\lambda = 1 + g^2/8\pi^2.$$

With the aid of (15), (13) and (11) the probability amplitude of the transition in question is found to be

$$S_N = K(16\pi)^N g^{N+2}\lambda^{1/N}\sum_{j=1}^{N}\lambda^{j-1}(j+1)\,N^{-3N/2}E^{N/2}, \quad (16)$$

where K is a coefficient which is independent of N. The mean number of created bosons is now found to be

$$\bar{N} = [16\pi g]^{3/5}E^{1/5}/2.7, \quad (17)$$

where E is the initial nucleon energy in the laboratory system.

The multiplicity represented by (17) agrees relatively well with some experimental high-energy data, but agrees somewhat less well (although the order of magnitude remains correct) at lower en-

ergies. This quite naturally reflects the important role of noncentral collisions in the latter case. The results interests us not so much from the standpoint of a quantitative analysis of the processes at high energies but because of its methodological significance, since it shows that field theory does not produce absurd results.

Further study is required to determine how the final results are affected by our hypotheses that antifermions play an unimportant part and that exact propagation functions may be replaced with c-number functions. This type of analysis, like the foregoing calculation, should not be based on perturbation theory and can in principle be conducted along the lines of the method proposed here.

The authors wish to thank E. L. Feĭnberg and D. S. Chernavskiĭ for several valuable comments.

[1] Lewis, Oppenheimer, and Wouthuysen, Phys. Rev. **73**, 127 (1948).

[2] W. Heitler and E. Janossy, Proc. Phys. Soc. (London) **A62**, 669 (1949).

[3] H. Fukuda and G. Takeda, Prog. Theoret. Phys. (Kyoto) **5**, 957 (1950).

[4] Umezawa, Takahashi, and Kamerfuchi, Phys. Rev. **85**, 505 (1952).

[5] F. J. Dyson, Phys. Rev. **75**, 1736 (1949).

[6] F. Bloch and A. Nordsieck, Phys. Rev. **52**, 54 (1937).

Translated by I. Emin
145

ON THE SINGULARITIES OF COSMOLOGICAL SOLUTIONS OF THE GRAVITATIONAL EQUATIONS

E. M. LIFSHITZ and I. M. KHALATNIKOV

Institute of Physics Problems, Academy of Sciences, U.S.S.R.

Submitted to JETP editor April 19, 1960

J. Exptl. Theoret. Phys. (U.S.S.R.) **39**, 800-808 (September, 1960)

We obtain a broad class of cosmological solutions of the gravitational equations, which contains seven arbitrary physically different functions of the spatial coordinates. This number is only one less than the number of functions necessary for the description of an arbitrary initial distribution of the matter and gravitational field in the general case.

1. FORMULATION OF THE PROBLEM

THE particular classes of cosmological solutions of the equations of gravitation, obtained in the preceding communication[1] (referred to henceforth as I), show that the presence of singularities is, in any case, a rather broad property of such solutions. This is evidenced by various exact solutions (i.e., those valid over all of space at all instants of time), obtained by different authors under definite, sometimes special, assumptions concerning their form (see, for example, references 2 and 3).

However, all these solutions can by themselves not answer the main question of whether the presence of a singularity is a general property of the cosmological solutions, not connected with any specific assumption regarding the character of the distribution of matter and of the gravitational field. An affirmative answer to this question would mean that the equations of gravitation have a general solution with a singularity and with as many arbitrary functions of the coordinates as are necessary to specify the arbitrary initial conditions at a certain instant of time. To the contrary, the lack of a solution (with singularity) with this number of arbitrary functions would denote that the case of arbitrary distribution of matter and field does not, generally speaking, lead to the presence of a singularity.

We thus arrive at the following formulation of the problem: assuming the singularity to exist, it is required to find near the singularity the form of the broadest class of solutions of the equations of gravitation in such a way, that we can judge whether this solution is general from the number of the arbitrary functions of the coordinates contained in this solution.

Among the arbitrary functions contained in any given solution of the equations of gravitation there are, generally speaking, such whose arbitrariness is merely due to the arbitrary choice of reference frame. We obviously need be interested only in the "physically different" arbitrary functions, the number of which cannot be reduced by any choice of reference frame. From physical considerations it is readily seen that the number of such functions should in the general case be equal to eight: the arbitrary initial conditions should specify the initial spatial distribution of the density of matter, its three velocity components, and four additional quantities which determine the free gravitational field (i.e., the field not connected with the matter). We can arrive at this last number, for example, by considering weak gravitational waves: by virtue of their transverse nature, their field is determined by two quantities (the components g_{ik}) which satisfy a second-order equation (the wave equation), and therefore the initial conditions for them should be specified by four functions of the coordinates.

We shall use here, as in I, a reference frame subject to conditions I (1.3): $g_{0\alpha} = g_{00} = -1$. L. D. Landau has indicated long ago that in such a system one of the equations of gravitation [Eq. I (1.4)] makes it immediately possible to prove that the determinant g must vanish within a finite time (this was also noted by Komar[4]). This fact, however, does not in itself prove in any manner the necessity for the existence of a true physical singularity in the solutions, since the singularity (the vanishing of g) may prove to be fictitious, and may disappear on going to other reference frames. Furthermore, V. V. Sudakov has indicated that in the given case such a fictitious singularity should exist by virtue of the character of the chosen ref-

erence frame. It is easily seen that in this system the time lines (i.e., the lines x^1, x^2, x^3 = const) represent a family of geodesics. But the lines of such a family, on which no special parallelness conditions are imposed, will generally intersect each other on certain hypersurfaces — four-dimensional analogs of the caustic surfaces in geometrical optics. On the other hand, the intersection of the coordinate lines denotes the vanishing of the corresponding components of the metric tensor, and the determinant g also vanishes. The metric will therefore have a singularity on the indicated hypersurfaces, but not a physical one.*

In the present communication we give a very broad class of solutions of the equations of gravitation, obtained during the course of the indicated program. These solutions have physical singularities, but the class is still not general; it contains seven arbitrary functions, i.e., only one less than required in the general case.

2. CASE OF EMPTY SPACE

We begin the construction of this solution with the case of empty space.

In the absence of matter, the right halves of the general equations I (1.4) — (1.6) are replaced by zeroes; we rewrite these equations in the form

$$R_0^0 = \frac{1}{2}\frac{\partial^2}{\partial t^2}\ln(-g) + \frac{1}{4}\varkappa_\alpha^\beta\varkappa_\beta^\alpha = 0, \tag{2.1}$$

$$R_\alpha^0 = \frac{1}{2}\frac{\partial^2}{\partial x^\alpha \partial t}\ln(-g) - \frac{1}{2}\varkappa_{\alpha;\ \beta}^{\beta} = 0, \tag{2.2}$$

$$R_\alpha^\beta = P_\alpha^\beta + \frac{1}{2\sqrt{-g}}\frac{\partial}{\partial t}(\sqrt{-g}\varkappa_\alpha^\beta) = 0. \tag{2.3}$$

We seek a first-approximation solution of these equations near the singularity (principal terms of the expansion) in the form

$$g_{\alpha\beta} = t^{2p_1}l_\alpha l_\beta + t^{2p_2}m_\alpha m_\beta + t^{2p_3}n_\alpha n_\beta, \tag{2.4}$$

where $\mathbf{l}$, $\mathbf{m}$ and $\mathbf{n}$ are three-dimensional vectors, which are functions of the coordinates. The exponents p_1, p_2, and p_3 may also be functions of the coordinates. The determinant of this tensor is

$$-g = (\mathbf{l}[\mathbf{m}\times\mathbf{n}])^2 t^{2(p_1+p_2+p_3)}. \tag{2.5}$$

The tensor $g^{\alpha\beta}$, which is the reciprocal of the tensor (2.4), can be written in the form†

$$g^{\alpha\beta} = \sum t^{-2p_1}\tilde{l}_\alpha\tilde{l}_\beta. \tag{2.6}$$

Here and below the summations are over the cyclic permutations of the vectors $\mathbf{l}$, $\mathbf{m}$, and $\mathbf{n}$ and of the numbers p_1, p_2, and p_3; we use the notation

$$\tilde{\mathbf{l}} = [\mathbf{m}\times\mathbf{n}]/(\mathbf{l}[\mathbf{m}\times\mathbf{n}]),\ \tilde{\mathbf{m}} = [\mathbf{n}\times\mathbf{l}]/(\mathbf{l}[\mathbf{m}\times\mathbf{n}]),\ \tilde{\mathbf{n}} = [\mathbf{l}\times\mathbf{m}]/(\mathbf{l}[\mathbf{m}\times\mathbf{n}]) \tag{2.7}$$

for the vectors which are "reciprocal" to the vectors $\mathbf{l}$, $\mathbf{m}$, and $\mathbf{n}$ (so that $\mathbf{l}\cdot\tilde{\mathbf{l}} = 1$, $\tilde{\mathbf{l}}\cdot\tilde{\mathbf{m}} = \tilde{\mathbf{l}}\cdot\tilde{\mathbf{n}} = 0, \ldots$). We have, furthermore,

$$\varkappa_{\alpha\beta} = \sum 2p_1 t^{2p_1-1}l_\alpha l_\beta, \qquad \varkappa_\alpha^\beta = t^{-1}\sum 2p_1 l_\alpha\tilde{l}_\beta,$$
$$\varkappa^{\alpha\beta} = \sum 2p_1 t^{-2p_1-1}\tilde{l}_\alpha\tilde{l}_\beta. \tag{2.8}$$

Substitution of (2.5) and (2.8) in (2.1) leads to

$$p_1 + p_2 + p_3 = p_1^2 + p_2^2 + p_3^2. \tag{2.9}$$

We now make the assumption that in Eq. (2.3) the three-dimensional curvature tensor P_α^β does not contribute to the principal terms of the equation.* Then the principal terms are of order t^{-2} and vanish if $p_1 + p_2 + p_3 = 1$. Together with relation (2.9) we obtain, therefore,

$$p_1 + p_2 + p_3 = 1, \qquad p_1^2 + p_2^2 + p_3^2 = 1. \tag{2.10}$$

These two equations relate the three functions p_1, p_2, and p_3 and consequently only one of these is independent.† With this, p_1, p_2, and p_3 never

*The analytic form of the metric near such a fictitious singularity will be indicated in another communication.

†The vector-operation symbols (vector products, the operations curl, grad, etc.) must be understood throughout in a purely formal manner, as operations on the components of the vectors $\mathbf{l}$, $\mathbf{m}$, and $\mathbf{n}$ as if the coordinates x^1, x^2, x^3 were Cartesian.

*There are apparently no broad classes of solutions which do not satisfy this condition. A relatively narrow class (which will be given later on) is obtained for constant values of p_1, p_2, and p_3 equal to s_1, s_2, and 1 respectively, where s_1 and s_2 are two numbers that satisfy the condition $s_1 + s_2 = s_1^2 + s_2^2$.

Relation (2.9) [i.e., Eq. (2.1)] is satisfied also when $p_1 = p_2 = p_3 = 1$, i.e., when $g_{\alpha\beta} = t^2 a_{\alpha\beta}$, where the $a_{\alpha\beta}$ are functions of the coordinates. Then Eq. (2.3) yields $P_{\alpha\beta} = -2a_{\alpha\beta}$; this means that the space has a constant negative curvature (independent of the coordinates of the point). The corresponding space-time metric can be written with the aid of "four-dimensional spherical coordinates" χ, θ, φ in the form

$$-ds^2 = -dt^2 + t^2[d\chi^2 + \mathrm{sh}^2\chi\,(d\theta^2 + \sin^2\theta\cdot d\varphi^2)]$$

(see, for example, reference 5, Sec. 104). But the transformation $r = t\sinh\chi$, $\tau = t\cosh\chi$ transforms such a metric simply to the Galilean metric

$$-ds^2 = -d\tau^2 + dr^2 + r^2(d\theta^2 + \sin^2\theta d\varphi^2).$$

†The constant numbers p_1, p_2, and p_3, which are related by Eqs. (2.9), were first used in the exact solution of Eqs. (2.1) — (2.3), indicated by Taub,[6] corresponding to a completely homogeneous (but not isotropic) empty space:

$$-ds^2 = -dt^2 + t^{2p_1}dx_1^2 + t^{2p_2}dx_2^2 + t^{2p_3}dx_3^2.$$

When $p_1 = p_2 = 0$ and $p_3 = 1$, the transformation $x_1 = x$, $x_2 = y$, $t\sinh x_3 = z$, $t\cosh x_3 = \tau$ makes this metric Galilean, i.e., the singularity is fictitious. At these values of p_1, p_2, and p_3 the singularity is also fictitious for the metric (2.4) (although the latter is, naturally, not Galilean). We exclude these values from further consideration.

have the same value simultaneously, and two of them are equal only in the triplets 0, 0, 1 and $-\frac{1}{3}$, $\frac{2}{3}$, $\frac{2}{3}$. In all other cases p_1, p_2, p_3 are all different, one being negative and the other two positive. We shall arrange these values in the order $p_1 < p_2 < p_3$. The quantities p_1, p_2, and p_3 run through their values in the following respective intervals

$$-\tfrac{1}{3} \leqslant p_1 \leqslant 0, \qquad 0 \leqslant p_2 \leqslant \tfrac{2}{3}, \qquad \tfrac{2}{3} \leqslant p_3 \leqslant 1.$$

They can be represented in parametric form as

$$p_1 = \frac{-s}{1+s+s^2}, \qquad p_2 = \frac{s(1+s}{1+s+s^2},$$
$$p_3 = \frac{1+s}{1+s+s^2}, \tag{2.11}$$

as the parameter s runs through values from 0 to 1. The figure shows the curves that determine any two of the values p_1, p_2, or p_3 once the third is specified (the three values lie on one vertical line).

The conditions (2.10) ensure the vanishing of the contribution $\sim t^{-2}$ from the second term in Eq. (2.3); in accordance with the assumption made, it is necessary also to ensure the absence of terms of the same order from the tensor P_α^β.

Inasmuch as the metric has an essentially different time dependence along the directions **l**, **m**, and **n**, it is convenient to "project" all the tensors on these directions. Denoting the corresponding projections by the subscripts l, m, and n we determine them in the following manner:

$$P_{ll} = P_{\alpha\beta}\tilde{l}_\alpha\tilde{l}_\beta, \qquad P_{lm} = P_{\alpha\beta}\tilde{l}_\alpha\tilde{m}_\beta, \ldots \tag{2.12}$$

In this notation we have, in particular,

$$g_{ll} = t^{2p_1}, \qquad g_{mm} = t^{2p_2}, \qquad g_{nn} = t^{2p_3}.$$

The "mixed" tensor components are defined accordingly as

$$P_l^l = P_{ll}/g_{ll} = t^{-2p_1}P_{ll}, \qquad P_l^m = P_{lm}/g_{mm} = t^{-2p_2}P_{lm}, \ldots \tag{2.13}$$

The calculation of the components of the tensor $P_{\alpha\beta}$ from the general formulas with the aid of the metric tensor (2.4) leads to the following expressions for the highest-order terms:

$$P_l^l = -P_m^m = -P_n^n = \frac{(\mathbf{l}\ \mathrm{curl}\ \mathbf{l})^2}{2(\mathbf{l}\,[\mathbf{m}\times\mathbf{n}])^2}t^{-2(1-2p_1)},$$
$$P_{lm} = 2\frac{(\mathbf{l}\ \mathrm{curl}\ \mathbf{l})\,p_{1,n}}{(\mathbf{l}\,[\mathbf{m}\times\mathbf{n}])}\ln t\cdot t^{2(p_1-p_2)},$$
$$P_{ln} = -2\frac{(\mathbf{l}\ \mathrm{curl}\ \mathbf{l})\,p_{1,m}}{(\mathbf{l}\,[\mathbf{m}\times\mathbf{n}])}\ln t\cdot t^{2(p_1-p_2)},$$
$$P_{mn} = 2\ln^2 t\cdot(p_{2,n}p_{1,m} + p_{3,m}p_{1,n} - p_{1,m}p_{1,n}). \tag{2.14}$$

The letters l, m, and n following the comma in the subscripts denote here differentiation in the corresponding direction, in accordance with the definition

$$f_{,l} = \tilde{l}_\alpha\partial f/\partial x^\alpha, \ldots$$

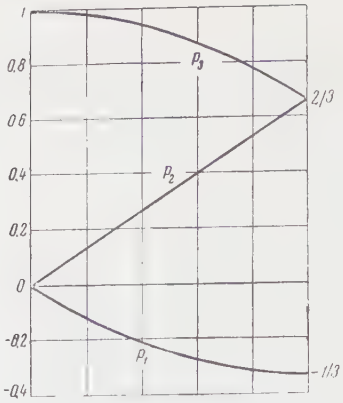

Since $p_1 < 0$, we see that the power of $1/t$ in the diagonal components $P_l^l, \ldots$, does not exceed 2. To satisfy Eqs. (2.3) it is therefore necessary in any case that these terms vanish, i.e., we must have

$$\mathbf{l}\ \mathrm{curl}\ \mathbf{l} = 0. \tag{2.15}$$

We note that this condition has a simple geometrical meaning. The vector satisfying this condition can be represented in the form $\mathbf{l} = \psi\ \mathrm{grad}\ \varphi$ (ψ and φ are two scalar functions), so that $l_\alpha l_\beta dx^\alpha dx^\beta = \psi^2 d\varphi^2$. This means that the direction of the vector **l** at each point of space can be chosen as the direction of the coordinate x^1 (so that the surfaces $\varphi = \mathrm{const}$ become the surfaces $x^1 = \mathrm{const}$). It is well known that in the general case of an arbitrary three-dimensional vector field this is, generally speaking, impossible.

If condition (2.15) is satisfied, the principal terms in the components of the tensor $P_{\alpha\beta}$ are found to be of the following order of magnitude

$$P_l^l \sim P_m^m \sim P_n^n \sim \ln^2 t,$$
$$P_{lm} \sim t^{2(p_2-p_3)}\ln t, \qquad P_{ln} \sim P_{mn} \sim \ln^2 t, \tag{2.16}$$

and in the main do not influence the equations (2.3).

It remains for us to satisfy Eqs. (2.2). The largest terms in these equations could have an order $t^{-1}\ln t$: these terms appear when differentiating the exponents in the derivatives of $g_{\beta\gamma}$ with respect to the coordinates contained in the expression

$$\varkappa^\beta_{\alpha;\,\beta} = \frac{1}{\sqrt{-g}}\frac{\partial}{\partial x^\beta}(\sqrt{-g}\varkappa^\beta_\alpha) - \frac{1}{2}\varkappa^{\beta\gamma}\frac{\partial g_{\beta\gamma}}{\partial x^\alpha}.$$

However, by virtue of (2.10), these terms cancel out identically:

$$\varkappa^{\beta\gamma}\frac{\partial g_{\beta\gamma}}{\partial x^\alpha} = 4\sum p_1 t^{-2p_1-1}\tilde{l}_\beta\tilde{l}_\gamma\cdot\sum t^{2p_1}\ln t\frac{\partial p_1}{\partial x^\alpha}l_\beta l_\gamma$$
$$= 4\frac{\ln t}{t}\sum p_1\frac{\partial p_1}{\partial x^\alpha} = 2\frac{\ln t}{t}\frac{\partial}{\partial x^\alpha}(p_1^2+p_2^2+p_3^2) = 0.$$

Therefore the principal terms are those of order $1/t$. The first term in (2.2) in this approximation vanishes, and the calculation of the derivative $\kappa^{\beta}_{\alpha;\beta}$ leads to

$$R^0_\alpha = -\frac{1}{t\,(\mathbf{l}\,[\mathbf{m}\times\mathbf{n}])}\sum l_\alpha \{[\mathbf{m}\times\mathbf{n}]\,\nabla p_1 + (p_3 - p_1)\,\mathbf{m}\,\mathrm{curl}\,\mathbf{n} + (p_1 - p_2)\,\mathbf{n}\,\mathrm{curl}\,\mathbf{m}\} = 0. \tag{2.17}$$

Projecting this equation on the directions $\mathbf{l}$, $\mathbf{m}$, and $\mathbf{n}$ we obtain the three relations

$$\begin{aligned}
&[\mathbf{m}\times\mathbf{n}]\,\nabla p_1 + (p_3 - p_1)\,\mathbf{m}\,\mathrm{curl}\,\mathbf{n} + (p_1 - p_2)\,\mathbf{n}\,\mathrm{curl}\,\mathbf{m} = 0,\\
&[\mathbf{n}\times\mathbf{l}]\,\nabla p_2 + (p_1 - p_2)\,\mathbf{n}\,\mathrm{curl}\,\mathbf{l} + (p_2 - p_3)\,\mathbf{l}\,\mathrm{curl}\,\mathbf{n} = 0,\\
&[\mathbf{l}\times\mathbf{m}]\,\nabla p_3 + (p_2 - p_3)\,\mathbf{l}\,\mathrm{curl}\,\mathbf{m} + (p_3 - p_1)\,\mathbf{m}\,\mathrm{curl}\,\mathbf{l} = 0.
\end{aligned} \tag{2.18}$$

The following terms of the expansion of the metric tensor

$$g_{\alpha\beta} = g^{(0)}_{\alpha\beta} + h_{\alpha\beta} \tag{2.19}$$

[where $g^{(0)}_{\alpha\beta}$ is given by (2.4)] are expressed in terms of the quantities contained in (2.4). We shall not repeat here the corresponding calculations, but will indicate only that the first correction terms have the following orders of magnitude:

$$h^l_l \sim h^m_m \sim h^n_n \sim h^n_l \sim h^n_m \sim t^{2(1-p_3)}\ln^2 t \tag{2.20}$$

(the component h_{lm} is found to be of relatively higher order of smallness and in this sense enters in the next approximation).

Expression (2.4) contains a total of ten different functions of the coordinates: three components for each of the three vectors $\mathbf{l}$, $\mathbf{m}$, and $\mathbf{n}$, and one of the functions p_1, p_2, or p_3. These ten functions are connected by the four relations (2.15) and (2.18). In addition, the reference frame which we are using admits also of arbitrary transformation of the three spatial coordinates in terms of each other. Therefore the solution obtained contains merely $10 - 4 - 3 = 3$ physically different arbitrary functions of the coordinates. This is one less than required to specify the arbitrary initial conditions in vacuum.*

3. SOLUTION IN A SPACE FILLED WITH MATTER

Let us show now that the presence of matter does not change the solution obtained, and that the initial conditions for the distribution and motion of the matter can be specified in a fully arbitrary manner.

To gain an idea of the orders of magnitude of the energy density ϵ and of the components of the four-velocity of the matter u_i, it is convenient to use the hydrodynamic equations of motion of matter, which are contained, as is well known, in the equations of gravitation (the equations $T^k_{i,k} = 0$):

$$\frac{1}{\sqrt{-g}}\frac{\partial}{\partial x^i}(\sqrt{-g}\,u^i\sigma) = 0, \tag{3.1}$$

$$(p+\varepsilon)\,u^k\left\{\frac{\partial u_i}{\partial x^k} - \frac{1}{2}u^l\frac{\partial g_{kl}}{\partial x^i}\right\} = -\frac{\partial p}{\partial x^i} - u_i u^k\frac{\partial p}{\partial x^k} \tag{3.2}$$

(see, for example, reference 7, Sec. 125). Here σ is the entropy density; for the ultrarelatistic equation of state $p = \epsilon/3$ the entropy is $\sigma \sim \epsilon^{3/4}$.

We make an assumption (which will be confirmed by the results obtained) that the principal terms in (3.1) and (3.2) are those which contain the derivatives with respect to time; then Eq. (3.1) and the spatial components of (3.2) (the temporal component yields nothing new) give:

$$\frac{\partial}{\partial t}(\sqrt{-g}\,u_0\varepsilon^{3/4}) = 0, \qquad 4\varepsilon\frac{\partial u_\alpha}{\partial t} + u_\alpha\frac{\partial \varepsilon}{\partial t} = 0,$$

hence

$$t u_0\varepsilon^{3/4} = \mathrm{const}, \qquad u_\alpha\varepsilon^{1/4} = \mathrm{const},$$

where the symbol "const" stands for quantities independent of the time. In addition, we have from the identity $u_i u^i = -1$, considering that all the covariant components u_α are of the same order

$$u_0^2 \approx u_n u^n = u_n^2 t^{-2p_3}$$

(we again use the projections on the directions $\mathbf{l}$, $\mathbf{m}$, and $\mathbf{n}$, i.e., we represent the three-dimensional vector $\mathbf{u}$ in the form $\mathbf{u} = u_l\mathbf{l} + u_m\mathbf{m} + u_n\mathbf{n}$).

From these relations we obtain

$$\varepsilon \sim t^{-2(1-p_3)}, \qquad u_0^2 \sim t^{-(3p_3-1)}, \qquad u_\alpha \sim t^{(1-p_3)/2}, \tag{3.3}$$

after which we can readily verify that the terms discarded in (3.1) and (3.2) are actually small compared with those retained.

We now estimate the components of the energy-momentum tensor T^k_i, contained in the right halves of Eqs. I (1.4) — (1.6). In Eq. I (1.4) we have

$$T^0_0 \sim \varepsilon u_0^2 \sim t^{-(1+p_3)}.$$

Inasmuch as $p_3 < 1$, this quantity is of lower order in $1/t$ than the principal terms in the left side of the equation ($\sim t^{-2}$). The same holds for Eqs. I (1.6); the spatial components of the tensor T^k_i, "projected" on the directions $\mathbf{l}$, $\mathbf{m}$, and $\mathbf{n}$, are of the order of magnitude

$$T^l_l \sim \varepsilon \sim t^{-2(1-p_3)}, \qquad T^m_m \sim \varepsilon u_m u^m \sim t^{-(1+2p_3-p_3)},$$

$$T^n_n \sim \varepsilon u_n u^n \sim t^{-(1+p_3)}, \tag{3.4}$$

*The solution with two arbitrary functions, obtained in Section 4 of I for the case of empty space, corresponds to the particular case of constant values p_1, p_2, and p_3, equal to $-\frac{1}{3}$, $\frac{2}{3}$, and $\frac{2}{3}$.

Recently Harrison[3] found a series of exact solutions of a special type. These solutions have singularities which can be reduced to the type (2.4) (with different constant values of p_1, p_2 and p_3) or to the type mentioned in footnote *, page 559. We are grateful to Harrison for a preprint of his paper.

which are all smaller than t^{-2}.

On the other hand, in Eq. I (1.5) we have

$$T_\alpha^0 \sim \varepsilon u_0 u_\alpha \sim 1/t,$$

i.e., the same order of magnitude as in the left side of the equation. This circumstance, however, also leaves the character of the solution unchanged. Actually, in accordance with (3.3), we write

$$\varepsilon = \varepsilon^{(0)} t^{-2(1-p_3)}, \qquad \mathbf{u} = \mathbf{u}^{(0)} t^{(1-p_3)/2} \tag{3.5}$$

for the first terms of the expansion of these quantities; here

$$u_0^2 \approx u_n^{(0)2} t^{-(3p_3-1)}.$$

Equating expression (2.17) for R_α^0 to the quantity $T_\alpha^0 = 4\epsilon u_\alpha u^0/3$, we obtain in lieu of (2.18)

$$[\mathbf{m}\times\mathbf{n}]\nabla p_1 + (p_3 - p_1)\,\mathbf{m}\,\mathrm{curl}\,\mathbf{n} + (p_1 - p_2)\,\mathbf{n}\,\mathrm{curl}\,\mathbf{m}$$

$$= -\tfrac{4}{3}\varepsilon^{(0)} u_l^{(0)} u_n^{(0)},\ldots \tag{3.6}$$

Thus only the connection between the functions contained in (2.4) changes, and this connection now includes the new functions $\epsilon^{(0)}$ and $\mathbf{u}^{(0)}$.

The form of the following terms of the expansion of the metric tensor also changes, and the first terms following (2.4) are precisely the terms connected with the presence of matter.

To calculate these terms, we write $g_{\alpha\beta}$ in the form (2.19). Here

$$g^{\alpha\beta} = g^{(0)\alpha\beta} - h^{\alpha\beta}, \qquad \varkappa_{\alpha\beta} = \varkappa^{(0)}_{\alpha\beta} + \dot{h}_{\alpha\beta},$$

$$\varkappa_\alpha^\beta = \varkappa_\alpha^{(0)\beta} + \dot{h}_\alpha^\beta - \varkappa_\alpha^{(0)\gamma} h_\gamma^\beta + \varkappa_\gamma^{(0)\beta} h_\alpha^\gamma \tag{3.7}$$

(the dot denotes differentiation with respect to t). From I (2.1) and I (2.3) we obtain the following equations for $h_{\alpha\beta}$:

$$R_0^0 = \tfrac{1}{2}(\ddot{h} + \varkappa_\alpha^{(0)\beta}\dot{h}_\beta^\alpha) = T_0^0, \tag{3.8}$$

$$R_\alpha^\beta = \frac{1}{2}\left(\ddot{h}_\alpha^\beta + \frac{1}{t}\dot{h}_\alpha^\beta + \frac{1}{t}\varkappa_\alpha^{(0)\beta}\dot{h} - \varkappa_\alpha^{(0)\gamma}\dot{h}_\gamma^\beta + \varkappa_\gamma^{(0)\beta}\dot{h}_\alpha^\gamma\right) = T_\alpha^\beta, \tag{3.9}$$

where $h = h_\alpha^\alpha$ [in the calculation of R_α^β it is necessary to take into account the fact that the $\kappa_\alpha^{(0)\beta}$ are proportional to 1/t, whereas $\kappa_\gamma^{(0)\gamma} = 2/t$; the contribution to R_α^β from the "perturbation" of the tensor P_α^β is of smaller order of magnitude than the terms in (3.9)]. Since these equations do not contain derivatives with respect to coordinates, we can directly change in these equations to projections on $\mathbf{l}$, $\mathbf{m}$, and $\mathbf{n}$; considering that only

$$\varkappa_l^{(0)l} = 2p_1/t, \qquad \varkappa_m^{(0)m} = 2p_2/t, \qquad \varkappa_n^{(0)n} = 2p_3/t,$$

differ from zero, we obtain from (3.9) equations of the form

$$\frac{1}{2}\left(\ddot{h}_l^l + \frac{1}{t}\dot{h}_l^l + \frac{p_1}{t}\dot{h}\right) = T_l^l, \ldots \tag{3.10}$$

$$\frac{1}{2}\left(\ddot{h}_l^m + \frac{1 + 2p_3 - 2p_1}{t}\dot{h}_l^m\right) = T_l^m, \ldots \tag{3.11}$$

Of the three "diagonal" components (3.4) of the energy-momentum tensor, the one containing the highest power of 1/t is T_n^n. Therefore in calculating h_l^l, h_m^m and h_n^n, we can omit T_l^l and T_m^m for the right halves of (3.10), and retain only $T_n^n = 4\epsilon u_n u^n/3$. As a result we obtain

$$h_l^l = -\frac{p_1}{1-p_3}h, \qquad h_m^m = -\frac{p_2}{1-p_3}h, \qquad h_n^n = 2h,$$

$$h = \frac{8\varepsilon^{(0)} u_n^{(0)2}}{3(1-p_3)(2-p_3)} t^{1-p_3}, \qquad h_l^n = \frac{8\varepsilon^{(0)} u_l^{(0)} u_n^{(0)}}{3(1-p_3)(1+p_3-2p_1)} t^{1-p_3},$$

$$h_m^n = \frac{8\varepsilon^{(0)} u_m^{(0)} u_n^{(0)}}{3(1-p_3)(1+p_3-2p_2)} t^{1-p_3}. \tag{3.12}$$

These corrections are of higher order of magnitude than the first correction terms in the absence of matter (on the other hand, the component h_{lm} is again found to be of relatively higher order of smallness).

Equation (3.8) is satisfied by the expressions (3.12) identically. On the other hand, the equation $R_\alpha^0 = T_\alpha^0$, which we did not write out, would come in only in the determination of the following expantion terms of the energy and velocity.

Thus, the solution obtained for the gravitation equations represents a very broad class of solutions with singularities. It contains seven arbitrary functions of the coordinates: the three functions which enter in the absence of matter, the function ϵ^0 and the three functions $u_\alpha^{(0)}$.*

The character of variation of the metric $t \to 0$ in this solution is such that at each point of space the linear distances diminish along two directions (as t^{p_2} and t^{p_3}) and increase along the third (as $t^{-|p_1|}$); the volumes decrease here in proportion to t. The laws of these variations (i.e., the values of p_1, p_2, and p_3) vary in space and are determined by the initial conditions.

The density of matter becomes infinite at each point in space as $\epsilon \sim t^{-2(1-p_3)}$. This is clear evidence of the physical (not fictitious) nature of the singularity in the given solution (we note also that in the case of empty space the singularity is not fictitious because the scalars made up of the components of the curvature four-tensor R_{iklm}, for example, the scalar $R_{iklm}R^{iklm}$, do not become infinite). The velocity of motion of matter tends in this solution (in the reference frame considered here) to the velocity of light as $t \to 0$.† Actually,

*It can be shown that the higher terms of the expansion of the metric contain no other arbitrary function.

†In the particular case when p_1, p_2 and p_3 have the constant values $-\frac{1}{3}$, $\frac{2}{3}$, and $\frac{2}{3}$, the matter can be "written in" into the solution (20.4) in another, particular manner, by which its velocity tends to zero as $t \to 0$. This is the solution developed in I [formulas I(4.2) and (4.3)]; in this solution the matter brings only two, and not four arbitrary new functions, i.e., the initial conditions for this solution should have a certain particular character.

as $t \to 0$, the three-dimensional scalar $u_\alpha u^\alpha \approx u_n u^n$ goes to infinity as $t^{-3(p_3-1)}$. This means that the matter moves at any point essentially along the direction **n**, while the absolute magnitude of its ordinary three-dimensional velocity **v** tends to unity as

$$\sqrt{1-v^2} \sim t^{(3p_3-1)/2}.$$

The proper time τ of the moving matter is connected with the time t by means of $d\tau = dt\sqrt{1-v^2}$. Therefore

$$\tau \sim t^{(3p_3+1)/2}.$$

In the attached reference frame, the energy density goes to infinity, consequently, in accordance with the law

$$\varepsilon \sim \tau^{-4(1-p_3)/(3p_3+1)}.$$

The solution obtained, however, is still not general, for the general solution should contain eight arbitrary functions of the coordinates. The fact that this solution is incomplete manifests itself, in particular, in its stability properties. The general solution, by definition, is completely stable: no small perturbations can alter its character, since it admits of arbitrary initial conditions. The present solution, however, is unstable (if terms quadratic in the perturbations are taken into account) under perturbations of a definite type — perturbations connected with the appearance of the nonvanishing quantity **l** curl **l**. The question of the existence or absence of a general solution with singularity is closely related with the problem of the character of this instability, and calls for a separate investigation.

In conclusion, we are sincerely grateful to Academician L. D. Landau for continuing interest in our work and for many discussions. We are also grateful to V. V. Sudakov for informing us of his results.

[1] E. M. Lifshitz and I. M. Khalatnikov, JETP **39**, 149 (1960), Soviet Phys. JETP **12**, 108 (1961).

[2] E. Schucking and O. Herkmann, Onzieme conseil de physique Solvay. Bruxelles (1958).

[3] B. K. Harrison, Phys. Rev. **116**, 1285 (1959).

[4] A. Komar, Phys. Rev. **104**, 544 (1956).

[5] L. D. Landau and E. M. Lifshitz, Теория поля (Field Theory), 3d Ed. Fizmatgiz, 1960.

[6] A. H. Taub, Ann. of Math. **53**, 472 (1951).

[7] L. D. Landau and E. M. Lifshitz, Механика сплошных сред (Mechanics of Continuous Media), Gostekhizdat, 1954.

Translated by J. G. Adashko
146

COORDINATE CONDITIONS IN THE EINSTEIN THEORY OF GRAVITATION

I. G. FIKHTENGOL'TS

Submitted to JETP editor April 17, 1960

J. Exptl. Theoret. Phys. (U.S.S.R.) 39, 809-813 (September, 1960)

It is proved that the coordinate conditions employed by Einstein, Infeld, and Hoffman in their derivation of the equations of motion for a system of masses, cannot be obtained from the requirement that the gravitational field Lagrangian be invariant under some family of coordinate transformations. The application of these coordinate conditions to the astronomical problem of an isolated mass system is shown to be inexpedient.

We shall show that the coordinate conditions, employed by Einstein, Infeld, and Hoffman[1-3] in their work on the problem of the motion of an isolated mass system, cannot be derived from the requirement that the field Lagrangian be invariant* under some family of coordinate transformations.

To prove the above assertion we first find the general transformation law for the gravitational field Lagrangian under the replacement of the coordinates x_0, x_1, x_2, x_3 by the new coordinates x'_0, x'_1, x'_2, x'_3. Starting from the known transformation law of the Christoffel symbol of the second kind

$$\Gamma'^{\alpha}_{\mu\nu}=\frac{\partial x'_\alpha}{\partial x_\rho}\frac{\partial x_\sigma}{\partial x'_\mu}\frac{\partial x_\tau}{\partial x'_\nu}\Gamma^{\rho}_{\sigma\tau}+\frac{\partial x'_\alpha}{\partial x_\rho}\frac{\partial^2 x_\rho}{\partial x'_\mu \partial x'_\nu},$$

we obtain

$$L'=L+Q/\sqrt{-g}. \tag{1}$$

Here

$$L=g^{\mu\nu}(\Gamma^{\beta}_{\mu\alpha}\Gamma^{\alpha}_{\nu\beta}-\Gamma^{\alpha}_{\mu\nu}\Gamma^{\beta}_{\alpha\beta}), \tag{2}$$

$$Q=(P^{\beta}_{\mu\alpha}P^{\alpha}_{\nu\beta}-P^{\alpha}_{\mu\nu}P^{\beta}_{\alpha\beta})\mathfrak{G}^{\mu\nu}+P^{\nu}_{\mu\nu}\frac{\partial\mathfrak{G}^{\mu\alpha}}{\partial x_\alpha}-P^{\alpha}_{\mu\nu}\frac{\partial\mathfrak{G}^{\mu\nu}}{\partial x_\alpha}, \tag{3}$$

$$P^{\alpha}_{\mu\nu}=\frac{\partial x'_\sigma}{\partial x_\mu}\frac{\partial x'_\tau}{\partial x_\nu}\frac{\partial^2 x_\alpha}{\partial x'_\sigma \partial x'_\tau}, \tag{4}$$

$$\mathfrak{G}^{\mu\nu}=\sqrt{-g}\,g^{\mu\nu}. \tag{5}$$

Greek indices take on the values 0, 1, 2, and 3.

The expression for the function Q can be considerably simplified by making use of the identity

$$P^{\beta}_{\mu\alpha}P^{\alpha}_{\nu\beta}-P^{\alpha}_{\mu\nu}P^{\beta}_{\alpha\beta}=\partial P^{\alpha}_{\mu\alpha}/\partial x_\nu-\partial P^{\alpha}_{\mu\nu}/\partial x_\alpha.$$

We then obtain

$$Q=\frac{\partial}{\partial x_\alpha}(P^{\nu}_{\mu\nu}\mathfrak{G}^{\mu\alpha}-P^{\alpha}_{\mu\nu}\mathfrak{G}^{\mu\nu}). \tag{6}$$

Equations (1) and (6) express the law of transformation for the function L. If in addition we make use of the known transformation law for the determinant g, we find that the transformation law for the Lagrangian

$$\mathcal{L}=\sqrt{-g}\,L \tag{7}$$

is given by the formula

$$\mathcal{L}'\left|\frac{D(x'_0, x'_1, x'_2, x'_3)}{D(x_0, x_1, x_2, x_3)}\right|-\mathcal{L}=Q. \tag{8}$$

The fact that under arbitrary coordinate transformations the difference on the left hand side of Eq. (8) is equal to a sum of derivatives with respect to x_α [see Eq. (6)], corresponds precisely to the general covariance property of Einstein's gravitation equations. Starting from the established transformation law for the gravitational field Lagrangian we conclude that the condition, that the field Lagrangian be invariant under arbitrary coordinate transformations, is given by*

$$\frac{\partial}{\partial x_\alpha}(P^{\nu}_{\mu\nu}\mathfrak{G}^{\mu\alpha}-P^{\alpha}_{\mu\nu}\mathfrak{G}^{\mu\nu})=0. \tag{9}$$

It is important to note that the conditions of invariance of the field Lagrangian under arbitrary families of coordinate transformations reduce to equations, that are linear with respect to the quantities $\mathfrak{G}^{\mu\nu}$.

We pass now to a consideration of the coordinate conditions

$$\partial\gamma_{0k}/\partial x_k-\partial\gamma_{00}/\partial x_0=0, \qquad \partial\gamma_{ik}/\partial x_k=0, \tag{10}$$

employed by Einstein, Infeld, and Hoffman[1-3] in

*More precisely, from the requirement of relative invariance of the field Lagrangian (see Fikhtengol'ts,[4] denoted in the following by I). The word "relative" has been omitted for the sake of brevity. In what follows it is understood that the word invariance, as applied to the field Lagrangian, means relative invariance.

*In the case of infinitesimally small coordinate transformations the condition (9) reduces to the condition I(17).

their derivation of the equations of motion of an isolated system of masses. In the conditions (10)

$$\gamma_{\mu\nu} = h_{\mu\nu} - \tfrac{1}{2}\eta_{\mu\nu}\eta^{\alpha\beta}h_{\alpha\beta}, \tag{11}$$

where the quantities $h_{\mu\nu}$ and $h^{\mu\nu}$ are respectively given by the equations*

$$g_{\mu\nu} = \eta_{\mu\nu} + h_{\mu\nu}, \qquad g^{\mu\nu} = \eta^{\mu\nu} + h^{\mu\nu}, \tag{12}$$

with

$$\eta_{00} = \eta^{00} = 1, \qquad \eta_{0i} = \eta^{0i} = 0, \qquad \eta_{ik} = \eta^{ik} = -\delta_{ik}. \tag{13}$$

Latin indices take on the values 1, 2, and 3.

Let us express the conditions (10), which we shall call the Einstein-Infeld conditions, with the help of the fundamental tensor $g_{\mu\nu}$. It follows from Eqs. (11) — (13) that

$$\gamma_{\mu\nu} = \eta_{\mu\nu} + g_{\mu\nu} - \tfrac{1}{2}\eta_{\mu\nu}\eta^{\alpha\beta}g_{\alpha\beta},$$

and therefore the conditions (10) become

$$\begin{aligned} &\frac{\partial \gamma_{0k}}{\partial x_k} - \frac{1}{2}\frac{\partial}{\partial x_0}(g_{00} + g_{11} + g_{22} + g_{33}) = 0, \\ &\frac{\partial g_{ik}}{\partial x_k} + \frac{1}{2}\frac{\partial}{\partial x_i}(g_{00} - g_{11} - g_{22} - g_{33}) = 0. \end{aligned} \tag{14}$$

In order to prove that the Einstein-Infeld conditions cannot be obtained from the requirement that the field Lagrangian be invariant under some family of coordinate transformations it is sufficient to show, as a consequence of Eq. (9), that the conditions (14) do not reduce to equations linear in $\mathfrak{G}^{\mu\nu}$.

The proof will be carried out under the assumption that the metric deviates little from a Galilean metric. In that case we can set approximately (see Fock[5])†

$$\begin{aligned} &\mathfrak{G}^{00} = 1 + 4U/c^2 + 4S/c^4, \quad \mathfrak{G}^{0i} = 4U_i/c^3 + 4S_i/c^5, \\ &\mathfrak{G}^{ik} = -\delta_{ik} + 4S_{ik}/c^4. \end{aligned} \tag{15}$$

Going over from the quantities $\mathfrak{G}^{\mu\nu}$ to the quantities $g_{\mu\nu}$, we obtain in the corresponding approximation

$$\begin{aligned} &g_{00} = -\tfrac{1}{2}(\mathfrak{G}^{00} + \mathfrak{G}^{11} + \mathfrak{G}^{22} + \mathfrak{G}^{33}) + \tfrac{3}{8}(\mathfrak{G}^{00} - 1)^2, \\ &g_{0i} = \mathfrak{G}^{0i} - \tfrac{1}{2}(\mathfrak{G}^{00} - 1)\mathfrak{G}^{0i}, \\ &g_{ik} = -\tfrac{1}{2}[\mathfrak{G}^{00} - \mathfrak{G}^{11} - \mathfrak{G}^{22} - \mathfrak{G}^{33} - \tfrac{1}{4}(\mathfrak{G}^{00} - 1)^2]\delta_{ik} - \mathfrak{G}^{ik}. \end{aligned} \tag{16}$$

We conclude that, with Eqs. (16) taken into account, the Einstein-Infeld conditions become in the approximation corresponding to Eq. (15)

$$\begin{aligned} &\frac{\partial \mathfrak{G}^{0\mu}}{\partial x_\mu} = \tfrac{3}{8}\frac{\partial}{\partial x_0}(\mathfrak{G}^{00} - 1)^2 + \tfrac{1}{2}\frac{\partial}{\partial x_k}[(\mathfrak{G}^{00} - 1)\mathfrak{G}^{0k}], \\ &\frac{\partial \mathfrak{G}^{ik}}{\partial x_k} = \tfrac{1}{8}\frac{\partial}{\partial x_i}(\mathfrak{G}^{00} - 1)^2. \end{aligned} \tag{17}$$

It is clear from the relations (17) that the Einstein-Infeld conditions do not reduce to equations linear in $\mathfrak{G}^{\mu\nu}$, and, consequently, that these conditions cannot be obtained from the requirement of invariance of the field Lagrangian under some family of coordinate transformations.

If an even rougher approximation than Eq. (15) is used to find the quantities $\mathfrak{G}^{\mu\nu}$, namely, if we set

$$\mathfrak{G}^{00} = 1 + 4U_c c^2, \qquad \mathfrak{G}^{0i} = 4U_i c^3, \qquad \mathfrak{G}^{ik} = -\delta_{ik} \tag{15'}$$

and then pass from the quantities $\mathfrak{G}^{\mu\nu}$ to the quantities $g_{\mu\nu}$, then we find

$$\begin{aligned} &g_{00} = 1 - \tfrac{1}{2}(\mathfrak{G}^{00} - 1), \qquad g_{0i} = \mathfrak{G}^{0i}, \\ &g_{ik} = -[1 + \tfrac{1}{2}(\mathfrak{G}^{00} - 1)]\delta_{ik}. \end{aligned} \tag{16'}$$

Thus in the approximation corresponding to Eq. (15') the relation between $g_{\mu\nu}$ and $\mathfrak{G}^{\mu\nu}$ becomes linear. In this approximation the Einstein-Infeld conditions become linear in $\mathfrak{G}^{\mu\nu}$, too. Furthermore, it follows directly from Eqs. (14) and (16') that in this approximation the Einstein-Infeld conditions coincide with harmonic coordinate conditions (see also Fock[6]).

We show now that in approximations higher than those discussed above, the use of the Einstein-Infeld coordinate conditions in the astronomical problem of an isolated mass system is inexpedient. In order to be convinced of that it is sufficient to discuss the simplest such system, namely the system consisting of a single spherically symmetric mass. As is well known, for this simple case an exact solution of the Einstein gravitation equations is available. It is this solution (in the region outside the mass) that we shall use. Assuming that at large distances from the mass m, which serves as the source of the gravitational field, the field is Newtonian, and that at infinity the space-time metric becomes Galilean, we have

$$\begin{aligned} &g_{00} = 1 - 2\alpha/\rho, \quad g_{0i} = 0, \\ &g_{ik} = -\frac{1}{r^2}\left\{\rho^2\delta_{ik} + \left[\frac{1}{1 - 2\alpha/\rho}\left(\frac{d\rho}{dr}\right)^2 - \frac{\rho^2}{r^2}\right]x_i x_k\right\}. \end{aligned} \tag{18}$$

Here $\alpha = \gamma m/c^2$ is the gravitational radius of the mass m (γ is Newton's constant of gravitation) and ρ is an arbitrary function of the variable $r = \sqrt{x_1^2 + x_2^2 + x_3^2}$. It is of course understood, that the Eq. (18) for the components of the fundamental tensor is valid in only those coordinate systems,

*Following Einstein et al.,[1-3] we set $x_0 = ct$.

†The difference between the expressions (15) and the corresponding expressions (67.04) in Fock's book[5] is due to the fact that in this paper we follow Einstein et al.[1-3] and set $x_0 = ct$, whereas Fock uses in the relevant discussion $x_0 = t$.

for which both the assumed property of a spherically symmetric field, as well as the stationary property of the spherically symmetric gravitational field in the region outside the mass, hold true. To determine the function $\rho(r)$ it is necessary to invoke additional (coordinate) conditions. In the Schwarzschild solution it is assumed that $\rho = r$ (see, e.g., Landau and Lifshitz[7]). If harmonic coordinate conditions are used then, as is shown in Fock's book, $\rho = r + \alpha$. If, however, the Einstein-Infeld coordinate conditions are used, then, as a consequence of Eqs. (14) and (18), we obtain the following equation for the function ρ:

$$\frac{d}{dr}\left[\frac{1}{1-2\alpha/\rho}\left(\frac{d\rho}{dr}\right)^2-\frac{2\rho^2}{r^2}+\frac{2\alpha}{\rho}\right]+\frac{4}{r}\left[\frac{1}{1-2\alpha/\rho}\left(\frac{d\rho}{dr}\right)^2-\frac{\rho^2}{r^2}\right]=0. \tag{19}$$

The r-dependence of the function ρ determined by this equation is rather complicated. If we limit ourselves in the determination of ρ/r to quantities of order $(\alpha/r)^3$ then we can set

$$\rho/r=1+\alpha/r+2\alpha^2/r^2+\varphi\alpha^3/r^3. \tag{20}$$

with the function $\varphi(r)$ determined, as a consequence of Eq. (19), by the following approximate equation:

$$\frac{d^2\varphi}{dr^2}-\frac{2}{r}\frac{d\varphi}{dr}=-\frac{2}{r^2}. \tag{21}$$

Equation (21) may be integrated by elementary means. It follows directly from Eqs. (20) and (21) that, when use is made of the Einstein-Infeld coordinate conditions, the quantity ρ/r cannot be expressed as a power series in α/r or, what is the same, in U/c^2, where U is the Newtonian potential of the mass m serving as the source of the gravitational field. The indicated complex character of the dependence $\rho = \rho(r)$ is not, however, due to the intrinsic physical properties of the spherically symmetric gravitational field, but arises solely from the inappropriateness of the Einstein-Infeld coordinate conditions to the problem of an isolated system of masses.

[1] Einstein, Infeld, and Hoffman, Ann. Math. **39**, 65 (1938).

[2] A. Einstein and L. Infeld, Ann. Math. **41**, 455 (1940).

[3] A. Einstein and L. Infeld, Canad. J. Math. **1**, 209 (1949).

[4] I. G. Fikhtengol'ts, JETP **35**, 1457 (1958), Soviet Phys. JETP **8**, 1018 (1959).

[5] V. A. Fock, Теория пространства, времени и тяготения (Theory of Space, Time and Gravitation), Gostekhizdat, 1955.

[6] V. A. Fock, JETP **38**, 108 (1960), Soviet Phys. JETP **11**, 80 (1960).

[7] L. D. Landau and E. M. Lifshitz, Теория поля (Field Theory), Gostekhizdat, 1948 (Eng. Transl., Addison-Wesley, 1951).

Translated by A. M. Bincer
147

LATERAL DISTRIBUTION OF HIGH ENERGY NUCLEAR-ACTIVE PARTICLES IN THE CORE OF EXTENSIVE ATMOSPHERIC SHOWERS

A. A. EMEL'YANOV and O. I. DOVZHENKO

P. N. Lebedev Physics Institute, Academy of Sciences, U.S.S.R.

Submitted to JETP editor April 20, 1960

J. Exptl. Theoret. Phys. (U.S.S.R.) 39, 814-821 (September, 1960)

The lateral distribution of high-energy nuclear-active particles in the core of extensive atmospheric showers is considered. The mean-square radius for nuclear-active particles with energies $\geq 5 \times 10^{11}$ ev is computed from the angular distribution of secondary particles emitted in multiple-production processes, as predicted by the Landau hydrodynamic theory. It is shown that the mean-square radius depends not only on the angles of emission of the secondary particles during multiple production but also on the diffraction scattering of the nuclear-active particles by nuclei of air atoms.

1. There are many known experimental papers devoted to the lateral characteristics of the nuclear-active component of extensive atmospheric showers (EAS) of cosmic rays.[1,2] One of the tasks of these investigations is to study the angular distribution of the secondary particles produced when high-energy nuclear-active particles collide with the nuclei of air atoms. For this purpose, the form of the lateral-distribution function of the flux density of the nuclear-active particles of energy higher than specified is determined in different experiments. Since the nuclear-active cascade is accompanied by a large number of electrons produced by the π^0 mesons which are created in the same interaction events as the $\pi^{\pm}$ mesons and the nucleons, one might think that an investigation of the lateral characteristics of the electron-photon component would explain several detailed features of the elementary act. However, it has been shown by many authors (see, for example, reference 3) that the lateral distribution of the electron-photon component is practically independent of the lateral and angular distributions of the π^0 mesons. It follows therefore that the lateral distribution of the π^0 mesons is very narrow, and consequently a study of the lateral characteristics of the electron-photon component (except perhaps at very short distances from the axis) does not make it possible to evaluate the angular distribution of the secondary nuclear-active particles in the elementary act.

The situation is different with $\pi^{\pm}$ and nucleons, the lateral distributions of which (in the case of high energies) are determined by the angular distribution of the particles during the acts of multiple generation and by elastic scattering on the nuclei of the air atoms (diffraction scattering).

2. Let us consider the passage of high-energy nuclear-active particles through the atmosphere. Let $P(E, t, \mathbf{r}, \theta)$ be the flux density of the nuclear-active particles of the EAS. Here E is the energy of the nuclear-active particles, t the height of observation in nuclear-interaction ranges, $\mathbf{r}$ the radius vector in a plane perpendicular to the shower axis, and θ the vector of direction of motion of the particle. The function P satisfies the following kinetic equation:[4]

$$\partial P(E, t, \mathbf{r}, \theta)/\partial t + \theta\, \partial P(E, t, \mathbf{r}, \theta)/\partial \mathbf{r} = -P(E, t, \mathbf{r}, \theta) + \int_{E}^{\infty}\int_{\Omega} P(E', t, \mathbf{r}, \theta+\chi)\,\varphi_L(E', E, \theta+\chi, \theta)\,dE'd\Omega + \int_{\Omega}[P(E, t, \mathbf{r}, \theta+\chi) - P(E, t, \mathbf{r}, \theta)]\,d\sigma(\chi), \qquad (1)$$

where $\varphi_L(E', E, \theta+\chi, \theta)$ is the probability that a particle of energy E', traveling at an angle $\theta + \chi$ to the shower axis, will have an energy E after colliding with the nucleus of the air atom, and will be deflected by an angle χ; $d\sigma(\chi)$ is the cross section for the deflection of a nuclear-active particle by an angle χ as a result of diffraction scattering.*

We shall consider nuclear-active particles of very high energies ($E \gg Mc^2$), and can therefore put $\theta \ll 1$ and $\chi \ll 1$.

For the function φ_L, which characterizes the multiple particle production processes, we use an

*We neglect the diffraction-generation effect.

expression that follows from the hydrodynamic theory of interaction of particles of very high energies,[5] with allowance for the fact that the distribution of the secondary particles along the direction $\theta + \chi$ has azimuthal symmetry:

$$\varphi_L(E', E, \theta+\chi, \theta)\,dE'\,d\Omega \approx \frac{2}{3} N_{E'} \frac{\exp\{-(\eta-\eta_c')^2/2L\}\,dE'd\Omega}{\sqrt{2\pi L}\;2\pi p_\perp c}\,\delta\left(\chi - \frac{p_\perp c}{E}\right),$$

$$\eta \approx \ln\frac{E}{Mc^2}, \qquad L \approx 0.5\,\eta', \qquad N_{E'} \approx 2.3\,e^{\eta'/\eta},$$

$$\eta_c' \approx \frac{1}{2}\left[\eta' - \ln\frac{n_0+1}{2}\right],$$

n_0 is the average number of nucleons in a "tunnel" of the air-atom nucleus, and $p_\perp$ is the momentum acquired by a secondary particle in the direction perpendicular to the direction of motion of the primary particle. According to Milekhin,[5] $p_\perp \approx 3\mu c$,* where μ is the pion mass. The function φ_L is normalized to the total number of particles produced by a primary particle of energy E'.

It must be especially emphasized that we assume that the π mesons and the nucleons interact in the same manner with the nuclei of the air atoms. It is possible that account should be taken of the difference between π-mesons interactions and nucleon interactions. This would lead to a system of kinetic equations which are genetically related, but such an analysis is not believed desirable in the present paper.

In addition to scattering that takes place during the nuclear-interaction events accompanied by multiple particle production, one must allow also for the so-called diffraction scattering, which occurs without loss of primary-particle energy, since it is found that the effective angles are of the same order of magnitude in diffraction scattering as in multiple-production events. The total cross section of diffraction scattering σ_{dif} is equal to the multiple-production cross section σ_{mp}:

$$\sigma_{dif} = \sigma_{mp} \approx \pi R^2 A^{2/3},$$

where A is the atomic weight of air and $R \approx 1.3 \times 10^{-13}$ cm.

The cross section σ_{dif} which we use for diffraction scattering contains one natural assumption, namely that the nucleus is a non-transparent "black ball" for fast nuclear-active particles.[6]

To simplify the kinetic equation (1), we use the condition $\chi \approx 1$ and expand the function $P(E, t, \mathbf{r}, \theta + \chi)$ in powers of χ:[7]

*By $p_\perp$ is meant the mean-squared value of the transverse momentum.

$$P(\theta+\chi) = P(\theta) + \frac{\partial P}{\partial\theta}\chi + \frac{1}{2}\left(\frac{\partial^2 P}{\partial\theta_x^2}\chi_x^2 + \frac{\partial^2 P}{\partial\theta_y^2}\chi_y^2 + \frac{\partial^2 P}{\partial\theta_x\partial\theta_y}\chi_x\chi_y\right) + \ldots \qquad (2)$$

Here χ_x and χ_y are the components of the vector χ in a plane tangent to the unit sphere at the point θ:

$$\chi_x = \chi\cos\varphi, \quad \chi_y = \chi\sin\varphi.$$

Let us average Eq. (2) over φ with allowance for the azimuthal symmetry

$$\int_0^{2\pi} P(\theta+\chi)\,d\varphi \approx \int_0^{2\pi} P(\theta)\,d\varphi + \frac{\pi}{2}\chi^2\Delta_\theta P + \ldots, \qquad (3)$$

where, in view of the smallness of χ, we discard terms with higher powers of χ.

We substitute (3) in the right half of (1). The integral that determines the multiple-production processes assumes the form

$$\int_E^\infty\int_\Omega P(E', t, \mathbf{r}, \theta+\chi)\,\varphi_L(E', E, \theta+\chi, \theta)\,dE'd\Omega = L[P(E', t, \mathbf{r}, \theta)] + (p_\perp c/2E)^2\,\Delta_\theta L[P(E', t, \mathbf{r}, \theta)],$$

$$L[P(E', t, \mathbf{r}, \theta)] = \int_E^\infty P(E', t, \mathbf{r}, \theta)\,\varphi_L(E', E, \theta+\chi, \theta)\,dE'. \qquad (4)$$

The integral that describes the diffraction scattering is transformed into

$$\int_0^\pi\int_0^{2\pi}[P(E, t, \mathbf{r}, \theta+\chi) - P(E, t, \mathbf{r}, \theta)]f(\chi)\sin\chi\,d\chi\,d\varphi \approx \frac{\pi}{2}\,\Delta_\theta P(E, t, \mathbf{r}, \theta)\int_0^{\chi_m} f(\chi)\chi^3\,d\chi. \qquad (5)$$

Here $f(\chi)$ is determined from the expression for the diffraction-scattering cross section $d\sigma(\chi) = f(\chi)\,d\chi$, and χ_m is the maximum angle of deflection, taking account of the transparency of the edge of the nucleus to nuclear-active particles. We note that the expression for $f(\chi)$, which follows from the "black ball" model,[6]

$$f(\chi) = \frac{1}{\pi}\left|J_1\left(\frac{E}{\mu c^2}\sin\chi\right)/\sin\chi\right|,$$

leads to a divergent expression for the mean-squared deflection angle $\overline{\chi^2}$. Taking into account the fact that we know the structure of the edge of the nucleus, we introduce the mean-squared angle of diffraction scattering $\overline{\chi^2} = (b\mu c^2/E)^2$, and then (5) is transformed to

$$(b\mu c^2/2E)^2\,\Delta_\theta P(E, t, \mathbf{r}, \theta). \qquad (6)$$

The parameter b should be determined experimentally, for example, from emulsion data. We thus write finally expression (4) in the form

$$\frac{\partial P(E,\ t,\ \mathrm{r},\ \theta)}{\partial t}+\theta\frac{\partial P(E,\ t,\ \mathrm{r},\ \theta)}{\partial \mathrm{r}}=-P(E,\ t,\ \mathrm{r},\ \theta)$$
$$+\left(\frac{b\mu c^2}{2E}\right)^2\Delta_\theta P(E,\ t,\ \mathrm{r},\ \theta)$$
$$+\left[1+\left(\frac{p_\perp c}{2E}\right)^2\Delta_\theta\right]L[P(E',\ t,\ \mathrm{r},\ \theta)]. \qquad (7)$$

3. Let us now determine the mean-squared angle and the radius of deflection of the nuclear-active particles. Following the usual procedure of calculating the moments of the function P(E, t, r, θ),[7] we integrate (7) with respect to t from 0 to ∞ and then multiply by θ^2 and integrate over all of space and all the solid angles. As a result we obtain

$$P_1(E)-L[P_1(E')]=\left(\frac{b\mu c^2}{E}\right)^2P_0(E)+\left(\frac{p_\perp c}{E}\right)^2L[P_0(E')], \qquad (8)$$

$$P_0(E)=\int_0^\infty\int_{\mathrm{r}}\int_{\Omega}P(E,\ t,\ \mathrm{r},\ \theta)\,dt\,d\mathrm{r}\,d\theta,$$

$$P_1(E)=\int_0^\infty\int_{\mathrm{r}}\int_{\Omega}P(E,t,\mathrm{r},\theta)\,\theta^2\,dt\,d\mathrm{r}\,d\theta. \qquad (8')$$

Hence

$$\overline{\theta^2}=P_1(E)/P_0(E). \qquad (8'')$$

Next, multiplying (7) by $\theta\cdot\mathrm{r}$ and carrying out the same integrations, we obtain

$$P_2(E)-L[P_2(E')]=P_1(E), \qquad (9)$$

$$P_2(E)=\int_0^\infty\int_{\mathrm{r}}\int_{\Omega}P(E,\ t,\ \mathrm{r},\ \theta)\,(\theta\mathrm{r})\,dt\,d\mathrm{r}\,d\theta; \qquad (9')$$

and finally, multiplying (7) by r^2 and integrating over all space and all the solid angles, we get

$$P_3(E)-L[P_3(E')]=2P_2(E), \qquad (10)$$

$$P_3(E)=\int_0^\infty\int_{\mathrm{r}}\int_{\Omega}P(E,\ t,\ \mathrm{r},\ \theta)\,r^2\,dt\,d\mathrm{r}\,d\theta. \qquad (10')$$

The mean square of the deviations $\overline{r^2}$ is given by

$$\overline{r^2}=P_3(E)/P_0(E). \qquad (10'')$$

Thus, the problem of determining $\overline{\theta^2}$ and $\overline{r^2}$ reduces to a successive solution of very complicated integral equations (8), (9), and (10). These equations can be solved if we know the function $P_0(E)\,dE$, i.e., if we know the differential energy spectrum of the nuclear-active particles in the EAS. For this function we can use the expression

$$P_0(E)\,dE=AE^{-2}dE, \qquad A=\text{const}, \qquad (11)$$

which follows both from an examination of the altitude variation of the EAS under a variety of assumptions regarding the character of the elementary act,[8] and from experimental data.[2,10]

After substituting (11) in (8) we obtain

$$P_1(E)-L[P_1(E')]=\left(\frac{b\mu c^2}{E}\right)^2\frac{A}{E^2}$$
$$+\left(\frac{p_\perp c}{E}\right)^2\int_E^\infty\frac{A}{E'^2}\varphi_L(E',\ E)\,dE'. \qquad (12)$$

The solution of Eqs. (12), (9) and (10), carried out by the method of successive approximations, has made it possible to obtain the following expressions* for $\overline{\theta^2}$ and $\overline{r^2}$:

$$\overline{\theta^2}\approx 1.1\,(\mu c^2/E)^2\,[b^2+0.7\,(p_\perp/\mu c)^2], \qquad (13)$$

$$\overline{r^2}\approx 3.0\,(\mu c^2/E)^2\,[b^2+0.7\,(p_\perp/\mu c)^2]. \qquad (14)$$

For a comparison with the experimental data, it is necessary to obtain an expression for the mean-squared radius of particles of energy greater than specified, $\overline{r^2}\,(\geq E)$, since this quantity can be estimated experimentally.

By definition

$$\overline{r^2}(\geqslant E)=\int_E^\infty P_3(E')\,dE'\Big/\int_E^\infty P_0(E')\,dE'. \qquad (15)$$

Substituting in (15) the values of $P_3(E)$ and $P_0(E)$, we obtain

$$\overline{r^2}\,(\geqslant E)\approx(\mu c^2/E)^2\,[b^2+0{,}7\,(p_\perp/\mu c)^2]. \qquad (16)$$

We must qualify that the expressions obtained for $\overline{\theta^2}$, $\overline{r^2}$, and $\overline{r^2}\,(\geq E)$ are valid at very high energies ($E\gtrsim 5\times10^{11}$ ev), since we did not take into account the spontaneous decay of the pions.

To compare the value obtained for $\overline{r^2}\,(\geq E)$ with the experimental data, it is necessary to know the value of the diffraction parameter b. The value of b cannot be determined theoretically since the structure of the nucleon is unknown, and consequently we do not know the character of the "transparency" of the edge of the nucleus to fast pions. It is sensible to assume, however, that b ≈ 3 (this corresponds to a smearing of the nuclear edge $\sim\hbar/Mc$, where M is the nucleon mass). In this case $[\overline{r^2}\,(\geq10^{12}\text{ ev})]^{1/2}\approx 0.6$ m for an altitude of 3,860 m above sea level (Pamir). We assume here that $p_\perp\approx 3\mu c$, if we are to follow the hydrodynamic theory of multiple production.[5] This corresponds to a hydrodynamic system decay temperature $T_K\approx\mu c^2$ (the transverse momentum acquired by the particles through expansion of the hydrodynamic system at primary-particle energies $\sim10^{13}$ ev is much less than the transverse momentum obtained in thermal motion[9]).

From the results obtained in the investigation of the energy characteristics of the nuclear-active

*The computational accuracy of (13) and (14) is not lower than 10%.

component in the region of the core of the EAS,[10] it follows that $[\overline{r^2}\,(\gtrsim 10^{12}\ \text{ev})]^{1/2} \gtrsim 1\,\text{m}$. Thus, the experimental and theoretical values of the mean-squared radius are quite close to each other, although the experimental value is somewhat higher. There is little likelihood of attributing this difference to an underestimate of b (when $b \approx 6$ we have $\overline{r^2}_{\text{exp}} \approx \overline{r^2}_{\text{theor}}$). It is natural to assume that the transverse momentum $p_\perp$, acquired by the secondary particles during multiple production, is in fact higher for the faster particles than follows from the hydrodynamic theory, although $p \approx 3\mu c$ for the overwhelming majority of the secondary particles (this is confirmed by emulsion data[11]). In addition, the fastest particle can be a nucleon[12] with a transverse momentum considerably greater than $3\mu c$.

4. We see from the formula for $\overline{r^2}$ that for particles of energy $\gtrsim 5 \times 10^{11}$ ev, r enters into the lateral distribution function of the nuclear-active particles only in the combination rE. Since particles of such energies are observed only near the axis of the shower, we can use the Pomeranchuk-Migdal method[13,14] to calculate the lateral distribution function of the flux density of the nuclear-active particles. We seek a distribution function in the form

$$P(E,\ r,\ t) = P(E,\ t)\,F(rE/kE_\alpha), \tag{17}$$

where P(E, t) is the total number of nuclear-active particles with energies in the interval E, E + dE, at a depth t; E_α determines the value of $(\overline{r^2})^{1/2}$, and k = const. The normalizing factor A is determined from the condition

$$2\pi A \int_0^\infty F(rE/kE_\alpha)\,r\,dr = 1,$$

hence

$$A = E^2/2\pi(kE_\alpha)^2. \tag{18}$$

For the flux density of nuclear-active particles with energy $\geq E$ we have

$$\rho(E,\ r,\ t) = \frac{1}{2\pi(kE_\alpha)^2}\int_E^{E_0} P(E',\ r,\ t)E'^2 F\left(\frac{rE'}{kE_\alpha}\right)dE'. \tag{19}$$

To determine the functions P(E, t)dE we make use of the analytic expression derived by Fukuda, Ogita, and Ueda,[3]

$$P(E,t')\,dE = \frac{(1-\delta)\,\nu}{[4\pi\sqrt{(1-\delta)\,\nu t' y}]^{1/2}}$$
$$\times \exp\{-t' + \delta y + 2[(1-\delta)\,\nu t' y]^{1/2}\}\,dy, \tag{20}$$

where $y = \ln(E_0/E)$, t' is the depth in units of range of nuclear interaction from the point of shower production to the observation level, ν is the ratio of charged nuclear-active particles to the total number of particles produced during the multiple-generation act, and δ is the fraction of the energy retained by the nucleus after each interaction; the values of ν and δ were chosen by comparing the altitude variation with experiment: $\nu \approx 2/3$, $\delta \approx 1/2$. The function $F(rE/kE_\alpha)$ was chosen to be

$$F(rE/kE_\alpha) = e^{-rE/kE_\alpha}.$$

Then $k = 1/\sqrt{6}$ [this follows from the condition $\overline{r^2} = (E_\alpha/E)^2$, and for $r \lesssim \sqrt{\overline{r^2}}$ the choice of the specific form of the function F is immaterial].

To compare the experimental data with the calculated lateral distribution, account must be taken of the fluctuations in the depth of the onset of the shower, namely, that showers with a total of N particles at the observation level can be produced by primary nuclear-active particles of different energies, interacting at different altitudes from the observation level. In calculating $\rho(E, r, t)$ we used the dependence of the total number of particles $N = \xi(E_0, t')$, which follows from calculations of the altitude variation of the EAS under the assumption that the hydrodynamic theory of multiple production is valid.[9] In this case the range for the interaction of nuclear-active particles with nuclei of air atoms was assumed to be 75 g/cm^2.

Figure 1 shows a comparison of the experimentally-obtained and theoretically-calculated lateral distributions for particles with energy $\gtrsim 5 \times 10^{11}$ ev, for the case $E_\alpha \approx 1.5 \times 10^9$ ev (corresponding to $b \approx 6$ and $p_\perp \approx 3\mu c$).

It must be noted that the total number of nuclear-active particles with energy $\geq 5 \times 10^{11}$ ev in a shower with a large number of particles, $N = 10^5$, obtained by integrating expression (20) with respect to the energy for the Pamir altitude, is about one-fourth the experimentally obtained value. The theoretically-calculated lateral distribution was therefore normalized to the experimental value relative to the total number of nuclear-active particles of energy $\geq 5 \times 10^{11}$ ev.

Let us consider now the dependence $\rho(E, r, t)$ for fixed values of r and t, i.e., let us determine the energy spectra of the nuclear-active particles at different distances from the shower axis. The results of the calculation are shown by the solid lines of Fig. 2, which shows also the experimental values of $\rho(\geq E)$ taken from the paper of Dovzhenko, Zatsepin et al.[10] The calculation was carried out for $E \approx 1.5 \times 10^9$ ev.

In conclusion, the authors consider it their

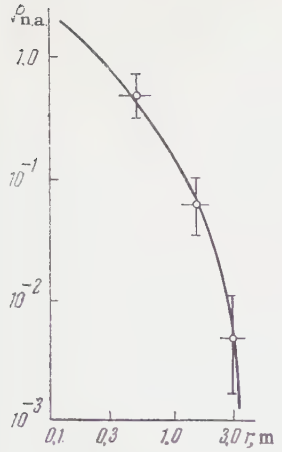

FIG. 1

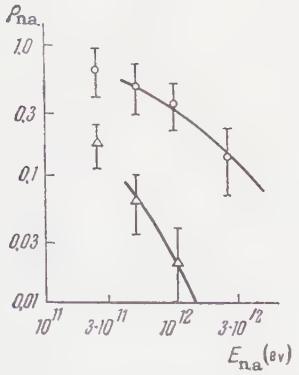

FIG. 2

FIG. 1. Lateral distribution of nuclear-active particles with energy $\geqslant 5 \times 10^{11}$ ev. The experimental points were borrowed from reference 10, and the solid curve $\rho_{n.a.}(r)$ is calculated by formulas (19) – (21).

FIG. 2. Energy spectra of nuclear-active particles for distances r from the shower axis ranging from zero to one meter (○) and from one to two meters (△) for a shower with a total number $N = 10^5$ particles.[10]

pleasant duty to thank G. T. Zatsepin, G. A. Milekhin, S. I. Nikol'skiĭ, and I. L. Rozental' for a discussion of the results obtained, A. A. Pomanskiĭ for acquainting them with the results of the calculation of the altitude variation of EAS by the Fermi-Landau model prior to publication, and also to G. Ya. Goryacheva and G. V. Minaeva for help with the numerical calculations.

[1] Nikol'skiĭ, Vavilov, and Batov, Dokl. Akad. Nauk SSSR **111**, 71 (1956), Soviet Phys.-Doklady **1**, 625 (1957).

[2] Abrosimov, Dmitriev, Kulikov, Massal'skiĭ, Solov'ev, and Khristiansen, JETP **36**, 751 (1959), Soviet Phys. JETP **9**, 528 (1959).

[3] Fukuda, Ogita, and Ueda. Progr. Theor. Phys. **21**, 29 (1959).

[4] L. Landau, Journ. Phys. **3**, 237 (1940).

[5] G. A. Milekhin, JETP **35**, 1185 (1958), Soviet Phys. JETP **8**, 829 (1959).

[6] A. I. Akhiezer and I. Ya. Pomeranchuk, Некоторые вопросы теории ядра (Certain Problems in Nuclear Theory), Gostekhizdat, 1952.

[7] S. Z. Belen'kiĭ, Лавинные процессы в космических лучах (Cascade Processes in Cosmic Rays), Gostekhizdat, 1948.

[8] S. I. Nikol'skiĭ and A. A. Pomanskiĭ, Proc. Intl. Conf. on Cosmic Rays, Moscow, 1959 (in press).

[9] G. A. Milekhin and I. L. Rozental', JETP **33**, 197 (1957), Soviet Phys. JETP **6**, 154 (1958).

[10] Dovzhenko, Zatsepin, Murzina, Nikol'skiĭ, and Yakovlev, op. cit. ref. 8.

[11] Debendetti, Garelli, Tallone, and Vigone, Nuovo cimento **4**, 1142 (1956).

[12] Vernov, Grigorov, Zatsepin, and Chudakov, Izv. Akad. Nauk SSSR Ser. Fiz. **19**, 493 (1955), Columbia Tech. Transl. p. 445.

[13] I. Ya. Pomeranchuk, JETP **14**, 1252 (1944).

[14] A. B. Migdal, JETP **15**, 313 (1945).

Translated by J. G. Adashko
148

INVESTIGATION OF THE STABILITY OF A PLASMA BY A GENERALIZED ENERGY PRINCIPLE

V. F. ALEKSIN and V. I. YASHIN

Physico-Technical Institute, Academy of Sciences, Ukrainian S.S.R.

Submitted to JETP editor April 23, 1960

J. Exptl. Theoret. Phys. (U.S.S.R.) 39, 822-826 (September, 1960)

Stability conditions are derived for a plasma possessing an anisotropic particle velocity distribution and located in a cylindrically symmetric magnetic field. Cases of longitudinal and azimuthal magnetic fields are considered.

1. INTRODUCTION

In the rare collisions when the magnetohydrodynamic approximation is not valid, the stability of a plasma can be investigated with the generalized energy principle, developed by Kruskal and Oberman,[1] according to which the necessary and sufficient condition for the stability of a plasma is that the change δW in the plasma energy be greater than or equal to zero under the possible perturbations.

The application of the generalized energy principle was confined heretofore to the proof of comparison theorems, without account of the charge neutrality of the plasma; it follows from these theorems that the energy change produced by the perturbations is bounded by the energy change in the magnetohydrodynamic approximation from below, and by the approximation of Chew, Goldberger, and Low from above. In the present paper we formulate, on the basis of this principle with allowance for the charge neutrality of the plasma, new comparison theorems for a plasma in a magnetic field which is constant along the force line. We also derive the conditions for the stability of a plasma with arbitrary anisotropic velocity distribution of the particles, located in a magnetic field with cylindrical symmetry. We consider the case of longitudinal and purely-azimuthal magnetic fields, which depend in an arbitrary manner on the distance to the symmetry axis. It is shown that the stability conditions of the plasma in the case of a homogeneous magnetic field remain the same if the field is dependent on the distance to the symmetry axis.

2. GENERALIZED ENERGY PRINCIPLE WITH ACCOUNT OF CHARGE NEUTRALITY OF THE PLASMA

The variation of the energy of a plasma located in a magnetic field $\mathbf{H}(\mathbf{r})$, described by an arbitrary distribution function $f(\mathbf{r}, v_{\parallel}^2, v_{\perp}^2)$, and dependent on the coordinates and on the velocity components parallel and perpendicular to the force lines of the magnetic field, is of the form[1]

$$\delta W = \frac{1}{2}\int d^3x \left\{\frac{Q^2}{4\pi} + [\boldsymbol{\xi}\times\mathbf{Q}]\operatorname{curl}\frac{\mathbf{H}}{4\pi} + (\boldsymbol{\xi}\nabla p_{\perp})\operatorname{div}\boldsymbol{\xi} + 2p_{\perp}(\operatorname{div}\boldsymbol{\xi} - \varkappa)^2 + (p_{\perp} - p_{\parallel})\left[n_i n_k \frac{\partial \xi_l}{\partial x_i}\left(\frac{\partial \xi_l}{\partial x_k} + \frac{\partial \xi_k}{\partial x_l}\right) + n_i n_k \xi_l \frac{\partial}{\partial x_l}\left(\frac{\partial \xi_l}{\partial x_k}\right) - \varkappa^2\right]\right\} + I, \tag{2.1}$$

$$I = -\frac{1}{2}\sum_i m_i \int\int\int \frac{H}{v_{\parallel}} d\mu\, d\varepsilon\, d^3x \left[\frac{f_1^{(i)2}}{\partial f_0^{(i)}/\partial \varepsilon} - \mu^2 H^2 \frac{\partial f_0^{(i)}}{\partial \varepsilon}(\operatorname{div}\boldsymbol{\xi} - \varkappa)^2\right],$$

$$\mathbf{Q} = \operatorname{curl}[\boldsymbol{\xi}\times\mathbf{H}], \qquad \varkappa = n_i n_k \partial \xi_i / \partial x_k, \qquad \mathbf{n} = \mathbf{H}/H, \tag{2.2}$$

where $f_0^{(i)}$ is the equilibrium distribution function of particles of type i (of mass m_i and charge e_i) in the $\mathbf{r}$, $\mathbf{v}$ space; $f_1^{(i)}$ is a small addition to $f_0^{(i)}$, due to the perturbations; the integration variables μ and ϵ are connected with the adiabatic invariant and the particle kinetic energy by the relations $\mu = v_{\perp}^2/2H$ and $\epsilon = (v_{\parallel}^2 + v_{\perp}^2)/2$; finally $p_{\parallel}$ and $p_{\perp}$ are the longitudinal and transverse components of the pressure tensor:

$$p_{\parallel} = \sum_i m_i \int\int \frac{H}{v_{\parallel}} f_0^{(i)} v_{\parallel}^2\, d\mu\, d\varepsilon, \qquad p_{\perp} = \sum_i m_i \int\int \frac{H^2}{v_{\parallel}} f_0^{(i)} \mu\, d\mu\, d\varepsilon. \tag{2.3}$$

The summation is over all types of particles. The distribution function is assumed normalized in the following manner:

$$\frac{1}{4\pi}\int f_0^{(i)} d^3v \equiv \int\int \frac{H}{v_{\parallel}} f_0^{(i)} d\mu\, d\varepsilon = n^{(i)}, \tag{2.4}$$

where $n^{(i)}$ is the density of particles of type i.

The condition for the equilibrium of a plasma with anisotropic pressure is of the form

$$\frac{\partial}{\partial x_k}[p_{\perp}\delta_{ik} + (p_{\parallel} - p_{\perp})n_i n_k] = [\operatorname{curl}\mathbf{H}\times\mathbf{H}]_i. \tag{2.5}$$

In minimizing δW with respect to $f_1^{(i)}$ one must, along with using the additional condition used by Kruskal and Oberman,[1]

$$\int_L \frac{dl}{v_\parallel}\left[v_\parallel^2 \varkappa \frac{\partial f_0^{(i)}}{\partial \varepsilon} + \mu H (\operatorname{div} \xi - \varkappa) \frac{\partial f_0^{(i)}}{\partial \varepsilon} - f_1^{(i)}\right] = 0, \quad (2.6)$$

(where the integration is along the magnetic force line L), take account also of the charge-neutrality condition of the plasma as a whole

$$\sum_i e_i \iint \frac{H}{v_\parallel}\left[(\mu H - v_\parallel^2)(\operatorname{div} \xi - \varkappa) \frac{\partial f_0^{(i)}}{\partial \varepsilon} - f_1^{(i)}\right] d\mu\, d\varepsilon = 0. \quad (2.7)$$

By minimizing δW and taking (2.6) and (2.7) into account, we get

$$f_1^{(i)} = (\lambda_i + e_i \tau / m_i)\, \partial f_0^{(i)} / \partial \varepsilon, \quad (2.8)$$

where $\lambda_i(\mu, \epsilon, L)$ and $\tau(r)$ are the Lagrange multipliers corresponding to conditions (2.6) and (2.7). From (2.6), (2.7), and (2.8) we obtain for these multipliers the system of integral equations

$$\lambda_i = \int_L \frac{dl}{v_\parallel}\left[v_\parallel^2 \varkappa + \mu H (\operatorname{div} \xi - \varkappa) - \frac{e_i}{m_i}\tau\right]\left(\int_L \frac{dl}{v_\parallel}\right)^{-1}, \quad (2.9)$$

$$\tau = \frac{\sum_i e_i \iint \frac{H}{v_\parallel}(\operatorname{div}\xi - \varkappa)(\mu H - \lambda_i) \frac{\partial f_0^{(i)}}{\partial \varepsilon} d\mu\, d\varepsilon}{\sum_i \frac{e_i^2}{m_i} \iint \frac{H}{v_\parallel} \frac{\partial f_0^{(i)}}{\partial \varepsilon} d\mu d\varepsilon}. \quad (2.10)$$

This system can be readily solved by assuming the magnetic field constant along the force line; we have then

$$\lambda_i - \frac{e_i}{m_i}\tau = \frac{1}{l}\int_L dl\,[v_\parallel^2 \varkappa + \mu H (\operatorname{div} \xi - \varkappa)] + \frac{e_i}{m_i}\left[(\operatorname{div} \xi - \varkappa) - \frac{1}{l}\int_L dl\,(\operatorname{div} \xi - \varkappa)\right] g, \quad (2.11)$$

$$g = \sum_i e_i \iint \frac{H^2}{v_\parallel} \frac{\partial f_0^{(i)}}{\partial \varepsilon}\, \mu\, d\mu\, d\varepsilon \Big/ \sum_i \frac{e_i^2}{m_i} \iint \frac{H}{v_\parallel} \frac{\partial f_0^{(i)}}{\partial \varepsilon} d\mu\, d\varepsilon, \quad (2.12)$$

where $\lambda = \int_L dl$ is the length of the magnetic force line L.

Account of the plasma neutrality modifies the comparison theorems. If the magnetic field is constant along the force line, we have in the isotropic and anisotropic cases, respectively,

$$\delta W \geqslant \delta W_H,$$

$$\delta W \leqslant \delta W_L - \frac{1}{2}\int d^3x g \sum_i e_i \iint \frac{H^2}{v_\parallel} \frac{\partial f_0^{(i)}}{\partial \varepsilon}\left[(\operatorname{div} \xi - \varkappa) - \frac{1}{l}\int_L (\operatorname{div} \xi - \varkappa) dl\right]^2 \mu d\mu d\varepsilon, \quad (2.13)$$

where δW_H is the change of energy in the magnetohydrodynamic approximation, and δW_L is the change in the approximation of Chew, Goldberger, and Low.

3. STABILITY OF A PLASMA IN A LONGITUDINAL MAGNETIC FIELD

Let us investigate the stability of a plasma in a magnetic field with anisotropic velocity distribution of the particles. We assume that the field has a cylindrical symmetry and is directed parallel to the symmetry axis. We then have in a cylindrical coordinate system $H_r = 0$, $H_\varphi = 0$, and $H = H_z(r)$. The plasma displacements $\xi(r)$ are represented in the form

$$\xi(r) = [\xi_r(r),\ \xi_\varphi(r),\ \xi_z(r)]\, e^{ikz + im\varphi}. \quad (3.1)$$

The expression for δW does not depend on the component of ξ parallel to the field. This shows that the most dangerous are the convective or interchange instabilities. Minimizing δW with respect to ξ_φ, we obtain

$$\delta W = \frac{k^2}{2}\int d^3x \left\{\eta \xi_r^2 + \frac{\eta\gamma}{m^2\gamma + k^2\eta r^2}\left(\frac{d}{dr} r\xi_r\right)^2\right\}, \quad (3.2)$$

$$\eta = H^2/4\pi + p_\perp - p_\parallel, \qquad \gamma = H^2/4\pi + 2p_\perp + 2q, \quad (3.3)$$

$$q = \frac{1}{2}\left\{\sum_i m_i \iint \frac{H^3}{v_\parallel} \frac{\partial f_0^{(i)}}{\partial \varepsilon} \mu^2 d\mu\, d\varepsilon - g \sum_i e_i \iint \frac{H^2}{v_\parallel} \frac{\partial f_0^{(i)}}{\partial \varepsilon} \mu\, d\mu\, d\varepsilon\right\}. \quad (3.4)$$

The second sum in (3.4) is connected with the condition of plasma charge neutrality, and is positive when $\partial f_0^{(i)}/\partial \epsilon < 0$.

The expression (3.2) leads to the sufficient conditions for the plasma stability

$$H^2/4\pi + p_\perp - p_\parallel \geqslant 0, \qquad H^2/4\pi + 2p_\perp + 2q \geqslant 0. \quad (3.5)$$

Given η and γ, the necessary and sufficient conditions for the stability of the plasma are obtained by minimizing (3.2) with respect to ξ_r and using the boundary conditions. These conditions can be chosen in the form $\xi_r(0) = \xi_r(R) = 0$, if the plasma density vanishes on the boundary $r = R$.

For a plasma in a constant and homogeneous field, analogous stability criteria were obtained by the method of normal oscillations in the work of Kitsenko and Stepanov.[2]

If the plasma is homogeneous and consists of electrons, i = 1, and of ions of one type, i = 2, and if the unperturbed distribution function has the form

$$f_0^{(i)} = \frac{2n_0 m_i^{3/2}}{T_\perp^{(i)}(2\pi T_\parallel^{(i)})^{1/2}} \exp\left(-\frac{m_i v_\parallel^2}{2T_\parallel^{(i)}} - \frac{m_i v_\perp^2}{2T_\perp^{(i)}}\right), \quad (3.6)$$

we obtain from (2.3) and (3.4)

$$p_\parallel = n_0 (T_\parallel^{(1)} + T_\parallel^{(2)}), \qquad p_\perp = n_0 (T_\perp^{(1)} + T_\perp^{(2)}),$$

$$q = -n_0 \left(\frac{T_\perp^{(1)2}}{T_\parallel^{(1)}} + \frac{T_\perp^{(2)2}}{T_\parallel^{(2)}} \right) + \frac{n_0}{2} \frac{(T_\parallel^{(1)} T_\perp^{(2)} - T_\parallel^{(2)} T_\perp^{(1)})^2}{T_\parallel^{(1)} T_\parallel^{(2)} (T_\parallel^{(1)} + T_\parallel^{(2)})}.$$

When $T_\parallel^{(1)} = T_\parallel^{(2)}$ and $T_\perp^{(1)} = T_\perp^{(2)}$, the stability conditions (3.5) become the same as the conditions obtained by Vedenov and Sagdeev,[3] provided the error in the cited paper is corrected.

4. STABILITY OF A PLASMA IN AN AZIMUTHAL MAGNETIC FIELD

Let us consider an azimuthal magnetic field with components $H_r = H_z = 0$, $H = H_\varphi(r)$. When investigating the stability of a plasma in such a field under displacements of the type (3.1), it is best to consider separately the cases of "necking," m = 0, and bending, m ≠ 0. As a result of minimizing δW with respect to ξ_z, we obtain by integrating over φ and z, with m = 0,

$$\delta W = \pi \int r\, dr \left\{ \left[\eta + 3p_\parallel + 2r \frac{dp_\perp}{dr} - \frac{(H^2/4\pi - p_\parallel)^2}{H^2/4\pi + 2p_\perp} \right] \frac{\xi_r^2}{r^2} + \frac{p_\perp - p_\parallel}{r} \frac{d}{dr} \xi_r^2 \right\}. \tag{4.1}$$

Integrating the second term in (4.1) by parts, we get

$$\delta W = \pi \int r\, dr \left[\frac{H^2}{4\pi} + p_\perp + 2p_\parallel + r \frac{d}{dr} (p_\perp + p_\parallel) - \frac{(H^2/4\pi - p_\parallel)^2}{(H^2/4\pi + 2p_\perp)} \right] \frac{\xi_r^2}{r^2}, \tag{4.2}$$

from which follows the necessary and sufficient condition for the plasma stability

$$\frac{H^2}{4\pi} + p_\perp + 2p_\parallel + r \frac{d}{dr} (p_\perp + p_\parallel) - \frac{(H^2/4\pi - p_\parallel)^2}{H^2/4\pi + 2p_\perp} \geqslant 0. \tag{4.3}$$

For m ≠ 0 the change in energy becomes, after integrating over φ and z and minimizing with respect to ξ_z,

$$\delta W = \pi \int r\, dr \left\{ \left[(m^2+1)\eta + 2r \frac{dp_\perp}{dr} - \eta \frac{k^2 r^2 \eta + m^2 \gamma}{m^2 \eta + k^2 r^2 \gamma} \right] \frac{\xi_r^2}{r^2} + \frac{1}{r} \left(\eta\gamma \frac{m^2 + k^2 r^2}{m^2 \eta + k^2 r^2 \gamma} - \frac{H^2}{4\pi} \right) \frac{d}{dr} \xi_r^2 + \frac{m^2 \eta \gamma}{m^2 \eta + k^2 r^2 \gamma} r^2 \left(\frac{d}{dr} \frac{\xi_r}{r} \right)^2 \right\}. \tag{4.4}$$

Integrating the second term in (4.4) by parts we obtain the sufficient stability conditions

$$H^2/4\pi + p_\perp - p_\parallel \geqslant 0, \qquad H^2/4\pi + 2p_\perp + 2q \geqslant 0, \tag{4.5}$$

$$(m^2-2)\eta - r\, d\eta/dr - (m^2\eta + k^2 r^2 \gamma)^{-2} \{ \eta\delta [m^2 (k^2 r^2 - m^2)\eta + k^2 (m^2 + k^2 r^2) r^2 \gamma] + m^2 r [k^2 r^2 \delta^2 d\eta/dr - (k^2 r^2 + m^2) \eta^2 d\delta/dr] \} \geqslant 0 \qquad (\delta = \eta - \gamma). \tag{4.6}$$

In an isotropic plasma δ = 0 and the stability criteria (4.3) and (4.6) become the same as those obtained by Kadomtsev[4]

$$-\frac{1}{2r^3} \frac{d}{dr} \left(r^2 \frac{H^2}{4\pi} \right)^2 - 2rp \frac{d}{dr} \left(\frac{H^2}{4\pi} \right) + 3p \frac{H^2}{4\pi} + 5p^2 \geqslant 0 \quad (m = 0),$$

$$(m^2 - 2) H^2 - r \frac{d}{dr} H^2 \geqslant 0 \qquad (m \neq 0).$$

Conditions (4.5) are then satisfied automatically.

In the case of long-wave perturbations, when kr ≪ 1, condition (4.6) assumes the simple form

$$(m^2 - 1) \left(\frac{H^2}{4\pi} + p_\perp - p_\parallel \right) - \frac{d}{dr} r \left(\frac{H^2}{4\pi} + 2p_\perp + 2q \right) \geqslant 0.$$

In conclusion, the authors are grateful to A. I. Akhiezer, K. N. Stepanov, and A. B. Kitsenko for valuable advice and a discussion of the results of the work.

[1] M. D. Kruskal and C. R. Oberman, Физика горячей плазмы и термоядерные реакции (Physics of Hot Plasma and Thermonuclear Reactions), Glavatom 1, 42 (1959).

[2] A. B. Kitsenko and K. N. Stepanov, JETP 38, 1840 (1960), Soviet Physics JETP 11, 1323 (1960).

[3] A. A. Vedenov and R. Z. Sagdeev, Физика плазмы и проблема управляемых термоядерных реакции (Physics of Plasma and the Problem of Controllable Thermonuclear Reactions), U.S.S.R. Acad. Sci. 3, 278 (1958).

[4] B. B. Kadomtsev, JETP 37, 1096 (1959), Soviet Physics JETP 10, 780 (1960).

Translated by J. G. Adashko
149

EQUATIONS FOR THE MANDELSTAM REPRESENTATION SPECTRAL FUNCTIONS

K. A. TER-MARTIROSYAN

Submitted to JETP editor April 23, 1960

J. Exptl. Theoret. Phys. (U.S.S.R.) 39, 827-840 (September, 1960)

On the basis of unitarity, a closed system of equations is derived for the Mandelstam-representation spectral functions, fully symmetric with respect to the three channels of the four-particle vertex. The question of consistency of equations obtained by applying unitarity in different channels is clarified. If the integral representation is written down with subtractions, one obtains a set of coupled equations for the one-variable and two-variable spectral functions. Consistent iteration of these equations corresponds to taking into account the contribution (or part of the contribution) from a number of Feynman diagrams consisting of two parts connected by two lines. This set of equations reduces to a Chew-Mandelstam type equation if the terms containing the two-variable spectral functions are neglected.

1. INTRODUCTION

It has been conjectured recently that it may be possible to construct quantum field theory directly from the unitarity conditions together with relations (of the dispersion type) arising from the analytic properties of the amplitudes.

Working along these lines Mandelstam[1-3] and Chew[4] constructed a scheme based on the assumption, that for not too high energies the nearest lying singularities (poles, branch points), i.e. the simplest two-particle terms in the unitarity relations, dominate the behavior of the amplitudes.* The two-particle into two-particle transition amplitudes involved in these terms may be expressed in terms of the integral representation proposed by Mandelstam.[1] At the same time a number of relations among the spectral functions of the integral representation can be obtained from the unitarity conditions and these relations may be considered as the basic equations of the theory. This system of equations for the spectral functions has not been obtained in closed form. This may be due to the fact that the three unitarity conditions, for the three channels of the four-particle vertex, are incompatible in the two-particle approximation (as was noted by Mandelstam).

As is shown below, this incompatibility is easily removed by taking into account on the right side of the unitarity condition an appropriate part of the contributions due to all many-particle processes. The corresponding terms have a simple interpretation in terms of diagrams, and when they are taken into account a closed system of equations is obtained for the spectral functions, fully symmetric with respect to the three channels.

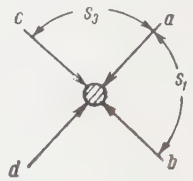

FIG. 1. The four-particle function – the amplitude for the processes $a+b \rightleftarrows c+d$, $a+d \rightleftarrows c+b$, $a+c \rightleftarrows b+d$

In the system of equations obtained from the Mandelstam representation with subtractions appear both spectral functions depending on two variables and on one variable. The iteration in the coupling constants of the resultant equations corresponds to a consistent taking into account of contributions (or a well defined part of the contributions) from Feynman diagrams consisting of two parts connected by two lines. If terms involving the two-variable spectral functions are neglected then the resultant equations are analogous to the equations obtained by Chew and Mandelstam[4] (for the meson-meson interaction), Cini and Fubini,[8] and a number of other authors.[9]

2. UNITARITY CONDITIONS

Let us consider the four-particle vertex function shown in Fig. 1, i.e., the two-particle into two-particle transition amplitude $A = A(s_1, s_2, s_3)$. This amplitude describes transitions in three channels: in the first channel for the reaction $a + b \rightleftarrows c + d$, in the second for the reaction

*This assumption is not as obvious as may seem at first sight, since infinitely distant singularities of the amplitude may be important (in this connection see discussion at the end of the article on the question of convergence of the integral representation).

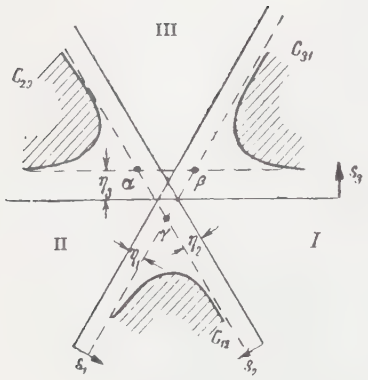

FIG. 2. The system of triangular coordinates s_1, s_2, s_3, with $s_1 + s_2 + s_3 = \nu$. The height of the small equilateral triangle in the center of the figure is equal to the sum of the squares of the masses (ν) of the four particles a, b, c, d; inside the dashed triangle $\alpha\beta\gamma$ the amplitude is real.

$a + d \rightleftarrows b + c$, in the third for the reaction $a + c \rightleftarrows b + d$ and it is a function of the invariants

$$s_1 = (p_a + p_b)^2 = (\varepsilon_a + \varepsilon_b)^2 - (\mathbf{p}_a + \mathbf{p}_b)^2,$$
$$s_2 = (p_a + p_d)^2, \quad s_3 = (p_a + p_c)^2,$$

which are equal to the square of the energy of the particles in the barycentric frame in the respective channel. (These invariants were denoted by Mandelstam[2,3] by s, u and t respectively.)

Since $s_1 + s_2 + s_3 = \nu$, where ν is the sum of the squares of the masses of the four particles in Fig. 1, it is convenient to discuss the amplitude A as a function of the position of the point $\xi = (s_1, s_2, s_3)$ in the triangular coordinates of Fig. 2. In these coordinates s_1, s_2 and s_3 represent the distances of an arbitrary point ξ in the plane of Fig. 2 from the sides of an equilateral triangle (shown by heavy lines in the center of Fig. 2), whose height is equal to ν. Since the sum of these distances is always equal to the height of the triangle the condition $s_1 + s_2 + s_3 = \nu$ is automatically fulfilled for any point ξ in the plane of Fig. 2.

If the particles a, b, c, and d of Fig. 1 are different then the unitarity conditions relate the amplitude A to a number of other four-particle vertex functions: $B^{(1)}$ and $C^{(1)}$ in the first channel [see Fig. (3a)], $B^{(2)}$ and $C^{(2)}$ in the second channel, and $B^{(3)}$ and $C^{(3)}$ in the third channel [the notation is obvious from Fig. (3)]. It follows from Fig. (3) that the unitarity conditions may be expressed in the form

$$A_1(s_1, s_2, s_3) = \zeta_1(s_1) \int B^{(1)*}(s_1, s_2', s_3')\, C^{(1)}(s_1, s_2'', s_3'')\, d\mathbf{n}_1/4\pi + \Delta_1(s_1, s_2, s_3), \quad (1)$$

$$A_2(s_1, s_2, s_3) = \zeta_2(s_2) \int B^{(2)*}(s_1', s_2, s_3')\, C^{(2)}(s_1'', s_2, s_3'')\, d\mathbf{n}_2/4\pi + \Delta_2(s_1, s_2, s_3), \quad (2)$$

$$A_3(s_1, s_2, s_3) = \zeta_3(s_3) \int B^{(3)*}(s_1', s_2', s_3)\, C^{(3)}(s_1'', s_2'', s_3)\, d\mathbf{n}_3/4\pi + \Delta_3(s_1, s_2, s_3). \quad (3)$$

Here A_1, A_2, A_3 stand for the absorptive part of the amplitude A in each of the three channels, so that, for example

$$A_1 = (2i)^{-1}(A(s_1 + i\tau_1, s_2, s_3) - A(s_1 - i\tau_1, s_2, s_3)),$$

and ζ_1, ζ_2, ζ_3 are functions determining the statistical weight* of the two-particle states (α_1, β_1), (α_2, β_2), (α_3, β_3) in Fig. (3), into which transitions from the initial state (of channel one, two and three) are allowed by all conservation laws. It is understood that the quantities $B^{(i)*}C^{(i)}$ ($i = 1, 2, 3$) in Eqs. (1) — (3) are summed over all possible types of these particles, in particular if the particles α_1, β_1 have spin then a summation over spin variables is understood. For brevity such summations will not be indicated; for the same reason we have written in these equations $B^{(i)*}C^{(i)}$ instead of $\frac{1}{2}(B^{(i)*}C^{(i)} + B^{(i)}C^{(i)*})$. The integration in Eqs. (1) — (3) is over the directions $\mathbf{n}$ of the momenta of the particles α_1 (or β_1) in the barycentric frame.

The amplitudes in Eqs. (1) — (3) depend on the invariants s_i, s_i', and s_i'' whose meaning is explained in Fig. 3 and in the caption to that figure.

The symbols Δ_1, Δ_2, and Δ_3 stand for contributions from terms corresponding to production of three or more particles. The quantity Δ_1 vanishes if s_1 is below the threshold for production of three particles (or four, if the transition from the initial state with particles a,b into a three-particle state is forbidden); similarly Δ_2 and Δ_3 vanish if s_2 and s_3 are below the corresponding thresholds.

If the amplitude A has pole terms then to the right side of Eq. (1) terms proportional to $\delta(s_1 - \mu_\alpha^2)$ should be added, where μ_α are the masses of the bound states. Similar terms must be added to Eqs. (2) and (3). The unitarity relations (1) — (3) also hold for each of the amplitudes $B^{(i)}$ and $C^{(i)}$. This is also true for all the fol-

*The quantities ζ depend on the normalization of all amplitudes. For the same normalization as used by Chew and Mandelstam,[4] where the cross sections and amplitudes are related by

$$\left(\frac{d\sigma}{d\Omega}\right)_1 = \frac{q_{cd}}{q_{ab}} \left| \frac{4}{\sqrt{s_1}} A \right|^2$$

(q_{ab} and q_{cd} are the momenta of the particles in the barycentric frame before and after the transition), the ζ_i are given by

$$\zeta_i = 4(\varkappa_i \sqrt{s_i})^{-1} q_{\alpha_i\beta_i}\theta(s_i - \eta_i),$$

where $q_{\alpha_i\beta_i} = [2\sqrt{s_i}]^{-1}[s_i - (\mu_{\alpha_i} - \mu_{\beta_i})^2]^{1/2}(s_i - \eta_i)^{1/2}$; $\eta_i = (\mu_{\alpha_i} + \mu_{\beta_i})$; $\varkappa_i = 2$, if the particles α_i and β_i are identical and $\varkappa_i = 1$ if they are different; the θ function is equal to unity if $s_i > \eta_i$ and equal to zero if $s_i < \eta_i$.

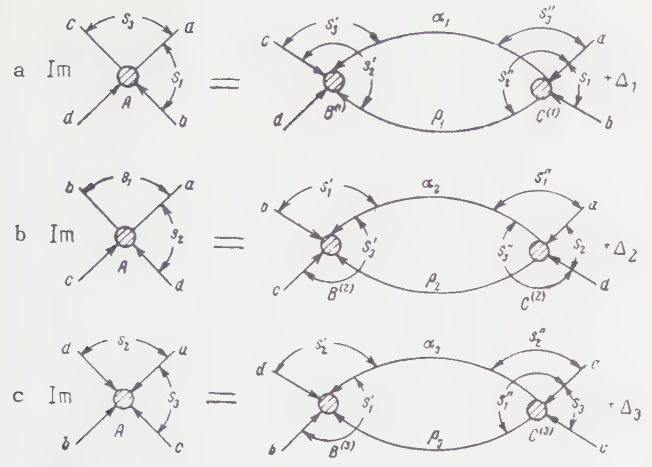

FIG. 3. The unitarity conditions in the three channels. On the left side of the equalities stand the absorptive parts of the amplitudes. The notation is:

a: $s_2' = (p_{\alpha_1}+p_d)^2$, $s_3' = (p_{\alpha_1}+p_c)^2$, $s_2'' = (p_b - p_{\alpha_1})^2$, $s_3'' = (p_a - p_{\alpha_1})^2$;

b: $s_1' = (p_b + p_{\alpha_2})^2$, $s_3' = (p_c + p_{\alpha_2})^2$, $s_1'' = (p_a - p_{\alpha_2})^2$, $s_3'' = (p_d - p_{\alpha_2})^2$;

c: $s_1' = (p_{\alpha_3} + p_b)^2$, $s_2' = (p_{\alpha_3} + p_d)^2$, $s_1'' = (p_c - p_{\alpha_3})^2$, $s_2'' = (p_a - p_{\alpha_3})^2$.

The same notation is used in Eqs. (1)–(3); to them corresponds the numbering of the channels of the amplitudes $B^{(i)}$ and $C^{(i)}$ (i = 1, 2, 3) used in what follows.

lowing relations which will always be written out, for the sake of brevity, for the A amplitude only.

We shall consider only the case of "normal"[5] relations between the masses of all particles, when the integral representation of Mandelstam is valid. In that case the left sides of Eqs. (1) – (3) may be expressed in the form[1]

$$A_1 = \frac{1}{\pi}\int_0^\infty \left[\frac{A_{12}(s_1,\sigma)}{\sigma - s_2} + \frac{A_{31}(\sigma, s_1)}{\sigma - s_3}\right] d\sigma,$$

$$A_2 = \frac{1}{\pi}\int_0^\infty \left[\frac{A_{23}(s_2,\sigma)}{\sigma - s_3} + \frac{A_{12}(\sigma, s_2)}{\sigma - s_1}\right] d\sigma,$$

$$A_3 = \frac{1}{\pi}\int_0^\infty \left[\frac{A_{31}(s_3,\sigma)}{\sigma - s_1} + \frac{A_{23}(\sigma, s_3)}{\sigma - s_2}\right] d\sigma, \qquad (4)$$

where the A_{ij} are real spectral functions. By making use of the one-dimensional integral representation for the amplitudes $B^{(i)}$ and $C^{(i)}$, Mandelstam showed that the first terms on the right sides of Eqs. (1) – (3) can be reduced to precisely the same form. We write out the expressions obtained by Mandelstam[1] for these terms, for relations (1), (2), and (3) respectively:

$$\frac{1}{\pi}\int_0^\infty \left[\frac{P_1(s_1,\sigma)}{\sigma - s_2} + \frac{Q_1(\sigma, s_1)}{\sigma - s_3}\right] d\sigma,$$

$$\frac{1}{\pi}\int_0^\infty \left[\frac{P_2(s_2,\sigma)}{\sigma - s_3} + \frac{Q_2(\sigma, s_2)}{\sigma - s_1}\right] d\sigma,$$

$$\frac{1}{\pi}\int_0^\infty \left[\frac{P_3(s_3,\sigma)}{\sigma - s_1} + \frac{Q_3(\sigma, s_3)}{\sigma - s_2}\right] d\sigma, \qquad (5)$$

where

$$Q_1(s_3, s_1) = \frac{1}{\pi^2}\iint_0^\infty \Gamma_1(m', m''; s_3, s_1)[B_3^{(1)*}C_3^{(1)} + B_2^{(1)*}C_2^{(1)}]\, dm'^2\, dm''^2, \qquad (5a)$$

$$P_1(s_1, s_2) = \frac{1}{\pi^2}\iint_0^\infty \Gamma_1'(m', m''; s_2, s_1)[B_2^{(1)*}C_3^{(1)} + B_3^{(1)*}C_2^{(1)}]\, dm'^2\, dm''^2. \qquad (5b)$$

Here $B_2^{(1)}$ stands for the absorptive part of the amplitude $B^{(1)}$ in the second channel, in which the variable s_2 has been replaced by m'^2, and s_3 by $\nu_1' - m'^2 - s_1$ (ν_1' stands for the sum of the squares of the masses of the four particles for the amplitude $B^{(1)}$), i.e., $B_2^{(1)} = B_2^{(1)}(s_1, m'^2, \nu_1' - m'^2 - s_1)$; the variables s_i, or the quantities by which these variables were replaced, are written throughout in the order s_1, s_2, s_3. Analogously

$$B_3^{(1)} = B_3^{(1)}(s_1, \nu_1' - m'^2 - s_1, m'^2),$$

$$C_2^{(1)} = C_2^{(1)}(s_1\, m''^2, \nu_1'' - m''^2 - s_1),$$

$$C_3^{(1)} = C_3^{(1)}(s_1, \nu_1'' - m''^2 - s_1, m''^2).$$

By Γ_1 is denoted the spectral function A_{31} of the box diagram, Fig. 4a, for which m′ and m″ are the masses of the particles corresponding to the vertical lines.* The function Γ_1 differs from zero beyond the curve $C_{31}^{(a)}$ (Fig. 5) corresponding to the singular points of the diagram in Fig. 4a;

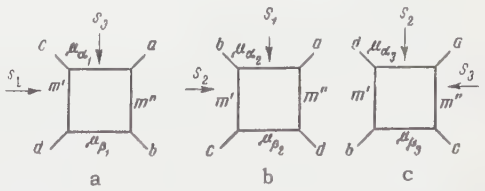

FIG. 4. Feynman diagrams for which the spectral functions are given by: a – the quantity Γ_1, b – the quantity Γ_2, and c – the quantity Γ_3. The quantities Γ_1', Γ_2' and Γ_3' stand for spectral functions of the same diagrams but with two particles in the left parts of each diagram interchanged.

*We give, for checking purposes, the value of Γ_1 corresponding to the normalization indicated in the footnote on p. 576. $\Gamma_1 = -8\pi\kappa_1^{-1}A_{13}^{(4)}$, where $A_{13}^{(4)}$ is given in Eq. (3.25) of the Mandelstam paper[2] (after exchanging particles to correspond to Fig. 4a).

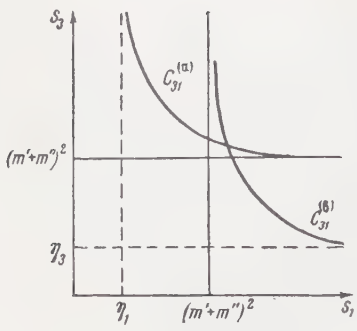

FIG. 5. The curves of singular points of the box diagrams, Fig. 4a ($C_{31}^{(a)}$) and Fig. 4c ($C_{31}^{(c)}$) with particles b and d interchanged (with $s_2 \to s_1$). The quantities Γ_1 and Γ_3' [in Eqs. (5a) and (5b)] are different from zero in the region beyond these curves.

this curve has in the $s_1 - s_2$ plane the asymptotes $s_1 = \eta_1 = (\mu_{\alpha_1} + \mu_{\beta_1})^2$ and $s_3 = (m' + m'')^2$. In particular, if either $s_1 < \eta_1$ or $s_3 < (m' + m'')^2$ then Γ_1 is certainly equal to zero. Similarly we denote by Γ_1' the spectral function A_{12} of the box diagram, Fig. 4a, in which the particles c and d (in the left part of the diagram) are exchanged.

All of the notation here introduced (including, in particular, the definitions in Fig. 3) is fully symmetric with respect to the three channels of the amplitude A; all of the relations for channel one [including, in particular, Eqs. (1) — (5)] go over into the corresponding relations for channel two by the cyclic permutation of the indices $1 \to 2$, $2 \to 3$, $3 \to 1$. One more cyclic permutation of all indices (i.e., the substitution $1 \to 3$, $2 \to 1$, $3 \to 2$) leads to the relations for channel three.

When this is taken into account it is easy to derive from Eqs. (5a) and (5b) the values of the quantities Q_2, Q_3 and P_2, P_3. The corresponding quantities Γ_2, Γ_3 and Γ_2', Γ_3' will represent the spectral functions of the diagrams, Fig. 4b and 4c, and (for Γ_2', Γ_3') the analogous diagrams obtained by interchanging particles in the left part of the diagrams. For example, for $P_3(s_3, s_1)$ we obtain from Eq. (5b)

$$P_3(s_3, s_1) = \frac{1}{\pi^2} \int_0^\infty\int\int \Gamma_3'(m', m''; s_1, s_3)[B_1^{(3)*} C_2^{(3)} + B_2^{(3)*} C_1^{(3)}]\, dm'^2\, dm''^2. \tag{5c}$$

The notation $B_j^{(3)}$ and $C_j^{(3)}$ ($j = 1, 2$) is analogous to that used in Eqs. (5a) and (5b); the spectral function Γ_3' of the diagram in Fig. 4c (with particles b and d in the left part of the diagram interchanged) is different from zero in the region beyond the curve $C_{31}^{(c)}$ in Fig. 5; it certainly vanishes if $s_3 < \eta_3$ [where $\eta_3 = (\mu_{\alpha_3} + \beta_3)^2$ or if $s_1 < (m' + m'')^2$.

The relations (4) and (5) were written without subtractions. The modifications introduced by subtractions are considered below.

The terms Δ_1, Δ_2, and Δ_3 in Eqs. (1) — (3) are equal to the difference of expressions (4) and (5). Therefore they may be represented in the same form as Eqs. (4) and (5).

$$\Delta_1 = \frac{1}{\pi}\int_0^\infty \left[\frac{u_1(s_1, \sigma)}{\sigma - s_2} + \frac{v_1(\sigma, s_1)}{\sigma - s_3}\right] d\sigma,$$

$$\Delta_2 = \frac{1}{\pi}\int_0^\infty \left[\frac{u_2(s_2, \sigma)}{\sigma - s_3} + \frac{v_2(\sigma, s_2)}{\sigma - s_1}\right] d\sigma,$$

$$\Delta_3 = \frac{1}{\pi}\int_0^\infty \left[\frac{u_3(s_3, \sigma)}{\sigma - s_1} + \frac{v_3(\sigma, s_3)}{\sigma - s_2}\right] d\sigma, \tag{6}$$

where u_1, u_2, u_3 and v_1, v_2, v_3 are real functions (the same kind of functions as A_{ij} and P_i, Q_i). Since $\Delta_1 \equiv 0$ if s_1 is below the threshold for production of three (four) particles, it follows that in that case $u_1 = v_1 = 0$. Analogously, u_2, v_2 and u_3, v_3 vanish respectively if s_2 and s_3 are below the same thresholds in the other two channels.

3. EQUATIONS FOR THE SPECTRAL FUNCTIONS A_{ij}

We substitute Eqs. (4) — (6) into Eqs. (1) — (3), analytically continue Eqs. (1) — (3) into the unphysical region — beyond the curves C_{12}, C_{23}, C_{31} in Fig. 2 — and equate in these regions the imaginary parts of both sides of the equalities (1) — (3). In this way we obtain six equations for the three spectral functions A_{12}, A_{23}, and A_{31} — two equations for each function. For example, from Eqs. (1) and (3) we obtain for A_{31}

$$A_{31}(s_3, s_1) = Q_1(s_3, s_1) + v_1(s_3, s_1),$$
$$A_{31}(s_3, s_1) = P_3(s_3, s_1) + u_3(s_3, s_1). \tag{7}$$

In the two-particle approximation, i.e., with $v_1 = u_3 = 0$, these equations are incompatible since Q_1 and P_3 are not equal to each other.

If s_1 is below the threshold for production of three (four) particles then v_1 vanishes; similarly u_3 vanishes if s_3 is below this threshold. In precisely the same way one notes that Q_1 vanishes for s_3 below the threshold for production of three (four) particles, and P_3 vanishes for s_1 below this threshold [see the above indicated properties of the quantities Γ_1 and Γ_3' in the integrals (5a) and (5c)].

An exception arises when all four of the amplitudes $B^{(1)}$, $C^{(1)}$ and $B^{(2)}$, $C^{(3)}$ in Eqs. (5a) and (5c) have poles. In that case one must extract from Eqs. (5a) and (5c) the contribution (which is the same in both integrals) arising from integration simultaneously over the poles of both the amplitudes B and C. This contribu-

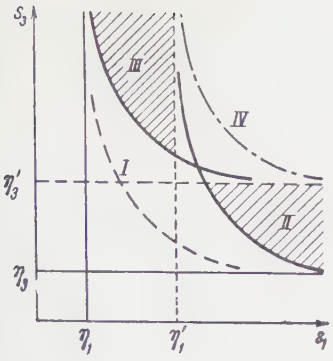

FIG. 6. Regions of nonvanishing values for the following quantities in Eq. (8): beyond the curve I – $A_{31}^{(0)}$, II – P_3, III – Q_1 and IV – δA_{31}. The symbols η_1' and η_3' denote thresholds for production of three (or four) particles. The spectral functions are correctly determined (within small corrections) only in the shaded regions of the figure.

tion is the spectral function $A_{31}^{(0)}$ of the box diagram, Fig. 4a,* when m'' and m' are equal to the pole values μ_{α_3} and μ_{β_3}. If we set

$$A_{31} = A_{31}' + A_{31}^{(0)}, \qquad Q_1 = Q_1' + A_{31}^{(0)}, \qquad P_3 = P_3' + A_{31}^{(0)},$$

then we obtain for A_{31}', Q_1' and P_3' equations of precisely the same form as Eq. (7), in which Q_1' certainly vanishes if s_3 is below the threshold for production of three particles, and P_3' certainly vanishes if s_1 is below this threshold. Consequently, the only difference between this case and others lies in the requirement that the contribution $A_{31}^{(0)}$ be extracted from the spectral function A_{31}.

We shall consider the quantities Q_1 and P_3 in Eq. (7) as known. Then a general solution of the two equations (7) for the three unknowns A_{31}, v_1 and u_3 will be given by

$$v_1 = P_3 + \delta A_{31}, \qquad u_3 = Q_1 + \delta A_{31}, \quad A_{31} = Q_1 + P_3 + \delta A_{31} \tag{8}$$

By δA_{31} we denote here some function of s_3 and s_1 which cannot be determined from Eq. (7). It is clear, however, that δA_{31} vanishes if either s_3 or s_1 is below the threshold for production of three (or four) particles. (If s_1 is below that threshold then $v_1 = P_3 = 0$, if s_3 is then $u_3 = Q_1 = 0$; in both cases $\delta A_{31} = 0$.)

In this manner the quantity A_{31} is expressed in Eq. (8) as a sum of two terms, $(Q_1 + P_3)$ and δA_{31}, of which the first vanishes if at least one of the variables is below the threshold for production of two particles, and the second vanishes if one of the variables is below the threshold for production of three (four) particles. Figure 6 shows in the $s_3 s_1$-plane those regions in which various terms of Eq. (8) fail to vanish.† In order to determine δA_{31} it is necessary to take correctly into account in the unitarity condition the contributions of terms corresponding to the production of three and more particles (requiring the discussion of, in addition to the four-particle function, diagrams involving a larger number of external lines — the five-particle, six-particle functions, etc.). It is natural to construct a theory by ignoring in the first approximation terms of the type δA_{31}, corresponding to distant singularities of the amplitude, i.e., to set $\delta A_{31} = 0$. It then follows from Eqs. (5a), (5c) and (8) that

$$A_{31} = \frac{1}{\pi^2}\int_0^\infty\!\!\int \{\Gamma_1(s_3, s_1)\,[B_3^{(1)*}C_3^{(1)} + B_2^{(1)*}C_2^{(1)}] + \Gamma_3'(s_1, s_3)\,[B_1^{(3)*}C_2^{(3)} + B_2^{(3)*}C_1^{(3)}]\}\,dm'^2 dm''^2. \tag{9a}$$

It is obvious that the remaining equations for A_{12} and A_{23} may be obtained from the above by one or two cyclic permutations of all the indices 1, 2, 3:

$$A_{12} = \frac{1}{\pi^2}\int_0^\infty\!\!\int \{\Gamma_2(s_1, s_2)[B_1^{(2)*}C_1^{(2)} + B_3^{(2)*}C_3^{(2)}] + \Gamma_1'(s_2, s_1)\,[B_2^{(1)*}C_3^{(1)} + B_3^{(1)*}C_2^{(1)}]\}\,dm'^2\,dm''^2, \tag{9b}$$

$$A_{23} = \frac{1}{\pi^2}\int_0^\infty\!\!\int \{\Gamma_3(s_2, s_3)\,[B_2^{(3)*}C_2^{(3)} + B_1^{(3)*}C_1^{(3)}] + \Gamma_2'(s_3, s_2)\,[B_3^{(2)*}C_1^{(2)} + B_1^{(2)*}C_3^{(2)}]\}\,dm'^2\,dm''^2. \tag{9c}$$

If the amplitudes $B^{(i)}$ and $C^{(i)}$ have poles then one must add on the right hand side of these equations the spectral functions $A_{31}^{(0)}$, $A_{12}^{(0)}$ and $A_{23}^{(0)}$ corresponding to the diagrams, Fig. 4a, b, c (with the masses m' and m'' equal to the pole values).

The system of equations (9), together with relations of the type of Eq. (4) for the absorptive parts of the amplitudes $B^{(i)}$ and $C^{(i)}$), form a complete system of equations for the spectral functions for all amplitudes.

At this time it is not clear whether these equations determine the spectral functions uniquely (and, if not, then what additional requirements must be imposed in order that the determination be unique).

4. EQUATIONS FOR THE ONE-VARIABLE SPECTRAL FUNCTIONS

In the majority of cases the integrals (4) — (6) over σ diverge. For example, the functions $A_{ij}(s, \sigma)$ in Eq. (4) for constant s not only do not fall off, but increase with σ (almost proportionally to σ). Therefore all the integral representations must be written with subtractions taken into account. We then obtain[2] instead of Eq. (4)

*Or of the identical to it diagram, Fig. 4c, with particles a and c interchanged, in which $m'' = \mu_{\alpha_1}$, and $m' = \mu_{\beta_2}$.

†The shaded region represents the region in which the spectral function A_{31} is correctly given by Eq. (8) (i.e., in this region higher order approximations will result in small corrections only).

$$A_1 = a_1(s_1) + \frac{1}{\pi}\int_0^\infty [\varphi(\sigma, s_2) A_{12}(s_1, \sigma) + \varphi(\sigma, s_3) A_{31}(\sigma, s_1)]\, d\sigma,$$

$$A_2 = a_2(s_2) + \frac{1}{\pi}\int_0^\infty [\varphi(\sigma, s_3) A_{23}(s_2, \sigma) + \varphi(\sigma, s_1) A_{12}(\sigma, s_2)]\, d\sigma,$$

$$A_3 = a_3(s_3) + \frac{1}{\pi}\int_0^\infty [\varphi(\sigma, s_1) A_{31}(s_3, \sigma) + \varphi(\sigma, s_2) A_{23}(\sigma, s_3)]\, d\sigma. \quad (4')$$

These relations differ from (4) only in the appearance on the right hand sides of the spectral functions a_1, a_2, a_3, which depend on one variable only, and in the replacement under the integral sign of $1/(\sigma - s_i)$ by the difference

$$\varphi(\sigma, s_i) = \frac{1}{\sigma - s_i} - \frac{1}{\sigma - s_{i0}} = \frac{s_i - s_{i0}}{(\sigma - s_i)(\sigma - s_{i0})},$$

where (s_{10}, s_{20}, s_{30}) is some point at which the subtraction is carried out.*

The one-dimensional integral representation with subtractions for the amplitude A is given by

$$A = F_1 + \frac{1}{\pi}\int_0^\infty [\varphi(m'^2, s_2) A_2 + \varphi(m'^2, s_3) A_3]\, dm'^2, \quad (10)$$

where A_2 and A_3 are determined in precisely the same way as the quantities $B_2^{(1)}$ and $B_3^{(1)}$ in Eqs. (5a), (5b), i.e.,

$$A_2 = A_2(s_1, m'^2, \nu - m'^2 - s_1),$$

$$A_3 = A_3(s_1, \nu - m'^2 - s_1, m'^2).$$

F_1 stands for the following function of s_1:

$$F_1(s_1) = a_0 + \frac{1}{\pi}\int_0^\infty \varphi(\sigma, s_1) a_1(\sigma)\, d\sigma + \frac{1}{\pi^2}\int_0^\infty\int_0^\infty \frac{(s_1 - s_{10}) A_{23}(m'^2, m''^2)\, dm'^2 dm''^2}{(\nu - m'^2 - m''^2 - s_1)(m'^2 - s_{20})(m''^2 - s_{30})}, \quad (10a)$$

where by a_0 we denote the value of A at the point s_{10}, s_{20}, s_{30} (it is convenient to choose this point inside the triangle $\alpha\beta\gamma$ in Fig. 2 because then a_0 is real). As can be verified by direct calculations, the substitution of Eqs. (4′) and (10a) into the Eq. (10) for A results in the two dimensional Mandelstam representation [cf. Mandelstam,[2] Eq. (2.13)] with one subtraction. Two more one dimensional representations analogous to Eq. (10) follow by one or two cyclic permutations of all indices in Eqs. (10) and (10a).

Let us also give the expression for the average of the amplitude A over the scattering angle ϑ_1 in channel one ($\cos\vartheta_1 = q_{ab}\, q_{cd}/q_{ab}\, q_{cd}$) For constant s_1 the quantities s_2 and s_3 are functions of this angle. We denote the average of A over $\cos\theta_1$ by $\langle A(s_1)\rangle_1$ and the average of the function φ in Eq. (10) by $l_i(m'^2, s_1) = \langle\varphi(m'^2, s_i)\rangle_1$, where $i = 2, 3$. All quantities are functions of s_1. According to Eq. (10)

$$\langle A(s_1)\rangle_1 = F_1(s_1) + \frac{1}{\pi}\int_0^\infty [l_2(m'^2, s_1) A_2 + l_3(m'^2, s_1) A_3]\, dm'^2. \quad (11)$$

We observe that l_2 and l_3 are simple logarithmic functions of m'^2 (cf. Mandelstam,[2] p. 1745); for example

$$l_3 = \left\langle \frac{1}{m'^2 - s_3} \right\rangle_1 - \frac{1}{m'^2 - s_{30}},$$

$$\left\langle \frac{1}{m'^2 - s_3} \right\rangle_1 = \frac{1}{4 q_{ab} q_{cd}} \ln \frac{m'^2 - s_3^{(-)}}{m'^2 - s_3^{(+)}},$$

where

$$s_3^{(\pm)} = (\sqrt{\mu_a^2 + q^2} - \sqrt{\mu_c^2 - q_{cd}^2})^2 - (q_{ab} \pm q_{cd})^2,$$

and q_{ab}, q_{cd} — the momenta of the particles before and after the transition in channel one — are given in terms of s_1 by well known formulas.

By one or two cyclic permutations of all indices in Eq. (11) we obtain analogous formulas for the average values of the amplitude A in channels two and three.

Calculations show (as was to be expected) that the subtractions have no effect at all on the form the Eq. (9) for the spectral functions. To verify this it is necessary to express the first (two-particle) term on the right side of the equalities (1) — (3) in a form analogous to Eq. (4′). For this purpose the amplitudes $B^{(i)}$ and $C^{(i)}$ must be expressed in Eqs. (1) — (3) as one dimensional representations of the form (10). This leads to rather unwieldy calculations. The required result may be obtained more simply by carrying out a subtraction directly in Eq. (5). To this end we average each of the quantities (5) over the scattering angle in the corresponding channel and add and subtract this average [denoted by Φ_1, Φ_2, or Φ_3, corresponding to the three quantities in Eq. (5)] from each of the quantities (5). As a result we obtain for the first term on the right side of Eq. (1)

$$\Phi_1(s_1) + \frac{1}{\pi}\int_0^\infty \{[\varphi(\sigma, s_2) - l_2(\sigma, s_1)] P_1(s_1, \sigma) + [\varphi(\sigma, s_3) - l_3(\sigma, s_1)] Q_1(\sigma, s_1)\}\, d\sigma, \quad (5')$$

*It is obvious that if the integrals over σ in Eq. (4) converge then the Eqs. (4) and (4′) are fully equivalent provided that

$$a_1(s_1) = \frac{1}{\pi}\int_0^\infty \left[\frac{A_{12}(s_1, \sigma)}{\sigma - s_{20}} + \frac{A_{31}(\sigma, s_1)}{\sigma - s_{30}}\right] d\sigma$$

(and analogously for a_2 and a_3). However even in this case it is more convenient for practical reasons to use the representation with subtractions since then the integrals converge faster.

and by averaging directly over cos ϑ the first term on the right side of Eq. (1) we easily find the value of Φ_1:

$$\Phi_1(s_1) = \zeta_1(s)\langle B^{(1)}(s_1)\rangle^* \langle C^{(1)}(s_1)\rangle_1. \qquad (5'a)$$

The representation (6) for the quantities Δ_i will be written in a form analogous to Eqs. (4') and (5'):

$$\Delta_1 = \delta a_1 + \frac{1}{\pi}\int_0^\infty \{\varphi(\sigma, s_2)\, u_1(s_1, \sigma) + \varphi(\sigma, s_3)\, v_1(\sigma, s_1)\}\, d\sigma, \qquad (6')$$

where $\delta a_1(s_1) = 0$ if s_1 is below the threshold for production of three (four) particles. By one or two cyclic permutations of all indices in Eqs. (5'), (5'a) and (6') we obtain the corresponding formulas for the other two channels.

We next substitute into the Eqs. (1) — (3) the formulas (4') — (6') and equate in the unphysical region (beyond the curves C_{12}, C_{23} and C_{31} in Fig. 2) the imaginary parts of both sides of the equations obtained from the equalities (1) — (3). We then obtain for the spectral functions A_{ij} the equations (9), as before. Equating the real parts of these equalities (or considering their average over the scattering angle in each of the channels) we obtain in addition the three equations for the three functions a_1, a_2, and a_3:

$$a_1(s) + \frac{1}{\pi}\int_0^\infty [l_2(\sigma, s)\, Q_1(s, \sigma) + l_3(\sigma, s)\, P_1(s, \sigma)]\, d\sigma = \zeta_1(s)\langle B^{(1)}(s)\rangle_1^* \langle C^{(1)}(s)\rangle_1, \qquad (9'a)$$

$$a_2(s) + \frac{1}{\pi}\int_0^\infty [l_3(\sigma, s)\, Q_2(s, \sigma) + l_1(\sigma, s)\, P_2(s, \sigma)]\, d\sigma = \zeta_2(s)\langle B^{(2)}(s)\rangle_2^* \langle C^{(2)}(s)\rangle_2, \qquad (9'b)$$

$$a_3(s) + \frac{1}{\pi}\int_0^\infty [l_1(\sigma, s)\, Q_3(s, \sigma) + l_2(\sigma, s)\, P_3(s, \sigma)]\, d\sigma = \zeta_3(s)\langle B^{(3)}(s)\rangle_3^* \langle C^{(3)}(s)\rangle_3. \qquad (9'c)$$

We have neglected on the right sides the terms δa_1, δa_2 and δa_3, different from zero only in the region beyond the threshold for production of three (four) particles, since their magnitude [as in the case of δA_{ij} in Eq. (9)] can only be found by correctly taking into account in Eqs. (1) — (3) terms corresponding to the production of three and more particles.

Equations (9) and (9'), together with the relations (4') and (11) (written for the amplitudes $B^{(i)}$ and $C^{(i)}$), form a complete system of equations for the spectral functions for all amplitudes* A, $B^{(i)}$, and $C^{(i)}$.

*It is of course understood that analogous equations are written for the spectral functions of all the amplitudes $B^{(i)}$ and $C^{(i)}$. If N four-particle functions are involved in all the unitarity conditions (1)–(3), then we get 6N equations for the 6N spectral functions.

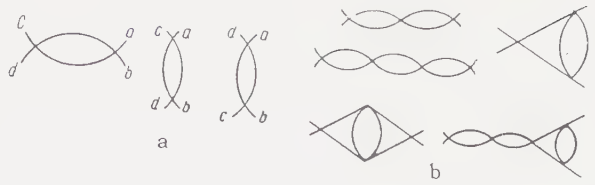

FIG. 7. Simpler diagrams of the "parquet" type,[6] whose contribution depends on one variable only. The contribution from a diagram always depends on one variable only, if the diagram consists of two parts to each of which are attached two external lines and which are joined by just one common point (or if two external lines are joined in a point).

5. ITERATIONAL SOLUTION. EQUATIONS OF THE CHEW-MANDELSTAM TYPE

The solution of the system of equations (9) and (9') is easily found in the form of a power series in the coupling constants. Let us discuss for simplicity the case when none of the amplitudes have poles. The case when poles are present is no different in principle. The coupling constants are the quantity a_0 and the analogous values $b_0^{(i)}$ and $c_0^{(i)}$ of the amplitudes $B^{(i)}$ and $C^{(i)}$ evaluated at the subtraction point (s_{10}, s_{20}, s_{30}). It follows from Eq. (9') that the $a_i(s)$ are of second order in the coupling constants, and from Eqs. (9) and (4') we find that the A_{ij} are of fourth order. In first approximation we substitute in Eq. (9') $\langle B^{(i)}\rangle_i \approx b_0^{(i)}$, $\langle C^{(i)}\rangle_i \approx c_0^{(i)}$ and neglect the second term on the left side. We then obtain for the $a_j(s)$ values that are of second order in the coupling constants

$$a_j(s) = \zeta_j(s)\, b_0^{(j)*} c_0^{(j)} \qquad (j = 1, 2, 3).$$

They correspond to the simplest type of diagrams, Fig. 7a. Accurate to second order terms we have from Eq. (4') that $A_i \approx a_i$.

The substitution of analogous expressions for $B_j^{(i)}$ and $C_j^{(i)}$ into Eqs. (10a), (11), and (9') results in expressions for a_j corresponding to more complex diagrams, Fig. 7b, of third and fourth order in the coupling constants (the number of such diagrams turns out to be precisely the same as in conventional perturbation theory). The substitution of these same values for $B_j^{(i)}$ and $C_j^{(i)}$ into the system of equations (9) leads to the appearance

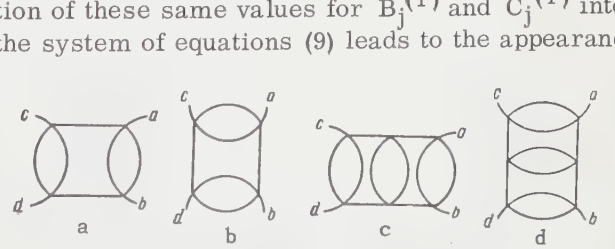

FIG. 8. Simpler diagrams, whose contribution depends on two variables.

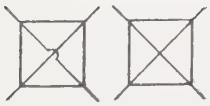

FIG. 9. Diagrams, whose contributions are not included in the Eqs. (9) and (9′).

of spectral functions for fourth order diagrams — "loaves," Fig. 8a, b. Here the term Q_1 in (1) corresponds to the "loaf," Fig. 8a, and the term P_3 (or the term v_1 in Eq. (7) which is equal to P_3 for $\delta A_{31} \approx 0$) to the rotated "loaf," Fig. 8b.

Already in this order in the coupling constants the significance (from the point of view of diagrams) of the terms Δ_i in the unitarity conditions (1) — (3) becomes clear. It is clear that diagrams of the type Fig. 8a, c (and similar chains with larger numbers of links) arise as a consequence of the first term on the right side of the unitarity condition (1). These diagrams correspond to two-particle intermediate states in channel one. Analogously the chain of vertical diagrams of the type Fig. 8b, d arises as a consequence of the first term in the unitarity relation (3) in channel three. From the point of view of channel one the latter type of diagrams corresponds not to two-particle, but to four-particle, six-particle, intermediate states, etc. But once these diagrams are definitely included in Eq. (3) then they must be included in Eq. (1), or else the relations (1) and (3) become mutually contradictory. It is precisely this contribution that is represented in Eq. (1) by the term Δ_1 [and in Eq. (7) by the term $v_1 \approx P_3$]; the terms Δ_2 and Δ_3 in Eqs. (2) and (3) have an analogous meaning. In particular, the contribution of these terms guarantees the necessary symmetry of the amplitude A in the variables s_1, s_2 and s_3.

Diagrams of the type shown in Fig. 9, as well as more complex ones (to which correspond spectral functions different from zero only when both variables lie in the region beyond the threshold for production of four and more particles), will never be generated by iteration of Eqs. (9) and (9′).* Their contribution is included in the here ignored terms δA_{ij}.

The indicated method of iteration of the equations was in fact described in detail by Mandelstam;[3] however he did not write down the closed system of equations (9) — (9′).

A possible approach to the solution of the system of equations (9) — (9′) consists of the following. We neglect in Eq. (9′) the terms containing the function A_{ij} (assuming that this neglect does not affect appreciably the values of the functions a_i). Then the system (9′) reduces to equations of the Chew-Mandelstam type:[4]

$$a_i(s) = \zeta_i(s)\langle B^{(i)}(s)\rangle_i \langle C^{(i)}(s)\rangle_i \qquad (i = 1, 2, 3), \tag{12}$$

where, according to Eqs. (11) and (10a),

$$\langle B^{(1)}(s)\rangle_1 = b_0^{(1)} + \frac{1}{\pi}\int_0^\infty [\varphi(\sigma, s) b_1^{(1)}(\sigma) + l_2(\sigma, s) b_2^{(1)}(\sigma) + l_3(\sigma, s) b_3^{(1)}(\sigma)]\, d\sigma. \tag{12a}$$

The value of $\langle C^{(1)}(s)\rangle_1$ is determined in precisely the same way, whereas the values of $\langle B^{(2)}\rangle_2$, $\langle B^{(3)}\rangle_3$ and $\langle C^{(2)}\rangle_2$, $\langle C^{(3)}\rangle_3$ follow by cyclic permutations of all indices. In this approximation the spectral functions A_{ij} can be determined from Eq. (9) by making the following substitution in the right hand sides of these equations

$$B_j^{(i)} = b_j^{(i)}(m'^2), \qquad C_j^{(i)} = c_j^{(i)}(m''^2),$$

in agreement with the formulas (4′) written for the amplitudes $B^{(i)}$. The resultant values of A_{ij} may be substituted into the Eq. (9′) in order to determine the corrections to the solutions of (12) and (12a). The possibility of such an iterational procedure with respect to the functions A_{ij} may be actually verified without difficulty.

For the case of an interaction of neutral mesons (when there is only one amplitude A of the $\pi\pi$ interaction and all the amplitudes $B^{(i)}$ and $C^{(i)}$ coincide with A) the equations (12) — (12a) are precisely the same as the equations of the Chew-Mandelstam theory.[4]

The system of equations (9) — (9′) will be discussed in detail for a number of specific cases in a paper to follow.

6. CONCLUSION

The systems of equations (9) and (9′) provide a solution to the problem of summing of all the contributions to the spectral functions a_i and A_{ij} from diagrams of the "parquet" type[6] (see Fig. 7 — 8), consisting (in an arbitrary part of them) of two parts connected by two lines only.

In the next higher approximation all diagrams must be taken into account, which are connected by three (four) lines; for this purpose one must include three- (or four-) particle intermediate states in the unitarity conditions.

At this time it is not yet possible to give a definite answer to the question: does the above sequence of approximations lead to rapidly converging (to the correct value) results. The neglect of dis-

*Consequently, in these equations we have taken into account the contributions from all diagrams of the type of Figs. 7 and 8, whose characteristic property is that by consecutive replacements of two points connected by two lines, by one, the diagrams simplify and reduce to a simple point.

tant singularities (i.e., of those parts of the spectral functions which begin to be nonvanishing in distant regions) can be justified provided that the integrals of the spectral representation converge rapidly. In that case the low energy region separates, and the behavior of various processes in this region does not depend on the behavior of various quantities (e.g., amplitudes, spectral functions, etc.) in the high energy region.

Apparently, this is the case in actuality. The fastest increase in the spectral functions A_{ij} is to be expected for the elastic scattering amplitude. In this case it follows from the optical theorem that two of the functions $A_{ij}(\sigma, \sigma')$ increase linearly (or almost linearly[7]) with increasing σ or σ'. At first sight it would seem that the integrals in the Mandelstam representation are logarithmically divergent (or only logarithmically convergent) even after one subtraction. In fact, however, even in this case the integrals in the Mandelstam representation (analogously to the integrals in the dispersion relations for the forward scattering amplitude, discussed already by Goldberger and Miyazawa) converge like a power (like $d\sigma/\sigma^2$). This is a consequence of crossing symmetry which precisely in the case of the elastic scattering amplitude leads to mutual cancellation of the fastest growing terms.* It is therefore quite likely that the scheme discussed above represents the first link in a chain of rapidly converging approximations.

*The author is grateful to I. Ya. Pomeranchuk, who called attention to this circumstance.

The author expresses his gratitude to V. N. Gribov, V. M. Shekhter, and A. A. Ansel'm for discussions on a number of questions in this paper and for interesting comments.

[1] S. Mandelstam, Phys. Rev. **112**, 1344 (1958).
[2] S. Mandelstam, Phys. Rev. **115**, 1741 (1959).
[3] S. Mandelstam, Phys. Rev. **115**, 1752 (1959).
[4] G. Chew and S. Mandelstam, Phys. Rev. **119**, 467 (1960).
[5] Karplus, Sommerfield, and Wichman, Phys. Rev. **111**, 1187 (1958).
[6] Pomeranchuk, Sudakov, and Ter-Martirosyan, Phys. Rev. **103**, 784 (1956). Dyatlov, Sudakov, and Ter-Martirosyan, JETP **32**, 767 (1957), Soviet Phys. JETP **5**, 631 (1957).
[7] V. N. Gribov, Nucl. Phys. (in press).
[8] M. Cini and S. Fubini, Ann. Phys. **3**, 352 (1960).
[9] W. R. Frazer and J. R. Fulco, Phys. Rev. **117**, 1603 and 1609 (1960). Oshida, Takahashi, and Ueda, Progr. Theor. Phys. **23**, 731 (1960).

Translated by A. M. Bincer
150

THE NEUTRAL ρ^0-MESON HYPOTHESIS IN THE LIGHT OF DATA ON ANTIPROTON ANNIHILATION

V. I. GOL'DANSKIĬ and V. M. MAKSIMENKO

P. N. Lebedev Physics Institute, Academy of Sciences, U.S.S.R.

Submitted to JETP editor April 26, 1960

J. Exptl. Theoret. Phys. (U.S.S.R.) **39**, 841-844 (September, 1960)

According to the Gell-Mann—Nishijima scheme, a neutral ρ^0 meson with zero strangeness should exist. The following decay modes for this particle have been indicated in the literature:

$$\rho^0 \to \pi^+ + \pi^- + \gamma, \quad \rho^0 = \pi_0^0 \to 2\gamma; \quad \rho^0 = \pi_{10}^0 \to 3\gamma.$$

The possible contribution of such decays (for various ρ^0-meson masses) in the annihilation of antiprotons is discussed from the viewpoint of the statistical theory of multiple processes. The data presently available on the yield of π^+, π^-, and π^0 mesons during annihilation are inconsistent with the existence of a π_0^0 meson with a mass smaller than 3.5 m_π and also with the existence of a π_{10}^0 meson with a mass smaller than 5.5 m_π. On the other hand, the $\rho^0 \to \pi^+ + \pi^- + \gamma$ decay not only does not contradict the experimental data, but even removes some difficulties connected with the determination of the interaction volume.

THE Gell-Mann—Nishijima scheme of elementary particles, both in its original form, and modified to take the conservation of the number of isofermions into account, predicts the existence of the not as yet observed neutral ρ^0 meson with isotopic spin and strangeness equal to zero. The possible properties of these mesons, and its decay modes in particular, have lately been frequently discussed in the literature.

The decay mechanism of the ρ^0 meson has been discussed in particular detail by Zel'dovich,[1] who used the most widely-accepted assumption that this meson is a pseudo-scalar particle with zero spin similar to a nucleon-antinucleon pair in the $0\,^1S_0$ state (according to the Bethe-Hamilton scheme[2]). In such a case, the most probable decay mode of the ρ^0 meson with a mass greater than the double mass of the π meson is the decay

$$\rho^0 \to \pi^+ + \pi^- + \gamma. \tag{1}$$

This decay is predominant also for $m_\rho > 3m_\pi$ and even for $m_\rho \gtrsim 4m_\pi$, since the 3π decay is forbidden, and the 4π decay (as are the decays into a greater number of π mesons) is strongly suppressed by the necessity of large orbital momenta in the final state.

For $m_\rho < 2m_\pi$, the predominant decay mode should be

$$\rho^0 \to 2\gamma. \tag{2}$$

Purely hypothetical variants of ρ^0 mesons are the "twin" of the usual π^0 meson, the so-called π_0^0 meson,[3] and also a particle close in mass to the π^0 meson having unit spin, the π_{10}^0 meson.[4] The proposed basic decay schemes of these particles are as follows:

$$\pi_0^0 \to 2\gamma, \tag{2'}$$

$$\pi_{10}^0 \to 3\gamma. \tag{3}$$

We shall not dwell on a description of all the attempts to find the ρ^0 meson and, in particular, the π_0^0 and π_{10}^0 mesons (see references 4—9), but, instead, we shall analyze those data that can now be deduced from experiments on antiproton annihilation.

The latest data on the annihilation of antiprotons stopping in hydrogen[10] reveal that π^+ and π^- mesons carry away $\frac{2}{3}(\pm 3\%)$ of the released energy, and π^0 mesons about $\frac{1}{3}$. Since the yield of π^0 mesons is determined from their decay γ rays, we can assume that, from the equality of the π^+, π^-, and π^0 meson yields, we can deduce the presence of one γ ray for each such meson. Therefore, the production of ρ^0 mesons having the decay mode (1) would correspond to a certain decrease of the γ-ray yield, while the production of ρ^0 mesons having a decay mode (2), or even more so (3), would lead to an increase in the γ-ray yield.

In view of the limitation stated above, we shall not discuss here the ratio of yields of π^+, π^-, and π^0 mesons in multimeson decays of heavy ρ^0

mesons ($m_\rho > 4m_\pi$). The corresponding relations can be obtained from the selection rules for the isotopic spin. It is clear, however, that the closer the mass of the ρ^0 meson to the maximum possible one (i.e., the mass of two nucleons), the smaller will, in general, be the role of the intermediate state in the possible variations of the relative yield of mesons of various signs.

Thus, we will consider three decay modes, types (1), (2), and (3):

$$\rho^0 \to \pi^+ + \pi^- + \gamma, \quad \rho^0 \to 2\gamma, \quad \rho^0 \to 3\gamma$$

and we shall compare the possible contribution of these processes to the yield of γ rays in the annihilation of antiprotons with the experimental data. In doing so, it is more convenient not to use the energy fractions of $\pi^\pm$ and π^0 mesons given above, but rather their average number per act of annihilation:[10]

$\bar{n}_{\pi^+} = 1.53 \pm 0.08$, $\bar{n}_{\pi^-} = 1.53 \pm 0.08$, $\bar{n}_{\pi^0} = 1.60 \pm 0.50$.

We shall assume, that, together with π^+, π^-, and π^0 mesons, ρ^0 mesons may be produced in the annihilation of antiprotons. In order to estimate their yield, we shall use the statistical theory of multiple production, assuming that the interaction strength for π^+ and ρ^0 mesons is the same, and, therefore, that the relative yield of ρ^0 mesons depends only on their mass, of which different values are used for the calculation.

The total number of emitted π^+ and π^- mesons is assumed to be given as $\bar{n}_{\pi\pm} = 3.06 \pm 0.12$, and, for different assumptions with respect to the ρ^0 mass, the number of half of the emitted γ rays, $n_\gamma/2$, is calculated. It is evident that, for the decay mode (1), the quantity $n_\gamma/2$ decreases with decreasing assumed mass of the ρ^0 meson, while, for the modes (2) and (3), the contrary is true.

The effective volume V in which, according to the theory, statistical equilibrium is attained between all secondary particles, is considered as an adjustable parameter, and is so chosen that the calculated value of $\bar{n}_{\pi\pm}$ for a given V is equal to the experimental one.

In order to calculate the statistical weights, the exact formulas were used.[11,12] The results of the calculations for the three decay modes are shown

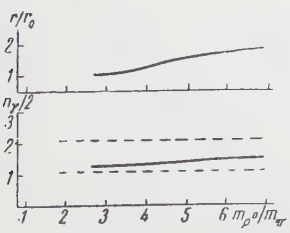

FIG. 1. Decay mode $\rho^0 \to \pi^+ + \pi^- + \gamma$.

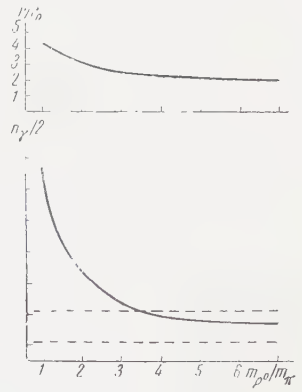

FIG. 2. Decay mode $\rho^0 \to 2\gamma$.

in Figs. 1—3. The dotted line denotes the experimental limits of the quantity $n_\gamma/2$ (equal, in the absence of ρ^0 mesons, to the number of π^0 mesons). In the upper part of the figures, the variation of the radius r of the effective volume $V = 4\pi r^3/3$ expressed in units of $r_0 = \hbar/m_\pi c$ is shown.

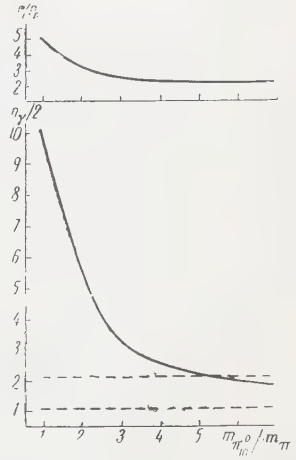

FIG. 3. Decay mode $\pi^0_{10} \to 3\gamma$.

As can be seen from Fig. 1, mode (1) does not contradict the experimental data (because of their low accuracy) for any value of the ρ^0-meson mass. The decay mode (2) (Fig. 2) would lead to a disagreement with the experiment, except for $m_\rho \geq 3.5\, m_\pi$. The decay mode (3) (Fig. 3) could be consistent with the available data only for the case of a very heavy ρ^0 meson with a mass not less than 5.5 π meson masses.

Thus, one can assume that the yield of mesons of various signs in antiproton annihilation definitely contradicts the existence both of π^0_0 mesons and, even more so, of π^0_{10} mesons.

It is interesting to note that, for the decay mode (1), one can obtain a better agreement between the calculation and the experiment for $r = r_0$. As is well known,[12] for such a value of r, the theory is in good agreement with the data on NN- and πN-collisions, but, for the case of annihilation, the

calculated number of π^0 mesons produced is underestimated by not taking the decay mode (1) into account, and it is found that it is necessary either to increase r, or to introduce additional assumptions.

In our calculations, we did not take the hypothetical resonance interaction of π mesons into account,[13,14] and also did not use the variant of statistical theory with the Lorentz-invariant phase volume[15] (see also reference 10). However, both in this and in the other case, the fraction of ρ^0 mesons will be smaller than in the estimates obtained above, which would tend to lessen any contradiction with the experiment.

[1] Ya. B. Zel'dovich, JETP **34**, 1644 (1958), Soviet Phys. JETP **7**, 1130 (1958).

[2] H. Bethe and G. Hamilton, Nuovo cimento **4**, 1 (1956).

[3] A. M. Baldin, Nuovo cimento **8**, 569 (1958).

[4] R. Ely and D. Frisch, Phys. Rev. Lett. **3**, 565 (1959).

[5] Akimov, Savchenko, and Soroko, Preprint, Joint Institute for Nuclear Research (1959).

[6] Booth, Chamberlain, and Rogers, Bull. Am. Phys. Soc. **4**, 8 (1959).

[7] Zinov, Konin, Korenchenko, and Pontecorvo, Preprint, Joint Institute for Nuclear Research (1959); JETP **36**, 1948 (1959), Soviet Phys. JETP **9**, 1386 (1959).

[8] V. I. Gol'danskiĭ and Ya. A. Smorodinskiĭ, JETP **36**, 1950 (1959), Soviet Phys. JETP **9**, 1387 (1959).

[9] Bernardini, Querzoli, Salvini, Silverman, and Stoppini, Nuovo cimento **14**, 268 (1959).

[10] E. Segré, Paper presented at the Ninth International Conference on High-Energy Physics, Kiev 1959.

[11] V. M. Maksimenko and I. L. Rozental', JETP **32**, 658 (1957), Soviet Phys. JETP **5**, 546 (1957).

[12] Belen'kiĭ, Maksimenko, Nikishov, and Rozental', Usp. Fiz. Nauk **62**, 1 (1957).

[13] F. Dyson, Phys. Rev. **99**, 1037 (1955).

[14] G. Takeda, Phys. Rev. **100**, 440 (1955).

[15] P. Strivastava and G. Sudarshan, Phys. Rev. **110**, 781 (1958).

Translated by H. Kasha
151

ELECTROMAGNETIC WAVES IN A HALF-SPACE FILLED WITH A PLASMA

Yu. N. DNESTROVSKIĬ and D. P. KOSTOMAROV

Moscow State University

Submitted to JETP editor April 27, 1960

J. Exptl. Theoret. Phys. (U.S.S.R.) **39**, 845-853 (September, 1960)

The propagation of electromagnetic waves across a magnetic field in half-space filled with a magnetoactive plasma is studied. It is assumed that the plasma is confined by a stationary magnetic field H, and the structure of this field is investigated for the case when the ratio of the plasma pressure to the magnetic pressure is small. It is demonstrated that, at large distances from the plasma boundary an electromagnetic wave with an electric vector parallel to the magnetic field H has the form of a plane wave with a propagation constant which is specified by the equation for an infinite plasma. The reflection and transmission coefficients are evaluated for a plane wave incident on the plasma from a vacuum.

IN the present paper we consider the problem of the penetration of an electromagnetic wave in a half-space filled with a plasma. Problems of this type have been investigated by many researchers.[1-6] A linearized kinetic equation together with Maxwell's equations were used to describe the process. The boundary condition at the plasma boundaries was that the electrons be specularly reflected.

Landau[1] considered the problem for a longitudinal electric field. A characteristic feature of the solution was that the field away from the boundary of the plasma was not a plane wave. With the aid of Landau's method, Silin[2] solved the problem for a plasma confined in a homogeneous magnetic field $\mathbf{H}_0$ perpendicular to its boundary (magnetoactive plasma). An investigation of the solution, carried out by Shafranov,[3] has shown that in this case the field is not a plane wave far away from the plasma boundary.

Shafranov has made an attempt to consider the penetration of the electromagnetic field into a plasma for an arbitrary direction of the field $\mathbf{H}_0$, but the solution has not been carried out in a consistent manner. While the equations and boundary conditions are rigorously formulated for the electromagnetic field, only general remarks are made regarding the electron distribution function. It is stated that the condition that the electrons be specularly reflected from the plasma boundary does not distort their distribution functions and therefore the kernel $K(\mathbf{r}, \mathbf{r}')$ of the integral relations between the field and the currents in the plasma depends, as previously, only on the quantity $R = |\mathbf{r} - \mathbf{r}'|$. This statement has not been proved. In our opinion, it is true only in the exceptional case when the field $\mathbf{H}_0$ is perpendicular to the plasma boundary. For such a direction of the magnetic field, the Larmor circles for the electrons do not intersect the plasma boundary, and therefore the distribution function is the same as in an unbounded plasma if the electrons are specularly reflected from the boundary. For any other direction of the magnetic field $\mathbf{H}_0$, the Larmor circles will intersect the plasma boundary and this should influence the distribution function.

In later investigations devoted to semi-bounded plasma,[4-6] the authors either referred to Shafranov's results,[3] or did not touch at all on problems related to the determination of the distribution function, confining themselves to unproved general remarks.

The problem can thus at present be considered as consistently solved only when the field $\mathbf{H}_0$ is perpendicular to the plasma boundary and is parallel to the direction of wave propagation.[2] In the present paper we solve this problem for the opposite case: the magnetic field is assumed parallel to the plasma boundary and perpendicular to the direction of wave propagation, and the electric vector is assumed polarized parallel to the magnetic field (ordinary wave). It is shown that the field away from the plasma boundary is in the form of a plane wave, the propagation constant of which is the root of the corresponding dispersion equation formulated for the infinite plasma. In solving the problem, an attempt is made to con-

struct a more accurate model for the plasma boundary, so as to replace the artificial specular-reflection boundary condition.

1. FORMULATION OF THE PROBLEM

Let a plasma filling the half-space $x > 0$ be located in a stationary magnetic field $\mathbf{H}(x)$ parallel to the z axis $[\mathbf{H}(x) = \{0, 0, H(x)\}]$; assume a specified electric field on the boundary of the plasma in the plane $x = 0$

$$E_x = E_y = 0, \qquad E_z = E_z(0, y)\, e^{-i\omega t}. \tag{1}$$

It is required to determine the field in the plasma, in the form of an outgoing wave as $x \to \infty$.

In solving this problem, we assume, as usual, that 1) the plasma is neutral on the average, 2) the electromagnetic wave does not act on the ions. 3) the electromagnetic wave disturbs little the electronic component of the plasma, and 4) the effect of the magnetic field of the wave can be neglected compared with the electric field and with the stationary magnetic field.

Let us proceed to discuss the conditions on the plasma boundary. We do not assume the usual hypothesis of specular reflection of the electrons from the boundary: this hypothesis necessitates an infinite magnetic field and is little justified physically in many cases. The model which we propose for the plasma boundary is based on the following premises: 1) there are no electrons in the region $x < 0$; 2) the electrons are confined in the region $x > 0$ by a stationary magnetic field $H(x)$, and 3) the stationary magnetic field becomes homogeneous away from the boundary, while the unperturbed electron distribution function is Maxwellian:

$$\lim_{x\to\infty} H(x) = H_0,$$

$$\lim_{x\to\infty} f_0 = N\,(m/2\pi T)^{3/2} \exp\left[-m\,(v_x^2 + v_y^2 + v_z^2)/2T\right]$$

(N is the electron density and T is the temperature in energy units).

Let us introduce the following notation: $\omega_0 = \sqrt{4\pi Ne^2/m}$ is the plasma frequency, $\omega_H = eH_0/mc$ is the Larmor frequency, $x_0 = \sqrt{2T/m}\,\omega_H^{-1}$ is the average Larmor radius, and $\mu_0 = 2T\omega_0^2/mc^2\omega_H^2 = 8\pi NT/H_0^2$ is the ratio of the plasma pressure to the magnetic pressure. The problem so formulated is solved approximately under the assumption that $\mu_0 \ll 1$. Terms of order μ_0^2 are neglected.

2. UNPERTURBED DISTRIBUTION FUNCTION AND STATIONARY MAGNETIC FIELD

Let F be the electron distribution function, satisfying the kinetic equation in the Vlasov form

$$\frac{\partial F}{\partial t} + \mathbf{v}\nabla F + \frac{e}{m}\left(\mathbf{E} + \frac{1}{c}[\mathbf{v}\times\mathbf{H}],\ \nabla_v F\right) = 0. \tag{2}$$

We change over from variables x, v_x, v_y, v_z to dimensionless variables α, β, γ, and δ:

$$\xi = x/x_0, \qquad v_x = \sqrt{2T/m}\beta\cos\delta,$$

$$v_y = \sqrt{2T/m}\beta\sin\delta, \qquad v_z = \sqrt{2T/m}\gamma$$

and represent the function F in the form

$$F = f_0(\xi,\ \beta,\ \gamma,\ \delta) + f(t,\ \xi,\ y,\ \beta,\ \gamma,\ \delta), \tag{3}$$

where f_0 is the unperturbed distribution function, while f is a small perturbation due to the electromagnetic wave. From the kinetic equation (2) and from Maxwell's equations we obtain a system for the determination of the function f_0 and of the stationary magnetic field $H(x)$

$$\beta\cos\delta\,\partial f_0/\partial\xi - (1 + g(\xi))\,\partial f_0/\partial\delta = 0; \tag{4}$$

$$\frac{dg}{d\xi} = -\frac{4\pi x_0 j_y}{cH_0} = -\frac{4\pi e x_0}{cH_0}\left(\frac{2T}{m}\right)^2 \int_0^{2\pi} \sin\delta\, d\delta \int_0^{\infty} \beta^2 d\beta \int_{-\infty}^{\infty} f_0\, d\gamma, \tag{5}$$

$$H(\xi) = H_0(1 + g(\xi)). \tag{6}$$

The unperturbed distribution function f_0 for the solution of (4) is chosen as

$$f_0 = N\left(\frac{m}{2\pi T}\right)^{3/2} e^{-(\beta^2+\gamma^2)}\,\eta\left(\xi + \int_0^{\xi} g(\sigma)\,d\sigma + \beta(\sin\delta - 1)\right), \tag{7}$$

where $\eta(\xi)$ is the step function, $\eta(\xi) = 1$ when $\xi > 0$ and $\eta(\xi) = 0$ when $\xi < 0$. The function (7) satisfies the conditions formulated above for confining the electrons in the half-space $x > 0$. The discontinuity line of the function (7)

$$\xi + \int_0^{\xi} g(\sigma)\,d\sigma + \beta(\sin\delta - 1) = 0$$

is the characteristic of Eq. (4).

Substituting (7) into (5) and carrying out several transformations, we obtain the following equation for the function $g(\xi)$, which characterizes the inhomogeneity of the magnetic field

$$g(\xi) = \mu_0 \frac{1}{\pi} \int_0^{2\pi} (1 + \sin\delta)\, d\delta \int_{\Phi}^{\infty} e^{-\Phi^3}\, \Phi^3 ds,$$

$$\Phi = \frac{1}{1 - \sin\delta}\left(s + \int_0^{s} g(\sigma)\,d\sigma\right). \tag{8}$$

A solution of this equation can be constructed in the form of a series in the parameter μ_0:

$$g(\xi) = \sum_{n=1}^{\infty} \mu_0^n g_n(\xi).$$

In the first approximation this yields

$$g(\xi) = \mu_0 g_1(\xi) + O(\mu_0^2), \tag{9}$$

where

$$g_1(\xi)=\frac{1}{2\pi}\int_0^{2\pi}\exp\left\{-\left(\frac{\xi}{1-\sin\delta}\right)^2\right\}\left[\left(\frac{\xi}{1-\sin\delta}\right)^2+1\right]\cos^2\delta d\delta. \tag{10}$$

Thus, the unperturbed distribution function f_0 and the stationary magnetic field $H(x)$ are given by (7) and (6), in which $g(\xi)$ is given by (9) and (10). We see that the inhomogeneity of the magnetic field is of order μ_0 and manifests itself only in a boundary zone of width $l \sim x_0$ $(\xi \sim 1)$. Upon further increase of x, the additional term tends to zero exponentially.

3. DETERMINATION OF THE ELECTRIC FIELD OF THE WAVE IN THE PLASMA

Let us proceed now to determine the alternating electromagnetic field excited in the plasma by the boundary mode (1). We consider first the case when

$$E_z|_{x=0}=E(0)\,e^{i(h_y y-\omega t)}. \tag{11}$$

The general case can be reduced to that given by expansion of the boundary field in a Fourier integral with respect to the variable y. We shall seek the functions f and E_z in the form

$$f(t,\ \xi,\ y,\ \beta,\ \gamma,\ \delta)=e^{i(h_y y-\omega t)}f(\xi,\ \beta,\ \gamma,\ \delta),$$

$$E_z(t,\ \xi,\ y)=e^{i(h_y y-\omega t)}E(\xi).$$

From the kinetic Eq. (2) and from Maxwell's equations we obtain the following linearized system of equations for the functions $f(\xi,\ \beta,\ \gamma,\ \delta)$ and $E(\xi)$:

$$\beta\cos\delta\frac{\partial f}{\partial\xi}-(1+g(\xi))\frac{df}{d\delta}+i\left(x_0h_y\beta\sin\delta-\frac{\omega}{\omega_H}\right)f$$
$$=-\frac{e}{m\omega_H}\left(\frac{m}{2T}\right)^{1/2}\frac{\partial f_0}{\partial\gamma}E(\xi), \tag{12}$$

$$\frac{d^2E}{d\xi^2}+x_0^2(k^2-h_y^2)E=-ik^2x_0^2\frac{4\pi e}{\omega_H}\left(\frac{2T}{m}\right)^2\int_0^{2\pi}d\delta\int_0^{\infty}\beta d\beta\int_{-\infty}^{\infty}f\gamma d\gamma, \tag{13}$$

where $k=\omega/c$. From (12), taking into account the expression (7) for the function f_0, we see that the function f is proportional to $(Ne/m\omega_H)\times(m/2T)^2$. Consequently, the integral term in Eq. (13) is of order μ_0. Thus, to determine the electric field accurate to terms of order μ_0 inclusive, it is sufficient to obtain the function f in the zero approximation with $g(\xi)=0$. In other words, the effect of the inhomogeneity of the stationary magnetic field can be neglected in determining the electric field with the degree of accuracy which we require. Taking this into account, we rewrite (12) as

$$\beta\cos\delta\partial f/\partial\xi-\partial f/\partial\delta+i(x_0h_y\beta\sin\delta-\omega/\omega_H)f$$
$$=(Ne/m\omega_H)(2T/m)^2E(\xi)\,2\gamma e^{-(\beta^2+\gamma^2)}\eta(\xi+\beta(\sin\delta-1)). \tag{14}$$

Let us consider the system (13) and (14). It is easy to write down a solution of (14) which is periodic in δ with period 2π. Such a solution is unique and has the form

$$f=i\frac{Ne}{m\omega_H}\left(\frac{m}{2T}\right)^2\varkappa\left(\frac{\omega}{\omega_H}\right)2\gamma e^{-(\beta^2+\gamma^2)}\eta(\xi+\beta(\sin\delta-1))$$
$$\times\int_{\delta-2\pi}^{\delta}\exp\left\{i\left[\frac{\omega}{\omega_H}(\alpha-\delta+\pi)+x_0h_y\beta(\cos\alpha-\cos\delta)\right]\right\}$$
$$\times E(\xi+\beta(\sin\delta-\sin\alpha))\,d\alpha, \tag{15}$$

$$\varkappa\left(\frac{\omega}{\omega_H}\right)=\frac{\omega}{\omega_H}\Big/2\pi\sin\frac{\omega}{\omega_H}\pi.$$

Substituting (15) and (13), we obtain an integro-differential equation for the field $E(\xi)$:

$$\frac{d^2E}{d\xi^2}+x_0^2(k^2-h_y^2)E=\mu_0\varkappa\left(\frac{\omega}{\omega_H}\right)\int_0^{2\pi}d\delta\int_{\delta-2\pi}^{\delta}$$
$$\times d\alpha\int_0^{\infty}E(\xi+\beta(\sin\delta-\sin\alpha))\times\eta(\xi+\beta(\sin\delta-1))$$
$$\times\exp\left\{-\beta^2+i\left[\frac{\omega}{\omega_H}(\alpha-\delta+\pi)\right.\right.$$
$$\left.\left.+x_0h_y\beta(\cos\alpha-\cos\delta)\right]\right\}\beta d\beta. \tag{16}$$

We are interested in a solution of (16) which assumes a specified value $E(0)$ when $\xi=0$ and behaves like an outgoing wave as $\xi\to\infty$. We shall seek such a solution in the form

$$E(\xi)=E_\infty(e^{ix_0h_x\xi}+u(\xi)). \tag{17}$$

Here $u(\xi)$ is a new unknown function, which must approach zero at infinity, while h_x and E_∞ are constants to be determined. According to (16), the function $u(\xi)$ should satisfy the following equation:

$$\frac{d^2u}{d\xi^2}+x_0^2(k^2-h_y^2)u=\mu_0\varkappa\left(\frac{\omega}{\omega_H}\right)\int_0^{2\pi}d\delta$$
$$\times\int_{\delta-2\pi}^{\delta}d\alpha\int_0^{\infty}u(\xi+\beta(\sin\delta-\sin\alpha))$$
$$\times\eta(\xi+\beta(\sin\delta-1))\exp\left\{-\beta^2+i\left[\frac{\omega}{\omega_H}(\alpha-\delta+\pi)\right.\right.$$
$$\left.\left.+x_0h_y\beta(\cos\alpha-\cos\delta)\right]\right\}\times\beta d\beta-e^{-ih_xx_0\xi}\mu_0\varkappa\left(\frac{\omega}{\omega_H}\right)$$
$$\times\int_0^{2\pi}d\delta\int_{\delta-2\pi}^{\delta}d\alpha\int_{\xi'}^{\infty}\exp\left\{-\beta^2+i\left[\frac{\omega}{\omega_H}(\alpha-\delta+\pi)\right.\right.$$
$$\left.\left.+x_0h_y\beta(\cos\alpha-\cos\delta)+x_0h_x\beta(\sin\delta-\sin\alpha)\right]\right\}$$
$$\times\beta d\beta-x_0^2D\left(\sqrt{h_x^2+h_y^2}\right)e^{-ix_0h_x\xi},$$

where $\xi'=\xi/(1-\sin\delta)$, and

$$D(h) = k^2 - h^2 - \pi \frac{\omega_0^2}{c^2} \varkappa\left(\frac{\omega}{\omega_H}\right) \int_0^{2\pi} \exp\left\{-\frac{x_0^2 h^2}{2}(1-\cos\varepsilon)\right\} \times \cos\frac{\omega}{\omega_H}(\varepsilon-\pi)\, d\varepsilon.$$

Let us put $h_x = (h^2 - h_y^2)^{-1/2}$, where h is the root of the equation

$$D(h) = 0. \tag{19}$$

This equation is a dispersion equation for waves of the type considered in an unbounded plasma. With this choice of h_x, the term that does not vanish at infinity drops out from Eq. (18). The amplitude E_∞ can be determined from the boundary condition at $\xi = 0$:

$$E(0) = E_\infty (1 + u(0)). \tag{20}$$

The solution of the integro-differential equation (18), which tends to zero at infinity, must satisfy the following integral equation

$$u(\xi) = \mu_0 L[u] + \mu_0 w(\xi), \tag{21}$$

where

$$L[u] = \varkappa\left(\frac{\omega}{\omega_H}\right) \int_0^{2\pi} d\delta \int_{\delta-2\pi}^{\delta} d\alpha \int_0^{\infty} \exp\left\{-\beta^2 + i\left[\frac{\omega}{\omega_H}(\alpha - \delta + \pi) + x_0 h_y \beta(\cos\alpha - \cos\delta)\right]\right\} \beta\, d\beta \times \int_\xi^\infty \frac{\sin[x_0\sqrt{k^2 - h_y^2}\,(\sigma-\xi)]}{x_0\sqrt{k^2-h_y^2}}\, \eta(\sigma + \beta(\sin\delta - 1))\, u(\sigma + \beta(\sin\delta - \sin\alpha))\, d\sigma, \tag{22}$$

$$w(\xi) = -\varkappa\left(\frac{\omega}{\omega_H}\right) \int_0^{2\pi} d\delta \int_{\delta-2\pi}^{\delta} d\alpha \int_\xi^\infty \frac{\sin[x_0\sqrt{k^2-h_y^2}\,(\sigma-\xi)]}{x_0\sqrt{k^2-h_y^2}} e^{i x_0 h_x \sigma}\, d\sigma \times \int_{\sigma'}^\infty \exp\left\{-\beta^2 + i\left[\frac{\omega}{\omega_H}(\alpha - \delta + \pi) + x_0 h_y \beta(\cos\alpha - \cos\delta) + x_0 h_x \beta(\sin\delta - \sin\alpha)\right]\right\} \beta\, d\beta \tag{23}$$

[here $\sigma' = \sigma/(1 - \sin\delta)$]. Equation (21) contains the small parameter μ_0 ahead of the integral term, and it is therefore natural to solve it by successive approximations. We shall seek the solution of (21) in the form

$$u(\xi) = \sum_{n=1}^{\infty} \mu_0^n u_n(\xi), \tag{24}$$

and determine the functions $u_n(\xi)$ from the recurrence formulas

$$u_1(\xi) = w(\xi), \qquad u_{n+1}(\xi) = L[u_n].$$

It is easy to show that (24) converges, and consequently that (21) is solvable at sufficiently small values of the parameter μ_0. To obtain a solution of (21) with the required degree of accuracy, it is sufficient to use the zeroth approximation

$$u(\xi) = \mu_0 w(\xi) + O(\mu_0^2). \tag{25}$$

The amplitude E_∞ of the wave at infinity is determined from Eq. (20):

$$E_\infty = E(0)(1 - \mu_0 w(0) + O(\mu_0^2)). \tag{26}$$

Thus, the electric field in the plasma, under boundary condition (11), is of the form

$$E_z(x, y) = E_\infty e^{i(h_x x + h_y y)}\{1 + \mu_0 e^{-i h_x x} w(x/x_0) + O(\mu_0^2)\}. \tag{27}$$

As $x \to \infty$, this field behaves like a plane wave with a propagation constant $h = (h_x^2 + h_y^2)^{1/2}$ which is determined by the dispersion equation for the unbounded plasma. The function $w(x/x_0)$ describes the distortion of the field at the plasma boundary. It differs noticeably from zero only in a boundary zone of width x_0, and tends exponentially to zero with increasing distance from the boundary.

If we neglect the motion of the electrons and assume that their temperature is zero, then Eq. (27) goes automatically into the elementary-theory equation for the interaction between the electromagnetic wave and the plasma in terms of the dielectric-constant tensor.

4. CASE OF LARGE WAVELENGTHS

In this section we shall consider in greater detail the case when

$$\mu = 2T\omega^2/mc^2\omega_H^2 = (kx_0)^2 \ll 1,$$

i.e., when the average Larmor radius of the electrons is much smaller than the wave length in vacuum.

Let us compare the parameters μ_0 and $\mu = \mu_0\omega^2/\omega_0^2$. In a cold plasma ($T = 0$), the ordinary wave can propagate transversely to the magnetic field if $\omega_0/\omega < 1$. Consequently, in a plasma with low temperature ($T \ll mc^2$) the parameter μ_0 for propagating waves should either be smaller than μ or of the same order. In this section we shall expand all the quantities in powers of the parameters μ, and consider at the same time that $O(\mu_0) \lesssim O(\mu)$.

Let us consider first the function $w(\xi)$, given by (23), which can be represented in the form [we use $\xi' = \xi/(1 - \sin\delta)$]

$$w(\xi) = w_0(\xi) + \sqrt{\mu}\, w_1(\xi) + O(\mu);$$

$$w_0(\xi) = -\frac{1}{4\pi}\int_0^{2\pi}\left[(1-\sin\delta)^2 e^{-\xi'/s} - 2\xi(1-\sin\delta)\int_{\xi'}^\infty e^{-\beta^3} d\beta\right] d\delta,$$

$$w_1(\xi) = -\frac{i}{8\pi}\int_0^{2\pi}\left\{\frac{(h_y - i h_x \omega/\omega_H)\cos\delta - (h_x + i h_y \omega/\omega_H)\sin\delta}{k(1-\omega^2/\omega_H^2)} \times \left[\xi(1-\sin\delta)e^{-\xi'/s} - (2\xi^2 + 3(1-\sin\delta)^2)\int_{\xi'}^\infty e^{-\beta^3} d\beta\right] + \frac{2h_x}{k}(1-\sin\delta)^2\int_{\xi'}^\infty e^{-\beta^3} d\beta\right\} d\delta. \tag{28}$$

In particular

$$w(0) = -\frac{3}{4} - \frac{i}{8}\left[5\frac{h_x}{k} - 3\frac{h_x + ih_y\omega/\omega_H}{k(1-\omega^2/\omega_H^2)}\right]\sqrt{\mu} + O(\mu). \tag{29}$$

Substituting (28) and (29) in (26) and (27), we get

$$E_\infty = E(0)\left\{1 + \frac{3}{4}\mu_0 + \frac{i}{8}\mu_0\sqrt{\mu}\left[5\frac{h_x}{k} - 3\frac{h_x + ih_y\omega/\omega_H}{k(1-\omega^2/\omega_H^2)}\right] + O(\mu^2)\right\}, \tag{30}$$

$$E_z(x,y) = E_\infty e^{i(h_x x + h_y y)}\left\{1 + \mu_0 e^{-ih_x x}\left[w_0\left(\frac{x}{x_0}\right) + \sqrt{\mu}\, w_1\left(\frac{x}{x_0}\right)\right] + O(\mu^2)\right\}. \tag{31}$$

With the aid of (30) and (31) we readily can construct a solution of the problem with the general boundary condition (1). Confining ourselves to terms of order μ, we obtain

$$E_z(x,y) = \frac{ih}{2}\left(1 + \frac{3}{4}\mu_0\right)\int_{-\infty}^{\infty} H_0^{(1)}\left(h\sqrt{x^2 + (y-\eta)^2}\right) \times \frac{xE_z(0,\eta)\,d\eta}{\sqrt{x^2 + (y-\eta)^2}} + \mu_0 w_0\left(\frac{x}{x_0}\right)E_z(0,y) + O(\mu^{3/2}). \tag{32}$$

The simplicity of formula (32) is due to the fact that E_∞ and $u(x/x_0)$ are independent of h_y at the degree of accuracy indicated above.

In conclusion let us consider the incidence of a plane electromagnetic wave with wave vector $\mathbf{k} = (k_x, k_y, 0)$ from vacuum, $x < 0$, on a half-space filled with plasma. We assume that the electric vector of the incident wave is polarized along the z axis, and obtain the solution of this problem accurate to terms of order μ inclusive.

In the region $x < 0$ the electric field has the form

$$E = E_0 e^{i(k_x x + k_y y)} + E_1 e^{i(-k_x x + k_y y)},$$

where E_0 is the specified amplitude of the incident wave. The field in the plasma is determined by the formula (31), where $h_y = k_y$. Using the conditions of the continuity of the functions $E_z(x, y)$ and $\partial E_z(x, y)/\partial x$ in the plane $x = 0$, we obtain the following system of equations for E_1 and E_∞:

$$E_0 + E_1 = E_\infty\left[1 - \frac{3}{4}\mu\omega_0^2/\omega^2 + O(\mu^{3/2})\right]$$

$$(E_0 - E_1)k_x = E_\infty h_x\left[1 - i\frac{\sqrt{\mu}}{2}\frac{\omega_0^2}{\omega^2}\frac{k}{h_x} + \mu\frac{\omega_0^2}{\omega^2}\left(\frac{3}{4} - \frac{1}{2}\frac{1 + ik_y\omega/h_x\omega_H}{1-\omega^2/\omega_H^2}\right) + O(\mu^{3/2})\right].$$

Hence

$$\frac{E_1}{E_0} = \frac{k_x - h_x}{k_x + h_x}\left\{1 - \mu\left[\frac{\pi}{2}\frac{k_x^2 - k_x h_x}{k^2} + \frac{k_x h_x}{k^2}\frac{2 - 3\omega^2/\omega_H^2}{1-\omega^2/\omega_H^2}\right] + i\left[\sqrt{\mu}\frac{\sqrt{\pi}h_x}{k} + \mu\frac{k_x h_y}{k^2}\frac{\omega_0^2}{\omega\omega_H}\frac{1}{1-\omega^2/\omega_H^2}\right] + O(\mu^{3/2})\right\} \tag{33}$$

$$\frac{E_\infty}{E_0} = \frac{2k_x}{k_x + h_x}\left\{1 + \mu\left[\frac{3}{4}\frac{\omega_0^2}{\omega^2} - \frac{(k_x - h_x)h_x}{2k^2}\frac{2 - 3\omega^2/\omega_H^2}{1-\omega^2/\omega_H^2} - \frac{\pi}{4}\frac{(k_x - h_x)^2}{k^2}\right] + i\left[\sqrt{\mu}\frac{\sqrt{\pi}}{2}\frac{\kappa_x - n_x}{k} + \mu\frac{(\kappa_x - n_x)k_y}{2k^2}\frac{1}{1-\omega^2/\omega_H^2}\frac{\omega_0^2}{\omega\omega_H}\right] + O(\mu^{3/2})\right\}. \tag{34}$$

In deriving these formulas we used the relations

$$k_x^2 - h_x^2 = k^2 - h^2 = k^2\omega_0^2\omega^{-2}(1 + O(\mu)).$$

If $|k_y| = |h_y| < h$, i.e., if h_x is real, we have

$$\left|\frac{E_1}{E_0}\right|^2 = \left(\frac{k_x - h_x}{k_x + h_x}\right)^2\left\{1 + \mu\frac{k_x h_x}{k^2}\left[\pi - 2\frac{2 - 3\omega^2/\omega_H^2}{1-\omega^2/\omega_H^2}\right] + O(\mu^{3/2})\right\}, \tag{35}$$

$$\left|\frac{E_\infty}{E_0}\right|^2 = \left(\frac{2k_x}{k_x + h_x}\right)^2\left\{1 + \mu\left[\frac{3}{2}\frac{\omega_0^2}{\omega^2} - \frac{h_x(k_x - h_x)}{k^2}\frac{(2 - 3\omega^2/\omega_H^2)}{1-\omega^2/\omega_H^2} - \frac{\pi}{4}\frac{(k_x - h_x)^2}{k^2}\right] + O(\mu^{3/2})\right\}, \tag{36}$$

$$\arg E_1 = \sqrt{\mu}\frac{\sqrt{\pi}k_x}{k} + \mu\frac{k_x k_y}{k^2}\frac{\omega_0^2}{\omega\omega_H}\frac{1}{1-\omega^2/\omega_H^2} + O(\mu^{3/2}), \tag{37}$$

$$\arg E_\infty = \sqrt{\mu}\frac{\pi}{2}\frac{k_x - h_x}{k} + \mu\frac{(k_x - h_x)k_y}{k^2}\frac{\omega_0^2}{\omega\omega_H}\frac{1}{2(1-\omega^2/\omega_H^2)} + O(\mu^{3/2}). \tag{38}$$

When $\mu = 0$, Eqs. (33) — (38) coincide with the corresponding formulas of elementary theory. It must be noted that the phases of the transmitted and reflected waves are more sensitive to variation of the electron temperature than the amplitudes.

[1] L. D. Landau, JETP **16**, 574 (1946).

[2] V. P. Silin, Тр. ФИАН (Transactions of the Physics Institute, Academy of Sciences) **6**, 199 (1955).

[3] V. D. Shafranov, JETP **34**, 1475 (1958), Soviet Phys. JETP **7**, 1019 (1958).

[4] K. N. Stepanov, JETP **36**, 1457 (1959), Soviet Phys. JETP **9**, 1035 (1959).

[5] B. N. Gershman, JETP **37**, 695 (1959), Soviet Phys. JETP **10**, 497 (1960).

[6] B. N. Gershman, JETP **38**, 912 (1960), Soviet Phys. JETP **11**, 657 (1960).

Translated by J. G. Adashko
152

ELECTRIC MONOPOLE TRANSITIONS IN THE THEORY OF NONAXIAL NUCLEI

V. S. ROSTOVSKIĬ

Moscow State University

Submitted to JETP editor April 29, 1960

J. Exptl. Theoret. Phys. (U.S.S.R.) **39**, 854-858 (September, 1960)

It is demonstrated that if the coupling between rotation and β vibrations is taken into account, electric monopole transitions become possible between nuclear rotational states possessing the same momenta and parities. The transition matrix elements between such states are calculated. The results are compared with the experiments.

THE theory of nonaxial nuclei, proposed by Davydov and Filippov[1] and developed in subsequent works, explains adequately the positions and many properties of the low-lying levels of even-even nuclei. According to this theory, for each non-zero J there exist several rotational states of given momentum and parity. It is interesting to consider the probability of electric monopole transitions between such states with emission of internal-conversion electrons. Church and Weneser[2] have shown that the E0-transition operator can be expanded in powers of the parameters $\alpha_{2\mu}$ of quadrupole deformation. Since the principal term in the expansion is a constant and does not produce any transitions (in view of the orthogonality of the wave functions of the initial and final states of the nucleus) and there is no linear term, it is necessary to take account of terms of higher order in $\alpha_{2\mu}$. The E0 transitions between the lower vibrational states with $J \neq 0$ are due here to terms of third and higher order in $\alpha_{2\mu}$. As noted by Grechukhin,[3] the E0-transition operator is a scalar, i.e., it is independent of the Euler angles that characterize the orientation of the nucleus in space, and consequently E0 transitions between rotational states are strictly forbidden in the adiabatic theory.

We investigate in this work the probability of E0 transitions between rotational states of nonaxial nuclei, with allowance for the coupling between the rotation and the β oscillations. It is assumed that the rotation and the β oscillations are adiabatically slow compared with the γ oscillations, but account is taken of the dependence of the equilibrium value of the nonaxiality parameter γ on β, indicated in the papers of Davydov and Filippov[4] and Wang Ling.[5]

The wave functions of the initial and final states of the nucleus are obtained from the equation

$$(\hat{T}_\beta + V_\beta + \hat{H}^r_{\beta\gamma} - E)\,\Psi = 0, \tag{1}$$

where

$$\hat{T}_\beta = \hbar^2 (2B\beta^2)^{-1} \frac{\partial}{\partial\beta}\left(\beta^2 \frac{\partial}{\partial\beta}\right), \qquad V_\beta = \frac{1}{2} C (\beta - \beta_0)^2,$$

$$\hat{H}^r_{\beta\gamma} = \hbar^2 (8B\beta^2)^{-1} \sum_{\varkappa=1}^{3} \hat{J}_\varkappa^2 \left[\sin\left(\gamma - \frac{2\pi\varkappa}{3}\right)\right]^{-2}. \tag{2}$$

If we replace in the operator $\hat{H}^r_{\beta\gamma}$ in Eq. (1) the values of β and γ in terms of the equilibrium values β_0 and $\gamma_0 \equiv (\beta_0)$, we can separate the variables in this equation, viz.,

$$(\hat{T}_\beta + V_\beta + \hat{H}^r_{\beta_0\gamma_0} - E^v_\nu - E^r_{J\tau})\, u_\nu(\beta)\, \varphi_{J\tau}(\theta_i) = 0, \tag{3}$$

where the vibrational wave function has the form

$$u_\nu(\beta) = \beta^{-1} H_\nu\left(\delta \frac{\beta - \beta_0}{\beta_0}\right) \exp\left[-\delta^2 (\beta - \beta_0)^2 / 2\beta_0^2\right], \tag{4}$$

and the vibration energy is $E^V_\nu = \hbar\omega_V (\nu + 1/2)$ (see, for example, reference 6). Here $\delta = (\hbar^{-2} BC)^{1/4} = (B\beta^2\hbar^{-1}\omega_V)^{1/2}$ is a dimensionless parameter, which can be determined if the energy of the first excited state with spin 0^+ is known; H_ν is the Hermite function of the first kind. The parameter ν is obtained from the condition that the wave function is bounded when $\beta = 0$, i.e., from the condition $H_\nu(-\delta) = 0$. The value of the rotation energy $E^r_{J\tau}$ and the rotational wave functions $\varphi_{J\tau}$ are given in the papers by Davydov and Filippov[1] and by Davydov and the author.[7]

Since the total momentum J is conserved, we seek the solution of (1) in the form of a superposition of rotation-vibration functions with given J:

$$\Psi_{\nu J\tau} = \sum_{\nu',\tau'} A^{\nu J\tau}_{\nu' J\tau'} u_\nu(\beta)\, \varphi_{J\tau}(\theta_i). \tag{5}$$

Then in the first approximation of perturbation theory

$$A^{\nu J\tau}_{\nu' J\tau'} = (E^{v}_{\nu} - E^{v}_{\nu'} + E^{r}_{J\tau} - E^{r}_{J\tau'})^{-1} \langle u_\nu \varphi_{J\tau} | \hat{H}^{r}_{\beta\gamma} - \hat{H}^{r}_{\beta_0\gamma_0} | u_{\nu'} \varphi_{J\tau'} \rangle, \quad \nu'\tau' \neq \nu\tau; \quad A^{\nu J\tau}_{\nu J\tau} = 1. \tag{6}$$

Expanding the perturbation operator and retaining the first-order terms, we obtain

$$\hat{H}^{r}_{\beta\gamma} - H^{r}_{\beta_0\gamma_0} = (\beta - \beta_0)\beta_0^{-1}[-2\hat{H}^{r}_{\beta_0\gamma_0} + \varepsilon\hat{F}], \tag{7}$$

where

$$\varepsilon = \beta\partial\gamma/\partial\beta|_{\beta=\beta_0,\ \gamma=\gamma_0}, \qquad \hat{F} = \partial\hat{H}^{r}_{\beta\gamma}/\partial\gamma|_{\beta=\beta_0,\ \gamma=\gamma_0}.$$

As shown by Chaban,[8] the distinction between rotational and vibrational motion is meaningful only when $\delta > 2$. We confine ourselves to these values of δ. Then when $n < 3$ the Hermite function of the first kind, $H_{\nu n}$, differs little from the Hermite polynomials with corresponding integral indices, H_n, and the differences $\nu_{n+1} - \nu_n - 1$ are small and tend rapidly to zero with increasing δ. Therefore, in calculating the matrix elements we can assume

$$H_{\nu_{n+1}} = H_{\nu_{n+1}}. \tag{8}$$

The perturbation operator (7), which is proportional to $(\beta - \beta_0)/\beta_0$, has here non-vanishing matrix elements only when $\nu - \nu' = \pm 1$.

Let us proceed to calculate the matrix element of the E0 transition. For collective models of the nucleus, the operator of the E0 transition, accurate to second-order terms in $\alpha_{2\mu}$ (with allowance for the constant volume of the nucleus), has the form

$$\hat{E0} = N\frac{3Z}{4\pi R^3}\int_V \left(\frac{r}{R}\right)^2 dV = N\frac{3Z}{4\pi}\left(\frac{4\pi}{5} + \beta^2\right),$$

$$N = \tfrac{1}{6}e^2\Phi_i(0)\,\Phi_f(0)\,R^2, \qquad \beta^2 = \sum_{\mu=-2}^{2} |\alpha_{2\mu}|^2. \tag{9}$$

Here N is a factor defined by the electron wave functions, Φ_i and Φ_f are the radial parts of the wave functions of the initial and final states of the electron, Z is the charge, and R is the radius of the nucleus.

The matrix elements of the transition between different rotational states, with allowance for the orthogonality of the rotational functions $\varphi_{J\tau}$, are written as

$$\langle \Psi_{pJ\tau_1} | \hat{E0} | \Psi_{qJ\tau_2} \rangle = N\frac{3Z}{4\pi}\sum_{\nu,\nu',\tau} A^{pJ\tau_1}_{\nu J\tau} A^{qJ\tau_2}_{\nu' J\tau} \langle u_\nu | \beta^2 | u_{\nu'} \rangle. \tag{10}$$

Let us consider the transitions between two lower levels of the nucleus with a given non-zero spin J. According to the theory of nonaxial nuclei, these levels are referred to a single lower vibrational state ν_0. Taking condition (8) into account, we obtain from (10)

$$\langle \Psi_{\nu_0 J1} | \hat{E0} | \Psi_{\nu_0 J2} \rangle = N\frac{3Z}{4\pi}\sqrt{2}\beta_0^2\delta^{-1}(A^{\nu_0 J1}_{\nu_1 J2} + A^{\nu_0 J2}_{\nu_1 J1}). \tag{11}$$

Using (6), (7) and (8) we find

$$A^{\nu_0 J1}_{\nu_1 J2} = -(\hbar\omega_v + E^{r}_{J2} - E^{r}_{J1})^{-1}(\delta\sqrt{2})^{-1}\varepsilon\langle\varphi_{J_1}|\hat{F}|\varphi_{J_2}\rangle. \tag{12}$$

The value of $A^{\nu_0 J_2}_{\nu_1 J_1}$ is obtained from (12) by interchanging the indices $\tau = 1$ and $\tau = 2$. Differentiating the equation $(\hat{H}^{r}_{\beta\gamma} - E^{r}_{J\tau})\varphi_{J\tau} = 0$ with respect to γ, we obtain

$$\langle\varphi_{J_1}|\hat{F}|\varphi_{J_2}\rangle = (E^{r}_{J_2} - E^{r}_{J_1})\langle\varphi_{J_1}|\frac{\partial}{\partial\gamma_0}\varphi_{J_2}\rangle. \tag{13}$$

Putting $x_J \equiv (\hbar\omega_V)^{-1}(E^{r}_{J_2}$ and $E^{r}_{J_1})$, we obtain finally

$$\langle \Psi_{\nu_0 21} | \hat{E0} | \Psi_{\nu_0 22} \rangle = -N\frac{3Z}{4\pi}\beta_0^2\delta^{-2}\varepsilon\frac{2x_J}{1-(x_J)^2}\langle\varphi_{J_1}|\frac{\partial}{\partial\gamma}\varphi_{J_2}\rangle. \tag{14}$$

We note that (14) cannot be used for transitions between two lower levels with spin 0^+, since these levels pertain to different vibrational states. The matrix element of the transition between these levels, calculated in accordance with (10), is

$$\langle \Psi_{\nu_0 0} | \hat{E0} | \Psi_{\nu_1 0} \rangle = 3ZN\sqrt{2}\beta_0^2\delta^{-1}/4\pi$$

and is independent of ϵ in first approximation.

For the case $J = 2$ we use the specific form of $\varphi_{2\tau}$ and $E^{r}_{2\tau}$, obtained by Davydov and Filippov.[1] We find

$$\langle\varphi_{21}\ \frac{\partial}{\partial\gamma}\varphi_{22}\rangle = \frac{4\sin^2 3\gamma}{9-8\sin^2 3\gamma}, \qquad \delta^{-2} = x_2\,\frac{2\sin^2 3\gamma}{3[9-8\sin^2 3\gamma]^{1/2}},$$

$$\langle \Psi_{\nu_0 21} | \hat{E0} | \Psi_{\nu_0 22} \rangle = -N\frac{3Z}{4\pi}\beta_0^2\varepsilon\frac{16\sin^4 3\gamma_0}{3[9-8\sin^2 3\gamma_0]^{1/2}}\frac{x_2^2}{1-x_2^2}. \tag{15}$$

The final result contains the parameter $\epsilon = \beta\partial\gamma/\partial\beta|_{\beta=\beta_0,\gamma=\gamma_0}$. Theoretical estimates of this parameter can be obtained from the papers of Davydov and Filippov[4] and of Wang Ling.[5] The plot given by Wang Ling of the dependence of the equilibrium value of the nonaxiality parameter γ on $s = \log(4TB\beta^3\hbar^{-2})$ can be extrapolated, with good accuracy, by means of the parabola $\gamma = (s^2 - 14s + 41)\pi/180$. This yields $\epsilon(\gamma_0) = -0.045 \times \sqrt{8+\gamma_0}$ (γ_0 in degrees). When γ_0 varies from 0 to 30°, ϵ changes from 0.13 to 0.28, i.e., merely by a factor of two.

The table lists the theoretical values of the matrix element ρ of the E0 transition between two lower levels with spin 2^+, calculated from (15):

$$\rho \equiv N^{-1}\langle \Psi_{\nu_0 21}\ \hat{E0}\ \Psi_{\nu_0 22}\rangle, \qquad N = \tfrac{1}{6}e^2\Phi_i(0)\,\Phi_f^*(0)\,R^2.$$

The literature data on the energy levels are indicated in the last column of the table and the values of β_0 are taken from the survey article by Davydov,[9] while γ_0 and δ are calculated on the

Nucleus	β_0	γ_0	δ	$-\varepsilon$	ρ_{theor}	Reference
Cd^{114}	0.20	24	1.85	0.26	0.095	[12]
Gd^{154}	0.30	13	2.6	0.21	0.046	[13]
Er^{166}	0.33	13	4.5	0.21	0.006	[12-14]
Os^{188}	0.18	19	3.0	0.23	0.014	[13]
Pt^{194}	0.15	30	2.4	0.28	0.040	[16]
Pt^{196}	0.13	30	2.4	0.28	0.030	[12]
Hg^{198}	0.11	22	1.9	0.25	0.045	[12,15]

basis of the paper by Chaban,[8] with the energy corrected for non-adiabatic rotation. For Pt^{196}, the 0^+ level is unknown. It follows from $E_{22}/E_{21} = 1.93 < 2$, that the non-adiabatic corrections are strong here, $\delta \sim 2$, and $\gamma_0 = 30°$. In the calculation of ρ_{theor} we used $\delta = 2.4$, obtained for the neighboring even-even nucleus Pt^{194}, which has a similar arrangement of the lower 2^+ levels.

The results obtained indicate that electric monopole transitions between rotational states of non-axial nuclei are possible and can serve as a criterion for the applicability of the adiabatic approximation. It is seen from (14) and (15) that the E0 transition must be sought primarily among the strongly-deformed nuclei with low-lying 0^+ level and small δ (we note that the non-adiabatic nature of the rotation influences these nuclei most strongly), and with large non-axiality (i.e., with $E_{22}/E_{21} \sim 2$).

Let us compare our results with the experimental data for Pt^{196} obtained by Gerholm and Peterson.[10] To determine ρ_{exp} they used the ratio of the reduced probabilities of the electric quadrupole transitions

$$B(E2;\ 22 \to 21)/B(E2;\ 21 \to 0) = 2,$$

given by the "free oscillation" theory of Scharf-Goldhaber and Weneser.[11] If we use the value 10/7 given by the theory of nonaxial nuclei for $\gamma = 30°$, the experimental value of ρ is found to be in the limits $0.013 \leq \rho_{exp} \leq 0.04$. The theoretical value $\rho_{theor} = 0.030$ is in good agreement with experiment.

In conclusion, I thank Professor A. S. Davydov for suggesting the problem and for valuable remarks.

[1] A. S. Davydov and G. F. Filippov, JETP **35**, 440 (1958), Soviet Phys. JETP **8**, 303 (1959).

[2] E. Church and J. Weneser, Phys. Rev. **103**, 1035 (1956).

[3] D. P. Grechukhin, JETP **38**, 1891 (1960), Soviet Phys. JETP **11**, 1359 (1960).

[4] A. S. Davydov and G. F. Filippov, JETP **36**, 1497 (1959), Soviet Phys. JETP **9**, 1061 (1959).

[5] Wang Ling, Научн. докл. высш. шк., Физ.-мат. науки (Scient. Reports of the Colleges, Phys.-Math. Sci.) **1**, 146 (1959).

[6] A. S. Davydov, and A. A. Chaban, JETP **33**, 547 (1957), Soviet Phys. JETP **6**, 428 (1958); A. S. Davydov and G. F. Filippov, JETP **33**, 723 (1957), Soviet Phys. JETP **6**, 555 (1958); A. S. Davydov, Теория атомного ядра (Theory of the Atomic Nucleus), Gostekhizdat, 1958, Sec. 24.

[7] A. S. Davydov and V. S. Rostovskiĭ, JETP **36**, 1788 (1959), Soviet Phys. JETP **9**, 1275 (1959).

[8] A. A. Chaban, JETP **38**, 1630 (1960), Soviet Phys. JETP **11**, 1174 (1960).

[9] A. S. Davydov, Izv. Akad. Nauk SSSR, Ser. Fiz. **23**, 792 (1959), Columbia Tech. Transl. p. 788.

[10] T. Gerholm and B. Peterson, Phys. Rev. **110**, 1119 (1958).

[11] G. Scharf-Goldhaber and J. Weneser, Phys. Rev. **98**, 212 (1955).

[12] B. S. Dzhelepov and L. K. Peker, Схемы распада радиоактивных ядер (Decay Schemes of Radioactive Nuclei), U.S.S.R. Acad. Sci. Press, 1958.

[13] B. S. Dzhelepov and L. K. Peker, Excited States of Deformed Nuclei, Preprint R-1 288, Joint. Inst. Nuc. Res., Dubna, 1959

[14] Jacob, Mihelich, Harmatz, and Handley, Bull. Am. Phys. Soc. **3**, 358 (1958).

[15] E. P. Grigor'ev and M. P. Avotina, Izv. Akad. Nauk SSSR, Ser. Fiz. **24**, 324 (1960), Columbia Tech. Transl., in press.

[16] M. Johns and J. MacArthur, Canad. J. Phys. **37**, 1205 (1959).

Translated by J. G. Adashko
153

ON MUTUAL FRICTION IN HELIUM II

Yu. G. MAMALADZE

Institute for Physics, Academy of Sciences, Georgian S. S. R.

Submitted to JETP editor April 25, 1960

J. Exptl. Theoret. Phys. (U.S.S.R.) **39**, 859-860 (September, 1960)

A possible method is indicated for deciding experimentally the question of the existence of a component parallel to the axis of rotation in the mutual friction force between the superfluid and normal components of rotating helium II.

THE mutual friction force acting on a unit mass of the superfluid component from the direction of the normal component in rotating helium II has been examined in a number of papers.[1-3] The force:

$$\mathbf{F}_{sn} = -\frac{\rho_n}{2\rho} B' \boldsymbol{\omega}\times[\mathbf{v}_n - \mathbf{v}_s] - \frac{\rho_n}{2\rho} B\left[\frac{\boldsymbol{\omega}}{\omega}[\boldsymbol{\omega}\times(\mathbf{v}_n - \mathbf{v}_s)]\right], \quad (1)$$

where $\boldsymbol{\omega} = \operatorname{curl} \mathbf{v}_S$ and B and B′ are the coefficients of mutual friction of Hall and Vinen. Both terms in (1) are perpendicular to $\boldsymbol{\omega}$.

The purpose of this note is to indicate the possibility of an experimental resolution of the question of the existence of a third term in the mutual friction force, parallel to $\boldsymbol{\omega}$, i.e., of the existence of an additional term in $\mathbf{F}_{sn}$ of the form

$$\frac{\rho_n}{2\rho} B'' \frac{\boldsymbol{\omega}}{\omega}[\boldsymbol{\omega}\times(\mathbf{v}_n - \mathbf{v}_s)]. \quad (2)$$

The coefficient B″ can be determined from the damping of the oscillations of a cylinder along its axis (coincident with the axis of rotation of the fluid).* The hydrodynamic equations for rotating helium II are solved[4] with the following boundary conditions, in order to derive the corresponding equations:

$$v_{nr}(R) = 0, \quad v_{n\varphi}(R) = \omega_0 R, \quad v_{nz}(R) = i\Omega z_0 \exp(i\Omega t), \quad (3)$$

where R is the radius of the cylinder, ω_0 the angular velocity of rotation, Ω the frequency of the oscillations and z_0 their amplitude.

This leads to the following expression for the force acting on the surface of unit length of an infinite hollow thin-walled cylinder, oscillating in a boundless liquid:

$$F_z = i2\pi R\eta_n \Omega\varkappa \left[\frac{H_1^{(1)}(\varkappa R)}{H_0^{(1)}(\varkappa R)} - \frac{J_1(\varkappa R)}{J_0(\varkappa R)}\right] z_0 \exp(i\Omega t), \quad (4)$$

where

$$\varkappa^2 = -\frac{i\Omega}{\nu_n}\left[1 + \left(\frac{\omega_0}{\Omega}\right)^2 \frac{\rho_n\rho_s B''^2/\rho^2}{1 + (\omega_0/\Omega)^2(\rho_n B''/\rho)^2} - i\frac{\omega_0}{\Omega}\frac{\rho_s B''/\rho}{1 + (\omega_0/\Omega)^2(\rho_n B''/\rho)^2}\right]$$

$$(\operatorname{Im}(\varkappa) > 0). \quad (5)$$

Here η_n and ν_n are the dynamic and kinematic viscosities of the normal component, and H and J are the Hankel and Bessel functions.

Equation (5) leads to a penetration depth $1/\operatorname{Im}(\kappa) \sim \sqrt{2\nu_n/\Omega}$. For $R \sim 1$ cm, the quantity κR can therefore be considered large, and taking the asymptotic expansions of the Bessel functions we easily obtain the following equation:

$$\frac{\gamma_2 - \gamma_1}{l_2 - l_1} = \frac{\pi R\sqrt{2\eta_n\rho\Omega}}{m}\left(1 + \frac{\omega_0}{2\Omega}\frac{\rho_s}{\rho}B''\right), \quad (6)$$

which is valid for

$$(\omega_0\rho_n B''/\Omega\rho)^2 \ll 1, \qquad (\omega_0/\Omega)^2\rho_n\rho_s B''^2/\rho^2 \ll 1,$$

$$R/\operatorname{Im}(\varkappa) \gg 1.$$

Here γ_2 and γ_1 are the damping coefficients for the cylinder immersed to the depths l_2 and l_1: m is the mass of the oscillating system. Edge effects are automatically removed by subtracting γ_1 from γ_2. It is assumed that the oscillating system is "heavy" ($\Omega_2 = \Omega_1 = \Omega$).

It is convenient to use the following equation for determining B″:

$$(\gamma_2 - \gamma_1)/(\gamma_2 - \gamma_1)_{\omega_0=0} = 1 + (\omega_0\rho_s/2\Omega\rho)B''. \quad (7)$$

If B″ = 0, the damping is independent of the speed of rotation. If this is not the case we shall find a linear increase in damping with increasing ω_0.

The author is grateful to É. L. Andronikashvili, S. G. Matinyan, and D. S. Tsakadze for discussions.

*According to I. L. Bekarevich and I. M. Khalatnikov (private communication) an additional term should also be introduced into the force $\mathbf{F}_{sn}$ containing the product of ω and $\operatorname{curl}(\omega/\omega)$. Actually, in the case considered of the oscillations of a cylinder along the vortex lines, $\operatorname{curl}(\omega/\omega) = 0$.

[1] H. E. Hall and W. F. Vinen, Proc. Roy. Soc. **A238**, 204, 215 (1956).

[2] E. M. Lifshitz and L. P. Pitaevskiĭ, JETP **33**, 535 (1957), Soviet Phys. JETP **6**, 418 (1958).

[3] L. P. Pitaevskiĭ, Thesis, Institute for Physics Problems, U.S.S.R. Academy of Sciences (1958).

[4] Yu. G. Mamaladze and S. G. Matinyan, JETP **38**, 184 (1960), Soviet Phys. JETP **11**, 134 (1960).

Translated by R. Berman
154

PARTICLE COLLISIONS IN A HIGH-TEMPERATURE PLASMA

O. V. KONSTANTINOV and V. I. PEREL'

Institute for Technical Physics, Academy of Sciences, U.S.S.R.

Submitted to JETP editor April 30, 1960

J. Exptl. Theoret. Phys. (U.S.S.R.) 39, 861-871 (September, 1960)

We obtain a transport equation for a high-temperature plasma. The effective cross sections for electron-electron and electron-ion collisions are evaluated without an artificial cutoff of the interaction. We elucidate the role of the plasma oscillations for plasma kinetics. We show that one must take into account the influence of the ions on the screened interaction when considering electron-ion collisions.

IN a previous paper[1] we obtained a generalized transport equation for electrons which interacted with one another, with phonons, and with neutral impurity centers. We apply here the method developed in reference 1 to the case of a quasi-neutral plasma.

It is well known that in the case of the Coulomb interaction the total bremsstrahlung scattering cross section diverges logarithmically. The usual transport equation in which only pair collisions are taken into account is therefore inapplicable in that case. This difficulty is usually eliminated by cutting off the impact parameter at distances of the order of the Debye radius. Larkin[2] evaluated rigorously the transition probability for a fast electron passing through an electron gas in equilibrium the space charge of which was compensated by a smeared-out positive charge.

The problem whether one can describe only pair collisions even after some renormalization of the interaction remains, however, not cleared up. The present paper is devoted to an elucidation of that problem.*

We also take into account the motion of the ions and we investigate their role in the screening of the interaction. We hope later on to use the transport equation obtained here to calculate more accurate values of the transport coefficients.

*A short note by Balescu[3] is devoted to related problems; in this note he gives without proof and without stating the limits of its applicability an equation for the distribution function of an electron gas with a smeared-out positive charge. This equation, however, is not in the form of the usual transport equation with pair collisions, and this makes it difficult to interpret it physically.

1. EQUATIONS FOR THE SINGLE-PARTICLE DENSITY MATRICES OF THE ELECTRONS AND THE IONS

We consider a system consisting of interacting electrons and ions. The Hamiltonian H of the system is of the form*

$$H = H_0 + U,$$
$$H_0 = \sum_k (\varepsilon_k a_k^+ a_k + E_k A_k^+ A_k), \qquad U = U_{ee} + U_{ei} + U_{ii}. \tag{1}$$

Here

$$U_{ee} = \tfrac{1}{2} \sum_{q+q',\, f,\, f'} u_{q-q'}\, a_q^+\, a_{q'}\, a_f^+ a_{f'}\, \delta_{q+f,\, q'+f'},$$

$$U_{ei} = -\sum_{q+q',\, f,\, f'} u_{q-q'}\, a_q^+ a_{q'}\, A_f^+ A_{f'}\, \delta_{q+f,\, q'+f'},$$

$$U_{ii} = \tfrac{1}{2} \sum_{q+q',\, f,\, f'} u_{q-q'},\, A_q^+\, A_{q'}\, A_f^+ A_{f'}\, \delta_{q+f,\ q'+f'};$$

k, q, and f are wave vectors, $\epsilon_k = \hbar^2 k^2/2m$ is the electron energy, $E_k = \hbar^2 k^2/2M$ is the ion energy, A_k^+ and a_k^+ are creation operators for an ion and an electron, respectively, $u_\gamma = V^{-1} 4\pi e^2 \gamma^{-2}$, and V is the volume of the system.

Let there be a weak electromagnetic field in the system. The extra term in the density matrix F_t of the system (the matrix is proportional to the electrical field E_μ) is of the form [see Eq. (1) of reference 1]

$$F_t = \int_{-\infty}^{0} d\tau \int dx E_\mu\, (\mathbf{x}, t + \tau) \int_0^\beta d\lambda\, [J_\mu^e\, (\mathbf{x}, \tau + i\hbar\lambda) + J_\mu^i\, (\mathbf{x}, \tau + i\hbar\lambda)]\, F_0.$$

*The electrons and ions are assumed to have no spin. This is permissible, since exchange effects are small under the conditions of interest to us (vide infra).

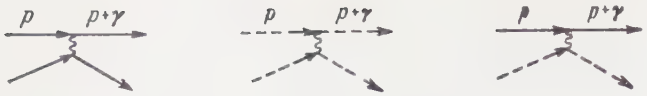

FIG. 1

Here J^e_μ and J^i_μ are the electron and ion current-density operators, $F_0 = Z^{-1}\exp(-\beta H')$, $Z = \mathrm{Sp}\exp(-\beta H')$, $H' = H - \mu\hat{N}$, $\hat{N}$ is the total particle number operator (electrons and ions), and μ is the chemical potential.

As in reference 1, we can determine the correction to the single-particle density matrices of the electrons and ions, respectively

$$f_{pp'}(t) = \int_{-\infty}^{0} d\tau \int dx E_\mu(\mathbf{x}, t+\tau) \int_0^\beta d\lambda\, \mathrm{Sp}\{F_0 a_p^+ a_{p'}[J^e_\mu(\mathbf{x}, \tau + i\hbar\lambda) + J^i_\mu(\mathbf{x}, \tau + i\hbar\lambda)]\},$$

$$\varphi_{pp'}(t) = \int_{-\infty}^{0} d\tau \int dx E_\mu(\mathbf{x}, t+\tau) \int_0^\beta d\lambda\, \mathrm{Sp}\{F_0 A_p^+ A_{p'}[J^0_\mu(\mathbf{x}, \tau + i\hbar\lambda) + J^i_\mu(\mathbf{x}, \tau + i\hbar\lambda)]\}. \quad (2)$$

Putting $E_\mu(\mathbf{x}, t) = E_\mu(\mathbf{x}, s)\exp[i(\kappa\cdot\mathbf{x}) + st]$ and following reference 1, we change to a diagram expansion of the functions $f_{pp'}$ and $\varphi_{pp'}$ in powers of the interaction. In any diagram there go to a terminal point τ either two electron or two ion lines with indices $\mathbf{k}$ and $\mathbf{k}'$ (the line $\mathbf{k}'$ enters into the terminal point τ and the line $\mathbf{k}$ starts from it) over which the summation is carried out. In the first case the terminal point τ corresponds to a factor

$$E(\varkappa, s)\, e^{st}\, (e\hbar/2m)(\mathbf{k} + \mathbf{k}')\delta_{\mathbf{k}', \mathbf{k}-\varkappa},$$

and in the second case to the same factor with e/m replaced by $-e/M$ (e is the electron charge, and m and M are the electron and ion mass respectively).

For diagrams occurring in the expansion of the function $f_{pp'}$ two electron lines go to the terminal point $-i\hbar\lambda$ (p' enters into the terminal point $-i\hbar\lambda$, and p starts from it). For the function $\varphi_{pp'}$ ion lines occur at the terminal point $-i\hbar\lambda$.

It is clear that there can be three types of points, corresponding to electron-electron, ion-ion, and electron-ion interactions (see Fig. 1). In the first two cases the point corresponds to a factor u_γ, and in the third case to $-u_\gamma$. The other factors corresponding to the points $1/i\hbar$, $-1/i\hbar$, and -1, and also factors corresponding to lines and intersections are defined in the same way as in Sec. 1 of reference 1. A free section

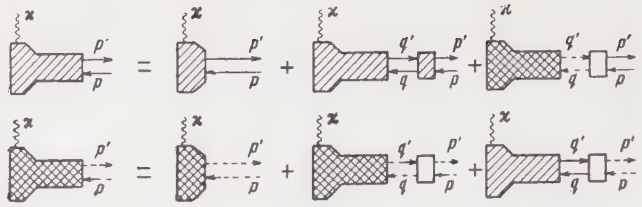

FIG. 2

can clearly arise not only when two electron lines are cut, but also when this happens to two ion lines.

The system of two generalized transport equations for the functions $f_{pp'}$ and $\varphi_{pp'}$ is depicted in Fig. 2 and is written down as follows

$$(s + i\omega_{p+\varkappa, p}) f_{p, p+\varkappa} = r_{p, p+\varkappa} + \sum_q f_{q, q+\varkappa} w^{ee}_{qp} + \sum_q \varphi_{q, q+\varkappa} w^{ie}_{qp}, \quad (3a)$$

$$(s + i\Omega_{p+\varkappa, p})\varphi_{p, p+\varkappa} = R_{p, p+\varkappa} + \sum_q \varphi_{q, q+\varkappa} w^{ii}_{qp} + \sum_q f_{q, q+\varkappa} w^{ei}_{qp}. \quad (3b)$$

Here $\hbar\omega_{kp} = \epsilon_k - \epsilon_p$, $\hbar\Omega_{kp} = E_k - E_p$, ϵ_k is the energy of an electron with wave vector k, and E_k the energy of an ion. The quantities $r_{p,p+\kappa}$, $R_{p,p+\kappa}$, and w_{qp} are defined in analogy with the quantities $r_{p,p+\kappa}$ and w_{qp} of reference 1. $r_{p,p+\kappa}$ and $R_{p,p+\kappa}$ differ from one another only in the kind of the last lines on the right. The quantities w_{qp} with different superscripts differ by the kind of extreme lines on the right and on the left.

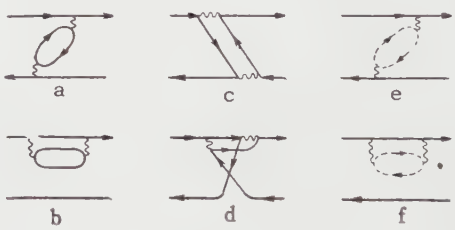

FIG. 3

2. EVALUATION OF THE COLLISION TERM

If the interaction potential were to decrease steeply at large distances, and were the particle concentration in the plasma low, we could confine ourselves in the quantity w to the diagrams proportional to the first power of the concentration. (We recall that the concentration arises from each reverse electron or ion line.) In Figs. 3 and 4 we have drawn possible types of such diagrams for w^{ee} and w^{ie} in the Born approximation. Account of these diagrams would lead to the usual collision term in the transport equation, linearized in the external field (as $s \to 0$ and $\kappa \to 0$).

FIG. 4

Diagrams of the type 3a and 3c lead to expressions arising when the electron-electron collision term is linearized; this term describes the arrival of electrons into the state p. Diagrams of the type 3b and 3d lead to the expression arising when the term corresponding to the departure of electrons is linearized. Diagrams of the kind 3e and 4a give the term describing the arrival of electrons into the state p through collisions with ions; diagrams of the kind 3f and 4b give correspondingly the term describing the departure. Diagrams for the quantities w^{ii} and w^{ei} are obtained from those for w^{ee} and w^{ie} by replacing electron lines by ion lines and the other way round.

In the Coulomb interaction case under consideration, however, it is impossible to restrict oneself to the above-mentioned diagrams since they diverge for small momentum transfers. To circumvent this divergence one must add to each of the diagrams of Figs. 3 and 4 diagrams of higher order in the concentration, but also of higher order of divergence with respect to the momentum transferred (which is the same as in the original diagram). We shall in the following consider the case of a nondegenerate gas. These diagrams will then differ from the original ones in that we must instead of each wavy line introduce a chain consisting of an arbitrary number of electron and ion loops (Fig. 5).

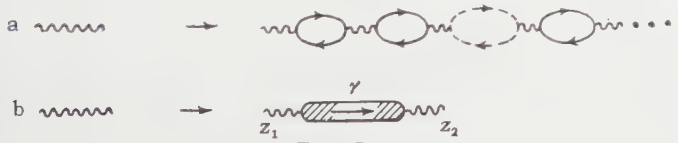

FIG. 5

The renormalization of the interaction can be done as follows: For the sake of convenience we assume for the time being that the renormalized wavy line is replaced not by a sum of chains, but by a block representing the sum of all possible diagrams which are fixed by two wavy lines in the points $z_1 = t_1 - i\hbar\lambda$ and $z_2 = t_2 - i\hbar\lambda$ on the horizontal section of the contour. We shall assume that all internal lines of the block cover the whole of the contour C. One understands easily that as $s \to 0$ the diagrams that contain points on vertical sections automatically contribute nothing to w, as there will be only one vertical free section in them.

We denote by z_2 the point which is most to the right so that $t_1 > t_2$ (all t are negative). This designation has a meaning for the modified diagrams (see reference 1) since in them the relative order of points on the horizontal sections remains unchanged in the integration. We assign to the block an arrow pointing from z_1 to z_2. Above the arrow we indicate the wave vector γ, which is transferred through the block from the point z_2 to z_1. It is clear that all arrows at the blocks will be directed from left to right. Such a block is drawn in Fig. 5b. We shall call it a plasmon line.

In the time representation the plasmon line corresponds to

$$L_\gamma(z_1, z_2) = \sum_{q, q'} \mathrm{Sp}\left\{e^{-\beta H_0} T_C \exp\left(\frac{1}{i\hbar}\int_C U_z\, dz\right)\right.$$
$$\left.\times (B_{q,\, q+\gamma})_{z_1} (B_{q'+\gamma,\, q'})_{z_2}\right\} Z^{-1}, \tag{4}$$

$$B_{kp} = a_k^+ a_p + A_k^+ A_p. \tag{5}$$

It is clear that

$$L_\gamma(z_1, z_2) = L_{-\gamma}(z_1, z_2).$$

Changing over from the interaction representation to the Heisenberg representation we see that

$$L_\gamma(z_1, z_2) = \sum_{q, q'} \mathrm{Sp}\left\{e^{-\beta H} T_C B_{q,\, q+\gamma}(z_1) B_{q'+\gamma,\, q'}(z_2)\right\} Z^{-1}.$$

If z_2 occurs earlier than z_1 on the contour C (regular plasmon line),

$$L_\gamma(z_1, z_2) = L_\gamma(t_1 - t_2)$$
$$= \sum_{q, q'} \mathrm{Sp}\left\{e^{-\beta H} B_{q,\, q+\gamma}(t_1)\, B_{q'+\gamma,\, q'}(t_2)\right\} Z^{-1}. \tag{6}$$

If the plasmon line is irregular,

$$L_\gamma(z_1, z_2) = \bar{L}_\gamma(t_1 - t_2)$$
$$= \sum_{q, q'} \mathrm{Sp}\left\{e^{-\beta H} B_{q'+\gamma,\, q'}(t_2)\, B_{q,\, q+\gamma}(t_1)\right\} Z^{-1}. \tag{7}$$

We put

$$L_\gamma(\tau) = \int_{-i\infty+\varepsilon}^{i\infty+\varepsilon} L_\gamma(\eta)\, e^{\eta\tau}\, d\eta, \qquad L_\gamma(\eta) = \int_0^\infty e^{-\eta\tau} L_\gamma(\tau)\, d\tau;$$

$$\bar{L}_\gamma(\tau) = \int_{-i\infty+\varepsilon}^{i\infty+\varepsilon} \bar{L}_\gamma(\eta)\, e^{\eta\tau}\, d\eta, \qquad \bar{L}_\gamma(\eta) = \int_0^\infty e^{-\eta\tau} \bar{L}_\gamma(\tau)\, d\tau. \tag{8}$$

Here $L_\gamma(\eta)$ and $\bar{L}_\gamma(\eta)$ are functions analytic in the right-hand half-plane of the complex variable η.

We can now formulate the rule for writing down the expressions corresponding to diagrams in which the integration over the time is performed. This rule remains as before, with one difference in that plasmon lines occur, each carrying an

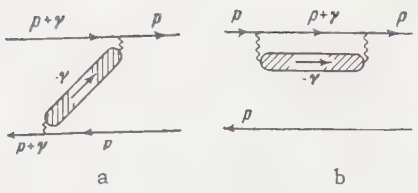

FIG. 6

"energy" $i\hbar\eta$. A regular plasmon line corresponds to the factor $L_\gamma(\eta)$ and an irregular one to $\bar{L}_\gamma(\eta)$. An integration of the form

$$(2\pi i)^{-1}\int_{-i\infty+\varepsilon}^{i\infty+\varepsilon} d\eta$$

is performed over all η.

When we define the direction of the plasmon lines as we have done above, they all enter a region that lies to the right of the vertical straight intersecting line. The factors which occur at the cuts through a plasmon line will thus be of the form $[s + i(\omega_{MN} + i\eta)]^{-1}$ and have thus a pole in the right-hand half-plane of η ($\mathrm{Re}\, s > 0$), where $L_\gamma(\eta)$ and $\bar{L}_\gamma(\eta)$ are analytical. One can thus integrate over η by closing the contour around the right-hand half-plane.

It is now easy to reduce all pertinent diagrams to expressions containing $L_\gamma(\eta)$. We show in the Appendix that the function $L_\gamma(\eta)$ is connected with the function $\tilde{K}_\gamma(\eta)$ by the simple equations (A5) and (A6). The latter can be evaluated by the method applied in Larkin's paper.[2]

In the final reckoning all the diagrams will thus be expressed in terms of $\tilde{K}_\gamma(\eta)$ as follows:

I. The sum of the diagrams 3a and 3e assumes after renormalization the form given in Fig. 6a. The sum of diagram 6a and the diagram with the opposite slope gives

$$w^{\mathrm{I}}_{p+\gamma,\,p} = \frac{u_\gamma^2}{2\pi i\hbar^2}\int_{-i\infty+\varepsilon}^{i\infty+\varepsilon} d\eta\left[\frac{\bar{L}_\gamma(\eta)}{s + i(\omega_{p+\gamma,\,p} + i\eta)}\right.$$

$$\left. + \frac{L_\gamma(\eta)}{s + i(\omega_{p,\,p+\gamma} + i\eta)}\right] = (u_\gamma^2/\hbar^2)[\bar{L}_\gamma(s + i\omega_{p+\gamma,\,p})$$

$$+ L_\gamma(s - i\omega_{p+\gamma,\,p})]$$

or, using Eq. (A6)

$$w^{\mathrm{I}}_{p+\gamma,\,p} = -(u_\gamma^2/\hbar^2)\,2\beta\hbar[1$$

$$- \exp(-\beta\hbar\omega_{p+\gamma,\,p})]^{-1}\mathrm{Im}\,\tilde{K}_\gamma(s + i\omega_{p+\gamma,\,p}). \qquad (9)$$

II. The renormalized diagrams 3b and 3f are given in Fig. 6b. The sum of diagram 6b and the diagram with the loop at the bottom gives

$$w^{\mathrm{II}}_{qp} = -\delta_{qp}\sum_\gamma w^{\mathrm{I}}_{p,\,p+\gamma}. \qquad (10)$$

III. The renormalization of the diagram 3c reduces to adding to it the diagrams given in Fig. 7.

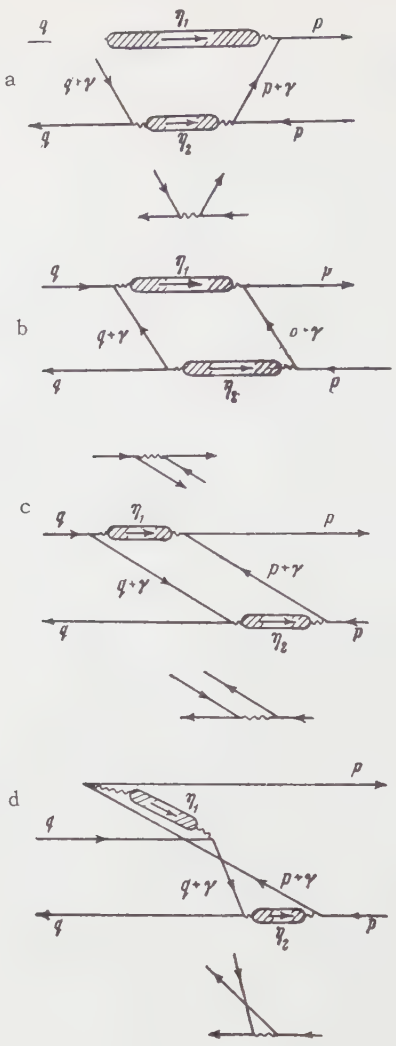

FIG. 7

One must also add the diagrams obtained from the diagrams of Fig. 7 by replacing one of the plasmon lines by a point in the places indicated on the figure. In each of these diagrams one must take into account the possibility of the transposal of a point (see reference 1) in those casse where such a transposal does not lead to the occurrence of additional irregular electron lines. (We recall that we are considering the nondegenerate case.) One verifies easily that one must transpose all those points where the electron lines form a sharp angle.

The diagram 7a corresponds to the expression (we have omitted for the sake of simplicity the integrals over η and the sum over γ)

$$(u_\gamma^4/\hbar^4)[s + i(\omega_{q+\gamma,\,q} + i\eta_1)]^{-1}[s + i(i\eta_1 + i\eta_2)]^{-1}[s$$

$$+ i(\omega_{p+\gamma,\,p} + i\eta_1)]^{-1}$$

$$\times[\bar{L}_\gamma(\eta_2) - L_\gamma(\eta_2)]\,L_\gamma(\eta_1)(n_{p+\gamma} - n_p).$$

The diagram 7b corresponds to the expression

$$(u_\gamma^4/\hbar^4)[s+i(\omega_{q+\gamma,q}+i\eta_1)]^{-1}[s+i(i\eta_1+i\eta_2)]^{-1}$$
$$\times[s+i(\omega_{p,p+\gamma}+i\eta_2)]^{-1}$$
$$\times[\bar{L}_\gamma(\eta_2)-L_\gamma(\eta_2)]L_\gamma(\eta_1)(n_{p+\gamma}-n_p).$$

The sum of these expressions and the expression corresponding to the diagram of Fig. 7c gives, as $s \to 0$,

$$(u_\gamma^4/\hbar^4)[s+i(\omega_{q+\gamma,q}+\omega_{p,p+\gamma})]^{-1}[s+i(\omega_{p+\gamma,p}+i\eta_1)]^{-1}$$
$$\times[s+i(\omega_{p,p+\gamma}+i\eta_2)]^{-1}[\bar{L}_\gamma(\eta_2)$$
$$-L_\gamma(\eta_2)]L_\gamma(\eta_1)(n_{p+\gamma}-n_p)$$

or, after integrating over η_1 and η_2

$$\frac{u_\gamma^4}{\hbar^4}\frac{n_{p+\gamma}-n_p}{s+i(\omega_{q+\gamma,q}+\omega_{p,p+\gamma})}[\bar{L}_\gamma(s+i\omega_{p,p+\gamma})$$
$$-L_\gamma(s+i\omega_{p,p+\gamma})]L_\gamma(s+i\omega_{p+\gamma,p}).$$

Collecting all other diagrams leading to the renormalization of diagram 3c and using Eqs. (A5) and (A6) we get the expression

$$\frac{u_\gamma^2}{\hbar^2}\frac{n_{p+\gamma}}{s+i(\omega_{q+\gamma,q}+\omega_{p,p+\gamma})}|1-\beta u_\gamma\tilde{K}_\gamma(s-i\omega_{p+\gamma,p})|^2.$$

The analogous renormalized diagram, which differs in slope from diagram 3c, leads to the complex conjugate expression. Thus

$$w_{qp}^{III}=\sum_\gamma 2\pi\frac{u_\gamma^2}{\hbar^2}\delta(\omega_{q+\gamma,q}-\omega_{p+\gamma,p})|1-\beta u_\gamma\tilde{K}_\gamma$$
$$\times(s-i\omega_{p+\gamma,p})|^2 n_{p+\gamma}. \quad (11)$$

IV. The renormalization of diagram 3d and of the analogous one with the loop at the bottom is performed in exactly the same way. The result is

$$w_{qp}^{IV}=-\sum_\gamma 2\pi\frac{u_\gamma^2}{\hbar^2}\delta(\omega_{q-\gamma,q}+\omega_{p+\gamma,p})|1-\beta u_\gamma\tilde{K}_\gamma$$
$$\times(s-i\omega_{p+\gamma,p})|^2 n_p. \quad (12)$$

The renormalization of the diagrams of the kind 4a and 4b leads to expressions differing from w_{qp}^{III} and w_{qp}^{IV} only in that $\omega_{q+\gamma,q}$ and $\omega_{q-\gamma,q}$ are replaced by $\Omega_{q+\gamma,q}$ and $\Omega_{q-\gamma,q}$.

Substituting the values of w evaluated in the foregoing into Eq. (3a) and using Eq. (A7) for K_γ we obtain the collision term of the transport equation for the electron distribution function in the form

$$S=S_{ei}+S_{ee};$$

$$S_{ee}=V^{-2}\sum_{\gamma,q}\frac{2\pi}{\hbar^2}\delta(\omega_{p+\gamma,p}-\omega_{q+\gamma,q})|A_\gamma(\omega_{p+\gamma,p})|^2$$
$$\times(f_{p+\gamma}n_q+n_{p+\gamma}f_q-f_p n_{q+\gamma}-n_p f_{q+\gamma}), \quad (13)$$

$$S_{ei}=V^{-2}\sum_{\gamma,q}\frac{2\pi}{\hbar^2}\delta(\omega_{p+\gamma,p}-\Omega_{q+\gamma,q})|A_\gamma(\omega_{p+\gamma,p})|^2$$
$$\times(f_{p+\gamma}N_q+n_{p+\gamma}\varphi_q-f_p N_{q+\gamma}-n_p\varphi_{q+\gamma}). \quad (14)$$

Here N_q is the equilibrium ion distribution function

$$A_\gamma(\omega_{p+\gamma,p})=\frac{u_\gamma V}{1+u_\gamma P_\gamma(s+i\omega_{p+\gamma,p})}. \quad (15)$$

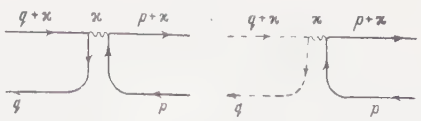

FIG. 8

3. THE SELF-CONSISTENT FIELD AND THE FREE TERM IN THE TRANSPORT EQUATION

In the foregoing we did not consider diagrams of the first order which occur in w_{qp} (see Fig. 8). These diagrams need not be renormalized, as the chains that renormalize them are taken into account when the transport equation is derived. Diagrams of this kind lead to the occurrence of a term

$$\sum_q(f_{q,q+\varkappa}-\varphi_{q,q+\varkappa})(i\varkappa\mathbf{v}_p)\frac{\partial n_p}{\partial\varepsilon_p}u_\varkappa$$

on the right-hand side of the transport equation for the electron distribution function. Here $\mathbf{v}_p$ is the velocity of an electron with wave vector p. We assumed that $\kappa \ll p$. This term describes the influence of the self-consistent electron and ion field.

We restrict ourselves in the quantity $r_{p,p+\kappa}$ to diagrams which do not contain the interaction. We have then

$$r_{p,p+\varkappa}=-e(\mathbf{E}_\varkappa\mathbf{v}_p)\frac{\partial n_p}{\partial\varepsilon_p},\qquad \mathbf{E}_\varkappa=\mathbf{E}(\varkappa s)e^{st+i\varkappa x}. \quad (16)$$

4. THE TRANSPORT EQUATION

If we take into account the fact that the electron distribution function $f_p(\mathbf{x}, t)$ can be expressed in terms of $f_{p,p+\kappa}(t)$ by the equation

$$f_p(\mathbf{x},t)=\int e^{i\varkappa x}f_{p,p+\varkappa}(t)\,d\varkappa, \quad (17)$$

we get finally from Eq. (3a)

$$\frac{\partial f_p}{\partial t}+(\mathbf{v}_p\nabla)f_p+e(\mathbf{E}\mathbf{v}_p)\frac{\partial n_p}{\partial\varepsilon_p}-e(\nabla\Psi,\mathbf{v}_p)\frac{\partial n_p}{\partial\varepsilon_p}=S_{ee}+S_{ei}, \quad (18)$$

$$\Psi(\mathbf{x},t)=e\int|\mathbf{x}-\mathbf{x}'|^{-1}V^{-1}\sum_q[f_q(\mathbf{x}',t)-\varphi_q(\mathbf{x}',t)]\,d\mathbf{x}'; \quad (19)$$

S_{ee} and S_{ei} are defined by Eqs. (13) and (14).

This equation has the standard form of a transport equation with pair-collisions, linearized with respect to the deviation of the distribution function from the equilibrium one. The quantity $A_\gamma(\omega_{p+\gamma,p})$ plays the role of an effective transition matrix element for all collisions.

We can use Eqs. (A7) to write $|A_\gamma(\omega_{p+\gamma,p})|^2$ in the form

$$|A_\gamma(\omega_{p+\gamma,p})|^2=\frac{(4\pi e^2)^2}{(\gamma^2+\Delta^2 I)^2+\Delta^4\Gamma^2}, \quad (20)$$

where

$$I = I_i + I_e, \qquad \Gamma = \Gamma_i + \Gamma_e,$$

$$I_e = (n_0\beta\hbar V)^{-1} \sum_q \frac{n_q - n_{q+\gamma}}{\omega_{q+\gamma,\,q} - \omega_{p+\gamma,\,p}}$$

$$\approx \frac{2}{\sqrt{\pi}} \int_0^\infty e^{-k^2}\, dk\, \frac{k^2}{k^2 - \beta\varepsilon_p \cos^2\psi}, \tag{21}$$

$$\Gamma_e = (n_0\beta\hbar V)^{-1}\pi \sum_q (n_q - n_{q+\gamma})\,\delta(\omega_{q+\gamma,\,q} - \omega_{p+\gamma,\,p})$$

$$\approx \sqrt{\pi\beta\varepsilon_p}\cos\psi \exp(-\beta\varepsilon_p \cos^2\psi), \tag{22}$$

$$I_i = (n_0\beta\hbar V)^{-1} \sum \frac{N_q - N_{q+\gamma}}{\Omega_{q+\gamma,\,q} - \omega_{p+\gamma,\,p}}$$

$$\approx \frac{2}{\sqrt{\pi}} \int_0^\infty e^{-k^2}\, dk\, \frac{k^2}{k^2 - \beta\varepsilon_p (M/m)\cos^2\psi}, \tag{23}$$

$$\Gamma_i = (n_0\beta\hbar V)^{-1}\pi \sum_q (N_q - N_{q+\gamma})\,\delta(\Omega_{q+\gamma,\,q} - \omega_{p+\gamma,\,p})$$

$$\approx \sqrt{\pi\beta\varepsilon_p\, M/m}\cos\psi \exp\left(-\beta\varepsilon_p \frac{M}{m}\cos^2\psi\right), \tag{24}$$

ψ is the angle between the vectors p and γ, $\Delta^2 = 4\pi n_0 e^2\beta$ is the inverse square of the Debye radius, and n_0 the electron (ion) concentration.

The approximate expressions given in Eqs. (21) – (24) are obtained by taking it into account that the characteristic momentum transferred is appreciably less than the thermal momentum ($\gamma \ll p$) both for the ions and for the electrons.

When electrons collide with one another, which corresponds to the term S_{ee} the values of the angle ψ need not be restricted. The quantities I_i and Γ_i can thus be neglected in the term S_{ee} by comparison with I_e and Γ_e, since $M/m \gg 1$. The ions do therefore practically not take part in the screening of the electron-electron interaction. One sees easily that in the case where the velocity of one of the colliding electrons is much less than thermal, the quantity A_γ corresponds to the first Born approximation for the scattering by the usual Debye potential.

If the electron velocities are not small compared with thermal, A_γ takes into account the deformation of the Debye cloud.

When the energies of both the colliding electrons are much higher than thermal, $|A_\gamma|^2$ has steep maxima in the points $\omega_{p+\gamma,p} = \pm\omega_0$ (ω_0 is the plasma frequency). This corresponds to such a process that one electron emits a plasmon and the other one absorbs it, or the other way round. The plasmons can thus not carry away any momentum from the electron system.

It is also clear from Eq. (13) that the term with the renormalized electron-electron collisions does not contribute to the momentum balance. Papers in which the influence of plasma oscillations on the conductivity was taken into account by assuming the plasmons to be an independent system, like the phonons, are thus incorrect.

In electron-ion collisions described by the term S_{ei}, the energy conservation law restricts the possible values of ψ to a region close to $\frac{1}{2}\pi$ since $\cos\psi \sim \sqrt{m/M}$. The quantities I_i and Γ_i are thus not small and it is not possible to neglect the influence of the ions in the screening of the electron-ion interaction. For the same reason ($\cos\psi \sim \sqrt{m/M}$) we can assume $I_e \approx 1$, $\Gamma_e = 0$ in the term S_{ei}.

One could obtain the transport equation for the ion distribution function by a completely analogous method from Eq. (3b). The Born approximation used here is practically nowhere suitable for ion-ion collisions. We shall therefore not write out this equation.

5. LIMITS OF APPLICABILITY

We assume when evaluating the collision term that $\kappa \to 0$, neglecting it compared with the transfer of the wave vector γ. It is clear from Eq. (20) that a characteristic value of γ is of the order of magnitude of the inverse Debye radius. When putting $\kappa \to 0$ we assume thus that the external electrical field changes little over a Debye radius.

The condition $s \to 0$ ($s = \nu - i\omega$) means that $\hbar\omega$ is much less than the characteristic energy transferred in a collision $\epsilon_{p+\gamma} - \epsilon_p \sim \hbar\omega_0$. Putting $s \to 0$, we assume thus that the frequency of the external field is much smaller than the plasma frequency.

When evaluating K_γ we made the same approximation as those in Larkin's paper[2] i.e., we assumed that the gas parameter is small: $(e^2/kT)^3 n_0 \ll 1$.

One can show that neglecting in w diagrams in which plasmon lines which carry different momenta intersect or are superimposed upon one another (see Figs. 9a and 9b) is valid under the same conditions. The same applies to replacing $r_{p,p+\kappa}$ by a free line.

Use of the Born approximation enables us to neglect diagrams of the kind drawn in Fig. 10. This presupposes that the condition $4\pi e^2/\hbar v_T \ll 1$

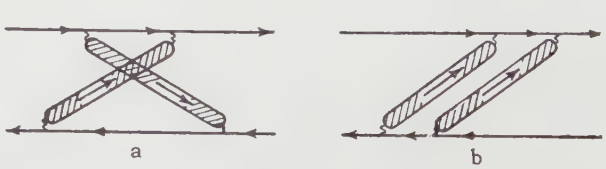

FIG. 9

FIG. 10

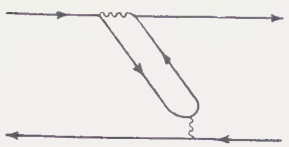

FIG. 11

is satisfied, where v_T is the thermal velocity of the electron.

Neglect of the exchange terms (see Fig. 11) presupposes that the electron de Broglie wavelength is small compared with the Debye radius.

In conclusion we express our gratitude to L. É. Gurevich for valuable advice and discussions.

APPENDIX

The evaluation of the quantity $L_\gamma(t_1 - t_2)$ is based upon the idea of analytical continuation which was stated in the paper by Abrikosov et al.[4] and is very close to the calculations given by Larkin.[2]

We consider the function (where $\lambda_1 > \lambda_2$)

$$K_\gamma(\lambda_1 - \lambda_2) = \sum_{q,q'} \mathrm{Sp}\,\{e^{-\beta H} B_{q,q+\gamma}(-i\hbar\lambda_1) \times B_{q'+\gamma,q'}(-i\hbar\lambda_2)\}\, Z^{-1}. \tag{A1}$$

Its Fourier coefficient

$$K_\gamma(\omega_n) = \beta^{-1} \int_0^\beta e^{i\omega_n \hbar\lambda} K_\gamma(\lambda)\, d\lambda$$

$\omega_n = 2\pi n/\beta\hbar$, $(n = 0, 1, 2, \ldots)$, expanded in terms of the eigenstates of the total Hamiltonian H is of the form

$$K_\gamma(\omega_n) = i(\beta\hbar)^{-1} \sum_{MN} e^{-\beta E_M} \rho_{MN}(\gamma) \left[\frac{1}{\omega_n - i\omega_{MN}} - \frac{1}{\omega_n + i\omega_{MN}}\right] Z^{-1},$$

$$\rho_{MN}(\gamma) = \Big|\sum_q B_{q,q+\gamma}\Big|^2_{MN}. \tag{A2}$$

We have used here the property $\rho_{MN}(\gamma) = \rho_{NM}(\gamma)$ which is a consequence of the fact that $\rho_{MN}(\gamma)$ is an even function of γ.

We denote the analytical continuation of the function $K_\gamma(\omega_n)$ of a discrete set of points ω_n onto the right-hand half-plane of the complex variable η by $\tilde{K}_\gamma(\eta)$

$$\tilde{K}_\gamma(\eta) = i(\beta\hbar)^{-1} \sum_{MN} e^{-\beta E_M} \rho_{MN}(\gamma) \left[\frac{1}{\eta - i\omega_{MN}} - \frac{1}{\eta + i\omega_{MN}}\right] Z^{-1}. \tag{A3}$$

If we now use Eqs. (6) – (8) we can write the quantities $L(\eta)$ and $\bar{L}(\eta)$ in the form

$$L_\gamma(\eta) = Z^{-1} \sum_{MN} e^{-\beta E_M} \rho_{MN}(\gamma) \frac{1}{\eta - i\omega_{MN}},$$
$$\bar{L}_\gamma(\eta) = Z^{-1} \sum_{MN} e^{-\beta E_M} \rho_{MN}(\gamma) \frac{1}{\eta + i\omega_{MN}}. \tag{A4}$$

Comparing Eqs. (A3) and (A4) we get

$$\bar{L}_\gamma(\eta) - L_\gamma(\eta) = i\beta\hbar\tilde{K}_\gamma(\eta), \tag{A5}$$

$$\bar{L}_\gamma(s + i\Omega) + L_\gamma(s - i\Omega) = -\beta\hbar(1 - e^{-\beta\hbar\Omega})^{-1} 2\,\mathrm{Im}\,\tilde{K}_\gamma(s + i\Omega). \tag{A6}$$

The last relation is only valid when $s \to 0$.

The expressions arising from the renormalization of the diagrams in section 2 contain the quantities L_γ and $\bar{L}_\gamma$ only in the combinations which occur in Eqs. (A5) and (A6).

If $K_\gamma(\omega_n)$ is approximated by a sum of chain diagrams we can use the method applied by Larkin[2] to get to the expression

$$\tilde{K}_\gamma(\eta) = \beta^{-1} \frac{P_\gamma(\eta)}{1 + u_\gamma P_\gamma(\eta)}, \qquad P_\gamma(\eta) = P_\gamma^{(e)}(\eta) + P_\gamma^{(i)}(\eta),$$

$$P_\gamma^{(e)}(\eta) = -\hbar^{-1} \sum_q \frac{n_{q+\gamma} - n_q}{i\eta + \omega_{q+\gamma,q}},$$

$$P_\gamma^{(i)}(\eta) = -\hbar^{-1} \sum_q \frac{N_{q+\gamma} - N_q}{i\eta + \Omega_{q+\gamma,q}}. \tag{A7}$$

[1] O. V. Konstantinov and V. I. Perel', JETP **39**, 197 (1960), Soviet Phys. JETP **12**, 142 (1961).

[2] A. I. Larkin, JETP **37**, 264 (1959), Soviet Phys. JETP **10**, 186 (1960).

[3] R. Balescu, Physica **25**, 324 (1959).

[4] Abrikosov, Gor'kov, and Dzyaloshinskiĭ, JETP **36**, 900 (1959), Soviet Phys. JETP **9**, 636 (1959).

Translated by D. ter Haar
155

ON THE EFFECT OF ACOUSTIC RESONANCE PULSES ON A NUCLEAR SPIN SYSTEM

A. R. KESSEL'

Physico-Technical Institute, Kazan' Branch, Academy of Sciences, U.S.S.R.

Submitted to JETP editor May 3, 1960

J. Exptl. Theoret. Phys. (U.S.S.R.) 39, 872-877 (September, 1960)

The effect of acoustic pulses of a resonance frequency ω and duration $t_\omega \ll T_2$ on a system of nuclear spins ($I > \frac{1}{2}$) is examined theoretically. It is shown that in contrast to the effect of an electromagnetic field on the spin system, a single acoustic pulse does not induce a free procession signal to the first approximation in $\hbar\omega/kT$. Two acoustic pulses produce a spin-echo signal which is equal in magnitude to that produced by electromagnetic pulses.

1. In recent years a number of experiments[1-6] has been performed which confirm the effect predicted by Al'tshuler[7] of ultrasonic resonance absorption in paramagnetic substances. This phenomenon differs from ordinary paramagnetic resonance absorption by the fact that here ultrasonic phonons are absorbed instead of photons. Experiments[1-6] have made it possible to measure the probabilities of transition between sublevels of paramagnetic particles under the influence of acoustic oscillations. In carrying this out the ultrasonic pulses were of such duration that a stationary mode had time to be established in the substance.

In order to study magnetic properties of matter in addition to resonance absorption the phenomena of spin echo and of nuclear induction have been successfully utilized in which electromagnetic pulses rotate the nuclear spins into a plane perpendicular to the constant magnetic field in which they then precess with the Larmor frequency. For example, two pulses each of duration t_ω spaced by a time interval τ produce a spin-echo signal, with the induced emf due to the rotation of the total magnetic moment of the sample M_0 being equal to[8]

$$\mathcal{E} = -nS\frac{\partial}{\partial t}\sum\hbar\gamma I_x(t) = -nSM_0\omega\sin(\gamma H_1 t_\omega) \times \sin^2(\gamma H t_\omega/2)\cos\omega(t-2\tau)\exp\left[-\frac{(t-2\tau)^2}{2T_2^2}\right], \quad (1)$$

where $t > t_\omega + \tau$, $2H_1$ is the amplitude of the pulse, γ is the gyromagnetic ratio, nS is the number of turns and the cross section of the receiver coil.

It appears to be of interest to carry out an investigation of similar phenomena stimulated by ultrasonic methods. In order to rotate a magnetic moment in a constant magnetic field a certain amount of energy has to be expended. As Al'tshuler has shown[7] the coefficient of sound absorption is usually larger than the coefficient of absorption for the electromagnetic field; moreover, modern sound emitters can produce energy fluxes equal in magnitude to the electromagnetic energy introduced into the sample in spin echo experiments. All this suggests that ultrasonic pulses can rotate magnetic moments no less effectively than the electromagnetic field.

The action of sound on spins may be explained by the following model. Suppose that an acoustic pulse of the Larmor frequency and of duration t_ω is introduced in the direction of the x axis into a substance containing nuclei possessing magnetic and quadrupole moments and situated in a constant magnetic field $\mathbf{H}_0(0, 0, H_0)$. Longitudinal acoustic oscillations will produce a time-dependent electric field gradient $\nabla E = (\nabla E)_0 \sin(\omega t - kx)$, which can be resolved into two components rotating in opposite directions.

We now go over into a system of coordinates rotating with the Larmor frequency,[8] in which the magnetic moment and one of the components of the gradient are stationary, while $\mathbf{H}_0$ and the second component rotating with double the Larmor frequency are not effective. In this coordinate system the quadrupole moment of the particle will begin to precess about the stationary gradient[9] with a certain frequency ω_Q and will be rotated through the angle $\varphi = \omega_Q t_\omega$. The magnetic moment rigidly coupled to the quadrupole moment will rotate simultaneously. The problem consists of selecting the conditions and the combinations of pulses which will rotate the magnetic moment in such a way that in the laboratory coordinate system it will precess in a plane perpendicu-

lar to $\mathbf{H}_0$ and will induce a measurable induced emf in the receiver coil.

2. We now proceed to a quantum-mechanical investigation of the effect of ultrasonic oscillations on a spin system. We assume that a crystal of cubic symmetry containing nuclei of quadrupole moment Q and spin I is situated in a constant magnetic field $\mathbf{H}_0$. At a time t = 0 we apply along the C_4 crystal axis an ultrasonic pulse of Larmor frequency and of duration t_ω. The acoustic pulse traverses the sample during the time t = d/v where d is the sample size and v is the velocity of sound. This leads to a retardation in the rotation between the nuclei in the ends of the sample by the angle $\varphi = \omega d/v$. We can show that, on the one hand, the acoustic pulse passing through the sample does not give rise to a total magnetic moment of the sample different from zero $M_x = \Sigma \hbar \gamma I_x(t)$ if the condition $\omega d/v < \pi$ is not satisfied, and, on the other hand, that $\mathscr{E}$ is proportional to $\omega^2 d$ and is greatly reduced when the condition $\omega d/v < \pi$ is satisfied. Therefore, it is more advantageous to utilize both the progressive and the reflected waves simultaneously. If we neglect absorption and reflection losses, then the oscillations of the particles of the substance can be represented in the form

$$u = u_1 + u_2 = A[\sin(\omega t - kx - kd) + \sin(\omega t + kx - kd)],$$

and the relative displacement of two neighboring particles is given by

$$\delta = 2Aa \sin kx \sin(\omega t - kd),$$

where A is the oscillation amplitude, a is the lattice constant.

The energy of the nucleus consists of a Zeeman and a quadrupole part:

$$\hat{\mathcal{H}} = -\gamma H_0 \hbar I_z - \sum_{i=-2}^{2} Q_i \nabla E^{-i} \qquad (2)$$

In a perfect cubic crystal $\nabla E^i \equiv 0$, and the nucleus is described by the eigenfunctions Ψ_m of the component of the spin along $\mathbf{H}_0$. During the time $0 \le t \le t_\omega$ the acoustic oscillations distort the cubic symmetry and produce a time-dependent electric field gradient. This leads[6] to nonvanishing terms in the sum (2)

$$Q_{\pm 1}\nabla E^{\mp 1} = -\hbar\omega_1 \sin kx \sin \omega t' [\hat{I}_\pm \hat{I}_z + \hat{I}_z \hat{I}_\pm],$$
$$Q_{\pm 2}\nabla E^{\mp 2} = \hbar\omega_2 \sin kx \sin \omega t' \hat{I}_\pm^2, \qquad (3)$$

where

$$\omega_1 = \frac{3e^2 Q q_1 A k}{8I(2I-1)\hbar} \sin 2\theta e^{\pm i\varphi}, \qquad \omega_2 = \frac{3e^2 Q q_1 A k}{8I(2I-1)\hbar} \sin^2\theta e^{\pm i2\varphi},$$

$q_1 = \partial(\nabla E^0)/\partial(\delta/a)$, $t' = t - (d/v)$, θ is the angle between $\mathbf{H}_0$ and the propagation vector $\mathbf{k}$, φ is the angle between the component of $\mathbf{k}$ in the xy plane and the x axis. In future we shall assume for the sake of simplicity that $\varphi = 0$. We write the nuclear spin wave function in the interval $0 \le t \le t_\omega$ in the following form

$$\Psi(t) = \sum_m C_m(t) \exp\{-iE_m t/\hbar\} \Psi_m, \qquad (4)$$

and after the acoustic pulse ($t > t_\omega$) it has the form

$$\Psi(t) = \sum_m C_m(t_\omega) \exp\{-iE_m(t - t_\omega)/\hbar\} \Psi_m. \qquad (5)$$

On substituting (2) — (4) into the Schrödinger equation we obtain a system of differential equations for $C_m(t)$. A solution of such a system for spin I = 1 and for an acoustic pulse of resonance frequency $\omega = \gamma H_0 = \omega_0$ will be given by

$$C_1(t) = -\frac{1}{\sqrt{2}} C_0(0) \sin\xi + C_1(0) \cos^2\frac{\xi}{2} - C_{-1}(0) \sin^2\frac{\xi}{2},$$
$$C_0(t) = C_0(0) \cos\xi + \frac{1}{\sqrt{2}}[C_1(0) + C_{-1}(0)] \sin\xi,$$
$$C_{-1}(t) = -\frac{1}{\sqrt{2}} C_0(0) \sin\xi + C_{-1}(0) \cos^2\frac{\xi}{2} - C_1(0) \sin^2\frac{\xi}{2}, \qquad (6)$$

where $C_m(0)$ are constants which specify the state before the beginning of the acoustic pulse at t = 0, $\xi = |\omega_1 \sin kx| t$. If the acoustic frequency is equal to $\omega = 2\omega_0$, i.e., if $\Delta m = 2$ transitions are induced, then

$$C_1(t) = C_1(0) \cos\eta + C_{-1}(0) \sin\eta, \qquad C_0(t) = C_0(0),$$
$$C_{-1}(t) = C_{-1}(0) \cos\eta - C_1(0) \sin\eta, \qquad \eta = |\omega_2 \sin kx| t. \qquad (7)$$

Table I gives the results of calculations of the time dependence of the average values of certain components of the spin and of the nuclear quadrupole moment. $\Psi(t)$ is given by (4) and (5) with the coefficients $C_m(t)$ given by (6), if the transitions $\Delta m = 1$ are induced, and given by (7) in the case of the $\Delta m = 2$ transitions. The average value, naturally, depends on the initial conditions at t = 0.

In order to evaluate the effect produced on the nucleus by two acoustic pulses we have to use the systems (5) or (6) twice, with the role of $C_m(0)$ being played the second time by $C_m(\tau)$ — the coefficients that specify the state of the nucleus immediately before the beginning of the second pulse at the instant $t = \tau$.

The result of such a calculation is given in Table II, where the first pulse induces the $\Delta m = 1$ transitions, and the second one induces the $\Delta m = 2$ transitions.

3. Until now we have considered individual nuclei. But in experiments the total effect of all the

TABLE I

	$C_m(0)=\delta_{1,m}$		$C_m(0)=\delta_{0,m}$		$C_m(0)=\delta_{-1,m}$	
	$\Delta m=1$	$\Delta m=2$	$\Delta m=1$	$\Delta m=2$	$\Delta m=1$	$\Delta m=2$
$\tilde{I}_x$	$-\frac{1}{2}\sin 2\xi \times \sin \omega t'$	0	$\sin 2\xi \times \sin \omega t'$	0	$-\frac{1}{2}\sin 2\xi \times \sin \omega t'$	0
$\tilde{Q}_1+\tilde{Q}_{-1}$	$-2\sin\xi \times \cos \omega t'$	0	0	0	$2\sin\xi \times \cos \omega t'$	0
$\tilde{Q}_2+\tilde{Q}_{-2}$	$-\sin^2\xi \times \cos 2\omega t'$	$-\sin 2\eta \times \cos \omega t'$	$2\sin^2\xi \times \cos 2\omega t'$	0	$-\sin^2\xi \times \cos 2\omega t'$	$\sin^2\eta \times \cos 2\omega t'$

TABLE II

	$\tilde{I}_y$
$C_m(0)=\delta_{1,m}$	$-\frac{1}{2}\sin 2\xi \cos\eta \sin \omega t' + \sin\xi \sin\eta \sin\omega(t'-2\tau)$
$C_m(0)=\delta_{0,m}$	$\sin 2\xi \cos\eta \sin \omega t'$
$C_m(0)=\delta_{-1,m}$	$-\frac{1}{2}\sin 2\xi \cos\eta \sin \omega t' - \sin\eta \sin\xi \sin\omega(t'-2\tau)$

nuclei in the sample is observed. Prior to the application of the acoustic pulse the population of the Zeeman levels was determined by the Boltzmann distribution

$$N_m = \frac{N}{2I+1} e^{-E_m/kT} = \frac{N}{2I+1}\left(1 + m\frac{\hbar\omega}{kT} + \ldots\right) \qquad (8)$$

(at room temperature $\hbar\omega/kT \sim 10^{-6}$). By utilizing the tables and the first two terms of the expansion of the exponential (8) we obtain the following expressions for the $\Delta m = 1$ transitions:

$$\Sigma\tilde{I}_x = \Sigma\{\tilde{Q}_2 + \tilde{Q}_{-2}\} = 0,$$

$$\Sigma\{\tilde{Q}_1 + \tilde{Q}_{-1}\} = 4\frac{N}{2I+1}\frac{\hbar\omega}{kT}\overline{\sin\xi}\cos\omega t' \exp\left[-\frac{t'^2}{2T_2^2}\right], \qquad (9)$$

and for the $\Delta m = 2$ transitions we obtain:

$$\Sigma\tilde{I}_x = \Sigma\{\tilde{Q}_1 + \tilde{Q}_{-1}\} = 0,$$

$$\Sigma\{\tilde{Q}_2 + \tilde{Q}_{-2}\} = -2\frac{N}{2I+1}\frac{\hbar\omega}{kT}\overline{\sin 2\eta}\cos 2\omega t' \exp\left[-\frac{2t'^2}{T_2^2}\right]. \qquad (10)$$

If the first transition is of $\Delta m = 1$ type, and the second transition is of $\Delta m = 2$ type, then

$$\Sigma\tilde{I}_y = 2\frac{N}{2I+1}\frac{\hbar\omega}{kT}\overline{\sin\xi\sin\eta}\sin\omega(t'-2\tau)\exp\left[-\frac{(t'-2\tau)^2}{2T_2^2}\right]. \qquad (11)$$

Here we have averaged over the frequency distribution which is assumed to be Gaussian.[8] The bar above the expression denotes averaging over the coordinate. If the pulses are so chosen that $\omega_1 t_\omega = \omega_2 t_\omega = \pi/2$, then we have $\overline{\sin\xi\sin\eta} = \frac{1}{2}$. A similar calculation for the case of spin $I = \frac{3}{2}$ gives

$$\Sigma\tilde{I}_y = \frac{N}{2I+1}\frac{\hbar\omega}{kT}\overline{\sin(2\sqrt{3}\xi)\sin(2\sqrt{3}\eta)} \times \sin\omega(t'-2\tau)\exp\left[-\frac{(t'-2\tau)^2}{2T_2^2}\right].$$

It may be seen from formulas (9) and (10) that up to quantities of the first order in $\hbar\omega/kT$ a free precession signal cannot be induced by a single acoustic pulse. However, in this case rotation of the components of the quadrupole moment of the nucleus takes place and, consequently, electric quadrupole radiation must be emitted with the components of the different nuclei rotating in the same phase. The intensity of the electric field of the radiation at small distances from the sample $R \sim k^{-1}$ is equal to[10]

$$E \approx \frac{1}{6}\frac{\partial^3}{\partial R^3}\frac{e}{R}\Sigma\{\tilde{Q}_{1,2} + \tilde{Q}_{-1,-2}\} \approx 10^{-60}\frac{\omega^5}{T},$$

where T is the absolute temperature, ω is the ultrasonic frequency, k is the wave number of the radiation. Because of its smallness this effect apparently cannot be observed by direct methods.

Two acoustic pulses produce a spin echo signal already in the first order of expansion (8)

$$\mathcal{E} = -nS\frac{2N}{2I+1}\gamma\frac{(\hbar\omega)^2}{kT}\sin\xi\sin\eta\cos\omega(t'-2\tau) \times \exp\left[-\frac{(t'-2\tau)^2}{2T_2^2}\right], \qquad (12)$$

which for $\omega_1 t_\omega = \omega_2 t_\omega = \pi/2$ is of the same magnitude as the signal (1) produced by two radio-frequency pulses with $\gamma H_1 t_\omega = \pi/2$.

4. In order for the spin-echo effect (1) and (12) to occur it is necessary[8] that the time t_ω during which the pulse acts on the spin system should be much smaller than T_2. On the other hand, the maximum effect will occur when $\omega_1 t_\omega = \omega_2 t_\omega = \pi/2$, so that the optimum condition is $T_2\omega_{1,2} \gg 1$.

It may be seen from this that in order to study

dynamic ultrasonic phenomena nuclear spin systems are more convenient since the relaxation times T_2 in electron spin systems are smaller by a factor of $10^3 - 10^6$. In order to estimate $\omega_{1,2}$ we utilize the relation[11] $A = (2J \cdot 10^7/\rho v \omega^2)^{1/2}$ cm, where ρ is the density of the substance, J is the intensity of sound in w/cm^2. According to formulas (3), and according to the data of Bolef and Menes,[6] we shall obtain for KI^{127} and KBr^{79} $\omega_{1,2} \sim 10^3 J^{1/2}$ sec^{-1}. The relaxation time T_2 in these substances is of the order of magnitude of 10^{-4} sec, so that we must use maximum sound intensities. It is known (cf., for example, reference 12), that in the pulsed mode it is possible to obtain from a quartz radiator a sound intensity of the order of 1000 w/cm^2.

Apparently, we must choose substances with large values of T_2, or extend it artifically. This can be done by changing somewhat the method used in the paper by Andrew, Bradbury, and Eades,[13] i.e., by producing a rotating field H_0, which ought to reduce the dipole line width. It is also known[14] that artificial introduction of defects into a sample leads under certain conditions to a narrowing of the nuclear resonance line by a factor of several fold. It should be remembered that T_2, which describes the decay of the spin-echo signal, is determined only by the so-called irreversible contributions to the line width,[15] so that consequently, we took for our estimate too low values of T_2, which were determined from the width of absorption lines produced both by reversible and irreversible contributions.

We can also use shorter pulse lengths such that $\omega_{1,2} t_\omega < \pi/2$. This will lead to a reduction in the signal amplitude which, if necessary, could be compensated by reducing the temperature.

The foregoing enables us to conclude that it is possible to select a substance and experimental conditions in such a way that the inequality $\omega_{1,2} T_2 > 1$ will be satisfied. This will make it possible to observe the effect of spin echos induced by ultrasonic oscillations.

The author is grateful to S. A. Al'tshuler and B. M. Kozyrev for discussion of the results and to R. A. Dautov for useful advice.

[1] W. G. Proctor and W. H. Tantilla, Phys. Rev. **104**, 1757 (1956).

[2] W. G. Proctor and W. A. Robinson, Phys. Rev. **104**, 1344 (1956).

[3] M. Menes and D. I. Bolef, Phys. Rev. **109**, 128 (1958).

[4] O. Kraus and W. H. Tantilla, Phys. Rev. **109**, 1052 (1958). Jennings, Tantilla, and Kraus, Phys. Rev. **109**, 1059 (1958).

[5] E. F. Taylor and N. Bloembergen, Phys. Rev. **113**, 431 (1959).

[6] D. I. Bolef and M. Menes, Phys. Rev. **114**, 1441 (1959).

[7] S. A. Al'tshuler, Doklady Akad. Nauk SSSR **85**, 1225 (1952); JETP **28**, 38 and 49 (1955), Soviet Phys. JETP **1**, 29 and 37 (1955).

[8] Bloom, Hahn, and Herzog, Phys. Rev. **97**, 1699 (1955). Das, Saha, and Roy, Proc. Roy. Soc. **A227**, 407 (1955).

[9] E. R. Andrew, Nuclear Magnetic Resonance, Cambridge, 1955.

[10] L. D. Landau and E. M. Lifshitz, Теория поля (Field Theory) OGIZ, 1948 [Engl. Transl., Addison Wesley, 1951].

[11] L. Bergman, Ultrasonics, (in German) Edwards Bros., 1944.

[12] C. E. Teeter, J. Acoust. Soc. Am. **18**, 488 (1947).

[13] Andrew, Bradbury, and Eades, Nature **183**, 62 (1959).

[14] T. Hashi, J. Phys. Soc. Japan **13**, 911 (1958).

[15] F. Reif, Phys. Rev. **100**, 1597 (1955).

Translated by G. Volkoff
156

QUANTUM OSCILLATIONS OF THERMODYNAMIC QUANTITIES FOR AN ARBITRARY FERMI SURFACE

M. Ya. AZBEL'

Physico-Technical Institute, Academy of Sciences, Ukrainian S.S.R.

Submitted to JETP editor May 6, 1960

J. Exptl. Theoret. Phys. (U.S.S.R.) **39**, 878-887 (September, 1960)

Thermodynamic quantities of an electron gas in a constant magnetic field **H** are calculated in the general case of a non-convex Fermi surface. It is shown that the presence of self-intersecting trajectories leads to quantum oscillations of these quantities as functions of H. It is pointed out that the experimentally observed oscillations corresponding to "anomalously weakly filled" bands may be due either to separated small surfaces, and are then described by the Lifshitz-Kosevich theory,[1] or to small bulges or depressions in the main large band, in which case they are described by the present theory.

1. INTRODUCTION

IN a series of papers by I. Lifshitz and Kosevich (see, for example, reference 1), it has been shown that, owing to the strong Fermi degeneracy of the electron gas, quantization of the energy levels of an electron with an arbitrary dispersion law $\epsilon = \epsilon(\mathbf{p})$ (ϵ is the energy, $\mathbf{p}$ is the quasimomentum) in a constant magnetic field $\mathbf{H}(0, 0, H)$ leads to an increment, which is periodically dependent on $1/H$ to the thermodynamic quantities. The period in the reciprocal of the magnetic field $\Delta(1/H)$ is equal to

$$\Delta(1/H) = eh/cS_m(\zeta), \tag{1}$$

where $S_m(\zeta)$ is the extremal (with respect to p_z) area of the intersection of the boundary Fermi surface $\epsilon(p) = \zeta$ with the plane $p_z = \text{const}$. Only this cross sectional area enters, for the reason (as is easy to understand) that the fundamental contribution to the oscillating part of the statistical sum for the smooth function $S(\zeta, p_z)$ will be made by just those electrons of the narrow layer close to the extremal (but, naturally, not equal to zero) sections, where, in the classical case, the majority of the electrons move with a period close to the given period in the region

$$\Delta p_z \sim p_0(\mu H/\varepsilon_0)^{1/2}, \quad p_0(\mu H/\varepsilon_0) \ll \Delta p_z \ll p_0 \tag{2}$$

(p_0 is of the order of the limiting momentum in the direction p_z, ϵ_0 is the limiting energy, $\mu = e\hbar/m^*c$, and $m^* = (2\pi)^{-1}\partial S/\partial\epsilon$ is the effective mass of the electron).

It is clear from (2) that the relative contribution of the periodic part of the thermodynamical quantities (which is comparable to the part which is monotonically dependent on the magnetic field) is also of order $(\mu H/\epsilon_0)^{1/2}$. Inasmuch as the part Ω which depends monotonically on H is even and, consequently, is proportional to $(\mu H/\epsilon_0)^2$, the absolute value of the periodic increment to Ω is proportional to $(\mu H/\epsilon_0)^{5/2}$, and the increment to the magnetic moment, which is linear in H, is proportional to $(\mu H/\epsilon_0)^{3/2}$.

If the Fermi surface is convex, then the only non-monotonic part of the statistical sum is connected with the extremal cross sections. In the case of a non-convex surface, the area of the cross section is generally not a smooth function: at a certain point $p_z^0(\zeta)$, which corresponds to the self-intersecting classical orbit in a magnetic field, a transition takes place from one cross section to two separate cross sections (Fig. 1), while the derivatives $\partial S/\partial\zeta$, $\partial S/\partial p_z$ at this point go to infinity logarithmically for all three areas.

It is natural to expect that these "singular" cross sections also contribute an oscillating part to the statistical sum (see also reference 2). It is physically clear that inasmuch as the picture of levels takes on the ordinary "non-singular" form at distances as small as the order of the distance between levels, i.e., of the order of

$$\Delta p_z \sim p_0 \mu H/\varepsilon_0, \tag{3}$$

then the irregular part, which is connected with self-intersection, will be at least $(\epsilon_0/\mu H)^{1/2}$ times smaller than the periodic part due to extremal sections. The absolute value of the irregular increment to the linear momentum is consequently proportional at least to $(\mu H/\epsilon_0)^2$

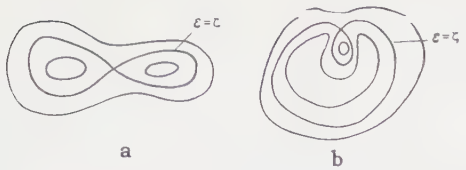

FIG. 1. a – case of "necking in," b – case of a "trough;" p_z = const.

[instead of $(\mu H/\epsilon_0)^{3/2}$ for the periodic part], while the contribution to Ω is proportional to $(\mu H/\epsilon_0)^3$ [instead of $(\mu H/\epsilon_0)^{5/2}$].

Thus the contribution to the oscillating terms from the cross sections with self-intersection is small in comparison with the known contribution of the extremal cross sections. However, the following circumstance must be kept in mind.

1. It is well known that the experimentally observed quantum oscillations (the De Haas-Van Alphen and the Shubnikov-De Haas effects) are brought about not by the main "large" bands, but by some anomalously weakly filled bands with density of the order of $10^{-2} - 10^{-6}$ electrons per atom. The genesis of these bands is completely unclear at the present time. It can be thought in each case that these bands are either separated small surfaces or small "bulges" or "depressions" in momentum space, which destroy the local bulge of the surface corresponding to a principal band.

Up to the present time only the first of these cases has been considered, although it does not follow at all that precisely this case takes place. Furthermore, it is difficult to ascertain experimentally which one of these actually does take place, since the oscillations have an entirely similar character in both cases, and the dependence of the amplitude of the oscillations on the magnetic field is difficult to determine unambiguously. The fact is that the amplitude of the oscillations is extremely sensitive to the mosaic structure, impurities, etc., and is least reliably established experimentally.

The interpretation of the observed effects can also be ambiguous. Thus, the directions in which one of the periods of the oscillations disappears can be interpreted either as the directions in which the cross sections with self-intersection disappear, or as the directions of open cross sections. Therefore, for explanation of this problem, it is necessary to draw upon resonance measurements in weak magnetic fields and on a study of quantum oscillations in high frequency and constant magnetic fields (see reference 3), in addition to a detailed investigation of the picture in strong magnetic fields. In such a case one makes use of the known noncentral character of cross sections with self-intersection and of the fact that the effective mass goes to infinity on these sections.

It is quite possible that both situations are realized in different metals.

2. Even if there is a case of a separated but non-convex surface, the "fine structure" due to self-intersection has quite an appreciable value, since for "small bands," $\epsilon_0/\mu H \sim 1 - 10^2$. Furthermore, the "fine structure" from similar bands can be larger (because of the smallness of the effective mass) than the principal structure from the "large" bands.

3. For a one-parameter family of directions of the constant magnetic field, there may in general be no cross section which is extremal in area, and the cross section with self-intersection may be the maximum in area. (Such a case exists, for example, for graphite.) In this case evidently only those oscillations remain which correspond to trajectories with self-intersection. In the investigation of the anisotropy of the effect, a sharp decrease in the amplitude of oscillations should be observed as one approaches a similar direction (this fall-off can also be ascribed to the approach to the open trajectories).

In the present paper, we calculate the thermodynamic potential Ω and the magnetic susceptibility in the general case of the presence of self-intersecting orbits.

2. GENERAL FORMULA FOR THE THERMODYNAMIC POTENTIAL Ω

1. It is well known that the thermodynamic quantities can be computed if the thermodynamic potential Ω, equal (per unit volume) to

$$\Omega = -\Theta \sum \ln\left[1 + \exp\left(\frac{\zeta - \varepsilon}{\Theta}\right)\right], \qquad \Theta = kT \tag{4}$$

is known. The summation is carried out over the quantum states, k is Boltzmann's constant, T is the temperature, ζ is the chemical potential.

Naturally, we will be interested only in the part of Ω connected with the electron gas, and therefore knowledge of the energy levels of the electrons in a constant magnetic field is sufficient in our case for the calculation of Ω. As was shown by the author,[2] the energy levels can be obtained from the two branches of the dispersion equation, which have the form

$$[2n_\pm(\varepsilon, p_z) + 1]\pi \equiv S_1 + S_2 + \varphi(k) \pm \cos^{-1}\{e^{-k\pi} \times (2\cos 2k\pi)^{-1/2}\cos(S_1 - S_2)\} = (2n+1)\pi, \tag{5}$$

in the case of the presence of "necking-in," and

in the case of the presence of a "trough"

$$[2n_{\pm}(\varepsilon, p_z) + 1]\pi \equiv S_1 - S_2 + \varphi(k) \pm \cos^{-1}\{e^{k\pi}(2\cosh 2k\pi)^{-1/2} \times \cos(S_1 + S_2)\} = (2n+1)\pi, \quad (6)$$

where n is an integer in each case,

$$\varphi(k) = 2\left\{k \ln\frac{|k|}{e} - \frac{1}{2i}\ln\frac{\Gamma(1/4 + ik)}{\Gamma(1/4 - ik)}\right\} - \tan^{-1}\tanh k\pi,$$

$$S(k) = \frac{c}{2e\hbar H}S(p_z), \quad k = \frac{\varepsilon - \varepsilon_0(p_z)}{2e\hbar H}c\sqrt{|m_x m_y|},$$

$$m_\alpha^{-1} = [\partial^2\varepsilon/\partial p_\alpha^2]_{p_x = p_y = 0}, \quad (7)$$

$\epsilon_0(p_z)$ is the energy for which self-intersection takes place for a given p_z; the origin of the coordinates is located at the point of self-intersection for the given p_z; the p_x and p_y axes are directed along the bisectors of the angles formed by the trajectories at the point of intersection, so that $m_x > 0$, $m_y < 0$. The quantity $S(p_z)$ is the area in momentum space; in the case of "necking in," S_1 corresponds to the area bounded by the orbits to the left of the p_x axis and S_2 to the right of p_x; in the case of a "trough," S_1 corresponds to the total area bounded by the orbit, including the area up to the p_y axis, while S_2 is the area of the "hole," including the area up to the p_y axis (see Fig. 2). Equations (5), (6) are applicable in the quasi-classical case, that is, for $S_{1,2}(k) \gg 1$ and, consequently, $n \gg 1$.

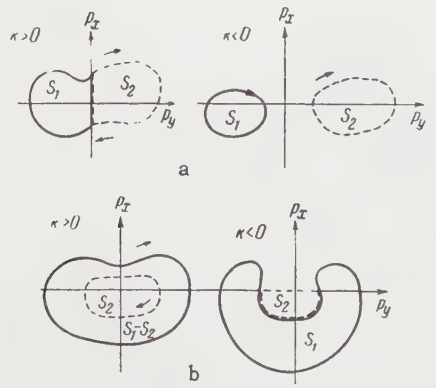

FIG. 2. a – case of necking in, b – case of a trough; the direction of the classical motion of the electron is shown by the arrow.

In accord with (5), (6), the energy depends on n and p_z and, as a function of these quantities, divides into two branches:

$$\varepsilon = \varepsilon_{\pm}(n, p_z). \quad (8)$$

(For simplicity, we shall not write down the spin component $\pm e\hbar/2m_0c$, m_0 is the mass of the free electron, since it can be established that it has no effect on either the general course of the discussion nor on the final formula if we take into account the spin pair before the statistical sum.)

2. Corresponding to (8), we have

$$\Omega \sim -2\Theta\int_{-\infty}^{\infty} dp_z \sum_{\pm}\sum_{n_{\pm}^{\min}}^{\infty} \ln\left\{1 + \exp\left(\frac{\zeta - \varepsilon_{\pm}(n, p_z)}{\Theta}\right)\right\}$$

$$(n_{\pm}^{\min} = \min_{\varepsilon} n_{\pm}(\varepsilon, p_z)). \quad (9)$$

The coefficient of proportionality is the same as in the case of free electrons considered by Landau,[4] and is equal to $eH/\hbar^2c$. This can be established, for example, by considering the electrons to be located in a box, where all the quantum numbers are discrete, and by calculating Ω as the dimensions of the box approach infinity. The thermodynamic potential is found either directly from Eq. (4) or by the equation

$$\Omega = -\int N(\zeta)\, d\zeta, \qquad N = \sum N_n |\psi_n|^2,$$

where $n \sim n_1, n_2, n_3$ are the quantum numbers, while ψ_n is the wave function (which is easily found in the quasi-classical region just as in reference 2). Detailed calculation shows that the Landau factor is not changed if there is degeneracy in the generalized momentum P_x, that is, if the levels are computed with accuracy up to $O(h^2)$, while the wave functions are computed with accuracy up to $O(h)$. Inasmuch as we are interested only in the oscillating part of $\Delta\Omega$ as a function of H^{-1}, and the lower levels ($n \sim 1$), as can be shown, give only the part of Ω proportional to H^2, summation in (9) with the previous accuracy can be carried out from $n = 0$. (Strictly speaking, this only makes it possible to calculate $\Delta\Omega$, since for $n \sim 1$ the fundamental equations (5), (6) are invalid.)

Thus Ω_1 (by Ω_1 we mean any function which has the same oscillating part as Ω) has the form

$$\Omega_1 = -\frac{2eH\Theta}{ch^2}\sum_{n=0}^{\infty}\int_{-\infty}^{\infty} dp_z\left[\ln\left(1 + \exp\left\{\frac{\zeta - \varepsilon_+(n, p_z)}{\Theta}\right\}\right) + \ln\left(1 + \exp\left\{\frac{\zeta - \varepsilon_-(n, p_z)}{\Theta}\right\}\right)\right]. \quad (10)$$

We now make use of Poisson's formula:

$$\sum_{n=0}^{\infty}\varphi(n) = \tfrac{1}{2}\varphi(0) + \int_0^{\infty}\varphi(n)\, dn + 2\,\mathrm{Re}\sum_{k=1}^{\infty}\int_0^{\infty} dn\,\varphi(n)\, e^{2\pi i k n}. \quad (11)$$

It can be shown that the first two components in (11) do not give terms which oscillate with the magnetic field and therefore can be omitted in Ω_1.

Integrating the remaining expression by parts, and carrying out the substitution of ϵ^+ for n in

the first integral, and ϵ^- in the second [such a substitution of variables is possible because of the monotonic character of $n_\pm(\epsilon)$, which is shown in reference 2, and which is determined by Eqs. (5) and (6)], and setting the lower limit of integration over ϵ_+ and ϵ_- at zero (since only $n \gg 1$ are important), we obtain

$$\Omega_1 = -\frac{2eH}{\pi ch^2}\,\mathrm{Im}\sum_{k=1}^{\infty}\frac{1}{k}\int_{-\infty}^{\infty}dp_z\int_0^{\infty}f_0\Big(\frac{\varepsilon-\zeta}{\Theta}\Big)\exp\{2\pi i k n_\pm(\varepsilon, p_z)\}\,d\varepsilon. \tag{12}$$

Making use of the formula

$$\sum_{k=1}^{\infty}\frac{\sin 2\pi kx}{\pi k} = \tfrac{1}{2} - x + [x] \equiv \psi(x) \tag{13}$$

(it is easy to establish the validity of this relation by expanding $\psi(x)$ in a Fourier series), where $[x]$ is the largest integer contained in x, we can write

$$\Omega_1 = -\frac{2eH}{ch^2}\int_{-\infty}^{\infty}dp_z\int_0^{\infty}f_0\Big(\frac{\varepsilon-\zeta}{\Theta}\Big)d\varepsilon\,\{\psi(n_+(\varepsilon, p_z)) + \psi(n_-(\varepsilon, p_z))\}. \tag{14}$$

Knowing Ω_1 it is easy to obtain the oscillating part ΔN of the number of electrons N. For this purpose, it suffices to know the value of N_1 which has the same oscillating part as N:

$$N_1(\zeta, H, \Theta) = -\frac{\partial\Omega}{\partial\zeta} = -\frac{2eH}{ch^2}\int_{-\infty}^{\infty}dp_z\int_0^{\infty}f_0'(\varepsilon)\,d\varepsilon\,\{\psi(n_+) + \psi(n_-)\}. \tag{15}$$

The fact that we have obtained the oscillation of a number of electrons should not be remarkable, since all the quantities were determined in the convenient independent variables ζ and H. Actually, $\zeta = \zeta(H)$, where the form of the function must again be found from the requirement of the constancy of the number of particles; the oscillating part of $\zeta(H)$ is again determined by the absence of oscillations in the number of particles.

Equation (15) takes on an especially simple form at absolute zero temperature, when $f_0'(\epsilon) = -\delta(\epsilon-\zeta)$ (the right-hand side is the Dirac δ function), and

$$\Delta N(\zeta, H, 0) = \frac{2eH}{ch^2}\int_{p_z^{\min}}^{p_z^{\max}}dp_z\,\{\psi(n_+(\zeta, p_z)) + \psi(n_-(\zeta, p_z))\}$$

$$(p_z^{\min} = [\min_{n_\pm} p_z(\varepsilon, n_\pm)]_{\varepsilon=\zeta}). \tag{16}$$

Comparing (14) and (16), we find

$$\Delta\Omega(\zeta, H, \Theta) = \int_0^{\infty}f_0\Big(\frac{\varepsilon-\zeta}{\Theta}\Big)\Delta N(\varepsilon, H, 0)\,d\varepsilon. \tag{17}$$

Thus the determination of $\Delta\Omega$ reduces to finding the fluctuations of the number of particles at absolute zero as a function of the chemical potential and the magnetic field. It is easy to see that, with accuracy up to terms exponentially small in ζ/Θ,

$$\Delta\Omega(\zeta, H, \Theta) = \int_0^{\zeta}\Delta N(x)\,dx + \Theta\int_0^{\infty}f_0(x)\,\{\Delta N(\zeta+\Theta x) - \Delta N(\zeta-\Theta x)\}\,dx. \tag{18}$$

3. We now calculate how the limiting transition to the ordinary formula comes about at $\epsilon = \zeta$ for p_Z far from the self-intersection. For such p_Z, we have $|k| \gg 1$, and, throwing away only terms which are exponentially small in Eqs. (5) and (6), we obtain the following expression for the integrand in (16):

a) when $k > 0$ for "necking-in" or when $k < 0$ for a "trough":

$$\psi(n_+) + \psi(n_-) = \psi\Big(\frac{S_1+S_2+\varphi}{\pi} - \frac{1}{2}\Big), \tag{19}$$

since

$$\psi(x+1) = \psi(x); \quad \psi(x+\tfrac{1}{2}) + \psi(x) = \psi(2x); \tag{20}$$

b) when $k > 0$ for "troughs" or when $k < 0$ for "necking-in":

$$\psi(n_+) + \psi(n_-) = \psi\Big(\frac{S_1+\varphi/2}{\pi} - \frac{1}{2}\Big) + \psi\Big(\frac{S_2+\varphi/2}{\pi} - \frac{1}{2}\Big), \tag{21}$$

since

$$\cos^{-1}\{\cos(S_1-S_2)\} = \frac{\pi}{2} - (-1)^{[(S_1-S_2)/\pi]}\,\psi\Big(\frac{S_1-S_2}{\pi}\Big), \tag{22}$$

$$\psi\{\alpha - \tfrac{1}{2} - \tfrac{1}{2}(-1)^{[\beta]}\psi(\beta)\} + \psi\{\alpha + \tfrac{1}{4} + \tfrac{1}{2}(-1)^{[\beta]}\psi(\beta)\} = \psi\Big(\alpha + \frac{\beta-1}{2}\Big) + \psi\Big(\alpha - \frac{\beta-1}{2}\Big). \tag{23}$$

One can establish the validity of the functional relationship (20) by making use of the definition of the function ψ and considering separately the cases $x - [x] > \frac{1}{2}$ and $x - [x] < \frac{1}{2}$. The relation (23) is obtained if we consider the even and odd $[\beta]$ separately and make use of Eq. (20).

As has already been shown,[2] the function $\varphi(k)$, which approaches zero as $1/|k|$ when $|k| \to \infty$, is retained in (19) and (21) because it gives a small correction to the usual rule of quasi-classical quantization for $|k| \gg 1$. The fact that Eqs. (19) and (21) in the quasi-classical case, for $\varphi(k) = 0$ in the variable ζ, H, give a fluctuation in the number of levels (proportional to the number of electrons), is self-evident.

We note that for $|k| \gg 1$, Eqs. (19) and (21) coincide with (16), (5), and (6) within experimental accuracy.

4. We now transform (16) to a form which is convenient for the calculation of ΔN. For brevity, we shall demonstrate all the transformations by an example of the "necking-in." We make use of the equation

$$\psi(n_+) = \frac{1}{\pi} \operatorname{Im} \sum_{l=1}^{\infty} \frac{1}{l} \exp\{2\pi i l n_+(p_z)\}. \qquad (24)$$

Let the condition $n'_+(p_z^{(k)}) = 0$ be satisfied at the points $p_z^{(k)}$. We circle these points with cuts of length $\omega \to 0$, and outside of these cuts we displace the integration contours in (16) upwards, where the derivative $n'_+ > 0$, and downward where $n'_+ < 0$ (Fig. 3). On the displaced portions, the series (24) converges and can be summed:

$$\psi(n_+) = \frac{1}{\pi} \operatorname{Im} \ln(1 - e^{2\pi i n_+}). \qquad (25)$$

Inasmuch as the integral over cuts of length 2ω [both from (24) and (25)] tend to zero as $\omega \to 0$,

FIG. 3

on the contour the cuts can be moved on the real axis ($\omega = 0$), and we can write the expression (25) under the integral everywhere. We can now again restore the contour to the real axis everywhere except for points on the axis where n_+ is equal to an integer. These points must be passed around from above if $n'_+ > 0$ at them, and below if $n'_+ < 0$.

Similar considerations are carried out for $\psi(n_-)$.

Summing $\psi(n_+)$ and $\psi(n_-)$, we obtain

$$\Delta N = \frac{2eH}{ch^2} \operatorname{Im} \int dp_z \ln(1 + 2tx + t^2); \qquad (26)$$

$$t = e^{if} = \exp\{i[S_1 + S_2 + k \ln(k^2/e^2)]\} \frac{\Gamma(1/4 - ik)}{\Gamma(1/4 + ik)} \frac{\cosh k\pi - i \sinh k\pi}{\sqrt{\cosh 2k\pi}},$$

$$x = (2 \cosh 2k\pi)^{-1/2} e^{-k\pi} \cos(S_1 - S_2),$$

$$1 + 2tx + t^2 = (1 - e^{2\pi i n_+})(1 - e^{2\pi i n_-}),$$

$$n_\pm = \exp\{if \pm i \cos^{-1} x\}. \qquad (27)$$

The integration is carried along the real axis everywhere where the expression $1 + 2tx + t^2 \neq 0$; points where this expression vanishes are surrounded from above or below in correspondence with the rule given above.

Integrating (26) by parts and discarding the monotonic part outside the integral sign, we obtain

$$\Delta N = \frac{2eH}{h^2 c} \operatorname{Im} \int p_z \, dp_z (2tx + t^2)'_{p_z} / (1 + 2tx + t^2), \qquad (28)$$

where the rule of going around the poles of the denominator remains as before.

5. Thus, as is seen from the foregoing, the behavior of the functions $n'_\pm(p_z)$ plays a vital role. We therefore investigate this function. First, we note that since only the p_z close to $p_z^0(\epsilon)$ are important, i.e., close to those p_z for which, for a given ϵ, there is self-intersection (this statement is clear physically and will be rigorously demonstrated in what follows), while for $p_z = p_z^0(\epsilon)$, by definition, $k = 0$, $v_x = v_y = 0$ and $d\epsilon_0/dp_z = \partial\epsilon_0/\partial p_z = v_z(\epsilon)$, then we have

$$\frac{2e\hbar H}{c} k(p_z) = \frac{dk}{dp_z}(p_z - p_z^0(\varepsilon)) = -(p_z - p_z^0(\varepsilon)) \sqrt{|m_x m_y|}\, v_z(\varepsilon)$$

$$(\varepsilon \approx \zeta), \qquad p_z = p_z^0(\zeta) - \frac{2\hbar\Omega(\zeta)}{v_z^0(\zeta)} k,$$

$$\Omega^{-1}(\zeta) = \frac{c}{eH} \sqrt{|m_x m_y|}\Big|_{\varepsilon=\zeta,\ p_z = p_z^0(\zeta)}. \qquad (29)$$

Here $v_z^0(\zeta) \neq 0$, since the four equalities $\epsilon = \zeta$, $v_x = v_y = v_z = 0$ are generally incompatible. It is clear that (29) is approximately true for any $|p_z - p_z^0(\epsilon)|$ which is small in comparison with the "width" in p_z of the surface $\epsilon(p) = \zeta$.

It is clear from (29) that $dn_\pm/dp_z \sim dn_\pm/dk$. From the definition of $n_\pm(k)$ according to (5), and from the form of S_1, S_2 for $k \ll k_0$, found in reference 2 [Eq. (1.10), where one must substitute the expression (29) in $S_{1,2}(\epsilon_0(p_z), p_z)$ and consider that $\epsilon_0(p_z) \approx \zeta$], it is easy to see that

$$n'_\pm(k) \sim [2 \ln k_0 + q(k)]/(2\pi), \quad q(k) \sim 1, \quad k_0 \sim \zeta/\hbar\Omega \gg 1.$$

For $k_0 \to \infty$, we have $n'_\pm(k) > 0$ for any k. Thus, in the case of interest to us, all the "dangerous" points on the p_z axis (for $k \ll k_0$) are bypassed from above.

3. CALCULATION OF THE FLUCTUATING PART OF Ω

1. We shall first compute the quantity ΔN. We divide the integration over p_z into three parts, corresponding to values of k in the interval $(-N, N)$ $(1 \ll N \ll k_0)$ and outside this interval.

For p_z corresponding to k outside the given interval, we have

$$1 + 2tx + t^2 = \begin{cases} 1 + e^{2i(S_1+S_2)}, & k \gg 1 \\ (1 + e^{2iS_1})(1 + e^{2iS_2}), & -k \gg 1 \end{cases}, \qquad (30)$$

and calculation can easily be carried out. In this region, naturally, terms appear which correspond

to $k = \pm N$ which are obviously contracted with similar terms obtained in integration in the interval corresponding to $-N \leq k \leq N$, and terms obtained by Lifshitz and Kosevich,[1] corresponding to the extremal values of the area at large distances from the cross section with self-intersection, where either $S_1'(p_z)$ or $S_2'(p_z)$ goes to zero for $k < 0$ or $(S_1 + S_2)'_{p_z}$ vanishes for $k > 0$.

One can show that, for example, for $v_z > 0$, the quantity $(S_1 + S_2)'_{p_z}$ vanishes in any case. In fact, for self-intersection, we have $p_z = p_z^0(\zeta)$ and $(S_1 + S_2)'_{p_z} = -\infty$. Consequently, with decrease of p_z, the positive quantity $S_1 + S_2$ close to this point increases and, since the quantity $S_1 + S_2$ must be equal to zero for $p_z = p_z^{\min}$, then $(S_1 + S_2)'_{p_z}$ must be equal to zero for some p_z. This extremum of $S_1 + S_2$ must correspond to $k \sim 1$ only close to the chosen directions of the magnetic field. However, in this case also, the terms obtained by Lifshitz and Kosevich are absent only for the given surface, while for other surfaces (on which $\epsilon(p) = \zeta$ is decomposed) they can be present.

We shall now make clear what yields the region corresponding to $-N \leq k \leq N$. In this region one can, by using Eqs. (26) and (29) and the fact that

$$S_{1,2} = S_{1,2}^0 + k \ln (k_0^{(1,2)} / e\,|k|), \qquad S_{1,2}^0 = S_{1,2}(\zeta, p_z^0(\zeta)),$$
$$k_0^{(1)} \sim k_0^{(2)} \gg 1, \qquad k_0^{(1,2)} \sim 1/H, \tag{31}$$

write ΔN in the form

$$\Delta N = \frac{2eH\Omega(\zeta)}{\pi\hbar c v_z^0(\zeta)} \operatorname{Im} \int_{-N+i0}^{N+i0} \ln(1 + 2tx + t^2)\, dk;$$

$$t = \exp\{i(S_1^0 + S_2^0) + ik \ln k_0^{(1)} k_0^{(2)}\}$$
$$\times \frac{\Gamma(1/4 - ik)}{\Gamma(1/4 + ik)} \frac{\cosh k\pi - i \sinh k\pi}{\sqrt{\cosh 2k\pi}},$$

$$x = e^{-k\pi}(2 \cosh 2k\pi)^{-1/2} \cos(S_1^0 - S_2^0 + k \ln k_0^{(1)} / k_0^{(2)}). \tag{32}$$

In the calculation of the above integral we consider the contour shown in Fig. 4, where $1 \ll N' \ll k_0$. The integral over the upper horizontal is exponentially small (in N'), the integrals along the verticals, which are the continuation of the contour on the horizontal axis, are not of interest to us. Therefore, the integral from $-N$ to N is essentially equal to the integral along the contour

$(-N, N;\ N, N + iN';\ N + iN',\ -N + iN';$
$-N + iN',\ -N).$

Inside this contour the quantity $1 + 2tx + t^2$ has, for $k_0 \gg 1$, pairs of poles located close to one another at the points $(1 + n/2)\,i/4$ $(n = 0, 1, \ldots)$ and roots near these points. The integral along

FIG. 4

the contour therefore reduces to the sum of integrals over contours surrounding each pair. Each of these integrals is equal to $2\pi i \Delta k$, where $\Delta k = k_p - k$ is the complex distance between the neighboring poles and the origin. Inasmuch as only the pair closest to the horizontal axis is important,

$$\Delta N = \frac{2\sqrt{\pi}eH\Omega(\zeta)}{hcv_z^0(\zeta)} (k_0^{(1)} k_0^{(2)})^{-1/4} \left\{ (k_0^{(2)} / k_0^{(1)})^{3/4} \sin\left(2S_1^0 - \frac{\pi}{4}\right) \right.$$
$$\left. + (k_0^{(1)} / k_0^{(2)})^{1/4} \sin\left(2S_2^0 - \frac{\pi}{4}\right) \right\} = \sum_{\alpha=1}^{2} A_\alpha \sin\left(2S_\alpha^0 - \frac{\pi}{4}\right); \tag{33}$$

it must be that

$$\Delta N \sim H / k_0^{1/2} \sim H^{3/2}.$$

Thus the amplitude of the fluctuations resulting from the self-intersecting cross sections is shown to be $(\epsilon_0/\mu H)$ times smaller than the amplitude of the oscillations from the extremal cross section; the oscillations have a simple periodic character with frequencies $2S_1^0$ and $2S_2^0$ [$S(k) \neq S(p_z)$!, see the definition (7) of the function $S(k)$].

In all the discussions given above it was not explicitly assumed that $\Omega \neq \infty$, that is, that neither m_x nor m_y is equal to zero. For the chosen directions of H (which form a single-parameter family) it is possible that $m_x = 0$ or that $m_y = 0$. Naturally this changes somewhat the structure of the levels and leads to an increase in the amplitude of oscillations [approximately by a factor of $(\epsilon_0/\mu H)^{1/4}$]. For isolated directions, where $m_x = m_y = 0$, the amplitude of the oscillations on cross sections with self-intersection can be shown to be of the same order as at the extremal.

Thus the picture of the quantum oscillations changes materially in the approach to certain chosen directions. We also note that in the case of a strong anisotropy, one of the values of $k_0^{(1,2)}$ can be shown to be of the order of unity. In this case, there arise complicated irregular oscillations.

2. Inasmuch as $S[\epsilon, p_z^0(\epsilon)]$ is a function of ϵ which does not have a logarithmic singularity, the calculation of $\Delta\Omega$ and its temperature dependence is carried out, starting from Eqs. (18), (33), with accuracy the same as given by Lifshitz and Kosevich,[1] and yields

$$\Delta\Omega(\zeta, H, \Theta) = \sum_{\alpha=1}^{2} \frac{2\pi e\hbar H}{\widetilde{m}_\alpha c} \frac{2\pi^2 c\Theta\widetilde{m}_\alpha / e\hbar H}{\sinh(2\pi^2 c\Theta\widetilde{m}_\alpha / e\hbar H)} A_\alpha \sin\left(2S_\alpha^0 - \frac{\pi}{4}\right), \tag{34}$$

$$\tilde{m}_\alpha = \frac{1}{2\pi}\frac{dS(\varepsilon, p_z^0(\varepsilon))}{d\varepsilon}. \quad (35)$$

From these formulas, it is easy to find all the thermodynamic quantities. Strictly speaking, one would have to compute the dependence of $\zeta(H)$, but it is easy to see that, as in reference 1, the consideration of this dependence does not change the form of the equations, in which one can write $\zeta(0)$ as before.

I am indebted to I. M. Lifshitz for valuable discussions.

[1] I. M. Lifshitz and A. M. Kosevich, JETP **29**, 730 (1959), Soviet Phys. JETP **2**, 636 (1956).

[2] M. Ya. Azbel', JETP (in press).

[3] M. Ya. Azbel', JETP **34**, 969, 1158 (1958), Soviet Phys. JETP **7**, 669, 801 (1958), Phys. Chem. Solids **7**, 105 (1958).

[4] L. D. Landau, Z. Physik **64**, 629 (1930).

Translated by R. T. Beyer
157

Letters to the Editor

EFFECT OF COLLISIONS OF RECOIL NUCLEI ON THE CROSS SECTION FOR RESONANCE SCATTERING OF GAMMA RAYS BY Ni^{60} NUCLEI

D. K. KAIPOV and Yu. K. SHUBNYĬ

Institute for Nuclear Physics, Academy of Sciences, Kazakh S.S.R.

Submitted to JETP editor April 17, 1960

J. Exptl. Theoret. Phys. (U.S.S.R.) **39**, 888-889 (September, 1960)

THE cross section for resonance scattering of γ rays by nuclei is very sensitive to the density of the source medium and to the lifetime of the level. To reduce the effect of collisions of recoil nuclei with surrounding molecules one usually uses sources in the gaseous state.[1,2] If the lifetime τ_γ of the level is less than $10^{-12} - 10^{-13}$ sec, investigation of the resonance effect with a liquid source can give some information concerning the nature of the interaction of the recoil nuclei with the surrounding atoms, and, in particular, concerning the mean free path of the recoil atom in the medium.

We have investigated the resonance scattering of γ rays with an energy of 1330 kev by Ni^{60} nuclei, using gaseous and liquid sources of Co^{60} in the compound $CoCl_2$. Earlier,[3] for a gaseous source, a value of $(17.1 \pm 3) \cdot 10^{-27}$ cm^2 was obtained for the average cross section for the resonance scattering.

A strong effect was also observed in using a liquid source (solution of $CoCl_2$ in HCl) with an activity ~ 40 mC. This enabled us to determine τ_γ by self-absorption to be $(1.14 \pm 0.37) \times 10^{-12}$ sec, which is in good agreement with the data of other authors.[4,5] The cross section for resonance scattering for the liquid source was found to be $(1.73 \pm 0.2) \times 10^{-27}$ cm^2.

The lifetime of the level τ_γ and the average cross section for resonance scattering $\bar{\sigma}$ are connected by the well-known relation

$$\bar{\sigma} = \frac{1}{2\tau_\gamma} \sigma_0 \pi h P(E_p). \qquad (1)$$

Here σ_0 is the cross section at resonance and $P(E_p)$ is the energy distribution of the γ quanta.

The slowing down of the recoil nuclei can be taken into account by introducing in (1) a factor $1 - \exp(-l/v\tau_\gamma)$, where v is the velocity of the recoil nucleus and l the mean free path of the recoil nucleus before collision. For a gaseous source $t_{coll} \gg \tau_\gamma$, and the factor is equal to 1. Using (1), we write the ratio of the cross section $\bar{\sigma}_1$ for the gaseous source to the cross section $\bar{\sigma}_2$ for the liquid source:

$$\bar{\sigma}_1 / \bar{\sigma}_2 = [1 - \exp(-l/v\tau_\gamma)]^{-1}. \qquad (2)$$

The value of τ_γ has been determined by various authors with sufficient accuracy to be $(1.1 \pm 0.1) \times 10^{-12}$ sec. Using for v the value 7.2×10^5 cm/sec, which is the velocity of the recoil nucleus for exact resonance, and noting that $\bar{\sigma}_1/\bar{\sigma}_2 = 9.9$, we obtain for l the value 8×10^{-8} cm. It should be mentioned that the width of the resonance line is very small (~ 1 ev), and the change in l because of the spread in recoil velocity is extremely small.

The value of l is determined both by the distance between molecules in the source and by the nature of the interaction of the recoil nucleus with the surrounding molecules. To get a picture of the effect of interaction, it is necessary to carry out similar experiments for different isotopes of Co. It should be mentioned that the contradiction in the determination of the lifetime of the 1.60-Mev level of Ce^{140} in references 6 and 7 is due to the neglect in reference 6 of the effect of collisions on the resonance scattering cross section.

The authors thank O. Suyarov for help in the measurements.

[1] N. N. Delyagin, JETP **37**, 1177 (1959), Soviet Phys. JETP **10**, 837 (1960).

[2] F. Metzger, Phys. Rev. **101**, 286 (1956).

[3] Akkerman, Kaipov, and Shubnyĭ, Vestn. Akad. Nauk, Kaz. S.S.R. (in press).

[4] F. Metzger, Phys. Rev. **103**, 983 (1956).

[5] Burgov, Terekhov, and Bizina, JETP **36**, 1612 (1959), Soviet Phys. JETP **9**, 1146 (1959).

[6] B. S. Dzhelepov and M. A. Dolgoborodova, Izv. Akad. Nauk, S.S.S.R., Ser. Fiz. **24**, 304 (1960), Columbia Tech. Transl., in press.

[7] S. Ofer and A. Schwarzschild, Phys. Rev. **116**, 725 (1959).

Translated by M. Hamermesh
158

COEFFICIENT OF SPIN CORRELATION IN pp SCATTERING AT 310 Mev AND 90° IN THE C.M.S.

I. M. VASILEVSKIĬ, V. V. VISHNYAKOV, E. ILESCU, and A. A. TYAPKIN

Joint Institute for Nuclear Research

Submitted to JETP editor June 27, 1960

J. Exptl. Theoret. Phys. (U.S.S.R.) **39**, 889-891 (September, 1960)

A phase shift analysis has been made of the data obtained in Berkeley from the complete set of experiments on elastic interaction of 310-Mev protons, which did not include investigations of the spin correlation of the scattered protons. We know that this analysis[1] has led to an ambiguous result. It was possible to separate from the possible solutions, five independent phase-shift sets, satisfactorily describing the experimental data. The solutions obtained led to different values of the coefficient $C_{nn}(90°)$, which determines the correlation between the spin components normal to the scattering plane. Thus, for the phase-shift sets numbered 1, 2, 3, 4, and 6, the values of $C_{nn}(90°)$ obtained were 0.158, 0.711, 0.300, 0.490, and 0.425, respectively.[2] In this connection, an experimental investigation of the spin correlation of the scattered protons at 310 Mev has become very important. However, the ambiguity of the analysis was subsequently greatly reduced through further extension and improvement of the nucleon-nucleon scattering phase-shift analysis itself.[3] The first analysis included 14 phase shifts, belonging to states up to H waves inclusive. In the new analysis[3] additional account was taken of states with higher orbital momenta, on the basis of the one-meson approximation developed by Chew[4] and by Okun' and Pomeranchuk.[5] This additional contribution was calculated in first approximation by perturbation theory, and added to the analysis merely one additional parameter, the pion-nucleon coupling constant g^2. The modified analysis made it possible to establish that only the first and second sets of phase shifts describe satisfactorily the experimental data for $g^2 \sim 14$. The value of the coefficient $C_{nn}(90°)$ becomes, in accordance with the new values of the phase-shift of the separated sets, equal to 0.38 for the first set and 0.61 for the second set.

The first experiments on the determination of $C_{nn}(90°)$, carried out in Liverpool at proton energies of 320 Mev and in Dubna at 315 Mev, favor the second phase-shift set.[6] Thus, the Liverpool group found the coefficient of spin correlation to be $C_{nn}(90°) = 0.75 \pm 0.11$. Our own measurements, in which the preliminary data of the calibration experiment on the determination of the polarizing ability of graphite analyzers were used, have yielded $C_{nn}(90°) = 0.7 \pm 0.3$.

We have now completed an experiment on the determination of the analyzing ability of the scatterers. The calibration experiment was carried out with a proton beam of energy approximately 160 Mev, the polarization of which was found to be 0.667 ± 0.027. The polarizing ability of the analyzers used in the measurements of the correlation asymmetry was found to be 0.28 ± 0.02. Considering that the coefficient C_{nn} cannot exceed unity, we obtained

$$C_{nn}(90°) = 0.84^{+0.10}_{-0.22}$$

We have thus obtained experimentally for the coefficient C_{nn} a large value, which is difficult to reconcile with the value predicted on the basis of the first phase-shift set.

From earlier experimental data for elastic pp scattering at 310 Mev, estimates have been made of the contribution of the singlet interaction b^2 and the contributions of the triplet interaction of the spin-orbit (c^2) and the tensor (h^2) types. Thus, Wolfenstein[7] found $15\% < b^2 < 60\%$, $35\% < c^2 < 70\%$, and $2\% < h^2 < 20\%$. According to Nurushev's[8] estimates, $b^2 \approx 25\%$, $c^2 \approx 62\%$, and $h^2 \approx 13\%$.

From the relations

$$b^2 = \frac{1}{2}(1 - C_{nn}),\ c^2 = \frac{1}{4}(1 + C_{nn} + 2D),$$

$$h^2 = \frac{1}{4}(1 + C_{nn} - 2D)$$

and from the value obtained for $C_{nn}(90°)$ and $D(90°) = 0.42$ (obtained by extrapolating the data of Chamberlain et al.[2]), the corresponding contributions are found to be $b^2 \approx 8\%$, $c^2 \approx 67\%$, and $h^2 \approx 25\%$.

The situation with respect to the separation of the phase shift sets that describe the elastic pp scattering at 310 Mev has been recently changed somewhat by a modified phase-shift analysis of the earlier experimental data.[9] The change in the analysis consisted of reducing the number of phase-shifts taken into account and extending the single-meson approximation to states with correspondingly lower orbital momenta. The analysis performed, which included 5, 7, and 9 phase shifts, has shown that if nine phase shifts are taken into account instead of the previous 14, and if the pion-

nucleon coupling constant g^2 is also taken into account, a fully satisfactory description of the same experimental data is obtained in the case of the second phase-shift set and even more so in the case of the first. At the same time, the coefficient $C_{nn}(90°)$, calculated from the new phase shifts, was found to be approximately 0.41 for either set. In this connection, MacGregor et al.[9] believe that to solve the problem of the two phase-shift sets it is necessary to measure the value of C_{kp} at 45°, which determines the correlation between the spin components in the plane of the main scattering.

However, the new analysis with the nine phase shifts and with the constant g^2 has led not only to the disappearance of the difference between the coefficients $C_{nn}(90°)$ corresponding to the first and second sets, but also to a value that contradicts the available experimental data. In our opinion, this discrepancy should be considered as an indication that nine phase shifts are not enough. If the analysis were to include the experimental values of $C_{nn}(90°)$ in the procedure with the nine phase shifts, then an excessive value would be obtained for the parameter χ^2 for both sets, similar to what takes place in the analysis of the experimental data in which the quantity C_{nn} is not included and only seven phase-shifts are taken into account.

While analyses with seven and nine phase shifts give preference to the first set of phase shifts over the second,[9] the inclusion of the larger experimentally-obtained value of the coefficient $C_{nn}(90°)$, with account of 14 phase shifts and the constant g^2, makes the two phase-shift sets equally probable, as indicated by Allaby et al.[10] For an unambiguous determination of the phase shift it is obviously necessary to carry out more exact measurements of several of the quantities included in the analysis.

[1] Stapp, Ypsilantis, Metropolis, Phys. Rev. **105**, 302 (1957).

[2] Chamberlain, Segre, Tripp, Wiegand, Ypsilantis, Phys. Rev. **105**, 288 (1957).

[3] Cziffra, MacGregor, Moravcsik, Stapp, Phys. Rev. **114**, 880 (1959).

[4] G. F. Chew, Phys. Rev. **112**, 1380 (1958).

[5] L. B. Okun' and I. Ya. Pomeranchuk, JETP **36**, 1717 (1959), Soviet Phys. JETP **9**, 1223 (1959).

[6] Ya. A. Smorodinskiĭ, Proc. International Conf. on High-Energy Physics, Kiev, 1960.

[7] L. Wolfenstein, Bull. Am. Phys. Soc. **1**, 36 (1956).

[8] S. B. Nurushev, JETP **37**, 301 (1959), Soviet Phys. JETP **10**, 212 (1960).

[9] MacGregor, Moravcsik, Stapp, Phys. Rev. **116**, 1248 (1959).

[10] Allaby, Ashmore, Diddens, Eades, Proc. Phys. Soc. **74**, 482 (1959).

Translated by J. G. Adashko
159

ON THE USE OF THE MÖSSBAUER EFFECT FOR STUDYING LOCALIZED OSCILLATIONS OF ATOMS IN SOLIDS

S. V. MALEEV

Leningrad Physico-Technical Institute, Academy of Sciences, U.S.S.R.

Submitted to JETP editor June 29, 1960

J. Exptl. Theoret. Phys. (U.S.S.R.) **39**, 891-892 (September, 1960)

THE Mössbauer effect consists in the emission (or resonant absorption) by a nucleus in a solid of a γ quantum with an energy which is precisely equal to the energy of the transition, because of the fact that the recoil momentum is transferred to the crystal as a whole.

Usually the nucleus which radiates the γ quantum is formed by the decay of some other nucleus. As a result of this process, the nucleus can with a very high probability leave its place in the lattice and get stuck somewhere at an interstitial position. But, even if the nucleus does not move about, if it should change its atomic number as a result of the decay the forces holding it in the lattice will change. Thus the nucleus emitting the Mössbauer quantum must be a lattice defect.

On the other hand it is well known (cf. reference 1) that the spectrum of oscillations of a defect atom in a lattice consists of a continuous spectrum, coinciding with the spectrum of oscillations of the ideal lattice, and of discrete frequencies which do not coincide with any of the frequencies of normal vibrations of the atoms of the ideal lattice. Vibrations with such frequencies (localized oscillations) cannot propagate through the lattice over any sizeable distance.

At the same time there is a finite probability that in the emission of a γ quantum there is simultaneously emitted or absorbed (the latter, naturally, only for sufficiently high temperatures, $T \gtrsim \hbar\omega_L$, where ω_L is the frequency of the local-

ized oscillation) a quantum of the localized oscillation. Thus, the spectrum of emitted γ quanta will consist of an unshifted line corresponding to the energy of the transition and of a continuous background corresponding to the emission and absorption simultaneously with the γ quantum of phonons from the continuous part of the spectrum of oscillations of the atom; on this background, there will be individual discrete peaks due to the emission and absorption of quanta of the localized oscillations.

These peaks can be observed in almost the same way as the unshifted line is observed. Namely, an absorber containing atoms in the ground state should be moved with such a velocity that the Doppler shift of its undisplaced absorption line will be equal to the frequency of the localized oscillation. One then will observe a stronger absorption than for neighboring frequencies. The velocity needed for this is obviously determined by the condition $\omega_L = v\omega/c$, where ω is the frequency of the γ line. If the energy of the transition is of the order of tens of kev, and $\hbar\omega_L \sim 0.01$ ev, $v \sim 10^3 - 10^4$ cm/sec. Such a velocity is not difficult to obtain by placing the absorber on the rim of a rotating disk.

[1] Maradudin, Mazur, Montroll, and Weiss, Revs. Modern Phys. **30**, 175 (1958).

Translated by M. Hamermesh
160

THE REALIZATION OF A MEDIUM WITH NEGATIVE ABSORPTION COEFFICIENT

V. K. ABLEKOV, M. S. PESIN, and I. L. FABELINSKIĬ

P. N. Lebedev Physics Institute, Academy of Sciences, U.S.S.R.

Submitted to JETP editor, June 30, 1960

J. Exptl. Theoret. Phys. (U.S.S.R.) **39**, 892-893 (September, 1960)

THE phenomenon of induced emission was predicted by Einstein.[1] The conditions for direct observation of this phenomenon were formulated by Fabrikant[2] and realized experimentally by Basov and Prokhorov,[3] Gordon, Zeiger, and Townes[4] in the microwave region of the spectrum, and by Butaev and Fabrikant[5] in the optical region of the spectrum.

In recent years there have appeared papers in which various means are proposed for realizing media with a negative absorption coefficient in the optical frequency range, but as yet there have been no reports of positive experimental realizations of these proposals.[6]

In the present work, it seems to us we have realized a medium which has a negative absorption coefficient in the visible region of the spectrum. For such a medium we use a gas discharge in a mixture of vapors of mercury and zinc.[7]

The negative absorption was studied at a temperature of the liquid electrodes of the gas discharge tube of 6 and 15° C, and the discharge current was varied from 8 to 15 amp. As a result of the measurements it was found that the transparency of the mercury-zinc discharge for the zinc line at 6362 A ($4^1P_1^0 - 4^1D_2$) is greater than unity and, under various conditions, changes from 1.5 to 10. Under these same conditions the transparency of the discharge for the 4722 A zinc line was less than unity and equal to ~ 0.9. The absolute value of the absorption coefficient k under the conditions of our experiments varied from 0.2 to 1.15. This makes it possible to estimate the concentration of excited atoms N_i in the 4^1D_2 level. In fact[2]

$$N_i = 8\pi |k| \Delta\nu/\lambda^2 A_{ik},$$

where $\Delta\nu$ is the half-width of the line, $\lambda = 6362$ A, A is the probability of spontaneous transition. For the 4^1D_2 level, $A_{ik} = 4 \times 10^7$ cm^{-1}.[8]

Setting $\Delta\nu = 10^{-2}$ cm^{-1} (the Doppler half-width), we obtain $N_i = 9 \times 10^9$ for $k = 0.2$, and $N_i = 5 \times 10^{10}$ for $k = 1.15$.

The estimate of N_i for the 4^1D_2 level made by us from measurements of the absolute intensity of the 6362-A line agree in order of magnitude with the computed values of N_i given above.

Let us state the physical reasons which in this case lead to such a break-down of the Boltzmann distribution of the atoms over the energy levels, so that one realizes a medium with a negative absorption in the optical frequency range.

According to Butaeva and Fabrikant,[5] $N_i/N_k = \alpha_i\tau_i/\alpha_k\tau_k$, where α_i and α_k are the numbers of acts of excitation per second to the levels E_i and E_k, while τ_i and τ_k are the lifetimes of atoms in these levels. In our case, the index i refers to the 4^1D_2 level, and k to the $4^1P_1^0$ level; then, if we disregard reabsorption of the 2138-A line, the ratio $\tau_i/\tau_k = 2.5 \times 10^{-8}/1.7 \times 10^{-9} \sim 15$.

Reabsorption of the 2138-A line can considerably reduce this ratio, but a rough estimate shows that this ratio remains ~ 1.

The ratio of the numbers of excitations, α_i/α_k, if we assume that the excitation occurs only because of electronic collisions, should be less than unity, but under the conditions we are considering there is a mechanism for selective excitation of the 4^1D_2 level which consists of the following: An atom of mercury has a 7^3S_1 level whose energy of excitation is only 133 cm^{-1} lower than the energy of the excited 4^1D_2 level of the zinc atom; i.e., the difference between the energies is of the order of the average energy of thermal motion of the atoms at room temperature. Therefore, we have very effective resonance collisions of the second kind between excited mercury atoms (7^3S_1) and unexcited zinc atoms, as a result of which there will occur an excitation of zinc atoms to the 4^1D_2 level. The number of mercury atoms in the discharge is very much greater than the number of zinc atoms, which guarantees a transfer of energy through collisions of the second kind.

It seems to us that this mechanism of excitation of approaching atoms by resonance collisions of the second kind in a gas discharge mixture can be extremely effective for producing a medium with a negative absorption coefficient. It seems that one can find a considerable number of examples of mixtures of atoms with nearby energy levels and with an asymmetry in the transfer of excitation by inelastic collisions of the second kind.

As an example, we may point to the mixture of cadmium and zinc atoms in which, in the diagram of energy terms, the interaction of the 5^3S_1 HgI and the 6^1S_0 CdI terms should produce a medium with a negative absorption coefficient for the infrared transition with $\lambda = 10394.7$ A and for the visible transition with $\lambda = 4413.06$ A.

The authors express their sincere gratitude to V. A. Fabrikant for valuable advice and useful discussion of the work.

[1] A. Einstein, Verh. Deutsch. Phys. Ges. **8**, 318 (1916).

[2] V. A. Fabrikant, Тр. ВЭИ (Trans. All-Union Electr. Inst.) No. 41, 236 (1940).

[3] N. G. Basov and A. M. Prokhorov, Doklady Akad. Nauk S.S.R. **101**, 47 (1955).

[4] Gordon, Zeiger, and Townes, Phys. Rev. **95**, 282 (1954).

[5] R. A. Butaeva and V. A. Fabrikant, Исследование по экспериментальной и теоретической физике (памяти Г. С. Ландсберга) [Investigations in Experimental and Theoretical Physics (in memoriam G. S. Landsberg)], U.S.S.R. Acad. Sci. Press, 1959, pages 62-70.

[6] A. L. Schawlow and C. H. Townes, Phys. Rev. **112**, 1940 (1958). A. Javan, Phys. Rev. Letters **3**, 87 (1959). J. Weber, Revs. Modern Phys. **31**, 681 (1959). Condell, Van Gunten, and Bennett, JOSA **50**, 184 (1960). S. G. Rautian and I. I. Sobel'man, JETP **39**, 217 (1960), Soviet Phys. JETP **12**, 000 (1961).

[7] Ablekov, Zaĭtsev, and Pesin, Приборы и техника эксперимента (Instrum. and Exp. Techniques) 1960 (in press).

[8] C. Allen, Astrophysical Quantities, London, Athlone Press, 1955.

Translated by M. Hamermesh
161

NUCLEAR ZEEMAN EFFECT IN Sn^{119}

N. N. DELYAGIN, V. S. SHPINEL', V. A. BRYUKHANOV, and B. ZVENGLINSKIĬ

Moscow State University

Submitted to JETP editor July 4, 1960

J. Exptl. Theoret. Phys. (U.S.S.R.) **39**, 894-896 (September, 1960)

THE resonance absorption of 23.8-kev γ quanta by Sn^{119} nuclei, resulting from the emission and absorption of γ quanta without energy loss to recoil (Mössbauer effect[1]), has been observed earlier by Alikhanov and Lyubimov[2] and by Barloutaud et al.[3] Alikhanov and Lyubimov studied, in particular, the influence of an external magnetic field on the magnitude of the resonance absorption effect. In our previous work[4] we measured the dependence of the resonant absorption of 23.8-kev γ quanta emitted in the decay of Sn^{119m} on the velocity of the source with respect to the absorber; we detected a hyperfine structure of the γ rays due to the splitting of the excited state of the Sn^{119} nucleus in the electric field of the white tin crystal.

In the present work we have investigated the dependence of the resonance absorption of 23.8-kev γ quanta by Sn^{119} nuclei on the source velocity under conditions where the absorber is in an external constant magnetic field. In this case, there is a Zeeman splitting of the absorption line, and one observes in the absorption spectrum a

hyperfine structure which enables one to determine the magnetic moment of the 23.8-kev excited state of Sn^{119}. The source of γ quanta was a foil of white metallic tin (94% Sn^{118} isotope), irradiated with thermal neutrons in a reactor.

It is not advisable to use metallic tin as the absorber in this case: If we have electric quadrupole and magnetic interactions of comparable magnitude, the hyperfine structure of the level will depend on the relative orientation of the magnetic field and the axis of the electric field gradient. Therefore, a unique interpretation of the results of the measurements (for a polycrystalline absorber) will become difficult.

In our experiment we used $SnNb_3$ alloy as absorber. As we have shown earlier,[4] there is no quadrupole splitting of the 23.8-kev level in a $SnNb_3$ crystal, and therefore, in a constant magnetic field, the hyperfine structure of the absorption line has the simple Zeeman form. The measurements were made with the source and absorber cooled to liquid nitrogen temperature. The experimental apparatus enabling us simultaneously to measure the whole absorption spectrum over a given interval of source velocity was described briefly earlier.[4] The absorber (20 mg/cm^2 of $SnNb_3$) was placed between the poles of a magnet which produced over the region of the absorber a constant homogeneous magnetic field of 12,150 oe. The measurements were made alternately with magnetic field and without field.

In the magnetic field the ground state of the Sn^{119} nucleus (spin $\frac{1}{2}$) splits into two sub-levels, and the excited state (spin $\frac{3}{2}$) into four sub-levels. Between the sub-levels of the excited and ground states six different M1 transitions are possible; as we change the velocity of the source, there occur successive overlappings of the six absorption lines with the two lines of the radiation (the hyperfine structure caused by the quadrupole interaction in the white tin crystal). Thus in the measured absorption spectrum one should observe twelve lines (over the whole range of positive and negative source velocities).

The form of the absorption spectrum will depend on the absolute values of the magnetic moments of the ground (μ_0) and excited (μ) states of the Sn^{119} nucleus, on the relative sign of these moments, and on the size of the quadrupole splitting Δ of the excited state in the tin crystal. The magnetic moment of the ground state of Sn^{119} is known to be -1.05 nuclear magnetons.[5]

The results of the measurements are shown in the figure (the ordinates give the counting rate in arbitrary units, and the abscissa the source velocity in mm/sec, or the corresponding energy shift in ev). Since the counting rate for negative values of the velocity did not differ within the limits of experimental error from the counting rate for positive velocities, we show on the figure only the half of the absorption spectrum for positive velocities. In the upper half of the figure is shown the absorption spectrum in the absence of the magnetic field, analogous to that obtained by us previously.[4] From this spectrum we again determined the separation Δ between the components of the hyperfine structure in the tin crystal; we obtained the value $(1.2 \pm 0.2) \times 10^{-7}$ ev, which is in good agreement with the value obtained previously.[4]

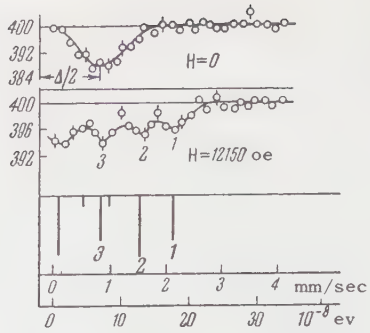

The absorption spectrum obtained when a magnetic field of 12,150 oe is applied to the absorber is shown in the middle part of the figure. Since the size of the magnetic splitting is comparable with the natural line width, not all of the lines in the spectrum are resolved, but this does not prevent a unique interpretation of the result. The position of the farthest absorption maximum (shown in the figure by the number 1) corresponds to an energy shift equal to $\mu H + \mu_0 H + \Delta/2$, if the signs of the magnetic moments of ground and excited state are opposite, and $\mu H - \mu_0 H + \Delta/2$ if these signs are the same (in the formulas, μ and μ_0 are the absolute values of the magnetic moments).

The overall appearance of the absorption spectrum enables us to make a choice between these two possibilities, since the experimental data agree with the theoretical computations of the absorption spectrum only for the case of opposite signs of μ and μ_0 (positive sign of μ). The computed absorption spectrum is shown in the lower part of the figure (disregarding the natural line width; the heights of the lines are proportional to their intensities). Thus, to determine the value of μ it is sufficient in principle to determine the position of just the single extreme absorption maximum.

Knowing the position of the three maxima

(1, 2, and 3 in the figure), we can independently determine, in addition to the value of μ, the values of the quantities Δ and μ_0, which is an additional check of the validity of the interpretation of the measured absorption spectrum. Thus, for the value of Δ we obtained $(1.9 \pm 0.2) \times 10^{-7}$ ev, which is in good agreement with the value obtained from the absorption spectrum in the absence of a magnetic field, and the value of μ_0 was found to be $-(1.1 \pm 0.3)$ nuclear magnetons in agreement with the available data. For the magnetic moment of the 23.8-kev excited state of Sn^{119} we found a value $\mu = +(1.9 \pm 0.4)$ nuclear magnetons. This value considerably exceeds the value predicted by the single-particle model (Schmidt lines), which shows that the 23.8-kev level in Sn^{119} in not a pure single-particle level. Such a conclusion is confirmed by the fact that the M1 transition with energy 23.8-kev is l-forbidden.

[1] R. L. Mössbauer, Z. Physik **151**, 124 (1959).

[2] A. I. Alikhanov and V. A. Lyubimov, Izv. Akad. Nauk S.S.S.R., Ser. Fiz. **24**, No. 9 (1960), Columbia Tech. Transl., in press.

[3] Barloutaud, Cotton, Picou, and Quidort, Compt. rend. **250**, 319 (1960). Barloutaud, Picou, and Tzara, Compt. rend. **250**, 2705 (1960).

[4] Delyagin, Shpinel', Bryukhanov, and Zvenglinskiĭ, JETP **39**, 220 (1960), Soviet Phys. JETP **12**, 159 (1961).

[5] N. F. Ramsey, in Experimental Nuclear Physics, ed. E. Segrè, John Wiley, 1953.

Translated by M. Hamermesh
162

THE DETERMINATION OF THE COEFFICIENTS OF DIFFUSION AND OF HEAT CONDUCTIVITY OF WEAK SOLUTION OF He^3 *IN HELIUM II*

T. P. PTUKHA

Institute for Physics Problems, Academy of Sciences, U.S.S.R.

Submitted to JETP editor July 13, 1960

J. Exptl. Theoret. Phys. (U.S.S.R.) **39**, 896-898 (September, 1960)

IF one wall of a reservoir containing a weak mixture of the isotopes He^3-He^4 is kept cold while heat is given out at the other, He^3 will be carried along by the thermal excitations and accumulate at the cold end. Diffusion and heat conductivity will cause a concentration gradient and a temperature gradient ∇T. By measuring the temperature gradient in the direction of the heat current in the steady state, and knowing the magnitude of this heat current, we can find the effective heat conductivity, κ_{eff}, which characterizes the processes of diffusion, thermal diffusion, and heat conductivity in the mixture.

To measure ∇T, four 35-μ phosphor-bronze wire resistance thermometers were used. The thermometers were made in such a way that their coils lay in one plane. The heat current was produced by a constantan heater with bifilar winding in the form of a flat disk. The lowest temperatures were obtained by pumping off He^3 vapor. The temperature of the He^3 bath was controlled by a temperature regulator[1] and kept constant to 10^{-4} °K.

Figure 1 shows the dependence of κ_{eff} on T. The circles and crosses correspond to results obtained with two different devices. The theoretical curves (dashed) calculated by Khalatnikov and Zharkov[2] are shown for comparison.

They determined the unknown constant for the interaction of an impurity with a roton, which is necessary for this calculation, from the experimental value of the diffusion coefficient found by Beenakker et al.[3] at T = 1.5°K. The existence of a minimum in the $\kappa_{eff}(T)$ curve indicates the existence of two heat transfer mechanisms in weak He^3-He^4 mixtures: heat transport due to the motion of thermal excitations, limited by the presence of He^3 (He^3 acts as a resistance to the propagation of heat), and heat transport by thermal conductivity (the diffusion of thermal excitations).

Values of the diffusion coefficient D in the temperature range from the λ point to T = 1.5°K were derived from the values of κ_{eff} for a concentration C = 0.1%. The results are shown in Fig. 2. The theoretical curve obtained from the equation[2]

$$D = \frac{kTt_{ip}}{m_3}\left(\frac{\rho_{n_0}}{\rho_n}\right)^2, \qquad (1)$$

is shown for comparison. Here k is Boltzmann's constant, ρ_{n_0} is the part of the normal density (ρ_n) of the mixture associated with the thermal excitations, and t_{ip} is the time characterizing the scattering of an impurity on a roton.

To determine t_{ip}, we normalized κ_{eff} to the experimental value at T = 1.6°K. The experimental values of the diffusion coefficient, taken from

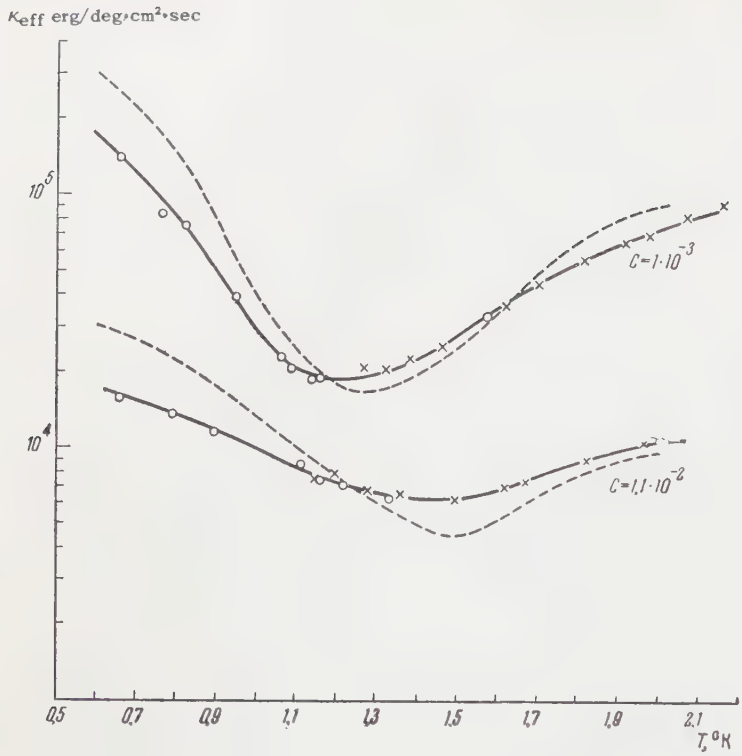

FIG. 1. Temperature dependence of the effective heat conductivity of mixtures with He^3 concentrations C = 0.1 and 1.1%. ($C = N_3m_3 \times (N_3m_3 + N_4m_4)^{-1}$, where N_3 and N_4 are the numbers of He^3 and He^4 atoms per unit volume and m_3 and m_4 are the masses of He^3 and He^4 atoms).

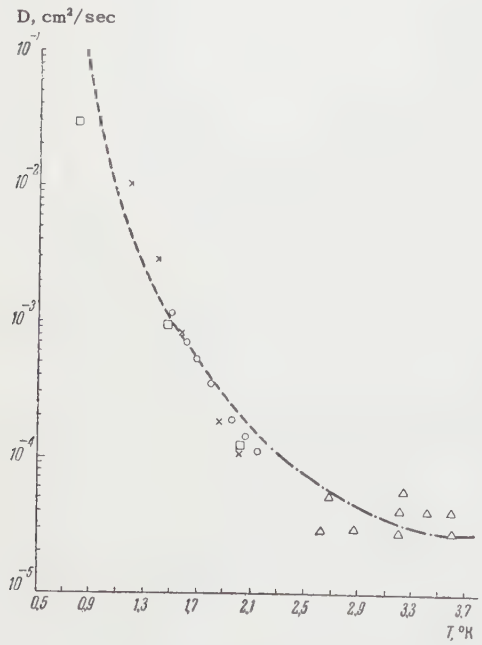

FIG. 2. Temperature dependence of the diffusion coefficient; ○ – results of the present work, × – reference 3, △ – references 4 and 5, □ – reference 6.

the work of Careri et al.[4,5] and of Beenakker et al.[3] are shown in Fig. 2. Since in the latter work there was an error in calculating the results, the values of D shown in Fig. 2 have been recalculated with the correct entropies of pure helium II, taken from the work of Kramers et al.[6] The values of D obtained by the spin-echo method by Garvin and Reich[7] are also included on the graph. Since they measured the diffusion coefficient under pressure,

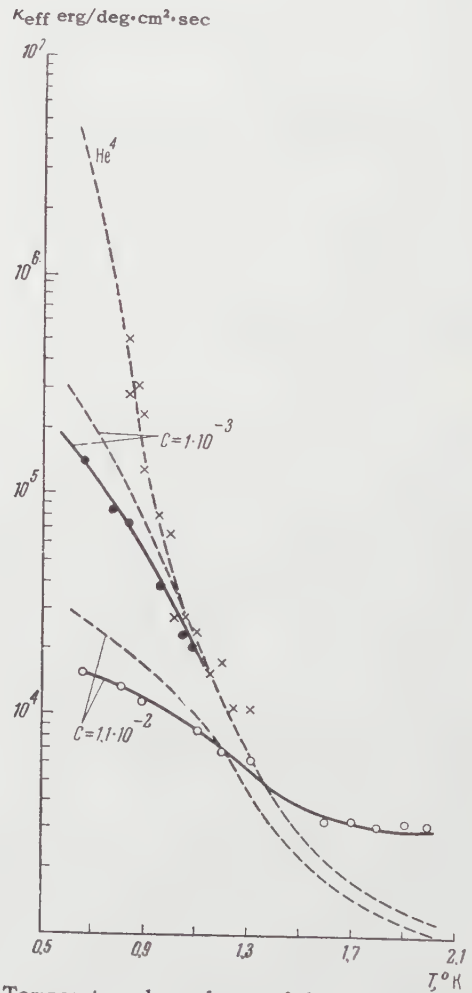

FIG. 3. Temperature dependence of the thermal conductivity, κ, of mixtures; ○ – results of the present work, × – from reference 8.

the values of D have been extrapolated roughly to the saturation vapor pressure.

Figure 3 shows the dependence of the thermal conductivity κ on T. For comparison, the thermal conductivity of He^4, obtained by Zinov'eva[8] from measurements of the attenuation of second sound, are shown. The dashed curves are theoretical, calculated from the results of Khalatnikov and Zharkov.[2] In this calculation the energy gap between the ground state of helium II and the lowest roton level was taken as $\Delta = 8.5°$ K. It can be seen from Fig. 3 that the thermal conductivity of weak solutions is little dependent on concentration in the temperature region between the λ point and 1.1° K. The curves for pure He^4 and for a mixture with C = 0.1% He^3 in He^4 diverge below 1.1° K. In this temperature region impurities influence the conductivity mechanism appreciably, reducing the mean free paths of rotons and phonons.

A more detailed discussion of the results and of the method, and the results of extending the measurements to lower concentrations will be published in the near future.

[1] A. N. Vetchinkin, Приборы и техника эксперимента (Instrum. and Exp. Techniques), in press.

[2] I. M. Khalatnikov and V. N. Zharkov, JETP **32**, 1108 (1957), Soviet Phys. JETP **5**, 905 (1957).

[3] Beenakker, Taconis, Lynton, Dokoupil, and van Soest, Physica **18**, 433 (1952).

[4] Careri, Reuss, Scaramuzzi, and Thomson, Proc. Int. Conference Low Temperature Physics and Chemistry, Univ. of Wisconsin Press (1958), p. 155.

[5] Careri, Reuss, and Beenakker, Nuovo cimento **13**, 148 (1959).

[6] Kramers, Wasscher, and Gorter, Physica **18**, 329 (1952).

[7] R. L. Garvin and H. A. Reich, Phys. Rev. **115**, 1478 (1959).

[8] K. N. Zinov'eva, JETP **31**, 31 (1956), Soviet Phys. JETP **4**, 36 (1957).

Translated by R. Berman
163

PARAMAGNETIC RESONANCE IN SINGLE-CRYSTAL TIN

M. S. KHAĬKIN

Institute for Physics Problems, Academy of Sciences, U.S.S.R.

Submitted to JETP editor June 14, 1960

J. Exptl. Theoret. Phys. (U.S.S.R.) **39**, 899-901 (September, 1960)

THE paramagnetic resonance of conduction electrons in metals has been investigated by Feher and Kip[1] on small particles and thin films of lithium, sodium, and beryllium, and was noted also in potassium. The theory of the effect was worked out by Dyson,[2] Azbel', Gerasimenko, and Lifshitz.[3,4] Experiments on paramagnetic resonance of large single crystals of metal have not yet been described in the literature.

In the present work, electron paramagnetic resonance was observed on a single crystal of very pure tin with $< 6 \times 10^{-5}$% of impurities.[5] The single crystal had dimensions of $11 \times 6 \times 1$ mm and served as the inner conductor of a strip-type resonator tuned to 9.35×10^9 cps. The measurements were carried out at a specimen temperature of 2.3° K by the frequency-modulation method.[6,7]

The results of the experiment are plotted in Fig. 1, in which are seen three paramagnetic-resonance signals. The copper parts of the resonator, prepared from copper of technical purity, give the wide line 1. The narrow symmetrical line 2 is the signal from $\sim 10^{-10}$ mole of crystalline diphenyl picryl hydrazyl, placed in the resonator for calibration. Line 3 is the paramagnetic resonance of the tin sample.

Rotation of the constant magnetic field in the plane perpendicular to the high-frequency magnetic field permits the observation of an apparent small anisotropy of the effect: the peak of the resonance moves by an amount which is of the order of its width. The significant change of the amplitude of the peak, which occurs during rotation of the field, is possibly explained[4] by a change of the angle of inclination of the field with respect to the sample surface. However, these aspects of the phenomenon are still not sufficiently clear from the experimental point of view.

In Fig. 2 is shown, on a larger scale, a record of the paramagnetic resonance of the electrons of tin (right-side peak) and of the calibration signal. The values of the constant magnetic field were recorded by a proton magnetometer (as in Fig. 1). From this graph it is possible to find the difference between the factor g_{Sn} for conduction electrons in tin and the factor $g_d = 2.0036$ for diphenyl

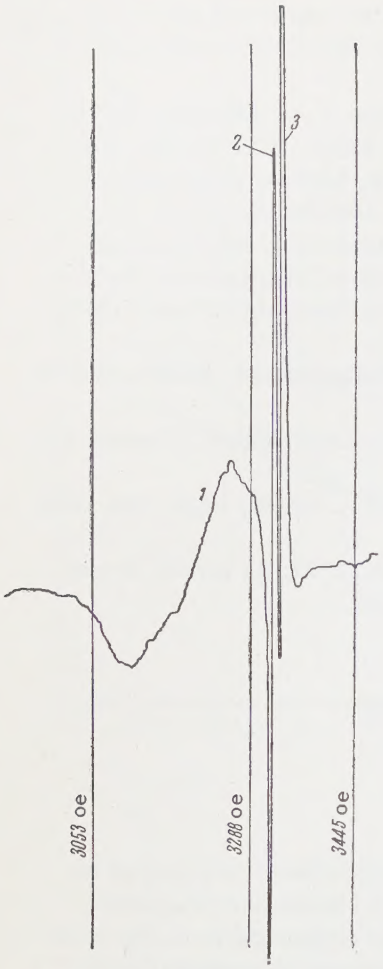

FIG. 1. Record of the experimental observation of paramagnetic resonance. Signals from three sources are seen: 1 – from the copper parts of the resonator, 2 – from diphenyl picryl hydrazyl, 3 – from single-crystal tin. The scale of the ordinate axis is proportional to the logarithmic derivative of the impedance of the sample with respect to the magnetic field, plotted along the abscissa.

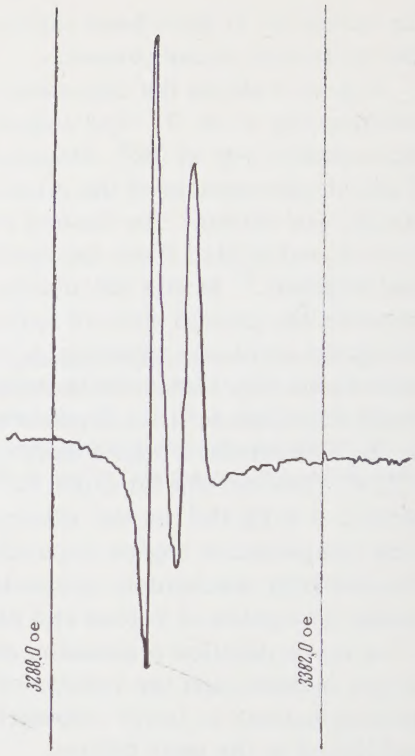

FIG. 2. Paramagnetic resonance of the conduction electrons of single-crystal tin (on the right), recorded simultaneously with the calibration signal of the paramagnetic resonance of diphenyl picryl hydrazyl. The variables along the coordinate axes are the same as in Fig. 1.

picryl hydrazyl

$$(g_{Sn} - g_d) / g_d = (H_d - H_{Sn}) / H_{Sn} = -(4.55 \pm 0.15) \cdot 10^{-3},$$

from which $g_{Sn} = 1.9945 \pm 0.0003$ (here H_d and H_{Sn} are the resonance values of the magnetic field).

The experiments described yield interesting data on the electron-spin relaxation times in single-crystal tin. Estimating the relaxation time T_2 after Dyson[2] as the reciprocal of width ΔH of the paramagnetic resonance line, which is ~ 4.5 oe (Fig. 2), we obtain $T_2 \sim 1.2 \times 10^{-8}$ sec. The more precise expression found by Kittel and derived in reference 1 gives

$$T_2 = 1.35 / \gamma \Delta H \approx 1.7 \cdot 10^{-8} \text{ sec}$$

(γ is the gyromagnetic ratio). This value of T_2 is, however, underestimated by 20 – 30% as a result of the line broadening due to the fact that the peak amplitude of modulation of the magnetic field was 1.7 oe. (For this reason the resonance line of diphenyl picryl hydrazyl in Fig. 2 is also broadened to ~ 2 oe.)

Considering the interaction of the spins with the lattice vibrations by means of orbital momentum, Elliot[8] found, that the corresponding relaxation time T_1 must be proportional to $\tau_R/(\Delta g)^2$ where τ_R is the electron mean-free-path time, estimated from the conductivity of the metal, and Δg is the deviation of the g factor of the electrons of the material from its value for a free electron. (A relaxation of this character was obtained by taking account of the scattering of electrons on impurities in the case of semiconductors.)

A more exact calculation of this effect was carried out by Andreev and Gerasimenko.[9] However, it is impossible to use their formulae to calculate T_1, for they took into account only the interaction of the electrons with the lattice vibrations, whereas under the conditions of the experiment the principal scattering was by the impurities. It can be noted only that T_1 must be large because of the large value of $\tau_R \approx 10^{-9}$ sec in the sample investigated, which indicates weak interaction between the electrons and the lattice. The value of τ_R in the experiments of Feher and Kip[1] was on the order of 10^{-14} sec.

The relaxation time $T_2 \approx 1.7 \times 10^{-8}$ sec means that the free path of the electron without changing spin orientation reaches 1 or 2 cm, whereas the electron free path determined by the conductivity of the metal is $l \approx 0.1$ cm. For a sample thickness of 0.1 cm this means that the electron can traverse the samples repeatedly, retaining its spin direction both as it collides within the metal and as it is scattered on its surface. This conclu-

sion can also be drawn from the results of Feher and Kip.[1]

However, for metal particles that are smaller than the depth of penetration of the electromagnetic field, these circumstances are not of such importance, whereas in the case of bulk metal they may be of decisive importance in polarizing the nuclei of the metal by Overhauser's method,[10] as discussed by Azbel' et al.[3] From their results it follows that in paramagnetic resonance of the metal electrons significant polarization of the nuclei in the bulk metal should take place to a depth

$$\delta \sim l\,(T_2/\tau_R)^{1/2} \approx 0.3 \text{ cm}.$$

Consequently, in a specimen 0.1 cm thick, with a high-frequency field applied at both sides, the polarization of the nuclei must be practically uniform throughout the volume. Since the sample thickness is less than the depth of spin diffusion δ, saturation of the resonance must be achieved in high-frequency fields which are significantly smaller than in the case of samples with thickness large compared to δ. This consideration clearly permits a significant reduction in the power rating of the generator and the expected Joule heating of the sample, which is of considerable experimental importance.

The author thanks P. L. Kapitza for his attention and interest in the work and Yu. A. Bychkov for useful discussions.

[1] G. Feher and A. F. Kip, Phys. Rev. **98**, 337 (1958).

[2] F. J. Dyson, Phys. Rev. **98**, 349 (1955).

[3] Azbel', Gerasimenko, and Lifshitz, JETP **32**, 1212 (1957), Soviet Phys. JETP **5**, 986 (1957).

[4] Azbel', Gerasimenko, and Lifshitz, JETP **35**, 691 (1958), Soviet Phys. JETP **8**, 480 (1959).

[5] V. B. Zernov and Yu. V. Sharvin, JETP **36**, 1038 (1959), Soviet Phys. JETP **9**, 737 (1959).

[6] M. S. Khaĭkin, JETP **37**, 1473 (1959), Soviet Phys. JETP **10**, 1044 (1960).

[7] M. S. Khaĭkin, Приборы и техника эксперимента (Instrum. and Exp. Techniques), in press.

[8] R. J. Elliott, Phys. Rev. **96**, 266 (1954).

[9] V. V. Andreev and V. I. Gerasimenko, JETP **35**, 1209 (1958), Soviet Phys. JETP **8**, 846 (1959).

[10] A. W. Overhauser, Phys. Rev. **92**, 411 (1953), G. R. Khutsishvili, Usp. Fiz. Nauk **71**, 9 (1960), Soviet Phys.-Uspekhi **3**, 285 (1960).

Translated by K. J. S. Cave
164